ABSTRACT

Generating Conjugated Boron Heterocycles
From Boroles

Sam Yruegas, Ph.D.

Mentor: Caleb D. Martin, Ph.D.

Much of the existing methodology for the construction of cyclic systems does not translate for boron-containing rings. With both limited routes and the restricted amount of commericially available reagents, significant progress is necessary to expand the library of known boracycles. Boroles, highly reactive four π-electron heterocycles, are a family of compounds with the potential to serve to as effective reagents to produce boron heterocycles with extended conjugation. The current work capitalizes on this ring expansion methodology to access six- and seven-membered heterocycles *via* 1,1- and 1,2-insertion reactions, respectively. These findings demonstrate that boroles, and their benzofused relatives 9-borafluorenes, are synthons for the construction of unique boracyclic architectures.

Generating Conjugated Boron Heterocycles From Boroles

by

Sam Yruegas, B.A.

A Dissertation

Approved by the Department of Chemistry and Biochemistry

_____

Patrick J. Farmer, Ph.D., Chairperson

Submitted to the Graduate Faculty of
Baylor University in Partial Fulfillment of the
Requirements for the Degree
of

Doctor of Philosophy

Approved by the Dissertation Committee

_____

Caleb D. Martin, Ph.D., Chairperson

_____

Patrick J. Farmer, Ph.D.

_____

Kevin K. Klausmeyer, Ph.D.

_____

John L. Wood, Ph.D.

_____

Alex Yokochi, Ph.D.

Accepted by the Graduate School

August 2019

_____

J. Larry Lyon, Ph.D., Dean

Page bearing signatures is kept on file in the Graduate School.

TABLE OF CONTENTS

LIST OF FIGURES

LIST OF TABLES

LIST OF SCHEMES

LIST OF NEW COMPOUNDS REPORTED

Compound	Formula/Structure	Page # for characterization details
2.12	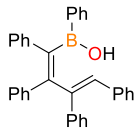	33
2.13	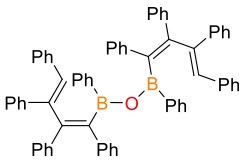	33
2.14	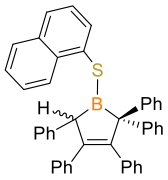	34
2.15	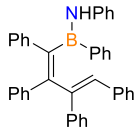	35
2.16	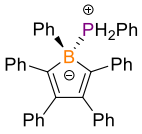	36
3.6	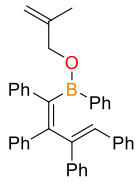	48
3.7	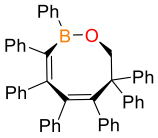	50

5.8	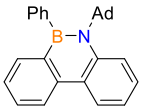	83
5.9	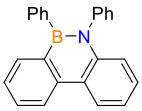	84
6.6	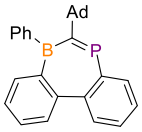	92
7.3	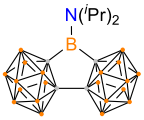	102
7.4	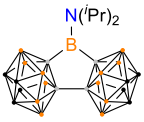	103
1.15-Ph·OPEt$_3$	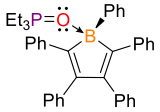	273
1.7-Ph·OPEt$_3$	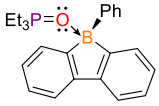	273

ACKNOWLEDGMENTS

Some very sage advice was imparted onto me very recently (said to me by Dr. Matt Conley, thanks Matt!). “We tend to forget the struggles we had to overcome to get here – just because it seems easy now, doesn’t mean it was easy then.” Hindsight is, at times, a terrible thing, and I did have my own set of trials and tribulations accompanied by the people who helped me trudge through them. I have not forgotten any of the kindness or actions of these individuals, and please let me say, I appreciate every one of you on these next few pages more than you’ll ever know.

I would like to thank my committee members for all the time and dedication they have provided these past five years. None of this work would have been possible without my mentor Caleb. It is a blessing to have someone believe in you so limitlessly. Thank you for the tough love, hard knocks, and constant belief that I could do more. Many times, I sat in your office, doubting myself, and always left feeling that I was going to make it work. The confidence I have in myself now emerged from the confidence you had in me. So from the bottom of my heart, thank you so much Caleb. I hope to continue to make you proud in all my future endeavors.

Pat, I have enjoyed our talks about low-carb meals, overcoming our glucose hurdles, and how important a Jablonski diagram is. KK, thank you for imparting all your Jedi X-ray crystallography knowledge as you are the Liam Neeson to my Ewan McGregor and I still have a lot to learn until I can get to Sir Alec Guinness level. Much thanks to Dr.

Alex Yokochi whom I hope enjoys all the X-ray crystallography I have to offer. Additional thanks to Dr. Sunghwan Lee for proceeding at my oral exam in 2016.

The #W6 original chemist, John Wood, continues to teach me about life, decision-making, and the endless pursuit of chemistry. I enjoyed our weekly meetings and updates as well as our frequent trashing of fondant (the worst edible decoration next to gum paste). Thank you for everything and please try not to stress too much.

Additional thanks go out to Kevin Shuford who always invited me into his office for a talk when I was feeling restless and stressed and Dr. Pennington for always having a smile and wave as I hustled back and forth from the lab to the spectrometer. The office staff was always helpful and available for all my events. Steve, you are the department MVP and the person who understood my college-and-band sister mania better than anyone. Much luck to Sam as he starts at Baylor in the fall. Ms. Barbara, you are an angel. Thank you for making sure we all got taken care of.

Special thanks go out to my undergraduate mentor Oleg V. Ozerov who has both supported and challenged me at every opportunity. I think he relishes this moment more than I do, but I am thankful for all advice, time, and mentorship. You are someone I look up to and want to be like in the future. Thanks for the caviar – I think I bought the wrong crackers for it though. Your cake is coming soon, I promise! Jess remains the pinnacle of awesomeness and is who I wanted to be when I started graduate school. Thank you for all your kindness and insight, even to this day. You are my woman chemist idol.

To my lab, past and current members, I love you guys! My job is only as great as it is in part to the fantastic labmates I have had over the years. Thomas, thanks for liking my lab tunes (although I have no idea how Irish rock got in there) and being my first glovebox

mate. My X-ray crystallography career started with some advice from Kexuan who was cautiously supportive of my methods and decidedly knew the best place to get crab in Waco. I learned a lot from Jon Barnard both in writing and chemistry. As my Lab Best Friend, every afternoon coffee was my favorite time of the day and your encouraging words profoundly touch me to this day. Kiran, you are the most enthusiastic person I know and our deskmate discussions helped to rejuvenate me when I was writing and wanted to be in the lab instead. Alba, I learned a lot about Spain and Catalan and appreciated someone to bond with over the Great British Bakeoff. Xiaojun, all the best to you in our group but honestly, you're already pretty awesome.

Jessica Baker, you amazing person! I learned so much teaching you and learning from you. I am so happy at your growth as both a chemist and as an individual and blessed to be included as a part of that. If I needed anyone to be honest, it would be you. I know we disagreed on a few things, but you always say you love thunderstorms, so what's a few raindrops between friends? Thank you for everything, love.

My partner in crime, Kristen Bluer, you are going to do great! Believe in yourself the way that I believe in you! I don't know what I would do without your great sensibility and dependability. Thanks for being my second in command, and at times, my plus one. I want you to know that you can accomplish anything you want with a dirty chai and a deep breath. I'm excited to see what's in store for you in the future and love you dearly!

To Leif Erickson Laperriere: I love your name. It has been an honor and privilege to stand by your side through two manuscripts, three zany glovebox adventures, and writing our thesis/dissertations. I have no doubt in my mind that you will succeed in all your future undertakings. You're going to kill it, kid.

To John and Tyler: when you get to be my age, you'll be sad that it's all over. Enjoy doing the chemistry and especially enjoy the learning. It's a beautiful ride. Also Tyler, thanks for looking out for me and I hope to never have a paperclip jar in the future (I hope yours disappears soon as well). I'm always here for you, buddy.

To all my "kids": each of you is amazing and it was such a great experience to be your mentor. Dayna taught me about history and Beyonce and I am so proud of her graduate school accomplishments. CJ is the sweetest kid and best Pokemon Go buddy, his dedication to his work is second to none. Jesse J. Martinez you are such a cool kid and you have an amazing path ahead of you. Just remember to look before you step and you'll be fine and remember I am always in your corner. Kate and Collin: outreach was a blast! Getting to see your bright, shining faces doing experiments made my day. Kate, I see great things for you, keep hustling! Interacting and teaching all of you was a highlight of my Ph.D.

Many thanks to the Farmer and Wood Labs for being supportive and making me feel welcome in a very collaborative and friendly community. Specifically, Heemal and Monica who assured me that knowledge would come in due time and talked to me about mechanisms, tacos, and books. Joyce who helped me organize a baby shower and is a talented chemist and crafter. Jacob Timmerman whose coffee drive-bys helped conceptualize ideas and outline game plans for success. Mike, Ottis, and Lasien – your lunch invitations were always a good day in our lab.

Much thanks to Nate, Tucker, and Mike Pettitt for all their help in CGSA events alongside all the other CGSA members, past and present. Immense thanks to Zach Winfield who I met at Graduate Recruitment Weekend and knew instantly we'd be best buds. Thanks for driving me around, teaching me how to make kolaches, and always having a listening

ear and helping hand. Also for getting me into Dungeons and Dragons which was always a good time!

Surviving graduate school was a success thanks to my family. My mom and sisters were always there to listen to my work stories, ask about my crystal structures, and rush to my rescue when I needed them. Thanks, Mom, for all your encouragement and maybe half a thanks for making sure I finished my manuscripts on time with your constant text message reminders, I love you. Cori thanks for imparting onto me all your business management skills alongside your excellent conflict resolution abilities. You are always right about everything, now and forever, I love you sissy. Carla thanks for letting me be your big sister when I could (love you). I'm so proud of you and your accomplishments. I can't wait to hear stories about your adventures at UTRGV and you should try out for mariachi because you're extremely talented! You are all three strong, independent women and thank you for sticking this out with me.

To all my tios, tias, and primos: te amo! Everyone brought something to the table. Thank you to Tio Gabe and Tia Chawie for spending dinner with me at The Grape (it was fun!) and their constant encouragement. Thanks to Tio Jerry and Tia Petra for taking care of me and being fiercely protective when I need them to be (love you tons). Thanks to Tia Becky and Tio Victor for believing in me and my work. Thanks to Tia Bonnie who knew how to cheer me up and my diabetes buddy. My Tio Rene, Tio Chacho, Tia Olga, and Tia Susie who fed me great food and company whenever I was home. Jerry, thanks for being the little brother I never had. Katie, you are so special. You work hard at everything you do, and I know nothing will stop you from achieving your goals. Carissa, my little ball of sunshine, I love how excited you get about science and I hope to only encourage you to

pursue your passions in the future. I also owe both of you new crystal growing kits but you are both naturals at it!

To my grandfather: thank you for making me the person that I am today. I love you and although being an electrician wasn't in the cards for me, I'm still happy we can share moments together like getting excited about going to Harbor Freight to buy tools. Leticia, gracias por todo el aliento y especialmente por el delicioso flan. Tony thanks for being a great brother-in-law and checking out my car every time I decided I was going to drive somewhere terrifying. To Debbie and Joe: thank you for including me in your family, it means the world to me.

A special thanks to all the dogs and their owners who encouraged me to get my own (Caleb and my family). Molly you were a sweetheart and a huge comfort to me. Olive is the cutest Lab(ador) assistant our group could ever have. Watson, Holmes, and Diesel always kept me company when I was away from home with their affection. Sherlock and Hercule are a constant delight in my life (though sometimes also a headache) and I am so lucky to have them.

Last, but certainly not least, Joshua B. Cox: I can say confidently you are the love of my life. The past five years have been a tumultuous ride that I've had the pleasure of sharing with you. Since the day I met you in a chemistry office on a summer day in 2012, I wanted to be just as good as you were in everything that you did and that continues to be my goal to this day. Thank you for all the chemistry advice, the life talks, the column suggestions, the low-carb meals, the sarcasm, the giant steel rolling pin, and washing the dishes (which I hate) as I put together this dissertation. Thank you for sticking by me through it all. I love you corazón!.

DEDICATION

To my mother Cala Yruegas, the best confidant, friend, and my undeterred champion! Gracias por todo lo que has hecho por mí estos veintisiete años. Te quiero hasta la luna y más allá!

CHAPTER ONE

Introduction

1.1 Aromatic Boron Heterocycles

Boron heterocycles have emerged as a key class of molecules due to the myriad of properties they possess, largely as a result of the incorporation of an electron deficient boron center.[1-2] Particularly, the empty p_z-orbital on boron can participate in π-conjugation when integrated into unsaturated cyclic systems.[3-4] One key feature of these compounds is the unique electronic properties that result from the integration of boron atoms into large organic cyclic frameworks culminating in their development as electronic materials, specifically as organic light emitting diodes (OLEDs).[5-8] Molecules, such as borane **1.1**, a B-doped polycyclic aromatic hydrocarbon, exhibit intense blue fluorescence showing great promise for use in OLEDs (Figure 1.1).[1] In a similar vein, B-doped pyrene frameworks (i.e. **1.2**) are currently being explored as possible n-channel organic semiconductors.[9]

Contemporarily, a surge of interest in biologically active boracycles has given rise to compounds such as an antitumor agent (**1.3**) featuring a 1,2-azaborine which inhibits binding to the CDK2 protein, even better than its phenyl analogue.[10] In addition, a similar ring system is an active antibacterial agent (**1.4**) that inhibits enoyl reductase in *Escherichia coli*.[11] Boron heterocycles have also shown potential as pharmaceuticals, specifically as antifungal agents. Tavaborole (**1.5**) and crisaborole (**1.6**) are commercially marketed as Kerydin® for treatment of the nail fungus onychomyscosis and nonsteroidal medication Eucrisa® for treatment of eczema, respectively.[12]

While it is invigorating to see the incorporation of the boron atom within these cyclic systems, synthetic barriers must be overcome to access these species. Much of the existing methodology for the construction of cyclic systems does not translate for boron-containing rings.[13-15] With both limited routes and the restricted amount of commericially available reagents, significant progress is necessary to expand the library of known boracycles. New synthetic approaches include harnessing boron-containing substrates that are high in potential energy and thermodynamically poised to react in order to furnish more stable products, such a set of compounds in this class are boroles.

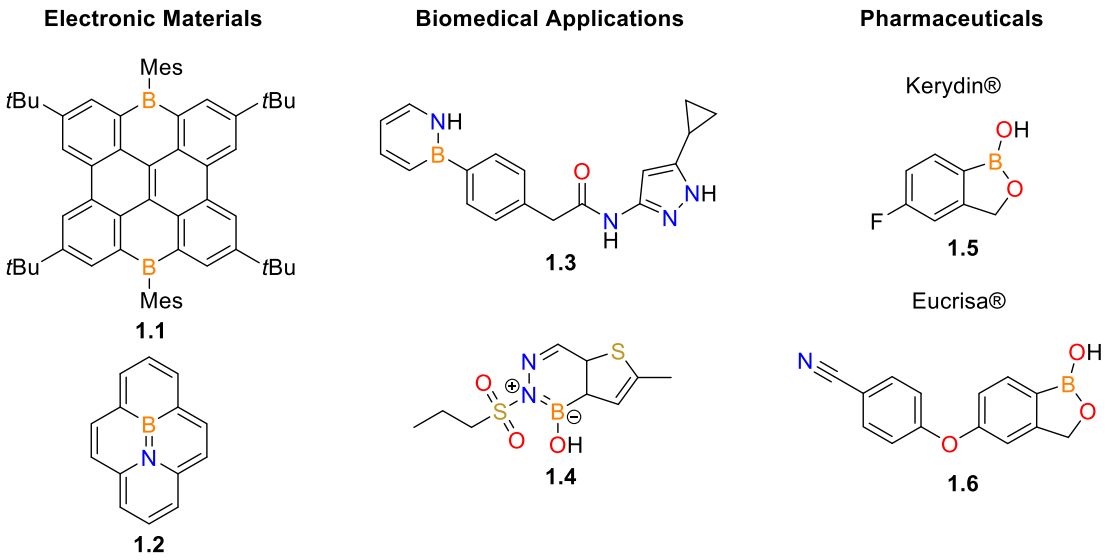

Figure 1.1. Examples of aromatic boron heterocycles.

1.2 Boroles

Boroles are metalloles containing four π-electrons within a strained five-membered ring. Boroles are also antiaromatic, and in conjunction with the aforementioned strain, engenders an energetically unfavourable structure.[16-18] Even though the first well known borole, pentaphenylborole (**1.7-Ph**, Figure 1.2), was synthesized in 1969 by Eisch[19] and coworkers, borole chemistry is relatively undeveloped. It was not until 2008, when its X-

ray crystal structure was reported that chemists probed its reactivity.[20] This report set the stage for a renewed renaissance of borole chemistry as exemplified by the exponential submission of publications thereafter. The combination of an antiaromatic species coupled with an activated diene backbone and Lewis acidic center results in a molecule with a unique and diverse reactivity.[21]

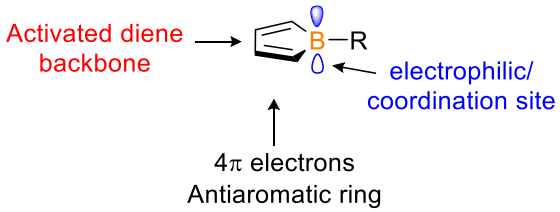

Figure 1.2. Properties of boroles (**1.7**).

1.2.1 Synthesis

Two general routes exist for the synthesis of boroles: direct salt metathesis with an aryl-substituted 1,4-dilithio-1,3-butadiene and corresponding dihalo- or haloborane[16, 22] or transmetallation from a tin or zirconium precursor (Scheme 1.1).[23-24] Braye and coworkers utilized the former route and reported the proposed synthesis of **1.7-Ph** as a colorless solid in 1961,[25] later debunked in 1969 by Eisch.[19] The salt metathesis method was reexamined by Robinson and coworkers in 2002 to access the B-bromo borole (**1.7-Br**), however, the reaction resulted in formation of fused boracycle **1.9** with a newly formed ethyl group on the adjacent carbon center, presumably derived from the solvent (Scheme 1.1).[26] As a result, few monocyclic boroles are made *via* this method and those known suffer from poor yields as intermediate **1.8** is difficult to manipulate.

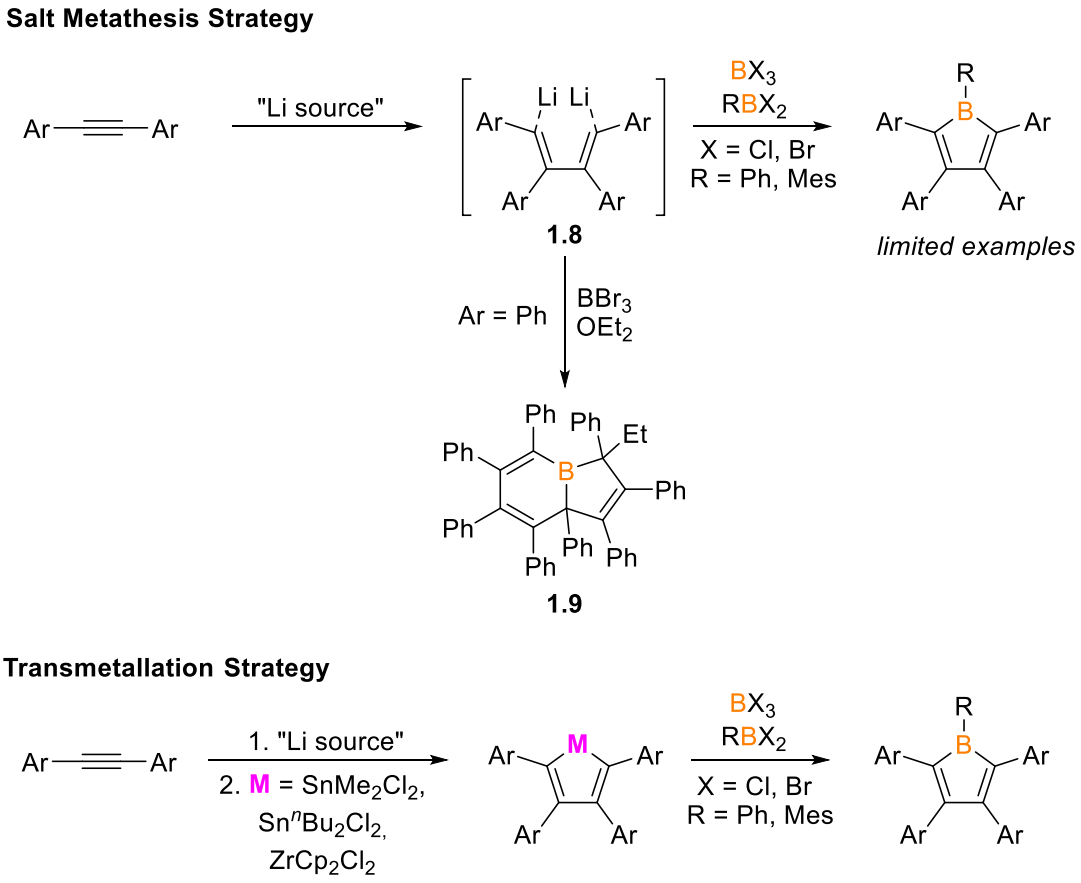

Scheme 1.1. General routes towards boroles.

The transmetallation route is the more popular method due to the relative ease involved in performing tin to boron exchange reactions and is known to work with a variety of diarylacetylenes granting access to functionalized species.[23] The original route developed by Eisch and coworkers remains the most commonly used methodology (Scheme 1.2)[27]. Early work in our group focused on the optimization of this route as well as adaptation to large scale, the details of which are elucidated in Appendix G.

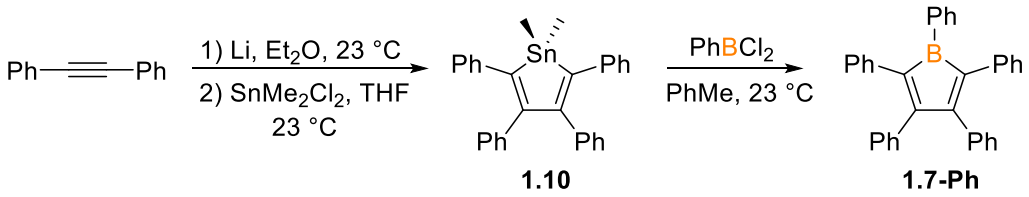

Scheme 1.2. Synthesis of **1.7-Ph**.

1.2.2 Brief Overview of Reactivity

The reactivity of **1.7-Ph** can be tentatively generalized in five categories: coordination, coordinative ring expansion, Diels-Alder cycloadditions, bond activation, and redox chemistry.[21] Due to the very Lewis acidic boron center of **1.7-Ph**, coordination of Lewis bases is facile including pyridines, ethers, phosphines, and carbenes.[28-33] Most rearrangements begin with coordination to the boron center, rendering the adjacent endocyclic B-C bond nucleophilic and poised to insert an unsaturated moiety. Our group, as well as Braunschweig and coworkers, reported the generation of the 1,2-azaborine species **1.11** *via* formal nitrene insertion from an azide, commonly referred to as a 1,1-insertion reaction (Scheme 1.3).[34-37] The method was expanded by Braunschweig and shown to work for several pentaarylboroles and azide partners. In 2015, our group demonstrated similar 1,1-insertion chemistry to give the first 1,2-phosphaborine species by incorporation of a P-Ph unit into the borole ring.[38]

The first instance of Diels Alder reactivity with **1.7-Ph** reported the borole acting as the diene with diphenylacetylene as the dienophile where the resulting product **1.12** rearranged to heptaphenylborepin upon heating.[39] Recently, it has also been shown that **1.7-Ph** can act as a dienophile in the presence of certain dienes.[40-41] Pentaphenylborole has also been shown to activate small molecules like CO and CO_2, resulting in rather unique reactivity.[42-44]

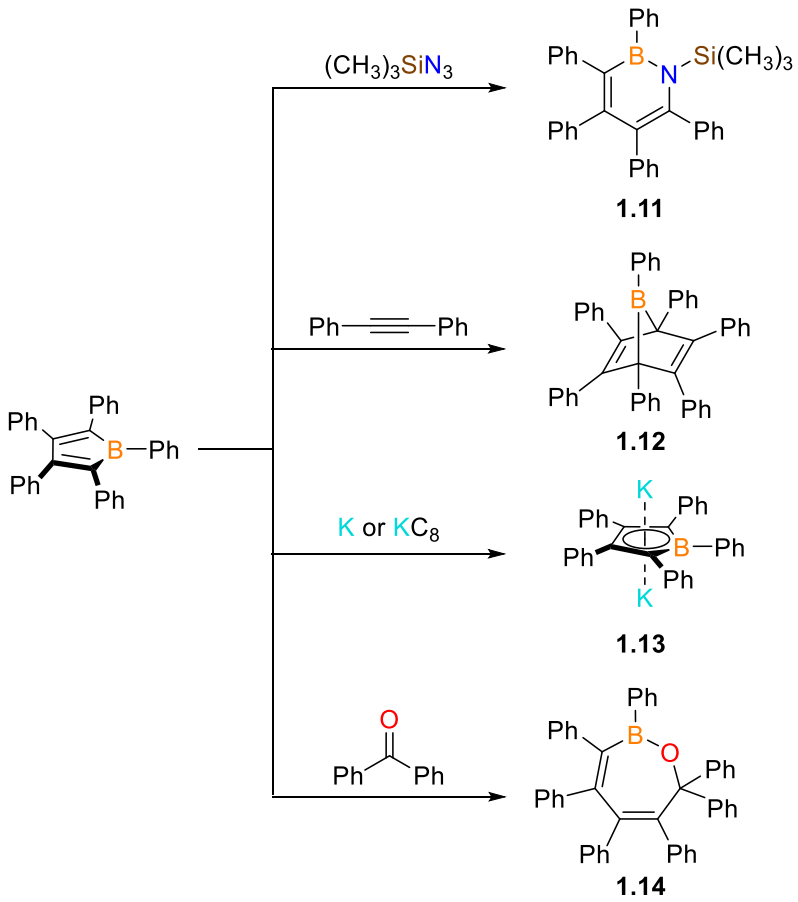

Scheme 1.3. Explored chemistry of pentaphenylborole.

The activation of E-H bonds is more straightforward. **1.7-Ph** can split H_2, adding each to the adjacent carbon center providing boracyclopent-3-ene as the *cis*- and *trans*-isomers.[45-50] The facile chemical reduction of monocyclic boroles allows access to 6π electron borole dianions which are garnering interest as a new class of ligands in transition metal chemistry.[32, 51-55] The reduction of **1.7-Ph** can be achieved by using K or KC_8 to give boroledііde **1.13**.

The 1,1-insertion methodology can be extended to other systems including 1,2- and 1,3-dipolar moieties to construct 7- and 8-membered boracycles. One example is shown in Scheme 1.3 demonstrating the ability of ketones (*i.e* benzophenone) to insert into **1.7-Ph**

to give 7-membered ring **1.14**.[56] This reactivity has been expanded to include nitriles, isocyanates, isothiocyanates, aldehydes, phosphaalkynes, diazoalkanes, azobenzenes, and ketenes.[56-62] Although this is only a brief introduction of **1.7-Ph**, its vast reactivity gives credence to its potential utility as a reagent to access large boron heterocycles.

1.3 9-Borafluorenes

The aforementioned reactivity is not limited to monocyclic boroles. Recent work demonstrates that dibenzofused boroles, otherwise known as 9-borafluorenes, may also be capable of analogous transformations. The scaffold of 9-borafluorene (**1.15**) was first reported by Köster and coworkers in 1963[63], further detailing the synthesis of various B-alkyl-, aryl-, and halo-substituted-9-borafluorenes. 9-Borafluorenes share similarities to their borole relatives including a Lewis acidic boron center and planarized ring system (Figure 1.3).[64-65]

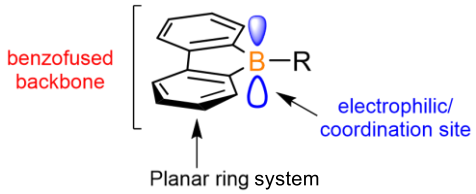

Figure 1.3. Properties of 9-borafluorenes (**1.15**).

The most relevant alteration is the biphenyl backbone instead of the 1,3-butadiene motif seen in monocyclic boroles, which impedes Diels Alder reactivity.[66] Interestingly, the dibenzoborole skeleton functions as an extended π-system, and when utilized in conjunction with known synthetic methods, could allow access to a diverse library of cyclic boron compounds.[67] Although 9-borafluorenes predate boroles (**1.7**), the body of work surrounding these molecules is rather minute. In that context, this introduction details the

synthesis and reactivity of several halo- and aryl-substituted 9-borafluorenes to fashion a comprehensive discussion.

1.3.1 Synthesis

While there are a few reported methods to generate 9-borafluorenes, the most common routes to access **1.15** are through a salt metathesis pathway or transmetallation approach utilizing tin precursors.[68-69] The salt metathesis route, unlike for boroles (**1.7**), is employed frequently for the synthesis of halogen substituted 9-borafluorenes, including the B-chloro derivative (**1.15-Cl**). The dilithiated species **1.16** is much easier to manipulate than **1.8** (Scheme 1.4). As a result, most 9-borafluorenes synthesized are generated from this route.[70-71]

Our group found the salt metathesis pathway to be inconsistent, and explored the transmetallation pathway, akin to that of **1.7**, which we were more familiar with. By optimizing this route, we could generate stannole **1.17** in multigram quantities (~20 g) easily and access 9-phenyl-9-borafluorene (**1.15-Ph**) and 9-chloro-9-borafluorene (**1.15-Cl**) *via* transmetallation.[72]

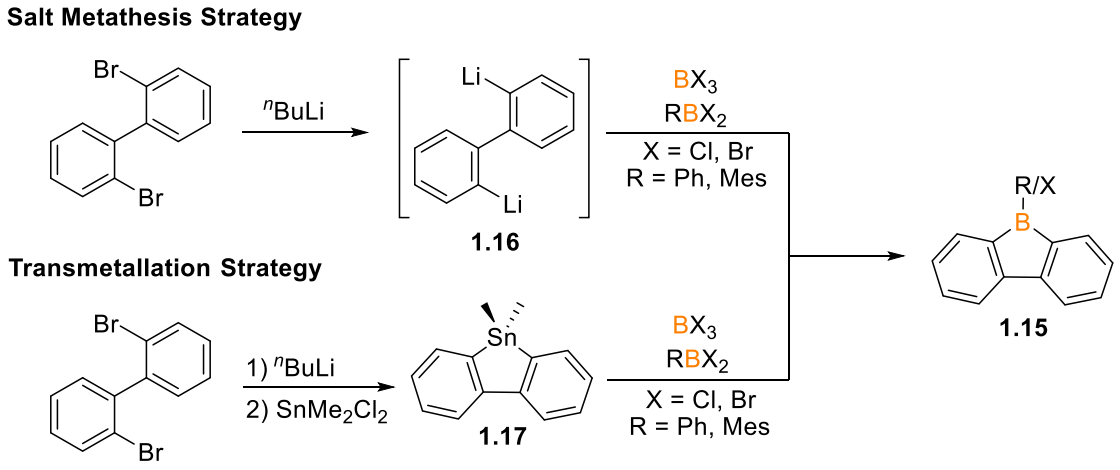

Scheme 1.4. General routes towards 9-borafluorenes.

1.3.2 Brief Overview of Reactivity

The reactivity of 9-borafluorenes is an emerging area of exploration. Therefore, only a few key examples are described in Scheme 1.5 to note the differences and similarities of **1.15** to **1.7-Ph**. The Lewis bases readily coordinate to the Lewis acidic boron center (**1.18**) just as **1.7-Ph** does.[62, 73-77] Amine-substituted-9-borafluorenes undergo spontaneous ring expansions, such as in the case of **1.19** where the nitrogen of the amine is incorporated into the ring to give a 1,2-azaborine containing product (Scheme 1.5).[78]

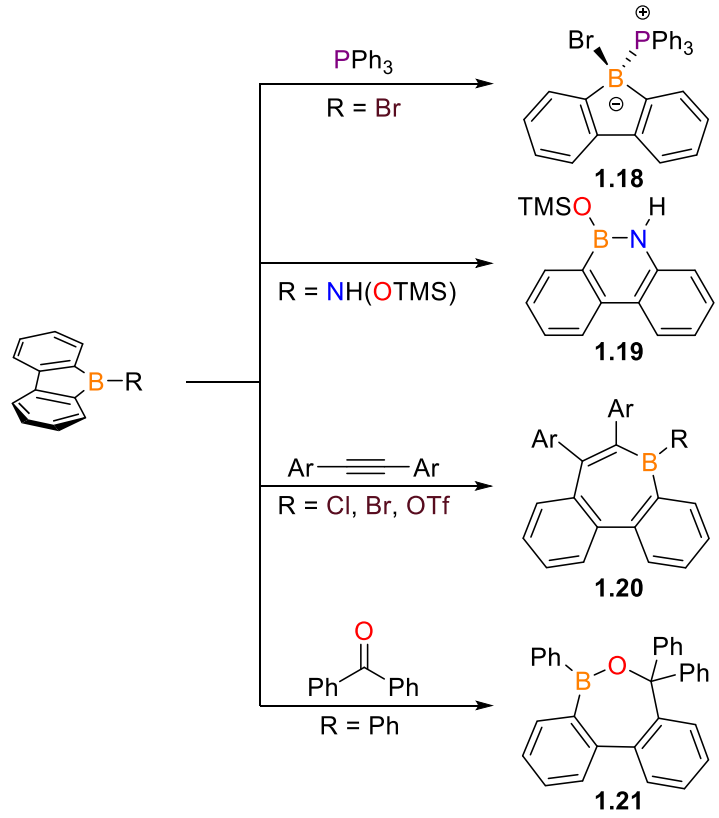

Scheme 1.5. Explored chemistry of 9-borafluorenes.

Work by Fukushima and coworkers showed insertion of a C_2 unit from an alkyne into the 9-borafluorene ring resulting in a 7-membered boracycle (**1.20**). In a more

traditional sense, aryl-substituted-9-borafluorenes can perform 1,2-insertions like their monocyclic relative.[66] Ketones can react to insert the carbonyl unit into the ring yielding the BO-containing 7-membered heterocycle **1.21** and this reactivity has been extended to include aldehydes, ketenes, isocyanates, carbodiimides, and diazoalkanes.[62, 79-80]

1.4 Properties of Boroles and 9-Borafluorenes

Boroles and 9-borafluorenes are antiaromatic compounds as well as Lewis acids. The methods of investigation of both properties are elucidated below as they play a significant role in the unraveling of borole reactivity pathways.

1.4.1 Lewis Acidity

The Gutmann-Beckett method is the most used Lewis acidity scale for measuring boron Lewis acids.[81] This method is used for boroles instead of the Child's method, which uses crotonaldehyde[82] and has functional groups that react with boroles (see Reactivity Sections 1.2.2 and 1.3.2). The Gutmann-Beckett method gauges the strength of the Lewis acid by adding an excess of a Lewis base probe, in this case triethylphosphine oxide (Et_3PO), to form a Lewis acid-base adduct. The adduct will have a new signal in the ^{31}P NMR spectrum shifted from the free phosphine oxide (41.0 ppm). From this data, an Acceptor Number (AN) scale can be extrapolated using the following formula $AN = 2.21 \times (\delta^{31}P_{sample} - 41.0)$. The larger the AN, the stronger the Lewis acid. The Gutmann-Beckett method is sensitive to solvent calibration, so it is important to perform the experiment with consistent variables. Figure 1.4 details Gutmann-Beckett values of **1.7-Ph**, several derivatives of **1.15**, versus the extremely Lewis acidic tris(pentafluorophenyl)borane ($B[C_6F_5]_3$)[83].

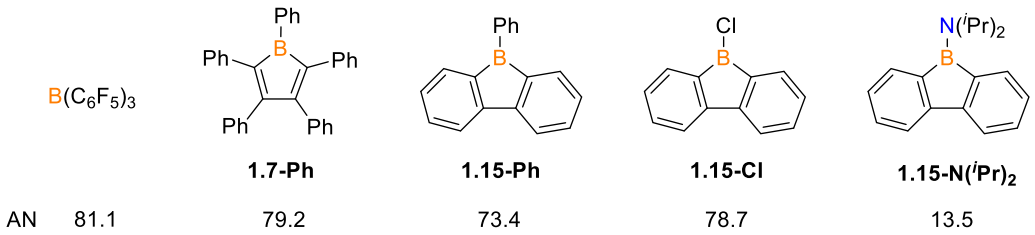

Figure 1.4. Gutmann-Beckett values for various boranes (all performed in C_6D_6).

1.4.2 Antiaromaticity and Aromaticity

The criteria for aromaticity was historically based upon the traditional definition of Hückel's (4n + 2)π electron rule.[84] While most criteria of aromaticity were reserved for organic species, it is now used for heteroatom-containing compounds. Previous computational methods, such as resonance stabilization energy (RSE) or aromatic stabilization energies (ASE), are based upon energetics and can be tedious to compute and are sometimes system dependent.[85-87] As chemistry develops and complex molecules arise, it becomes more difficult to rely on Hückel's rule as the only decree of aromaticity (Figure 1.5).

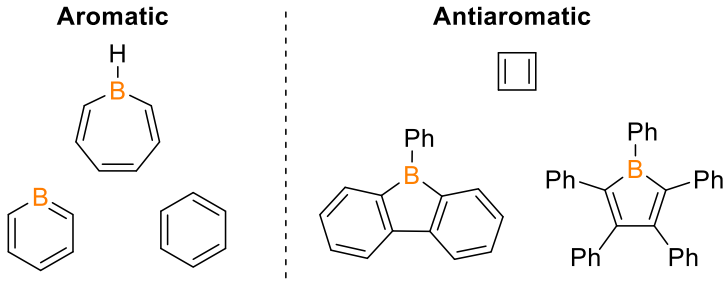

Figure 1.5. Examples of aromatic and antiaromatic compounds.

Schleyer and coworkers proposed the usage of nucleus-independent chemical shifts (NICS) as a gauge of aromaticity in 1996.[88] Under an applied magnetic field (B_0, Figure.

1.6), ring currents are induced in aromatic and antiaromatic compounds (orange rings, Figure 1.6) which then create a magnetic field (purple rings, Figure. 1.6).

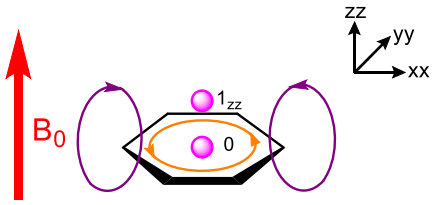

Figure 1.6. Diagram of aromatic ring current.

The induced field can then be sensed by a NICS probe, in this case a ghost atom (represented by the pink spheres), which then report a value of the absolute chemical shielding in parts per million. Typically, two values are considered to be the best gauge of aromaticity: NICS(0), defined as the shielding sensed at the center of the ring, and NICS(1)$_{zz}$, the shielding sensed 1 Å above the center of the ring in the direction of the zz-tensor out of the plane. Aromatic compounds are distinguished by having a large negative value (diatropic ring current), indicative of shielding. Antiaromatic compounds have large positive values (paratropic ring current) and the region is considered deshielded. Table 1.1 confirms that both **1.7-Ph** and **1.15-Ph** are antiaromatic *via* this method. NICS calculations of conjugated boron heterocycles can be useful in ascertaining both aromaticity and stability trends.[89-91]

Table 1.1. NICS(0) and NICS(1)$_{zz}$ Values of Benzene, **1.7-Ph**, and **1.15-Ph**[89]

Compounds		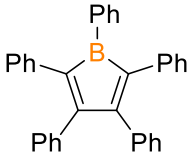	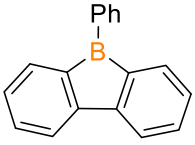
NICS(0)	-8.1	+12.9	+13.8
NICS(1)$_{zz}$	-29.0	+25.9	+23.9

1.5 Scope of the Dissertation and Attributions

For all intents and purposes, the work in this dissertation is focused on the reactivity of boroles and 9-borafluorenes accompanied by mechanistic studies, and in most cases, supported by computations.

Yruegas, S.; Huang, K.; Wilson, D. J. D.; Dutton, J. L.; Martin, C. D., *Dalton Trans*., **2016**, *45*, 9902-9911.

Chapter Two details the reactions of pentaphenylborole with E-H (E = Group 15 or 16) bonds to assess the lability of the endocyclic B-C bond. S.Y and C.D.M conceived the work and designed the experiments, S.Y acquired primary characterization data, K.H aided in X-ray crystallographic studies. D.J.D.W and J.L.D performed computational studies and composed manuscript drafts alongside S.Y and C.D.M.

Yruegas, S.; Wilson, C.; Dutton, J. L.; Martin, C. D., *Organometallics*, **2017**, *36*, 2581-2587.

Extending this work further, Chapter Three describes how pentaphenylborole induces the ring opening of epoxides to form different products based on the substitution of the epoxide. These results serve as a guidemap for determining methods of generating diverse boron-containing systems. S.Y and C.D.M conceived the work and designed the experiments, S.Y and C.W acquired primary characterization data, S.Y aided in X-ray crystallographic studies, and J.L.D performed computational studies and composed manuscript drafts alongside S.Y and C.D.M.

Yruegas, S.; Patterson, D. C.; Martin, C. D., *Chem. Commun*., **2016**, *52*, 6658-6661.

Yruegas, S.; Martin, C. D., *Chem. –Eur. J*., **2016**, *22*, 18358-18361.

Chapter Four identifies pentaarylboroles as potential precursors for the synthesis of hybrid inorganic/organic boron-containing benzene analogues that feature oxygen or sulfur as the lone-pair bearing heteroatom. The ability of boroles to perform single heteroatom insertions into the BC_4 ring allows access to a library of unusual aromatic species. S.Y and C.D.M conceived the work and designed the experiments, S.Y acquired primary characterization data and X-ray crystallographic data and performed computational studies. D.C.P acquired initial samples for X-ray analysis. Manuscript drafts were composed by S.Y and C.D.M.

Yruegas, S.; Martinez, J. J.; Martin, C. D., *Chem. Commun.,* **2018**, *54*, 6808-6811.

Chapters Five focuses on expanding the scope of the ring expansion methodology, established for pentaarylboroles in Chapter 2, to a benzofused borole, specifically 9-borafluorene, to generate 6-membered BN-containing heterocycles. S.Y and C.D.M conceived the work and designed the experiments, S.Y and J.J.M acquired primary characterization data, S.Y aided in X-ray crystallographic studies. Manuscript drafts were composed by S.Y and C.D.M.

Yruegas, S.; Barnard, J. H.; Al-Furaiji, K.; Dutton, J. L; Wilson, D. J. D; Martin, C. D., *Organometallics*, **2018**, *37*, 1515-1518.

Chapter Six investigates the reactivity of phosphaalkynes with 9-borafluorene both experimentally and mechanistically. The outcomes from these studies demonstrate the

utility of a family of boroles to act as reagents for the synthesis of fused boron heterocycles. S.Y and C.D.M conceived the work and designed the experiments, S.Y and J.H.B acquired primary characterization data, S.Y aided in X-ray crystallographic studies, and K. A-F, D.J.D.W, and J.L.D performed computational studies and composed manuscript drafts alongside S.Y and C.D.M.

Yruegas, S.; Axtell, J. C.; Kirlikovali, K. O.; Spokoyny, A. M.; Martin, C. D, *Chem. Commun.*, **2019**, *55*, 2892-2895.

Chapter Seven centers on the incorporation of a 1,1'-bis(*o*-carborane) scaffold to generate three-dimensional analogues of 9-borafluorene. The resulting species represent the first examples of 1,1'-bis(carboranyl)boranes and the beginning of an investigation of new unique boracyclic architectures utilizing carboranes. S.Y, A.M.S, and C.D.M conceived the work. S.Y, J.C.A, and C.D.M and designed the experiments, S.Y acquired primary characterization data and performed X-ray crystallographic studies. K.O.K performed computational studies. All authors aided in composition of manuscript drafts.

CHAPTER TWO

Probing the Reactivity of Pentaphenylborole with N-H, O-H, P-H, and S-H Bonds

This chapter published as: Yruegas, S.; Huang, K.; Wilson, D. J. D.; Dutton, J. L.; Martin, C. D., *Dalton Trans*., **2016**, *45*, 9902-9911.

2.1 Introduction

The chemistry of boroles has been an attractive subject due to the unique electronic structure of this five membered ring.[16-17, 19-20, 24, 27, 30-31, 51, 53, 68, 92-100] The antiaromatic four π electron heterocycle has displayed diverse reactivity with a variety of molecules.[18, 32-36, 38, 42, 45, 47-49, 54-58, 64, 78, 90, 101-121] A particularly interesting example of reactivity was reported by Piers and coworkers demonstrating that pentaaryl boroles (**1.7-Ph** and **2.1**) react with dihydrogen under ambient conditions to produce 1-bora-cyclopent-3-ene heterocycles *via* the introduction of the hydrogen atoms on the carbon centers adjacent to boron (**2.2** and **2.3**, Scheme 2.1).[45, 120] This was a significant discovery as an external Lewis base was not required, contrary to prototypical Frustrated Lewis Pairs.[122-127] Braunschweig and coworkers showed that pentaphenylborole (**1.7-Ph**) undergoes a hydrosilylation reaction with $HSiEt_3$ to afford the analogous silyl substituted 1-bora-cyclopent-3-ene (**2.4**).[49] Our group extended this work to other main group hydrides ($HGeEt_3$, HSn^nBu_3, and HBpin; pin = pinacol) which showed the same type of addition reactions (**2.5-2.7**).[50]

Protic systems react differently than non-polar H_2 and hydridic substrates. Piers and coworkers reported the reaction of phenol with **1.7-Ph** to rapidly produce the ring opened species **2.8** (Scheme 2.2). This result can be attributed to the lability of the endocyclic B-C bond, particularly upon coordination of the oxygen atom.[45] Although several

publications had reported that boroles were very water sensitive, this process had not been comprehensively studied.[19-20, 24, 27, 51, 92, 116]

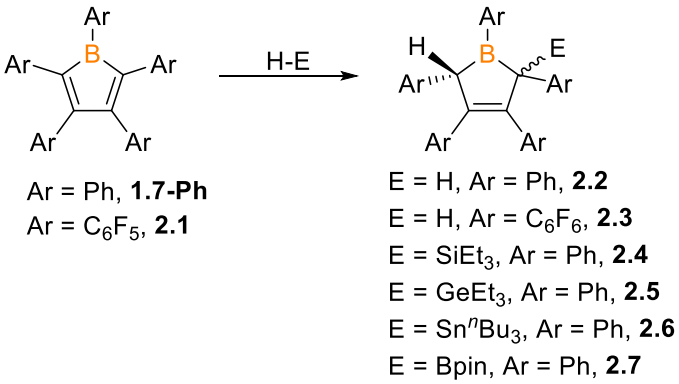

Scheme 2.1. Addition products from the reactions of H_2 and main group hydrides with boroles.

Marder and coworkers prepared boroles featuring bulky mesityl groups on boron (**1.7-Mes** and **1.7-^{F}Mes**) with the goal of protecting the electrophilic boron center as well as the labile B-C bonds.[116] A water stability study in comparison with the slightly smaller B-Mes derivative (**1.7-Mes**) showed a 600 fold increase in lifetime. The hydrolysis products formed (**2.9-2.11**) were analogous to the phenol protodeborylation ring opening reaction. Despite the second O-H group on water, only the activation of one bond occurred. However, this may have been a result of the bulky boroles that were studied, perhaps impeding further reactivity. Based on the diverse results with water, phenol, main group hydrides, and dihydrogen, we herein report a reactivity study of pentaphenylborole with various E-H (Group 15/16) bonds to unravel new reactivity pathways in borole chemistry. Boroles have interesting electronic properties and understanding their reactivity and stability with a wide variety of functional groups could facilitate the development of borole containing electronic materials.

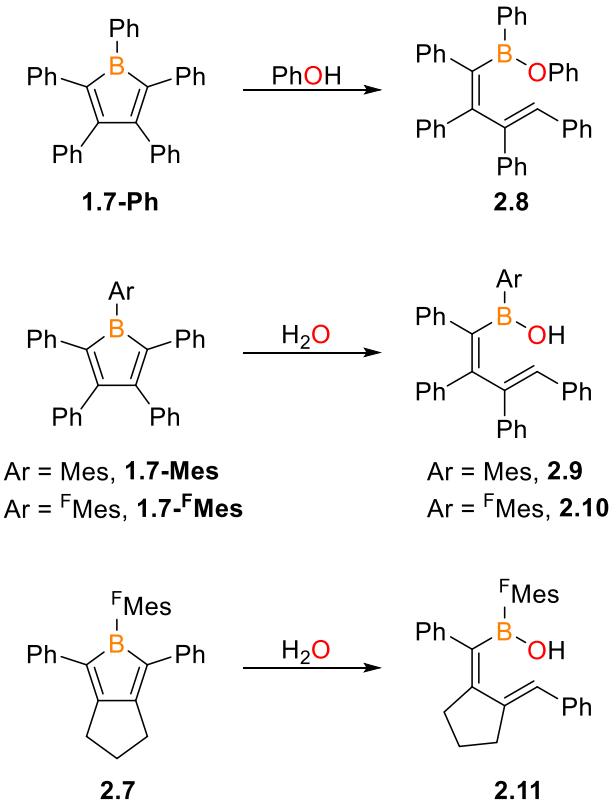

Scheme 2.2. Reactions of boroles with phenol and water.

2.2 Investigating the B-C Bond Cleavage of Pentaphenylborole

The 1:1 stoichiometric reaction of pentaphenylborole **1.7-Ph** with water in dichloromethane at 0 ˚C resulted in the rapid change of the blue color of pentaphenylborole to yellow (Scheme 2.3). Removing the solvent *in vacuo* and analyzing the redissolved residue in $CDCl_3$ by ^1H NMR spectroscopy showed two products in a ~3:1 ratio. The singlet at 5.44 ppm corresponding to the major species was assigned as a B-O*H* resonance due to its similarity to the B-O*H* resonance of **2.9** (5.92 ppm) and the major product accordingly assigned as the ring opened product **2.12**.[116] The FT-IR spectrum of the crude sample showed a diagnostic O-H stretch at 3404 cm^{-1} and crystals grown from a solution of diethyl ether and hexanes confirmed the identity as the protodeborylated product **2.12** (Figure 2.1).

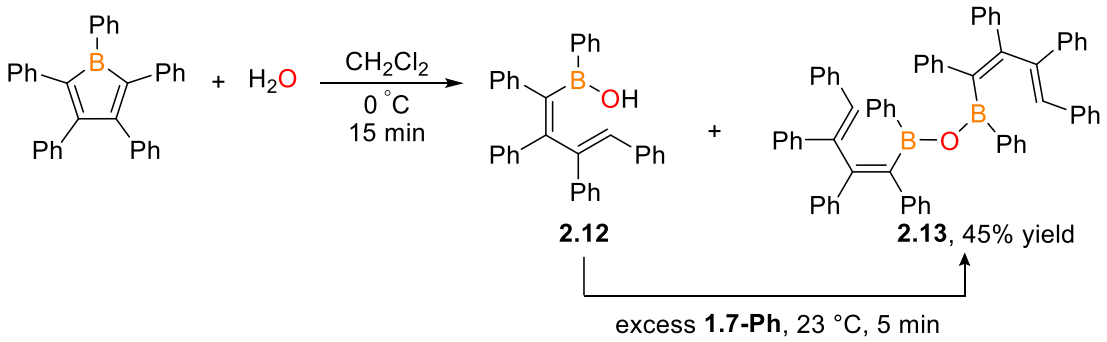

Scheme 2.3. Reaction of borole **1.7-Ph** with water.

The isolation of a pure sample of **2.12** proved to be difficult due to similar solubilities of the two compounds. Although bulky boroles only showed one product, a smaller borole may react in a 2:1 stoichiometry with water to generate a diboroxane species which was tentatively assigned as the minor product. The addition of excess borole to the reaction mixture converted all of **2.12** to the minor species indicated by ^{1}H NMR spectroscopy by the absence of the B-O*H* resonance at 5.44 ppm. Moreover, the FT-IR spectrum of the isolated powder lacked an O-H stretch. The ^{11}B{^{1}H} NMR shift of 45.7 ppm is indicative of a three-coordinate species and is comparable to other reported diboroxanes (e.g. tetraphenylboroxane δ = 46 ppm).[128-132] An X-ray diffraction study confirmed the identity as diboroxane **2.13**. The C_4 chains in **2.12** and **2.13** derived from the ring carbons are in twisted cis-configurations with dihedral angles ranging between 38.4(3)˚ and 42.6(2)˚. A notable feature in **2.13** is a surprisingly wide B-O-B angle, comparable to Mes_2B-O-BMes_2 [167.7(12)˚ *cf.* 165.5˚][129], likely a result of the steric bulk imposed by the contorted butadiene. This steric congestion also supports the observation of only a single protodeborylation in the reactions of boroles **1.7-Mes**, **1.7-^{F}Mes,** and **2.7** with water was likely a result of the bulk of the boroles tested.

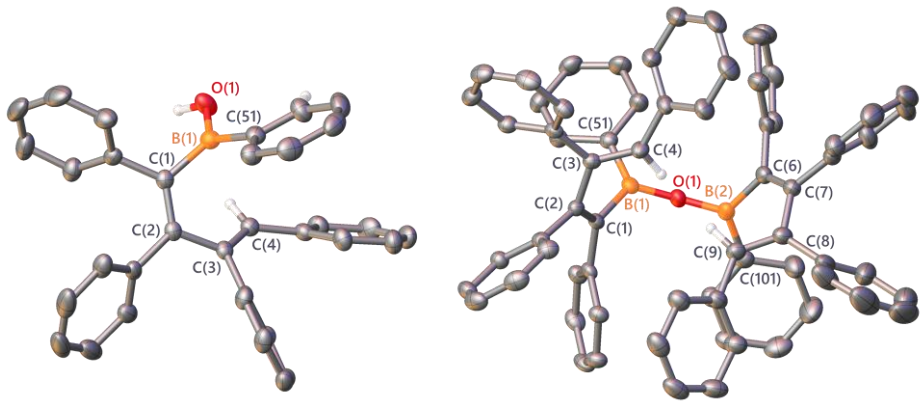

Figure 2.1. Solid-state structures of **2.12** (left) and **2.13** (right). Thermal ellipsoids are drawn at the 50% probability level. Hydrogen atoms have been omitted for clarity (other than those derived from H_2O). Selected bond lengths (Å) and angles (˚) for **2.12**: B(1)-O(1) 1.362(2), B(1)-C(1) 1.588(3), C(1)-C(2) 1.359(3), C(2)-C(3) 1.485(2), C(3)-C(4) 1.352(3), B(1)-C(51) 1.555(3), O(1)-B(1)-C(1) 117.95(18), O(1)-B(1)-C(51) 118.77(18), C(51)-B(1)-C(1) 122.90(16), C(1)-C(2)-C(3)-C(4) 40.2(2); For **2.13**: B(1)-O(1) 1.352(18), B(1)-C(1) 1.586(2), C(1)-C(2) 1.353(2), C(2)-C(3) 1.488(2), C(3)-C(4) 1.343(2), B(1)-C(51) 1.568(3), B(2)-O(1) 1.364(18), B(2)-C(6) 1.579(3), C(6)-C(7) 1.358(3), C(7)-C(8) 1.490(3), C(8)-C(9) 1.343(3), B(2)-C(101) 1.571(3), O(1)-B(1)-C(51) 118.40(15), O(1)-B(1)-C(1) 118.98(15), C(51)-B(1)-C(1) 121.82(15), C(1)-C(2)-C(3)-C(4) 42.6(2), O(1)-B(2)-C(101) 119.70(17), O(1)-B(2)-C(6) 119.00(17), C(101)-B(2)-C(6) 120.93(16), C(6)-C(7)-C(8)-C(9) 38.4(3), B(1)-O(1)-B(2) 167.7(12).

The ring opening reactivity of borole with water and an alcohol prompted us to examine the reaction with a thiol. The analogous 1:1 reaction of pentaphenylborole and 1-naphthalenethiol at room temperature rapidly resulted in the disappearance of the blue color of **1.7-Ph** (Scheme 2.4). The solvent was removed *in vacuo* and obtaining an ^{1}H NMR spectrum of the solids redissolved in $CDCl_3$ suggested conversion to one product with several broad peaks, all in the aryl region with the exception of a peak at 3.81 ppm. The broad signals resolved at -30 ˚C, notably the broad peak at 3.81 ppm became a sharp singlet integrating to one proton with respect to the 32 aryl protons and is shifted slightly downfield from 1-naphthalenethiol ($\delta = 3.60$). After work-up, a white powder was isolated in high yield (93%). A resonance in the $^{11}B\{^{1}H\}$ NMR spectrum was detected at $\delta = 76.0$ ppm, indicative of a three-coordinate boron center, and no S-H stretch (2550-2620 cm^{-1}) was present in the FT-IR spectrum of the product.

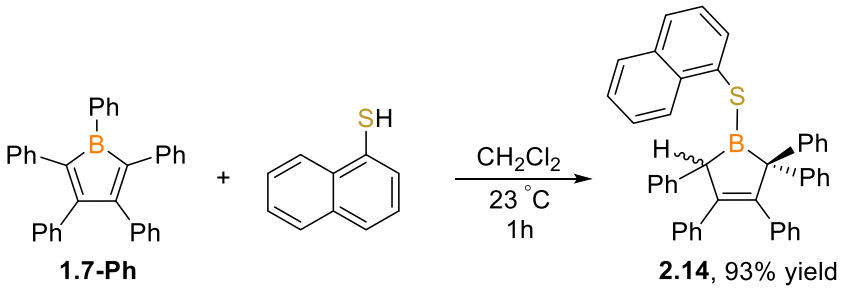

Scheme 2.4. Reaction of borole **1.7-Ph** with 1-naphthalenethiol.

Crystals suitable for an X-ray diffraction study were grown from a dichloromethane/toluene solution (1:3) and determined the identity of the product as the 1-boracyclopent-3-ene with a naphthalenethiolate group on the boron center as well as a phenyl group and proton introduced on the α-carbons of the five-membered ring (**2.14**, Figure 2.2). The boron-sulfur bond length is comparable to other thioboranes that exhibit B-S delocalization [1.782(4) Å *cf.* $Mes_2B(SCH_3)$ 1.787(6) Å].[133-135] The boracycle has a trigonal planar boron center [$\sum_{angles}$ = 359.9(5)˚] and features a distinct C-C double bond in the central ring [C(2)-C(3) = 1.348(3) Å]. The singlet observed at 3.81 ppm is assigned as the proton on the tertiary carbon adjacent to boron. While the introduction of groups to both α-carbon atoms is similar to the previously reported reactions of boroles with H_2 or main group hydrides, the final products are fundamentally different. With the thiol (S-H), the S-B bond is retained, and the Ph group migrates from the B atom, while with main group hydrides (E-H) the main group element migrates to the α-carbon while retaining the B-Ph bond.

The 1:1 reaction of aniline with pentaphenylborole at room temperature resulted in the rapid color change of blue to yellow accompanied with the formation of a precipitate (Scheme 2.5). After work-up, a white solid was isolated in 76% yield. Acquiring a ^{1}H NMR

spectrum of the crude solids redissolved in $CDCl_3$ showed the disappearance of the NH_2 resonance of the aniline at 3.55 ppm and the appearance of a new singlet at 6.44 ppm integrating in a 1:31 ratio with respect to the resonances in the aryl region. A broad singlet was observed in the $^{11}B\{^1H\}$ NMR spectrum at 41.4 ppm, characteristic of a three-coordinate boron center. The FT-IR spectrum showed an N-H stretch at 3388 cm^{-1} and an X-ray diffraction study on crystals grown from a dichloromethane solution *via* vapor diffusion into toluene, confirmed the product as the ring opened amino-borane **2.15**.

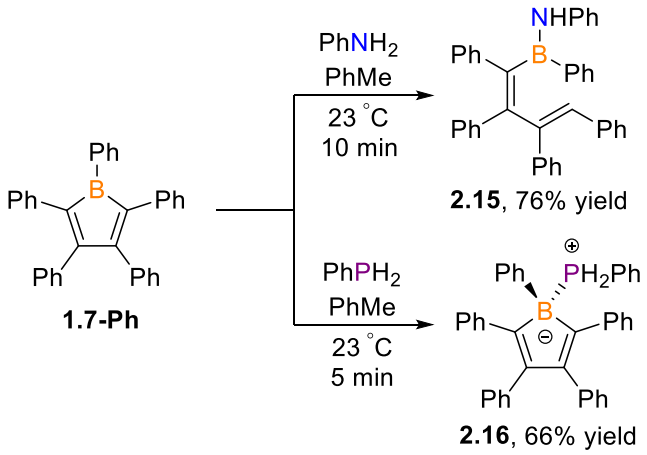

Scheme 2.5. Reaction of borole **1.7-Ph** with aniline and phenylphosphine.

To further examine this transformation, we performed the reaction at -40 ˚C in an NMR tube and analyzed the conversion by $^{11}B\{^1H\}$ NMR spectroscopy. At this temperature a signal corresponding to a four-coordinate species (δ = 1.3) was detected which was assigned as the pentaphenylborole-aniline adduct. After ten minutes, the four-coordinate species completely converted to the amino-borane product **2.15** (Appendix A: Figure A-21).[136] The B-N bond distance of 1.409(2) Å is similar to the B-N bond in borazine (1.42 – 1.43 Å) suggesting delocalization between boron and nitrogen.[133, 137-138] The butadiene chain is similar to the boroxines with a twisted *cis*-conformation [dihedral

angle C(1)-C(2)-C(3)-C(4) = 41.4(17)˚]. Interestingly, the addition of another equivalent of borole did not induce a second protodeborylation, even at elevated temperatures (at 23 ˚C in $CDCl_3$ or at 100 ˚C in toluene).

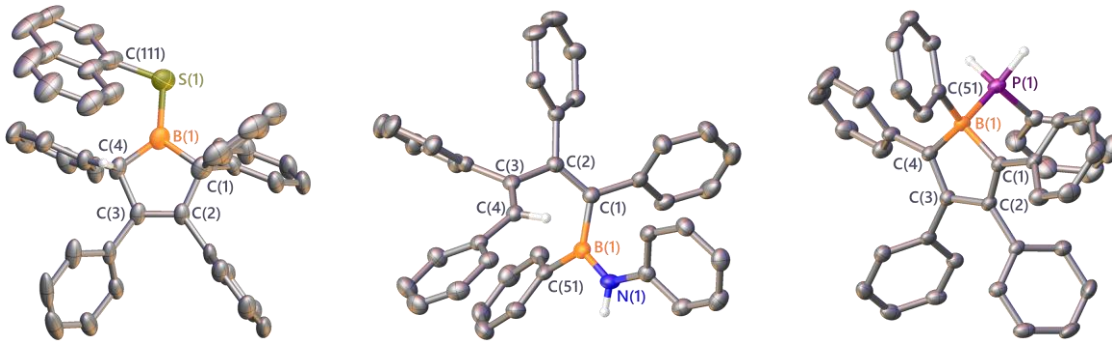

Figure 2.2. Solid-state structures of **2.14**-**2.16** (left to right). Thermal ellipsoids are at the 50% probability level. Hydrogen atoms have been omitted for clarity (other than those derived from the heteroatom of the substrates). Selected bond lengths (Å) and angles (˚) for **2.14**: S(1)-B(1) 1.785(3), B(1)-C(1) 1.607(3), C(1)-C(2) 1.544(3), C(2)-C(3) 1.348(3), C(3)-C(4) 1.526(3), B(1)-C(4) 1.580(4), S(1)-B(1)-C(1) 121.14(19), S(1)-B(1)-C(4) 129.35(19), C(1)-B(1)-C(4) 109.4(2), B(1)-C(1)-C(2) 100.37(18), B(1)-C(4)-C(3) 101.83(18); **2.15**: N(1)-B(1) 1.409(2), B(1)-C(1) 1.582(2), C(1)-C(2) 1.362(2), C(2)-C(3) 1.490(2), C(3)-C(4) 1.351(2), B(1)-C(51) 1.579(2), N(1)-B(1)-C(1) 123.43(15), N(1)-B(1)-C(51) 116.74(15), C(1)-B(1)-C(51) 119.23(15), C(1)-C(2)-C(3)-C(4) 41.4(17); **2.16**: P(1)-B(1) 1.993(3), B(1)-C(1) 1.616(3), C(1)-C(2) 1.351(3), C(2)-C(3) 1.479(3), C(3)-C(4) 1.365(3), B(1)-C(4) 1.627(3), P(1)-B(1)-C(1) 96.65(15), P(1)-B(1)-C(4) 104.24(16), P(1)-B(1)-C(51) 112.44 (17).

The addition of a stoichiometric equivalent of phenylphosphine to **1.7-Ph** in $CDCl_3$ at room temperature resulted in a rapid color change from blue to green and analysis of the crude reaction mixture by ^{31}P NMR spectroscopy showed a triplet at δ = -47.1 ppm (J = 366 Hz), shifted significantly downfield from free phenylphosphine (δ = -122 ppm). The corresponding doublet with a matching coupling constant was observed in the ^{1}H NMR spectrum at 5.77 ppm with a similar value to the other primary phosphine-borane adducts (J = 366 Hz *cf.* 360 - 380 Hz).[139-141] The $^{11}B\{^{1}H\}$ NMR shift is a sharp singlet at δ = -8.7 ppm, in the range of reported borole adducts.[30, 42, 57, 99] Crystals for an X-ray diffraction study were grown from a solution of dichloromethane *via* vapor diffusion into *n*-pentane and confirmed the identity as the Lewis acid/base complex **2.16**. The phosphorus-boron

bond distance of 1.993(3) Å is consistent with reported phosphine-borane adducts.[140, 142-143] Surprisingly, the phenylphosphine adduct (**2.16**) shows no evidence of B-C protonolysis at room temperature, or upon heating at 80 ˚C for several hours.

2.3 Computational DFT Studies

Computational DFT studies were undertaken to rationalize the different outcomes of the reactions of pentaphenylborole with the relatively similar reactants (Scheme 2.6). For computational efficiency, a model system of 2,3,4,5-tetramethyl-1-phenylborole (**1.7-Ph'**) was used in place of pentaphenylborole (**1.7-Ph**), and PhSH used in place of 1-naphthalenethiol. The M06-2X/6-31+G(d) optimised geometries of isolated products are consistent with the geometrical parameters derived from the crystal structures, which indicates that the optimized geometries for all structures are sufficiently accurate. The thermochemistry of each reaction was considered (Table 2.1), as it was hypothesized that initial adduct formation (**Int2.1**) was critical to the ring opening and related reactivity of boroles, and hence reaction energetics are listed relative to the adduct **Int2.1**. Experimental observations support this approach, with the detection of the initial adduct in the reaction with aniline and isolated adduct for phenylphosphine (**2.16**, for which it is also the final product). Adduct formation is calculated to be thermodynamically favoured with NH_2Ph (-33.3 kJ/mol) and PH_2Ph (-20.9 kJ/mol). In contrast, with H_2O and PhSH the formation of adduct **Int2.1** is calculated to be endergonic, although ΔG is very small (+9.9 and +7.8 kJ/mol, respectively). The endergonic nature of the formation of adducts **Int2.1** for H_2O and PhSH is consistent with no experimental observation of these species. The barrier to adduct formation was calculated to be only 35.9 and 22.2 kJ/mol for NH_2Ph and PH_2Ph, respectively. The formation of ring opened products from adduct **Int2.1** (**Prod2.1**) is

calculated to be exergonic for all reactants except PH_2Ph. The lack of observed reactivity with PH_2Ph beyond initial adduct formation (**2.16** *c.f.* **Int2.1**) may subsequently be rationalized on thermodynamic grounds. For water and aniline, the ΔG associated with the formation of the observed ring opened products (**Prod2.1** *c.f.* **2.12** and **2.15**) is calculated to be -148.9 and -81.0 kJ/mol respectively. The barriers to H-migration (**TS2.1**) are relatively low for H_2O and PhSH, and while the barrier for NH_2Ph is unexpectedly higher, the barriers are all consistent with the observed rapid reaction times.

The ΔG associated with the reaction of the ring opened H_2O product (**Prod2.1** *c.f.* **2.12**) with a second equivalent of borole to give **Prod2.3** (*c.f.* **2.13**) was calculated to be -39.0 kJ/mol. For the aniline product (**Prod2.3** *c.f.* **2.15**), ΔG for the reaction with a second equivalent of borole was calculated to be -39.1 kJ/mol. While the relevant transition state was not able to be located, it is believed that the reaction barrier for formation of the aniline bisborole complex (**Prod2.3**) must be significant in comparison to the H_2O reaction since no bisborole aniline product is observed in the experimental study.

Analysis of the structures and energetics of initial adduct formation (**Int2.1**) and the subsequent transition state (**TS2.1**) provides insight into the varied reactivity observed in the experimental study. After formation of **Int2.1**, further reactivity to **Prod2.1** (*via* H-migration and ring opening) or **Prod2.2** (*via* H and Ph migration for the ring closed species, **Int2.2** and **Int2.3**, respectively) requires either an initial H(-E) or Ph(-B) migration to an α-carbon of the borole ring. Migration of the boron-phenyl group was calculated to be unfavourable by 82-98 kJ/mol (**Int2.1** to **Int2.3**) for all complexes, whereas H-migration with thiophenol is favourable by 65 kJ/mol, and with phenylphosphine it is unfavourable by only 0.4 kJ/mol (**Int2.1** to **Int2.2**). With water and aniline, H-migration to an α-carbon

leads directly to the ring opened species (**Prod2.1** *c.f.* **2.12** and **2.15**). No stable minima were able to be located that corresponded to H-migration to an α-carbon.

Importantly, the stability of the H-migration intermediate (**Int2.2**) appears to be an indicator of further reactivity. For the water and aniline reactions, the absence of a stable minimum indicates that the reaction proceeds directly to borole ring opening (**Int2.1** to **Prod2.1**). With thiophenol, a stable minimum is identified (-65 kJ/mol from **Int2.1**), allowing subsequent phenyl migration from boron to the other α-carbon to form the ring closed product (**Prod2.2** *c.f.* **2.14**). A ring opened thiophenol product was identified, although it lies 38.8 kJ/mol higher in energy than the ring closed product **2.14** (**Prod2.1**). For PH_2Ph, a H-migration minimum was located, but it lies almost equal in energy to that of **Int2.1**.

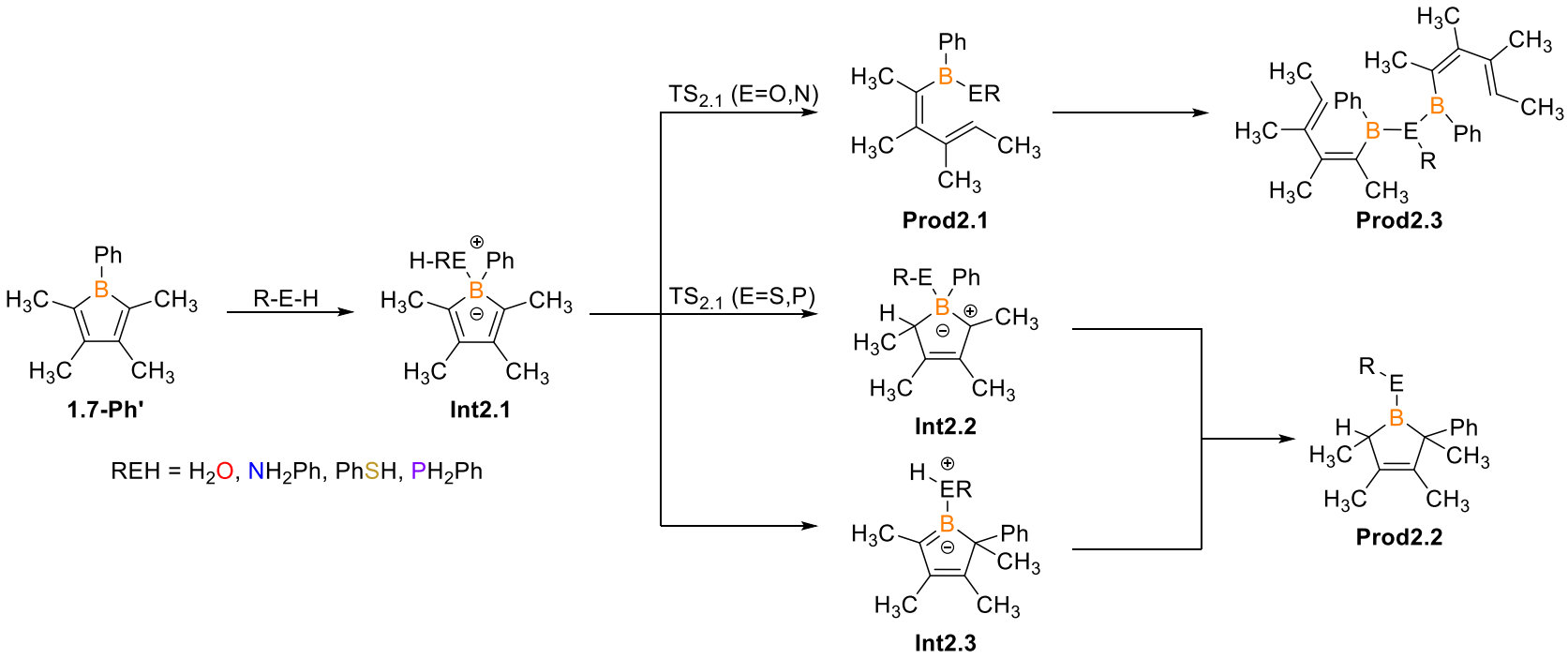

Scheme 2.6. Proposed mechanism for the reactions using 2,3,4,5-tetramethyl-1-phenylborole (**1.7-Ph'**) as a model system.

Table 2.1. M06-2X/6-31+G(d) Calculated Relative Free Energies (ΔG, kJ mol^{-1}) for the Reaction of 1-Phenyl-2,3,4,5-tetramethylborole (**1.7-Ph'**) with E-H Substrates, Relative to the Initial Adduct (**Int2.1**)

Compounds	Reactants	**Int2.1**	**$TS_{2.1}$**[a]	**Prod2.1**[b]	**Prod2.2**[c]	**Prod2.3**
H_2O	-9.9	0.0	57.7	-148.9	-187.6	-187.9
SHPh	-7.8	0.0	50.2	-87.7	-126.5	–
NH_2Ph	33.3	0.0	107.8	-81.0	-156.3	-120.2
PH_2PH	20.9	0.0	128.3	12.3	-47.9	92.2

[a]Transition state associated with H-migration from E (E = O, S, N, P) in **Int2.1**. [b]Ring opened product equivalent to **2.12** and **2.15**. [c]Addition product equivalent to **2.14** with H and Ph addition to α-carbons of the borole ring. [d]Product equivalent to the bisborole ring opened species **2.13**.

For all species, a second, more stable, product (**Prod2.2**) was identified that corresponds to the ring closed thiophenol product **2.14**. For water and aniline, there is no ready pathway to this product, as initial H-migration to an α-carbon is required (but no stable intermediate of type **Int2.2** is formed in each case). For PH_2Ph, a H-migration intermediate (**Int2.2**) was located only 0.4 kJ/mol lower in energy than **Int2.1**, but with a barrier of 128 kJ/mol, which is the largest barrier of the systems considered. Again, the importance of **$TS_{2.1}$** and **Int2.2** is highlighted.

The lability of the E-H bond and formation of stable H-migration intermediates (**Int2.2**) were identified as important factors from an analysis of the thermodynamics. It was subsequently hypothesized that the divergent reactivity may be related to the relative acidity of the substrate protons on the main group center of the adduct (**Int2.1**), as the second step in related ring opening reactions of boroles are a proton mediated B-C bond cleavage. Two different proxies for the acidity of the E-H protons in the adducts **Int2.1** were considered: the energy associated with simply removing a proton from the main group element of **Int2.1**, and the natural population analysis (NPA) charge on the protons in the adduct **Int2.1**, where a higher positive charge on the hydrogen atom indicates potential increased acidity. In the former case, pyridine was used as a model Bronsted base, in which

case the acidity is calculated as the ΔG of **Int2.1** + pyridine $\rightarrow$ [**Int2.1**-H]$^-$ + [pyridine+H]$^+$, by how readily **Int2.1** transfers a proton to pyridine.

The NPA charges on the E-H protons in the adducts **Int2.1** decrease from +0.52 for water to +0.42 for aniline, then there is a substantial drop to +0.148 in thiophenol and +0.019 in the phenylphosphine adduct. The energy associated with protonating pyridine increases from water (+379 kJ/mol) to aniline (+420 kJ/mol), with phenylphosphine (+426 kJ/mol) having the proton that is the most difficult to remove, in agreement with inferred acidity from the calculated proton charges. The thiophenol result (+356 kJ/mol) is an anomaly to the trend, having a small magnitude charge (less acidic proton) and yet it more readily protonates pyridine compared to the other adducts **Int2.1**.

While acidity is important, lability of the E-H and B-C bonds is also significant. The Wiberg bond indices (WBI) give an indication of the E-H and B-C bond strengths (Tables 2.2-2.3). For S-H and P-H in **Int2.1**, the WBIs are closest to unity (together with lower magnitude NPA charges on H), while the O-H and N-H WBIs are smaller (corresponding with higher magnitude NPA charges). The B-C bonds in the phenylphosphine adduct exhibit the highest WBIs, which is consistent with no observed reactivity beyond adduct **2.16**.

Calculated WBIs for E-B bonds (Table 2.3) indicate some multiple bond character in the ring opened species (**Prod2.1**), which arises from delocalization of the lone pairs from the heteroatom. A comparison with single-bond distances derived from the sum of single-bond covalent radii[144] indicates that the O-B and N-B bond distances are shorter than standard single bonds. Second-order perturbation analysis of NBO interactions indicates that this interaction is the most important stabilizing interaction in the ring opened

product for H_2O and NH_2Ph products (**Prod2.1** *c.f.* **2.12** and **2.15**). Delocalization from the lone pairs is most obviously manifested in the planarization of the N-atom in **2.15**.

Table 2.2. M06-2X/6-31+G(d) Calculated Proton Acidity (ΔG, kJ mol^{-1}) and B3LYP/def2-TZVPP Calculated NPA Charges (E) and Wiberg Bond Indices (WBI) of **Int2.1** Adducts

	Proton	NPA			WBI		
Compound	Acidity	H	E	B	E-H	B-C_1	B-C_2
H_2O	378.9	0.524	-0.761	0.575	0.718	0.884	0.875
HSPh	356.1	0.146	0.342	0.492	0.944	0.892	0.876
NH_2Ph	420.2	0.418	-0.655	0.414	0.795	0.897	0.873
PH_2PH	426.0	0.010	0.860	0.068	0.939	0.901	0.913

For PhSH, the energy stabilization from lone-pair donation of S to B is greater in the ring closed product (**Prod2.2** *c.f.* **2.14**) than in the unobserved ring opened species, **Prod2.1**. The calculated bond distance of 1.42 Å is also shorter than the 1.56 Å derived from single-bond covalent radii.

Table 2.3. B3LYP/def2-TZVPP Calculated E-B Bond Distances (Å), E-B Single Bond Distances (Å) from Covalent Radii, WBI for **Int2.1** and the Experimentally Observed Products[a]

	Int2.1		Experimentally observed species				Single-Bond [a]
Compound	R(E-B)	WBI	R(E-B)	WBI	Compound		R(E-B)
H_2O	1.724	0.460	1.374	0.958	**Prod2.1**	**2.12**	1.48
HSPh	2.235	0.524	1.793	1.326	**Prod2.2**	**2.14**	1.88
NH_2Ph	1.677	0.613	1.422	1.021	**Prod2.1**	**2.15**	1.56
PH_2PH	2.011	0.801	2.011	0.801	**Int2.1**	**2.16**	1.96

[a]Bond distances calculated from sum of single-bond covalent radii: B (0.85 Å), O (0.63 Å), S(1.03 Å), and P (1.11 Å).

The Lewis acidity of the ring opened product (**Prod2.1**) is a significant factor in predicting further reactivity with another equivalent borole. One measure of Lewis acidity is the electron affinity (EA). The reacting E-H compound is required to be less Lewis acidic

than the borole for a Lewis acid-base reaction to occur. The M06-2X/6-31+G(d) calculated vertical EA of 2,3,4,5-tetramethyl-1-phenylborole is -0.86 eV, with the ring opened products being -0.98 eV (H_2O), -1.04 eV (SH), -0.50 (NH_2Ph), and -0.19 eV (PH_2Ph). The NH_2Ph product (**Prod2.1**) is more Lewis acidic than the borole, which further supports the lack of reaction to form a bisborole complex (**Prod2.3**). In contrast, the H_2O ring opened product is less Lewis acidic (more negative EA) than the borole, and hence reaction with a second borole is expected (**Prod2.3** *c.f.* **2.13**). Interestingly, the PhSH ring opened product was the only other substrate that exhibited an EA more negative than that of H_2O.

The reactions of pentaphenylborole with substrates containing E-H (E = O, S, N, P) functional groups demonstrate multiple modes of reactivity with this antiaromatic species. The reactions with O-H and N-H containing substrates undergo protodeborylation to produce ring opened products with delocalized B-O and B-N bonds. Additionally, it was shown that a second protodeborylation could take place for H_2O. This differs from previous studies with larger boroles and water that only showed a single protodeborolation. A thiol reacted differently to produce a boracyclopent-3-ene heterocycle. In this case, the B-C bond was not cleaved and the phenyl group on boron migrated to the adjacent carbon. The reaction with phenylphosphine only showed adduct formation and no evidence of proton migration or ring opening. DFT calculations provide support for the observed reaction products and identify the initial adduct as a key intermediate in determining the final product. Ring opening may be linked to the lability of the E-H hydrogen in the initial adduct. Intriguingly, all the aforementioned reactivity is different to the addition products observed in previous studies with H_2, $HSiEt_3$, $HGeEt_3$, HSn^nBu_3, and HBpin.

2.4 Experimental Details

Phenylphosphine and 1-naphthalenethiol were purchased from Strem and Sigma-Aldrich Chemicals, respectively, and used as received. Aniline was purchased from Sigma-Aldrich and purified by distillation prior to use. In-house deionized water was used without further purification.

Computational Methods. All calculations were carried out within Gaussian 09.[145] Geometries of structures **2.12**-**2.16** were optimized using the M06-2X[146] density functional theory (DFT) method with an ultrafine pruned integration grid and optimized with the 6-31+G(d) basis set.[147-148] Geometry optimization of transition states typically employed the quadratic synchronous transit (QST) approach.[149] Stationary points were characterized as minima or transition states by calculating the Hessian matrix analytically at the same level of theory. All structures labelled as minima exhibit no imaginary frequencies; transition states exhibit one imaginary frequency. Thermodynamic corrections were taken from these calculations (standard state of T = 298.15 K and p = 1 atm). Intrinsic reaction coordinate (IRC) calculations using the local quadratic approximation were carried out to ensure transition states connected the appropriate local minima. Molecular orbital and natural bond orbital (NBO) analysis was calculated at the M06-2X/def2-TZVPP level of theory.

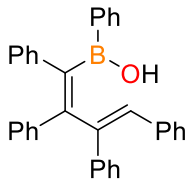

2.12

Generation of 2.12 (CCDC 1443358): A dichloromethane solution of **1.7-Ph** (56.0 mg, 0.130 mmol; 10 mL) was added drop wise via cannula transfer to a dichloromethane solution of degassed water (2.50 μL, 0.130 mmol; 1 mL) at 0 ˚C over a period of 15 minutes. Upon completion of the addition, the blue solution became yellow. The cold bath was removed, the solution stirred an additional 15 min, and the solvent removed *in vacuo* to produce a yellow oil. A mixture of products in a 75:25 ratio was determined by ^{1}H NMR and attempts to isolate pure **2.12** from this mixture were unsuccessful. Crystals of **2.12** for an X-ray diffraction study were grown by vapor diffusion of a diethyl ether solution of **2.12** into hexanes.

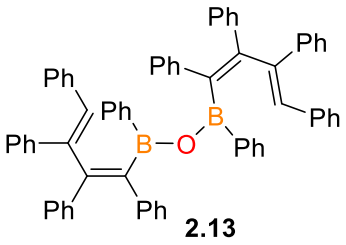

2.13

Isolation of 2.13 (CCDC 1443359): The appropriate amount of **1.7-Ph** (42.0 mg, 0.094 mmol; 3 mL) from the aforementioned mixture (determined by ^{1}H NMR analysis) was added dropwise over 5 minutes at room temperature (23 ˚C) to a solution of the yellow oil (1 mL). Removal of the solvent *in vacuo* gave a white solid that was washed with pentane (5 × 1 mL) and dried *in vacuo* to give **2.13** as a white powder. Yield: 32.2 mg, 45%; m.p 131-133 ˚C. Crystals for X-ray diffraction studies were grown by vapor diffusion of a diethyl ether solution of **2.13** into hexanes.

^{1}H NMR (600 MHz, $CDCl_3$): δ 7.59 (d, J = 12 Hz, 4H, C_6H_5), 7.26-7.23 (m, 6H, C_6H_5), 7.10-7.04 (m, 6H, C_6H_5), 7.00-6.93 (m, 19H, C_6H_5), 6.89-6.84 (m, 13H, C_6H_5), 6.47 (d, J = 6 Hz, 4H, C_6H_5);

$^{13}C\{^1H\}$ NMR (151 MHz, $CDCl_3$): δ 151.44, 147.03, 141.51, 139.37, 138.19, 137.23, 135.05, 132.79, 131.23, 131.02, 130.97, 130.74, 130.46, 127.86, 127.64, 127.50, 127.44, 126.88, 126.82, 126.52, 126.03;

$^{11}B\{^1H\}$ NMR (193 MHz, $CDCl_3$): δ 45.7 (br);

FT-IR (cm^{-1}(ranked intensity)): 3024(14), 1595(11), 1488(7), 1435(8), 1393(1), 1235(9), 1074(13), 1027(5), 913(6), 799(15), 752(2), 735(4), 624(12), 530(3), 500(10);

HRMS (ESI): calcd. for $C_{68}H_{52}B_2O$ $[M+Na]^+$: 929.4117; found 929.4167.

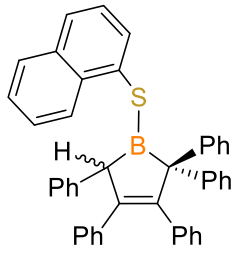

2.14

Synthesis of 2.14 (CCDC 1443360): At room temperature (23 ˚C), a dichloromethane solution of 1-naphthalenethiol (75.0 µL, 0.545 mmol; 1 mL) was added dropwise to a dichloromethane solution of **1.7-Ph** (242.0 mg, 0.545 mmol; 1 mL). The solution color changed from dark blue to yellow within 1 min. The solution was allowed to stir for 1 h, and the solvent removed *in vacuo*. The residue was washed with hexanes (3 × 3 mL) and dried *in vacuo* to furnish **2.14** as an off-white powder. Yield: 306.0 mg, 93%; m.p 138-140 ˚C. Crystals for X-ray diffraction studies were grown from a dichloromethane/toluene (1:3) solution.

^1H NMR (400 MHz, $CDCl_3$, -30 ˚C): δ 7.77 (dd, J = 16, 8 Hz, 2H, C_6H_5), 7.64 (d, J = 8 Hz, 2H, C_6H_5), 7.56 (d, J = 8 Hz, 2H, C_6H_5), 7.46-7.34 (m, 9H, C_6H_5), 7.10 (t, J = 8 Hz, 1H, C_6H_5), 7.04-6.99 (m, 2H, C_6H_5), 6.94 (t, J = 8 Hz, 2H, C_6H_5), 6.87-6.81 (m, 5H, C_6H_5),

6.72 (d, J = 8 Hz, 2H, C_6H_5), 6.67-6.59 (m, 3H, C_6H_5), 6.09 (d, J = 4 Hz, 2H, C_6H_5), 3.81 (s, 1H, *CH*);

$^{13}C\{^1H\}$ NMR (100 MHz, $CDCl_3$, -30 ˚C): δ 146.28, 144.51, 142.79, 142.54, 139.73, 137.99, 137.73, 133.90, 133.73, 132.92, 131.43, 130.69, 129.94, 129.24, 128.76, 128.61, 128.32, 128.26, 128.17, 128.08, 127.55, 127.35, 127.29, 126.63, 126.57, 126.48, 126.34, 126.28, 125.97, 125.34, 124.48, 77.36, 67.74, 51.45;

$^{11}B\{^1H\}$ NMR (128 MHz, $CDCl_3$, -30 ˚C): δ 76.0 (br);

FT-IR (cm^{-1}(ranked intensity)): 1595(15), 1486(6), 1438(13), 1165(8), 1089(9), 1022(7), 971(14), 862(10), 794(4), 768(2), 693(1), 577(3), 538(5), 462(11), 420(12);

HRMS (ESI): calcd. for $C_{44}H_{33}BS$ $[M+H]^+$: 605.2476; found 605.2403.

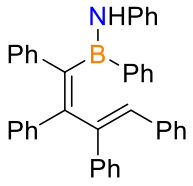

2.15

Synthesis of 2.15 (CCDC 1443361): At room temperature (23 ˚C), a toluene solution of aniline (38.0 μL, 0.412 mmol; 1 mL) was added drop wise to a toluene solution of **1.7-Ph** (183.0 mg, 0.412 mmol; 1 mL). The solution changed from dark blue to yellow within 1 min. The solution was stirred for 10 min, and the solvent removed *in vacuo*. The solids were washed with hexanes (5 × 1 mL) and dried *in vacuo* to produce **2.15** as a white powder. Yield: 168.1 mg, 76%; m.p 139-141 ˚C. Crystals for X-ray diffraction studies were grown by vapor diffusion of a dichloromethane solution of **2.15** into toluene.

^1H NMR (600 MHz, $CDCl_3$): δ 7.70 (d, J = 6 Hz, 2H, C_6H_5), 7.38-7.31 (m, 3H, C_6H_5), 7.16 (d, J = 6 Hz, 4H, C_6H_5), 7.10-7.08 (m, 4H, C_6H_5), 7.05-6.94 (m, 10H, C_6H_5), 6.86-

6.79 (m, 4H, *C*$_6$*H*$_5$), 6.65 (d, *J* = 12 Hz, 2H, *C*$_6$*H*$_5$), 6.59 (d, *J* = 6 Hz, 2H, *C*$_6$*H*$_5$), 6.44 (s, 1H, *NH*);

^{13}C{^{1}H} NMR (151 MHz, $CDCl_3$): δ 151.23, 147.37, 143.34, 142.03, 140.22, 138.64, 137.13, 133.23, 130.57, 130.39, 129.72, 128.91, 127.91, 127.70, 127.58, 127.51, 126.86, 126.76, 126.51, 125.93, 122.73, 120.52;

^{11}B{^{1}H} NMR (193 MHz, $CDCl_3$): δ 41.4 (br);

FT-IR (cm^{-1}(ranked intensity)): 3388(13), 3017(12), 1593(8), 1486(4), 1422(5), 1318(6), 1221(14), 1075(10), 1026(9), 916(11), 876(15), 752(2), 736(7), 690(1), 524(3);

HRMS (ESI): calcd. for $C_{40}H_{32}BN$ $[M+Na]^+$: 561.2557; found 561.2500.

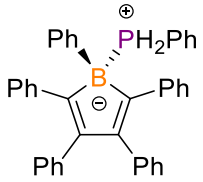

2.16

Synthesis of 2.16 (CCDC 1443362): At room temperature (23 ˚C), a toluene solution of phenylphosphine (26.0 μL, 0.230 mmol; 1 mL) was added dropwise to a toluene solution of borole **1.7-Ph** (104.0 mg, 0.230 mmol; 1 mL) resulting in a color change from dark blue to light green within 1 min accompanied by the formation of a precipitate. The solution was stirred for 5 min, and the solvent removed *in vacuo*. The yellow-green solid was washed with hexanes (5 × 1 mL) and dried in *vacuo* to give a yellow powder. Yield: 85.3 mg, 66%; m.p 96-98˚C. Crystals for X-ray diffraction studies were grown by vapor diffusion of a dichloromethane solution of **2.16** into pentane.

^{1}H NMR (600 MHz, $CDCl_3$): δ 7.56 (m, 1H, *C_6H_5*), 7.49-7.38 (m, 4H, *C_6H_5*), 7.23-7.13 (m, 5H, *C_6H_5*), 7.00-6.92 (m, 12H, *C_6H_5*), 6.81 (d, *J* = 6 Hz, 4H, *C_6H_5*), 6.55 (d, *J* = 12 Hz, 4H, *C_6H_5*), 5.77 (d, J_{PH} = 366 Hz, 2H, *PH*);

^{13}C{^{1}H} NMR (151 MHz, $CDCl_3$) δ 153.16, 141.31, 139.53, 134.06, 133.97, 133.78, 132.11, 130.16, 129.70, 128.97, 128.89, 127.71, 127.60, 127.39, 125.72, 125.64, 124.88;

^{31}P NMR (243 MHz, $CDCl_3$): δ -47.1 (t, J_{PH} = 366 Hz);

^{31}P{^{1}H} NMR (243 MHz, $CDCl_3$): δ -47.1 (s);

^{11}B{^{1}H} NMR (193 MHz, $CDCl_3$): δ -8.7 (br);

FT-IR (cm^{-1}(ranked intensity)): 1595(14), 1485(7), 1438(6), 1070(12), 1025(13), 866(9), 796(8), 778(3), 730(2), 697(1), 580(10), 544(4), 502(15), 456(11), 414(5);

HRMS (ESI): calcd. for $C_{40}H_{32}BP$ $[M+Na]^+$: 580.2330 found 580.2305.

CHAPTER THREE

Ring Opening of Epoxides Induced by Pentaphenylborole

This chapter published as: Yruegas, S.; Wilson, C.; Dutton, J. L.; Martin, C. D., *Organometallics*, **2017**, *36*, 2581-2587.

3.1 Introduction

In addition to protodeborylation-type reactions, boroles (*e.g.* **1.7-Ph** and **1.7-Mes**) react with a variety of substrates to generate six- and seven-membered heterocycles *via* 1,1- and 1,2-insertion reactions, respectively.[18, 21, 30, 34-36, 38-39, 42, 53, 56-59, 116-118, 121, 148, 150-155] Only two eight-membered heterocyclic motifs have been derived from this methodology, namely $BONC_5$ and BN_3C_4 rings (Scheme 3.1).[35, 117] The $BONC_5$ cyclic systems (**3.1-3.4**) are derived from the reaction of a nitrone and the BN_3C_4 system (**3.5**) by reaction with trimethylsilyl-azide (TMS-azide). In both reactions, the nitrone and azide act as 1,3-dipolar molecules that effectively insert into the boron-carbon bond of the borole.[35, 117] The mechanisms are initiated by forming a coordination complex in which the Lewis basic site of the substrate coordinates to the borole followed by attack of the adjacent nucleophilic B-C bond to insert atoms into the ring. The $BONC_5$ species proved to be air stable whereas the BN_3C_4 system ultimately converts to the thermodynamic 1,2-azaborine product *via* the expulsion of N_2 and loss of the coordinated borole. In this regard, epoxides can be classified as dipolar molecules where the highly strained three-membered ring makes the C-O bond poised to cleave and serve as a synthetic C_2O building block.

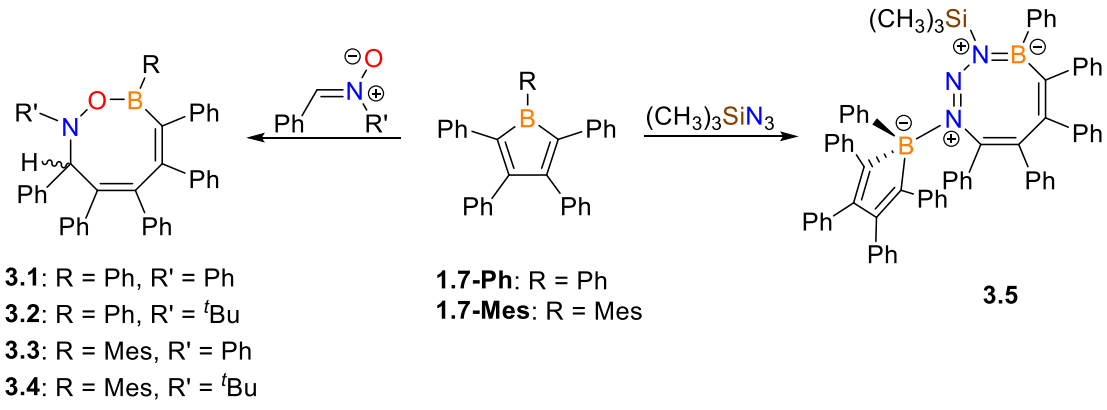

Scheme 3.1. $BONC_5$ and BN_3C_4 rings derived from reactions of boroles with nitrones and TMS-azide.

We envisioned the presence of the Lewis basic oxygen and adjacent electrophilic carbon atom may react with boroles similar to the aforementioned 1,3-dipoles to provide a facile route to eight-membered BOC_6 rings. To our surprise, three discrete products were obtained depending on the substitution on the epoxide, none of which are polymeric species, the typical products observed upon the addition of a Lewis acid to epoxides.[156-159]

3.2 Exploring the Ring Opening of Epoxides

The addition of a stoichiometric equivalent of isobutylene oxide to pentaphenylborole (**1.7-Ph**) in CH_2Cl_2 resulted in the immediate color change from the deep blue of borole to a pale yellow solution (Scheme 3.1). Removing the solvent *in vacuo*, redissolving the solids in $CDCl_3$, and acquiring a ^1H NMR spectrum revealed five singlets integrating in a 1:1:1:2:3 ratio (at 6.90, 4.88, 4.78, 4.32, and 1.63 ppm, respectively; Figure 3.2) presumably originating from the eight protons of the epoxide, in addition to the 25 aryl protons derived from the phenyl groups on pentaphenylborole.

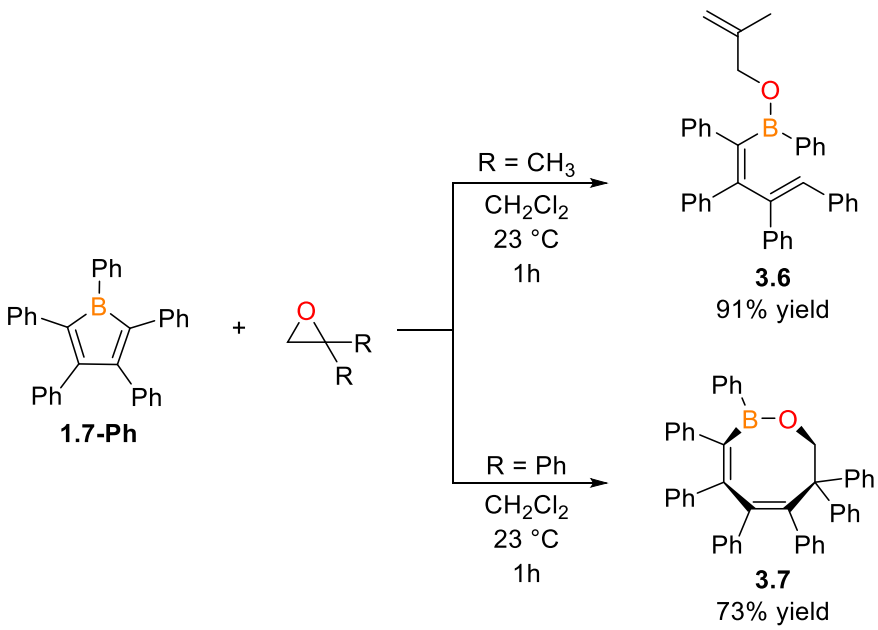

Scheme 3.1. Reactions of **1.7-Ph** with isobutylene oxide and 1,1-diphenylethylene oxide.

A single resonance was detected in the $^{11}B\{^{1}H\}$ NMR spectrum at 45.0 ppm, consistent with a three-coordinate species. An X-ray diffraction study on crystals grown *via* vapor diffusion of a CH_2Cl_2 solution into hexanes identified the compound as a ring opened borole with the pendent isobutylene oxide ring opened (**3.6**, Figure 3.1). An olefin on the pendent alkoxy group was assigned by the short C-C bond [C(6)-C(7) = 1.304 Å] and trigonal planar tertiary carbon center [$\sum_{angles}$C(6) = 359.87(15)°]. The butadiene chain of the product adopts a twisted *cis*-conformation [dihedral angle C(1)–C(2)–C(3)–C(4) = 42.04(6)°], consistent with previously reported ring opened borole species (**2.8-10**, **2.12** and **2.15**).

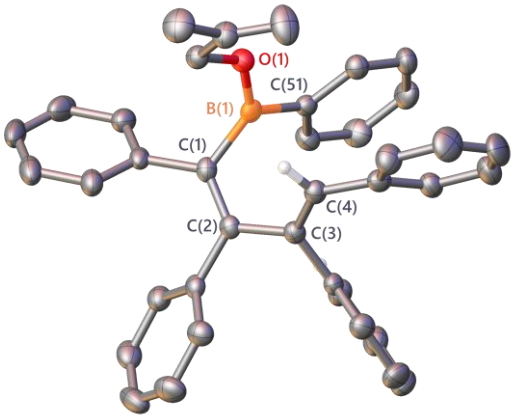

Figure 3.1. Solid-state structure of **3.6**. Hydrogen atoms have been omitted for clarity (other than the hydrogen atom derived from the protodeborylation of the epoxide) and ellipsoids are depicted at the 50% level. Selected bond lengths (Å) and angles (°) for **3.6**: B(1)–O(1) 1.360(2), B(1)–C(1) 1.585(3), C(1)–C(2) 1.356(2), C(2)–C(3) 1.483(2), C(3)–C(4) 1.354(2), B(1)–C(51) 1.563(3), O(1)-C(5) 1.428(2), C(5)-C(6) 1.495(3), C(6)-C(7) 1.304(3), C(6)-C(8) 1.501(3), O(1)–B(1)–C(1) 123.37(17), O(1)–B(1)–C(51) 114.97(17), C(51)–B(1)–C(1) 121.53(16), C(1)–C(2)–C(3)–C(4) 42.04(6).

The five singlets in the ^{1}H NMR spectrum could then be assigned accordingly. The downfield resonance at 6.90 ppm corresponds to the proton on the end of the butadiene chain, similar to reported ring opened borole species (**2.8-10**, **2.12** and **2.15**).[35, 45, 160] The two peaks at 4.88 and 4.78 ppm are assigned as the two diastereotopic vinyl protons, the singlet integrating to two at 4.32 ppm corresponds to the methylene group, and the peak at 1.63 ppm is assigned to the methyl group (Figure 3.2). We postulated that the isobutylene oxide underwent a protodeborylation pathway due to the acidic β-hydrogen atoms of the methyl groups to produce chain product **3.6**. Although an interesting transformation, we anticipated that a substrate lacking β-hydrogen atoms, specifically 1,1-diphenylethylene oxide, would circumvent a protodeborylation pathway and provide a feasible route to generate larger ring systems.

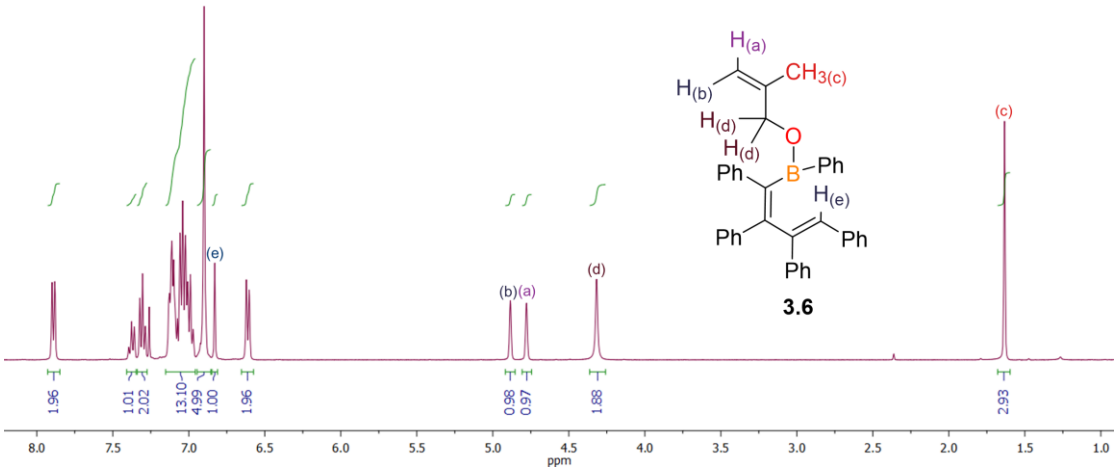

Figure 3.2. ^{1}H NMR spectrum of **3.6** in $CDCl_3$ with diagnostic peaks assigned.

The 1:1 stoichiometric reaction of 1,1-diphenylethylene oxide and **1.7-Ph** in dichloromethane immediately produced a colorless solution. Removing the solvent *in vacuo* and acquiring a ^{11}B{^{1}H} NMR spectrum of the redissolved solids in $CDCl_3$ revealed a signal at 46.3 ppm indicating a three-coordinate boron-containing product. Growing crystals for an X-ray diffraction study *via* diffusion of a CH_2Cl_2 into toluene unambiguously identified the product as an eight-membered BOC_6 heterocycle (**3.7**, Figure 3.3), resulting from the incorporation of the C_2O fragment of the epoxide into the borole. The methylene CH_2 is bound to the oxygen atom indicating C-O cleavage occurred selectively at the carbon with two phenyl groups. The eight-membered ring adopts a *pseudo*-boat conformation analogous to the systems derived from the nitrone and azide (**3.1-3.5**).[35, 117] The incorporated butadiene backbone has alternating double and single bond lengths [C(3)-C(4) = 1.349(5) Å, C(4)-C(5) = 1.511(5) Å, and C(5)-C(6) = 1.338(5) Å].

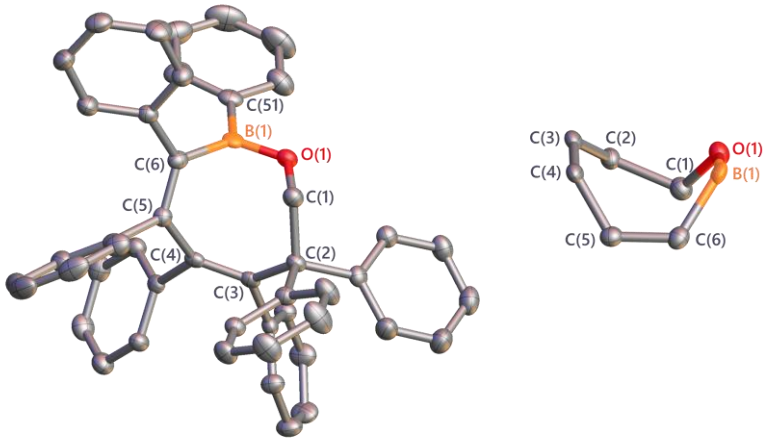

Figure 3.3. Solid-state structure of **3.7** (left) and view of the central BOC_6 ring (right). Hydrogen atoms have been omitted for clarity and ellipsoids are depicted at the 50% level. Selected bond lengths (Å) and angles (°) for **3.7**: B(1)-O(1) 1.375(5), O(1)–C(1) 1.435(4), C(1)–C(2) 1.551(5), C(2)–C(3) 1.569(5), C(3)–C(4) 1.349(5), C(4)–C(5) 1.511(5), C(5)-C(6) 1.338(5), C(6)–B(1) 1.577(5), B(1)-C(51) 1.552(5), B(1)–O(1)–C(1) 120.8(3), O(1)–C(1)–C(2) 113.7(3), C(1)–C(2)–C(3) 112.7(3), C(2)–C(3)–C(4) 128.3(3), C(4)–C(5)–C(6) 121.6(3), C(5)–C(6)–B(1) 118.3(3), C(6)–B(1)–O(1) 118.9(3), C(6)-B(1)-C(51) 124.0(3), O(1)-B(1)-C(51) 117.0(3).

Cyclohexene oxide differs from the other two epoxides by the fact that the fused cyclohexyl ring provides additional strain on the epoxide, making it more susceptible to polymerization. While it has β-hydrogen atoms, they are on rigid carbon centers in comparison to the free rotating methyl groups of isobutylene oxide. Reasonable expected outcomes with **1.7-Ph** and cyclohexene oxide were ring expansion, polymerization, or protodeborylation reactions. Interestingly, monitoring the 1:1 reaction with cyclohexene oxide with pentaphenylborole (**1.7-Ph**) in $CDCl_3$ by ^1H NMR spectroscopy showed that only half of the borole was consumed, while all of the epoxide reacted (Scheme 3.2). Doubling the stoichiometry of the cyclohexene oxide resulted in the consumption of both reagents to produce a yellow solution. Analysis by ^1H NMR revealed aryl protons integrating in a ratio of 25 to 16 with respect to a series of multiplets ranging from 2.06-0.72 ppm attributed to the cyclohexyl protons in addition to four multiplets between 5.00-3.00 ppm each integrating to one, likely derived from the protons on the α-carbon atoms

of the epoxide. Collectively, this data indicated that a single product was formed, in which two epoxides were incorporated in a non-symmetric manner.

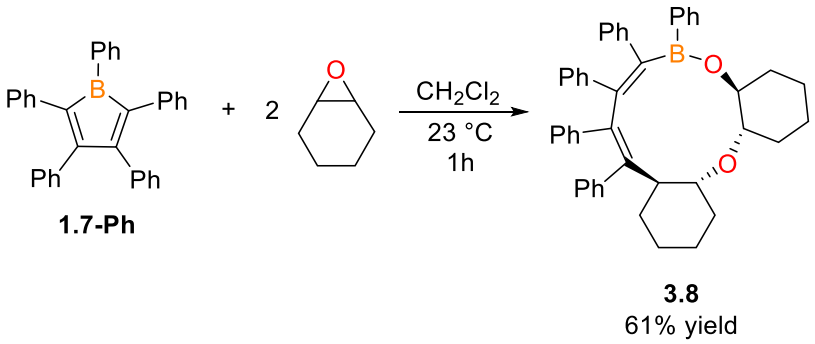

Scheme 3.2. Reactions of pentaphenylborole with cyclohexene oxide.

Crystals for an X-ray diffraction study were grown *via* vapor diffusion of a dichloromethane solution into toluene that revealed two epoxides inserted into the borole to form an eleven-membered BO_2C_8 ring (**3.8**, Scheme 3.2). Both C_2O linkages were inserted in the same B-C bond with the substituents on the cyclohexyl groups in an *anti*-orientation. Only a single diastereomer was observed and given the centrosymmetric space group (P-*1*), the other enantiomer is present in an equivalent ratio. This is also in agreement with the ^{1}H and ^{13}C NMR data, which both indicate a single diastereomer. Compound **3.8** represents the first structurally characterized eleven-membered boron-containing ring and only the second of such reported (Figure 3.4). The other example is a saturated BC_{10} system reported by Brown and co-workers in 1988 through five successive carbene insertions into a saturated BC_5 ring.[161]

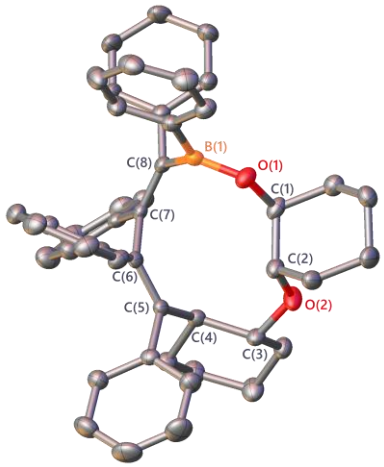

Figure 3.4. Solid-state structure of **3.8**. Hydrogen atoms have been omitted for clarity and ellipsoids are depicted at the 50% level. Selected bond lengths (Å) and angles (°) for **3.8**: B(1)-O(1) 1.364(2), O(1)–C(1) 1.441(2), C(1)–C(2) 1.528(3), C(2)-O(2) 1.431(2), O(2)–C(3) 1.441(2), C(3)–C(4) 1.537(2), C(4)–C(5) 1.541(2), C(5)-C(6) 1.353(2), C(6)–C(7) 1.512(2), C(7)–C(8) 1.353(2), C(8)–B(1) 1.588(3), B(1)-C(51) 1.558(3), B(1)–O(1)–C(1) 124.23(14), O(1)–C(1)–C(2) 108.03(15), C(1)–C(2)–O(2) 106.12(15), C(2)–O(2)–C(3) 119.74(14), O(2)–C(3)–C(4) 116.65(14), C(3)–C(4)–C(5) 118.40(14), C(4)–C(5)–C(6) 122.27(15), C(5)-C(6)-C(7) 122.82(16), C(6)-C(7)-C(8) 119.38(15), C(7)-C(8)-B(1) 124.66(15), C(8)-B(1)-O(1) 122.70(17), C(8)-B(1)-C(51) 122.48(15), O(1)-B(1)-C(51) 114.56(16).

3.3 Computational DFT Studies

The drastic difference in the products of the three reactions was surprising and prompted investigations into the mechanism. The reaction stoichiometry for all three epoxides were conducted in 1:2, 1:1, and 2:1 ratios and exclusively produced the three aforementioned products, confirming that the reaction outcome is independent of stoichiometry. Although three different products were obtained, the mechanisms are all believed to proceed by the initial coordination of the oxygen of the epoxide to the boron center to form adduct intermediates. Computational thermodynamic studies for all three reactions indicate that the adduct is higher in free energy with ΔG values of +44, +65 and +27 kJ/mol for adduct formation for the dimethyl (**Int3.1**), diphenyl (**Int3.2**), and cyclohexyl (**Int3.3**) epoxides with borole, respectively (Scheme 3.3).

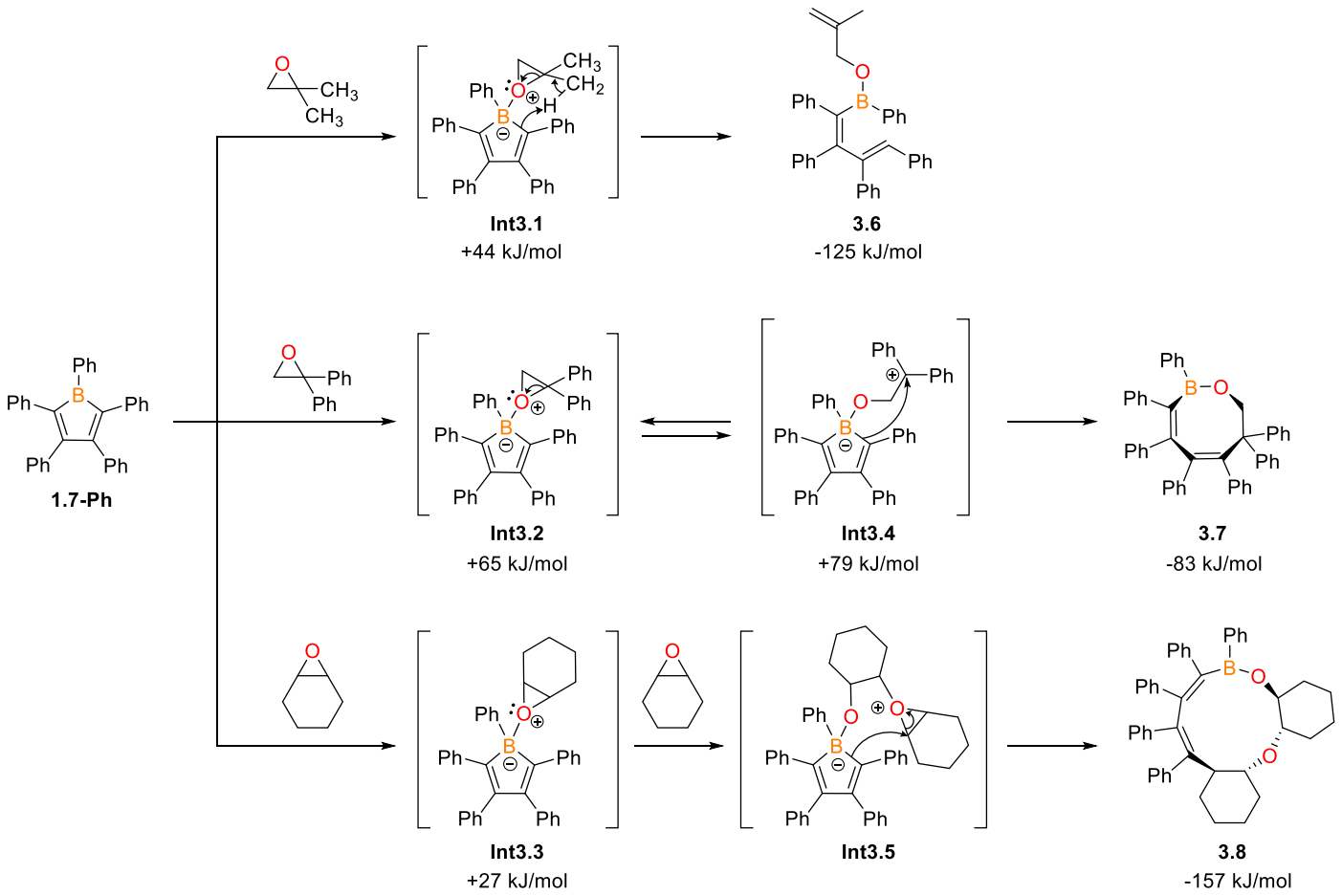

Scheme 3.3. Proposed mechanisms of the reactions of boroles and epoxides with corresponding calculated free energies (ΔG) underneath intermediates and final products with each reaction relative to the energies of **1.7-Ph** and the free epoxide being 0 kJ/mol.

The modest positive values are accessible for the reactions to proceed at room temperature as observed and consistent with the adducts not being isolable or observable species. For isobutylene oxide (**Int3.1**), the ring opened product formed by methyl deprotonation is slightly thermodynamically favored over the insertion product analogous to **3.7** by 3 kJ/mol, a negligible energetic difference, with an overall calculated ΔG for the reaction of -125 kJ/mol.[162] With respect to the 1,1-diphenylethylene oxide adduct (**Int3.2**), C-O bond cleavage at the carbon with two phenyl groups implies that the epoxide likely ring opens to form a tertiary carbocation that is poised for attack from the B-C bond (**Int3.4**) which lies 79 kJ/mol higher in energy than the initial reactants. This results in a ring expansion to incorporate the epoxide and form the BOC_6 ring (**Int3.4** to **3.7**), which has a calculated ΔG value of -83 kJ/mol from the starting materials.[163] The analogous carbocation for the dimethyl epoxide is much higher in energy at 118 kJ/mol, which is likely the root of the divergent reactivity for the two epoxides.

The mechanism for the cyclohexene oxide reaction differs in the fact that a second epoxide attacks the carbon of the coordinated epoxide of the adduct **Int3.3** and opens the coordinated epoxide to form **Int3.5**.[164] The B-C bond of the borole then attacks the pendent epoxide to furnish the 11-membered heterocycle product **3.8**. The observed result is the thermodynamic product (**3.8**, -157 kJ/mol) with respect to the other possibilities of ring opening *via* abstraction of the β-hydrogen analogous to **3.6** (-137 kJ/mol) or single insertion to generate an eight-membered ring product akin to **3.7** (-136 kJ/mol).

The reactions of pentaphenylborole with epoxides led to three diverse products dependent on the substitution on the epoxide. The reaction of isobutylene oxide resulted in the protodeborylation of the methyl group to generate the ring opened product whereas the

reaction with 1,1-diphenylethylene oxide generated the eight-membered ring that was initially expected. In the more constrained cyclohexene oxide, the β-hydrogen atoms were not deprotonated, but rather a second equivalent of epoxide reacted resulting in the insertion of two C_2O fragments into the boracycle to produce a rare 11-membered boron-containing ring. The postulated mechanisms are in agreement with thermodynamic calculations on the systems. These findings demonstrate that boroles have the potential to be effective reagents, in combination with the appropriate substrates, to controllably generate large ring systems.

3.4 Experimental Details

Isobutylene oxide and 1,1-diphenylethylene oxide were purchased from TCI America and Matrix Scientific, respectively, and used as received. Cyclohexene oxide was purchased from Sigma Aldrich and dried by storing over 4 Å molecular sieves.

Computational Methods. All calculations were carried out within Gaussian 09.[145] Geometries and single-point energies of all structures were optimized using the B3LYP[165] density functional theory (DFT) with the 6-31+G(d) basis set.[147-148]

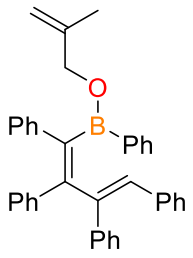

3.6

Synthesis of 3.6 (CCDC 1567465): At room temperature (23 ˚C), a solution of isobutylene oxide in CH_2Cl_2 (14.0 mg, 0.202 mmol) was added to a solution of **1.7-Ph** (90.0 mg, 0.202

mmol) in CH_2Cl_2 resulting in a color change from deep blue to pale yellow. The solution was allowed to stir for 1 h and the solvent removed in vacuo. The residue was washed with hexanes (3 x 3 mL) and dried in vacuo to give **3.6** as an off-white powder. Yield: 95.0 mg, 91%; m.p 110-111 ˚C. Single crystals for X-ray diffraction studies were grown from a CH_2Cl_2 solution of **3.6** by vapor diffusion into hexanes.

^{1}H NMR (400 MHz, $CDCl_3$): δ 7.89 (d, J = 8.0 Hz, 2H), 7.38 (t, J = 8.0 Hz, 1H), 7.30 (t, J = 8.0 Hz, 2H), 7.13-6.97 (m, 13H), 6.90 (m, 5H), 6.83 (s, 1H), 6.61 (d, J = 8.0 Hz, 2H), 4.88 (s, 1H), 4.78 (s, 1H), 4.32 (s, 2H), 1.63 (s, 3H);

^{13}C{^{1}H} NMR (151 MHz, $CDCl_3$): δ 152.46 (C_q), 147.10 (C_q), 146.52 (*CH*), 145.10 (*CH*), 142.71 (C_q), 142.32 (*CH*), 141.98 (C_q), 139.56 (C_q), 138.39 (C_q), 136.99 (C_q), 134.98 (*CH*), 134.37 (*CH*), 133.14 (*CH*), 131.70 (*CH*), 131.42 (*CH*), 131.22 (*CH*), 130.92 (*CH*), 130.84 (*CH*), 130.67 (*CH*), 130.42 (*CH*), 130.19 (*CH*), 129.94 (*CH*), 128.25 (*CH*), 127.72 (*CH*), 127.66 (*CH*), 127.56 (*CH*), 127.09 (*CH*), 126.96 (*CH*), 126.76 (*CH*), 126.19 (*CH*), 110.85 (CH_2), 109.96 (*CH*), 71.14 (CH_2), 67.06 (*CH*), 19.38 (CH_3), peaks assigned *via* ^{13}C{^{1}H} DEPT experiments;

^{11}B{^{1}H} NMR (193 MHz, $CDCl_3$): δ 45.0 (br);

FT-IR (cm^{-1}(ranked intensity)): 3022(14), 1596(10), 1488(12), 1435(5), 1328(1), 1243(6), 1074(7), 1028(11), 892(3), 810(13), 767(15), 750(2), 735(8), 604(9), 528(4);

HRMS (ESI): calcd. for $C_{38}H_{33}BONa$ $[M+Na]^+$: 539.2523; found 539.2530;

Elemental Analysis: calculated for $C_{38}H_{33}BO$: C, 88.37; H, 6.44; Found: C, 84.41; H, 6.30.

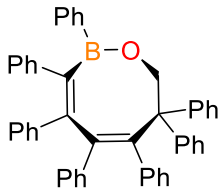

3.7

Synthesis of 3.7 (CCDC 1567466): At room temperature (23 ˚C), a solution of 1,1-diphenylethylene oxide in CH_2Cl_2 (36.0 mg, 0.185 mmol) was added to a solution of **1.7-Ph** (82.0 mg, 0.185 mmol) in CH_2Cl_2 resulting in a color change from deep blue to yellow. The solution was allowed to stir for 1 h and the solvent removed *in vacuo*. The residue was washed with hexanes (3 x 3 mL) and dried *in vacuo* to give **3.7** as a white powder. Purity and identity of **3.7** has been verified by ^{1}H and $^{13}C\{^{1}H\}$ NMR spectroscopy. Yield: 86.2 mg, 73%; m.p. 141-142 ˚C. Single crystals for X-ray diffraction studies were grown from a CH_2Cl_2 solution of **3.7** by vapor diffusion into toluene.

^{1}H NMR (600 MHz, $CDCl_3$): δ 8.07 (d, 2H), 7.54-7.45 (m, 5H), 7.20-7.02 (m, 9H), 6.97-6.87 (m, 10H), 6.74-6.68 (m, 3H), 6.64 (dt, J = 6.0, 18.0 Hz, 2H) 6.54 (t, J = 6.0 Hz, 1H), 6.38 (d, J = 6.0 Hz, 1H), 6.05 (d, J = 6.0 Hz, 2H), 5.77 (d, J = 6.0 Hz, 1H), 5.48 (d, J = 6.0 Hz, 1H);

$^{13}C\{^{1}H\}$ NMR (151 MHz, $CDCl_3$): δ 151.24 (C_q), 148.67 (C_q), 146.28 (C_q), 145.67 (C_q), 143.05 (C_q), 142.43 (C_q), 140.89 (C_q), 139.96 (C_q), 138.78 (C_q), 136.31 (*CH*), 135.96 (*CH*), 132.42 (*CH*), 131.92 (*CH*), 131.25 (*CH*), 130.84 (*CH*), 130.08 (*CH*), 129.62 (*CH*), 129.37 (*CH*), 128.38 (*CH*), 128.31 (*CH*), 128.16 (*CH*), 127.48 (*CH*), 127.20 (*CH*), 126.88 (*CH*), 126.36 (*CH*), 126.24 (*CH*), 126.19 (*CH*), 125.83 (*CH*), 125.49 (*CH*), 124.86 (*CH*), 81.15 (CH_2), 62.23 (C_q), peaks assigned *via* $^{13}C\{^{1}H\}$ DEPT experiments;

$^{11}B\{^{1}H\}$ NMR (128 MHz, $CDCl_3$): δ 46.3 (br);

FT-IR (cm^{-1}(ranked intensity)): 3055(15), 1597(9), 1488(6), 1438(7), 1332(13), 1269(1), 1180(14), 1074(11), 1030(4), 760(3), 736(10), 637(5), 582(8), 555(2), 516(12);

HRMS (ESI): calcd. for $C_{48}H_{37}BONa$ $[M+Na]^+$: 663.2838; found 663.2831.

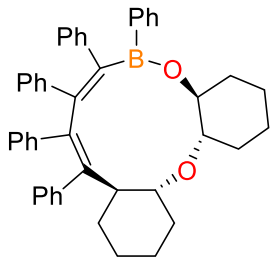

3.8

Synthesis of 3.8 (CCDC 1567467): At room temperature (23 ˚C), a solution of cyclohexene oxide in CH_2Cl_2 (80.0 mg, 0.820 mmol) was added to a solution of **1.7-Ph** (182.0 mg, 0.410 mmol) in CH_2Cl_2 resulting in a color change from deep blue to orange. The solution was allowed to stir for 1 h and the solvent removed *in vacuo*. The residue was washed with hexanes (3 x 3 mL) and dried *in vacuo* to give **3.8** as a yellow powder. Purity and identity of **3.8** has been verified by ^1H and $^{13}C\{^1H\}$ NMR spectroscopy. Yield: 159.0 mg, 61%; m.p. 206-207 ˚C. Single crystals for X-ray diffraction studies were grown from a CH_2Cl_2 solution of **3.8** by vapor diffusion into toluene.

^{1}H NMR (400 MHz, $CDCl_3$): δ 7.32 (d, J = 8.0 Hz, 2H), 7.20-6.98 (m, 13H), 6.92 (d, J = 8.0 Hz, 5H), 6.81 (d, J = 4.0 Hz, 2H), 6.64 (t, J = 8 Hz, 2H), 6.54 (t, J = 8.0 Hz, 1H), 4.73 (m, 2H), 3.87 (m, 1H), 3.21 (t, J = 8.0 Hz, 1H), 2.06 (m, 2H), 1.88-1.63 (m, 5H), 1.48-1.40 (m, 3H), 1.31-1.26 (m, 2H), 1.19-1.13 (m, 1H), 0.97-0.94 (m, 1H), 0.81-0.72 (m, 2H);

^{13}C{^{1}H} NMR (151 MHz, $CDCl_3$): δ 150.24 (C_q), 144.96 (C_q), 144.93 (C_q), 143.02 (C_q), 142.85 (C_q), 142.39 (C_q), 142.18 (C_q), 140.85 (C_q), 134.68 (*CH*), 131.05 (*CH*), 130.98 (*CH*), 129.87 (*CH*), 129.07 (*CH*), 127.99 (*CH*), 127.79 (*CH*), 127.45 (*CH*), 126.92 (*CH*),

126.72 (*CH*), 126.60 (*CH*), 126.30 (*CH*), 125.58 (*CH*), 125.56 (*CH*), 78.18 (*CH*), 75.07 (*CH*), 74.57 (*CH*), 49.20 (*CH*), 34.98 (*CH$_2$*), 30.60 (*CH$_2$*), 30.48 (*CH$_2$*), 29.20 (*CH$_2$*), 24.99 (*CH$_2$*), 24.19 (*CH$_2$*), 22.06 (*CH$_2$*), 21.94 (*CH$_2$*), peaks assigned *via* $^{13}C\{^1H\}$ DEPT experiments;

$^{11}B\{^1H\}$ NMR (128 MHz, $CDCl_3$): δ 43.5 (br);

FT-IR (cm^{-1}(ranked intensity)): 2930(3), 1596(12), 1487(7), 1437(6), 1277(4), 1158(9), 1071(1), 1053(13), 1022(14), 750(11), 737(8), 656(2), 546(5), 529(10), 470(15);

HRMS (ESI): calcd. for $C_{46}H_{45}BO_2Na$ $[M+Na]^+$: 663.3413; found 663.3417.

CHAPTER FOUR

Oxygen and Sulfur-Atom Insertion into Boroles as a Route to 1,2-Oxaborines and 1,2-Thiaborines

This chapter published as: Yruegas, S.; Patterson, D. C.; Martin, C. D., *Chem. Commun*., **2016**, *52*, 6658-6661 and Yruegas, S.; Martin, C. D., *Chem. –Eur. J*., **2016**, *22*, 18358-18361.

4.1 Introduction

Over the last decade, significant effort has been put forth toward the development of hybrid organic/inorganic analogues of benzene.[1, 13, 166-168] In particular, the azaborine series has garnered interest due to their potential in electronic materials and pharmaceuticals.[15, 168-181] Out of the three isomers, 1,2-azaborine (**4.1**, Figure 4.1) is the most stable, and the chemistry of this species is the most advanced.[155, 182-186] Despite the blossoming research of 1,2-azaborines, the boron-oxygen and boron-sulfur analogues 1,2-oxaborine (**4.2**) and 1,2-thiaborine (**4.3**), have been in comparison, largely neglected.

Letzinger and Nazy proposed the boron-oxygen containing phenanthrene analogue (**4.4**) in 1959, suggesting it as a possible product from the isomerization of 2,2'-tolandiboronic acid.[187] Later that year, Dewar and coworkers conclusively reported the synthesis of the phenanthrene analogue as well as the bicyclic naphthalene derivative (**4.5**).[188-189] The polycyclic systems containing the unsaturated 1,2-BOC_4 ring are much more developed than species lacking fused aryl groups.[44, 190-198] In fact, there are only three discrete 1,2-oxaborine systems known in the literature. The first 1,2-oxaborine **4.6** was synthesized in 1973 by the condensation of an alkyl phenyl ketone and a borane.[199] Ashe and coworkers reported the synthesis of **4.7** in 2007 *via* a carbenoid ring expansion route

and reported the only X-ray crystallographic characterization of a 1,2-oxaborine that featured chromium bound to the B-phenyl group of **4.7** (**4.8**).[200]

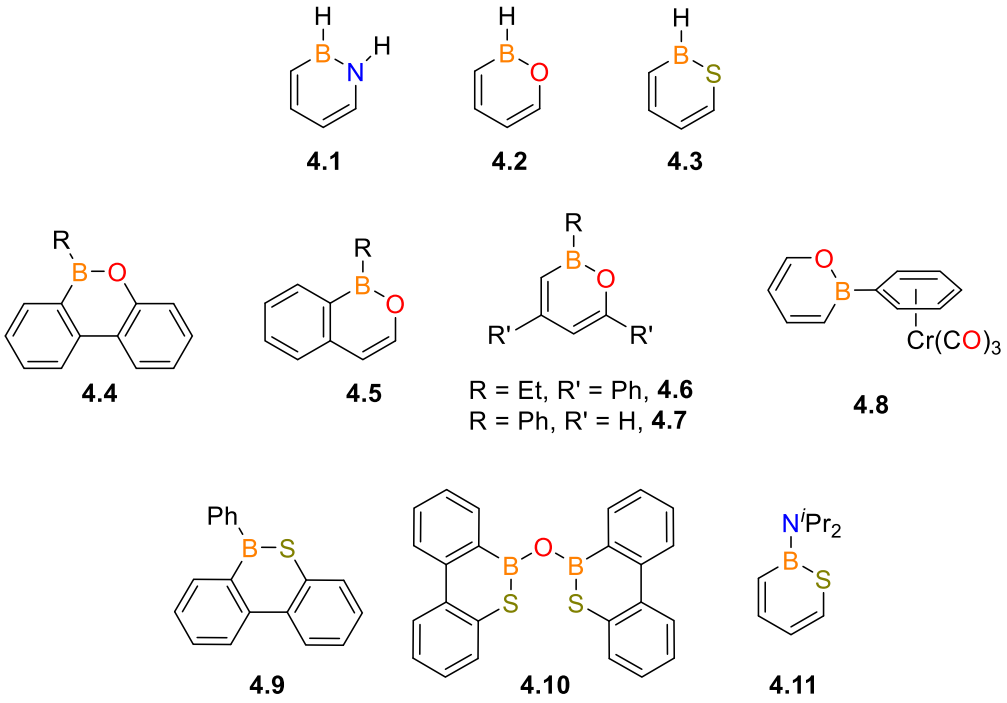

Figure 4.1. Unsaturated B–N, B–O, and B–S containing heteroarenes.

For sulfur, the reported derivatives are limited to two fused polycyclic systems, specifically phenanthrene analogues (**4.9** and **4.10**) and only a singular example of a 1,2-thiaborine exists, reported by Ashe (**4.11**).[135, 191, 201] The synthetic methodology to prepare **4.11** involved a carbenoid insertion into a 1,2-thiaborole generating the 1,2-thiaborine in relatively low yields.[135] Notably, this complex features a diisopropylamino group on the boron atom and exhibits a short B-N bond of 1.407 Å, indicative of a significant B-N π-interaction that inevitably diminishes endocyclic participation of the boron p-orbital, hence, disrupting the aromaticity. Disorder in the solid-state structure, specifically with the

carbon and sulfur atoms adjacent to boron, prevented an accurate analysis of the endocyclic metrical parameters.

As described in Chapter Three, boroles are effective reagents for the generation of six-, seven-, and eight-membered unsaturated heterocycles *via* ring expansion reactions. Given this, boroles could be a potential precursor to 1,2-oxaborine and 1,2-thiaborine species by the simple reaction with an oxygen or sulfur atom source.

4.2 Oxygen Insertion into Boroles

An early investigation by Eisch, treating pentaphenylborole with O_2 and subsequent work up by column chromatography, led to the isolation of tetraphenylfuran.[27] In 2015, upon analysis of an aerated solution of a borole, Marder and coworkers reported the observation of a peak by GC-MS corresponding to an ion with the mass of borole and an oxygen atom [M + 16] and indicated that it "may suggest the insertion of one oxygen atom into the borole."[116] These findings prompted us to investigate the chemistry of boroles with oxygen atom sources as a potential route to 1,2-oxaborines. To re-examine oxygen gas as a reagent, O_2 was bubbled through a $CDCl_3$ solution of pentaphenylborole (**1.7-Ph**), resulting in the change of the blue solution to orange. Acquiring *in situ* $^{11}B\{^1H\}$ and ^1H NMR spectra revealed an indiscernible complex mixture.

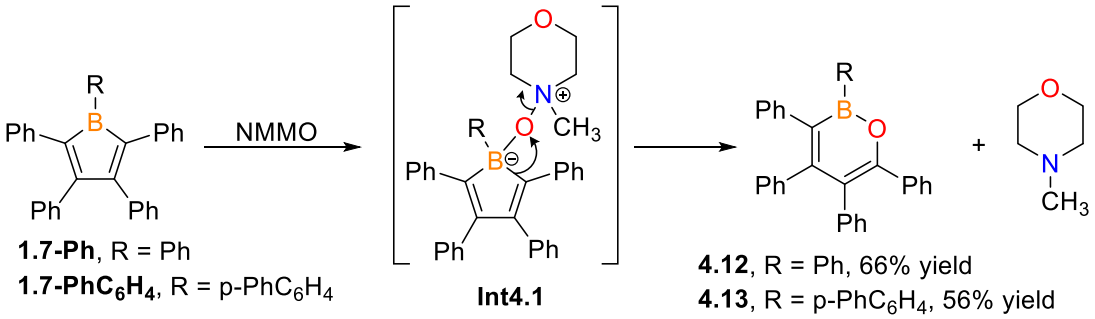

1.7-Ph, R = Ph
1.7-PhC$_6$H$_4$, R = p-PhC$_6$H$_4$

Int4.1

4.12, R = Ph, 66% yield
4.13, R = p-PhC$_6$H$_4$, 56% yield

Scheme 4.1. Reaction of boroles with N-methylmorpholine-N-oxide (NMMO) and proposed intermediate **Int4.1**.

To explore an alternative oxygen atom source, the 1:1 stoichiometric reaction of pentaphenylborole (**1.7-Ph**) with N-methylmorpholine-N-oxide (NMMO) was investigated. The room temperature reaction (23 ˚C) in $CDCl_3$ resulted in the rapid disappearance of the blue color of **1.7-Ph** to a bright yellow solution (Scheme 4.1). Monitoring the reaction *via in situ* $^{11}B\{^1H\}$ NMR spectroscopy after 1 minute revealed one resonance: a sharp singlet at 6.4 ppm indicative of a four-coordinate boron center (Figure 4.2). After 30 min, the resonance in the four-coordinate region disappeared, converging to a broad peak at 38.4 ppm in the three-coordinate region. Acquiring an ^1H NMR spectrum revealed free N-methylmorpholine, as well as a series of aryl resonances. Scaling up the reaction in dichloromethane, removal of the volatiles *in vacuo*, and recrystallization from a 3:1 chloroform/*n*-pentane solution gave the boron-containing species in 66% yield. An X-ray diffraction study on the crystals determined the identity as the desired pentaphenyl-1,2-oxaborine (**4.12**, Scheme 4.1).

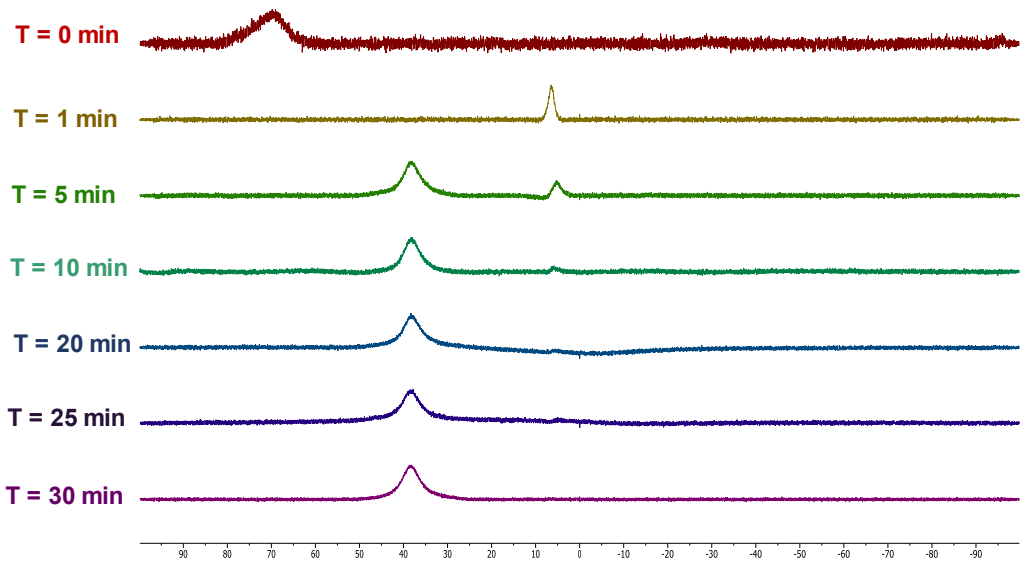

Figure 4.2. Stacked $^{11}B\{^1H\}$ NMR spectra of the reaction of **1.7-Ph** with N-methylmorpholine-N-oxide to give **4.12**.

Given that 1,2-azaborines bearing phenyl groups on boron and the ring carbon atoms have been found to be highly disordered,[183] we believed that this was also likely in **4.12** with the same pentaphenyl substitution. To circumvent this, the analogous species with a biphenyl group on the boron of the borole (**1.7-PhC$_6$H$_4$**) was reacted with NMMO to produce a species with a similar $^{11}B\{^1H\}$ NMR spectroscopic signature (δ = 38.8 *cf.* **1.7-Ph** δ = 38.4), and the B-biphenyl complex **4.13** was isolated in 56% yield.

The biphenyl group allowed us to confidently distinguish the boron from the carbon atoms and analyze the metrical parameters (Figure 4.3). The central BOC$_4$ ring in **4.13** is highly planar with a maximum deviation from planarity of 0.029 Å. The boron and endocyclic carbon atoms of the BOC$_4$ ring are all trigonal planar [$\sum$angles: B1 = 359.9(2)˚, C1 = 360.0(2)˚, C2 = 360.0(2)˚, C3 = 360.0(2)˚, and C4 = 360.0(2)˚], and the oxygen atom is more obtuse than a typical two coordinate oxygen [124.47(12)˚]. The endocyclic carbon bonds lie between single and double bonds, but do exhibit some diene character [C(1)-C(2)

1.379(2) Å, C(2)-C(3) 1.450(2) Å, and C(3)-C(4) 1.368(2) Å], slightly more than the extent of reported 1,2-azaborines.[155, 166, 183] The B-O bond length [1.380(2) Å] is comparable to reported B-O lengths of oxoboranes [*cf.* 1.351(7) Å] which indicates delocalization of the π-electrons between the boron and oxygen.[202-203] It is also noteworthy that the endocyclic B-C bond [1.527(2) Å] is slightly shorter than the exocyclic bond [1.568(2) Å].

The formation of 1,2-oxaborines **4.12** and **4.13** is believed to occur *via* a mechanism proceeding by the coordination of NMMO to the boron center to generate adduct intermediate **Int4.1**, which corroborates the observed four-coordinate boron peak by *in situ* $^{11}B\{^{1}H\}$ NMR spectroscopy. The endocyclic B-C bond is rendered nucleophilic upon coordination and can then attack the oxygen atom to undergo a 1,1-insertion generating the 1,2-oxaborines while liberating N-methylmorpholine as the by-product.

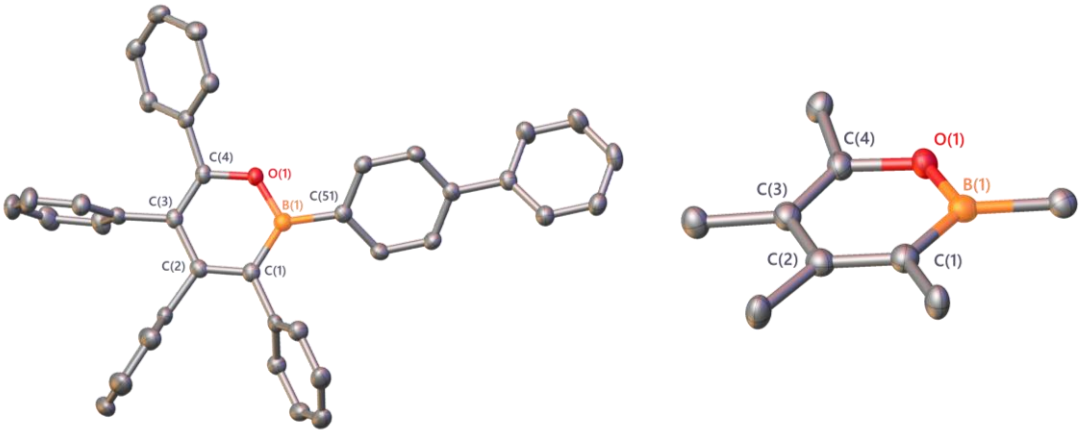

Figure 4.3. Solid-state structure of **4.13** (left). Thermal ellipsoids are drawn at the 50% probability level and hydrogen atoms have been omitted for clarity. Selected bond lengths (Å) and angles (°): B(1)–O(1) 1.380(2), B(1)–C(1) 1.527(2), C(1)–C(2) 1.379(2), C(2)–C(3) 1.450(2), C(3)–C(4) 1.368(2), C(4)–O(1) 1.356(17), B(1)–C(51) 1.568(2), O(1)–B(1)–C(51) 113.00(13), O(1)–B(1)–C(1) 116.79(14), C(4)–O(1)–B(1) 124.47(12), C(51)–B(1)–C(1) 130.11(14), C(4)–C(3)–C(2) 119.72(13), C(1)–C(2)–C(3) 121.43(13), C(2)–C(1)–B(1) 116.76(13). Simplified view along the BOC_4 plane of **4.13** (right, carbon atoms from aryl groups except *ipso* carbons have been removed).

Nucleus independent chemical shifts (NICS), one of the prime computational measures of aromaticity, have not been reported for 1,2-oxaborines. To gauge the aromatic nature of 1,2-oxaborines, NICS values of **4.12**, **4.13**, and related boron heterocycles were calculated from optimized geometries using the Gaussian 09 suite [GIAO HSE06/6-311+G(d,p) basis set, Table 4.1]. The diatropic ring currents were determined by a series of ghost atoms placed in the center [NICS(0)] and 1 Å above [$NICS(1)_{zz}$] the ring. The parent 1,2-oxaborine **4.2** has only slightly diminished ring current in comparison to its 1,2-azaborine counterpart **4.1** [**4.2**: NICS(0) -3.08, $NICS(1)_{zz}$ = -16.60 *c.f.* **4.1**: NICS(0) -5.15, $NICS(1)_{zz}$ = -20.15], both of which are less than benzene [NICS(0) -8.18, $NICS(1)_{zz}$ = -29.68].

The incorporation of a phenyl group on boron shows a decrease in the NICS value, and a reduction is also observed upon adding phenyl groups to the four carbon atoms. Hexaphenylbenzene and hexaphenyl-1,2-azaborine show this effect as well, but all species still retain appreciable aromatic character. The NICS values are virtually identical for **4.12** and **4.13**, indicating changing the biphenyl for phenyl group has minimal effect. The NICS calculations, coupled with the planarity of the BOC_4 ring and delocalized bond lengths, indicate that 1,2-oxaborines feature a moderate degree of aromaticity.

The UV-Vis absorption spectra of **4.12** and **4.13** both have lowest-energy absorption maxima at λ = 333 nm (**4.12**: ε = 12,000 $Lmol^{-1}cm^{-1}$, **4.13**: ε = 11,000 $Lmol^{-1}cm^{-1}$). In comparison, this value is significantly red-shifted with respect to hexaphenylbenzene (lowest-energy maximum at λ = 244 nm) and slightly red-shifted from hexaphenyl-1,2-azaborine (lowest-energy absorption maxima λ = 315 nm).[183]

Table 4.1. Nuclear Independent Chemical Shifts (NICS) of **4.12**, **4.13**, and Related Cyclic Systems (in ppm)

Compound	NICS(0)	$NICS(1)_{zz}$
	-8.18[a]	-29.68[a]
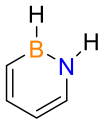	-5.15[a]	-20.15[a]
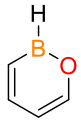	-3.08	-16.60
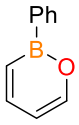	-1.63	-12.25
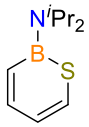	-3.28	-5.88
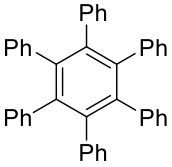	-5.47	-22.85
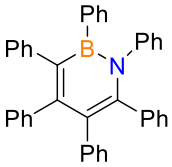	-2.60	-14.61
4.12	-1.35	-8.54
4.13	-0.67	-8.41
4.14	-3.47	-12.75
4.15	-2.33	-12.72

[a]Literature values.[48]

4.3 Exploring Sulfur Atom Insertion into Boroles

Elemental sulfur, commercially available as the cyclic octatomic allotrope S_8, is known to act as a sulfur atom source for the synthesis of heterocyclic systems.[204-208] We believed this could be exploited harmoniously with the aforementioned borole insertion chemistry and conveniently be used to access 1,2-thiaborine species in a single step.

The reaction of pentaphenylborole **1.7-Ph** with excess sulfur at 65 ˚C in benzene transformed from a blue suspension of borole into a yellow solution after 16 h (Scheme 3.2). Acquiring an *in situ* $^{11}B\{^1H\}$ NMR spectrum of the yellow solution revealed only a single resonance at 50.8 ppm, shifted upfield from pentaphenylborole (δ = 65.0). Subsequent work-up allowed the isolation of the product in 44% yield of which the identity was determined to be 1,2-thiaborine **4.14** by an X-ray diffraction study. Interestingly, the $^{11}B\{^1H\}$ NMR signal is significantly different than the documented shift of the diisopropylamino species **4.11** (35.8 ppm)[135] suggesting a different electronic structure. With B-phenyl and C-phenyl adjacent to sulfur in **4.14**, it could not be determined if disorder was present in the solid-state structure, therefore the B-biphenyl borole **1.7-PhC$_6$H$_4$** was reacted with S_8 to prepare a derivative that would differentiate these two positions and permit the accurate analysis of the bonding.

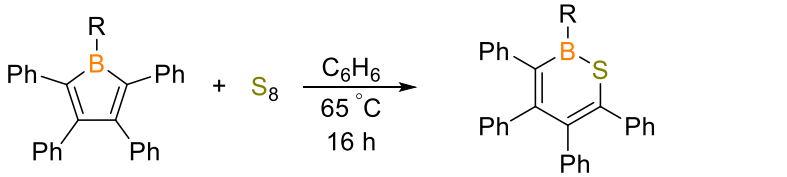

1.7-Ph, R = Ph
1.7-PhC$_6$H$_4$, R = *p*-PhC$_6$H$_4$

4.14, R = Ph, 44% yield
4.15, R = *p*-PhC$_6$H$_4$, 42% yield

Scheme 4.2. Reaction of boroles **1.7-Ph** and **1.7-PhC$_6$H$_4$** with elemental sulfur to generate 1,2-thiaborines **4.14** and **4.15**.

The analogous reaction of elemental sulfur with **1.7-PhC$_6$H$_4$** readily produced 1,2-thiaborine **4.15** with a similar $^{11}B\{^1H\}$ NMR spectroscopic signature of 51.1 ppm in a 42% yield (Scheme 4.2). An X-ray diffraction study on crystals grown allowed the assertion of the metrical parameters of 1,2-thiaborine species **4.15** (Figure 4.4). A key structural feature of **4.15** is the highly planar central BSC_4 ring with a maximum deviation from planarity of 0.049 Å. The boron and endocyclic carbon atoms are all within experimental error of trigonal planar geometries [∑angles: B1 = 359.9(7)˚, C1 = 360.0(8)˚, C2 = 359.8(2)˚, C3 = 359.7(7)˚, and C4 = 360.0(7)˚]. The sulfur atom displays a more obtuse bond angle than $(CH_3)_2S$ [106.55(7)˚ *c.f.* 99.1˚].[209] The C-C bonds within the BSC_4 ring are all intermediary between single and double bonds but contain slight diene character [C(1)–C(2) 1.383(2) Å, C(2)–C(3) 1.458(2) Å, and C(3)–C(4) 1.367(2) Å] similar to the extent observed in 1,2-azaborines, 1,2-oxaborines, and 1,2-phosphaborines.[34, 38, 152] The B-S bond length is consistent with delocalization of a lone-pair on sulfur to the p-orbital on boron, analogous to diorganothiaboranes [1.7934(17) Å *c.f.* $Mes_2B(SCH_3)$ 1.787(6) Å].[134]

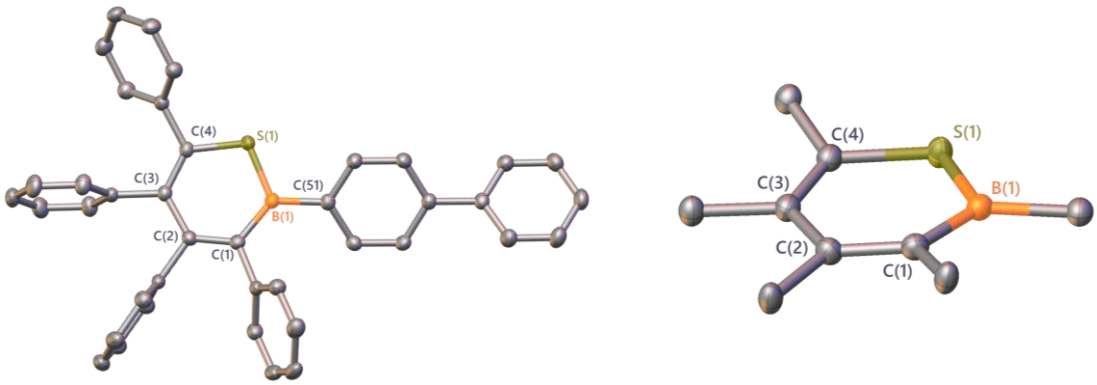

Figure 4.4. Solid-state structure of **4.15** (left). Thermal ellipsoids are depicted at the 50 % probability level and hydrogen atoms have been omitted for clarity. Selected bond lengths [Å] and angles [°]: B(1)−S(1) 1.7934(17), B(1)−C(1) 1.525(2), C(1)−C(2) 1.383(2), C(2)−C(3) 1.458(2), C(3)−C(4) 1.367(2), C(4)−S(1) 1.7325(14), S(1)-B(1)-C(1) 117.79(11), C(4)-S(1)-B(1) 106.55(7), C(51)-B(1)-C(1) 128.25(13), C(4)-C(3)-C(2) 123.92(13), C(1)-C(2)-C(3) 125.02(13), C(2)-C(1)-B(1) 122.51(13). Simplified view of the central BSC_4 ring of **4.15** (right, carbon atoms from aryl groups except *ipso* carbons have been removed).

In order to compare **4.11** with **4.14** and **4.15**, optimized geometries for the three systems were computed using density functional theory (DFT) with the exchange-correlation approximation HSE06 hybrid functional and the Pople basis 6-311+G(d,p).[145] The calculated bond lengths for **4.15** are in agreement with the X-ray structural data (Table 4.2). Unsurprisingly, **4.14** and **4.15** are virtually identical with the switch from a phenyl to a biphenyl group on boron leaving the parameters unaffected. The most striking difference in the parameters is the lengthened B-S bond for **4.11** (**4.11** = 1.8552 Å *c.f.* **4.14** = 1.8006 Å and **4.15** = 1.8013 Å). This feature coupled with the short B-N bond indicates the B-S delocalization is significantly lessened in **4.11** in comparison to **4.14** and **4.15** as well as implies a greater degree of aromaticity in **4.14** and **4.15**.

Table 4.2. Computed and Experimental Bond Lengths [Å] of 1,2-Thiaborines

Entry	4.11[a]	Computed 4.14[a]	Computed 4.15	Experimental 4.15
B(1)-S(1)	1.8552	1.8006	1.8013	1.7934
B(1)-C(1)	1.5389	1.5249	1.5254	1.5250
C(1)-C(2)	1.3587	1.3849	1.3848	1.3830
C(2)-C(3)	1.4317	1.4508	1.4509	1.4580
C(3)-C(4)	1.3485	1.3727	1.3726	1.3670
C(4)-S(1)	1.7277	1.7326	1.7325	1.7325
B(1)-N(1)	1.4191	N/A	N/A	N/A

[a]Due to the inherent disorder of both **3** and **6**, only their computational bond lengths are shown.

The UV-Vis absorbance spectra of 1,2-thiaborines **4.14** and **4.15** have lowest-energy maxima at λ = 340 nm and λ = 345 nm, respectively, which is substantially red-shifted in relation to hexaphenylbenzene (lowest-energy maximum at λ = 244 nm).[38] Fluorescence studies have not been reported previously for the 1,2-thiaborine species. Fluorescence maxima for the 1,2-thiaborines species were determined at 392 nm and 400 nm for **4.14** and **4.15**, respectively with corresponding Stokes' shifts of 52 nm and 55 nm.

The calculated HOMO/LUMO gaps for hexaphenylbenzene and the 1,2-thiaborine species are consistent with the observed red shift in the UV spectra [6.29 eV *c.f.* 4.60 eV].[38]

To assess the aromaticity, nuclear independent chemical shift (NICS) values were computed using the [GIAO HSE06/6-311+G(d,p)] basis set.[86] Compounds **4.11**, **4.14**, and **4.15** have comparable NICS(0) values, but vary when examining $NICS(1)_{zz}$ [Table 4.1L **4.11**: NICS(0) = −3.28, $NICS(1)_{zz}$ = −5.88, **4.14**: NICS(0) −3.47, $NICS(1)_{zz}$ = −12.75, **4.15**: NICS(0) = −2.33, $NICS(1)_{zz}$ = −12.72]. The values for **4.14** and **4.15** also exceed those for the analogous **4.12** [NICS(0) −1.35, $NICS(1)_{zz}$ = −8.54] and are on par with their nitrogen counterparts [NICS(0) −2.60, $NICS(1)_{zz}$ = −14.61]. The NICS values indicate that the herein reported penta-aryl species **4.14** and **4.15** are more aromatic than **4.11** and reveals that the aromaticity is hampered when π-donors are present on the boron atom.

The results presented build upon the rich chemistry of boroles, taking advantage of the high reactivity of these species to prepare 1,2-oxaborines and 1,2-thiaborines. The chemistry of these heterocycles has an exciting future given the diverse applications of their ubiquitous all carbon relative, benzene.

4.4 Experimental Details

N-methylmorpholine N-oxide and elemental sulfur were purchased from Sigma-Aldrich Chemicals and used as received.

Reaction of **1.7-Ph** with O_2: A $CDCl_3$ solution of **1.7-Ph** was prepared in a quartz NMR tube equipped with a septum. Oxygen gas was bubbled directly into the solution via a long needle and using a 22 gauge needle attached to a bubbler to prevent back-flow. An immediate color change from blue to orange occurred. ^{1}H and $^{11}B\{^{1}H\}$ NMR spectra were acquired revealing a complex mixture.

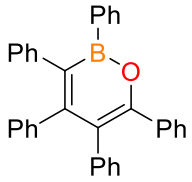

4.12

Synthesis of 4.12 (CCDC 1457937): At room temperature (23 ˚C), a dichloromethane solution (1 mL) of N-methylmorpholine N-oxide (78.0 mg, 0.664 mmol) was added dropwise to a dichloromethane solution of borole **1.7-Ph** (295.0 mg, 0.664 mmol). The solution color changed from dark blue to yellow within 1 min. The solution was allowed to stir for 1 h, and the solvent removed *in vacuo*. The residue was recrystallized by vapor diffusion of *n*-pentane into chloroform giving **4.12** as an off-white crystalline material. Yield: 204.0 mg, 66%; m.p 159-160 ˚C. Crystals for an X-ray diffraction study were grown by vapor diffusion of a *n*-pentane solution of **4.12** into chloroform.

^{1}H NMR (600 MHz, $CDCl_3$): δ 7.60 (d, J = 6.0 Hz, 2H), 7.42 (dd, J = 9.6, 6.0 Hz, 2H), 7.34 (t, J = 6.0 Hz, 1H), 7.26-7.21 (m, 5H), 7.14-7.06 (m, 3H), 7.04-7.01 (m, 3H), 6.99-6.97 (m, 2H), 6.94-6.89 (m, 5H), 6.74 (dd, J = 12.0, 6.0 Hz, 2H);

^{13}C{^{1}H} NMR (151 MHz, $CDCl_3$): δ 158.97, 153.82, 142.31, 139.40, 139.04, 138.06, 136.83, 136.67, 135.14, 132.04, 130.08, 130.00, 129.95, 129.71, 128.36, 127.85, 127.81, 127.68, 127.58, 126.90, 126.47, 125.96, 125.46, 123.87;

^{11}B{^{1}H} NMR (193 MHz, $CDCl_3$): δ 38.4 (br);

FT-IR (cm^{-1}(ranked intensity)): 1586(15), 1561(7), 1487(10), 1459(14), 1438(3), 1345(9), 1291(5), 1072(13), 1025(6), 754(2), 720(11), 692(1), 636(4), 587(8), 544(12);

HRMS (ESI): calcd. for $C_{34}H_{25}BO$ $[M+Na]^+$: 483.1897; found 483.1885;

Elemental Analysis: calculated for $C_{34}H_{25}BO$: C, 88.70; H, 5.47. Found: C, 88.20; H, 5.57;

UV-Vis (CH_2Cl_2) λ_{max} (333 nm): ε = 12,000 $Lmol^{-1}$ cm^{-1}; (305 nm): ε = 7500 $Lmol^{-1}$ cm^{-1}; (282 nm): ε = 5600 $Lmol^{-1}$ cm^{-1};

Fluorescence (CH_2Cl_2) λ_{em} 388 nm; Stokes shift (CH_2Cl_2) 55 nm (4,300 cm^{-1}).

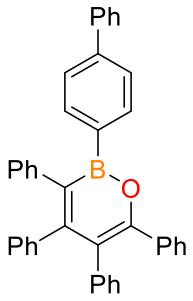

4.13

Synthesis of 4.13 (CCDC 1457938): At room temperature (23 ˚C), a dichloromethane solution (1 mL) of N-methylmorpholine N-oxide (26.0 mg, 0.225 mmol) was added dropwise to a dichloromethane solution of borole **1.7-PhC$_6$H$_4$** (117.0 mg, 0.225 mmol). The solution color changed from dark blue to yellow within 1 min. The solution was allowed to stir for 1 h, and the solvent removed *in vacuo*. The residue was recrystallized by vapor diffusion of *n*-pentane into chloroform giving **4.13** as an off-white crystalline material. Yield: 68.0 mg, 56%; m.p 191-192 ˚C**.** Crystals of **4.13** for an X-ray diffraction study were grown by vapor diffusion of *n*-pentane solution of **4.13** into chloroform.

^{1}H NMR (600 MHz, $CDCl_3$): δ 7.65 (d, *J* = 6.0 Hz, 2H), 7.60 (d, *J* = 6.0 Hz, 2H), 7.48 (d, *J* = 12.0 Hz, 2H), 7.43-7.40 (m, 4H), 7.33 (t, *J* = 12.0 Hz, 1H), 7.24-7.22 (m, 3H), 7.14-7.12 (m, 2H), 7.09-7.07 (m, 1H), 7.03-7.00 (m, 5H), 6.94-6.89 (m, 5H), 6.75 (m, 2H); **^{13}C{^{1}H} NMR** (151 MHz, $CDCl_3$): δ 158.97, 153.90, 142.44, 142.35, 141.20, 139.39, 139.17, 138.06, 136.70, 135.66, 132.05, 130.09, 129.96, 129.73, 128.83, 128.39, 127.87, 127.82, 127.75, 127.48, 127.25, 126.91, 126.48, 126.28, 125.98, 125.52, 123.91;

$^{11}B\{^1H\}$ NMR (193 MHz, $CDCl_3$): δ 38.8 (br);

FT-IR (cm^{-1}(ranked intensity)): 1584(9), 1486(12), 1497(15), 1439(5), 1297(3), 1070(11), 1026(14), 836(4), 752(2), 712(7), 692(1), 639(10), 589(8), 554(13), 532(6);

HRMS (ESI): calcd. for $C_{40}H_{29}BO$ $[M+Na]^+$: 559.2211; found 559.2196;

Elemental Analysis: calculated for $C_{40}H_{29}BO$: C, 89.55; H, 5.45. Found: C, 88.52; H, 5.48;

UV-Vis (CH_2Cl_2) λ_{max} (333 nm): ε = 11,000 $Lmol^{-1}$ cm^{-1}; (295 nm): ε = 17,000 $Lmol^{-1}$ cm^{-1};

Fluorescence (CH_2Cl_2) λ_{em} 387 nm; Stokes shift (CH_2Cl_2) 54 nm (4,200 cm^{-1}).

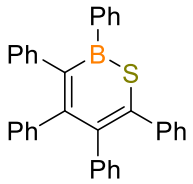

4.14

Synthesis of 4.14 (CCDC 1507212): At room temperature (23 ˚C), elemental sulfur in benzene (75.8 mg, 2.37 mmol; 1 mL) was added to a benzene solution of borole **1.7-Ph** (334.0 mg, 0.752 mmol; 1mL) in a pressure-tube and the mixture stirred for 16 h at 65 ˚C. Over this time, the solution gradually changed from dark blue to yellow. Copper metal was then added to the yellow solution and stirred overnight at 90 ˚C to remove excess sulfur. The solvent of the supernatant was removed *in vacuo* and the residue washed with hexanes (3 × 2 mL) and dried *in vacuo* to furnish the **4.14** as an off-white powder. Yield: 159.0 mg, 44%; m.p 160-161 ˚C. Single crystals for X-ray diffraction studies were grown by vapor diffusion of a dichloromethane solution of **4.14** into toluene.

^{1}H NMR (600 MHz, $CDCl_3$): δ 7.28 (m, 2H), 7.24 (m, 1H), 7.21-7.20 (m, 2H), 7.18-7.14 (m, 5H), 6.99-6.96 (m, 2H), 6.94-6.92 (m, 1H), 6.85-6.81 (m, 7H), 6.80-6.78 (m, 3H), 6.74 (m, 2H);

^{13}C{^{1}H} NMR (151 MHz, $CDCl_3$): δ 158.97, 153.82, 142.31, 139.40, 139.04, 138.06, 136.83, 136.67, 135.14, 132.04, 130.08, 130.00, 129.95, 129.71, 128.36, 127.85, 127.81, 127.68, 127.58, 126.90, 126.47, 125.96, 125.46, 123.87;

^{11}B{^{1}H} NMR (193 MHz, $CDCl_3$): δ 50.8 (br);

FT-IR (cm^{-1}(ranked intensity)): 1596(15), 1542(13), 1485(7), 1440(4), 1334(11), 1262(3), 1070(9), 1027(10), 927(8), 783(14), 750(12), 732(1), 599(6), 578(5), 558(2);

HRMS (ESI): calcd. for $C_{34}H_{26}BS$ $[M+H]^+$: 477.1849; found 477.1881;

Elemental Analysis: calculated for $C_{34}H_{25}BS$: C, 85.71; H, 5.29; Found: C, 88.20; H, 5.57;

UV-Vis (CH_2Cl_2) λ_{max} (340 nm): ε = 12,000 $Lmol^{-1}$ cm^{-1}, (260 nm): ε = 4,200 $Lmol^{-1}$ cm^{-1};

Fluorescence (CH_2Cl_2) λ_{em} 392 nm; Stokes shift (CH_2Cl_2) 52 nm (3,900 cm^{-1}).

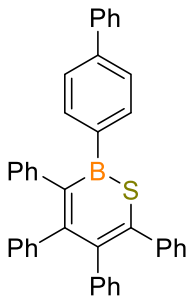

4.15

Synthesis of 4.15 (CCDC 1507213): At room temperature (23 ˚C), elemental sulfur in benzene (50.0 mg, 1.56 mmol; 1 mL) was added to a benzene solution of borole **1.7-PhC$_6$H$_4$** (210.0 mg, 0.403 mmol; 1mL) in a pressure-tube and the mixture stirred for 16 h at 65 ˚C. Over this time, the solution gradually changed from dark blue to yellow. Copper

metal was then added to the yellow solution and stirred overnight at 90 ˚C to remove excess sulfur. The solvent of the supernatant was removed *in vacuo* and the residue washed with hexanes (3 × 2 mL) and dried *in vacuo* to furnish the **4.15** as an off-white powder. Yield: 93.0 mg, 42%; m.p 165-166 ˚C**.** Single crystals for X-ray diffraction studies were grown by vapor diffusion of a dichloromethane solution of **4.15** into toluene.

^{1}H NMR (600 MHz, $CDCl_3$): δ 7.40 (d, *J* = 6.0 Hz, 2H), 7.25-7.19 (m, 5H), 7.13 (t, *J* = 6.0 Hz, 1H), 7.05 (m, 3H), 7.00-6.97 (m, 4H), 6.83 (t, *J* = 6.0 Hz, 2H), 6.78 (t, *J* = 6.0 Hz, 1H), 6.73 (d, *J* = 6.0 Hz, 2H), 6.68-6.62 (m, 7H), 6.75 (d, *J* = 6.0 Hz, 2H);

^{13}C{^{1}H} NMR (151 MHz, $CDCl_3$): δ 158.07, 145.87, 144.99, 143.58, 142.01, 141.88, 141.44, 140.99, 140.67, 139.39, 138.74, 134.49, 131.78, 130.46, 130.40, 129.96, 128.81, 127.77, 127.44, 127.39, 127.35, 127.16, 126.97, 126.62, 126.25, 125.81, 125.55, 125.12;

^{11}B{^{1}H} NMR (193 MHz, $CDCl_3$): δ 51.1 (br);

FT-IR (cm^{-1}(ranked intensity)): 1597(9), 1485(6), 1440(7), 1331(12), 1257(2), 1071(10), 1026(13), 913(15), 828(8), 764(4), 744(14), 731(1), 578(5), 562(3), 496(11);

HRMS (ESI): calcd. for $C_{40}H_{29}BSNa$ $[M+Na]^+$: 575.1982; found 575.1960;

Elemental Analysis: calculated for $C_{40}H_{29}BS$: C, 86.96; H, 5.29. Found: C, 88.52; H, 5.48;

UV-Vis (CH_2Cl_2) λ_{max} (345 nm): ε = 10,000 $Lmol^{-1}$ cm^{-1}, (260 nm): ε = 17,000 $Lmol^{-1}$ cm^{-1};

Fluorescence (CH_2Cl_2) λ_{em} 400 nm; Stokes shift (CH_2Cl_2) 55 nm (4,000 cm^{-1}).

CHAPTER FIVE

Intermolecular Insertion Reactions of Azides Into 9-Borafluorenes to Generate 9,10-B,N-Phenanthrenes

This chapter published as: Yruegas, S.; Martinez, J. J.; Martin, C. D., *Chem. Commun.,* **2018**, *54*, 6808-6811.

5.1 Introduction

Polycyclic aromatic hydrocarbons (PAHs) are emerging as candidates for organic photovoltaics and organic field effect transistors (OFETs) due to their unique conducting properties. [210-211] The incorporation of an isoelectronic B-N unit in place of a C=C unit in PAHs alters the photophysical properties, often resulting in a red-shift in the absorbance and fluorescence that can be desirable for utility in the aforementioned applications.[6, 14, 168, 212-215] Benzene and carbonaceous PAHs can be isolated from fossil fuel deposits, combustion residue, and natural products, whereas their B,N-doped analogues are not naturally occurring, and hence, must be accessed synthetically. [3, 13, 216-218]

Boroles, antiaromatic BC_4 heterocycles[18] (i.e. **1.7-Ph**), have been shown to undergo ring expansion reactions *via* insertion into the endocyclic B-C bond to generate an array of unsaturated boracycles (see Chapters Three and Four for previous examples).[21, 35-36, 38, 42, 44, 56-59, 117, 121, 150-152, 183, 219-223] Noteworthy is the reactivity with organic azides to produce highly substituted 1,2-azaborines[5e, f, i,] (**5.1**, Figure 5.1a), B,N-containing analogues of benzene.[224] Despite the rich insertion chemistry of boroles, the reactivity of their benzo-fused relatives, 9-borafluorenes (**1.15**), has not been explored with organic azides. 9-Borafluorenes have a reduced degree of antiaromaticity, and as a result, are less reactive.[64,

[69, 225] To date, an air-stable borole has yet to be reported, but 9-borafluorenes with sufficient bulk on boron are air stable compounds that can be subjected to column chromatography.[65, 67, 116, 226-228]

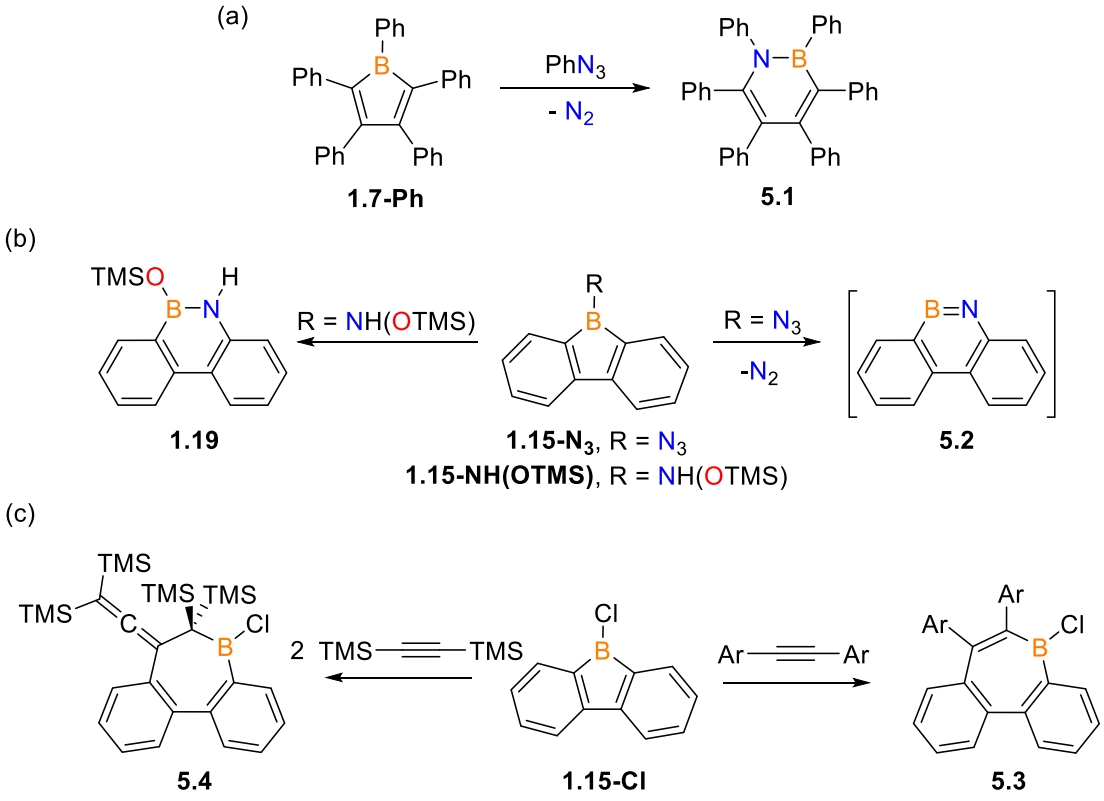

Figure 5.1. (a) Example of a formal nitrene insertion of an azide into a borole, (b) intramolecular nitrogen atom insertion of 9-*N*-substituted 9-borafluorenes, and (c) intermolecular insertion reactivity of **1.15-Cl** with alkynes.

Although scarce, examples of 9-borafluorenes undergoing insertion into the endocyclic B-C bond have been reported. Work by the groups of Köster and Wagner demonstrated that endocyclic B-C bond cleavage was observed by the addition of hydride sources.[74, 229-232] Bettinger and coworkers prepared 9-azido-9-borafluorene (**1.15-N3**), which upon thermolysis, produced B,N-phenanthryne **5.2** that was confirmed by a trapping experiment with TMSCl.[68, 70, 233] In another report, the same group demonstrated that an

appropriately substituted 9-borafluorene [**1.15-NH(OTMS)**] underwent a spontaneous ring expansion to incorporate the nitrogen of the amine into the ring to give the 1,2-azaborine containing product **1.19**.[78] Both of the previous insertion reactions were intramolecular with the nitrogen bound to boron inserting into the B-C bond. With respect to intermolecular insertion reactions, a singular report exists by Fukushima and coworkers on the reaction of alkynes with 9-chloro-9-borafluorene (**1.15-Cl**, Figure 5.1c). Reactions with diarylacetylenes furnished unsaturated aryl-fused borepin heterocycles *via* the insertion of the C_2 unit into the B-C bond (**5.3**) whereas bis(trimethylsilyl)acetylene reacted in a 2:1 stoichiometry to generate a seven-membered ring with an exocyclic allene **5.4**.[234]

Inspired by the prior intramolecular nitrogen insertion by Bettinger and the intermolecular alkyne insertion, we hypothesized that intermolecular reactions of 9-borafluorenes with organic azides could produce 1,2-azaborines with two fused arenes, namely 9,10-B,N-phenanthrenes. The only reaction of this sort documented is that of **1.15-Cl** with trimethylsilyl-azide, which generated **1.15-N$_3$** by a metathesis reaction.[68, 70] This metathesis pathway can be circumvented by avoiding the pairing of trimethylsilyl-azide with a B-halide substituted 9-borafluorene. In this chapter, we describe the reactions of azidobenzene and 1-azidoadamantane with 9-borafluorenes as a method to generate 9,10-B,N-phenanthrenes.

5.2 Reactions of Azides with 9-Borafluorenes

The stoichiometric reaction of **1.15-Cl** and azidobenzene in *n*-pentane underwent an instant color change from yellow to orange accompanied by gas evolution which subsided after 3h (Scheme 5.1). Acquiring an *in situ* $^{11}B\{^1H\}$ NMR spectrum of the orange solution revealed a single resonance at 35.5 ppm, shifted upfield considerably from **1.15-Cl**

(64.0 ppm).[68] After work-up, a single product was isolated that was identified by single crystal X-ray diffraction studies as the 9,10-B,N-phenanthrene complex **5.5**, generated *via* the formal nitrene insertion into the B-C bond and concomitant release of N_2 gas (Figure 5.2, Table 5.1).

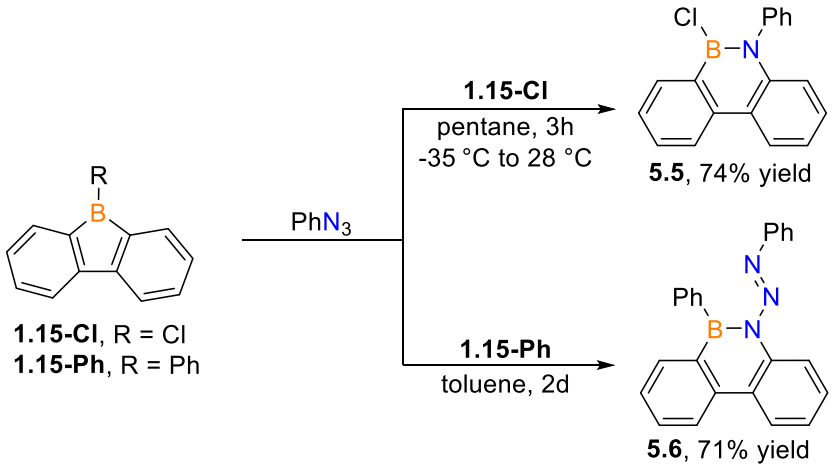

Scheme 5.1. Reactions of azidobenzene with 9-borafluorenes **1.15-Cl** and **1.15-Ph**.

A critical step determined in the intermolecular ring expansion methodology of the related monocyclic borole chemistry is coordination of the substrate to the Lewis acidic boron center which enables B-C bond cleavage.[21] The Gutmann-Beckett method is an experimental Lewis acidity scale that gauges the strength of the Lewis acid by addition of Et_3PO and analyzing the change in the ^{31}P NMR spectroscopic shift from the free phosphine oxide (41.0 ppm).[83, 235] An Acceptor Number (AN) is then calculated from the resultant ^{31}P adduct signal [AN = 2.21 x (δ_{sample} – 41.0)] in which a larger AN signifies a stronger Lewis acid. Rupar and coworkers measured the AN for **1.15-Cl** as 78.7 in benzene,[67] which is comparable to the value for **1.7-Ph** (AN = 79.2) that we measured by the analogous experiment in the same solvent and aligns with their comparable reactivity with azidobenzene. 9-Phenyl-9-borafluorene (**1.15-Ph**) is a convenient reagent to access

given the commercial availability of $PhBCl_2$, which undergoes transmetallation with the stannole precursor.[69] Conducting the analogous Gutmann-Beckett experiment with **1.15-Ph** indicated an acceptor number of 73.4, signifying weaker Lewis acidity in comparison to **1.15-Cl** and **1.7-Ph**.

To determine if the weaker Lewis acid **1.15-Ph** could undergo intermolecular ring expansion, it was reacted with azidobenzene. An immediate color change from yellow to orange was observed upon the addition of azidobenzene to a solution of **1.15-Ph** in toluene, but no gas evolution was seen over 48 h. Monitoring the reaction *via in situ* $^{11}B\{^1H\}$ NMR spectroscopy showed a major peak at 36.9 ppm, similar to **5.5** (35.5 ppm), and comparable to known B,N-phenanthrene species.[78, 196] The volatiles were stripped *in vacuo* and the resultant solids washed with *n*-pentane to isolate a bright yellow powder. X-ray diffraction studies identified the product as the *N*-diazene functionalized 9,10-B,N-phenanthrene complex **5.6**, in this case, incorporating the whole azide into the product. Contrary to the aforementioned result where the α-nitrogen of the azide inserted into the B-C bond, the γ-nitrogen inserted instead. Heating the reaction at 110 ˚C did not alter the outcome, exclusively forming **5.6** with no evidence of a formal nitrene-insertion/N_2 elimination product. [236]

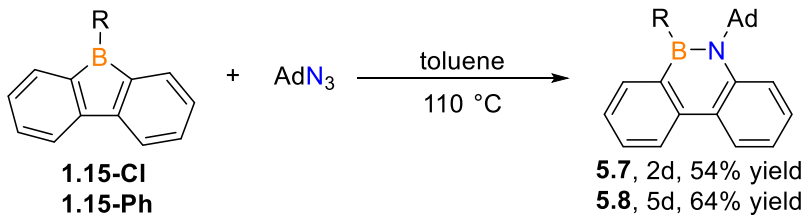

Scheme 5.2. Reactions of 1-azidoadamantane with 9-borafluorenes **1.15-Cl** and **1.15-Ph**.

To further assess the ability of the 9-borafluorenes to perform ring expansion, we investigated the chemistry with 1-azidoadamantane (AdN_3, Scheme 5.2). The addition of a stoichiometric amount of AdN_3 to a toluene solution of **1.15-Cl** or **1.15-Ph** at room temperature showed no evidence of reactivity by ^{1}H and $^{11}B\{^{1}H\}$ NMR spectroscopy or color change. Heating the reaction mixtures to 110 ˚C, and monitoring by $^{11}B\{^{1}H\}$ NMR spectroscopy, showed consumption of the 9-borafluorene starting material after 2d for **1.15-Cl** and 5d for **1.15-Ph** with the emergence of new peaks at 40.1 and 40.0 ppm, respectively. X-ray diffraction studies identified the products as the B,N-phenanthrenes **5.7** and **5.8**. Subsequent work-up gave off-white solids in 54% (**5.7**) and 64% (**5.8**) yields. Acquiring ^{1}H NMR spectra of the redissolved solids in $CDCl_3$ revealed signals in the alkyl region for the adamantyl groups integrating in a 15:8 (**5.7**) and 15:13 (**5.8**) ratio with respect to the resonances in the aryl region confirming 1:1 reactions.

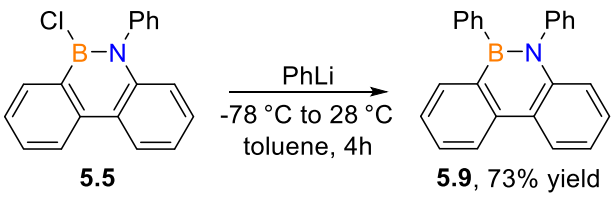

5.5 **5.9**, 73% yield

Scheme 5.3. Demonstrating the capability of B–Cl substitution of **5.5** to give **5.9**.

We were curious if the B,N-phenanthrene with phenyl groups on both boron and nitrogen could be accessed, as its synthesis has not been reported and **5.6** was the only observed product in the reaction of **1.15-Ph** and azidobenzene. The chloride in **5.5** serves as a synthetic handle for modifying the substitution at boron *via* transmetallation with a nucleophile.[237] Dissolving **5.5** in toluene, then adding phenyllithium in $^{n}Bu_2O$ at -78 ˚C, followed by removal of the solvent *in vacuo*, gave a light-yellow powder. Crystals grown

for an X-ray diffraction study identified the compound as the 9,10-B,N-phenanthrene **5.9**, which has a $^{11}B\{^{1}H\}$ NMR spectroscopic signature at 39.3 ppm in $CDCl_3$ (Scheme 5.3).

Table 5.1. Salient Bond Lengths (Å) and Angles [°] in Compounds **5.5**, **5.6**, **5.7**, and **5.8**

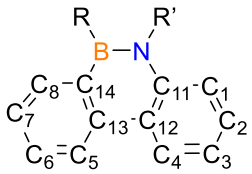

5.5 R = Cl, R' = Ph
5.6 R = Ph, R' = N_2Ph
5.7 R = Cl, R' = Ad
5.8 R = Ph, R' = Ad

Entry	**5.5**	**5.6**	**5.7**	**5.8**
B(1)–N(1)	1.402(3)	1.426(3)	1.416(2)	1.431(2)
N(1)-C(11)	1.420(3)	1.433(3)	1.429(2)	1.433(2)
C(11)-C(12)	1.411(3)	1.431(3)	1.431(2)	1.412(2)
C(12)-C(13)	1.474(3)	1.390(3)	1.469(3)	1.461(2)
C(13)-C(14)	1.411(3)	1.418(3)	1.408(3)	1.406(2)
C(14)-B(1)	1.525(3)	1.414(3)	1.534(3)	1.554(3)
N(1)-N(2)		1.427(3)		
N(2)-N(3)		1.246(3)		
N(1)-N(2)-N(3)		110.37(17)		

The 9,10-B,N-phenanthrene products **5.5-5.8** share similarities with the exception of noticeable puckering observed for **5.7** and **5.8** (max. deviation from planarity = 0.135 and 0.120 Å, respectively) due to the bulky adamantyl group. The B-N bond lengths range between 1.40-1.43 Å, indicating delocalization of the π-electrons between the boron and nitrogen atoms.[183, 219, 223] The diazene complex **5.6** is in the *E*-conformation with the two exocyclic nitrogen atoms adopting bent geometries and a N-N bond distance consistent with a double bond [N(2)-N(3) 1.246(3) Å].[36] Due to the identical substitution on boron and nitrogen of **5.9**, the boron and nitrogen atoms in the central ring are positionally disordered in the solid-state structure preventing an accurate discussion on bond lengths and angles of this molecule (Appendix D: Figure D-43).[238]

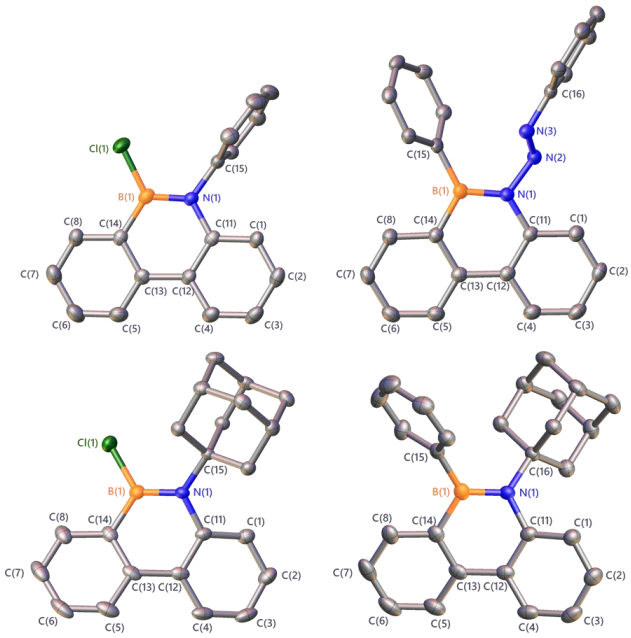

Figure 5.2. Solid-state structure of **5.5**, **5.6**, (top left to right) **5.7**, and **5.8** (bottom left to right). Thermal ellipsoids are depicted at the 50 % probability level and hydrogen atoms have been omitted for clarity.

The UV-Vis absorption and fluorescence data for all compounds are listed in Table 5.2. The absorbance values are significantly red-shifted with respect to their fully carbonaceous relative, phenanthrene (lowest-energy maximum at λ = 240 nm),[239] and in accordance with known 9,10-B,N-phenanthrenes (lowest-energy absorption maxima λ = 310-325 nm).[78] The carbonaceous analogue of **5.9** is known, 9,10-diphenylphenanthrene, which has lowest-energy absorption maxima and emissions red-shifted in comparison to **5.9** (λ_{max} = 351 nm *c.f.* 331 nm and λ_{em} = 392 nm *c.f.* 355 nm).[240] Noteworthy, **5.6** has the largest molar extinction coefficient (24,300 $Lmol^{-1}cm^{-1}$) presumably due to the diazene moiety being in conjugation with the B,N-phenanthrene π-system.[36] The fluorescence spectra of the compounds show emissions in the 350-360 nm range with moderate Stokes shifts.

Table 5.2. UV-Vis and Fluorescence Values for **5.5-5.9** (Spectra Collected in CH_2Cl_2 Under an Atmosphere of N_2)

Entry	**5.5**	**5.6**	**5.7**	**5.8**	**5.9**
R	Cl	Ph	Cl	Ph	Ph
R'	Ph	N=N-Ph	Ad	Ad	Ph
λ_{max} [nm]	329	319	328	331	331
ε [L mol^{-1} cm^{-1}]	11 100	24 300	3 700	3 700	12 500
λ_{em} [nm]	352	357	353	357	355
Stokes shift [cm^{-1}]	23	38	25	26	24

In summary, we have demonstrated the ability of 9-borafluorenes to undergo the first intermolecular heteroatom insertion reactions with organic azides to synthesize 9,10-B,N-phenanthrenes in a single synthetic step. The reactions with **1.15-Cl** gave products with a B-Cl bond that permits facile substitution at the boron center in the product. In one case, a diazene functionalized 9,10-B,N-phenanthrene compound was generated as the ɣ-nitrogen was incorporated into the ring rather than the α-nitrogen. Absorbance studies showed that the doped B,N-phenanthrenes are red-shifted in comparison to phenanthrene. These results demonstrate an intermolecular approach that can be utilized to install heteroatoms into boroles with fused rings to construct hybrid organic/inorganic fused arene systems.

5.3 Experimental Details

2'-2'-Dibromobiphenyl was purchased from Ark Pharm, boron trichloride in hexanes (1M) from Acros Organics, triethylphosphine oxide from Alfa Aesar, dichlorophenylborane from Beantown Chemicals, azidobenzene from Enamine, and 1-azidoadamantane and phenyllithium in dibutyl ether (1.8 M) from Sigma Aldrich, respectively. All reagents were used as received.

Note: The following synthesis is adapted from the previous preparation of **1.15-Ph** by Piers and coworkers.[69] In our hands, this route was higher yielding than the prior synthesis for **1.15-Cl** by going through the corresponding 9,9-dimethyl-9-stannafluorene, an air-stable intermediate, instead of the lithiation route which was found to be exceedingly sensitive.

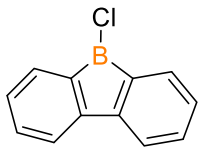

1.15-Cl

Synthesis of 1.15-Cl: A solution of 9,9-dimethyl-9-stannafluorene (2.56 g, 8.51 mmol) in toluene (50 mL) was cooled to 0 ˚C upon which BCl_3 in hexanes (1 M, 8.5 mL, 8.51 mmol) was added dropwise over 10 min. The reaction mixture was then stirred for 14 h at 23˚C. The volatiles were removed *in vacuo* to give an orange powder. The Me_2SnCl_2 by-product was removed by sublimation (40 ˚C, 0.2 Torr) and the resultant yellow residue was crystallized in *n*-pentane to give bright yellow crystals of **1.15-Cl**. Yield: 1.24 g, 73%;

^{1}H NMR (600 MHz, $CDCl_3$): δ 7.55 (d, J = 12.0 Hz, 2H), 7.38-7.34 (m, 4H), 7.15 (td, J = 12.0, 6.0 Hz, 2H);

^{11}B{^{1}H} NMR (193 MHz, $CDCl_3$): δ 63.8 (br);

The spectroscopic data matches the literature values.[69]

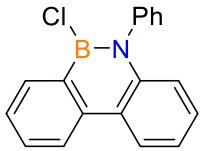

5.5

Synthesis of 5.5 (CCDC 1819488): A cold (-35 ˚C) solution of azidobenzene (0.152 g, 1.27 mmol) in *n*-pentane (2 mL) was added dropwise to a *n*-pentane solution (2 mL) of **1.15-Cl** (0.253 g, 1.27 mmol) and stirred for 3 h, after which the solvent was removed *in vacuo*. The residue was washed with hexanes (3 x 2 mL) and dried *in vacuo* to give **5.5** as a yellow powder. Single crystals for X-ray diffraction studies were grown from a *n*-pentane solution of **5.5** by vapor diffusion into toluene. Yield: 0.272 g, 74%; m.p 92-94 ˚C;

^{1}H NMR (400 MHz, $CDCl_3$): δ 8.54-8.41 (m, 2H), 8.39 (d, J = 8.0 Hz, 1H), 7.82 (td, J = 8.0, 1.2 Hz, 1H), 7.61-7.55 (m, 4H), 7.52-7.48 (m, 1H), 7.31-7.29 (m, 2H), 7.25-7.23 (m, 1H), 6.82-6.78 (m, 1H) ;

^{13}C{^{1}H} NMR (151 MHz, $CDCl_3$): δ 143.00, 141.95, 139.08, 135.14, 132.32, 129.97, 129.21, 128.26, 127.86, 126.99, 124.19, 123.67, 122.32, 122.22, 118.90;

^{11}B{^{1}H} NMR (193 MHz, $CDCl_3$): δ 35.5 (br);

FT-IR (cm^{-1}(ranked intensity)): 1591(12), 1481(7), 1444(9), 1363(8), 1281(15), 1259(3), 1170(11), 950(6), 752(1), 739(13), 721(4), 698(2), 598(5), 560(10), 429(14);

HRMS (CI^+) for $C_{18}H_{13}BClN$ [M^+], calcd: 289.0829; found 289.0829;

UV-Vis (CH_2Cl_2) λ_{max} (329 nm): ε = 11,100 $Lmol^{-1}$ cm^{-1}, (318 nm): ε = 7,700 $Lmol^{-1}$ cm^{-1};

Fluorescence (CH_2Cl_2) λ_{em} 352 nm; Stokes shift (CH_2Cl_2) 23 nm (2,000 cm^{-1}).

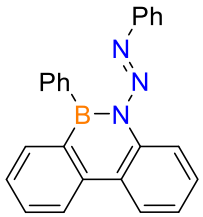

5.6

Synthesis of 5.6 (CCDC 1819489): A solution of azidobenzene (0.145 g, 1.22 mmol) in toluene (1 mL) was added to a toluene solution (1 mL) of **1.15-Ph** (0.293 g, 1.22 mmol) and stirred for 2 d at 23 ˚C. The solvent was removed *in vacuo* to yield a yellow residue. The residue was washed with *n*-pentane (3 x 2 mL) and dried *in vacuo* to give **5.6** as a yellow powder (the estimated purity by ^{1}H NMR 90%). Single crystals for X-ray diffraction studies were grown from a dichloromethane solution of **5.6** by vapor diffusion into toluene. Yield: 0.312 g, 71%; m.p 120-121 ˚C;

^{1}H NMR (600 MHz, C_6D_6): δ 8.31 (d, *J* = 12.0 Hz, 1H), 8.27 (d, *J* = 6.0 Hz, 1H), 7.71-7.68 (m, 2H), 7.52 (t, *J* = 6.0, 1H), 7.29 (t, *J* = 6.0, 1H), 7.24-7.19 (m, 6H), 7.16-7.15 (m, 2H), 7.09 (t, *J* = 6.0, 2H), 7.04-6.99 (m, 2H);

^{13}C{^{1}H} NMR (151 MHz, $CDCl_3$): 148.24, 138.89, 138.74, 138.48, 137.63, 133.02, 131.90, 131.41, 130.91, 129.73, 129.22, 128.49, 127.92, 127.24, 126.92, 126.53, 124.09, 123.83, 123.34, 122.93, 122.15, 121.94, 119.01, 116.49;

^{11}B{^{1}H} NMR (193 MHz, $CDCl_3$): δ 36.9 (br)**;**

FT-IR (cm^{-1}(ranked intensity)): 1598(13), 1481(7), 1429(9), 1291(11), 1229(3), 1140(12), 1002(4), 771(8), 745(1), 718(5), 705(2), 685(6), 638(15), 564(14), 516(10);

HRMS (CI^+) for $C_{24}H_{18}BN_3$ [M^+], calcd 359.1593; found 359.1597;

UV-Vis (CH_2Cl_2) λ_{max} (319 nm): ε = 24,300 $Lmol^{-1}$ cm^{-1};

Fluorescence (CH_2Cl_2) λ_{em} 357 nm; Stokes shift (CH_2Cl_2) 38 nm (3,400 cm^{-1}).

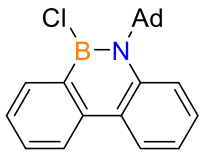

5.7

Synthesis of 5.7 (CCDC 1819490): A solution of 1-azidoadamantane (0.026 g, 0.15 mmol) in toluene (1 mL) was added to a toluene solution (1 mL) of **1.15-Cl** (0.029 g, 0.15 mmol) in a pressure tube and heated for 2 d at 110 ˚C, upon which the solvent was removed *in vacuo*. The yellow residue was washed with acetonitrile (3 x 2 mL) and dried *in vacuo* to give **5.7** as an off-white powder. Single crystals for X-ray diffraction studies were grown from a dichloromethane solution of **5.7** by vapor diffusion into hexanes. Yield: 0.028 g, 54%; m.p 117-118 ˚C;

^{1}H NMR (400 MHz, $CDCl_3$): δ 8.22 (d, J = 8.0 Hz, 1H), 8.14 (d, J = 8.0 Hz, 1H), 8.07 (dd, J = 8.0, 1.6 Hz, 1H), 7.73-7.66 (m, 2H), 7.46 (t, J = 8.0 Hz, 1H), 7.27-7.22 (m, 1H), 7.18 (m, 1H), 2.50 (s, 6H), 2.19 (s, 3H), 1.73 (q, J = 12.0 Hz, 6H);

^{13}C{^{1}H} NMR (151 MHz, $CDCl_3$): δ 140.00, 139.33, 133.65, 132.05, 128.01, 126.49, 125.26, 124.75, 123.73, 121.79, 61.28, 43.14, 36.48, 30.92;

^{11}B{^{1}H} NMR (193 MHz, $CDCl_3$): δ 40.0 (br)**;**

FT-IR (cm^{-1}(ranked intensity)): 2905(4), 1597(9), 1478(11), 1441(14), 1333(15), 1304(6), 1230(2), 1176(12), 1137(13), 1065(7), 948(8), 888(10), 759(5), 741(1), 616(3);

HRMS (CI^+) for $C_{22}H_{23}BClN$ [M^+], calcd 347.1612; found 347.1608;

UV-Vis (CH_2Cl_2) λ_{max} (328 nm): ε = 3,700 $Lmol^{-1}$ cm^{-1};

Fluorescence (CH_2Cl_2) λ_{em} 353 nm; Stokes shift (CH_2Cl_2) 25 nm (2,200 cm^{-1}).

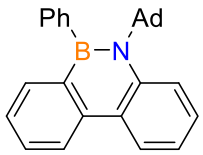

5.8

Synthesis of 5.8 (CCDC 1819491): A solution of 1-azidoadamantane (0.037 g, 0.21 mmol) in toluene (1 mL) was added to a toluene solution (1 mL) of **1.15-Ph** (0.050 g, 0.21 mmol) in a pressure tube and heated for 5 d at 110 ˚C, after which the solvent was removed *in vacuo*. The yellow residue was washed with acetonitrile (3 x 2 mL) and dried *in vacuo* to give **5.8** as an off-white powder. Single crystals for X-ray diffraction studies were grown from a dichloromethane solution of **5.8** by vapor diffusion into hexanes. Yield: 0.052 g, 64%; m.p 178-179 ˚C;

^{1}H NMR (600 MHz, $CDCl_3$): δ 8.26 (d, J = 12.0 Hz, 1H), 8.21 (d, J = 12.0 Hz, 1H), 8.06 (d, J = 6.0 Hz, 1H), 7.89 (d, J = 12.0 Hz, 1H), 7.65 (t, J = 6.0 Hz, 1H), 7.59 (d, J = 12.0 Hz, 2H), 7.43 (t, J = 6.0 Hz, 2H), 7.39-7.36 (m, 2H), 7.32 (t, J = 6.0 Hz, 1H), 7.22 (t, J = 6.0 Hz, 1H), 2.26 (s, 6H), 2.01 (s, 3H), 1.54 (q, J = 12.0 Hz, 6H);

^{13}C{^{1}H} NMR (151 MHz, $CDCl_3$): δ 145.02, 141.06, 139.03, 137.10, 135.54, 132.60, 131.07, 130.40, 128.27, 127.32, 127.16, 125.92, 125.41, 124.67, 123.51, 121.63, 121.19, 61.74, 44.72, 36.38, 30.79;

^{11}B{^{1}H} NMR (193 MHz, $CDCl_3$): δ 42.1 (br);

FT-IR (cm^{-1}(ranked intensity)): 2903(3), 1596(10), 1482(6), 1427(8), 1305(12), 1257(2), 1062(5), 936(14), 906(9), 785(13), 745(1), 729(7), 704(4), 632(11), 580(15);

HRMS (CI^+) for $C_{28}H_{28}BN$ [M^+], calcd 389.2314; found 389.2315;

UV-Vis (CH_2Cl_2) λ_{max} (331 nm): ε = 8,200 $Lmol^{-1}$ cm^{-1};

Fluorescence (CH_2Cl_2) λ_{em} 357 nm; Stokes shift (CH_2Cl_2) 26 nm (2,200 cm^{-1}).

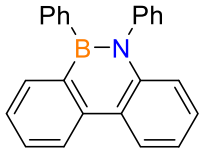

5.9

Synthesis of 5.9 (CCDC 1819492): To a solution of **5.5** (0.298 g, 1.03 mmol) in toluene (5 mL) was added a solution of phenyllithium in dibutyl ether (1.9 M, 0.59 mL, 1.13 mmol) at -78 ˚C. The reaction was stirred at this temperature for 1 h upon which the cold bath was removed and the solution warmed to 23 ˚C and stirred 3 h. The volatiles were removed *in vacuo* and the resultant orange residue was washed with hexanes (3 x 10 mL), filtered, and dried *in vacuo* to give **5.9** as a yellow powder. Single crystals for X-ray diffraction studies were grown from a dichloromethane solution of **5.9** by vapor diffusion into toluene. Yield: 0.248 g, 73%; m.p 176-178 ˚C;

^{1}H NMR (600 MHz, $CDCl_3$): δ 8.58-8.55 (m, 2H), 7.87 (d, J = 6.0 Hz, 1H), 7.78 (t, J = 6.0 Hz, 1H), 7.45 (t, J = 6.0 Hz, 1H), 7.33-7.30 (m, 4H), 7.25-7.24 (m, 3H), 7.18 (m, 3H), 7.13 (d, J = 6.0 Hz, 2H), 6.94-6.91 (m, 1H);

^{13}C{^{1}H} NMR (151 MHz, $CDCl_3$): δ 144.29, 142.00, 138.89, 137.64, 133.02, 131.42, 129.73, 129.23, 127.92, 126.96, 126.93, 126.43, 124.22, 124.09, 121.98, 121.94, 119.01;

^{11}B{^{1}H} NMR (193 MHz, $CDCl_3$): δ 39.3 (br)**;**

FT-IR (cm^{-1}(ranked intensity)): 1594(8), 1552(13), 1483(5), 1427(10), 1352(7),1323(9), 1298(3), 1023(14), 751(2), 742(15), 724(4), 697(1), 653(11), 619(6), 577(12);

HRMS (CI^+) for $C_{24}H_{18}BN$ [M^+], calcd 331.1532; found 331.1534;

UV-Vis (CH_2Cl_2) λ_{max} (331 nm): ε = 12,500 $Lmol^{-1}$ cm^{-1}, (319 nm): ε = 11,300 $Lmol^{-1}$ cm^{-1};

Fluorescence (CH_2Cl_2) λ_{em} 355 nm; Stokes shift (CH_2Cl_2) 24 nm (2,100 cm^{-1}).

CHAPTER SIX

Boraphosphaalkene Synthesis via Phosphaalkyne Insertion into 9-Borafluorene

This chapter published as: Yruegas, S.; Barnard, J. H.; Al-Furaiji, K.; Dutton, J. L; Wilson, D. J. D; Martin, C. D., *Organometallics*, **2018**, *37*, 1515-1518.

6.1 Introduction

Phosphorus is often labelled the "carbon copy" due to the similarities of its chemistry to carbon, particularly in unsaturated systems.[241-242] Cyclic species can act as ligands through conjugated π-systems akin to unsaturated cyclic hydrocarbons,[243-246] while the corresponding P≡C and P=C containing molecules (phosphaalkynes and phosphaalkenes, respectively) have reactivity reminiscent to their multiply bonded carbonaceous counterparts.[247-251] The chemistry of phosphaalkynes in many ways mimics that of alkynes, debatably more closely than that of their lighter congeners, nitriles. Nitriles coordinate Lewis acidic centers *via* the lone pair on nitrogen, whereas phosphaalkynes are inversely polarized and as a result are poor σ donors.[252-254] In addition, the diminished dipole moment of phosphaalkynes results in dienophile reactivity in pericyclic processes analogous to alkynes that is rarely observed for nitriles.[255-256]

In the few reported reactions of phosphaalkynes with boron species, the products are the result of addition reactions or Diels-Alder processes (Figure 6.1). The reaction of catecholborane (HBCat, Cat = catechol) and tert-butylphosphaalkyne results in a double hydroboration to produce primary phosphine **6.1** with the carbon quaternized by the introduction of the two BCat groups.[257] Stephan and coworkers reported that Piers' borane [$HB(C_6F_5)_2$] undergoes a single hydroboration with phosphaalkynes to

1,2-boraphosphaalkene dimer **6.2**, with the inverse selectivity forging P-B and C-H bonds.[258] This 1,2-boraphosphaalkene dimer dissociates upon the addition of Lewis bases (pyridine and isocyanide) to give the 1,2-boraphosphaalkene adducts. BBr_3 was claimed to react with tert-butylphosphaalkyne to generate 1,3-boraphosphaalkene **6.3** as a mixture of the E/Z isomers, but no characterization details supporting this complex were provided.[259]

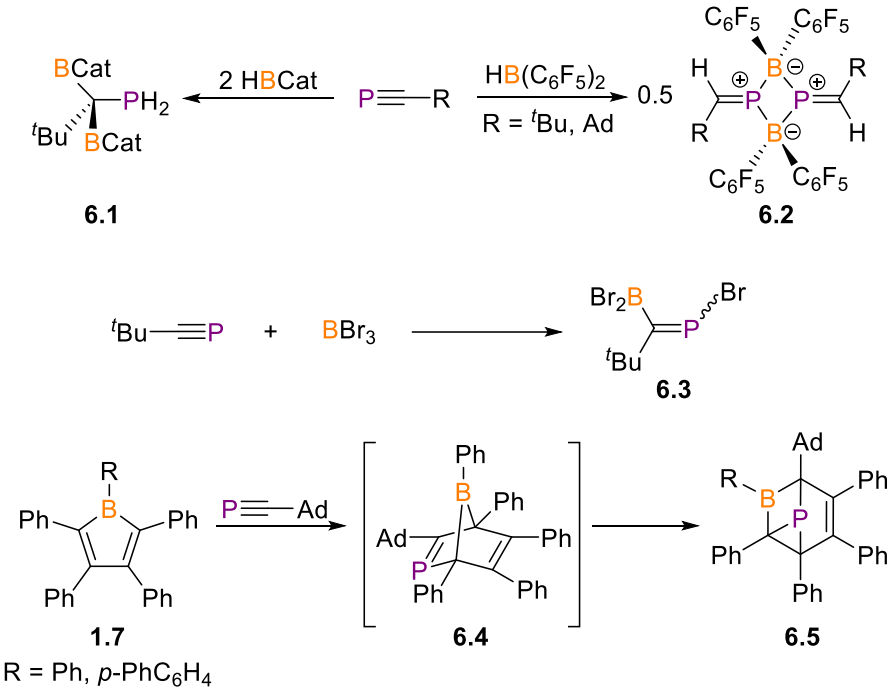

Figure 6.1. Reported reactions of boron species with phosphaalkynes (Cat = catechol, Ad = 1-adamantyl).

Our group reported the reactivity of antiaromatic boroles (**1.7**) with 1-adamantylphosphaalkyne to produce 1-phospha-6-boratricyclo-hept-3-enes (**6.5**),[59] which DFT calculations indicated proceeded via a [4 + 2] cycloaddition and subsequent rearrangement. In the borole reaction, while the initial step is similar to that of the cycloaddition observed with alkynes, the alkyne Diels-Alder adduct ultimately rearranged to a borepin.[39, 121, 150-151] Unsaturated 1,2-dipolar molecules with more pronounced dipole moments (nitrile, ketone, aldehyde, imines, isocyanates, isothiocyanates) coordinate to

boroles and subsequently insert to furnish seven-membered unsaturated boron heterocycles.[56-58]

9-Borafluorenes (**1.15**) are relatives of boroles with two aryl groups fused to the BC_4 core that decrease the degree of antiaromaticity and Lewis acidity[46, 67, 69, 228, 260] but readily form adducts with Lewis bases.[68, 73-74, 261] The biphenyl backbone should decrease the likelihood of a Diels-Alder pathway as diene reactivity would require disrupting the aromaticity of both arenes. 9-Borafluorenes have also been demonstrated to undergo insertions into the endocyclic B-C bonds (see Chapter 1 and Chapter 5 for examples). Herein, we examine the reactivity of 1-adamantylphosphaalkyne with 9-phenyl-9-borafluorene and probe the mechanism computationally.

6.2 Reaction of Phosphaalkyne with 9-Borafluorenes

The 1:1 stoichiometric reaction of **1.15-Ph** and 1-adamantyl phosphaalkyne in CH_2Cl_2 at room temperature was monitored by *in situ* $^{31}P\{^1H\}$ NMR spectroscopy indicating conversion of the phosphaalkyne signal (δ = -68) after 40 min to a major product at 199 ppm (Figure 6.2). This downfield spectroscopic signature lies in the region of known phosphaalkenes[262] and a single resonance was detected by $^{11}B\{^1H\}$ NMR spectroscopy at 69.4 ppm, representative of a three-coordinate boron environment, shifted slightly downfield from **1.15-Ph** (δ = 65).[69] After isolation, acquiring a ^1H NMR spectrum of the redissolved solids in $CDCl_3$ confirmed a 1:1 stoichiometric reaction based on the aromatic (7.71-7.15 ppm) and aliphatic (2.03-1.69 ppm) resonances integrating in a 13:15 ratio.

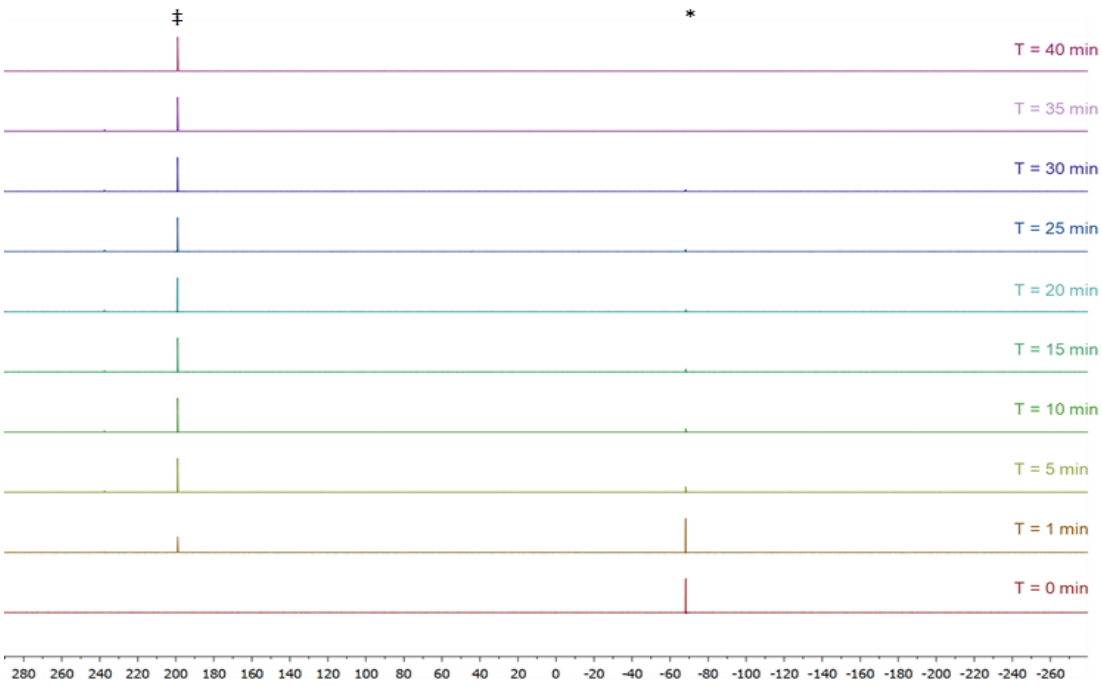

Figure 6.2. $^{31}P\{^{1}H\}$ NMR stacked plot of in situ reaction of **6.6** with 1-adamantylphoshaalkyne (‡ = **6.6**, * = 1-adamantylphosphaalkyne).

Single crystals for X-ray diffraction studies were grown by the vapor diffusion of a saturated *n*-pentane solution of the crude extract into hexanes and the structure was determined to be the 1,3-phosphaborepin product **6.6** (Scheme 6.1). The 1-adamantylphosphaalkyne underwent a formal 1,2-insertion into the endocyclic B-C bond of **1.15-Ph** to give **6.6** (Figure 6.3). The central BPC_5 ring of **6.6** adopts a boat-like conformation, with an interplanar angle for the biphenyl moiety of 44.95(5)˚. In regard to the boraphosphaalkene moiety, the P=C distance of 1.6847(12) Å and the C-P-C angle of 107.07(8)˚ are consistent with a P=C double bond[263-266] and matches the observed downfield $^{31}P\{^{1}H\}$ NMR shift of 199 ppm. The C=P-C angle of 107.06(6)˚ is more obtuse than the typical angle for phosphaalkenes (~100˚).[267] Both boron and the carbon of the phosphaalkene [C(1)] are trigonal planar [∑angles boron = 359.93(16)˚, carbon = 359.99(13)˚], but despite the planarity of the adjacent boron and carbon centers, the two

are not co-planar [interplanar angle = 75.95(4)˚]. Moreover, the B-C bond is a single bond [1.5536(17) Å][266] and the P=C bond is not elongated, indicating negligible π-interaction between boron and the phosphaalkene.

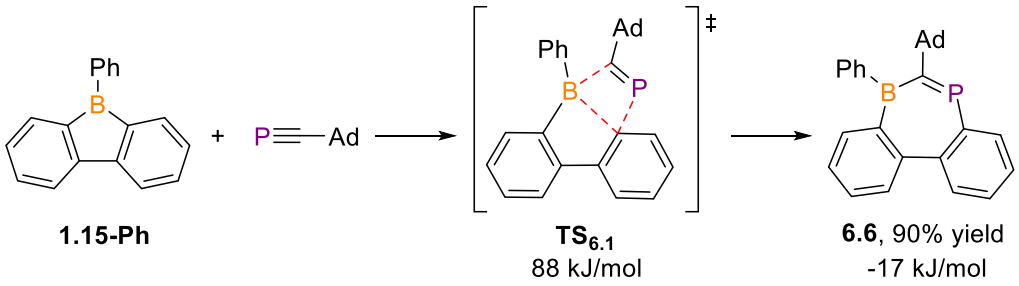

Scheme 6.1. Mechanism for the insertion reaction of 1-adamantylphosphaalkyne with **1.7-Ph**. M06-2X/def2-TZVP relative free energies are represented relative to the starting materials.

The reaction pathway was investigated using computational methods as insertion reactions of 9-borafluorenes are rare in the literature.[268] To enable a direct comparison, we employed the same methods as the previous investigation of the reactivity of pentaphenylborole **1.7-Ph**. The isolated product **6.6** is considerably different than that of the reaction of 1-adamantylphosphaalkyne with boroles (**1.7**) where the sole product is **6.5**, suggesting an alternative pathway. The insertion reaction between **1.15-Ph** and 1-adamantylphosphaalkyne to give **6.6** was found to be linked *via* a single transition state (**TS$_{6.1}$**, Scheme 6.1) involving cleavage of an endocyclic B-C bond by the P≡C unit of the phosphaalkyne and concomitant formation of B-C and P-C bonds. The calculated $\Delta G^{\ddagger}$ for the transition state (**TS$_{6.1}$**) is 88 kJ/mol, with $\Delta G°$ for the overall reaction being -17 kJ/mol, indicating a thermodynamically favored product (**6.6**). Despite significant effort, attempts to locate a transition state similar to **6.3** from **1.15-Ph** and 1-adamantylphosphaalkyne were unsuccessful. A Diels-Alder adduct akin to **6.3** could be found from the product **6.6** with a high corresponding $\Delta G^{\ddagger}$ for the transition state, 176 kJ/mol higher in energy than **6.6**. The

tripodal phosphine product (*c.f.* **6.4**) itself is thermodynamically unfavorable by 133 kJ/mol with respect to the reactants (150 kJ/mol higher than the observed product **6.6**, Appendix E: Scheme E-1).

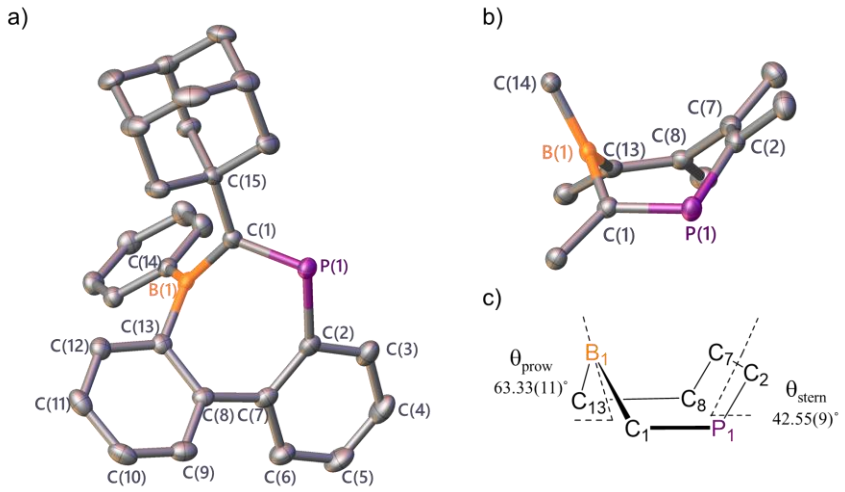

Figure 6.3. (a) Solid-state structure of **6.6**. Hydrogen atoms have been omitted for clarity, and ellipsoids are depicted at the 50% level. Selected bond lengths (Å) and angles (˚) for **6.6**: B(1)−C(1) 1.5536(17), C(1)−P(1) 1.6847(12), P(1)−C(2) 1.8385(13), C(2)−C(7) 1.4136(18), C(7)−C(8) 1.4869(17), C(8)−C(13) 1.4009(17), C(13)−B(1) 1.4013(17); C(13)−B(1)−C(1) 115.32(10), C(13)−B(1)−C(14) 120.71(10), C(14)−B(1)−C(1) 123.90(11), C(15)−C(1)−B(1) 124.10(10), C(15)−C(1)−P(1) 120.92(18), B(1)−C(1)−P(1) 144.97(8), C(1)−P(1)−C(2) 107.06(6). (b) The 1,3-BPC_5 core of **6.6**. (c) Diagram illustrating the dihedral planes defining the deviation of the ring from planarity into a boatlike conformation.

The calculations clearly rationalize the contrast in products generated between reaction of 1-adamantylphosphaalkyne with **1.7** and **1.15-Ph** due to alternative mechanisms. The rationale for preferential Diels-Alder reactivity for **1.7** is that a Diels-Alder process in **1.15-Ph** requires disruption of the aromaticity in both of the phenyl groups whereas this is not the case for **1.7** which has clear diene character in the organic backbone. This bond metathesis pathway differs from the modelled 1,2-insertion reactions with borole that form adduct intermediates en route to the seven membered ring products.[57]

In summary, 9-phenyl-9-borafluorene reacts with 1-adamantylphosphaalkyne under ambient conditions to give a ring expanded P,B-containing product that is the first

characterized 1,3-boraphosphaalkene. The reactivity is significantly different than the analogous reaction with pentaarylboroles which do not have fused aryl groups, rationalized by computational mechanistic studies that indicate the observed pathway is thermodynamically favored. The modelled bond metathesis ring expansion pathway is unique from the precedented Diels-Alder and coordination mechanisms in borole chemistry. The results demonstrate the potential of ring expansion reactions to insert unsaturated organic substrates into borafluorenes to prepare a wealth of seven membered rings with fused aryl groups.

6.3 Experimental Details

Adamantylphosphaalkyne was purchased from Santa Cruz Biotechnology and used as received.

Computational Methods. All theoretical calculations were performed within the Gaussian 09 and Gaussian 16 programs.[145, 269] Geometry optimizations without symmetry constraints were carried out with the M06-2X[146] density functional together with the 6-31+G(d) basis set[147] for both minima and transition state structures. All calculations employed an ultrafine integration grid. Harmonic vibrational frequencies were calculated analytically at the same level of theory in order to characterize stationary points as minima or transition states on the potential energy surface. The vibrational frequencies also enabled standard thermochemical properties under standard conditions (1 atm and 298 K) to be determined within the harmonic limit. The quadratic synchronous transit (QST) method[149] was also utilized to locate transition states. For all transition states, intrinsic reaction coordinate (IRC)[270] analysis was carried out to ensure connectivity between all minima and transition states along the reaction pathway. Single point energy calculations were performed at the

M06-2X/6-31+G(d) optimized geometries with M06-2X/def2-TZVPP[146, 271] calculations. Solvent effects were included with polarizable continuum model (PCM) self-consistent reaction field (SCRF) together with Truhlar's SMD solvation model,[272] with parameters for dichloromethane. All reported ΔG values are M06-2X/def2-TZVPP electronic energies (inclusive of solvent effects) with M06-2X/6-31+G(d) gas phase thermochemical corrections, defined as M06-2X/def2-TZVPP(CH_2Cl_2,SMD) //M06-2X/6-31+G(d). Molecular orbital (MO) and natural bonding orbital (NBO) evaluation were carried out at the B3LYP/def2-TZVP level of theory.[273]

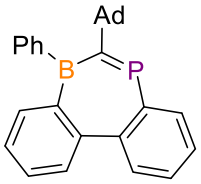

6.6

Synthesis of 6.6 (CCDC 1837570): 1-Adamantylphosphaalkyne (36.0 mg, 0.200 mmol) in CH_2Cl_2 (1 mL) was added to a solution of **1.15-Ph** (48.0 mg, 0.200 mmol) in CH_2Cl_2 (3 mL) at 23 ˚C. The mixture was stirred for 40 min giving a pale-yellow solution. The solvent was removed *in vacuo* and the solids washed with *n*-pentane (0.5 mL) to give an off-white powder. Yield: (75.0 mg, 90%) Single crystals for X-ray diffraction studies were grown from a *n*-pentane solution of **6.6** by vapor diffusion into hexanes. m.p 108 – 110 ˚C.

^{1}H NMR (600 MHz, $CDCl_3$) δ 7.70 (dd, J = 18.0, 6.0 Hz, 1H, *Ar*), 7.64 (d, J = 12.0 Hz, 1H, *Ar*), 7.62 (d, J = 6.0 Hz, 2H, *Ar*), 7.46 – 7.40 (m, 4H, *Ar*), 7.37 (t, J = 6.0 Hz, 1H, *Ar*), 7.24 (t, J = 6.0 Hz, 2H, *Ar*), 7.20 (t, J = 6.0 Hz, 1H, *Ar*), 7.16 (t, J = 12.0 Hz, 1H, *Ar*), 2.03 (s, 9H, *Ad*), 1.72 (dd, J = 12.0, 6.0 Hz, 6H, *Ad*) ppm;

$^{13}C\{^1H\}$ NMR (151 MHz, $CDCl_3$) δ 151.16 (br, *Ar*), 143.48 (d, *J* = 7.6 Hz, *Ar*), 139.17 (*Ar)*, 138.13 (*Ar)*, 137.77 (*Ar)*, 136.66 (*Ar)*, 136.41 (*Ar)*, 133.06 (*Ar)*, 130.60 (*Ar)*, 128.45 (*Ar)*, 128.36 (*Ar)*, 127.62 (*Ar)*, 126.95 (*Ar)*, 125.91 (*Ar)*, 125.72 (d, *J* = 12.0 Hz, *Ar*), 123.72 (*Ar*), 46.09 (d, *J* = 15.1 Hz, *Ad*), 45.87 (d, *J* = 15.1 Hz, *Ad*), 36.79 (*Ad*), 29.24 (*Ad*) ppm;

^{31}P NMR (243 MHz, $CDCl_3$) δ 199.0 ppm;

$^{31}P\{^1H\}$ NMR (243 MHz, $CDCl_3$) δ 199.0 ppm;

$^{11}B\{^1H\}$ NMR (192 MHz, $CDCl_3$) δ 69.4 ppm (br, s);

FT-IR (ranked intensity, cm^{-1}) 2898 (2), 2845 (15), 1591 (7), 1433 (4), 1241 (3), 883 (10), 744 (1), 695 (8), 650 (12), 617 (5), 596 (13), 556 (14), 500 (9), 471 (6), 416 (11);

HRMS (CI^+) for $C_{29}H_{28}BP$ (M^+), calcd: 418.2021; found: 418.2022;

Elemental Analysis: calculated for $C_{29}H_{28}BP$: C, 83.26; H, 6.75. Found: C, 82.00; H, 7.10*;

UV-Vis (CH_2Cl_2) λ_{max} (256 nm): ε = 16,000 $Lmol^{-1}cm^{-1}$, (340 nm): ε = 1,500 $Lmol^{-1}cm\text{-}^{1}$

Note: The elemental analysis values received were high, likely due to decomposition during shipment. The purity of compound **6.6 is established from the multinuclear NMR data.*

CHAPTER SEVEN

Generating Boracycles featuring Carborane Scaffolds

This chapter published as: Yruegas, S.; Axtell, J. C.; Kirlikovali, K. O.; Spokoyny, A. M.; Martin, C. D, *Chem. Commun.*, **2019**, *55*, 2892-2895.

7.1 Introduction

Polyhedral carborane clusters are viewed as three-dimensional aromatic analogues to the ubiquitous two-dimensional aromatic arenes (e.g. benzene).[274-276] These species share high delocalization within the cage and ring resulting in high kinetic stability.[277-281] The significant difference is that carboranes exhibit three-dimensional aromaticity while benzene is a classical π aromatic molecule. Due to their unique steric profile and electronic structure, *o*-carboranes have been explored as a substitute for phenyl groups in molecules. The lability of the C-H vertices (pKa = 22 *c.f.* benzene = 43) of *o*-carborane facilitates selective derivatization to incorporate carboranes into molecular architectures.[282-309] 1,1'-Bis(*o*-carborane, **7.2**) can be viewed as a three-dimensional analogue to a biphenyl unit, a common ligand scaffold in organometallic chemistry (**7.1**, Figure 7.1).[310-321] The facile manipulation and high stability has resulted in complexes featuring **7.2** being investigated in medicine and electronic materials.[277, 322-331]

9-Borafluorenes (**1.15**) contain a biphenyl backbone linked by a three-coordinate boron center and have been recognized as attractive targets for molecular sensors,[227-228, 332] reagents for the synthesis of polycyclic aromatic hydrocarbons[62, 70, 72, 78, 215, 333-335] as well as components in organic light emitting diodes (OLEDs)[4, 8, 336] and organic photovoltaics (OPVs).[337] The vacant p_z orbital on the boron center extends conjugation throughout the

three fused rings. We envisioned that 1,1'-bis(*o*-carborane) could replace the biphenyl framework in 9-borafluorenes to generate a species with a three-dimensional backbone.

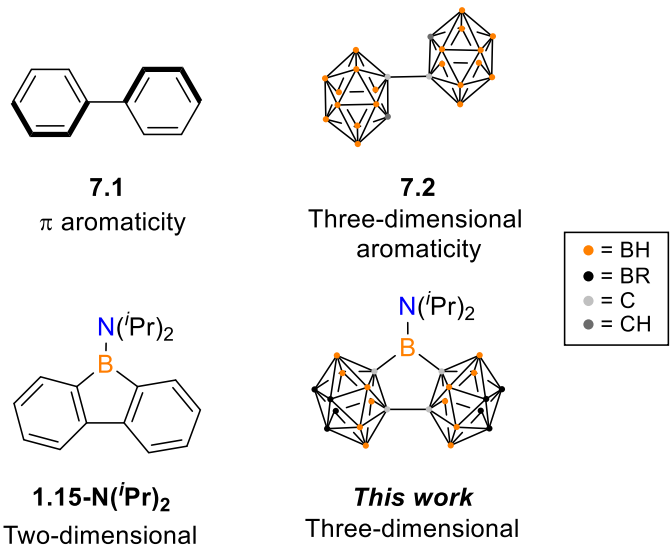

Figure 7.1. Relationship of biphenyl (**7.1**) to 1,1'-bis(*o*-carborane) (**7.2**) and the corresponding chelated boranes investigated in this work.

7.2 Approaches Towards a Three-Dimensional Analogue of 9-Borafluorene

The initial strategies to access the target [1,1'-bis(*o*-carboranyl)]boranes were inspired by effective methods for the synthesis of 9-borafluorenes, specifically transmetallation of a stannole or dilithiated species with RBX_2 (R = Ph, Mes).[67, 69, 338] The corresponding [1,1'-bis(*o*-carboranyl)]stannole[319] was recently reported and the [1,1'-bis(*o*-carboranyl)]dilithium species[339] has been generated and utilized *in situ*. Unfortunately, all attempts to access the [1,1'-bis(*o*-carboranyl)]borane *via* these reagents were unsuccessful (Appendix F: Tables F-1 and F-2). In addition, the transmetallation reaction with the [1,1'-bis(*o*-carboranyl)]magnesium species did not generate the desired boracycle (Table F-3). Potassium bis(trimethylsilyl)amide [K(HMDS)] is also an effective base for the deprotonation of the C-H vertices and the resultant salt, **K_2[7.2]**, is easier to

generate and offers enhanced solubility in comparison to the dilithiated reagent.[320, 340] After several attempts using a variety of conditions (Table F-4), the room temperature generation of **K_2[7.2]** in THF followed by addition of $(^i Pr)_2NBCl_2$ proved to be an effective method to furnish the desired [1,1'-bis(*o*-carboranyl)]borane **7.3**. Acquiring a $^{11}B\{^1H\}$ NMR spectrum of the crude reaction mixture showed a three-coordinate peak at 32.9 ppm, slightly shifted from $(^i Pr)_2NBCl_2$ (31.3 ppm), coupled with the disappearance of one of the diagnostic signals corresponding to **7.2** (-2.2 ppm) and emergence of a singlet at 1.7 ppm, suggesting restricted rotation about the C-C bond in **7.2**.[341] After isolation, the product was dissolved in $CDCl_3$ and the subsequent ^1H NMR spectrum contained no C-H carborane signal at 3.51 ppm, indicating successful deprotonation of the carboranyl moieties and the product was isolated in 89% yield (Scheme 7.1).

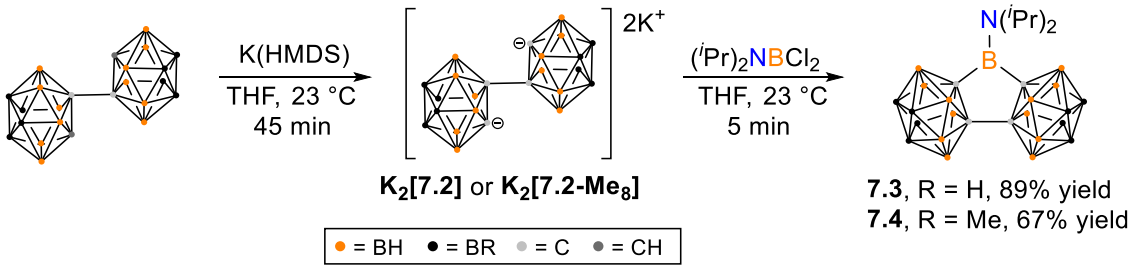

Scheme 7.1. Synthesis of **7.3** and **7.4**.

The identity of **7.3** was further confirmed based on single crystal X-ray diffraction studies (Figure 7.2). The synthetic route was compatible with the octa-methylated variant **7.4**[342] featuring a $^{11}B\{^1H\}$ NMR resonance at 33.7 ppm corresponding to the $(^i Pr)_2NB$-center, and a singlet at 6.0 ppm resulting from κ^2-C,C′-chelation of the bis(*o*-carborane). X-ray diffraction studies confirmed the structural identity of **7.4**, which was isolated in 67% yield (Figure 7.2).

7.3 Characterization of Three-Dimensional 9-Borafluorenes

A notable structural feature of **7.3** and **7.4** are highly planar central BC_4 rings (maximum deviation from planarity = 0.029 Å and 0.011 Å, respectively), which is comparable to their borafluorene counterpart **1.15-N(*i*Pr)$_2$** (0.020 Å). The boron atom of the central ring and adjacent nitrogen atom of **7.3** are trigonal planar [Σangles: B(1) = 360.0(18)˚ and N(1) = 360.0(17)˚, Table 7.1].

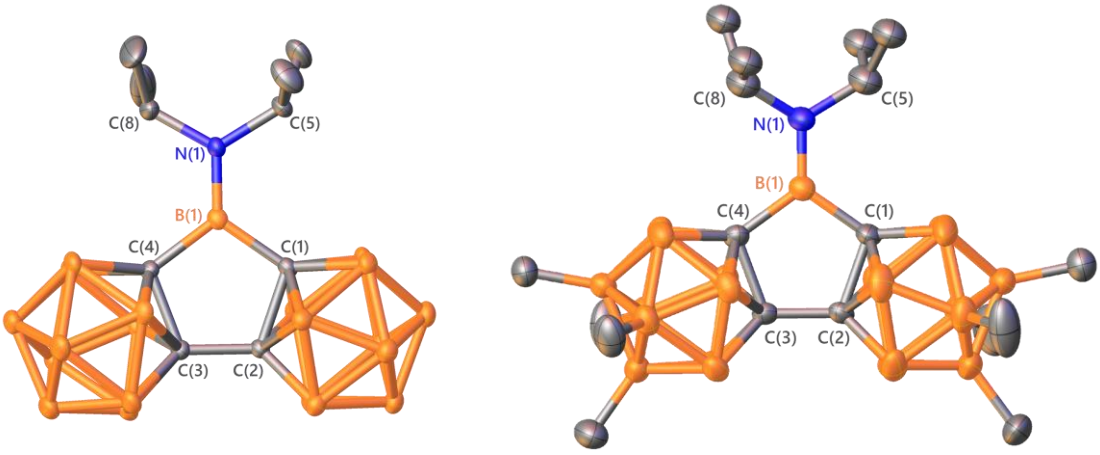

Figure 5.2. Solid-state structures of **7.3** and **7.4** (left to right). Thermal ellipsoids are depicted at 50% probability and hydrogen atoms are removed for clarity. The diisopropyl group in **7.4** is positionally disordered and only the major component is shown.

Positional disorder of the isopropyl groups on the nitrogen atom of **7.4** prevents an in-depth analysis of the metrical parameters of the substituents. The endocyclic carbon-carbon bonds of **7.3** and **7.4** are longer than **1.15-N(*i*Pr)$_2$**[67] [**7.3**: C(1)–C(2) 1.649(3) Å, C(2)–C(3) 1.528(3) Å, and C(3)–C(4) 1.649(3) Å, **7.4**: C(1)–C(2) 1.652(3) Å, C(2)–C(3) 1.524(3) Å, and C(3)–C(4) 1.646(3) Å, **1.15-N(*i*Pr)$_2$**: C(1)–C(2) 1.418(3) Å, C(2)–C(3) 1.474(3) Å, and C(3)–C(4) 1.413(3) Å] but contracted from the parent **7.2**[291] [C(1)–C(2) 1.630(3) Å, C(2)–C(3) 1.528(3) Å, and C(3)–C(4) 1.649(3) Å]. The B–N bond lengths of **7.3** and **7.4** are slightly shorter compared to previously reported B–N length of **1.15-**

N(*i*Pr)$_2$ [1.371(3) Å and 1.384(4) Å *c.f.* 1.396(3) Å][67, 343-344] indicating strong π-donation from the nitrogen lone pair to boron.[345]

Table 7.1. Salient Bond Lengths (Å) and Angles [°] in Compounds **7.3**, **7.4**, and **1.15-N(*i*Pr)$_2$**

Entry	**7.3**	**7.4**	**1.15-N(*i*Pr)$_2$**
B(1)-C(1)	1.631(3)	1.622(4)	1.593(3)
C(1)-C(2)	1.649(3)	1.652(3)	1.418(3)
C(2)-C(3)	1.528(3)	1.524(3)	1.474(3)
C(3)-C(4)	1.649(3)	1.646(3)	1.413(3)
C(4)-B(1)	1.630(3)	1.626(4)	1.601(3)
B(1)-N(1)	1.371(3)	1.384(4)	1.396(3)
N(1)-B(1)-C(4)	126.06(19)	125.50(2)	128.97(13)
C(1)-B(1)-N(1)	125.61(18)	125.40(2)	127.51(19)
C(1)-B(1)-C(4)	108.33(16)	109.00(2)	103.44(17)
B(1)-N(1)-C(5)	119.94(17)	*	120.90(2)
B(1)-N(1)-C(8)	120.09(18)	*	119.76(18)
C(5)-N(1)-C(8)	119.96(16)	*	119.35(19)

*The diisopropyl group in **7.4** is positionally disordered, barring discussion of these bond angles.

The UV-Vis spectra of **7.3** and **7.4** in CH_2Cl_2 (Figure 7.3) exhibit absorption maxima at 232 and 233 nm, respectively, blueshifted from **1.15-N(*i*Pr)$_2$** (248 nm).[67] Cyclic voltammetry (CV) measurements conducted on **7.3** show an irreversible one-electron reduction at -1.86 V versus the ferrocenium/ferrocene couple (Fc^+/Fc). In comparison, **7.4** exhibits an irreversible reduction at -2.09 V whereas **1.15-N(*i*Pr)$_2$** showed only a reversible reduction at -2.95 V, indicating that the bis(*o*-carboranyl) backbone imparts an electron-withdrawing effect facilitating reduction (Figure 7.4).[67]

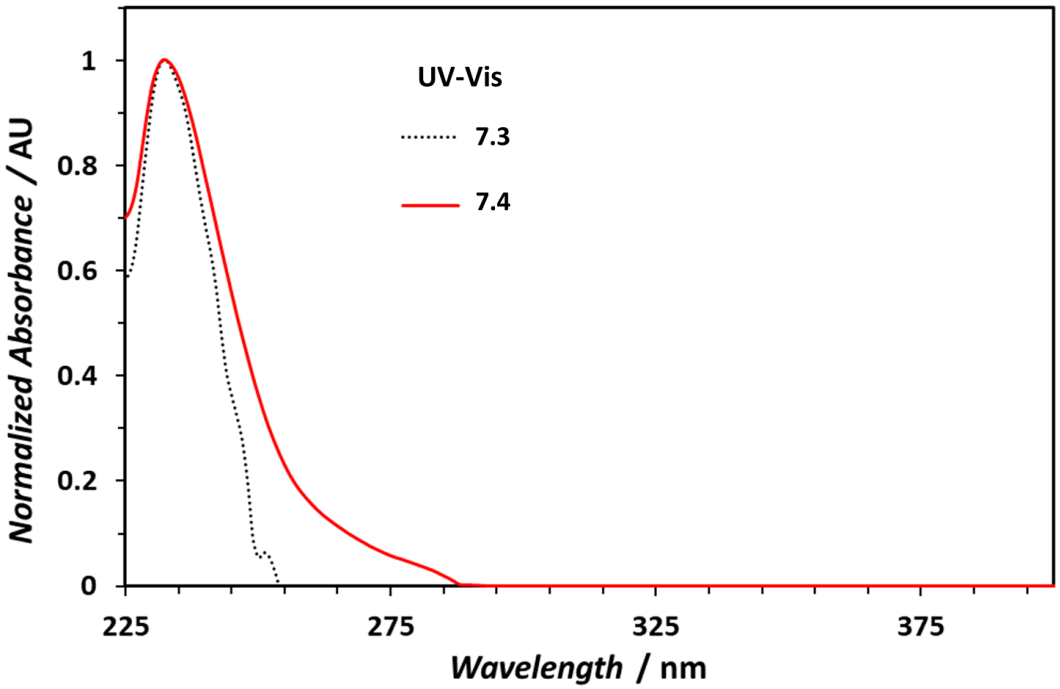

Figure 7.3. UV-Vis absorption emission spectra for **7.3** and **7.4** obtained from solutions of CH_2Cl_2 (λ_{max} = 232 and 233 nm respectively).

In order to understand the electronic effects of the bis(*o*-carboranyl) ligand scaffold, density functional theory (DFT) calculations were carried out. The geometries of **1.15-N(*i*Pr)$_2$**, **7.3**, and **7.4** were optimized based on the X-ray structure of **7.3** at the PBE-D3(BJ)/TZP level, and single-point calculations were carried out at the B3LYP-D3(BJ)/TZ2P level of theory (Appendix F: Figure F-18). The frontier orbital diagrams for **7.3** and **7.4** are similar, where the highest occupied molecular orbital (HOMO) is predominantly of π-character with respect to the B–N fragment, and the lowest occupied molecular orbital (LUMO) primarily resides on the bis(*o*-carboranyl) borane fragment. In contrast to the HOMO for **1.15-N(*i*Pr)$_2$** is entirely on the biphenyl fragment with no contribution from the amine, and the LUMO for **1.15-N(*i*Pr)$_2$** is localized on the biphenyl borane fragment. The HOMO-LUMO gaps for **7.3** and 7.**4** are comparable (5.99 eV and 6.03 eV, respectively), and significantly larger than **1.15-N(*i*Pr)$_2$** (4.17 eV). These data

corroborate similar absorption maxima for **7.3** and **7.4** as well as a bathochromic shift relative to the absorption maximum of **1.15-N(^{i}Pr)$_2$** (Figure 7.3). The calculated higher-lying LUMO for **7.4** (-1.74 eV) relative to that of 7**.3** (-2.05 eV) is consistent with the observed more negative reduction potential for **7.4** (-2.09 V and -1.86 V, respectively; Figure 7.4).

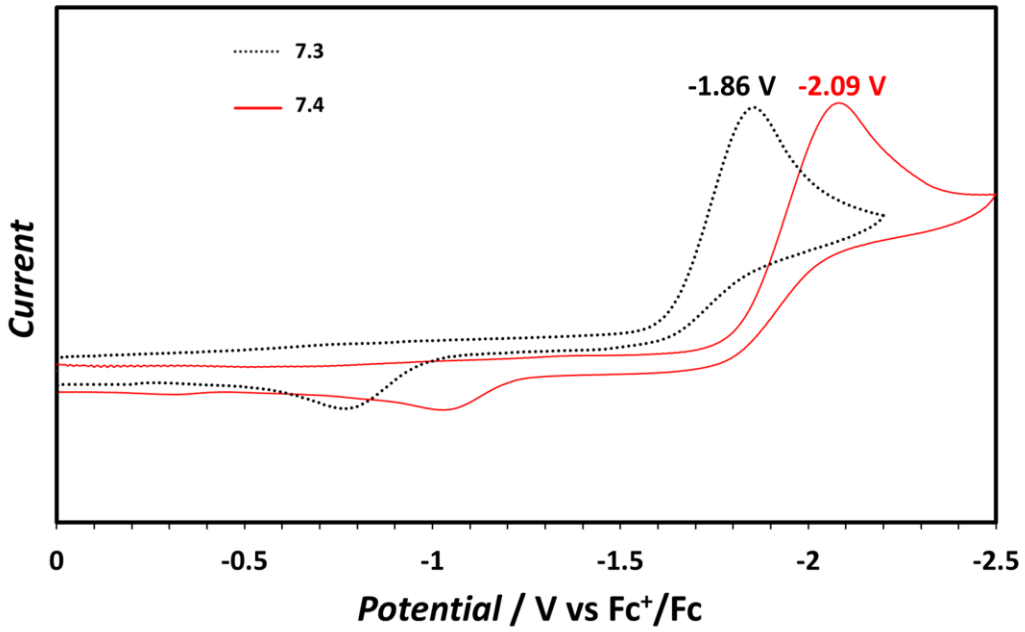

Figure 7.4. Cyclic voltammograms of **7.3** and **7.4** recorded in anhydrous tetrahydrofuran with 0.1 M [N^{n}Bu4][PF$_6$] and referenced to the ferrocenium/ferrocene redox couple (Fc^+/Fc; scan rate = 0.1 V s^{-1}).

To experimentally gauge Lewis acidity, the Gutmann-Beckett method was utilized.[81, 83] This method involves the addition of an excess of Et_3PO to a solution of the borane and monitoring the change in chemical shift of the $^{31}P\{^1H\}$ NMR signal (δ^{31P}_{sample} − 41.0). Multiplying this value by 2.21 gives the acceptor number (AN), where a greater AN signifies stronger Lewis acidity. The AN of **1.15-N(^{i}Pr)$_2$** is 13.5 in C_6D_6[67] and performing the analogous study with 7**.3** gave an AN value of 15.3. Methyl substitution at the peripheral boron vertices have an inductive effect, in this case acting as

electron-withdrawing groups.[292, 346-348] Subsequent Gutmann-Beckett studies of **7.4** corroborated this hypothesis with an AN of 20.3, aligning with an increase of Lewis acidity at the boron center.

In summary, we have taken advantage of the lability of the C-H bonds of 1,1'-bis(*o*-carborane) to access 9-borafluorene analogues with a three-dimensional backbone. These species represent the first examples of 1,1'-bis(carboranyl)boranes and feature a highly planar central ring with enhanced Lewis acidity in comparison to 9-borafluorenes. Methyl substitution at the 8,9,10,12-B-vertices results in an increase of the overall Lewis acidity of the molecule. The results demonstrate the potential of utilizing bis(*o*-carboranes) as biphenyl analogues to create unique boracyclic architectures.

7.4 Experimental Details

O-carborane and triethylphosphine oxide were purchased from Health Consumer Research and Alfa Aesar and used as received. Dichloro(diisopropylamino)borane and potassium bis(trimethylsilyl)amide [(K(HMDS)] were purchased from Sigma-Aldrich Chemicals and used as received. 1,1′-bis(*o*-carborane, **7.2**) and 9,9′,10,10′,11,11′,12,12′-octamethyl-bis(*o*-carborane, **7.2-BMe$_8$**) were synthesized according to published procedures.[315, 342]

Computational Methods. Density functional theory calculations were performed with ADF 2014 Suite version 2014.04[349-351] using Slater-type orbitals. Geometry optimizations were performed using PBE-D3(BJ)[352-353] with TZP (double-ζ core, triple-ζ valence + 1 polarization function) basis sets and single point calculations were performed using B3LYP-D3(BJ)[352, 354-356] with TZ2P (double-ζ core, triple-ζ valence + 2 polarization functions) basis sets.

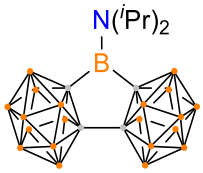

7.3

Synthesis of 7.3 (CCDC 1884761): To a solution of K(HMDS) (345.0 mg, 1.730 mmol) in tetrahydrofuran (2 mL) was added a solution of 7**.2** (248.0 mg, 0.860 mmol) in tetrahydrofuran (2 mL) at 23 ˚C. Upon completion of the addition, the clear solution became orange and the mixture was stirred for an additional 45 min. Dichloro(diisopropylamino)borane (166.0 µL, 0.946 mmol) was added dropwise and stirred for 5 min before removing the solvent *in vacuo*. The residue was extracted with CH_2Cl_2 (2 mL), filtered, and the solvent removed *in vacuo* resulting in a tan residue. The product was purified *via* recrystallization by dissolving the residue in a minimal amount of Et_2O (~2 mL) and storing at -35 ˚C overnight. The supernatant was decanted to produce white crystals. Yield: (304.0 mg, 89%); Crystals of **7.3** for X-ray diffraction studies were grown by the slow evaporation of a concentrated CH_2Cl_2 solution into hexanes at ambient temperature. m.p (231 – 232 ˚C);

^{1}H NMR (600 MHz, $CDCl_3$) δ 4.44 (quint, J = 6.0 Hz, 2H), 2.92 – 1.74 (m, 20H), 1.38 (d, J = 6.0 Hz, 12H) ppm;

^{1}H{^{11}B} NMR (600 MHz, $CDCl_3$) δ 4.44 (quint, J = 6.0 Hz, 2H), 3.21 (s, 3H), 2.59-2.02 (m, 17H), 1.38 (d, J = 6.0 Hz, 12H) ppm;

^{13}C{^{1}H} NMR (101 MHz, $CDCl_3$) δ 75.34, 52.01, 24.78 ppm;

^{11}B NMR (128 MHz, $CDCl_3$) δ 32.9 (s, 1B), 2.78 (d, 2B), -1.8 to -12.0 (m, 18B) ppm;

^{11}B{^{1}H} NMR (128 MHz, $CDCl_3$) δ 32.9 (s, 1B), 1.7 (s, 2B), -3.1 to -11.2 (m, 18B) ppm;

FT-IR (ranked intensity, cm^{-1}) 2972 (12), 2577 (1), 1519 (13), 1491 (4), 1463 (10), 1370 (6), 1177 (3), 1112 (5), 1065 (8), 981 (15), 912 (14), 813 (7), 732 (2), 714 (11), 647 (9);

HRMS (CI) for $C_{10}H_{33}B_{21}N$ $(M\text{-}H)^+$, calcd: 394.4712; found: 394.4709;

UV-Vis (CH_2Cl_2) λ_{max} (233 nm): ε = 12,600 $Lmol^{-1}cm^{-1}$

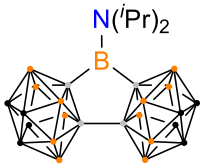

7.4

Synthesis of 7.4 (CCDC 1884762): To a solution of K(HMDS) (351.0 mg, 1.760 mmol) in tetrahydrofuran (2 mL) was added a solution of 7**.2-BMe8** (351.0 mg, 0.880 mmol) in tetrahydrofuran (2 mL) at 23 ˚C. Upon completion of the addition, the clear solution became orange and the mixture was stirred for an additional 45 min. Dichloro(diisopropylamino)borane (155.0 µL, 0.882 mmol) was added dropwise and stirred for 5 min before removing the solvent *in vacuo*. The residue was extracted with CH_2Cl_2 (2 mL), filtered, and the solvent removed *in vacuo* resulting in a tan powder. The product was purified *via* recrystallization by dissolving the tan residue in a minimal amount of *n*-pentane (~1 mL) and storing at -35 ˚C overnight. The supernatant was decanted to produce white crystals. Yield: (300.0 mg, 67%); Crystals of 7**.4** for X-ray diffraction studies were grown by the slow evaporation of a concentrated diethyl ether solution into hexanes at -35 ˚C. m.p (189 – 192 ˚C);

^{1}H NMR (400 MHz, $CDCl_3$) δ 4.44 (quint, J = 4.0 Hz, 2H), 3.48 – 1.54 (m, 12H), 1.36 (d, J = 4.0 Hz, 12H), 0.20 – 0.17 (m, 11H), 0.10 – 0.05 (m, 3H), 0.00 – -0.05 (m, 10H) ppm; $^1H\{^{11}B\}$ NMR (600 MHz, $CDCl_3$) δ 4.44 (quint, J = 6.0 Hz, 2H), 3.03 (s, 3H), 2.37 – 1.88

(m, 9H), 1.36 (d, J = 6.0 Hz, 12H) 0.19 – 0.17 (m, 11H), 0.10 – 0.05 (m, 3H), 0.00 – -0.05 (m, 10H) ppm;

$^{13}C\{^{1}H\}$ NMR (101 MHz, $CDCl_3$) δ 77.36, 67.50, 51.66, 24.88, -2.66 ppm;

^{11}B NMR (128 MHz, $CDCl_3$) δ 33.7 (s, 1B), 11.3 (s, 2B), 5.9 (s, 2B), 1.4 (s, 4B), -5.2 to -13.1 (m, 12B) ppm;

$^{11}B\{^{1}H\}$ NMR (128 MHz, $CDCl_3$) δ 33.7 (s, 1B), 11.3 (s, 2B), 6.0 (s, 2B), 1.1 (s, 4B), -6.8 to -13.7 (m, 12B) ppm;

FT-IR (ranked intensity, cm^{-1}) 2905 (9), 2700 (15), 2584 (4), 1516 (11), 1489 (2), 1465 (12), 1386 (14), 1369 (7), 1309 (3), 1182 (5), 1114 (1), 1025 (6), 958 (10), 783 (13), 750 (8);

HRMS (CI) for $C_{18}H_{50}B_{21}N$ (M^+), calcd: 509.5970; found: 509.5973;

UV-Vis (CH_2Cl_2) λ_{max} (233 nm): ε = 13,300 $Lmol^{-1}cm^{-1}$

CHAPTER EIGHT

Synopsis and Future Directions

8.1 General Synopsis

This dissertation has described the reactivity of pentaarylboroles and 9-borafluorenes, demonstrating their ability to act as reagents for generating new boron-containing compounds. Chapter Two disclosed experimental and computational studies on the relative lability of the endocyclic B-C bond of pentaphenylborole (**1.7-Ph**) when reacted with different E-H-containing partners.[160] Substrates containing O-H and N-H bonds underwent protodeborylation to give ring opened products **2.12** and **2.15** with a second protodeborylation occurring with H_2O (**2.13**, Scheme 8.1).

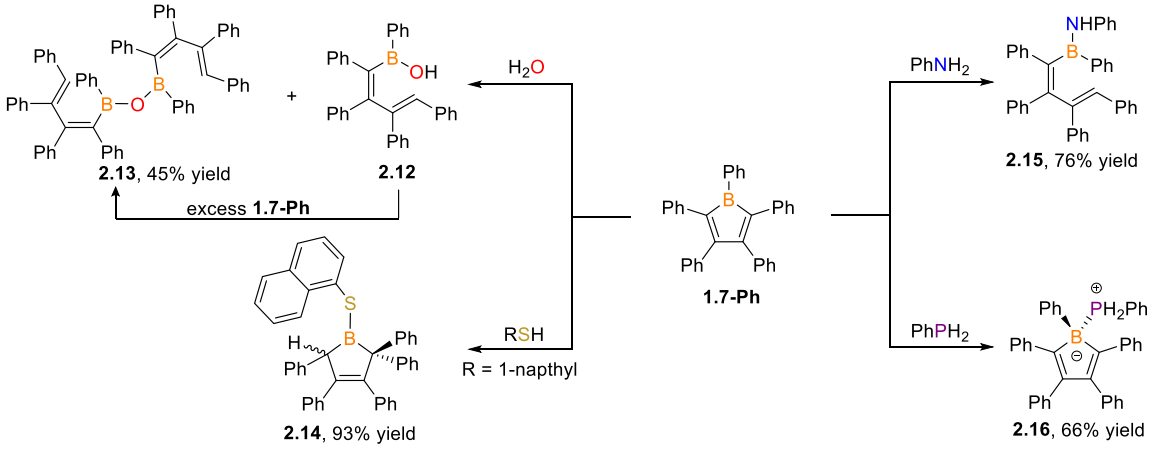

Scheme 8.1. Different modes of E-H activation.

Descending the row, S-H containing substrates resulted in a boracyclopent-3-ene framework (**2.14**), where the phenyl group on boron migrated to the adjacent carbon. The reaction of **1.7-Ph** with phenylphosphine produced adduct **2.16** with no evidence of proton

migration or ring opening, even at elevated temperatures. These investigations identify the adduct as a key intermediate in accessing the products alongside the lability of the B-C bond.

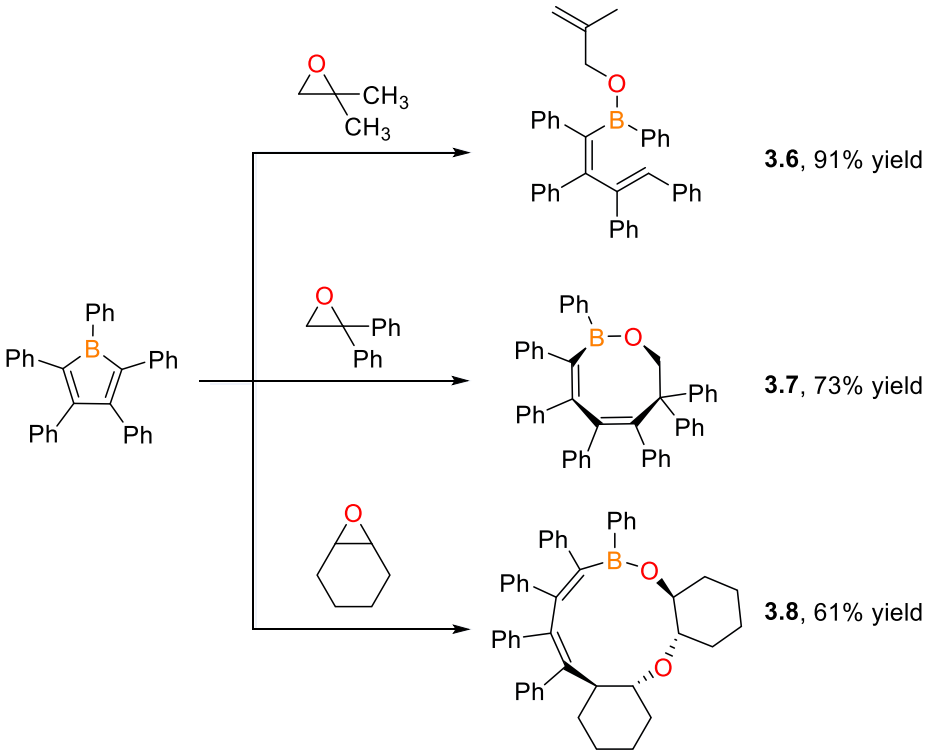

Scheme 8.2. Ring opening of epoxides.

Chapter Three extended this work further by describing the ring opening of epoxides by pentaphenylborole.[222] Interestingly, different products were formed based on the substitution of the epoxide. The availability of β-hydrogens at the epoxide resulted in protodeborylation of the methyl group to generate the ring opened product **3.6** (Scheme 8.2). Utilizing an epoxide without β-hydrogens gave the eight-membered ring **3.7** instead. Unexpectedly, the reaction of cyclohexene oxide with **1.7-Ph** furnished a rare 11-membered boracycle **3.8** from the insertion of two C_2O units into the BC_4 ring. The vastly

different products demonstrate the potential of boroles to be effective reagents for the construction of large boron-containing ring systems.

Chapter Four identifies pentaarylboroles as potential precursors for the synthesis of hybrid inorganic/organic boron-containing benzene analogues that feature oxygen or sulfur as a two π-electron contributor to the aromatic 6π electron ring.[152, 154] The results presented build upon the rich chemistry of boroles, taking advantage of the high reactivity of these species to prepare 1,2-oxaborines and 1,2-thiaborines (Scheme 8.3). The chemistry of these heterocycles has an exciting future given the diverse applications of their ubiquitous all carbon relative, benzene.

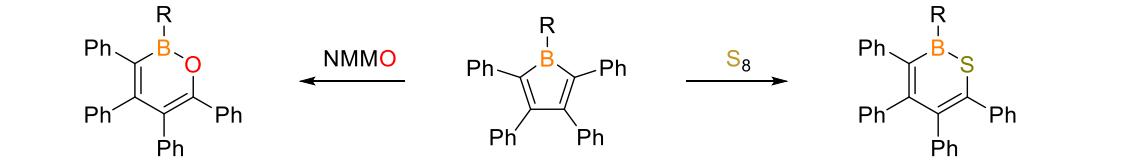

4.12, R = Ph, 66% yield
4.13, R = p-PhC_6H_4, 56% yield

1.7-Ph
1.7-PhC_6H_4

4.14, R = Ph, 44% yield
4.15, R = *p*-PhC_6H_4, 42% yield

Scheme 8.3. Generation of 1,2-oxaborines and 1,2-thiaborines from insertion reactions with pentaphenylborole.

Chapters Five and Six expand the scope of ring expansion methodology established from Chapters Two, Three, and Four for pentaarylboroles to a benzofused borole, specifically 9-borafluorene, to generate 6- and 7-membered BN- and BC=P-containing heterocycles (Scheme 8.4).[72, 333] The outcomes from these studies demonstrate that the unsaturated BC_4 rings with extended conjugation can also act as reagents for the synthesis of polycyclic aromatic hydrocarbons.

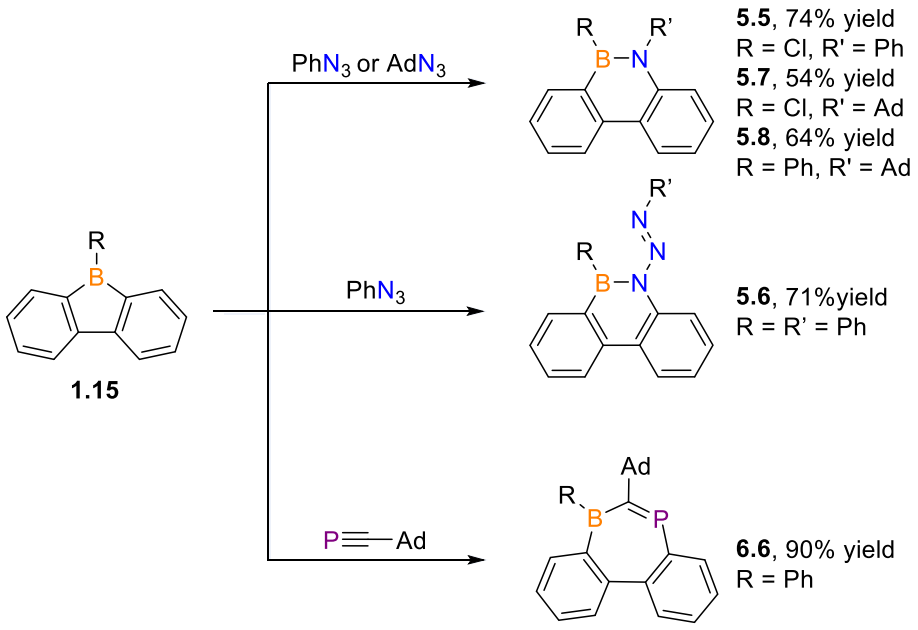

Scheme 8.4. Ring expansion reactions of 9-borafluorenes with azides and phosphaalkyne.

Chapter Seven described a new synthetic avenue in accessing 9-borafluorene analogues with a three-dimensional backbone.[357] The resulting species represent the first examples of 1,1'-bis(carboranyl)boranes and the beginning of an investigation of new unique boracyclic architectures utilizing carborane scaffolds (Figure 8.1).

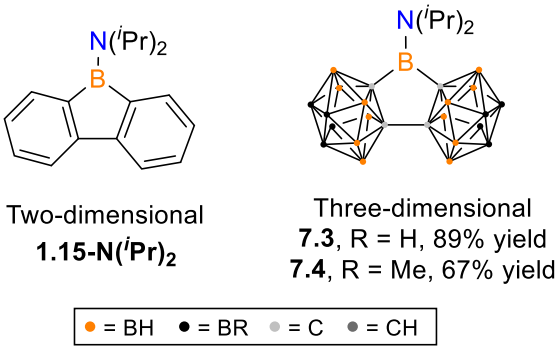

Figure 8.1. Synthesis of new 1,1'-bis(carboranyl)boranes.

8.2 Final Remarks

In summary, the chemistry disclosed in this dissertation elucidates the reactivity of pentaarylboroles and 9-borafluorenes, experimentally and computationally. The results reveal mechanistic insight enabling others to further pursue this vein of main group chemistry. Although several substrates are examined in this body of work, there remains other borole relatives and a vast library of small molecules that will rely on this foundation as the chemistry is pursued further.

APPENDICES

APPENDIX A

General Experimental Details and Supplementary Information for Chapter Two

General Experimental Details

All manipulations were performed under an inert atmosphere in a nitrogen-filled MBraun Unilab glovebox. Solvents were purchased from commercial sources as anhydrous grade, dried further using a JC Meyer Solvent System with dual columns packed with solvent-appropriate drying agents and stored over molecular sieves. $CDCl_3$ and C_6D_6 for NMR spectroscopy were purchased from Cambridge Isotope Laboratories and dried by stirring for 3 days over CaH_2, distilled, and stored over 4 Å molecular sieves. Compounds **1.7-Ph**, **1.7-PhC$_6$H$_4$**, 9,9-dimethyl-9-stannafluorene, and **1.15-Ph** were prepared *via* the literature procedures.[27, 59, 69]

Multinuclear NMR spectra were recorded on Bruker 400 or 600 MHz spectrometers. FT-IR spectra were recorded on a Bruker Alpha ATR FT-IR spectrometer on solid samples. High resolution mass spectra (HRMS) were obtained at the University of Texas at Austin Mass Spectrometry Center on a Micromass Autospec Ultima spectrometer using CI or at the Baylor University Mass Spectrometry Center on a Thermo Scientific LTQ Orbitrap Discovery spectrometer using +ESI. Melting points were measured with a Thomas Hoover Uni-melt capilliary melting point apparatus and are uncorrected. Elemental analyses (C and H) were performed by Atlantic Microlab, Inc. (Norcross, GA). UV-Vis spectra were recorded using an Agilent 8453 UV-Vis spectrophotometer. Solutions were prepared in a nitrogen filled glovebox and measured in screw capped quartz cuvettes for UV-Vis spectroscopy.

For the Gutmann−Beckett studies, samples were prepared in a 1:2 stoichiometric ratio of Lewis acid:Et_3PO. Subsequent ^{31}P NMR spectroscopy was done in C_6D_6. Samples were prepared in a glovebox under a N_2 atmosphere.

Cyclic voltammetry experiments were performed in an argon filled glovebox using a CH Instruments Model 1140 electrochemical analyzer with a platinum working electrode and a platinum wire auxiliary electrode. The reference electrode was AgCl coated silver wire and was referenced by the standard ferrocene/ferrocinium redox couple (0.56 V in THF) as an internal standard.

Single crystal X-ray diffraction data were collected on a Bruker D8 quest using Mo-K_α radiation (λ = 0.71073 Å). Crystals were selected under paratone oil, mounted on MiTeGen micromounts, and immediately placed in a cold stream of N_2. Structures were solved and refined using SHELXTL[358] and figures were produced using OLEX2.[359]

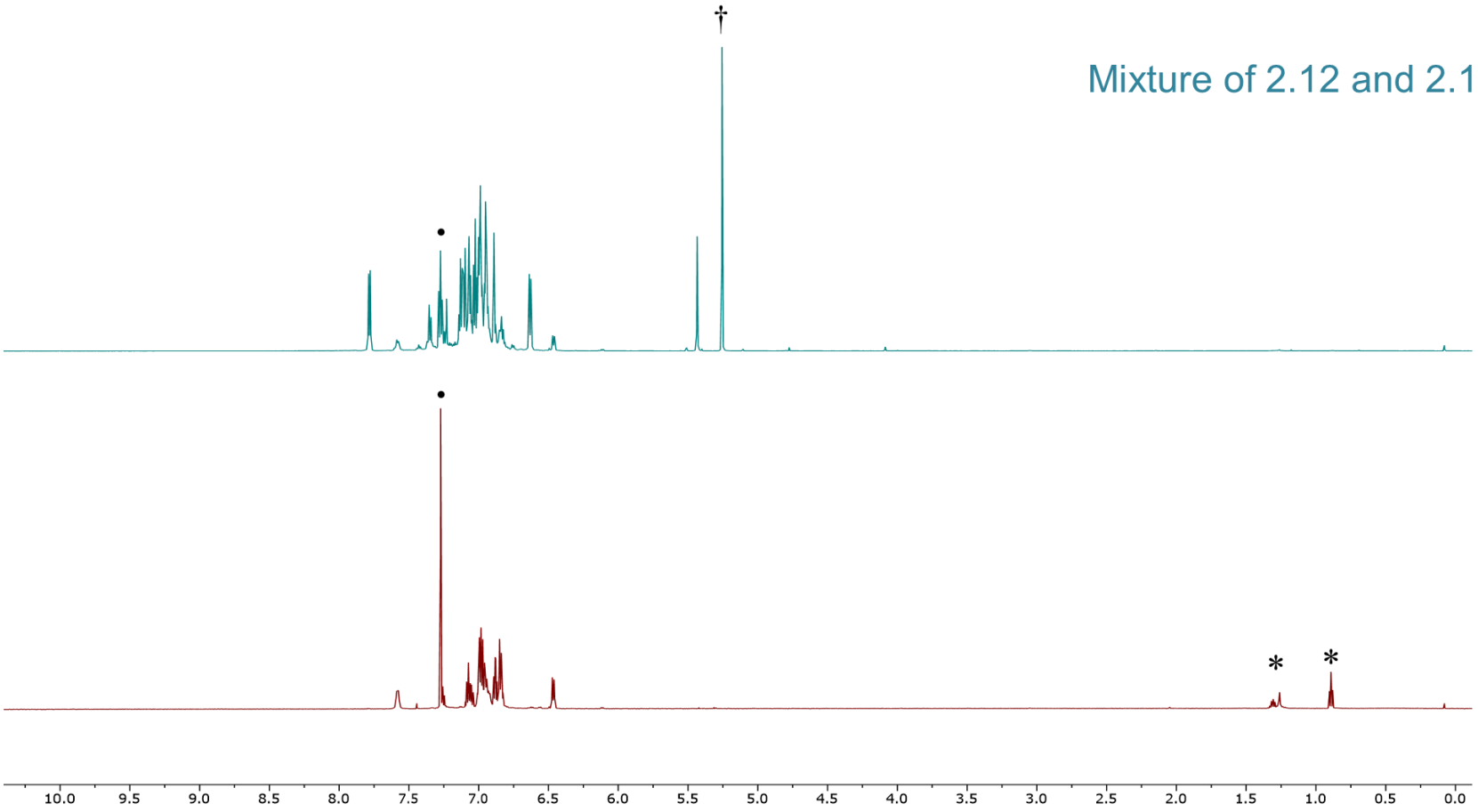

Figure A-1: Stacked plot of crude ^{1}H NMR spectra of the reaction of **1.17-Ph** with H_2O (top) and isolated **2.13** (bottom) in $CDCl_3$ († CH_2Cl_2, * hexanes, • $CDCl_3$).

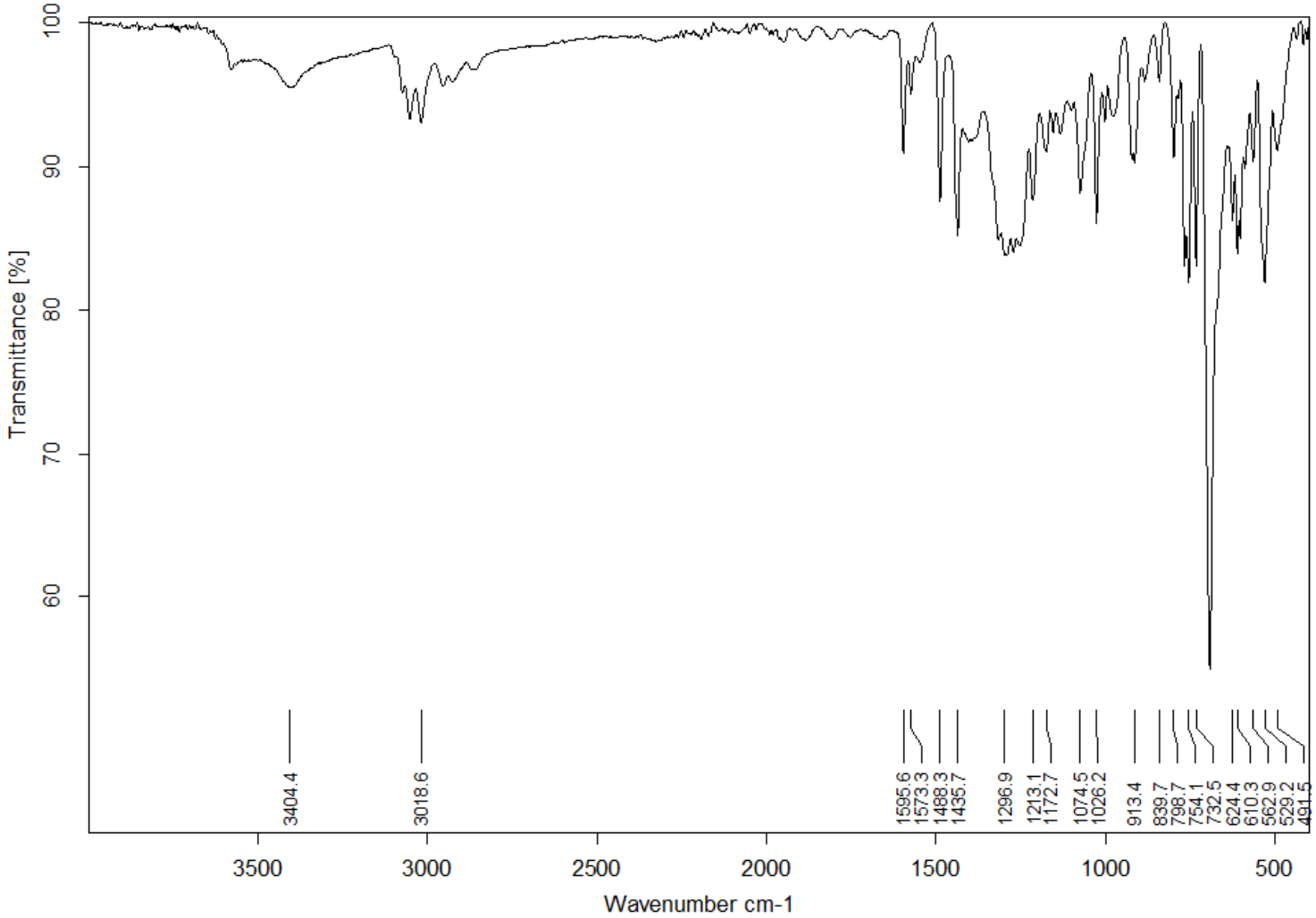

Figure A-2: FT-IR spectrum of crude reaction of **1.7-Ph** with H_2O.

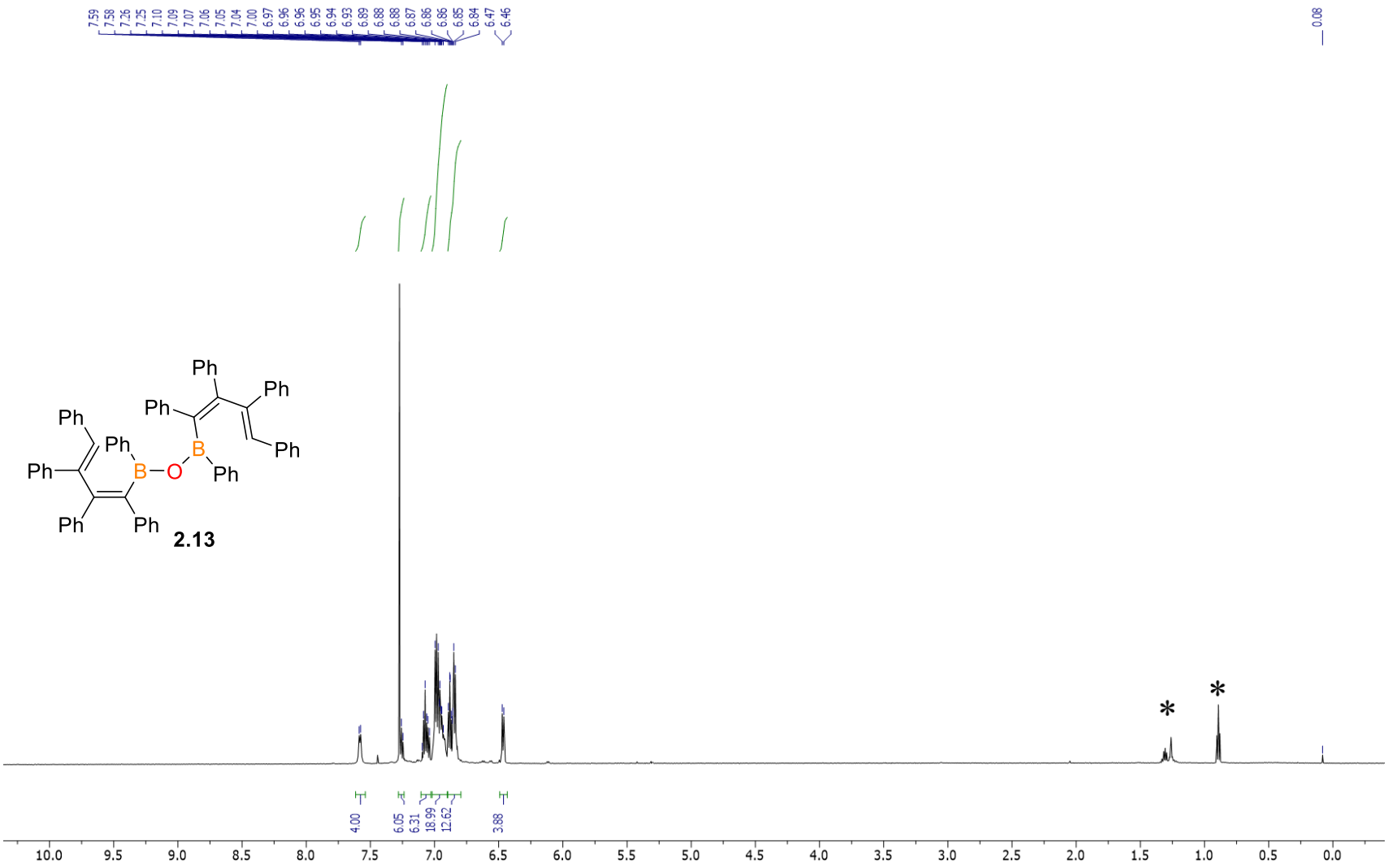

Figure A-3: ^{1}H NMR spectrum of **2.13** in $CDCl_3$ (*hexanes).

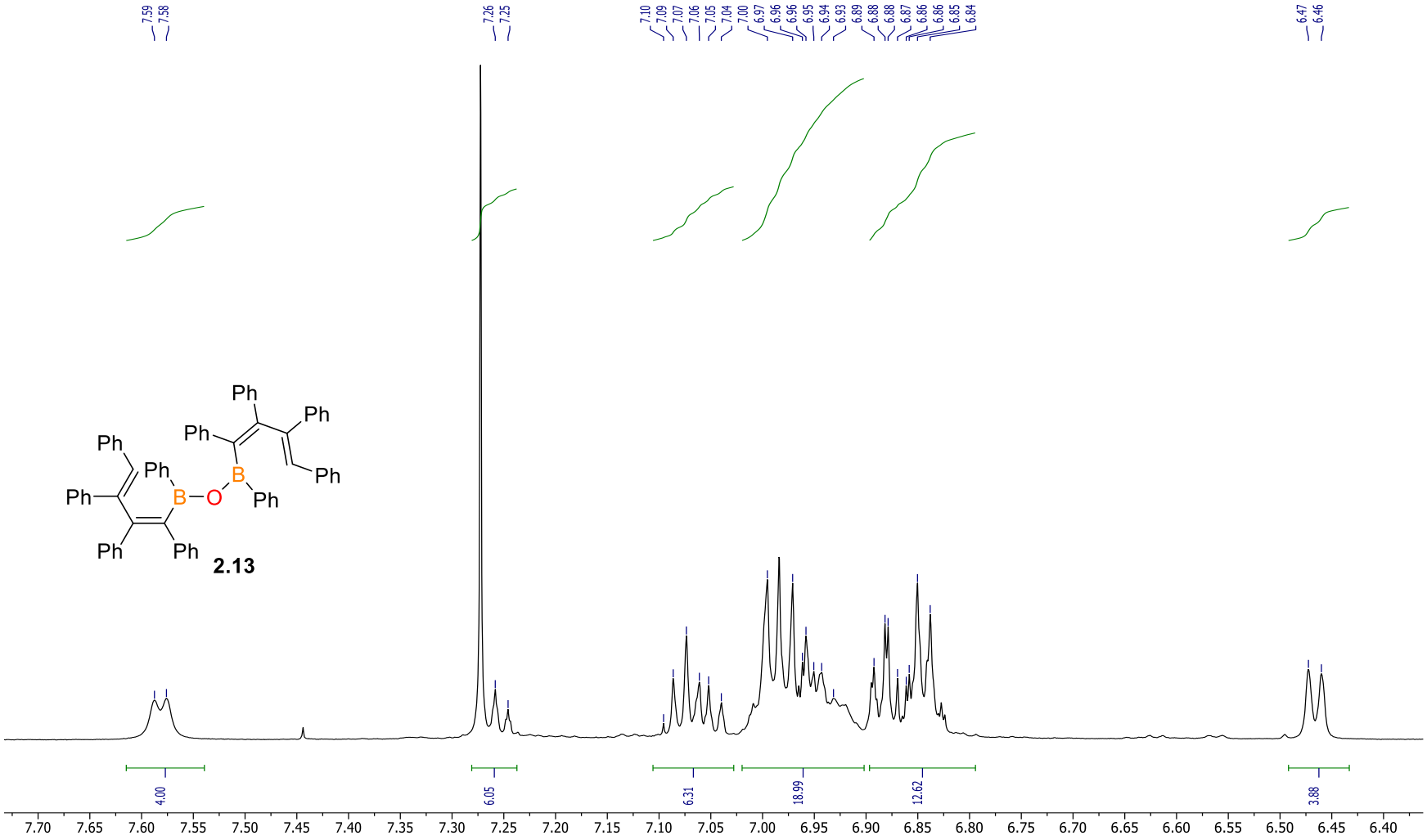

Figure A-4: Expansion of aromatic region of ^{1}H NMR spectrum of **2.13** in $CDCl_3$.

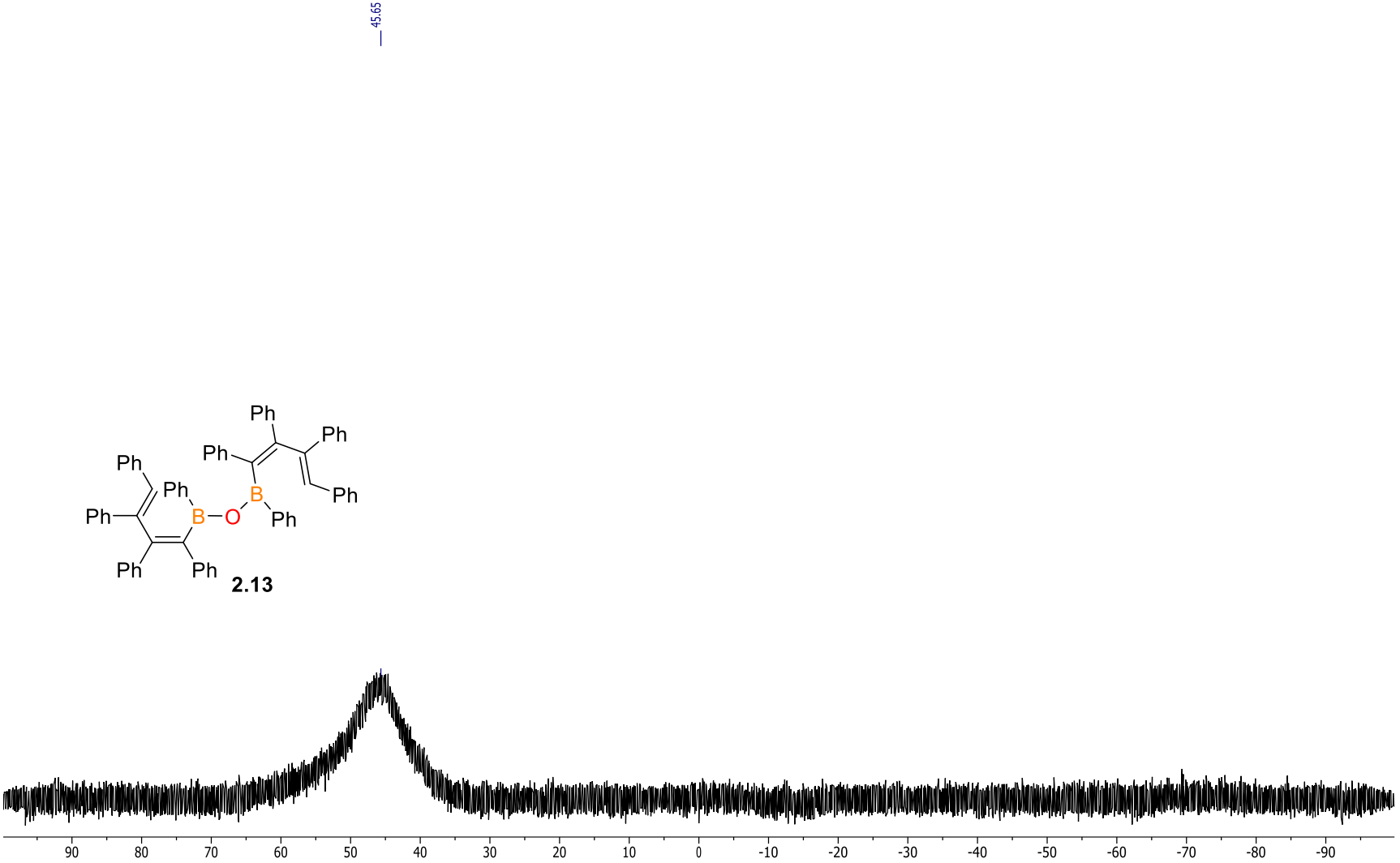

Figure A-5: $^{11}B\{^{1}H\}$ NMR spectrum of **2.13** in $CDCl_3$.

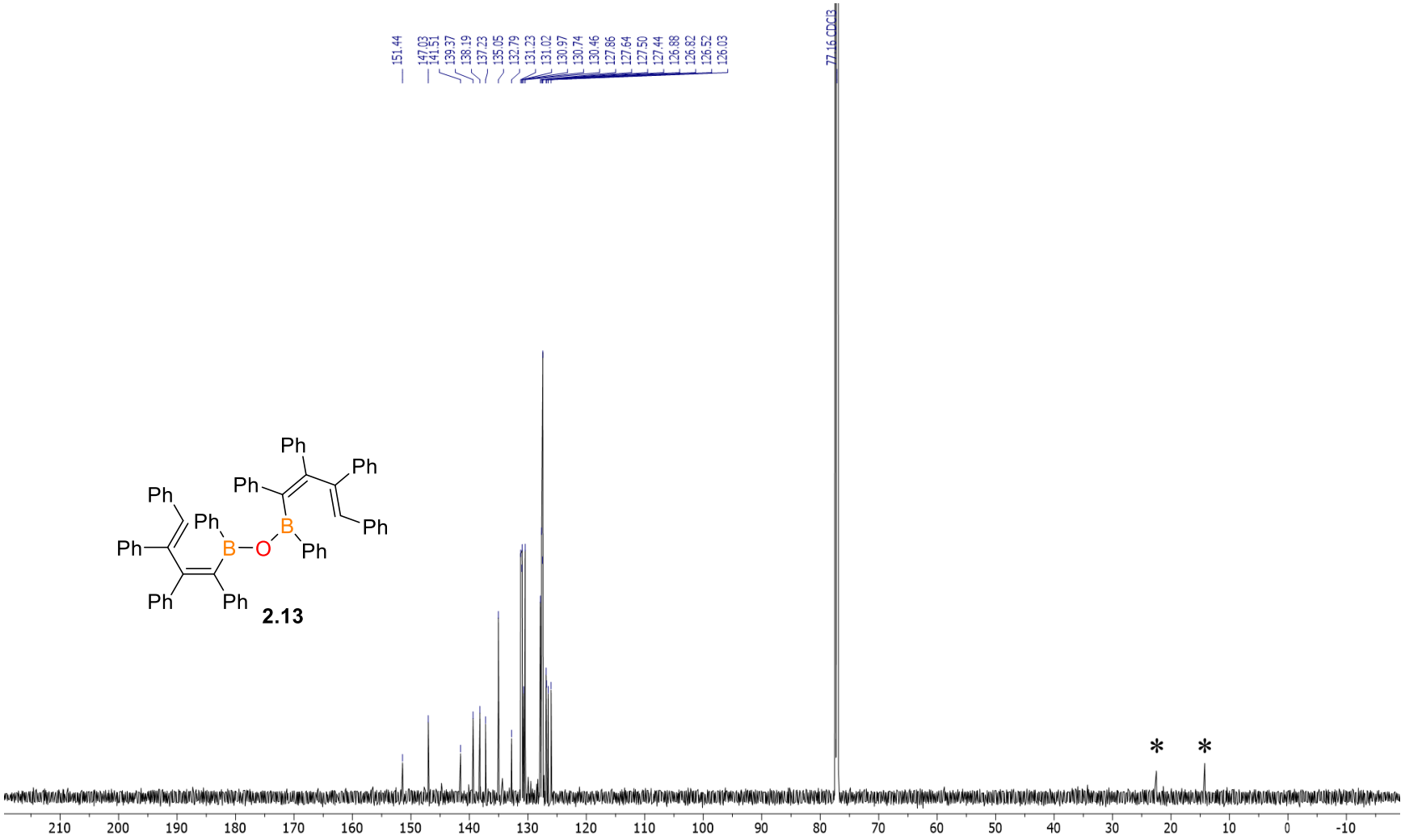

Figure A-6: $^{13}C\{^{1}H\}$ NMR spectrum of **2.13** in $CDCl_3$ (*hexanes).

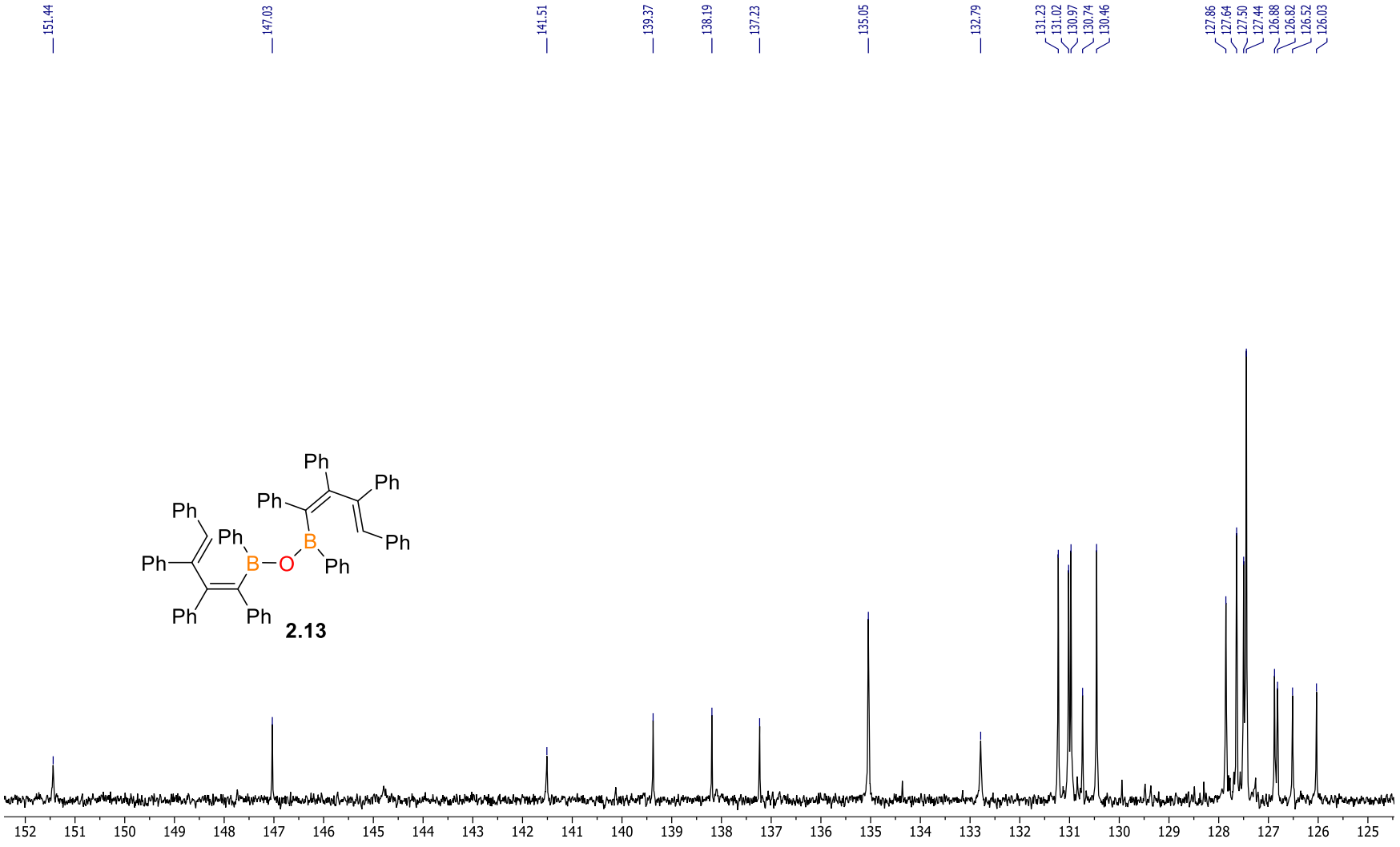

Figure A-7: Expansion of $^{13}C\{^{1}H\}$ NMR spectrum of **2.13** in $CDCl_3$.

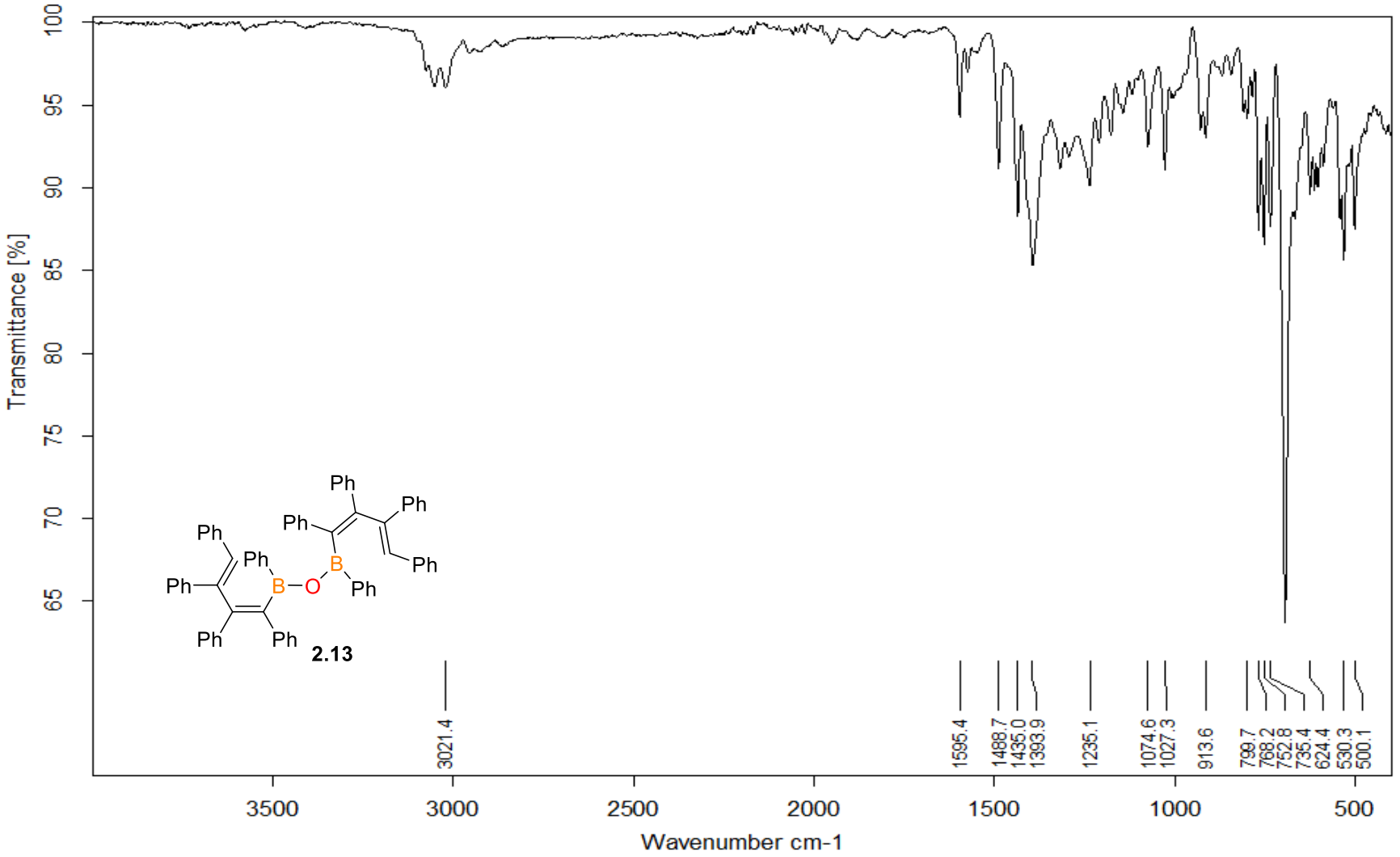

Figure A-8: FT-IR spectrum of **2.13**.

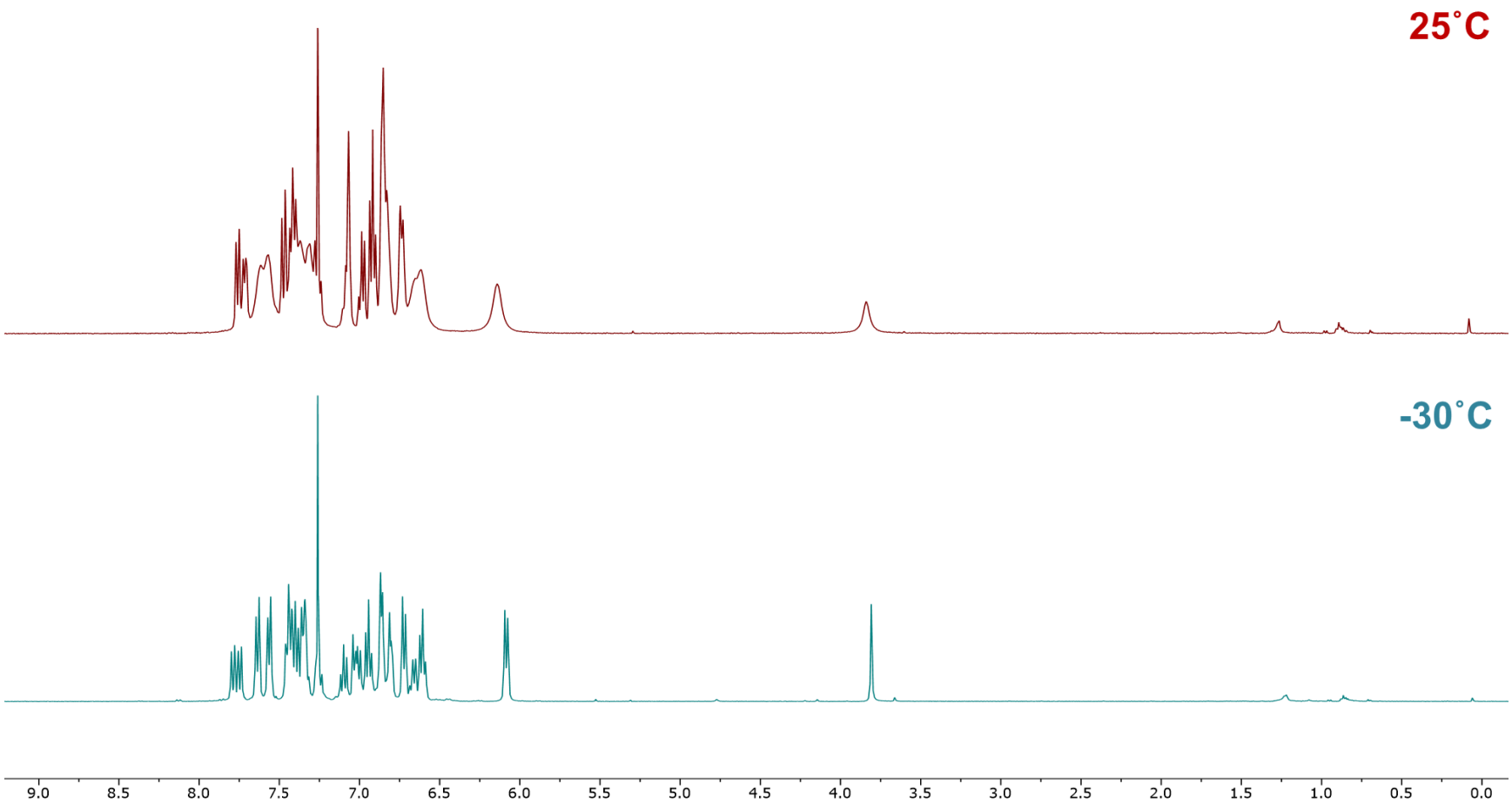

Figure A-9: ^{1}H NMR of **2.14** at 25 ˚C and -30 ˚C in $CDCl_3$.

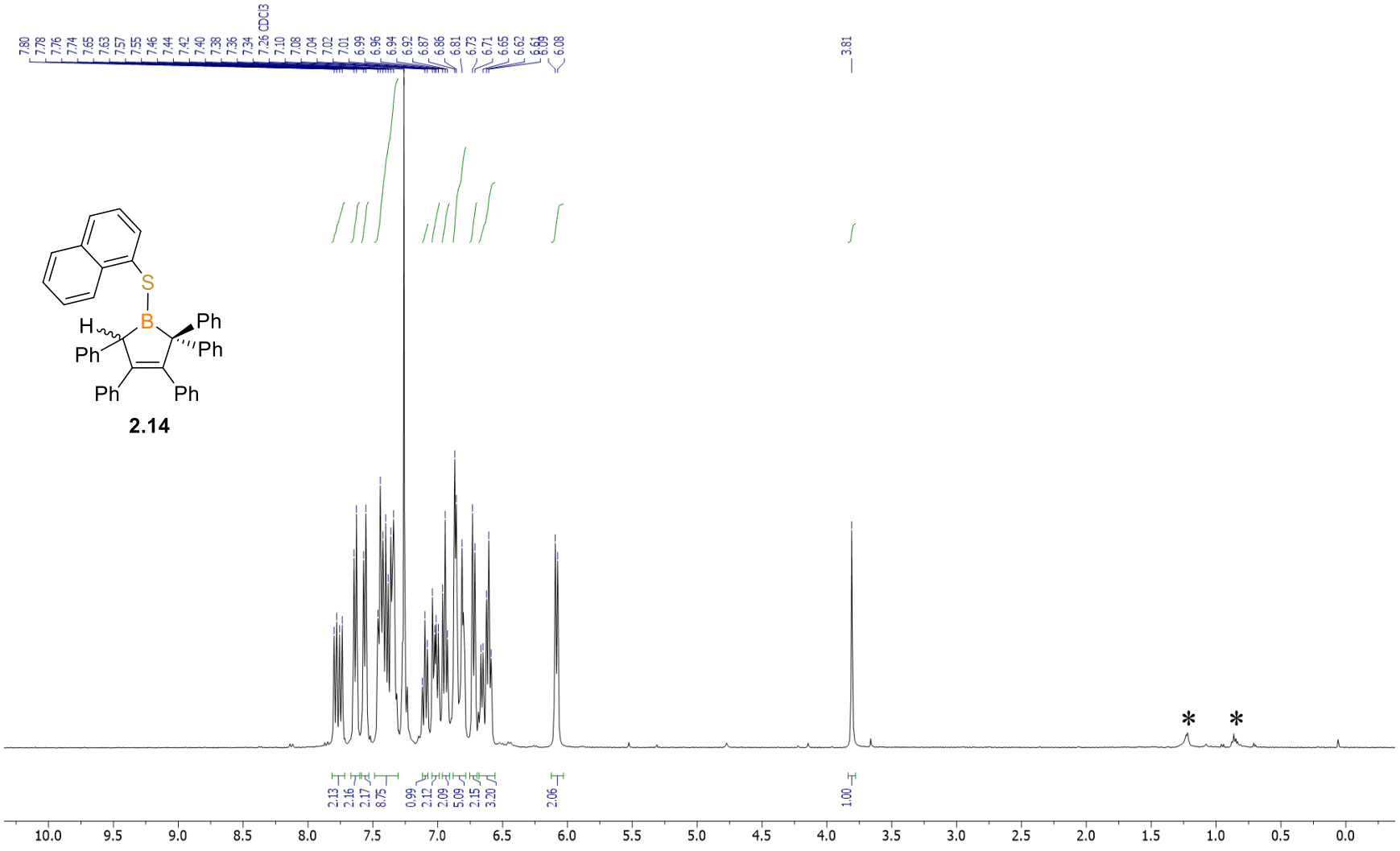

Figure A-10: ^{1}H NMR spectrum of **2.14** in $CDCl_3$ at -30 ˚C (*hexanes).

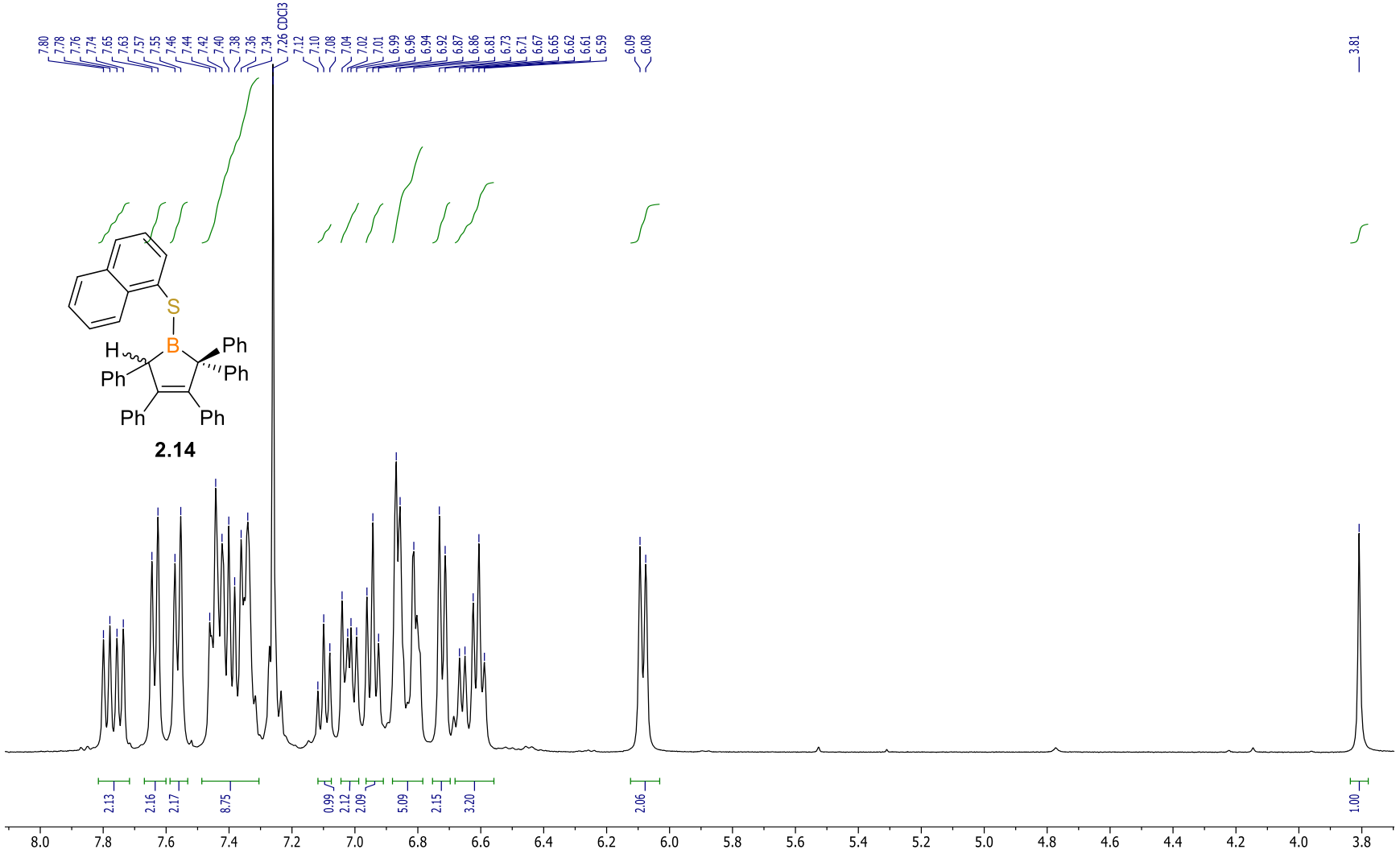

Figure A-11: Expansion of ^{1}H NMR spectrum of **2.14** in $CDCl_3$ at -30 ˚C.

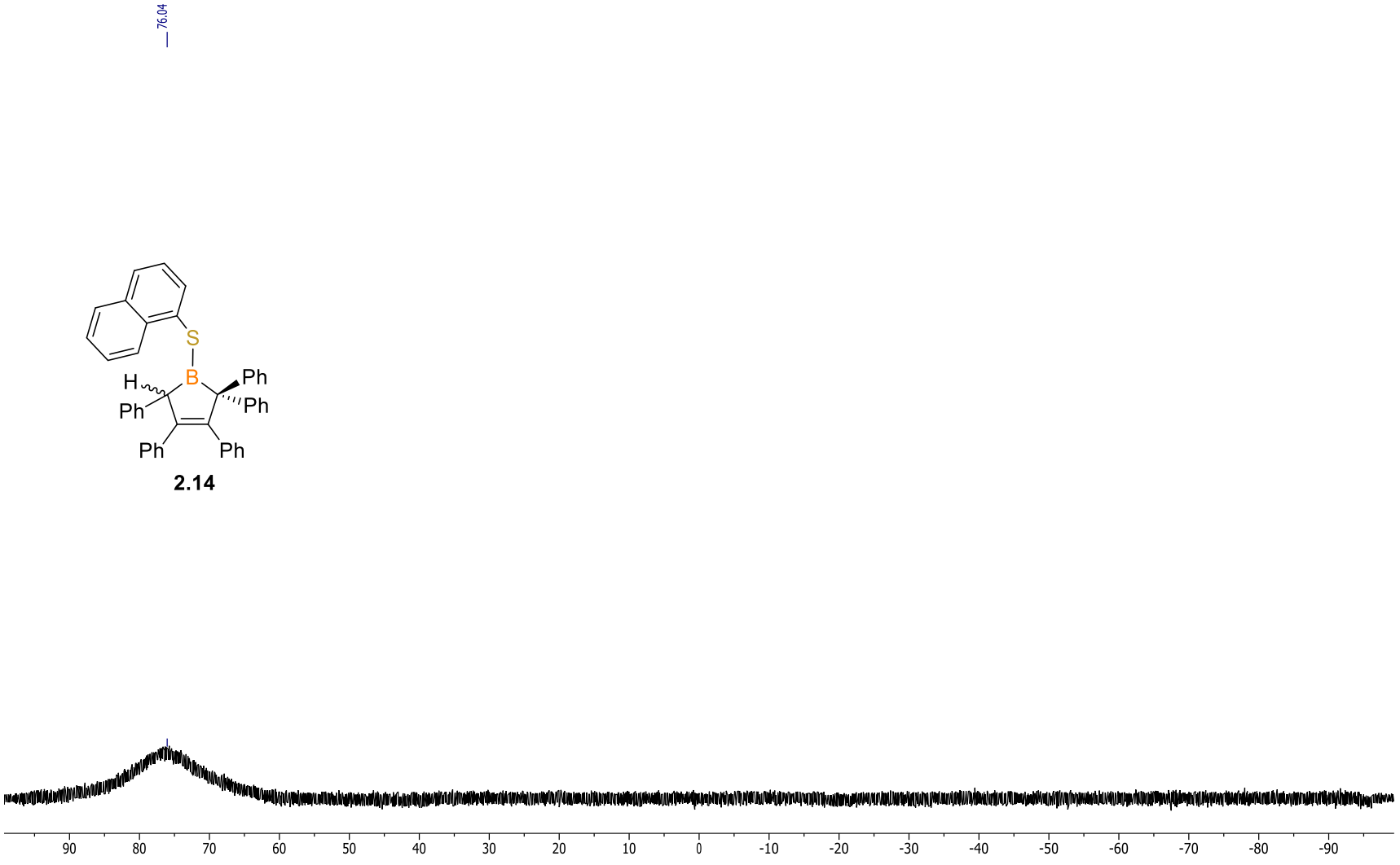

2.14

Figure A-12: $^{11}B\{^{1}H\}$ NMR spectrum of **2.14** in $CDCl_3$ at -30 ˚C.

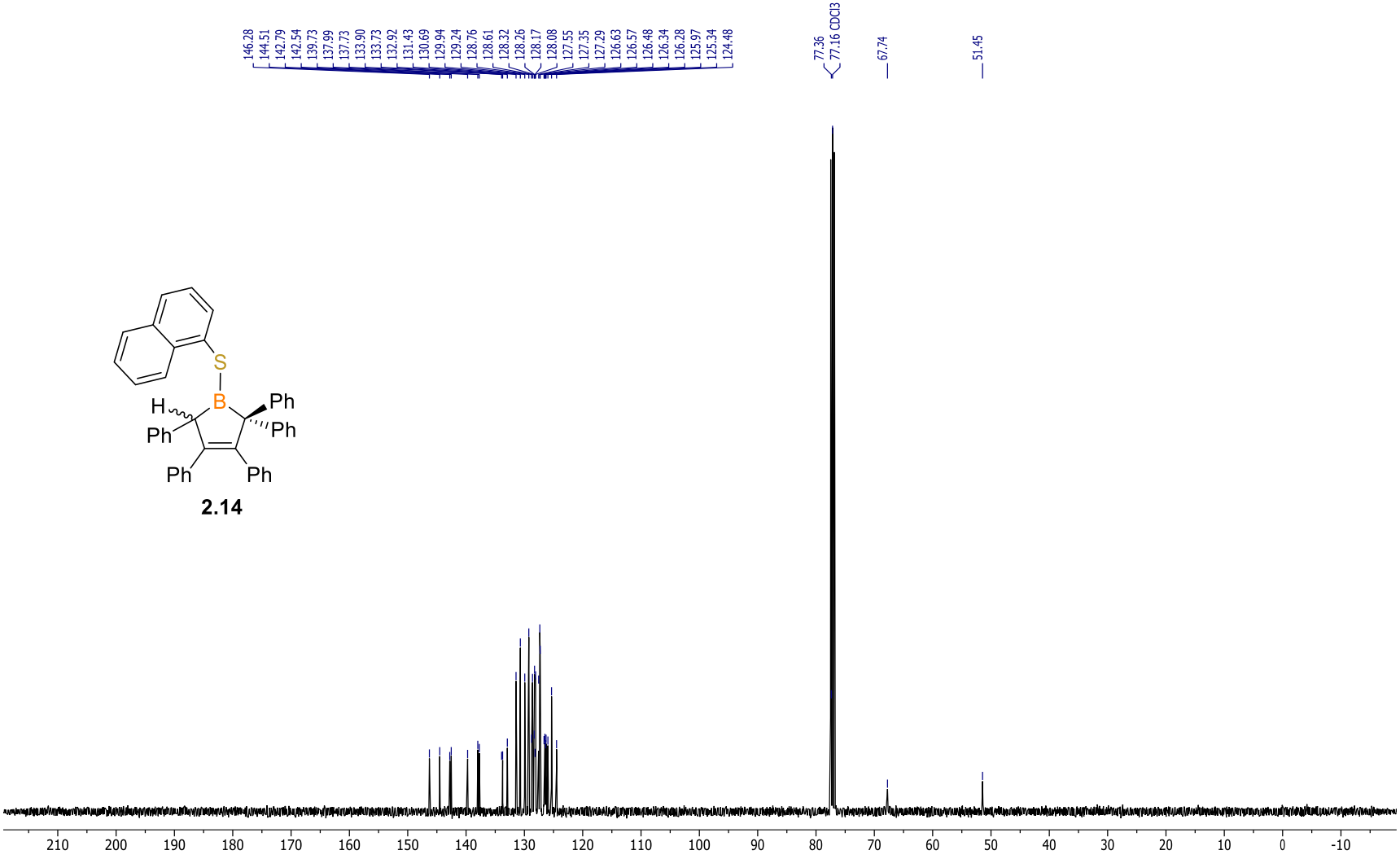

Figure A-13: $^{13}C\{^{1}H\}$ NMR spectrum of **2.14** in $CDCl_3$ at -30 ˚C.

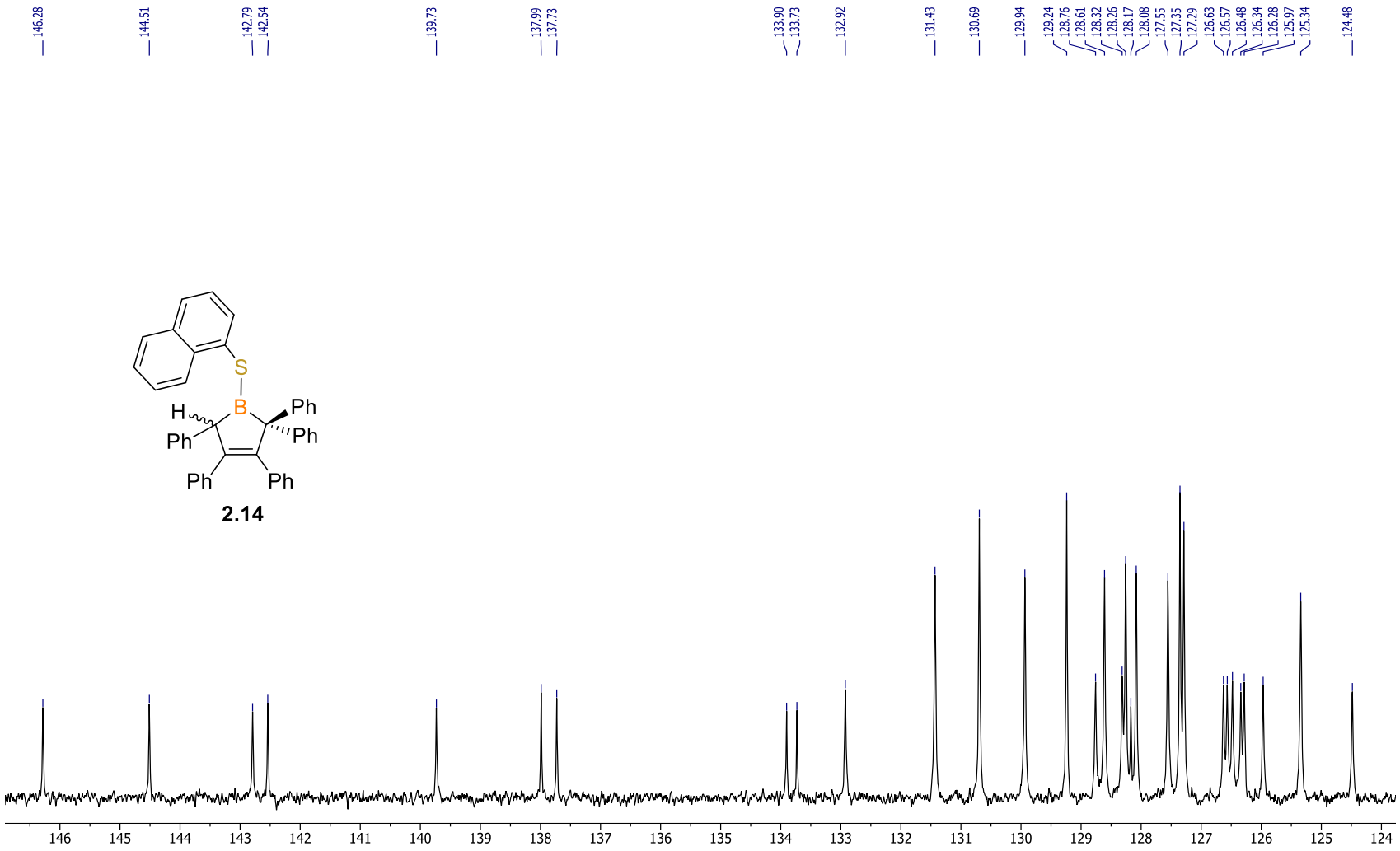

Figure A-14: Expansion of $^{13}C\{^{1}H\}$ NMR spectrum of **2.14** in $CDCl_3$ at -30 ˚C.

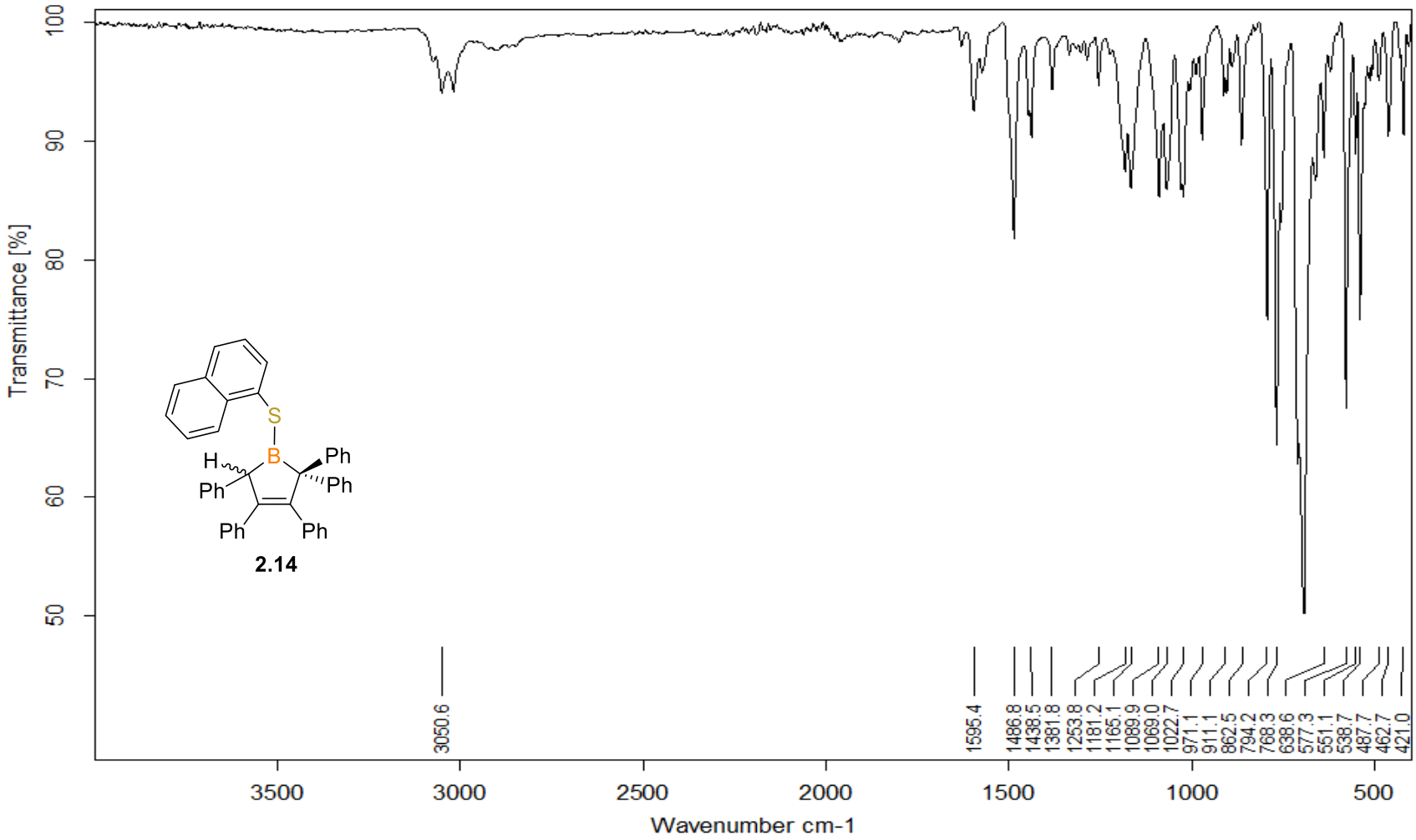

Figure A-15: FT-IR spectrum of **2.14**.

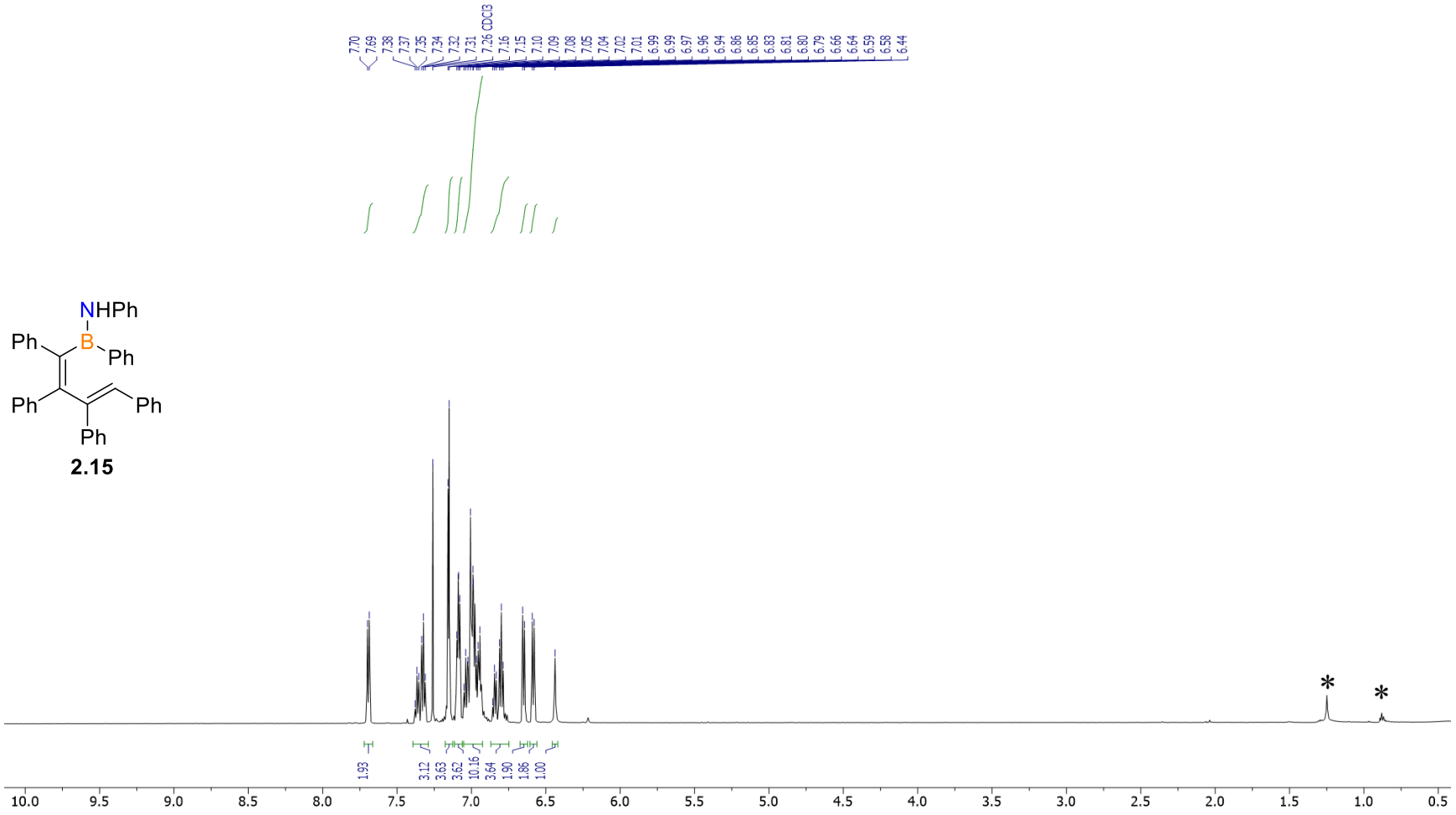

Figure A-16: ^{1}H NMR spectrum of **2.15** in $CDCl_3$ (*hexanes).

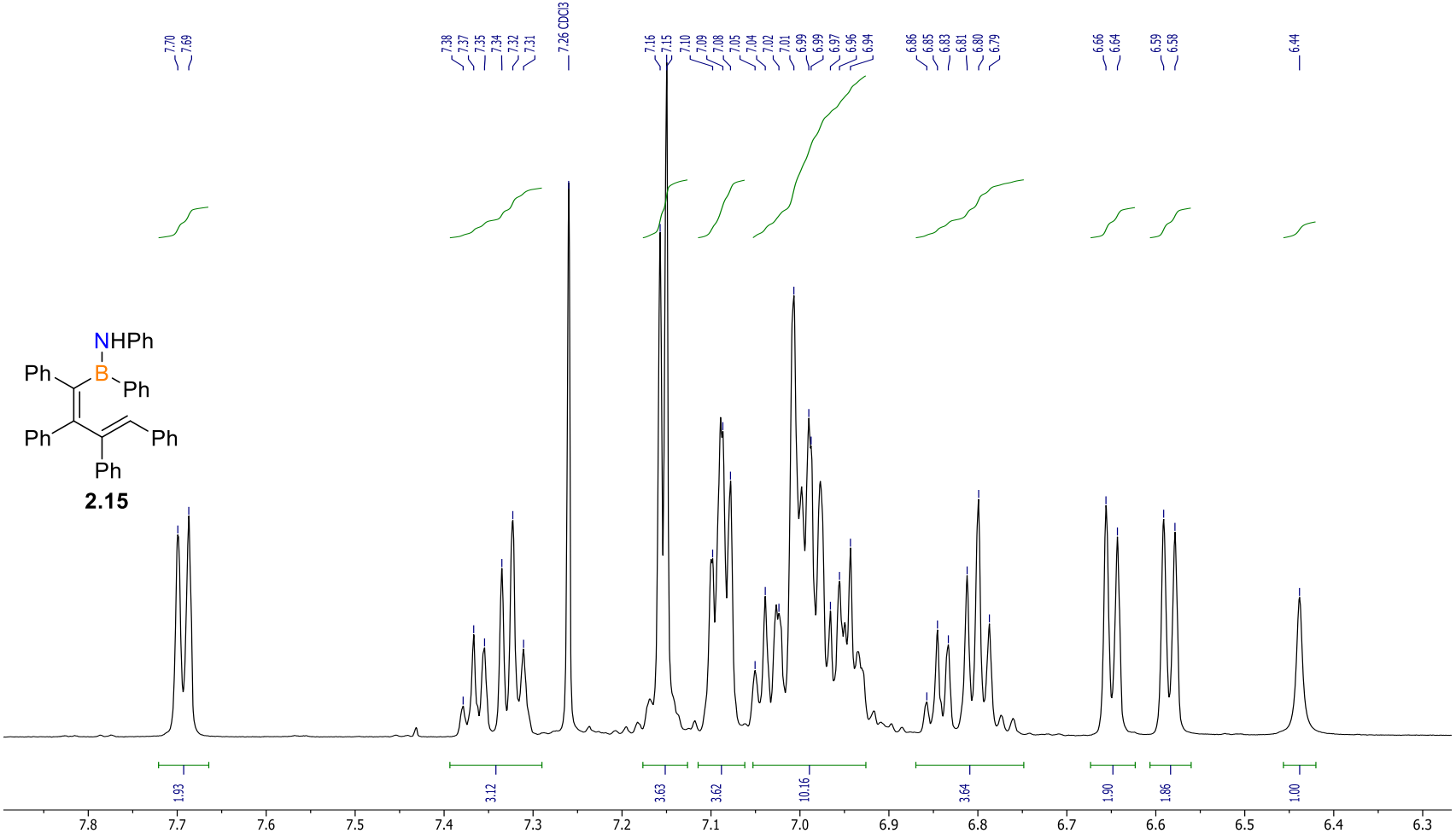

Figure A-17: Expansion of aromatic region of ^{1}H NMR spectrum of **2.15** in $CDCl_3$.

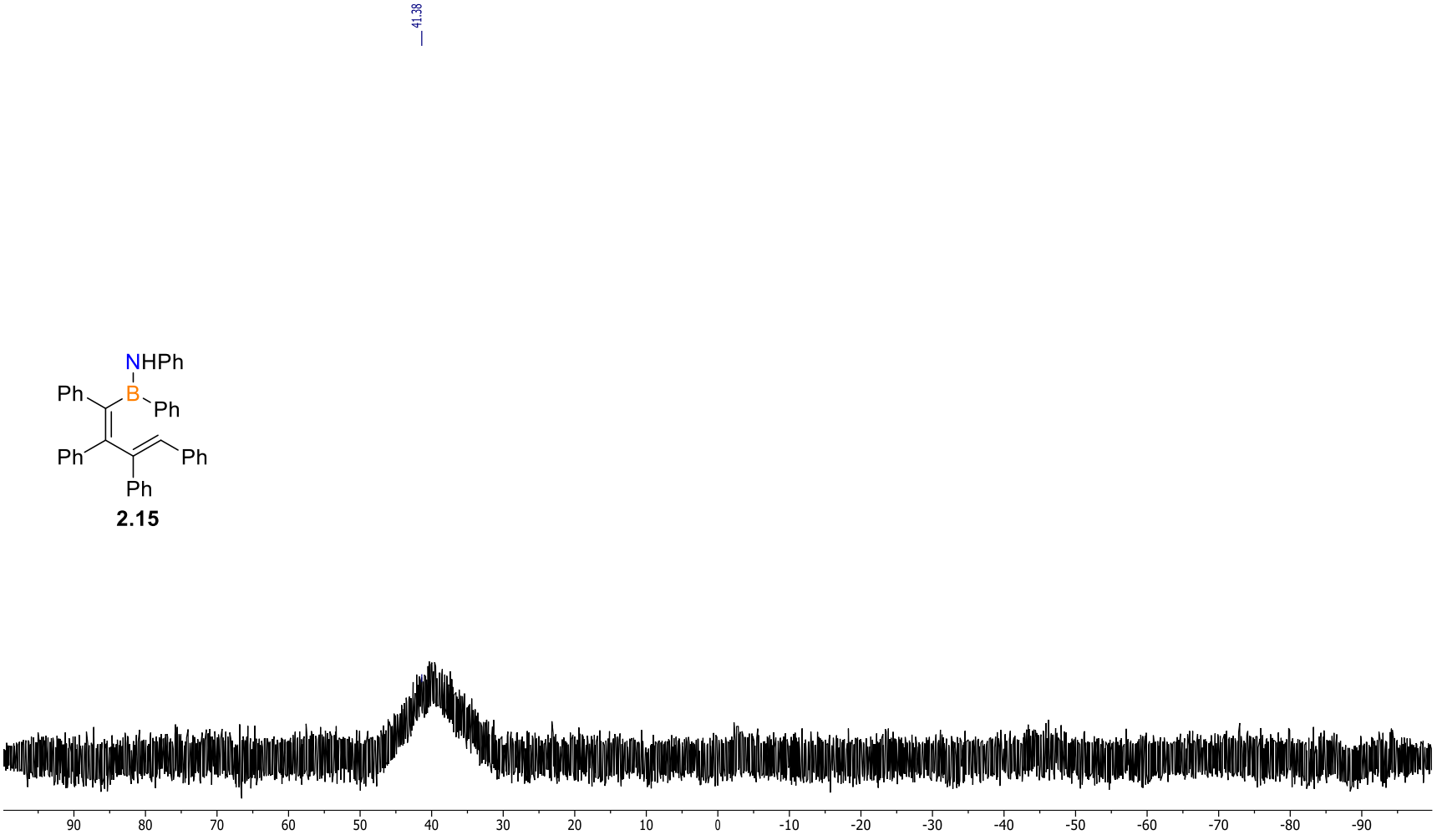

Figure A-18: $^{11}B\{^{1}H\}$ NMR spectrum of **2.15** in $CDCl_3$.

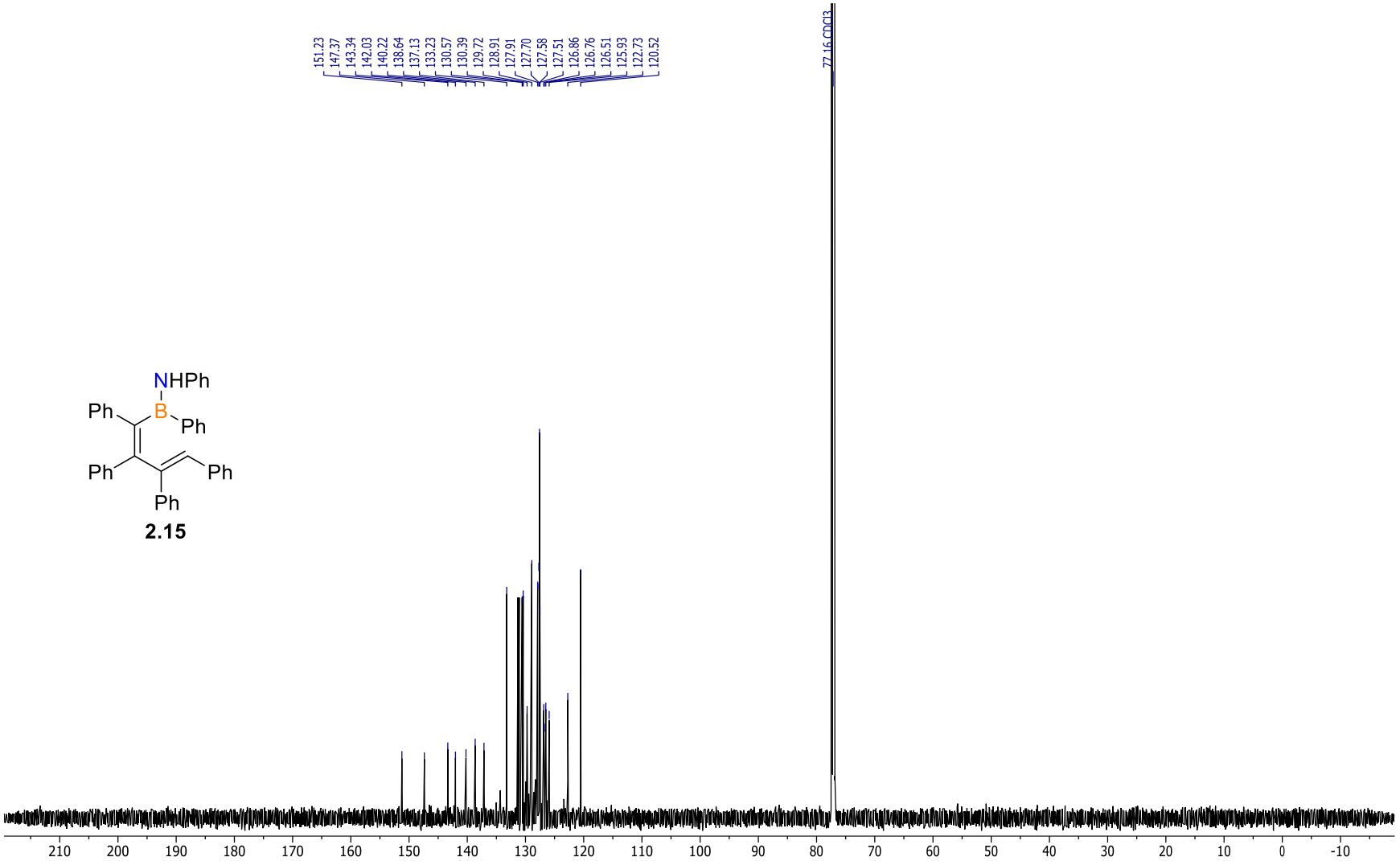

Figure A-19: $^{13}C\{^{1}H\}$ NMR spectrum of **2.15** in $CDCl_3$.

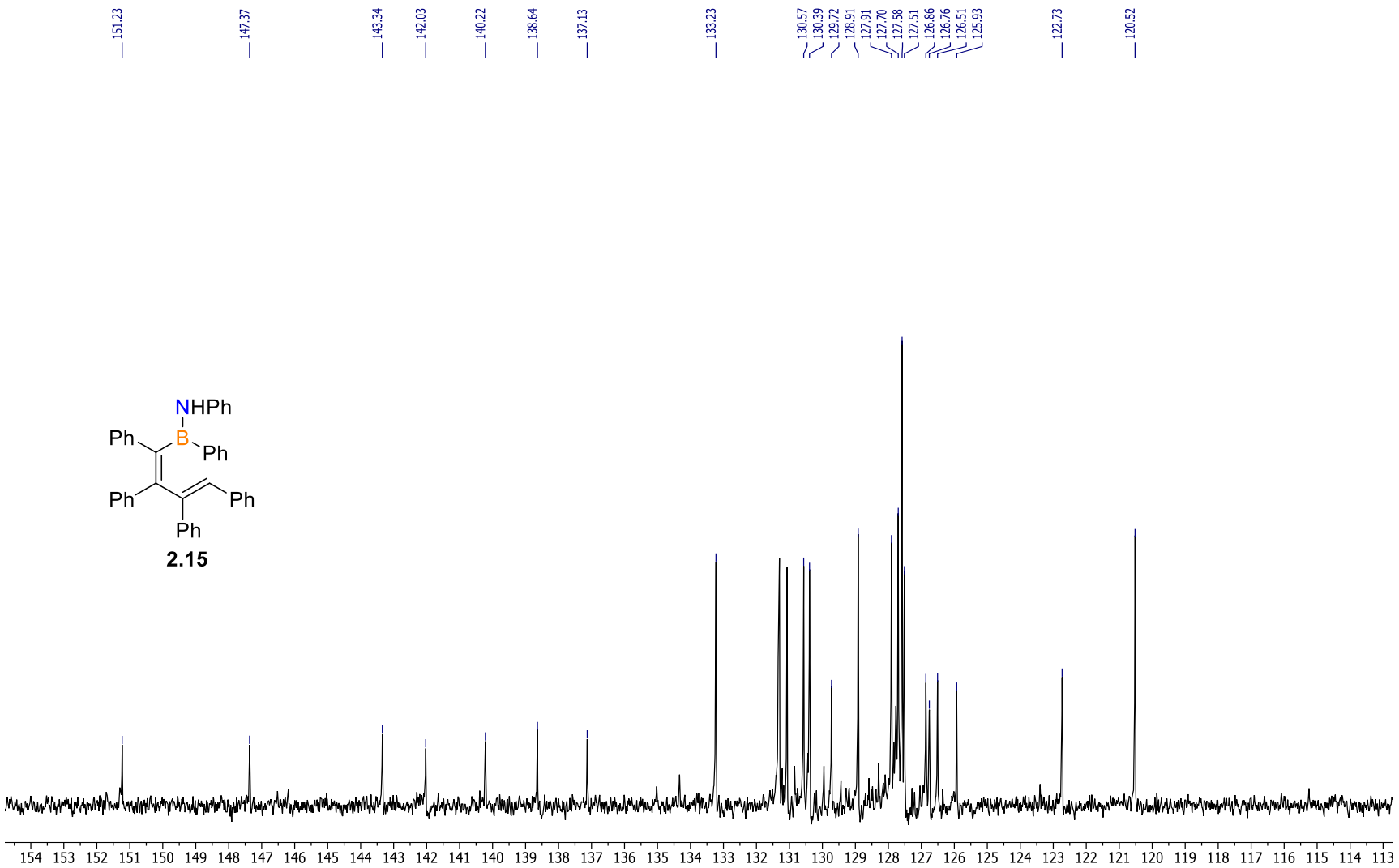

Figure A-20: Expansion of $^{13}C\{^{1}H\}$ NMR spectrum of **2.15** in $CDCl_3$.

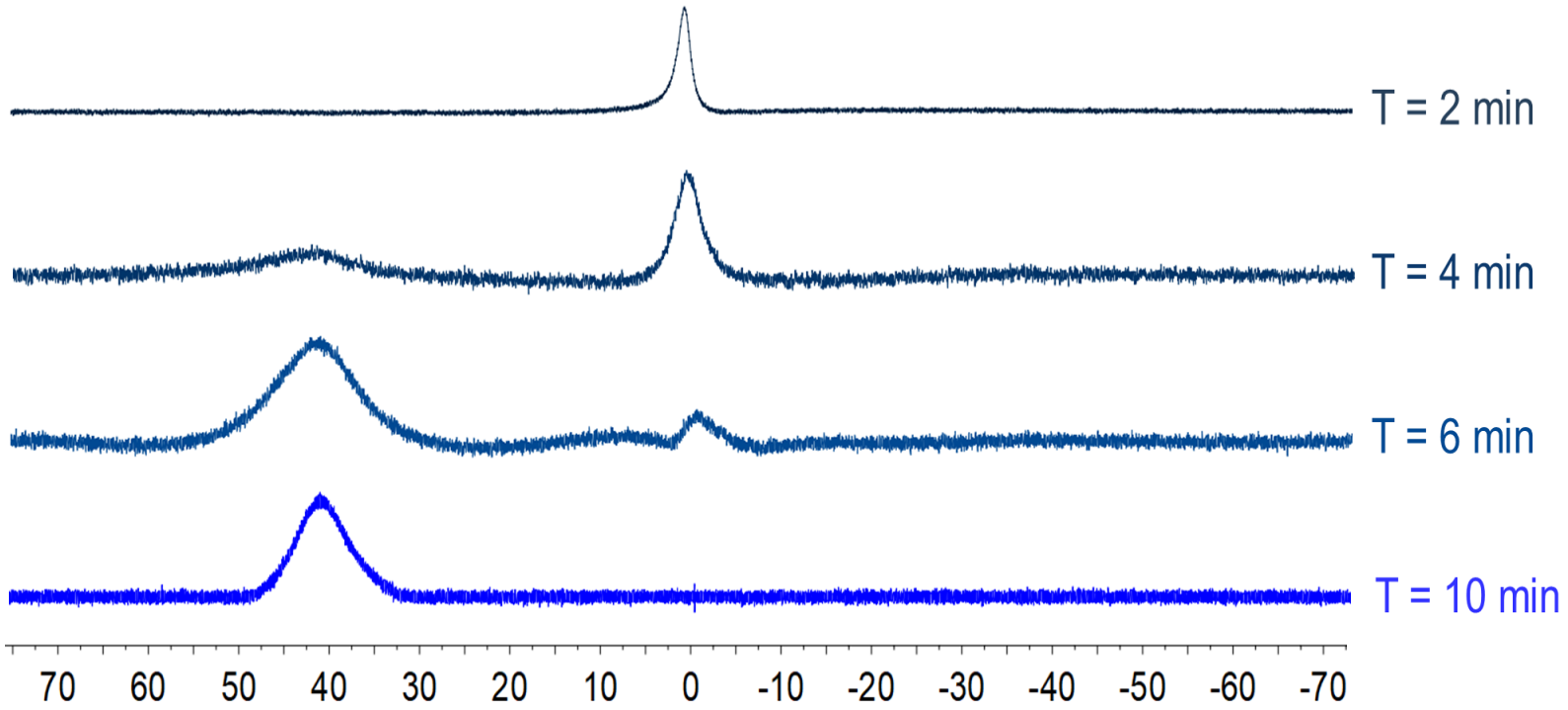

Figure A-21: Stacked plot of crude $^{11}B\{^{1}H\}$ NMR spectra of the reaction of **1.7-Ph** with aniline at -40˚C in $CDCl_3$ over a period of ten minutes.

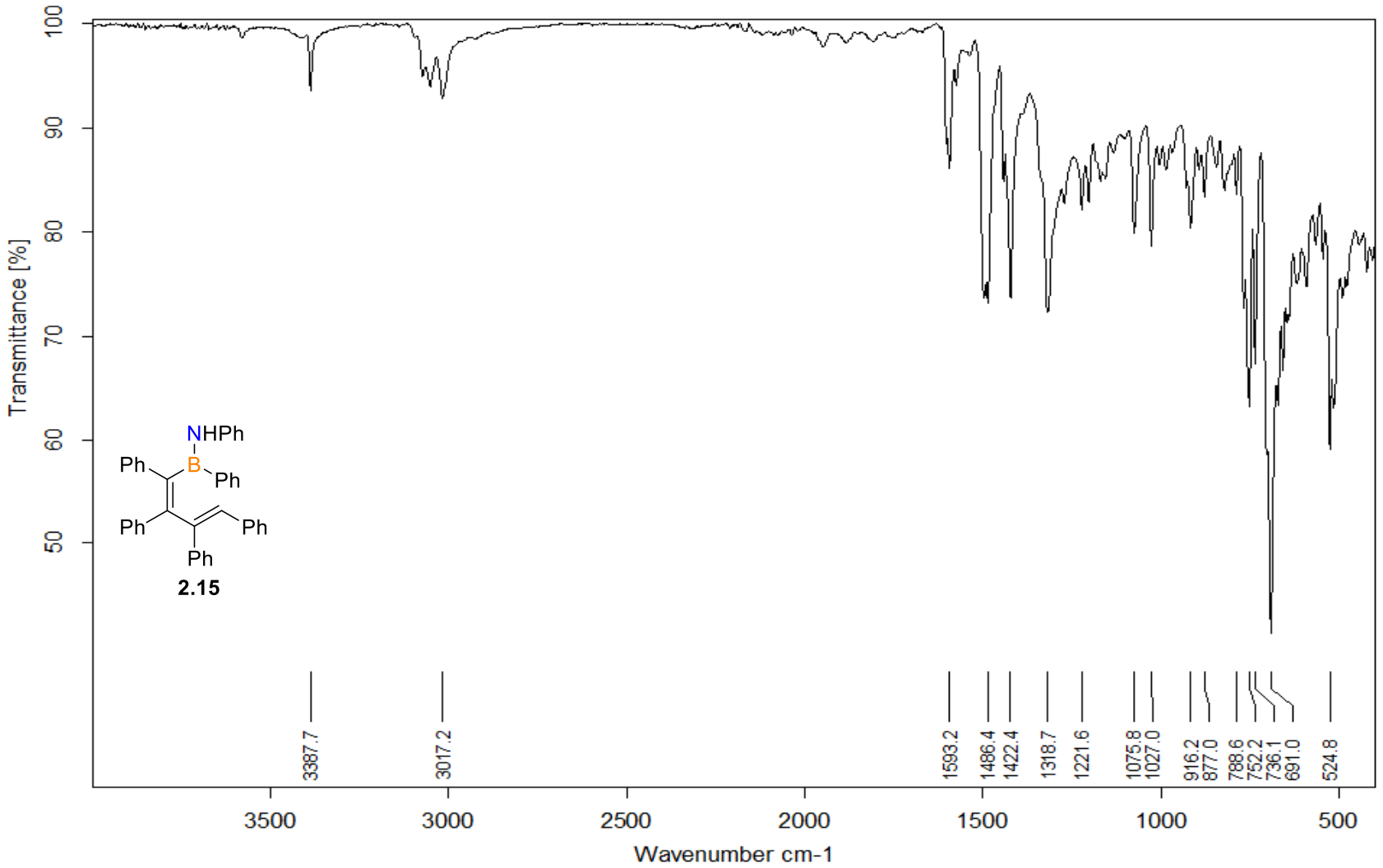

Figure A-22: FT-IR spectrum of **2.15**.

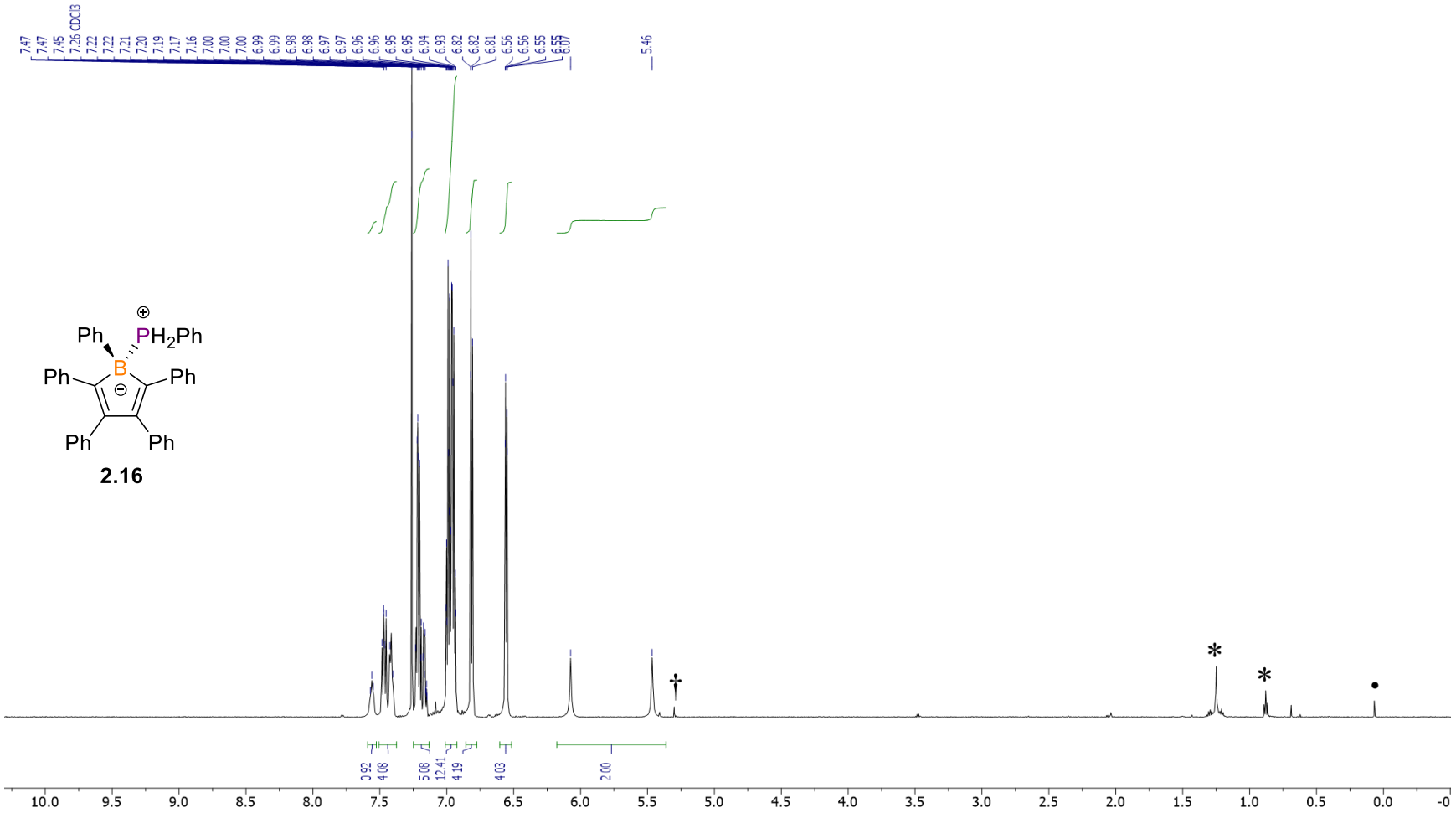

Figure A-23: ^{1}H NMR spectrum of **2.16** in $CDCl_3$ († CH_2Cl_2, * *n*-pentane, • silicone grease).

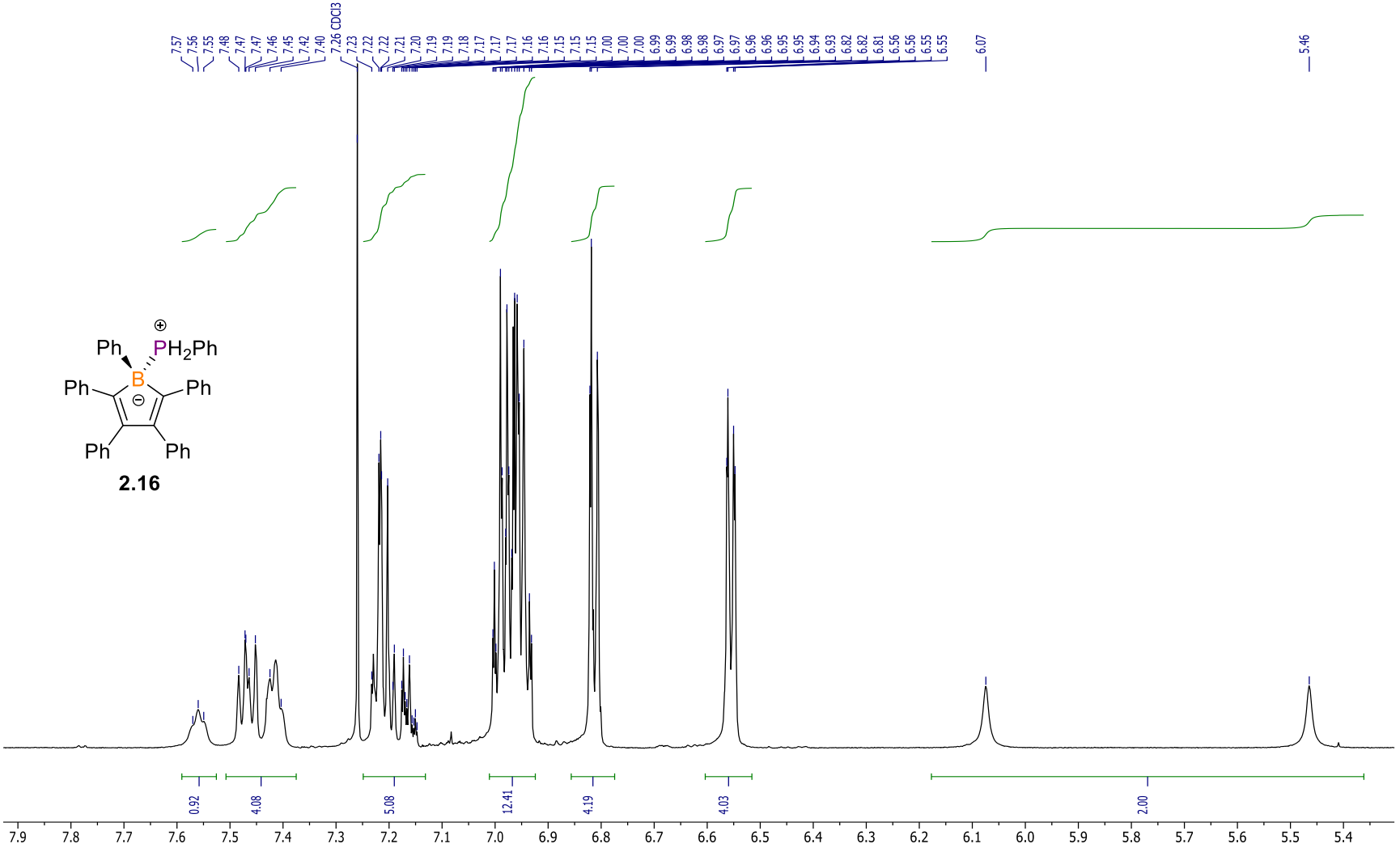

Figure A-24: Expansion of ^{1}H NMR spectrum of **2.16** in $CDCl_3$.

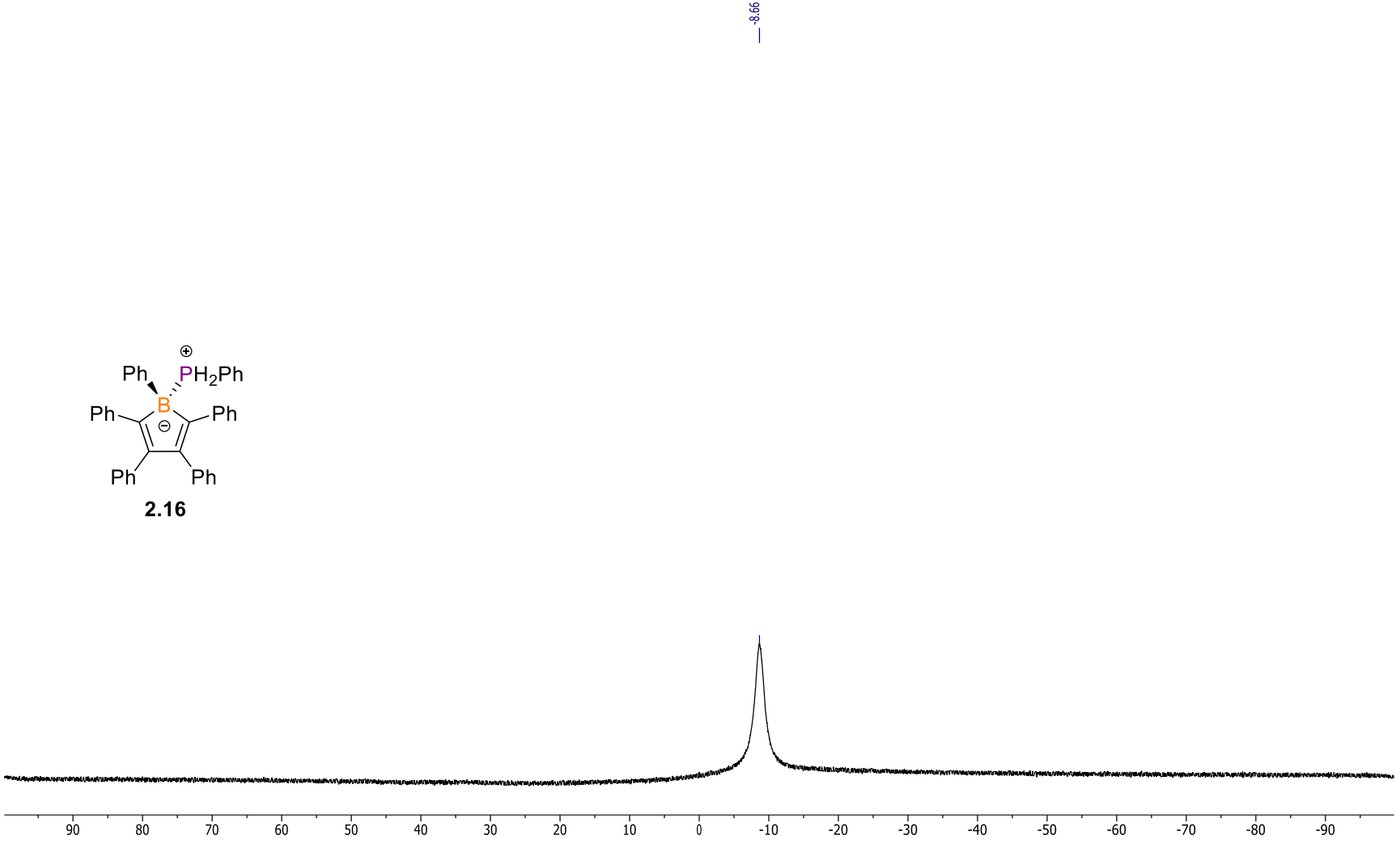

Figure A-25: $^{11}B\{^{1}H\}$ NMR spectrum of **2.16** in $CDCl_3$.

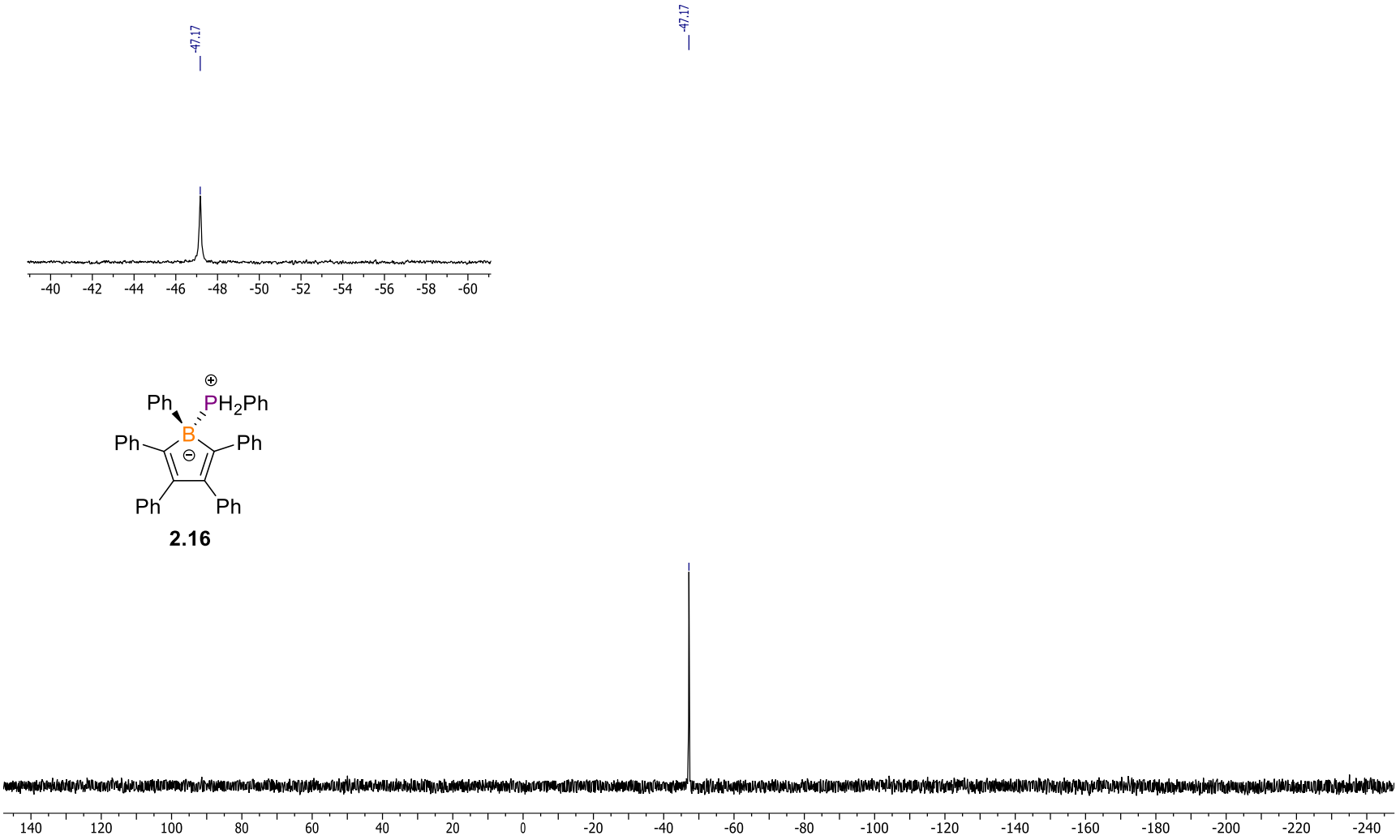

Figure A-26: $^{31}P\{^{1}H\}$ NMR spectrum of **2.16** in $CDCl_3$.

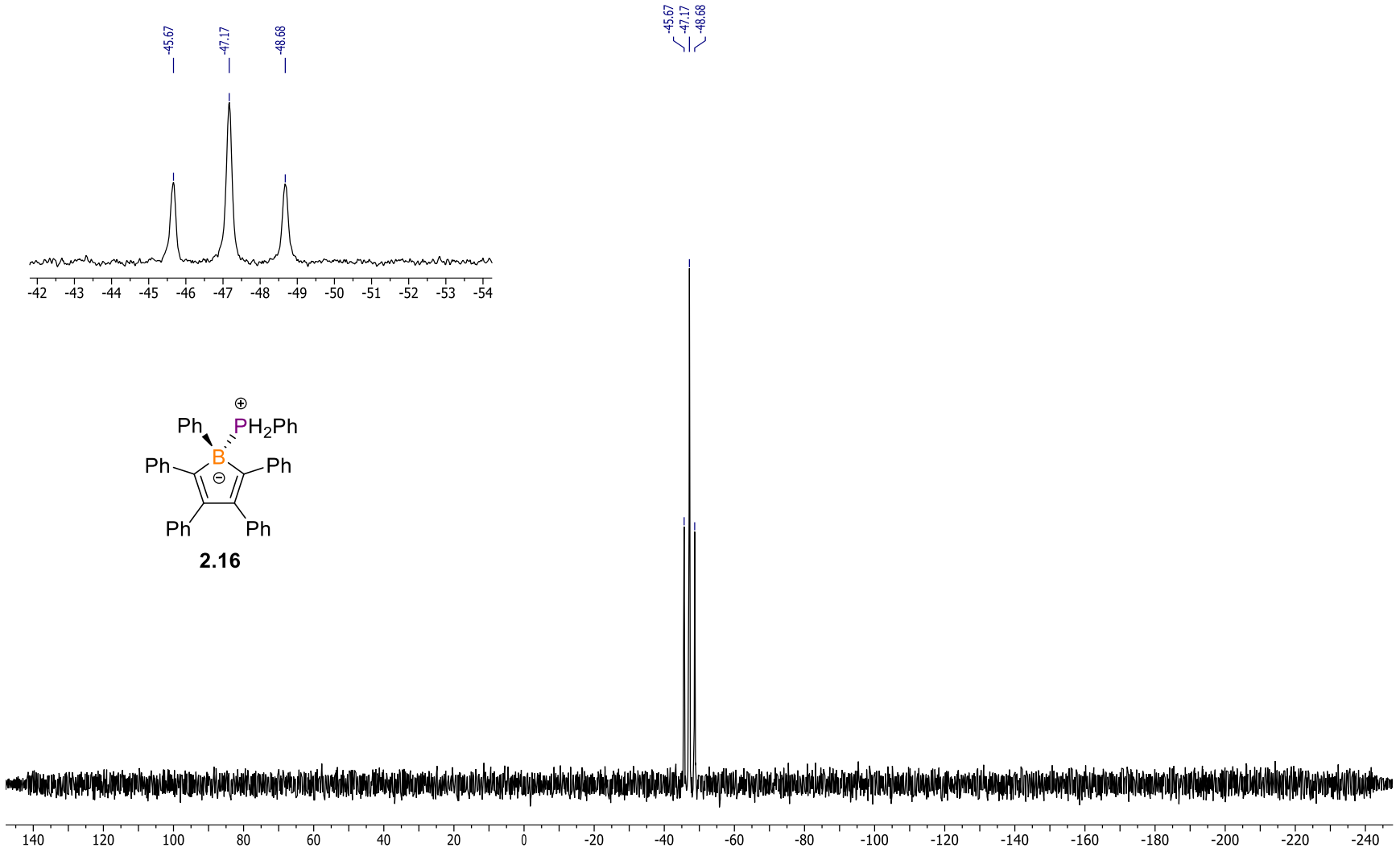

Figure A-27: ^{31}P NMR spectrum of **2.16** in $CDCl_3$.

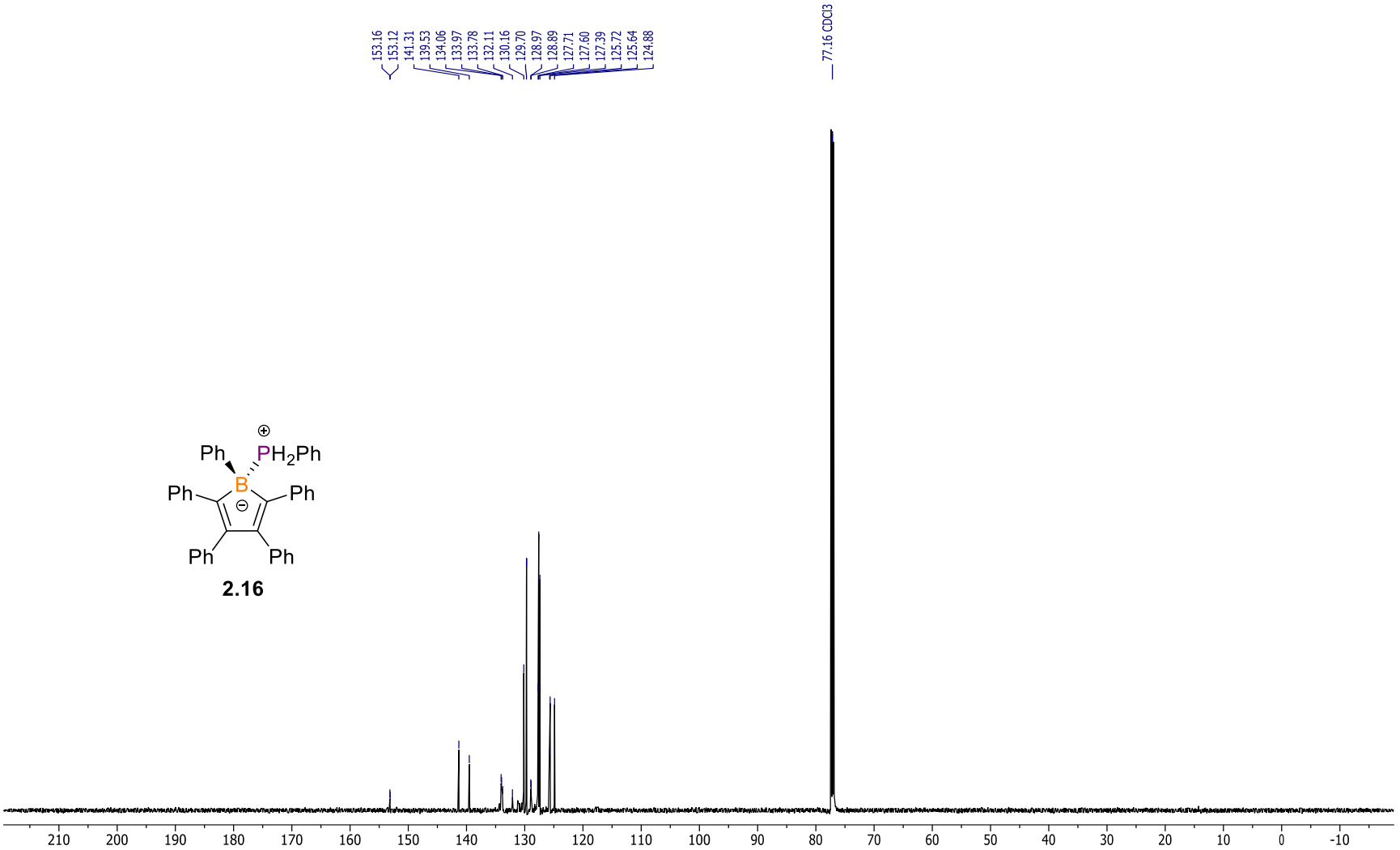

Figure A-28: $^{13}C\{^{1}H\}$ NMR spectrum of **2.16** in $CDCl_3$.

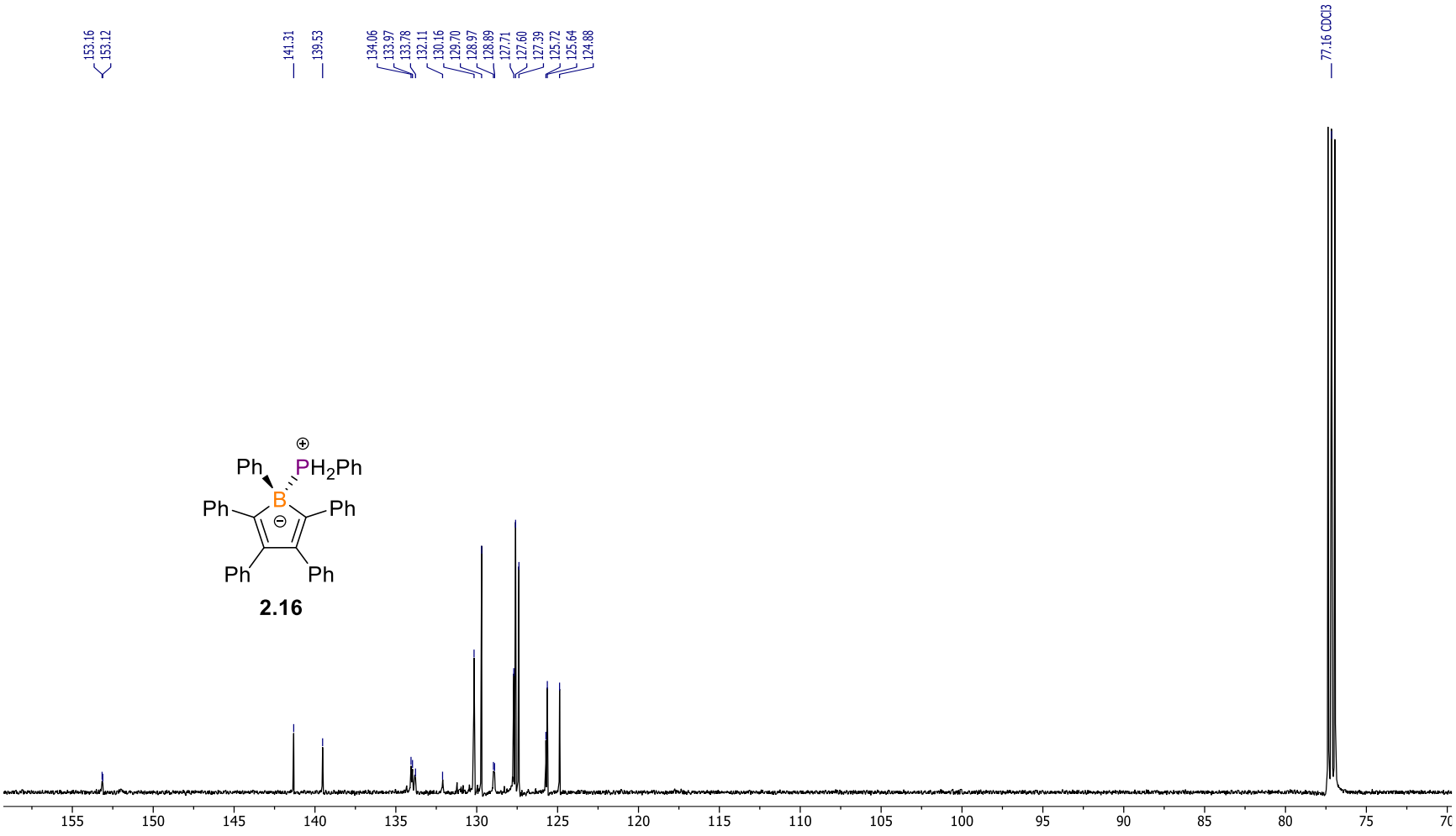

Figure A-29 Expansion of $^{13}C\{^{1}H\}$ NMR spectrum of **2.16** in $CDCl_3$.

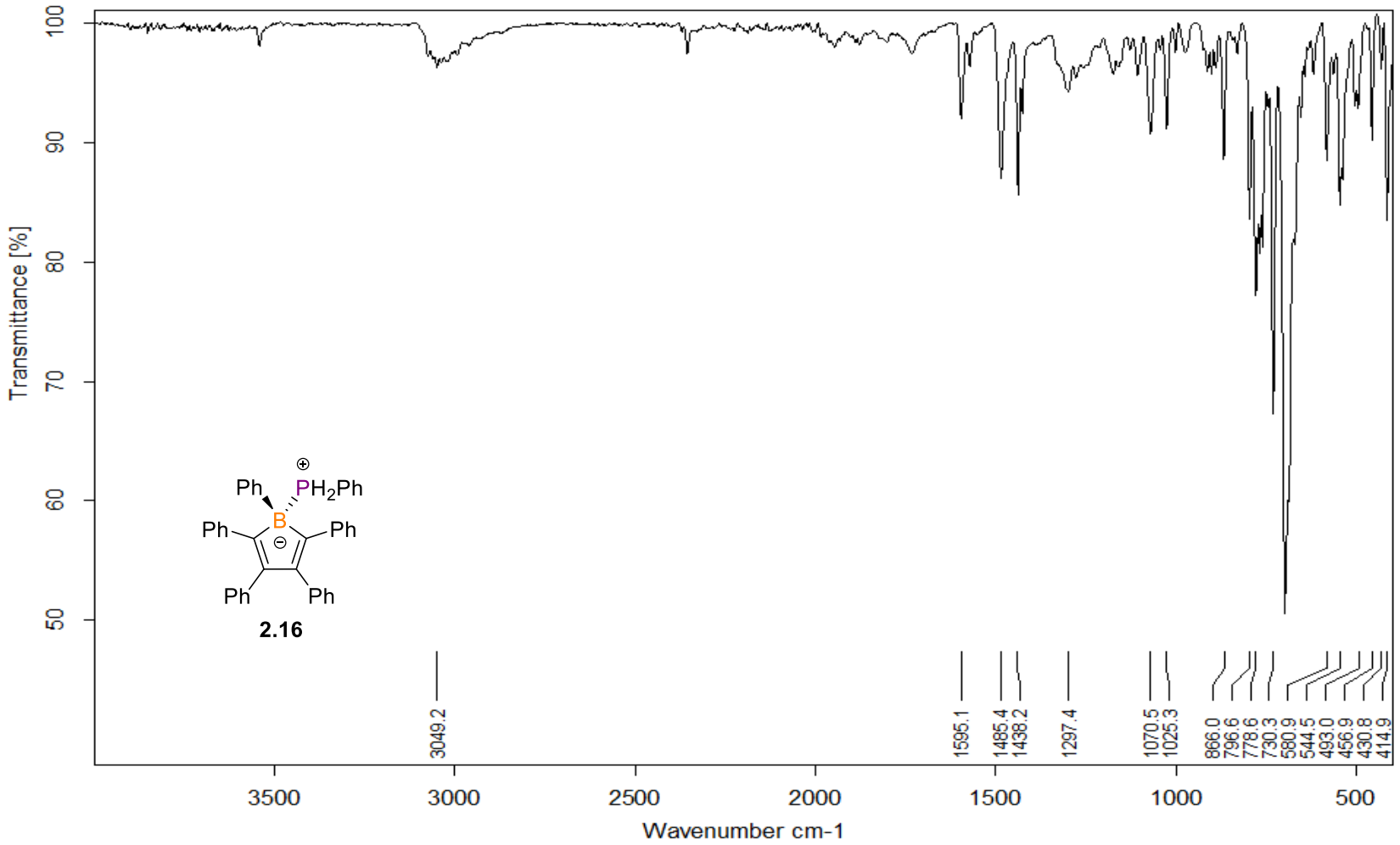

Figure A-30: FT-IR spectrum of **2.16**.

Table A-1: Crystallographic Data for **2.12**-**2.16**.

X-Ray Crystallography details: Crystals were selected under paratone oil, mounted on micromounts then immediately placed in a cold stream of N_2. Structures were solved and refined using SHELXTL[358]. For compounds **2.13** and **2.16**, the *n*-pentane and *n*-hexane solvates were found to be disordered to an extent that could not be modeled and the contribution of the solvate was removed from the reflection data using the squeeze function in the PLATON software suite.[360] For compound **2.15**, the toluene solvent molecule in the unit cell was disordered on an inversion center and was removed from the reflection data using the squeeze function in the PLATON software suite.[360]

Entry	**2.12**	**2.13**	**2.14**	**2.15**	**2.16**
CCDC	1443358	1443359	1443360	1443361	1443362
Empirical formula	$C_{34}H_{27}BO$	$C_{68}H_{52}B_2O$	$C_{44}H_{33}BS$	$C_{40}H_{32}BN$	$C_{40}H_{32}BP$
FW (g/mol)	462.36	906.71	604.57	537.47	554.43
Crystal system	Monoclinic	Monoclinic	Triclinic	Triclinic	Monoclinic
Space group	*P2₁/n*	*C2/c*	*P-1*	*P-1*	*C2/c*
a (Å)	16.1884(9)	47.9860(16)	8.5301(6)	10.1357(6)	14.7877(6)
b (Å)	9.1325(6)	10.1805(3)	9.7269(7)	12.1343(7)	12.3571(6)
c (Å)	18.4471(13)	22.1076(7)	19.5345(15)	14.8636(9)	35.9892(16)
α (deg)	90	90	87.469(2)	70.2320(17)	90
β (deg)	108.626(2)	91.302(2)	86.921(2)	73.1203(19)	95.394(3)
γ (deg)	90	90	82.647(2)	85.9647(18)	90
V (Å^3)	2584.4(3)	10797.2(6)	1604.0(2)	1645.44(17)	6547.3(5)
Z	4	8	2	2	8
D_c (mg m^{-3})	1.188	1.230	1.252	1.085	1.125
radiation, λ (Å)	0.71073	0.71073	0.71073	0.71073	0.71073
temp (K)	150(2)	150(2)	150(2)	150(2)	150(2)
$R1[I>2\sigma I]^a$	0.0529	0.0876	0.0562	0.0488	0.0717
$wR2(F^2)^a$	0.1502	0.1365	0.1539	0.1279	0.1297
GOF (S)^a	1.085	1.047	1.055	1.088	1.124

[a] $R1(F[\mathrm{I} > 2(\mathrm{I})]) = \sum\|\|F_o| - |F_c\|\| / \sum |F_o|$; $wR2(F^2\ [\text{all data}]) = [w(F_o^2 - F_c^2)^2]^{1/2}$; $S(\text{all data}) = [w(F_o^2 - F_c^2)^2/(n - p)]^{1/2}$ (n = no. of data; p = no. of parameters varied; $w = 1/[^2(F_o^2) + (aP)^2 + bP]$ where $P = (F_o^2 + 2F_c^2)/3$ and a and b are constants suggested by the refinement program.

Cartesian Coordinates of M06-2X / 6-31+G(d) optimised geometries

Reactants

1.7-Ph'

E_{SCF} = -568.311763727 Hartree
Singlet, neutral

6	3.618646	1.497053	-0.160491
6	2.316844	0.760468	-0.063760
6	2.316835	-0.760458	0.063713
6	1.064900	-1.262522	0.081890
5	0.106853	0.000033	0.000157
6	1.064922	1.262574	-0.081610
6	0.696584	2.711556	-0.239272
1	1.534200	3.322980	-0.589491
1	-0.122103	2.831485	-0.958302
1	0.351515	3.147895	0.707687
6	-1.449007	0.000019	0.000076
6	-2.180700	-1.110302	-0.461240
6	-3.572946	-1.109097	-0.477689
6	-4.271000	-0.000047	-0.000173
6	-3.573081	1.109039	0.477457
6	-2.180833	1.110312	0.461248
1	-1.649250	1.984865	0.826872
1	-4.114994	1.973220	0.851729
1	-5.357700	-0.000073	-0.000268
1	-4.114752	-1.973298	-0.852069
1	-1.649010	-1.984823	-0.826788
6	0.696561	-2.711492	0.239711
1	0.351834	-3.148049	-0.707275
1	1.534083	-3.322807	0.590349
1	-0.122356	-2.831306	0.958494
6	3.618626	-1.497107	0.160099
1	4.255380	-1.279208	-0.706217
1	4.181442	-1.188278	1.050184
1	3.476222	-2.578512	0.207183
1	4.181163	1.188255	-1.050777
1	3.476294	2.578470	-0.207459
1	4.255657	1.279053	0.705609

H_2O

E_{SCF} = -76.3837661933 Hartree
Singlet, neutral

8	0.000000	0.116389	0.000000
1	0.770604	-0.465524	0.000000
1	-0.770604	-0.465586	0.000000

thiophenol (PhSH))

E_{SCF} = -630.296445793 Hartree
Singlet, neutral

16	2.282897	-0.082928	-0.004779
6	0.509059	-0.000242	0.001300
6	-0.197786	-1.207061	0.002887
6	-0.192317	1.208408	-0.002003
6	-1.589731	-1.200157	0.000920
6	-1.585463	1.205879	-0.000996
1	0.344887	2.153096	-0.005752
6	-2.291334	0.004640	-0.000416
1	-2.118639	2.152200	-0.002200
1	-3.376766	0.007024	-0.000585
1	0.341627	-2.150493	0.007529
1	-2.126949	-2.144076	0.002144
1	2.494917	1.240294	0.065183

aniline (NH_2Ph)

E_{SCF} = -630.296445793 Hartree
Singlet, neutral

6	-1.169737	1.200785	0.003859
6	0.221724	1.205853	-0.005845
6	0.935284	0.000177	-0.008908
6	0.221618	-1.205811	-0.005711
6	-1.169516	-1.200944	0.003493
6	-1.878419	0.000047	0.008990
1	-1.702940	2.147407	0.007372
1	0.764366	2.148303	-0.017977
1	0.764869	-2.147929	-0.016868
1	-1.703169	-2.147315	0.006603
1	-2.963562	-0.000340	0.016804
7	2.332117	-0.000105	-0.076976
1	2.775217	0.835831	0.283241
1	2.774674	-0.835867	0.284388

phenylphosphine (PH_2Ph)

E_{SCF} = -574.046105321 Hartree
Singlet, neutral

6	1.603028	1.216497	-0.000002
6	0.211259	1.200131	0.000004
6	-0.489442	-0.013543	0.000008
6	0.236904	-1.207998	0.000009
6	1.633143	-1.195069	-0.000001
6	2.317268	0.016775	-0.000007
1	2.132277	2.165136	-0.000005
1	-0.336946	2.139189	0.000005
1	-0.292995	-2.157434	0.000019
1	2.182122	-2.132233	-0.000002
1	3.403303	0.030366	-0.000013

15	-2.334902	-0.119903	0.000012
1	-2.568604	0.826527	1.029332
1	-2.568593	0.826241	-1.029573

H_2O reaction

Intermediate 2.1 (adduct)

E_{SCF} = -644.711587639 Hartree
Singlet, neutral

5	0.123006	0.003940	0.502062
8	0.002850	0.142304	2.222232
1	-0.796269	0.635972	2.477755
1	0.781089	0.647518	2.517137
6	0.986635	1.280213	0.029611
6	2.178712	0.802632	-0.389626
6	3.313516	1.558792	-1.021723
1	3.483664	1.219139	-2.051508
1	3.125199	2.634508	-1.053116
1	4.252753	1.396790	-0.478531
6	2.288295	-0.691261	-0.192979
6	3.563153	-1.404536	-0.546958
1	3.827004	-1.242587	-1.599467
1	4.407674	-1.036192	0.049823
1	3.483982	-2.482411	-0.387012
6	1.154254	-1.212272	0.320306
6	0.920997	-2.638356	0.727562
1	1.832197	-3.245753	0.721889
1	0.497963	-2.681726	1.740059
1	0.190469	-3.134494	0.075294
6	0.504243	2.699958	-0.059286
1	1.260687	3.394905	-0.438097
1	-0.372589	2.768845	-0.716683
1	0.178447	3.083619	0.920266
6	-1.409136	-0.084486	0.057038
6	-2.342331	0.881599	0.472405
1	-2.016650	1.725404	1.086560
6	-3.682535	0.832675	0.091397
1	-4.376220	1.595613	0.435177
6	-4.124541	-0.188551	-0.747869
1	-5.165776	-0.232126	-1.055067
6	-3.217002	-1.146406	-1.197960
1	-3.550910	-1.940075	-1.861266
6	-1.882933	-1.093044	-0.794273
1	-1.188498	-1.846815	-1.157241

Transition State $_{2.1}$ ($TS_{2.1}$, H-migration from Int2.1)

E_{SCF} = -644.686180576 Hartree
Singlet, neutral

5	-0.085790	-0.303813	0.638245
8	-0.115133	-0.710160	2.199399
1	0.653738	-0.335077	2.660668
1	-0.825532	0.227491	1.884559
6	-1.084968	-1.311987	-0.091965
6	-2.206289	-0.647475	-0.453547
6	-3.427615	-1.182097	-1.148375
1	-3.648803	-0.614198	-2.060352
1	-3.298467	-2.228392	-1.434312
1	-4.315631	-1.117475	-0.506713
6	-2.130626	0.777782	-0.046524
6	-3.114857	1.772406	-0.584953
1	-2.992305	1.878500	-1.670999
1	-4.143169	1.431406	-0.417275
1	-2.993221	2.756896	-0.127929
6	-1.057407	1.079036	0.745027
6	-0.618508	2.486350	1.080740
1	-1.389948	3.045401	1.624419
1	0.280530	2.475188	1.707563
1	-0.364909	3.064540	0.182784
6	-0.805164	-2.774645	-0.216967
1	-1.625067	-3.348205	-0.660109
1	0.097791	-2.941437	-0.817847
1	-0.595854	-3.190364	0.778325
6	1.387264	-0.060164	0.096320
6	2.470936	-0.768919	0.633596
1	2.300147	-1.483329	1.439041
6	3.768048	-0.599269	0.145930
1	4.589913	-1.161567	0.581669
6	4.005826	0.286907	-0.901941
1	5.013084	0.424211	-1.285208
6	2.940072	0.995521	-1.458836
1	3.117547	1.687081	-2.278351
6	1.650605	0.821725	-0.961979
1	0.826262	1.378646	-1.405496

Product 2.1 (Prod2.1, ring open product)

E_{SCF} = -644.768236585 Hartree
Singlet, neutral

6	0.061727	2.337356	2.050295
6	-0.814997	1.287987	1.436032
6	-1.381378	1.285143	0.217057
6	-2.099324	0.076970	-0.270466
6	-1.554997	-1.154378	-0.141363
6	-2.304917	-2.400697	-0.593332
1	-3.250723	-2.536182	-0.053208
1	-2.547891	-2.357317	-1.661421
1	-1.708715	-3.306384	-0.441285
5	-0.125682	-1.384312	0.482021
8	0.025565	-2.265467	1.525665
1	-0.814880	-2.614844	1.851923
6	1.208184	-0.758781	-0.065365
6	2.395062	-0.873745	0.674123

1	2.375042	-1.409599	1.620030
6	3.586766	-0.311923	0.218622
6	3.613867	0.368775	-0.998338
1	4.541706	0.805554	-1.357767
6	2.447766	0.483064	-1.756415
1	2.467434	1.005557	-2.709069
6	1.260467	-0.075291	-1.288809
1	0.352398	0.016700	-1.881708
1	4.494412	-0.406085	0.808659
6	-3.437037	0.324524	-0.930355
1	-4.036852	-0.585579	-0.995534
1	-4.013587	1.075116	-0.378424
1	-3.304566	0.706057	-1.951501
6	-1.330030	2.446125	-0.746280
1	-2.335882	2.836596	-0.941478
1	-0.718187	3.269904	-0.377133
1	-0.916597	2.126961	-1.711126
1	-0.980129	0.410202	2.062083
1	-0.281947	2.594512	3.058167
1	1.083701	1.946988	2.147072
1	0.112197	3.256360	1.463869

Product 2.2 (Prod2.2, ring-closed product)

E_{SCF} = -644.787635586 Hartree
Singlet, neutral

6	-0.077757	0.294173	0.792333
6	-0.980014	-0.935185	0.683744
6	-0.656497	-2.129637	1.532960
1	-0.807698	-1.903496	2.595973
1	-1.263597	-3.004328	1.289102
1	0.399883	-2.401698	1.412123
6	-1.984541	-0.809263	-0.204631
6	-3.027949	-1.835220	-0.541730
1	-4.025057	-1.496792	-0.233391
1	-3.070348	-1.994085	-1.627361
1	-2.844447	-2.800295	-0.064397
6	-2.003208	0.523818	-0.942577
1	-1.712574	0.351709	-1.995059
6	-3.368701	1.229120	-0.942661
1	-3.721176	1.402910	0.080981
1	-3.317666	2.201613	-1.448019
1	-4.133114	0.641130	-1.462562
5	-0.856091	1.299563	-0.165568
8	-0.582259	2.627670	-0.187361
6	1.299039	0.038808	0.182079
6	2.465159	0.611659	0.705050
1	2.414610	1.230825	1.594726
6	3.704797	0.401202	0.101446
1	4.592845	0.855399	0.532505
6	3.809092	-0.385179	-1.043106
1	4.775105	-0.549975	-1.511228
6	2.657383	-0.960029	-1.578480
1	2.720443	-1.578900	-2.469439
6	1.421239	-0.749425	-0.972888
1	0.532362	-1.214502	-1.393961
6	-0.004313	0.824982	2.232332
1	-1.010633	0.877696	2.662718
1	0.605238	0.176846	2.874602
1	0.418275	1.834137	2.264126
1	-1.136295	3.133683	-0.797937

Product 2.3 (Prod2.3, bis-borole product)

E_{SCF} = -1213.12019435 Hartree
Singlet, neutral

6	2.853151	1.883162	-1.964085
6	2.118366	0.592382	-1.755168
1	1.065324	0.701985	-1.491745
6	2.597460	-0.658133	-1.858787
6	1.721986	-1.813084	-1.514670
6	1.006862	-1.795348	-0.368166
5	1.143357	-0.626150	0.683844
8	0.000000	0.000000	1.091821
5	-1.143357	0.626150	0.683844
6	-1.006862	1.795348	-0.368166
6	-1.721986	1.813084	-1.514670
6	-2.597460	0.658133	-1.858787
6	-2.118366	-0.592382	-1.755168
1	-1.065324	-0.701985	-1.491745
6	-2.853151	-1.883162	-1.964085
1	-3.799545	-1.759585	-2.494013
1	-2.236363	-2.588287	-2.531407
1	-3.071643	-2.353841	-0.996432
6	-3.993981	0.992070	-2.323705
1	-3.974614	1.480072	-3.305312
1	-4.628012	0.108273	-2.400945
1	-4.476426	1.688656	-1.628222
6	-1.723613	2.935968	-2.525732
1	-2.697532	3.440046	-2.538827
1	-0.967414	3.693720	-2.319832
1	-1.553015	2.545646	-3.535501
6	0.000000	2.853425	0.030919
1	0.224587	3.576199	-0.756560
1	-0.346805	3.414322	0.908229
1	0.944873	2.376996	0.322855
6	-2.469319	0.262868	1.444930
6	-3.645140	1.006921	1.274562
1	-3.631008	1.865716	0.607391
6	-4.816572	0.670852	1.944623
1	-5.716579	1.261567	1.800739
6	-4.832606	-0.426330	2.804961
1	-5.746022	-0.693216	3.328699

6	-3.674063	-1.175152	2.997827
1	-3.682432	-2.025647	3.673182
6	-2.505195	-0.826645	2.326331
1	-1.597479	-1.403432	2.488158
6	2.469319	-0.262868	1.444930
6	2.505195	0.826645	2.326331
1	1.597479	1.403432	2.488158
6	3.674063	1.175152	2.997827
1	3.682432	2.025647	3.673182
6	4.832606	0.426330	2.804961
1	5.746022	0.693216	3.328699
6	4.816572	-0.670852	1.944623
1	5.716579	-1.261567	1.800739
6	3.645140	-1.006921	1.274562
1	3.631008	-1.865716	0.607391
6	0.000000	-2.853425	0.030919
1	-0.944873	-2.376996	0.322855
1	-0.224587	-3.576199	-0.756560
1	0.346805	-3.414322	0.908229
6	1.723613	-2.935968	-2.525732
1	1.553015	-2.545646	-3.535501
1	2.697532	-3.440046	-2.538827
1	0.967414	-3.693720	-2.319832
6	3.993981	-0.992070	-2.323705
1	4.628012	-0.108273	-2.400945
1	4.476426	-1.688656	-1.628222
1	3.974614	-1.480072	-3.305312
1	2.236363	2.588287	-2.531407
1	3.071643	2.353841	-0.996432
1	3.799545	1.759585	-2.494013

Intermediate 2.3 (Ph migration)

E_{SCF} = -644.678173148 Hartree
Singlet, neutral

6	-0.122966	-0.242751	0.894435
6	-1.175870	-1.150765	0.265019
6	-1.039257	-2.638388	0.390082
1	-1.088510	-2.969133	1.437850
1	-1.820663	-3.173659	-0.156346
1	-0.070172	-2.982063	-0.000747
6	-2.177869	-0.424755	-0.296539
6	-3.411163	-0.984816	-0.950713
1	-4.314006	-0.634427	-0.434858
1	-3.490958	-0.645983	-1.991206
1	-3.427699	-2.077239	-0.950565
6	-1.979533	1.050269	-0.227813
6	-2.945620	2.005689	-0.871252
1	-3.956197	1.934174	-0.445539
1	-2.632172	3.050265	-0.742797
1	-3.047858	1.835714	-1.952438
5	-0.761515	1.159342	0.510344
8	0.151881	2.397780	0.755254
6	1.222195	-0.260228	0.194279
6	2.396859	0.162655	0.841511
1	2.386629	0.359464	1.911135
6	3.609438	0.278652	0.147855
1	4.502904	0.591954	0.681572
6	3.673997	-0.023098	-1.206515
1	4.613469	0.057961	-1.744993
6	2.512953	-0.443082	-1.865199
1	2.549428	-0.683922	-2.924293
6	1.309714	-0.552745	-1.179777
1	0.404776	-0.863251	-1.697016
6	-0.035548	-0.494052	2.410340
1	-1.048060	-0.515306	2.825367
1	0.449706	-1.453776	2.631219
1	0.517001	0.287679	2.944430
1	-0.044537	3.107406	0.118521
1	1.085477	2.099684	0.622682

SHPh reaction

Intermediate 2.1 (adduct)

E_{SCF} = -1198.62846574 Hartree
Singlet, neutral

5	0.909672	0.196451	0.295373
6	0.204529	1.634782	0.277930
6	-0.861127	1.545591	1.105885
6	-1.873273	2.604244	1.438000
1	-1.884737	2.821408	2.513425
1	-1.678295	3.540468	0.909468
1	-2.885602	2.270783	1.171708
6	-0.987598	0.173169	1.707240
6	-2.163644	-0.167051	2.576738
1	-2.231064	0.503912	3.442014
1	-3.103508	-0.062391	2.016769
1	-2.108391	-1.191791	2.952933
6	0.012244	-0.646096	1.312919
6	0.143509	-2.101532	1.669679
1	-0.825570	-2.584990	1.845194
1	0.655076	-2.661652	0.874206
1	0.745103	-2.251491	2.576594
6	0.643892	2.841210	-0.498898
1	0.032891	3.728316	-0.302496
1	1.686150	3.094809	-0.266936
1	0.610851	2.655473	-1.583482
6	2.464325	-0.033683	0.052752
6	3.149627	0.531517	-1.037675
1	2.598528	1.125244	-1.765902
6	4.519910	0.354214	-1.216132
1	5.019251	0.802282	-2.071151
6	5.251324	-0.393611	-0.292762
1	6.320910	-0.531343	-0.425284
6	4.600133	-0.959754	0.801202
1	5.162222	-1.539814	1.528391
6	3.225103	-0.784847	0.962595

1	2.733177	-1.229772	1.824221
6	-1.677307	-0.646290	-1.333418
6	-2.421753	0.517233	-1.526504
1	-1.938975	1.420247	-1.890673
6	-3.784263	0.515319	-1.230662
1	-4.363549	1.422141	-1.376912
6	-4.398566	-0.640401	-0.752941
1	-5.460223	-0.638365	-0.525350
6	-3.646476	-1.800649	-0.566229
6	-2.283376	-1.805691	-0.847730
1	-1.693883	-2.702409	-0.674463
1	-4.117801	-2.703000	-0.188415
16	0.070790	-0.552082	-1.635845
1	0.343153	-1.863062	-1.499125

$TS_{2.1}$ (H-migration from Int2.1)

E_{SCF} = -1198.60693916 Hartree
Singlet, neutral

5	-1.002452	0.247374	0.321311
6	0.005824	-0.298765	1.395109
6	0.998233	0.619323	1.540499
6	2.257718	0.483971	2.346401
1	2.409126	1.350186	3.001358
1	2.236877	-0.409224	2.974568
1	3.134079	0.412890	1.688013
6	0.762470	1.809704	0.702406
6	1.661635	3.001621	0.817934
1	1.563013	3.464271	1.808189
1	2.709394	2.692676	0.716350
1	1.450652	3.759802	0.062033
6	-0.333755	1.676918	-0.123682
6	-0.969188	2.769130	-0.946154
1	-1.049051	2.486316	-2.003346
1	-1.986883	2.971509	-0.592375
1	-0.407593	3.706579	-0.901324
6	-0.006150	-1.677796	1.982568
1	0.996063	-2.044589	2.229150
1	-0.606318	-1.712571	2.901553
1	-0.464965	-2.381311	1.277206
6	-2.517651	-0.082509	0.101274
6	-3.254148	-0.685361	1.132610
1	-2.756231	-0.936497	2.066240
6	-4.613972	-0.960720	0.991045
1	-5.162286	-1.421953	1.807849
6	-5.265911	-0.649478	-0.200134
1	-6.323642	-0.867999	-0.317408
6	-4.553097	-0.057515	-1.243861
1	-5.054261	0.182677	-2.177415
6	-3.199495	0.226751	-1.088089
1	-2.658799	0.684467	-1.914513
6	1.761899	-0.899705	-1.146015
6	2.346978	-1.990637	-0.487748
1	1.730325	-2.847395	-0.230221
6	3.701380	-1.975196	-0.169290
1	4.144402	-2.829514	0.334845
6	4.489431	-0.868232	-0.492972
1	5.546362	-0.859319	-0.243165
6	3.913846	0.220543	-1.144438
6	2.557849	0.205993	-1.473126
1	2.112589	1.047355	-1.998232
1	4.521544	1.081471	-1.409850
16	0.034578	-0.912635	-1.541993
1	-0.088770	0.627216	-0.980186

Product 2.1 (Prod2.1, ring opened product)

E_{SCF} = -1198.66272915 Hartree
Singlet, neutral

6	2.226496	1.260946	2.661616
6	1.152376	1.373354	1.623141
6	1.255033	2.025426	0.453130
6	0.195038	1.921115	-0.577426
6	-0.314412	0.722210	-0.951317
6	-1.408541	0.665886	-2.003082
1	-2.360714	1.063047	-1.625091
1	-1.131504	1.259347	-2.882830
1	-1.597147	-0.357662	-2.338634
5	0.218826	-0.613607	-0.339821
16	-0.924210	-1.872147	0.320969
6	-2.524804	-1.075854	0.333100
6	-2.758164	0.078811	1.084227
6	-4.013353	0.682625	1.062879
6	-5.047185	0.129518	0.307267
1	-6.025100	0.601455	0.293132
6	-4.821233	-1.035819	-0.423221
6	-3.563897	-1.637715	-0.411681
1	-3.379621	-2.536913	-0.993132
1	-5.621938	-1.475756	-1.010627
1	-4.183510	1.585409	1.642503
1	-1.956008	0.512208	1.673832
6	1.729893	-1.044289	-0.361602
6	2.256834	-2.008595	0.514684
1	1.607226	-2.474003	1.253188
6	3.601821	-2.369504	0.473736
1	3.985434	-3.111185	1.168878
6	4.454164	-1.779300	-0.459161
1	5.502691	-2.061670	-0.495648
6	3.953899	-0.825378	-1.345030
1	4.611715	-0.363711	-2.076528
6	2.610021	-0.462426	-1.290183
1	2.230614	0.291330	-1.977094
6	-0.292804	3.213986	-1.196670
1	0.081775	4.086239	-0.654495
1	0.015633	3.308145	-2.246207
1	-1.388018	3.253598	-1.181720
6	2.489674	2.819653	0.080974

1	2.335813	3.389720	-0.839344
1	2.790802	3.520734	0.866031
1	3.329321	2.134664	-0.096144
1	0.229966	0.832175	1.831599
1	3.018547	2.001507	2.524776
1	1.821036	1.369816	3.672648
1	2.691088	0.265996	2.602222

Product 2.2 (Prod2.2, ring closed product)

E_{SCF} = -1198.68090192 Hartree
Singlet, neutral

6	-1.482594	0.481043	0.811685
6	-1.775258	1.828011	0.146266
6	-3.159263	2.396337	0.269363
1	-3.360034	2.715680	1.299848
1	-3.320458	3.259368	-0.380758
1	-3.907368	1.634222	0.018015
6	-0.723792	2.365479	-0.496548
6	-0.692693	3.670870	-1.239193
1	-0.112766	4.423418	-0.690774
1	-0.205178	3.543791	-2.214215
1	-1.690128	4.082646	-1.409736
6	0.549937	1.531493	-0.426858
1	0.840850	1.216376	-1.443889
6	1.737986	2.309287	0.172588
1	1.515654	2.626443	1.198587
1	2.645995	1.699869	0.192795
1	1.953551	3.208711	-0.414952
5	0.062636	0.301847	0.444941
16	0.974111	-1.115931	1.057114
6	2.597548	-0.943872	0.325698
6	2.764114	-1.005602	-1.059537
6	4.034688	-0.862274	-1.613082
1	4.158090	-0.902324	-2.691473
6	5.143667	-0.676710	-0.787947
6	4.978591	-0.641808	0.595811
6	3.708428	-0.775461	1.154299
1	3.573047	-0.733361	2.231300
1	5.838635	-0.503463	1.244489
1	6.133004	-0.566733	-1.221706
1	1.899524	-1.165048	-1.698300
6	-2.272641	-0.643341	0.143571
6	-2.898512	-1.663393	0.867904
1	-2.867709	-1.660408	1.952792
6	-3.571363	-2.698771	0.217200
1	-4.051228	-3.476601	0.804799
6	-3.631206	-2.737998	-1.172822
1	-4.155365	-3.543897	-1.677970
6	-3.011880	-1.727974	-1.909060
1	-3.051936	-1.741989	-2.994829
6	-2.343266	-0.696105	-1.257389
1	-1.875325	0.094487	-1.841165
6	-1.712578	0.555408	2.331062
1	-1.177736	1.416508	2.746412
1	-2.777293	0.669526	2.570174
1	-1.344246	-0.339275	2.843957

Intermediate 2.3 (Ph migration from Int2.1)

E_{SCF} = -1198.5929058 Hartree
Singlet, neutral

5	0.035882	0.618515	0.470521
6	1.001063	0.163572	-0.717013
6	1.780837	1.469496	-0.897372
6	2.851158	1.541570	-1.942803
1	3.396685	2.488476	-1.917453
1	3.579715	0.730255	-1.807804
1	2.435616	1.427261	-2.953987
6	1.354602	2.441930	-0.052307
6	1.877946	3.850103	0.024058
1	2.684220	4.035269	-0.689430
1	1.079784	4.575596	-0.177774
1	2.260271	4.072257	1.028208
6	0.259577	1.990923	0.844431
6	-0.339167	2.914361	1.864604
1	0.404558	3.278664	2.586580
1	-0.787589	3.805237	1.402743
1	-1.135552	2.426561	2.442588
6	0.221681	-0.151588	-2.006835
1	0.892621	-0.401637	-2.839552
1	-0.472474	-0.991820	-1.878343
1	-0.368906	0.724000	-2.297739
6	1.915747	-0.970331	-0.276741
6	2.814228	-0.750639	0.781964
1	2.841379	0.236340	1.240579
6	3.653294	-1.758755	1.238099
1	4.340610	-1.558717	2.055924
6	3.616683	-3.027183	0.649766
1	4.272748	-3.816825	1.004578
6	2.733544	-3.261705	-0.396807
1	2.695507	-4.239772	-0.869345
6	1.892811	-2.241790	-0.856690
1	1.220774	-2.451886	-1.683417
6	-2.733367	-0.533795	0.449333
6	-3.077303	0.583083	-0.305285
1	-2.382335	1.419014	-0.371431
6	-4.301821	0.592023	-0.969731
1	-4.585703	1.457894	-1.560146
6	-5.155744	-0.508108	-0.883769
1	-6.106037	-0.497676	-1.409047
6	-4.790904	-1.624218	-0.132492
6	-3.569517	-1.643336	0.540108
1	-3.269692	-2.509914	1.123064
1	-5.452052	-2.483276	-0.072414
16	-1.141413	-0.590428	1.324214

1	-1.493037	0.175292	2.376476

Intermediate 2.2 (H migration from Int2.1)

E_{SCF} = -1198.65663263 Hartree
Singlet, neutral

5	-0.899049	0.195063	-0.126033
6	-0.207552	1.295856	0.748594
6	0.937907	1.832600	-0.035432
6	1.817885	2.904361	0.540202
1	2.690959	3.104235	-0.085081
1	1.266317	3.845868	0.656696
1	2.176443	2.629043	1.540180
6	1.060384	1.199759	-1.223165
6	2.179167	1.350058	-2.208286
1	2.860240	2.168695	-1.964335
1	2.764958	0.420241	-2.234727
1	1.795750	1.516241	-3.221499
6	-0.053319	0.202145	-1.497453
6	-0.958697	0.681604	-2.650652
1	-1.762298	-0.039479	-2.831325
1	-1.426441	1.642510	-2.403764
1	-0.400035	0.810472	-3.584941
6	-0.819886	2.123624	1.850550
1	-0.086563	2.444213	2.598588
1	-1.258018	3.023084	1.398676
1	-1.624750	1.582442	2.356859
6	-2.405587	-0.268273	-0.005727
6	-3.432423	0.687359	0.025464
1	-3.175500	1.745852	0.025017
6	-4.777315	0.315784	0.049924
1	-5.551537	1.078138	0.072570
6	-5.125723	-1.033310	0.050124
1	-6.171059	-1.328449	0.073825
6	-4.122796	-2.003098	0.021905
1	-4.386342	-3.057463	0.024304
6	-2.783826	-1.619234	-0.008125
1	-2.010358	-2.385862	-0.024009
6	1.807174	-0.975507	0.829707
6	2.976647	-0.304257	1.197773
1	2.921422	0.526350	1.894754
6	4.203078	-0.702881	0.673094
1	5.107368	-0.172469	0.956755
6	4.270947	-1.783803	-0.206570
1	5.228957	-2.095421	-0.612094
6	3.108330	-2.468370	-0.556985
6	1.877096	-2.062210	-0.045533
1	0.964883	-2.582697	-0.325044
1	3.156168	-3.315801	-1.234461
16	0.233091	-0.500169	1.503188
1	0.376286	-0.765604	-1.794250

NH_2Ph reaction

Intermediate 2.1 (adduct)

E_{SCF} = -855.827803989 Hartree
Singlet, neutral

7	-0.222563	-1.464846	-0.434711
5	0.577013	-0.036937	-0.068754
6	0.180785	1.053973	-1.188183
6	-0.474132	2.055677	-0.563381
6	-1.011412	3.327493	-1.158857
1	-0.548427	4.209999	-0.699627
1	-0.832808	3.382754	-2.235725
1	-2.092745	3.416275	-0.992053
6	-0.631220	1.782200	0.906406
6	-1.331141	2.781406	1.785863
1	-0.838274	3.761050	1.748484
1	-2.367382	2.936051	1.459127
1	-1.357523	2.460797	2.829968
6	-0.077585	0.601071	1.259128
6	0.007302	0.026231	2.643115
1	-0.442623	0.662828	3.412283
1	-0.491103	-0.952197	2.708036
1	1.055558	-0.147761	2.923638
6	0.554484	0.972157	-2.638599
1	0.158868	1.793153	-3.246444
1	1.646410	0.962297	-2.755296
1	0.198917	0.034689	-3.100815
6	2.146079	-0.405215	-0.003557
6	2.748628	-1.455653	-0.713443
1	2.150408	-2.114151	-1.346682
6	4.123624	-1.699114	-0.661763
1	4.550127	-2.524792	-1.225718
6	4.944897	-0.879141	0.106289
1	6.014872	-1.061534	0.151882
6	4.377600	0.181818	0.814697
1	5.009003	0.831698	1.415271
6	3.004579	0.406538	0.758921
1	2.575555	1.238051	1.316177
6	-1.670354	-1.441679	-0.297639
6	-2.434824	-0.748734	-1.231446
1	-1.952664	-0.236549	-2.057890
6	-3.818020	-0.701643	-1.073249
1	-4.418217	-0.159340	-1.797336
6	-4.428779	-1.338789	0.005689
1	-5.506863	-1.294906	0.124904
6	-3.651891	-2.036810	0.927979
6	-2.268583	-2.092877	0.775524
1	-1.659724	-2.636418	1.493890
1	-4.118943	-2.540589	1.768471
1	0.171557	-2.195083	0.164550
1	0.028669	-1.721157	-1.393313

TS $_{2.1}$ (H-migration from Int2.1)

E_{SCF} = -855.780235608 Hartree
Singlet, neutral

7	-0.722062	-0.650195	1.058617
5	0.472262	0.029648	0.186075
6	-0.083461	0.837818	-1.070537
6	0.114952	2.165772	-0.886686
6	-0.227227	3.289677	-1.825503
1	-0.660452	2.915253	-2.755544
1	-0.947189	3.984817	-1.374662
1	0.661837	3.876403	-2.087283
6	0.753054	2.438422	0.418906
6	1.329597	3.793219	0.709180
1	2.170917	4.002699	0.035435
1	0.585407	4.579132	0.535476
1	1.687491	3.873331	1.737857
6	0.870657	1.345550	1.231735
6	1.723761	1.299215	2.478383
1	1.412166	2.039356	3.225198
1	1.663226	0.312559	2.951536
1	2.783773	1.477511	2.256614
6	-0.698135	0.172429	-2.263937
1	-1.338472	-0.662825	-1.956033
1	-1.297757	0.846499	-2.883925
1	0.093328	-0.258173	-2.892187
6	1.713161	-0.951905	-0.037407
6	1.514835	-2.331708	-0.182944
1	0.506742	-2.739681	-0.107845
6	2.577053	-3.200120	-0.442284
1	2.392705	-4.265622	-0.552180
6	3.871072	-2.699372	-0.562976
1	4.702143	-3.370716	-0.760069
6	4.091418	-1.327380	-0.430224
1	5.097562	-0.927656	-0.526123
6	3.024173	-0.470913	-0.171049
1	3.207617	0.598246	-0.073208
6	-2.079416	-0.775834	0.684150
6	-2.818525	0.354600	0.315290
1	-2.342396	1.330923	0.334888
6	-4.147939	0.222335	-0.075350
1	-4.706750	1.107209	-0.366681
6	-4.768228	-1.026913	-0.078465
1	-5.807338	-1.123290	-0.377213
6	-4.041416	-2.148929	0.316076
6	-2.705771	-2.026954	0.691310
1	-2.136857	-2.908120	0.980489
1	-4.510875	-3.128476	0.324234
1	-0.209709	0.522221	1.463491
1	-0.395684	-1.432541	1.621028

Product 2.1 (Prod2.1, ring opened product)

E_{SCF} = -855.857441688 Hartree
Singlet, neutral

6	1.829924	0.747178	2.998271
6	1.056163	1.183218	1.790160
6	1.507059	1.840177	0.707105
6	0.604859	2.073260	-0.452316
6	-0.145818	1.068408	-0.957787
6	-1.099660	1.302713	-2.119790
1	-1.849328	2.071633	-1.896604
1	-0.555992	1.626325	-3.016351
1	-1.645310	0.390134	-2.377618
5	0.003142	-0.411064	-0.440435
7	-1.124884	-1.207425	-0.099068
1	-0.966336	-2.206045	-0.009824
6	-2.481340	-0.862171	0.063196
6	-2.876935	0.429733	0.431295
6	-4.228188	0.730626	0.580836
6	-5.204526	-0.245390	0.387312
1	-6.255653	-0.004550	0.511271
6	-4.811882	-1.537248	0.040281
6	-3.464460	-1.842615	-0.123188
1	-3.164444	-2.848907	-0.407792
1	-5.557139	-2.313025	-0.110409
1	-4.516846	1.738625	0.865361
1	-2.125248	1.193148	0.605594
6	1.402325	-1.147045	-0.435128
6	1.685432	-2.194646	0.456160
1	0.936789	-2.494393	1.189087
6	2.921205	-2.839445	0.457167
1	3.117991	-3.637458	1.168106
6	3.906492	-2.454688	-0.451662
1	4.870229	-2.956221	-0.457101
6	3.648870	-1.419711	-1.350072
1	4.411989	-1.115434	-2.061543
6	2.414217	-0.773277	-1.333034
1	2.227200	0.042665	-2.028752
6	0.609685	3.471220	-1.029043
1	0.660516	4.225722	-0.236258
1	1.482677	3.624271	-1.677785
1	-0.281176	3.666740	-1.629816
6	2.917013	2.351983	0.546950
1	2.925439	3.435831	0.383307
1	3.544226	2.139760	1.413646
1	3.385795	1.887744	-0.330395
1	0.001764	0.902209	1.799038
1	2.843836	1.150059	3.029798
1	1.316126	1.043119	3.919478
1	1.908762	-0.348331	3.010949

Product 2.2 (Prod2.2, ring closed product)

E_{SCF} = -855.877016076 Hartree
Singlet, neutral

6	-1.335471	0.297141	0.776613
6	-1.981278	1.580836	0.253541
6	-3.449130	1.792583	0.489554
1	-3.656068	1.932522	1.558317
1	-3.841181	2.664531	-0.038936
1	-4.019013	0.912694	0.166547
6	-1.122285	2.421142	-0.350709
6	-1.437068	3.772222	-0.926589
1	-0.991365	4.570554	-0.320060
1	-1.012046	3.865941	-1.934146
1	-2.510001	3.966890	-0.991717
6	0.313930	1.919705	-0.413588
1	0.623726	1.869204	-1.470470
6	1.294687	2.852112	0.326279
1	0.984682	2.981857	1.370071
1	2.312013	2.447381	0.327271
1	1.330703	3.845697	-0.134843
5	0.175050	0.486336	0.262197
6	2.511606	-0.588321	0.173457
6	3.061484	0.126022	-0.895912
6	4.422251	0.030671	-1.175060
1	4.832459	0.593386	-2.008773
6	5.251837	-0.787815	-0.410269
6	4.701665	-1.516818	0.642765
6	3.344918	-1.416316	0.934585
1	2.923031	-1.976642	1.766013
1	5.330931	-2.164508	1.246343
1	6.310776	-0.862257	-0.636579
1	2.420669	0.740784	-1.517772
6	-1.941620	-0.946881	0.142176
6	-2.251351	-2.101669	0.869564
1	-2.112659	-2.122244	1.946385
6	-2.756353	-3.240331	0.236229
1	-2.991289	-4.121365	0.827359
6	-2.965476	-3.247427	-1.138759
1	-3.360550	-4.131407	-1.630518
6	-2.665699	-2.101803	-1.878493
1	-2.826715	-2.090077	-2.953002
6	-2.160981	-0.971738	-1.245243
1	-1.937562	-0.080369	-1.829061
6	-1.384803	0.266985	2.315694
1	-1.000626	1.209779	2.719696
1	-2.408648	0.132209	2.687193
1	-0.772406	-0.541086	2.733306
7	1.139433	-0.511994	0.493244
1	0.814660	-1.332998	0.998659

Intermediate 2.3 (Ph migration from Int2.1)

E_{SCF} = -855.798569123 Hartree
Singlet, neutral

6	-1.646752	0.004182	0.801565
6	-2.539214	0.837739	-0.108147
6	-3.938045	0.381733	-0.393167
1	-4.547906	0.336936	0.521152
1	-4.455348	1.039286	-1.097237
1	-3.944099	-0.631438	-0.821919
6	-1.897693	1.956430	-0.533215
6	-2.483571	3.025716	-1.414684
1	-2.449006	4.001901	-0.914879
1	-1.907859	3.127565	-2.343191
1	-3.523024	2.824378	-1.684766
6	-0.495896	2.066860	-0.049556
6	0.371591	3.217675	-0.481011
1	-0.010540	4.186600	-0.128209
1	1.394566	3.119754	-0.101431
1	0.445616	3.292915	-1.575385
5	-0.319178	0.904295	0.775471
6	-1.253332	-1.330259	0.201126
6	-0.933861	-2.445195	0.991092
1	-1.103686	-2.418549	2.065067
6	-0.429270	-3.622027	0.422705
1	-0.194425	-4.468067	1.063406
6	-0.245300	-3.715112	-0.951544
1	0.138084	-4.628888	-1.395986
6	-0.577951	-2.618558	-1.756478
1	-0.447616	-2.678360	-2.833915
6	-1.067845	-1.449316	-1.189843
1	-1.301157	-0.589584	-1.814012
6	-2.267481	-0.112628	2.204082
1	-2.585463	0.880496	2.537662
1	-3.143194	-0.775982	2.210153
1	-1.567691	-0.500694	2.957577
7	0.958105	0.335078	1.538116
1	1.125212	0.864191	2.397312
6	2.189735	0.282128	0.748630
6	3.168904	1.246968	0.938761
6	2.334006	-0.733707	-0.190661
6	4.324285	1.200401	0.158593
1	3.028960	2.035683	1.674343
6	3.494942	-0.774360	-0.956418
1	1.545262	-1.470847	-0.328892
6	4.488596	0.191390	-0.786724
1	5.092750	1.954905	0.294361
1	3.618803	-1.563008	-1.691951
1	5.389167	0.156281	-1.391706
1	0.716664	-0.622861	1.827633

Product 2.3 (Prod2.3, Bisborole)

E_{SCF} = -1424.20745325 Hartree
Singlet, neutral

6	-2.744843	-2.444425	2.459307
6	-1.976970	-2.385551	1.173227
1	-0.912744	-2.168454	1.243961
6	-2.483823	-2.567264	-0.056817
6	-1.619006	-2.363109	-1.243821
6	-0.944972	-1.201076	-1.398907
5	-1.203987	0.067496	-0.495415
7	-0.085162	0.843616	-0.003041
5	1.214302	0.260228	0.403352
6	1.240849	-0.840783	1.526046
6	2.088069	-1.898485	1.545822
6	2.908995	-2.255964	0.366374
6	2.320960	-2.428396	-0.828579
1	1.235944	-2.353069	-0.867300
6	3.031298	-2.717274	-2.117305
1	4.056891	-3.062316	-1.959489
1	2.499877	-3.476639	-2.701540
1	3.078028	-1.809964	-2.735879
6	4.403213	-2.409480	0.567924
1	4.692196	-2.180637	1.598011
1	4.750600	-3.423575	0.338114
1	4.944142	-1.713152	-0.083133
6	2.212424	-2.806168	2.751385
1	2.352439	-2.243514	3.681110
1	1.297493	-3.402954	2.866986
1	3.043085	-3.508324	2.642152
6	0.366322	-0.557883	2.738840
1	0.028821	-1.469248	3.244336
1	0.914614	0.038042	3.483123
1	-0.524136	0.015130	2.457904
6	2.538784	0.944344	-0.109322
6	3.739411	0.868817	0.614430
1	3.753132	0.332959	1.561553
6	4.909296	1.467809	0.151196
1	5.823010	1.401528	0.736024
6	4.906002	2.149929	-1.064912
1	5.816986	2.614238	-1.432714
6	3.725713	2.241832	-1.803610
1	3.715018	2.778483	-2.748267
6	2.558403	1.655608	-1.321493
1	1.637918	1.754556	-1.893627
6	-0.197698	2.259506	0.146600
6	-0.794300	3.044661	-0.846884
6	-0.901116	4.422497	-0.690070
6	-0.395766	5.045051	0.451779
6	0.214421	4.272244	1.437215
6	0.307287	2.890174	1.289145
1	0.769028	2.289690	2.070503
1	0.615705	4.742859	2.330226
1	-0.474056	6.121567	0.569160
1	-1.373895	5.013709	-1.469133
1	-1.175414	2.563443	-1.744339
6	-2.686666	0.591227	-0.321474
6	-3.091526	1.266959	0.842284
1	-2.357092	1.485264	1.615783
6	-4.411946	1.666500	1.029794
1	-4.700729	2.175257	1.945525
6	-5.360989	1.426324	0.034379
1	-6.389382	1.749226	0.171709
6	-4.982016	0.771376	-1.135848
1	-5.714905	0.580995	-1.915509
6	-3.663063	0.346989	-1.298798
1	-3.384849	-0.191533	-2.203297
6	-0.043728	-0.969414	-2.598289
1	0.875491	-0.445789	-2.310927
1	0.248485	-1.895278	-3.104084
1	-0.546658	-0.331443	-3.339946
6	-1.533272	-3.512389	-2.228490
1	-2.223390	-4.316776	-1.959908
1	-1.755017	-3.199236	-3.254871
1	-0.522723	-3.941634	-2.228098
6	-3.935200	-2.925769	-0.300951
1	-4.229155	-3.849236	0.210631
1	-4.584142	-2.118047	0.058931
1	-4.139026	-3.050040	-1.368552
1	-2.231014	-3.064554	3.203033
1	-2.837857	-1.437388	2.889461
1	-3.755434	-2.838572	2.322919

PH_2Ph reaction

Intermediate 2.1 (adduct)

E_{SCF} = -1142.39033135 Hartree
Singlet, neutral

15	-0.019809	-0.223255	1.497999
5	0.957082	0.020152	-0.242691
6	0.229046	-1.154184	-1.064207
6	-0.798194	-0.584171	-1.747776
6	-1.818694	-1.261009	-2.620030
1	-1.778369	-0.882077	-3.648863
1	-1.675244	-2.343745	-2.657706
1	-2.835228	-1.069845	-2.250226
6	-0.865396	0.880703	-1.519667
6	-1.984768	1.698619	-2.100068
1	-2.049124	1.578637	-3.188360
1	-2.952869	1.382701	-1.685713
1	-1.859748	2.763846	-1.888376
6	0.130073	1.317831	-0.705133
6	0.307452	2.739708	-0.237793
1	0.833747	3.348367	-0.986025
1	-0.645889	3.244369	-0.032577
1	0.913151	2.786516	0.675920
6	0.606105	-2.607362	-1.055103
1	-0.010787	-3.219001	-1.721705
1	1.653858	-2.736395	-1.355356

1	0.525939	-3.044661	-0.047128
6	2.528021	0.020942	0.055960
6	3.171856	-1.054963	0.691565
1	2.586125	-1.917101	1.011157
6	4.547258	-1.062509	0.917952
1	5.012351	-1.912149	1.411200
6	5.325905	0.019060	0.506828
1	6.398637	0.018628	0.679005
6	4.715273	1.097930	-0.130016
1	5.313455	1.943315	-0.460186
6	3.336850	1.095266	-0.346125
1	2.878382	1.941977	-0.851826
6	-1.826962	-0.186626	1.375678
6	-2.518496	-1.312790	0.919966
1	-1.982481	-2.236152	0.712482
6	-3.894689	-1.246398	0.709816
1	-4.427759	-2.123266	0.354474
6	-4.581364	-0.056428	0.946573
1	-5.653062	-0.005755	0.778137
6	-3.893041	1.069448	1.398185
6	-2.517989	1.005906	1.610184
1	-1.980889	1.890231	1.945708
1	-4.424617	1.998722	1.579666
1	0.243207	0.730668	2.501177
1	0.239459	-1.403595	2.227861

$TS_{2.1}$ (H-migration from Int2.1)

E_{SCF} = -1142.33678722 Hartree
Singlet, neutral

5	-0.920908	-0.025205	-0.117621
6	-0.598829	0.970854	1.089960
6	-1.298814	2.148411	0.936537
6	-1.262011	3.358360	1.830484
1	-0.560358	3.223934	2.656869
1	-0.964731	4.259290	1.280130
1	-2.248428	3.558934	2.266314
6	-2.099318	2.116497	-0.261592
6	-2.920672	3.296666	-0.684982
1	-3.606304	3.587168	0.119528
1	-2.281067	4.166510	-0.883288
1	-3.510833	3.091154	-1.579894
6	-1.899907	0.938171	-0.998058
6	-2.691801	0.525813	-2.212646
1	-3.000171	1.366334	-2.843330
1	-2.111149	-0.166771	-2.831166
1	-3.594694	-0.015296	-1.904774
6	0.298702	0.632473	2.240667
1	1.077028	-0.075353	1.937348
1	0.779704	1.498479	2.708338
1	-0.298649	0.122232	3.008767
6	-1.225987	-1.566372	0.127384
6	-0.212195	-2.533009	0.215468
1	0.824638	-2.230366	0.071569
6	-0.495215	-3.872779	0.481132
1	0.313946	-4.596077	0.542827
6	-1.814475	-4.284775	0.664000
1	-2.040174	-5.328105	0.866643
6	-2.841704	-3.345187	0.583731
1	-3.874070	-3.654537	0.726091
6	-2.544946	-2.008075	0.321309
1	-3.358795	-1.285993	0.271785
6	2.362112	0.306343	-0.689610
6	2.946223	1.200594	0.214588
1	2.371245	2.053679	0.569548
6	4.251780	1.003293	0.658832
1	4.693425	1.701789	1.363810
6	4.993374	-0.080927	0.190942
1	6.013343	-0.231327	0.532091
6	4.423511	-0.968114	-0.721923
6	3.114379	-0.777639	-1.159688
1	2.674023	-1.477882	-1.865890
1	4.997741	-1.812456	-1.092561
1	-0.693972	1.570526	-1.479269
15	0.632410	0.572596	-1.225215
1	0.611438	-0.152377	-2.434385

Product 2.1 (Prod2.1, ring opened product)

E_{SCF} = -1142.38487989 Hartree
Singlet, neutral

6	2.150715	1.422692	2.770914
6	1.144984	1.548719	1.667040
6	1.331057	2.093736	0.451225
6	0.281899	1.965360	-0.591479
6	-0.243699	0.750416	-0.869959
6	-1.309982	0.589442	-1.939232
1	-1.005432	1.089499	-2.866813
1	-1.491960	-0.463661	-2.175103
1	-2.272826	1.017109	-1.629080
5	0.272696	-0.537304	-0.149384
15	-0.911833	-1.588436	0.966154
1	-0.877219	-2.818233	0.266902
6	-2.590176	-1.013704	0.506522
6	-3.031117	0.217327	1.010446
6	-4.284690	0.719799	0.668931
6	-5.128652	-0.011877	-0.166194
1	-6.107947	0.376345	-0.430132
6	-4.710035	-1.249746	-0.652638
6	-3.450030	-1.744953	-0.320871
1	-3.127831	-2.702699	-0.722963
1	-5.362479	-1.829513	-1.299659
1	-4.604704	1.681206	1.060924
1	-2.383990	0.794934	1.667872
6	1.742570	-1.051376	-0.320193
6	2.327294	-1.976089	0.564586
1	1.756221	-2.335445	1.419140
6	3.633080	-2.425726	0.388166

1	4.065503	-3.130190	1.093192
6	4.384461	-1.972574	-0.696863
1	5.401469	-2.326872	-0.840743
6	3.826040	-1.064380	-1.595656
1	4.406359	-0.711402	-2.443832
6	2.524365	-0.606673	-1.401837
1	2.097993	0.110349	-2.100427
6	-0.145765	3.218146	-1.324459
1	0.109323	4.119743	-0.759993
1	0.330092	3.294557	-2.311491
1	-1.228317	3.218670	-1.488347
6	2.611414	2.770527	0.024489
1	2.410213	3.575751	-0.689022
1	3.167221	3.195629	0.863118
1	3.260724	2.043652	-0.482892
1	0.161894	1.130816	1.884859
1	3.108681	1.886522	2.526866
1	1.777683	1.862003	3.702960
1	2.340938	0.359907	2.971656

Product 2.2 (Prod2.2, ring closed product)

E_{SCF} = -1142.4027099 Hartree
Singlet, neutral

6	-1.322852	0.425012	0.723792
6	-1.664154	1.863314	0.321486
6	-2.970294	2.448204	0.775400
1	-2.991517	2.548050	1.868237
1	-3.159244	3.436739	0.350404
1	-3.803935	1.791451	0.499005
6	-0.695032	2.472967	-0.384361
6	-0.698814	3.887073	-0.890483
1	0.007671	4.509670	-0.327618
1	-0.381144	3.916582	-1.940296
1	-1.682072	4.358224	-0.821005
6	0.534564	1.605752	-0.624992
1	0.762066	1.544489	-1.702662
6	1.790252	2.172079	0.078365
1	1.641756	2.221287	1.163901
1	2.672837	1.555590	-0.114993
1	2.005340	3.187876	-0.271748
5	0.062394	0.212682	-0.040141
6	2.636378	-1.155126	-0.146962
6	3.400256	-0.906501	-1.293210
6	4.750577	-0.572972	-1.190389
1	5.326838	-0.374195	-2.089538
6	5.360935	-0.506908	0.060560
6	4.614255	-0.776886	1.207824
6	3.261158	-1.092093	1.104967
1	2.682006	-1.277457	2.006712
1	5.084011	-0.730888	2.186340
1	6.413608	-0.252733	0.142158
1	2.934151	-0.972204	-2.273786
6	-2.348996	-0.580205	0.219285
6	-2.785823	-1.670150	0.980353
1	-2.431613	-1.802967	1.997923
6	-3.683155	-2.601226	0.453570
1	-4.007324	-3.437661	1.066641
6	-4.163355	-2.461258	-0.844907
1	-4.861740	-3.185657	-1.253356
6	-3.739329	-1.377695	-1.615322
1	-4.106635	-1.253562	-2.630246
6	-2.844317	-0.452971	-1.088417
1	-2.522691	0.392717	-1.694008
6	-1.092886	0.336950	2.246716
1	-0.403165	1.124381	2.569156
1	-2.033647	0.466856	2.796507
1	-0.661490	-0.625581	2.542871
15	0.840449	-1.494635	-0.353984
1	0.561012	-2.129060	0.880217

Intermediate 2.3 (Ph migration from Int2.1)

E_{SCF} = -1142.3609863 Hartree
Singlet, neutral

6	-1.805079	0.263162	0.791666
6	-2.433102	1.366557	-0.059423
6	-3.893719	1.297994	-0.383550
1	-4.510574	1.393403	0.521219
1	-4.205910	2.081756	-1.078575
1	-4.144550	0.328053	-0.834699
6	-1.534923	2.324571	-0.401737
6	-1.816934	3.568548	-1.199028
1	-1.602621	4.467585	-0.607725
1	-1.179374	3.617691	-2.090456
1	-2.857180	3.627048	-1.527743
6	-0.173260	2.035776	0.105859
6	0.968579	2.962107	-0.202035
1	0.776347	3.979287	0.166268
1	1.904598	2.624249	0.255438
1	1.146680	3.053311	-1.283947
5	-0.287096	0.795828	0.844201
6	-1.860562	-1.082206	0.084681
6	-2.231842	-2.269171	0.724447
1	-2.552573	-2.250723	1.761886
6	-2.212123	-3.494658	0.047845
1	-2.510359	-4.399136	0.571650
6	-1.823854	-3.557094	-1.284522
1	-1.811819	-4.506708	-1.811514
6	-1.455207	-2.377899	-1.941057
1	-1.155182	-2.408928	-2.985293
6	-1.472812	-1.164777	-1.265325
1	-1.188206	-0.246504	-1.776849
6	-2.469383	0.246038	2.179456
1	-2.435657	1.252540	2.609208

1	-3.520251	-0.070008	2.126615
1	-1.958072	-0.428593	2.876847
15	1.129061	-0.265137	1.497413
1	1.627837	-0.089901	2.805698
6	2.667909	-0.263104	0.525250
6	3.901949	-0.507064	1.135196
6	2.600016	-0.020724	-0.849434
6	5.065208	-0.518302	0.369353
1	3.958909	-0.685536	2.206512
6	3.766411	-0.036720	-1.611122
1	1.636800	0.192763	-1.307921
6	4.996546	-0.285214	-1.003925
1	6.023364	-0.705003	0.844767
1	3.713755	0.152134	-2.678999
1	5.904298	-0.292220	-1.600054
1	0.736388	-1.615557	1.579900

Intermediate 2.2 (H migration from Int2.1)

E_{SCF} = -1142.39255562 Hartree
Singlet, neutral

5	-0.914661	0.112565	-0.034088
1	0.319289	-0.922736	-1.753752
6	-0.279366	1.344126	0.643581
6	0.879309	1.778695	-0.090445
6	1.798923	2.875582	0.370458
1	1.295554	3.850296	0.357602
1	2.138474	2.706229	1.399106
1	2.688952	2.946935	-0.260250
6	1.034194	1.021744	-1.223636
6	2.200311	1.100290	-2.159091
1	2.432175	2.133867	-2.438684
1	3.096531	0.681778	-1.677808
1	2.013162	0.527225	-3.071472
6	-0.089274	0.047637	-1.439354
6	-1.000546	0.549723	-2.583593
1	-0.449015	0.667866	-3.524471
1	-1.817310	-0.159488	-2.748344
1	-1.447293	1.516516	-2.325359
6	-0.752052	2.101465	1.845365
1	0.056277	2.339591	2.547672
1	-1.164231	3.062895	1.505362
1	-1.546313	1.569566	2.376412
6	-2.467621	-0.236421	0.047878
6	-2.944832	-1.553247	-0.046844
1	-2.229528	-2.373116	-0.094416
6	-4.308049	-1.840852	-0.070956
1	-4.644323	-2.871784	-0.145432
6	-5.241474	-0.806616	0.006253
1	-6.305407	-1.026650	-0.007777
6	-4.797071	0.510436	0.101883
1	-5.514903	1.324629	0.159927
6	-3.428534	0.784124	0.120238
1	-3.100345	1.821164	0.181390
15	0.121321	-1.072648	1.376520
6	1.858557	-1.106296	0.830398
6	2.852338	-0.255989	1.338699
6	2.221307	-2.024729	-0.166761
6	4.160428	-0.316704	0.865590
1	2.594654	0.462383	2.113752
6	3.527062	-2.085023	-0.648967
1	1.470596	-2.705676	-0.563184
6	4.500354	-1.228338	-0.135753
1	4.914689	0.349941	1.274705
1	3.785446	-2.803274	-1.421824
1	5.519810	-1.274664	-0.507806
1	0.302763	-0.254243	2.517620

Product 2.3 (Prod2.3, bisborole)

E_{SCF} = -1710.69376701 Hartree
Singlet, neutral

6	-4.021670	-0.805726	2.867939
6	-3.153405	-1.474188	1.847831
1	-2.080760	-1.333714	1.975977
6	-3.560431	-2.176268	0.778608
6	-2.574319	-2.646286	-0.224124
6	-1.650328	-1.811772	-0.761592
5	-1.634185	-0.285713	-0.407338
15	-0.000009	0.539601	0.000346
5	1.634132	-0.285802	0.407667
6	1.650257	-1.811913	0.761735
6	2.574047	-2.646456	0.223987
6	3.560142	-2.176431	-0.778810
6	3.153038	-1.474282	-1.847950
1	2.080379	-1.333683	-1.975860
6	4.021001	-0.805868	-2.868355
1	5.061723	-1.132749	-2.819184
1	3.649868	-0.980015	-3.883316
1	4.011576	0.279718	-2.699793
6	5.010464	-2.461016	-0.470653
1	5.124037	-3.395607	0.086445
1	5.629654	-2.526936	-1.367922
1	5.410921	-1.656659	0.160390
6	2.625184	-4.113818	0.597190
1	3.005609	-4.266165	1.615268
1	1.621506	-4.552576	0.564174
1	3.259382	-4.680644	-0.088586
6	0.639260	-2.363960	1.749421
1	-0.157750	-2.929439	1.246537
1	1.114255	-3.040607	2.468618
1	0.157094	-1.562599	2.315183
6	2.923510	0.604216	0.538433
6	3.869270	0.301426	1.531569
1	3.695440	-0.551655	2.183350
6	5.023633	1.064233	1.694261
1	5.733232	0.814513	2.477944

6	5.270146	2.140554	0.846177	6	-5.269816	2.141179	-0.846072
1	6.172499	2.733275	0.964309	1	-6.172059	2.734050	-0.964287
6	4.353296	2.453161	-0.156517	6	-5.023466	1.064727	-1.694041
1	4.541133	3.288586	-0.824582	1	-5.733090	0.815048	-2.477716
6	3.191804	1.701391	-0.297778	6	-3.869234	0.301749	-1.531252
1	2.480667	1.963986	-1.077809	1	-3.695534	-0.551429	-2.182940
6	0.000152	2.359479	0.000081	6	-0.639285	-2.363761	-1.749250
6	-0.560246	3.071455	-1.067662	1	-0.157092	-1.562351	-2.314924
6	-0.568388	4.463009	-1.062275	1	0.157705	-2.929259	-1.246368
6	0.000497	5.162142	-0.000330	1	-1.114248	-3.040337	-2.468529
6	0.569206	4.463180	1.061822	6	-2.625721	-4.113562	-0.597626
6	0.560718	3.071630	1.067619	1	-3.260158	-4.680364	0.087952
1	1.002981	2.530212	1.899296	1	-3.006049	-4.265615	-1.615785
1	1.014860	5.001432	1.892820	1	-1.622153	-4.552557	-0.564558
1	0.000632	6.247902	-0.000489	6	-5.010832	-2.460612	0.470479
1	-1.013908	5.001127	-1.893432	1	-5.629530	-2.528934	1.367926
1	-1.002639	2.529903	-1.899184	1	-5.411909	-1.654857	-0.158389
6	-2.923437	0.604477	-0.538120	1	-5.124365	-3.393876	-0.088832
6	-3.191583	1.701764	0.297990	1	-3.650525	-0.979245	3.882998
1	-2.480437	1.964302	1.078032	1	-4.012756	0.279794	2.698874
6	-4.352943	2.453721	0.156619	1	-5.062243	-1.133115	2.818823
1	-4.540658	3.289238	0.824603				

.

APPENDIX B

Supplementary Information for Chapter Three

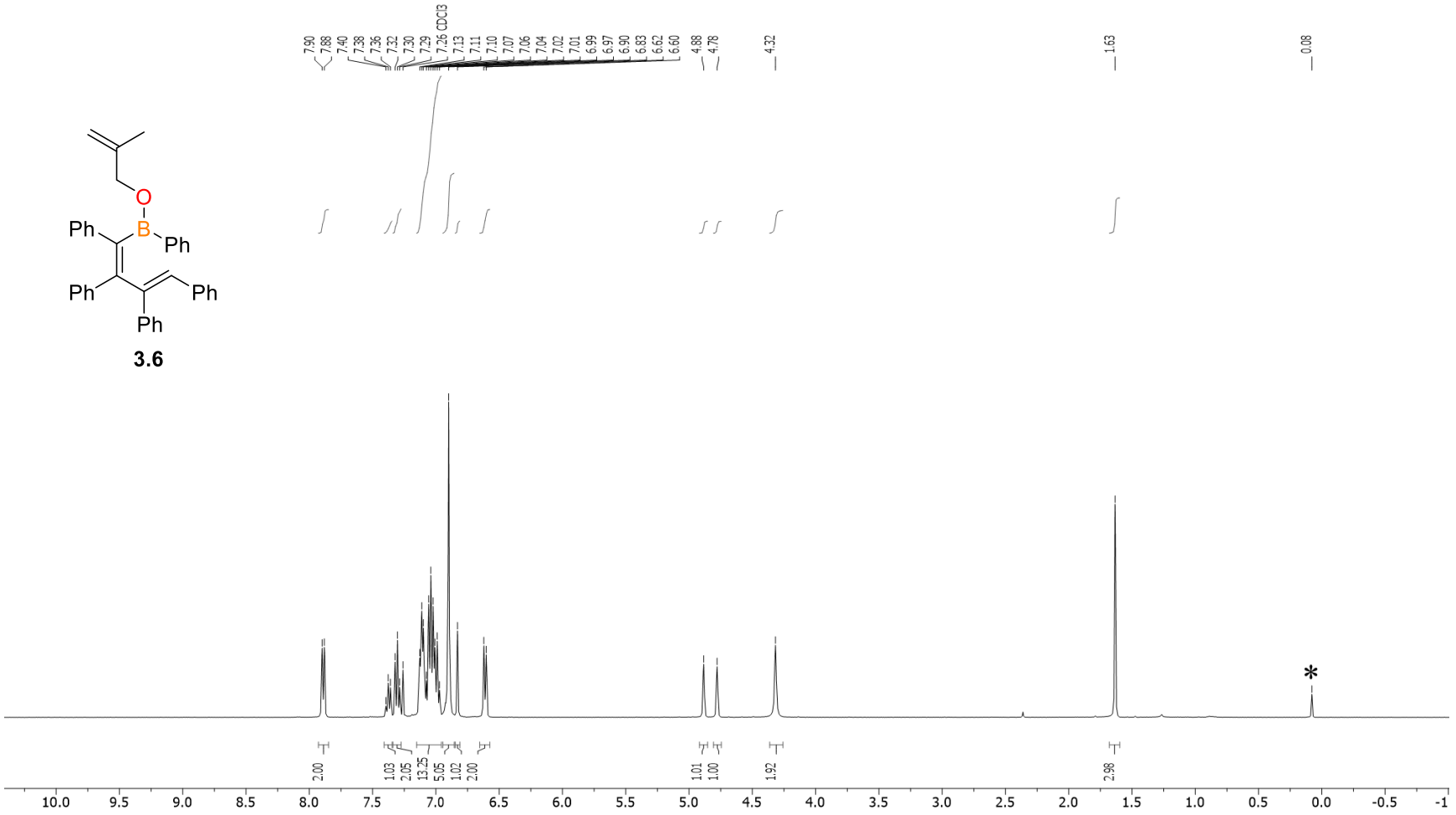

Figure B-1: ^{1}H NMR spectrum of **3.6** in $CDCl_3$ (*grease).

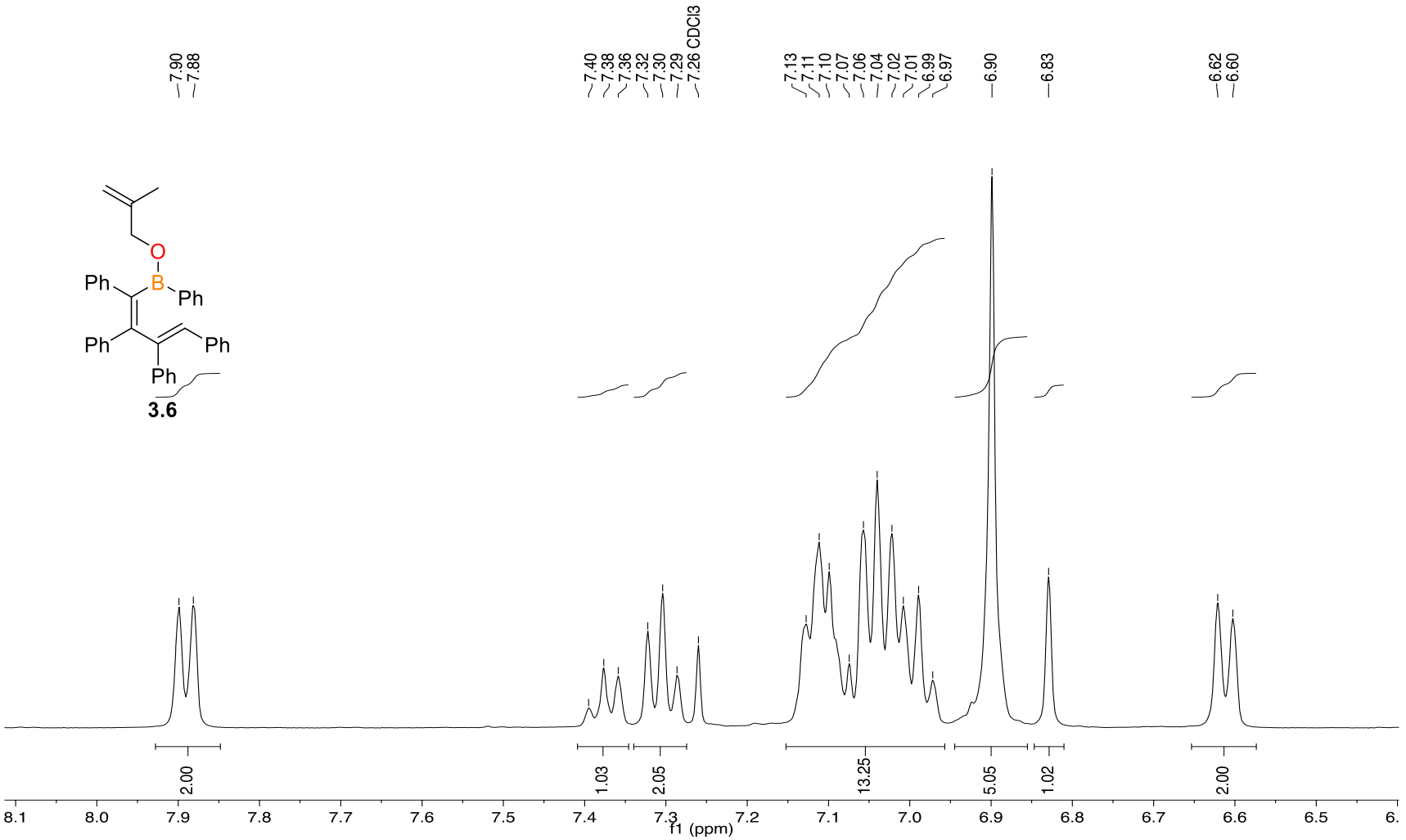

Figure B-2: Expansion of ^{1}H NMR spectrum of **3.6** in $CDCl_3$ (aryl region).

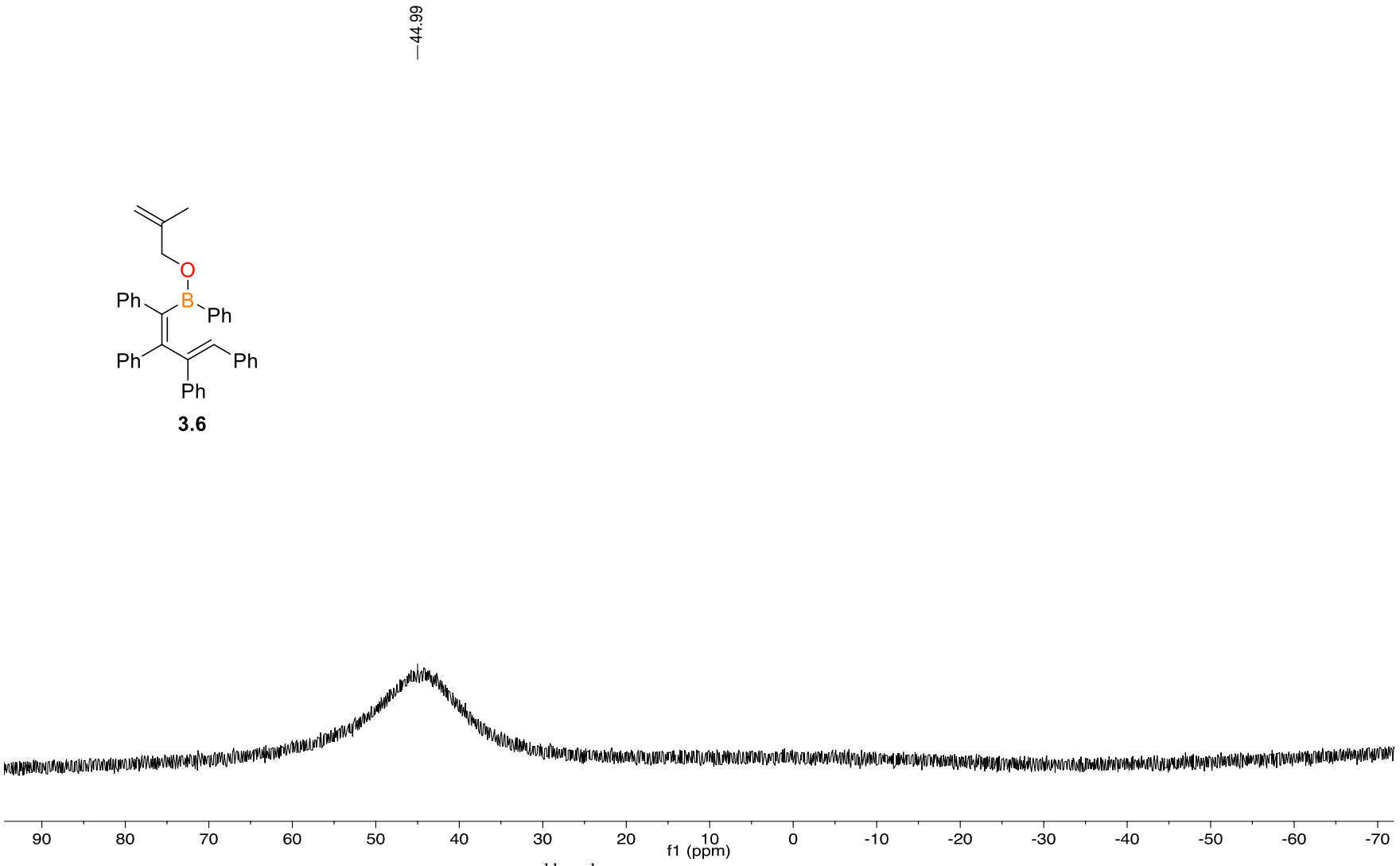

Figure B-3: $^{11}B\{^{1}H\}$ NMR spectrum of **3.6** in $CDCl_3$.

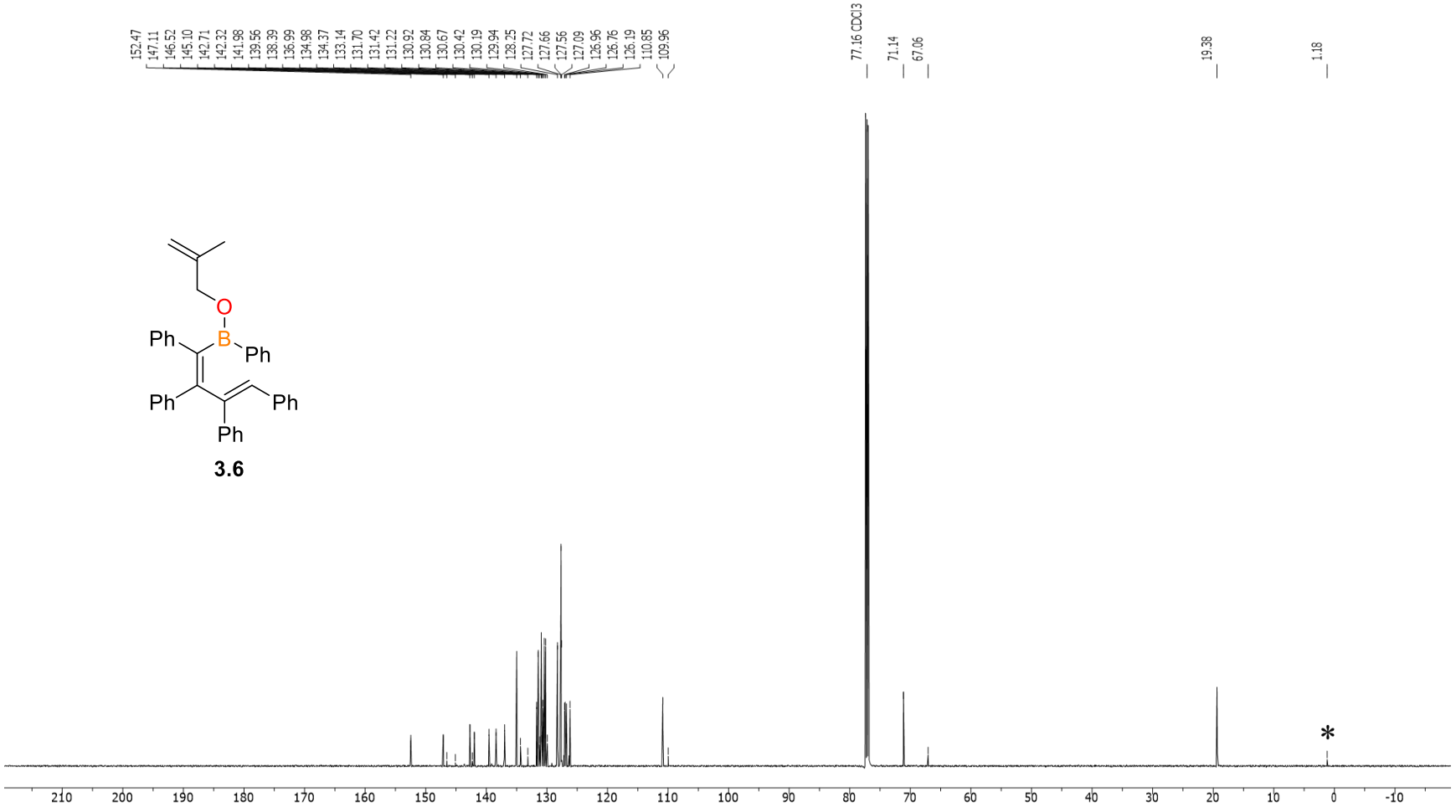

Figure B-4: $^{13}C\{^{1}H\}$ NMR spectrum of **3.6** in $CDCl_3$ (*grease).

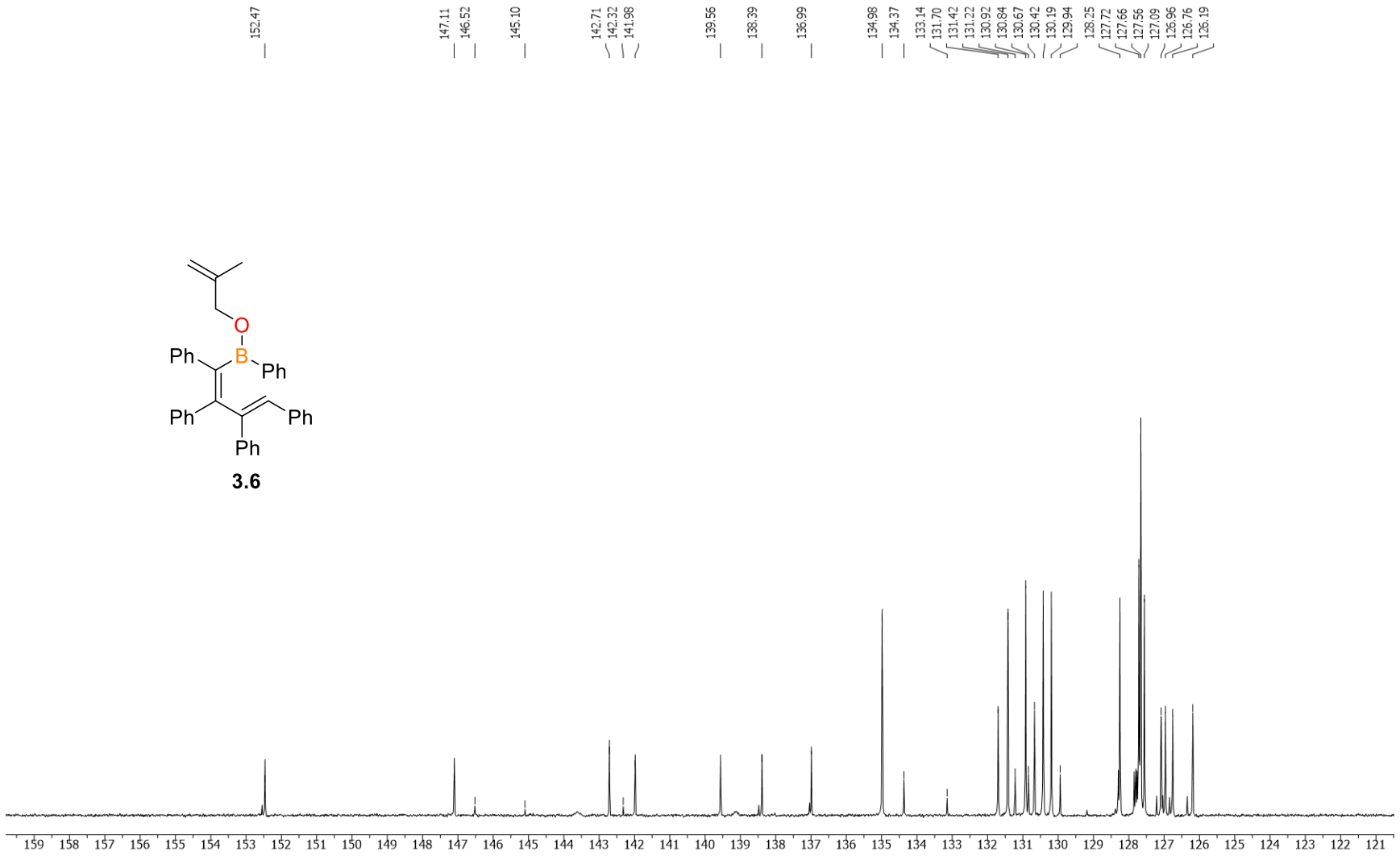

Figure B-5: Expansion of $^{13}C\{^{1}H\}$ NMR spectrum of **3.6** in $CDCl_3$ (aryl region).

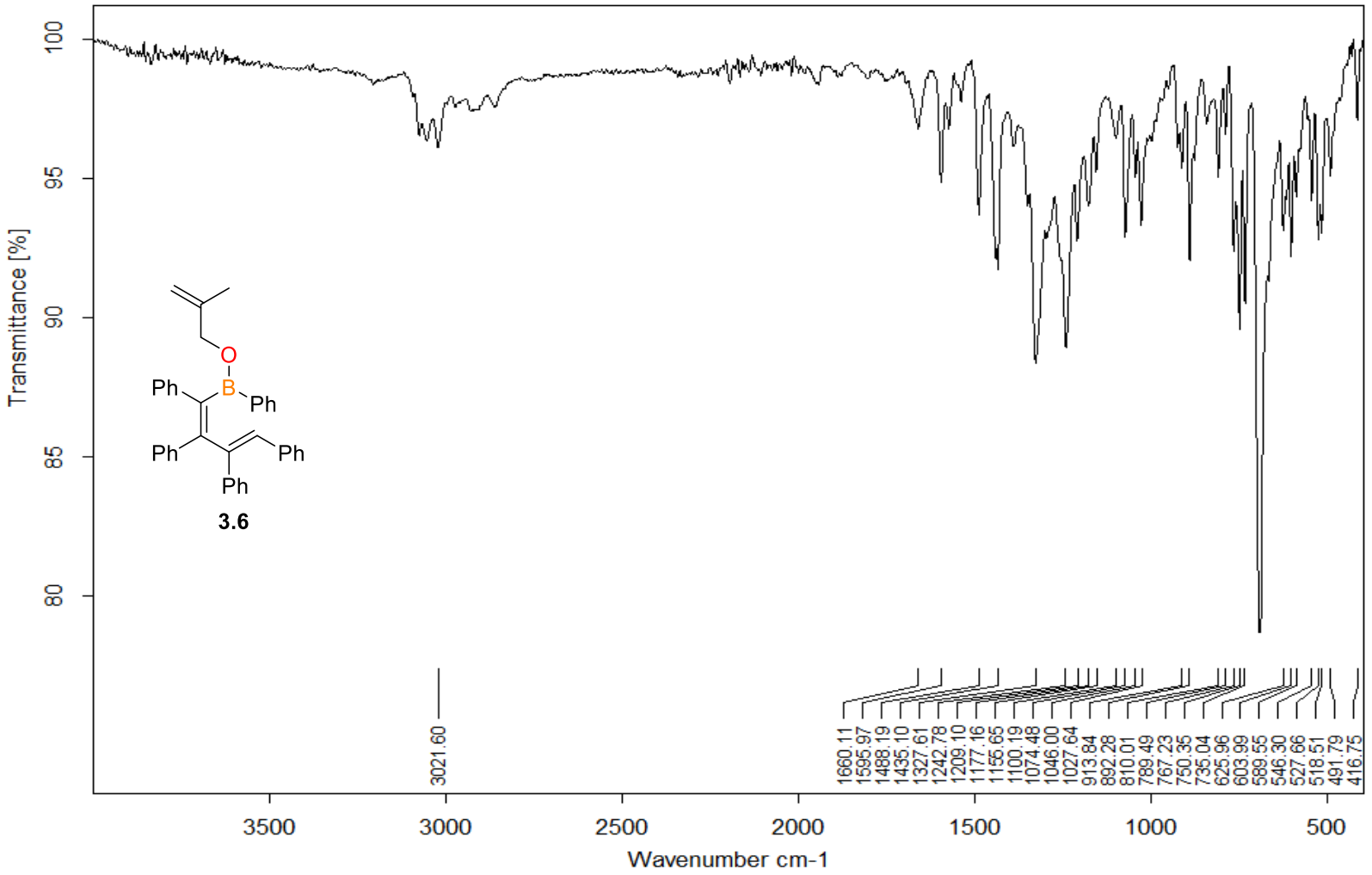

Figure B-6: FT-IR spectrum of **3.6**.

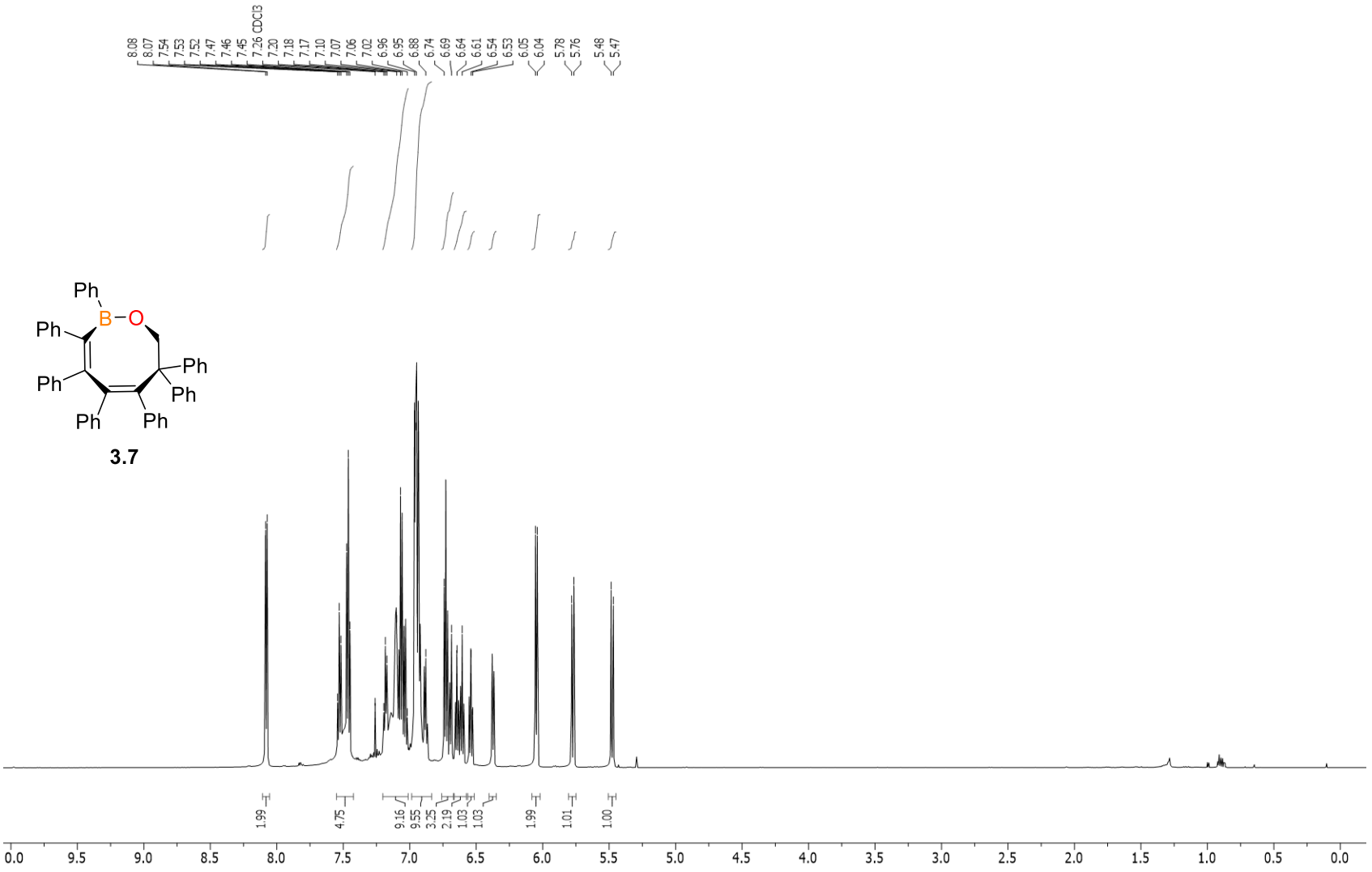

Figure B-7: ^{1}H NMR spectrum of **3.7** in $CDCl_3$.

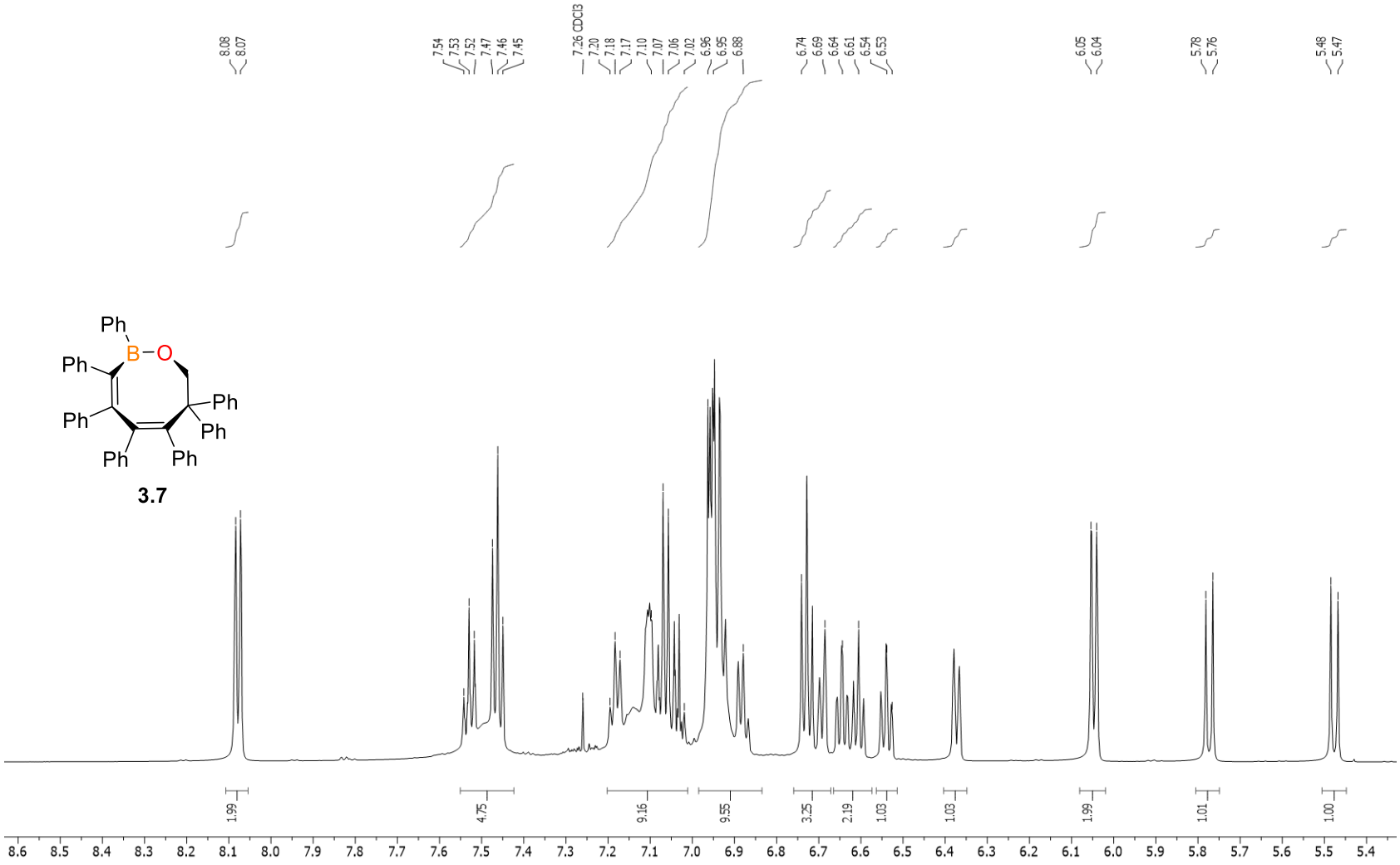

Figure B-8: Expansion of ^{1}H NMR spectrum of **3.7** in $CDCl_3$ (aryl region).

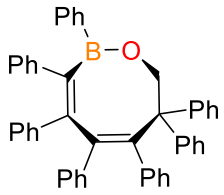

3.7

Figure B-9: $^{11}B\{^{1}H\}$ NMR spectrum of **3.7** in $CDCl_3$.

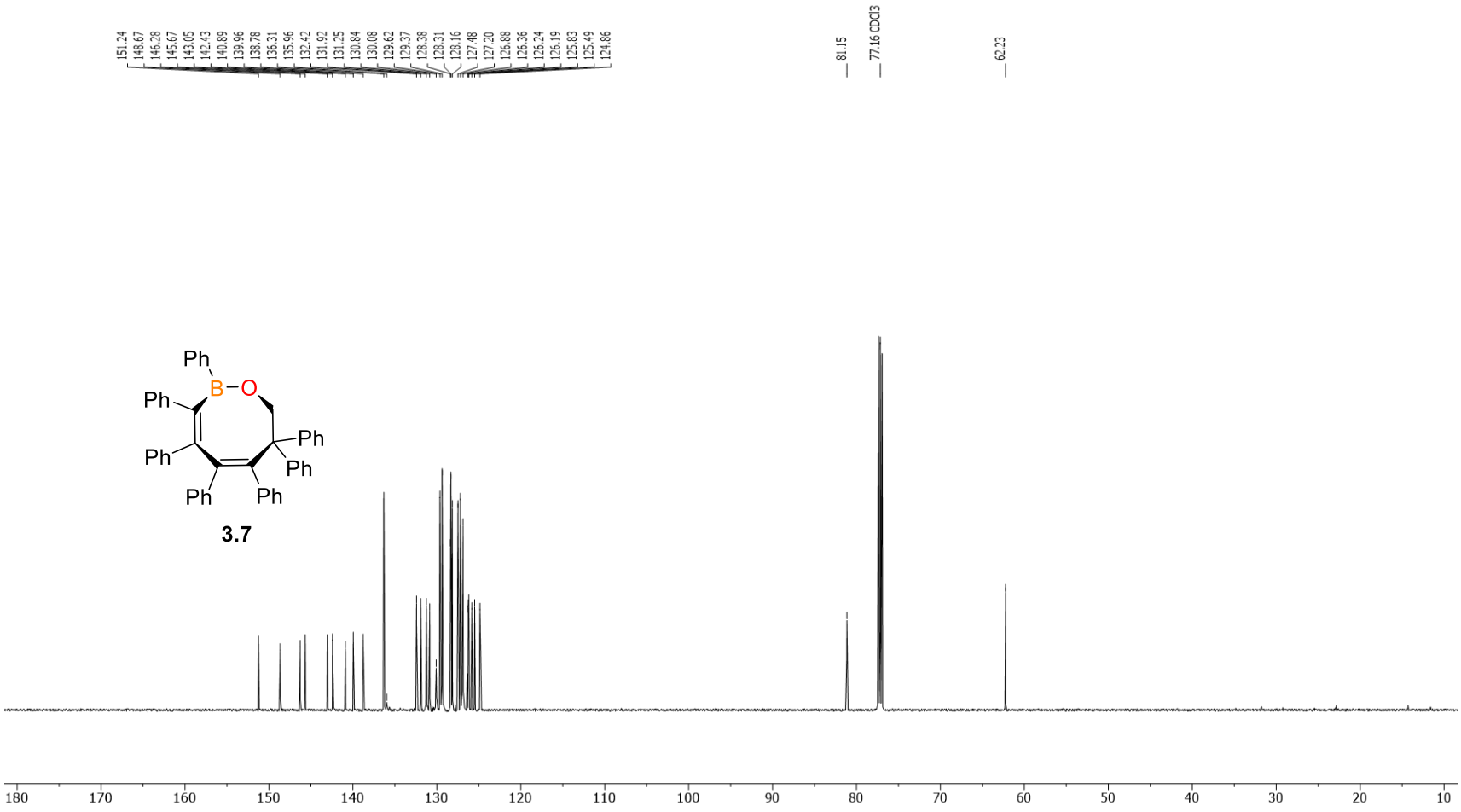

Figure B-10: $^{13}C\{^{1}H\}$ NMR spectrum of **3.7** in $CDCl_3$.

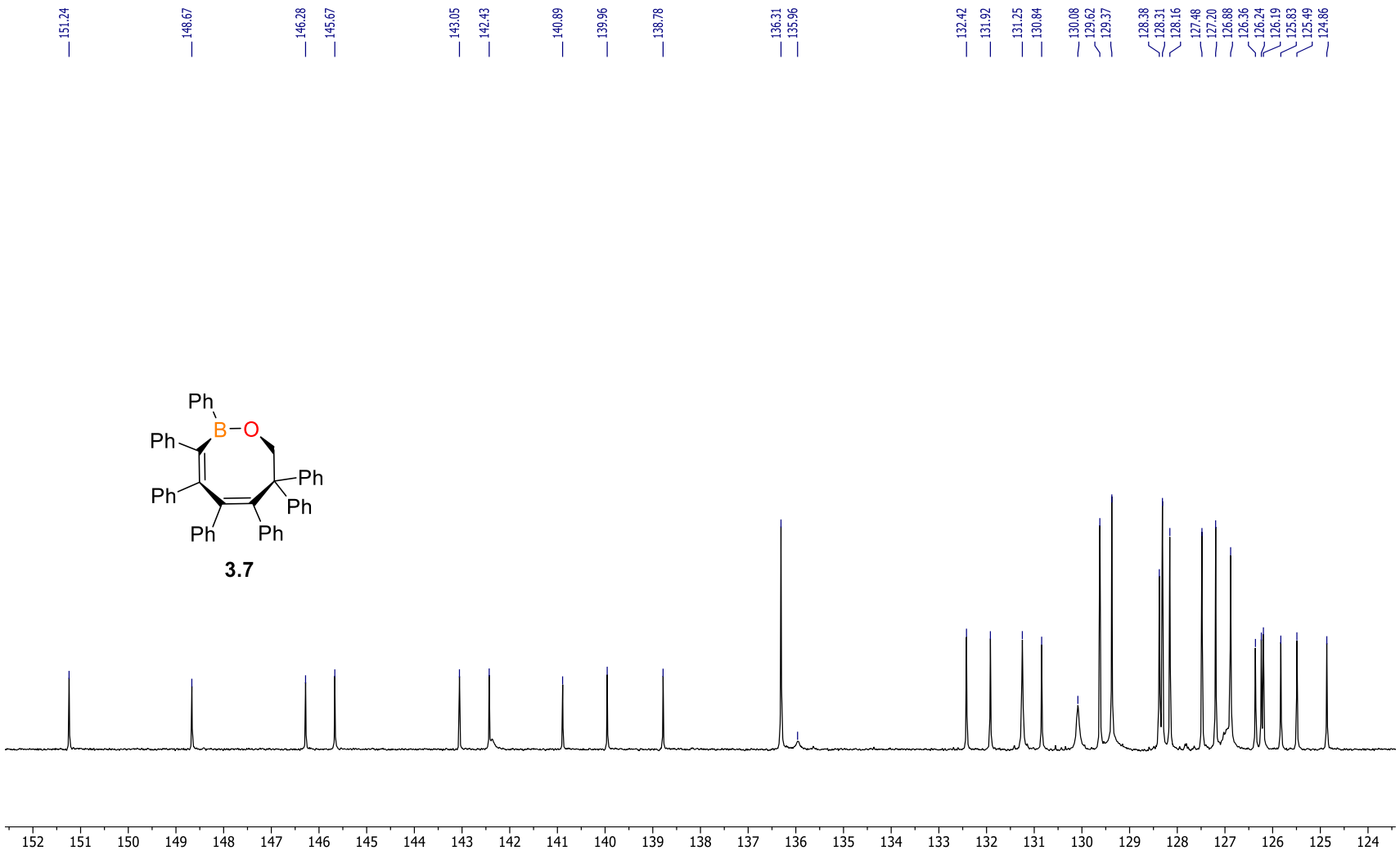

Figure B-11: Expansion of $^{13}C\{^{1}H\}$ NMR spectrum of **3.7** in $CDCl_3$ (aryl region).

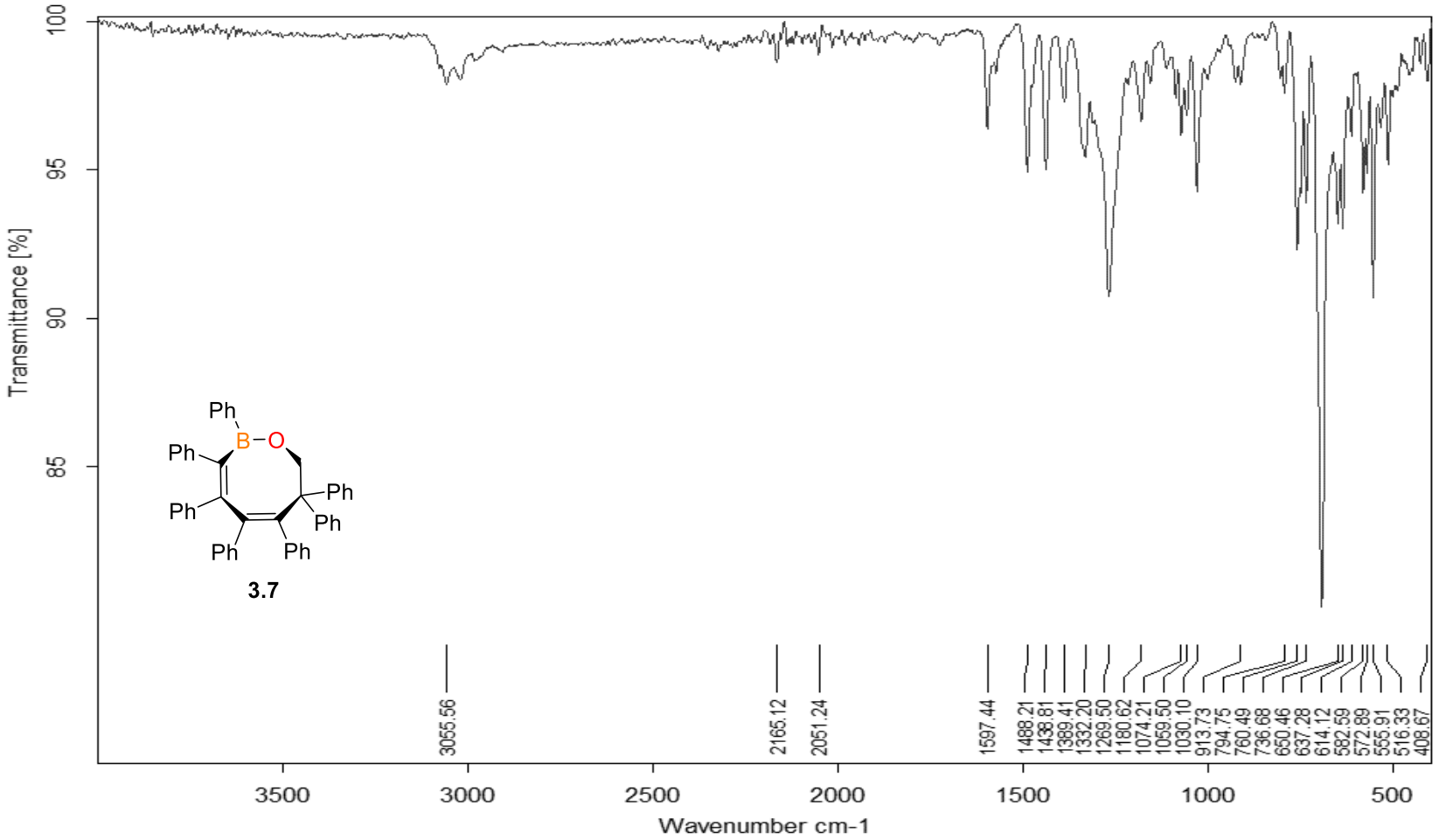

Figure B-12: FT-IR spectrum of **3.7**.

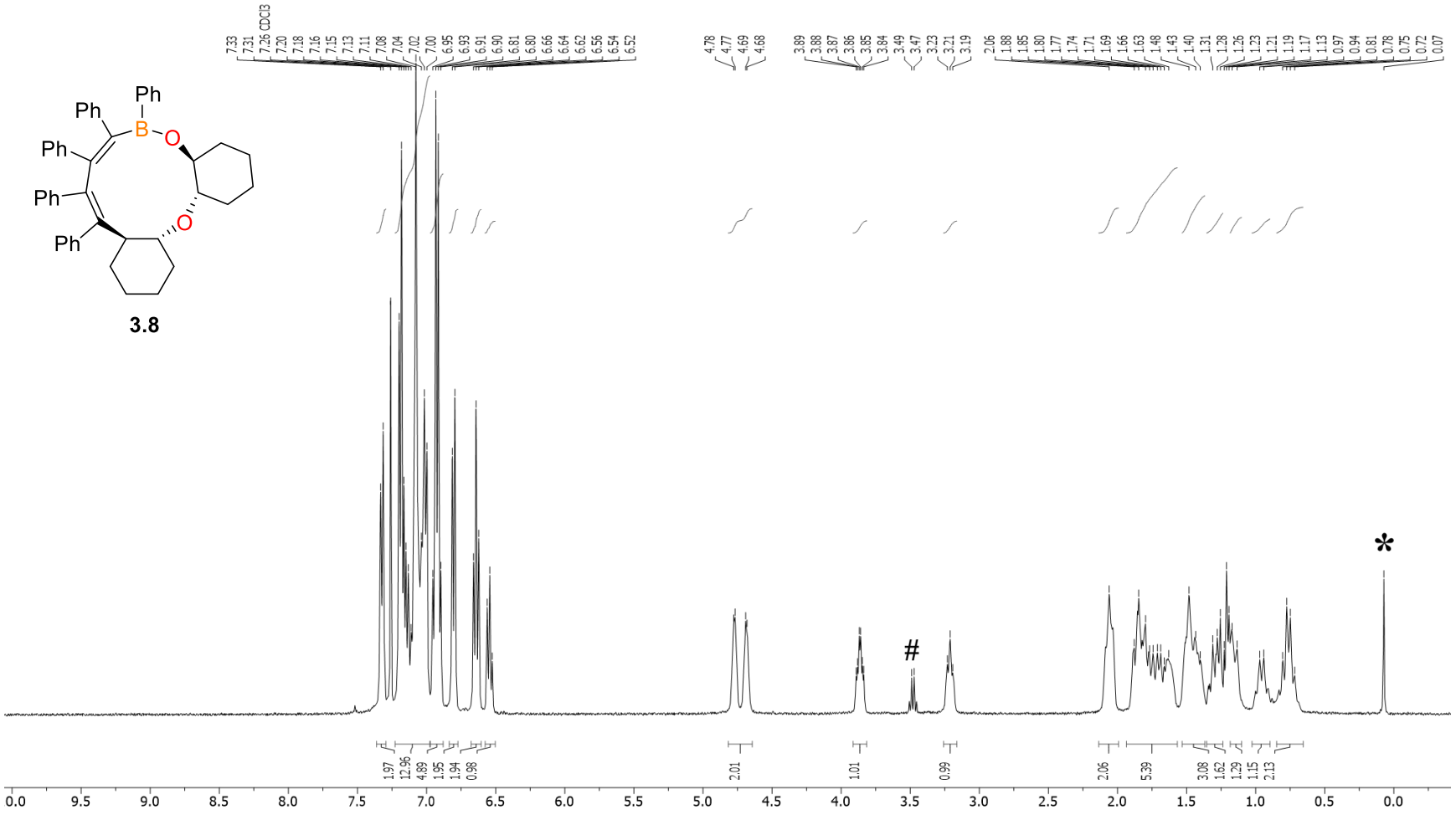

Figure B-13: ^{1}H NMR spectrum of **3.8** in $CDCl_3$ (*grease, #diethyl ether).

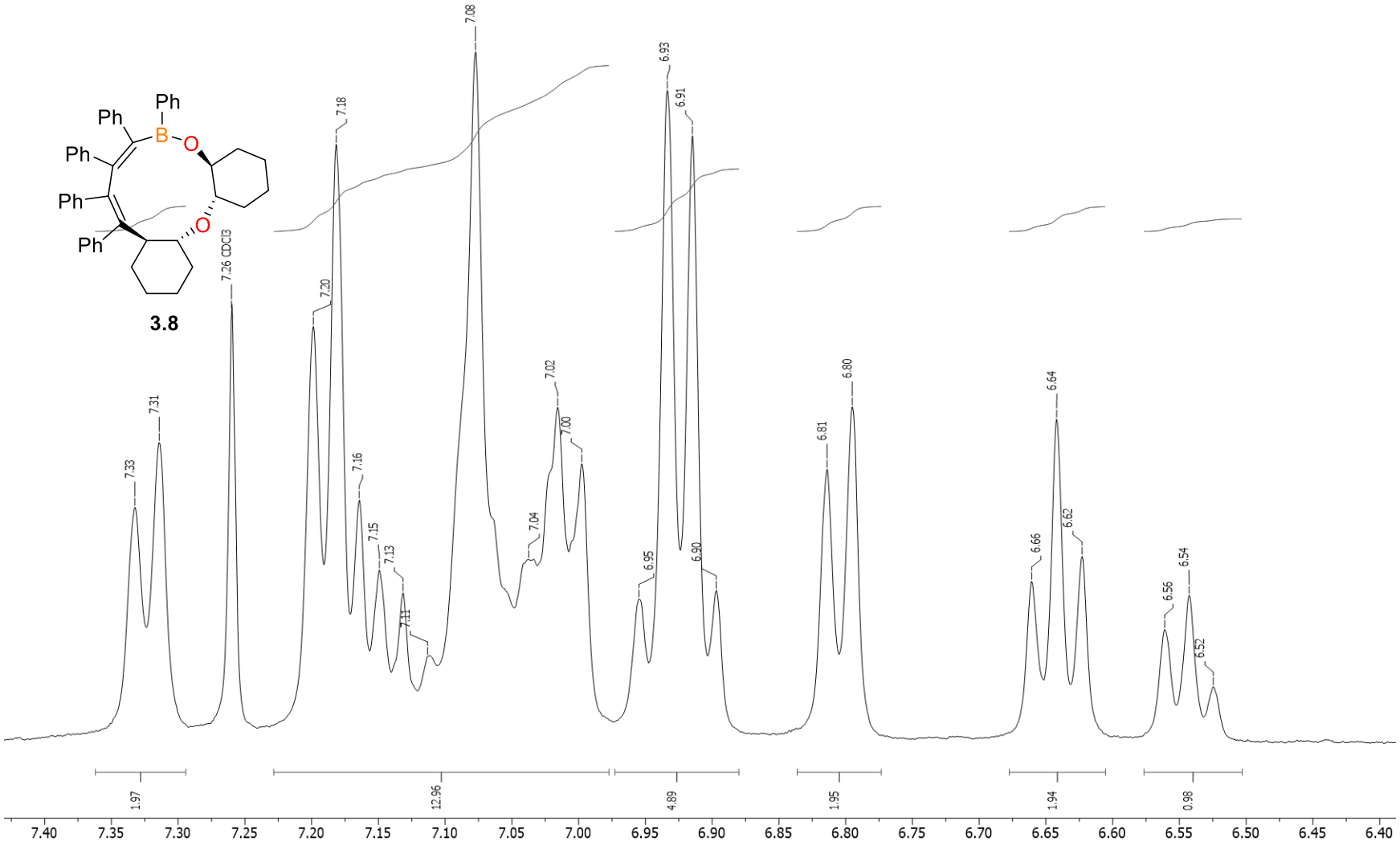

Figure B-14: Expansion of ^{1}H NMR spectrum of **3.8** in $CDCl_3$ (aryl region).

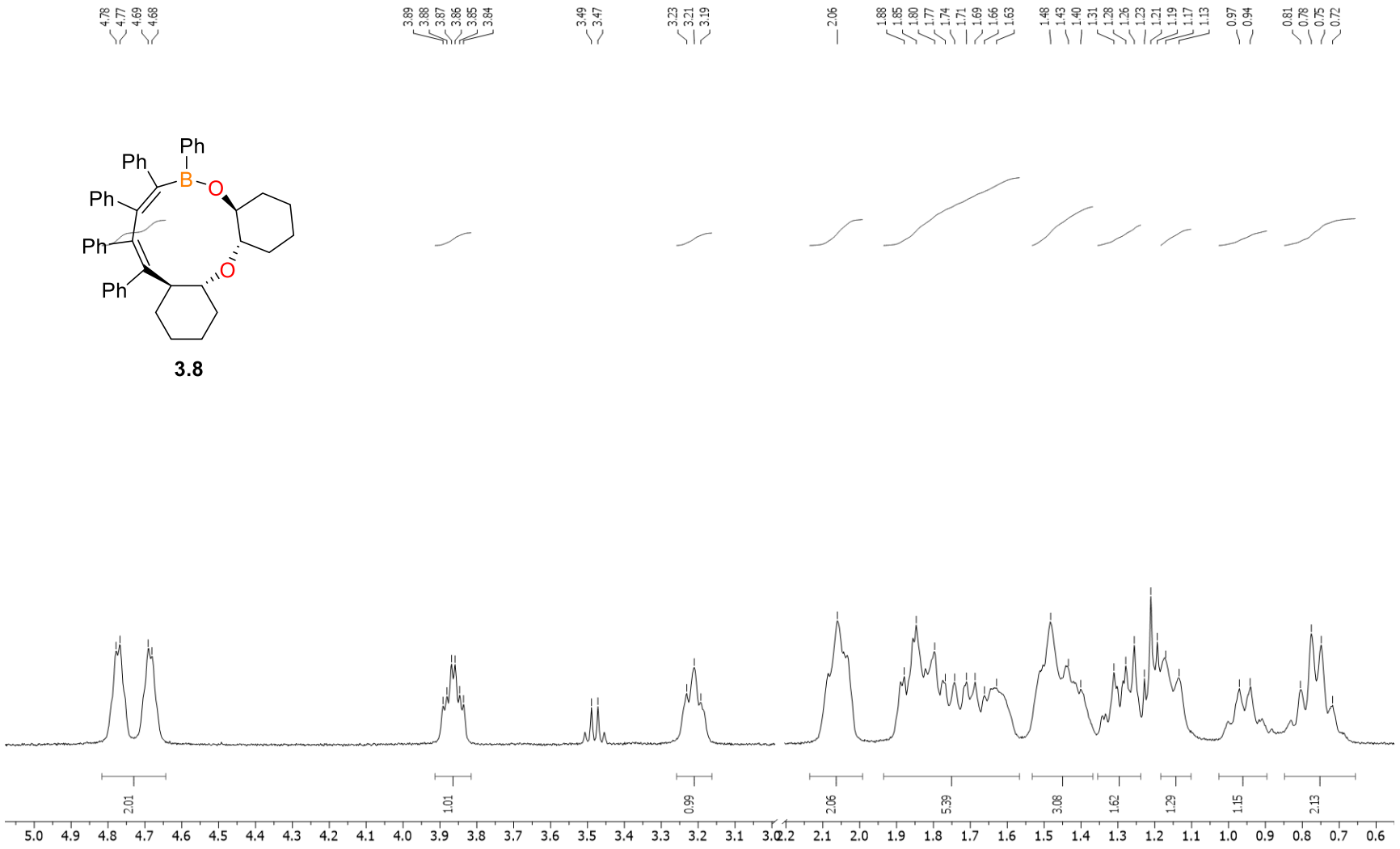

Figure B-15: Expansion of ^{1}H NMR of **3.8** in $CDCl_3$ (aliphatic region).

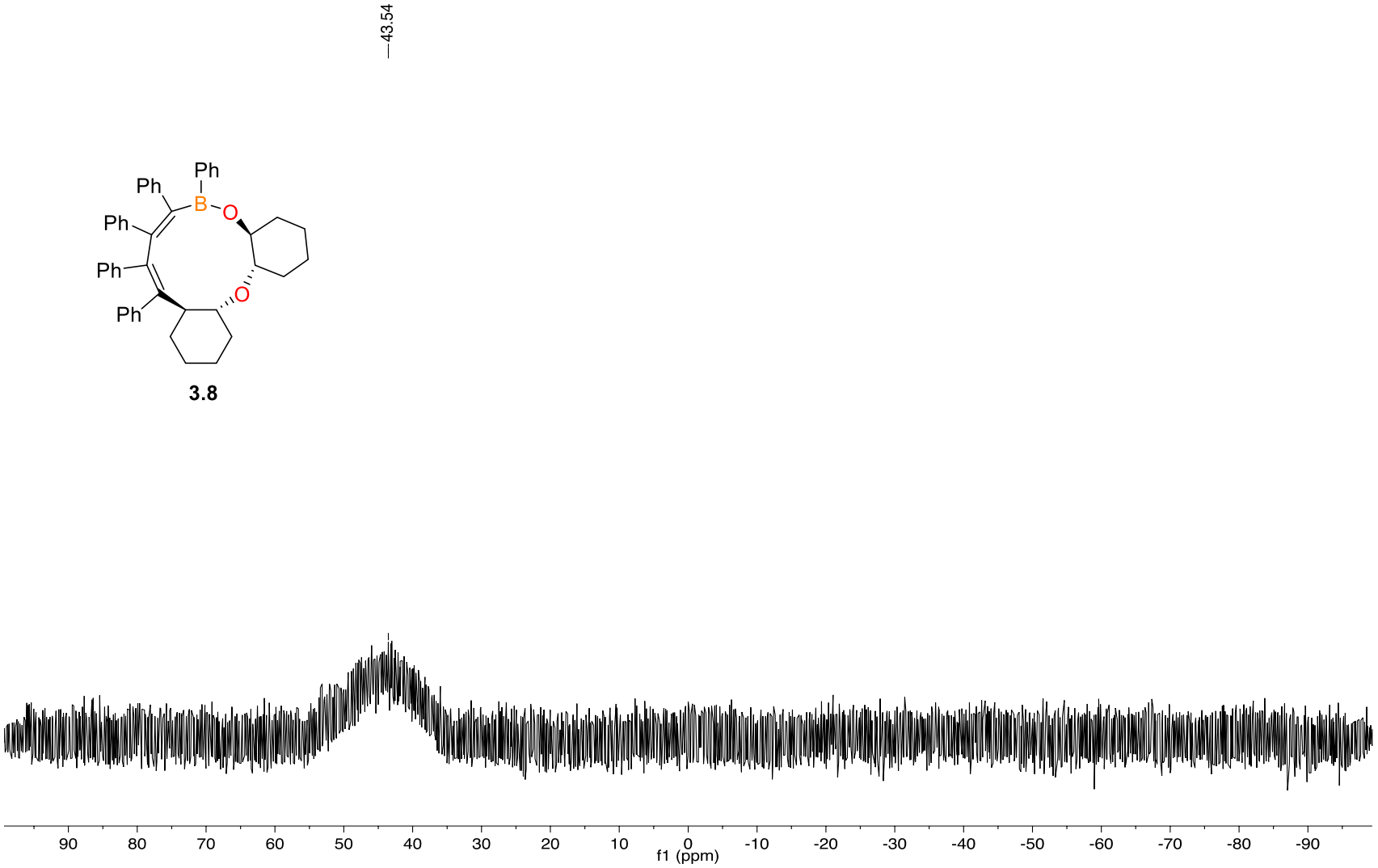

Figure B-16: $^{11}B\{^{1}H\}$ NMR spectrum of **3.8** in $CDCl_3$.

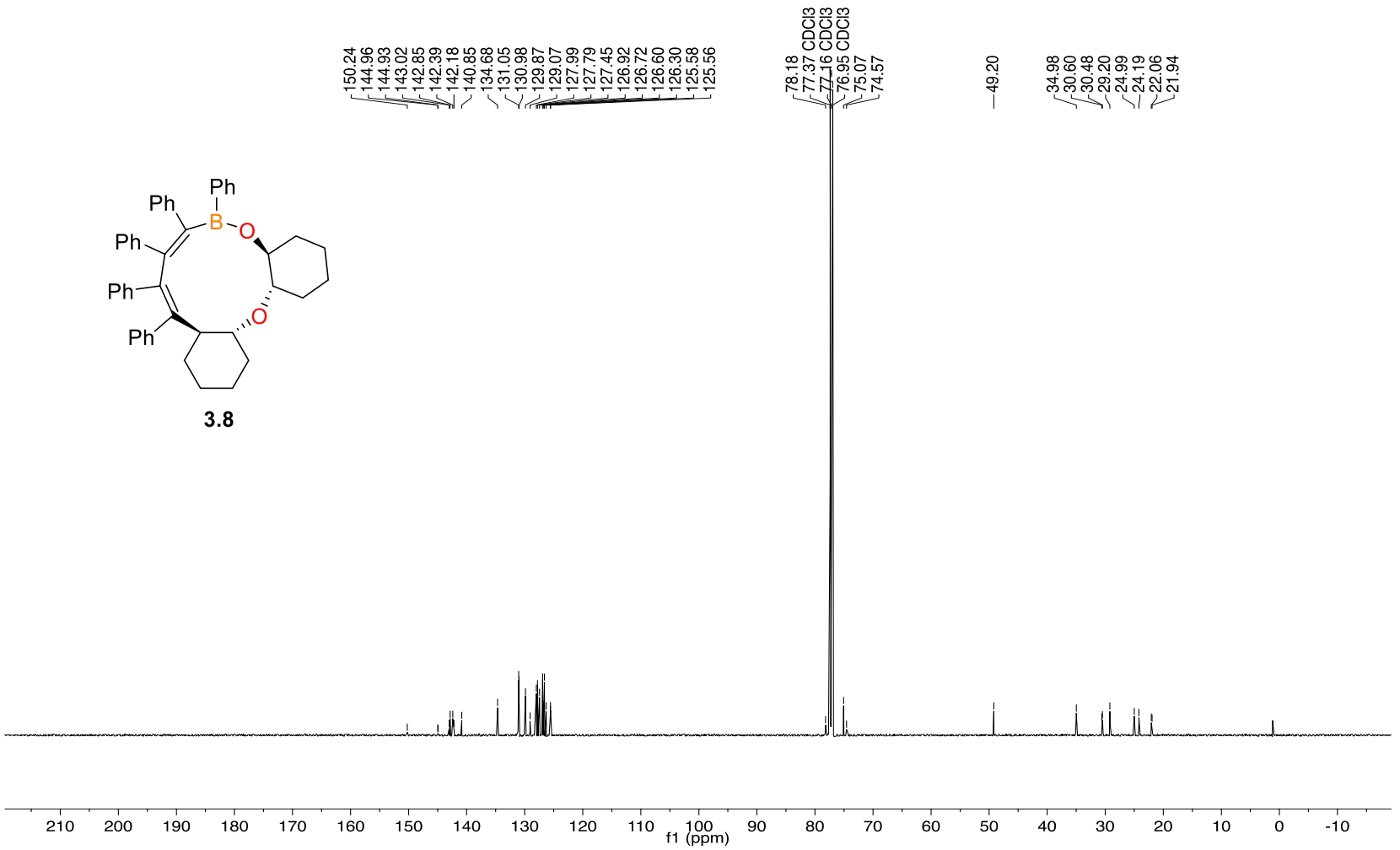

Figure B-17: $^{13}C\{^{1}H\}$ NMR spectrum of **3.8** in $CDCl_3$.

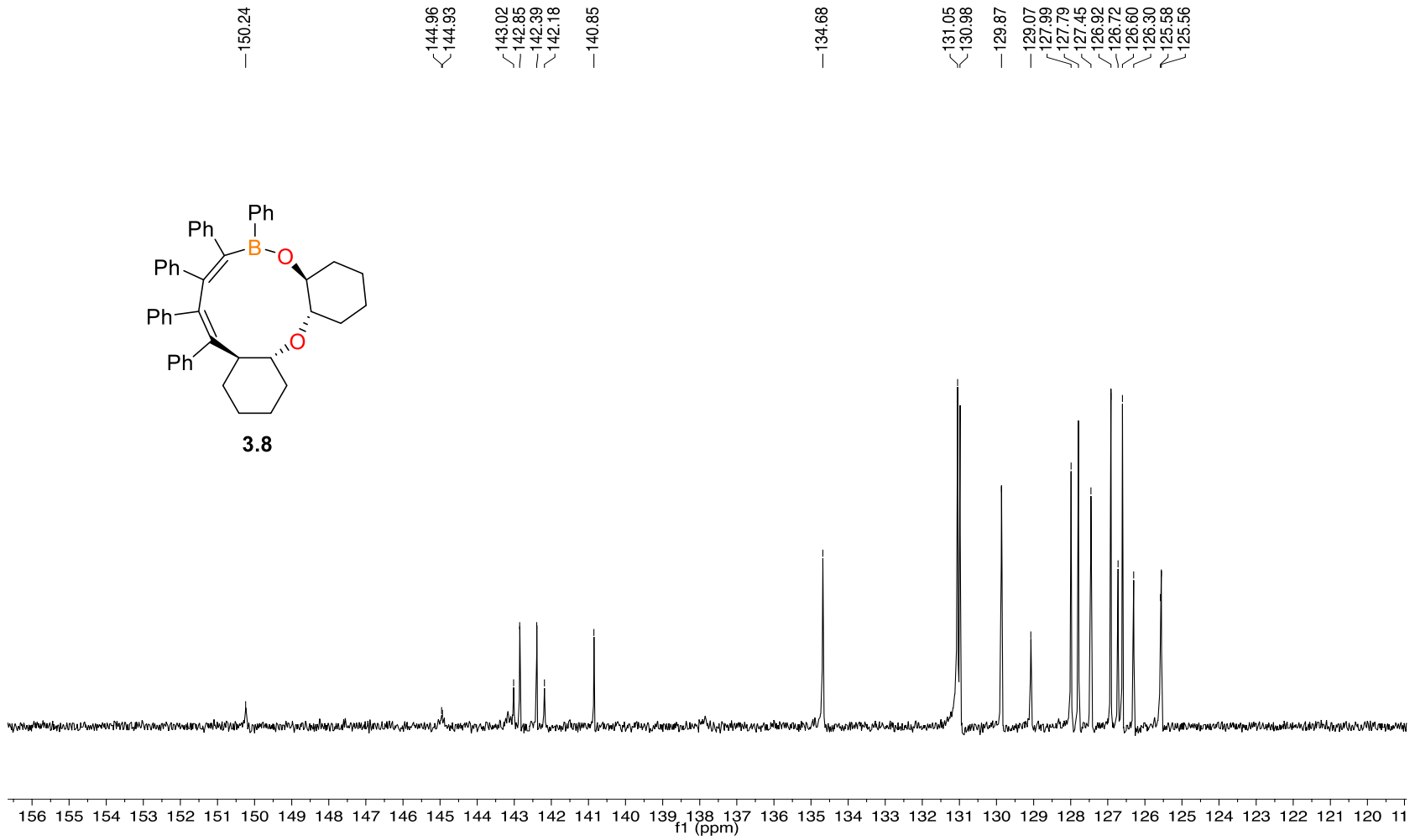

Figure B-18: Expansion of $^{13}C\{^{1}H\}$ NMR spectrum of **3.8** in $CDCl_3$ (aryl region).

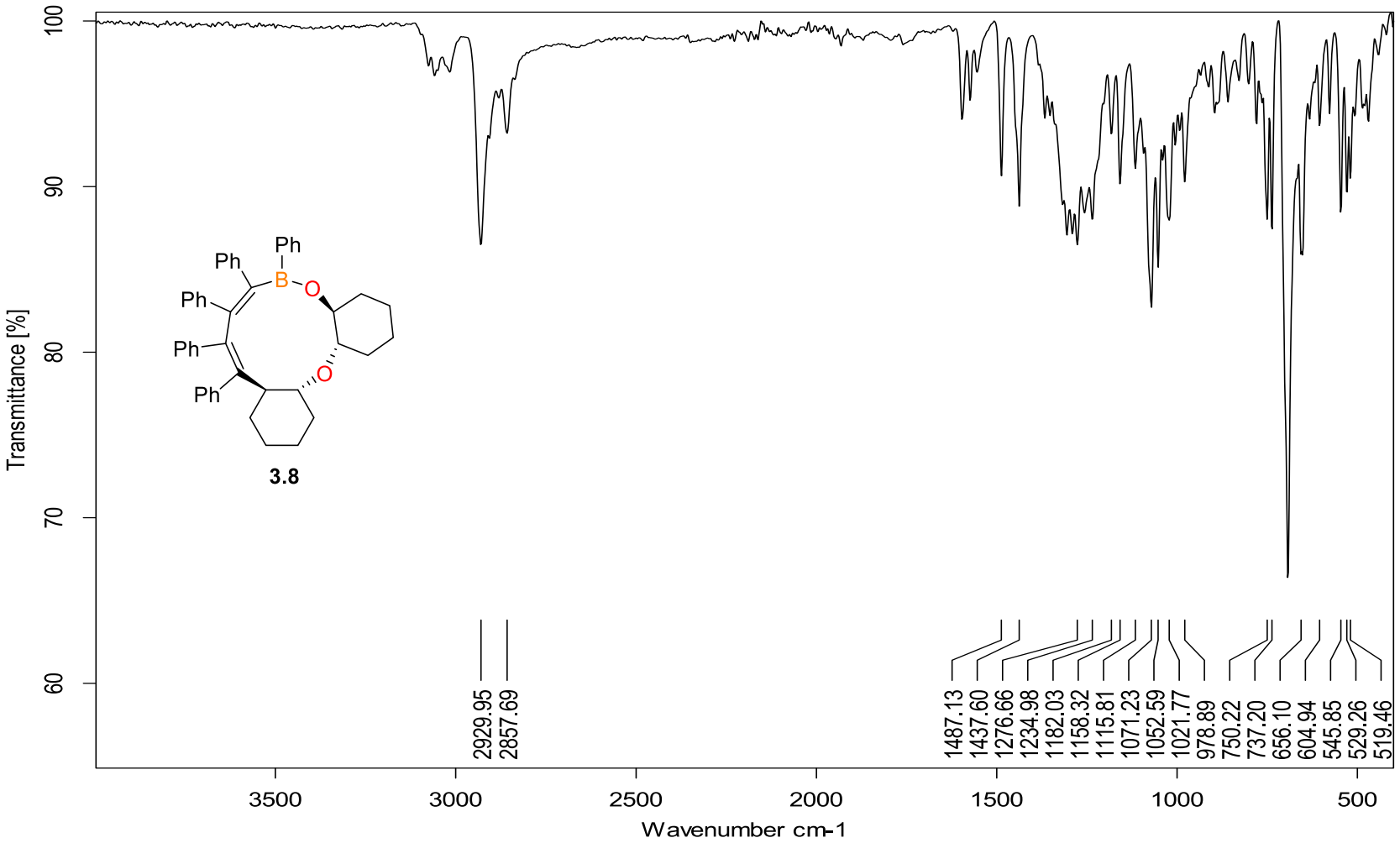

Figure B-19: FT-IR spectrum of **3.8**.

Table B-1: Crystallographic Data for **3.6-3.8**.

Entry	**3.6**	**3.7**	**3.8**
CCDC	1567465	1567466	1567467
Empirical formula	$C_{38}H_{33}BO$	$C_{48}H_{37}BO$	$C_{46}H_{45}BO_2$
FW (g/mol)	516.45	640.59	640.63
Crystal system	Triclinic	Triclinic	Triclinic
Space group	*P-1*	*P-1*	*P-1*
a (Å)	10.8110(7)	10.0123(19)	11.9143(10)
b (Å)	11.2201(8)	12.407(3)	12.2386(10)
c (Å)	13.9894(8)	14.530(3)	13.8415(11)
α (deg)	91.363(2)	83.153(7)	88.644(3)
β (deg)	105.304(2)	80.646(7)	72.819(3)
γ (deg)	112.355(2)	86.380(6)	69.847(3)
V (Å^3)	1499.00(17)	1767.7(7)	1803.3(3)
Z	2	2	2
D_c (mg m^{-3})	1.144	1.204	1.180
radiation, λ (Å)	0.71073	0.71073	0.71073
temp (K)	150(2)	150(2)	150(2)
$R1[I>2\sigma I]^a$	0.0575	0.0511	0.0621
$wR2(F^2)^a$	0.1697	0.1398	0.1729
GOF (S)^a	1.081	1.001	1.087

[a] $R1(F[\mathrm{I} > 2(\mathrm{I})]) = \sum\|\|F_o\| - |F_c\|\|/ \sum |F_o|$; $wR2(F^2\ [\text{all data}]) = [w(F_o^2 - F_c^2)^2]^{1/2}$; $S(\text{all data}) = [w(F_o^2 - F_c^2)^2/(n - p)]^{1/2}$ (n = no. of data; p = no. of parameters varied; $w = 1/[^2(F_o^2) + (aP)^2 + bP]$ where $P = (F_o^2 + 2F_c^2)/3$ and a and b are constants suggested by the refinement program.[1,2]

APPENDIX C

Supplementary Information for Chapter Four

Figure C-1: Crude ^{1}H NMR spectrum of the reaction of **1.7-Ph** with O_2.

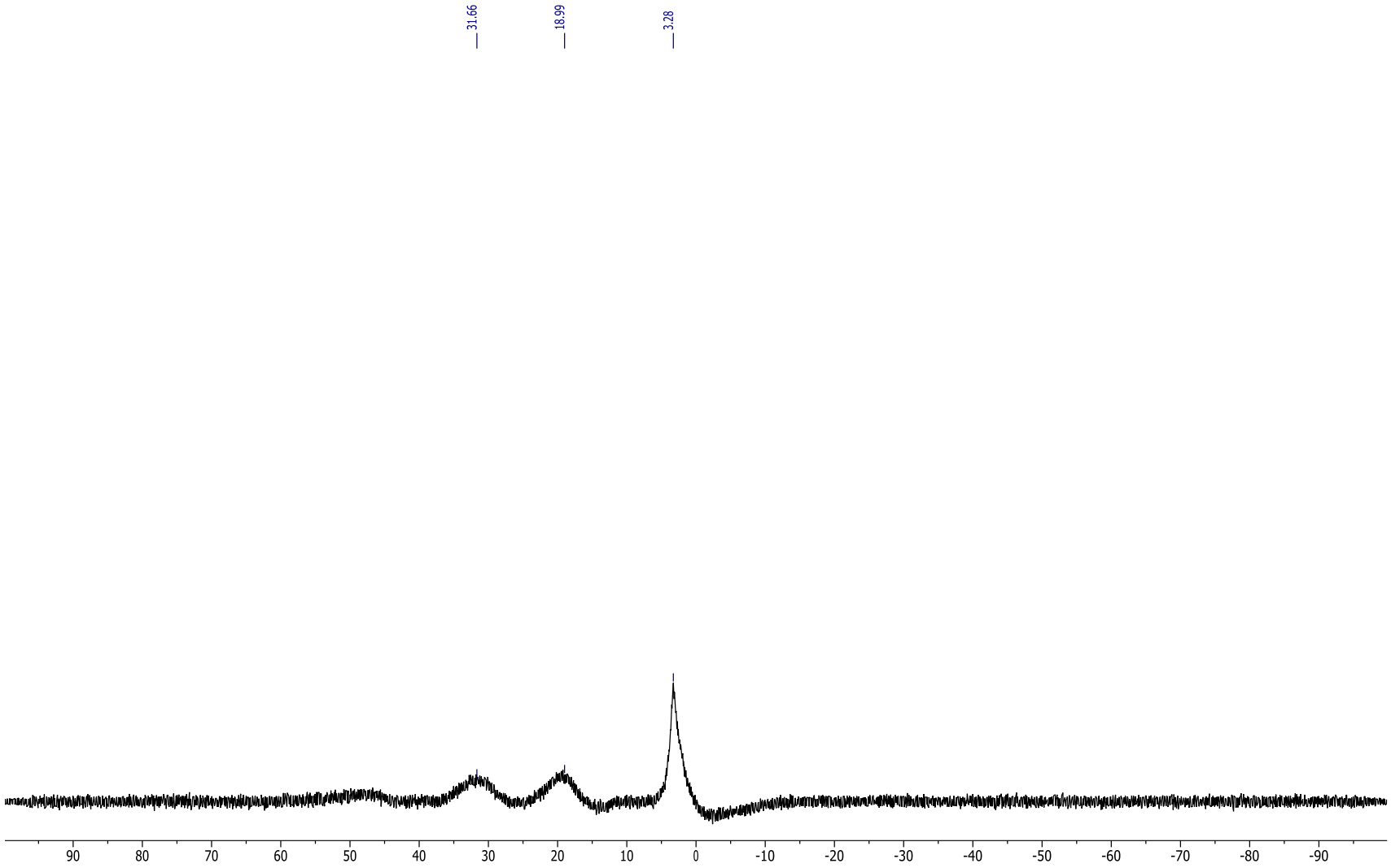

Figure C-2: Crude $^{11}B\{^{1}H\}$ NMR spectrum of the reaction of **1.7-Ph** with O_2.

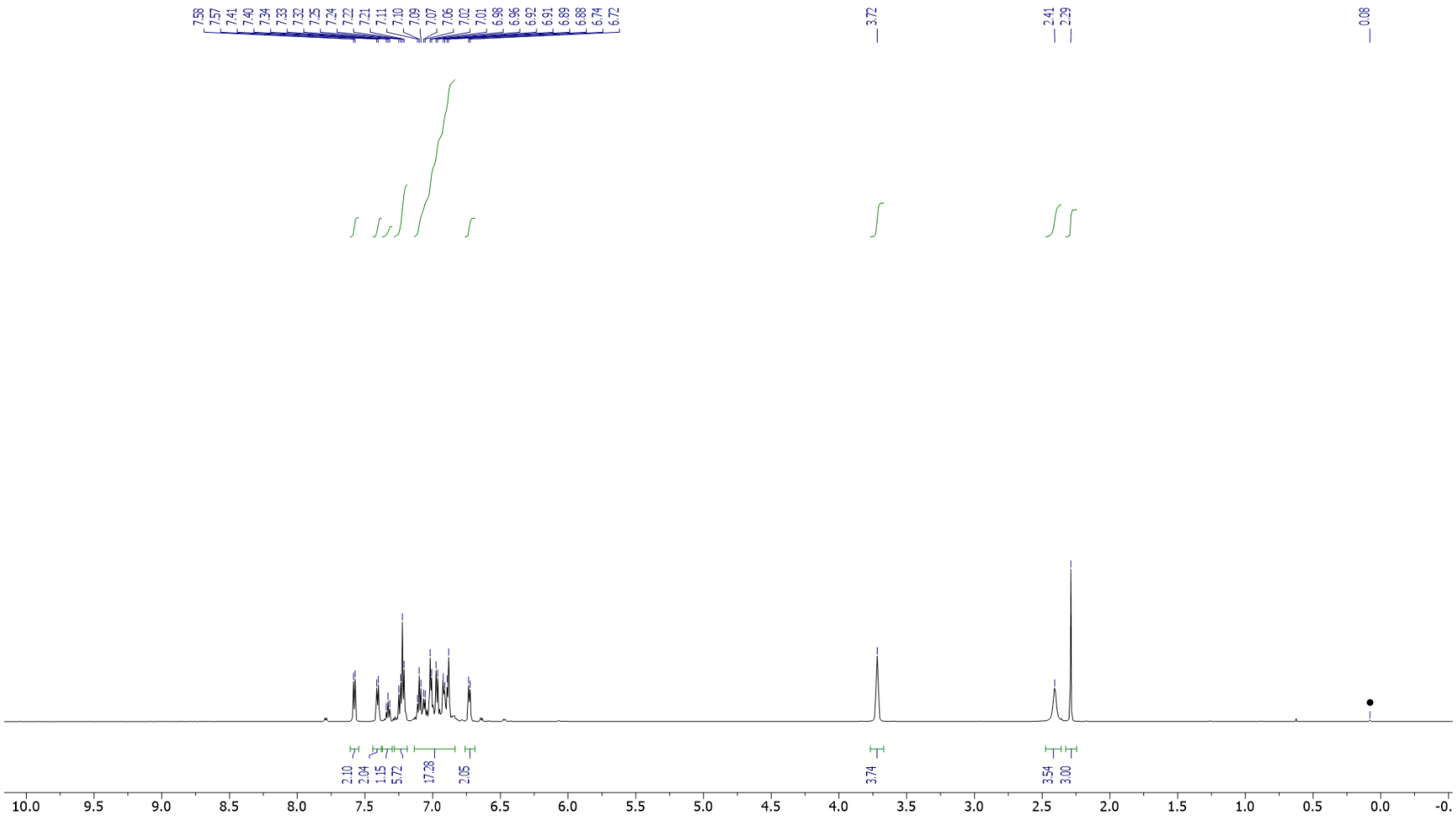

Figure C-3: Crude ^{1}H NMR spectrum of the reaction of **1.7-Ph** with N-methylmorpholine-N-oxide after 30 min (• grease).

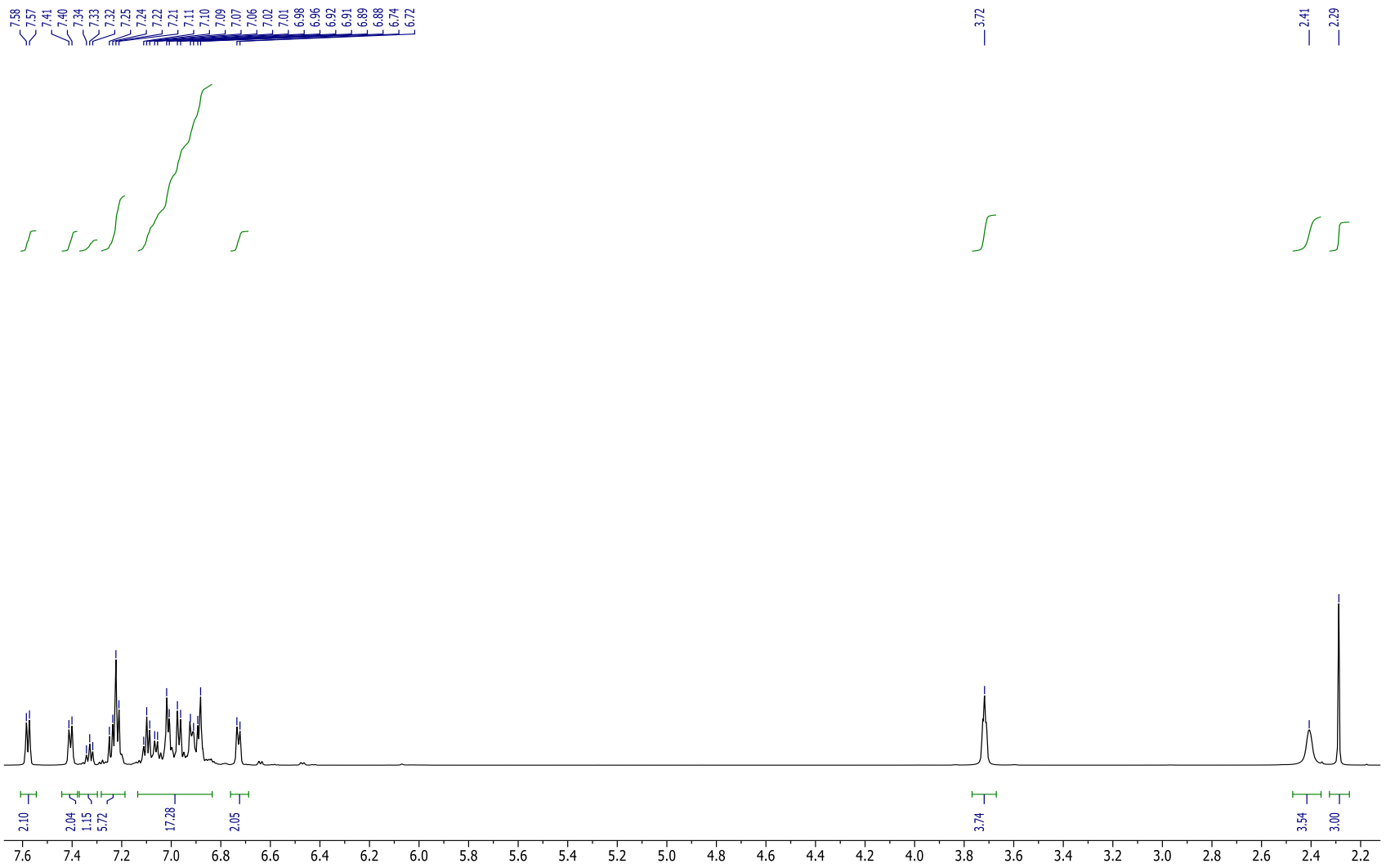

Figure C-4: Expansion of the crude ^{1}H NMR spectrum of the reaction of **1.7-Ph** with N-methylmorpholine-N-oxide after 30 min.

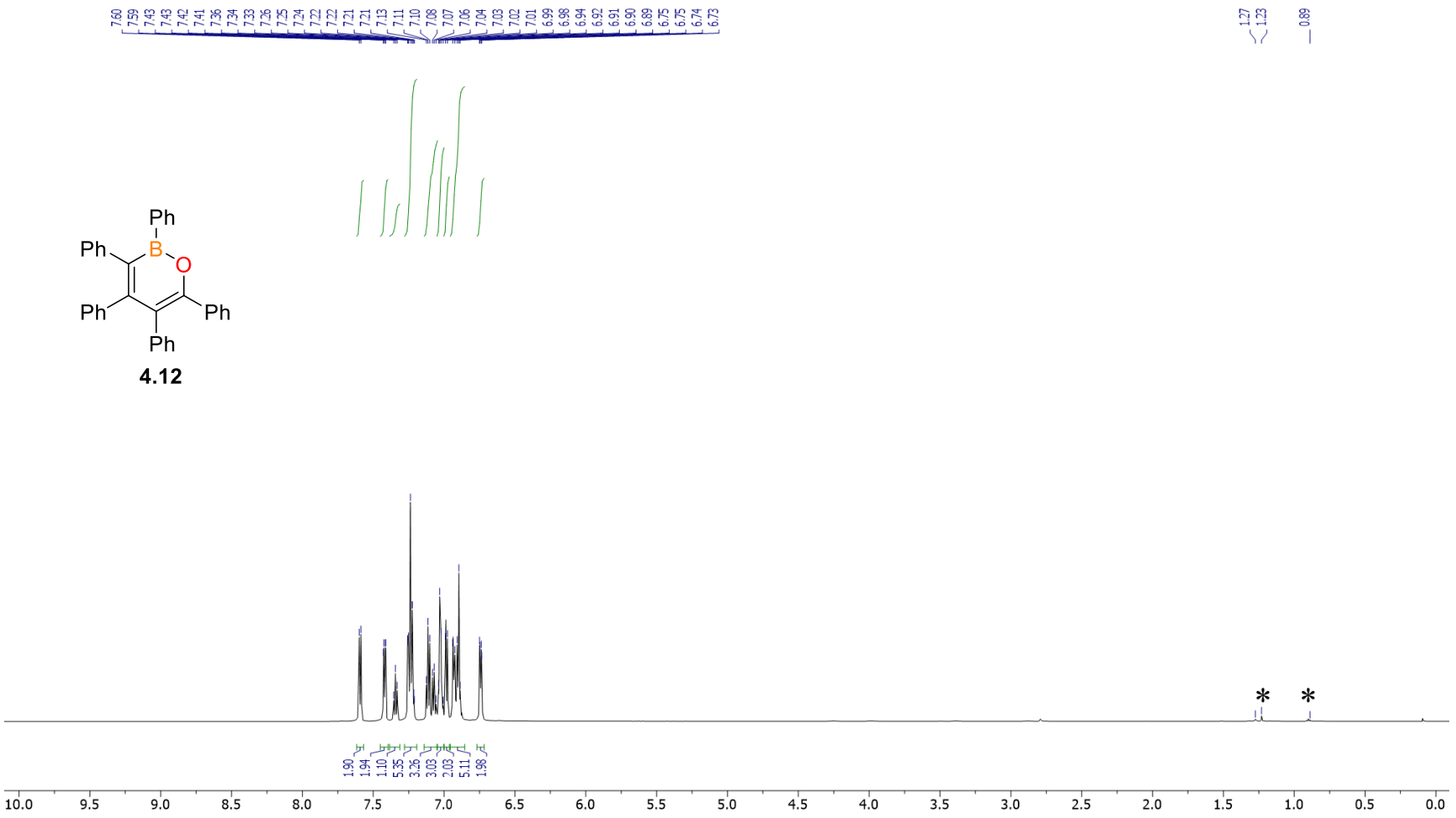

Figure C-5: ^{1}H NMR spectrum of **4.12** in $CDCl_3$ (* *n*-pentane).

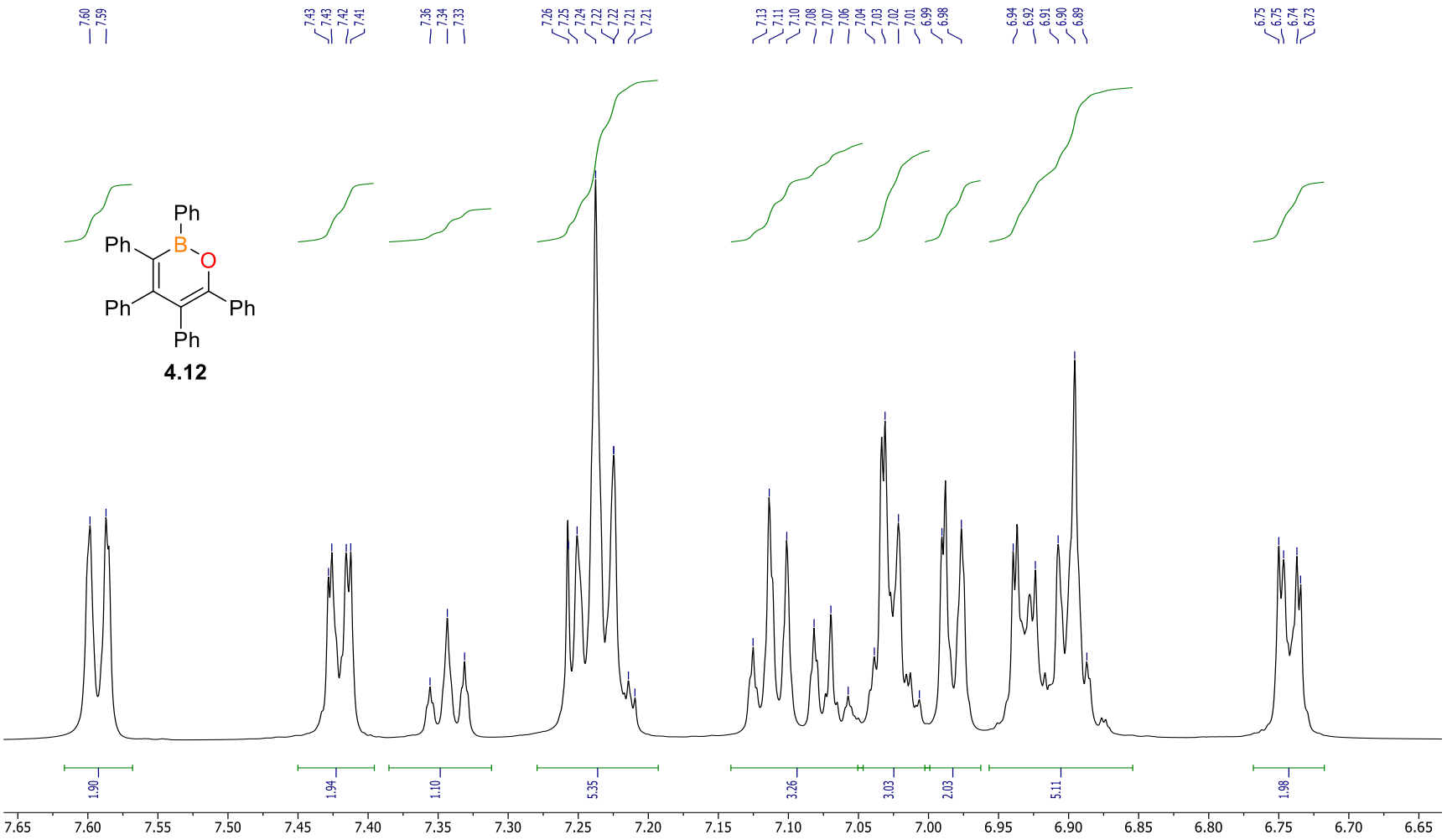

Figure C-6: Expansion of ^{1}H NMR spectrum of **4.12** in $CDCl_3$.

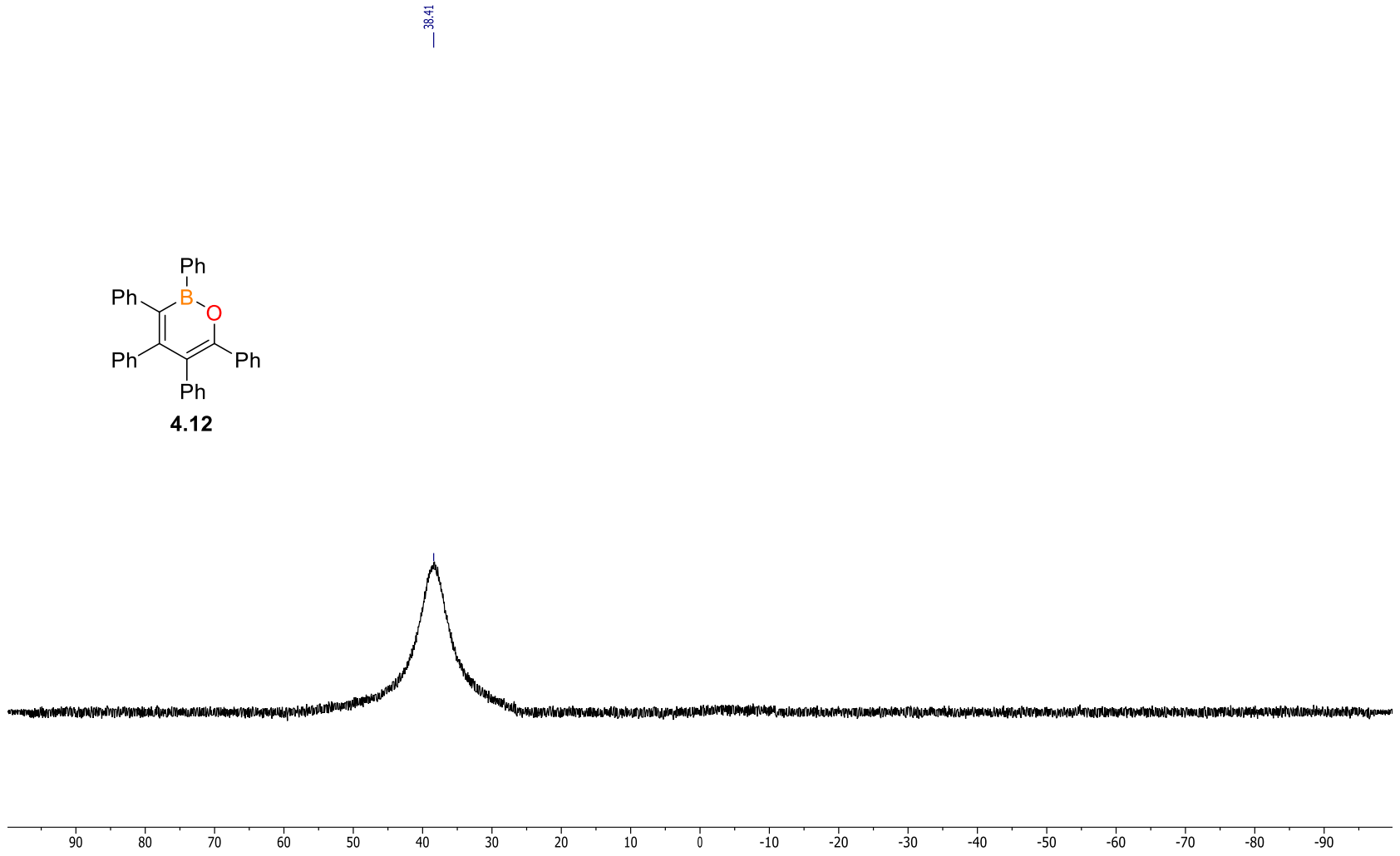

Figure C-7: $^{11}B\{^{1}H\}$ NMR spectrum of **4.12** in $CDCl_3$.

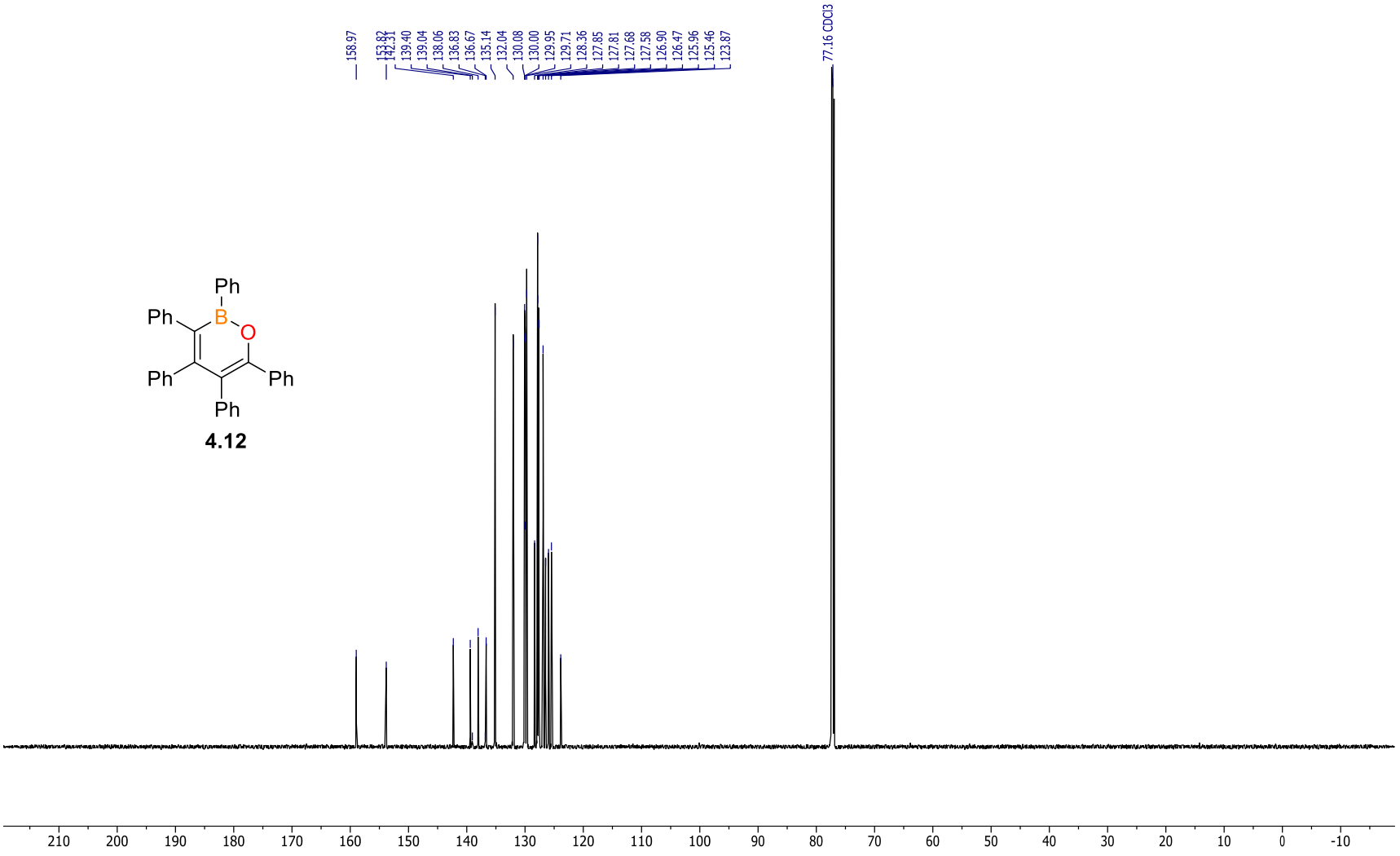

Figure C-8: $^{13}C\{^{1}H\}$ NMR spectrum of **4.12** in $CDCl_3$.

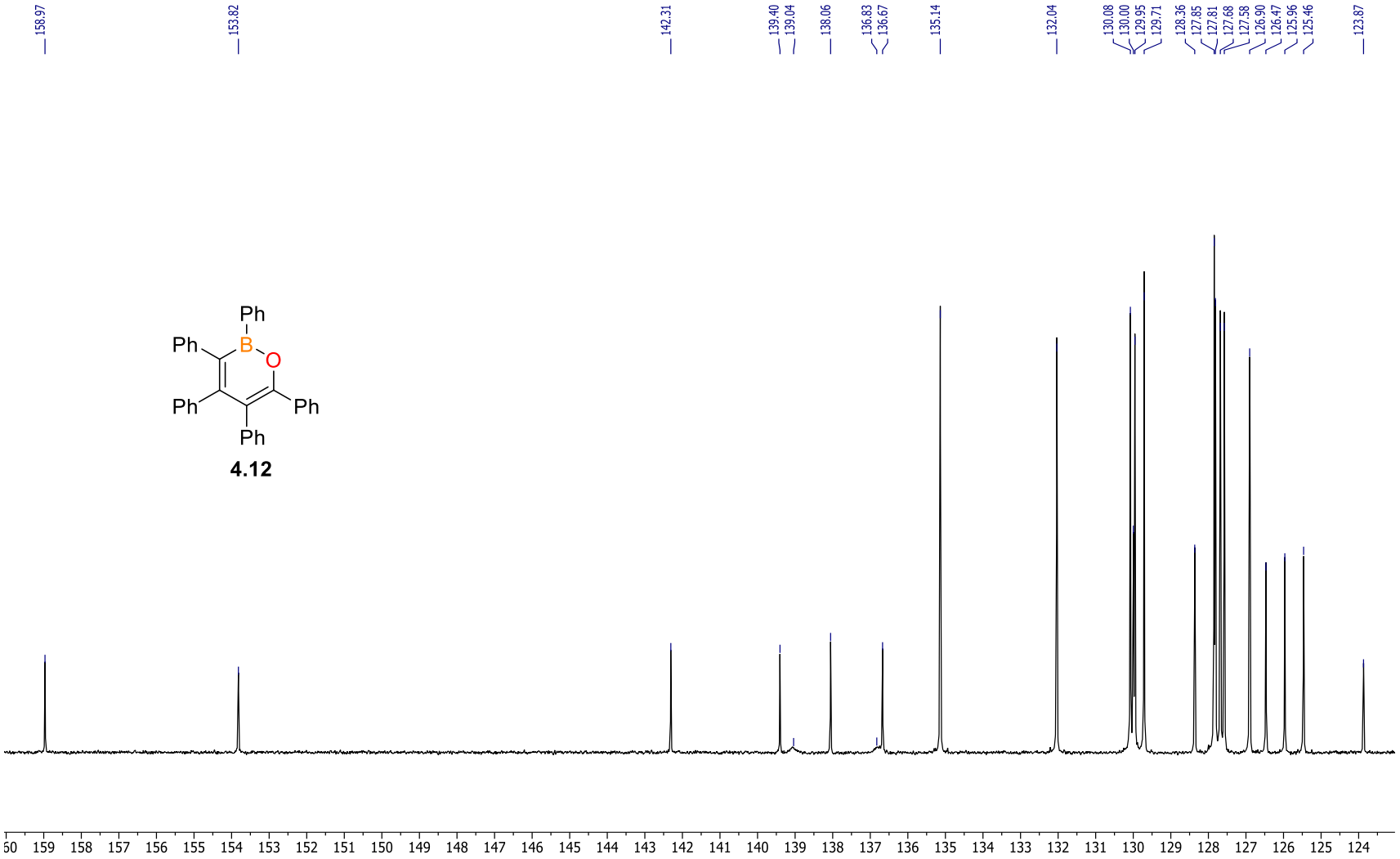

Figure C-9: Expansion of $^{13}C\{^{1}H\}$ NMR spectrum of **4.12** in $CDCl_3$.

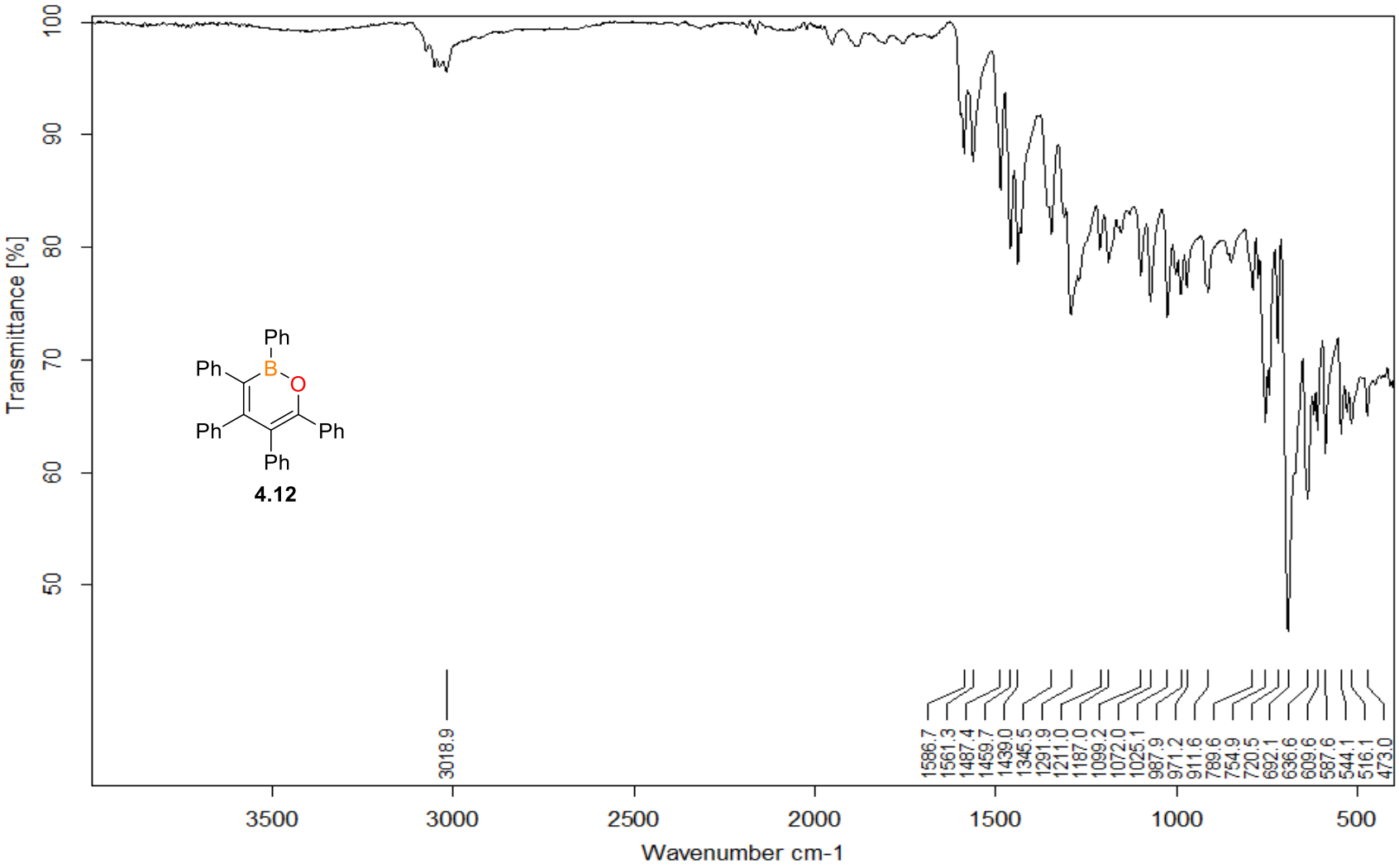

Figure C-10: FT-IR spectrum of **4.12**.

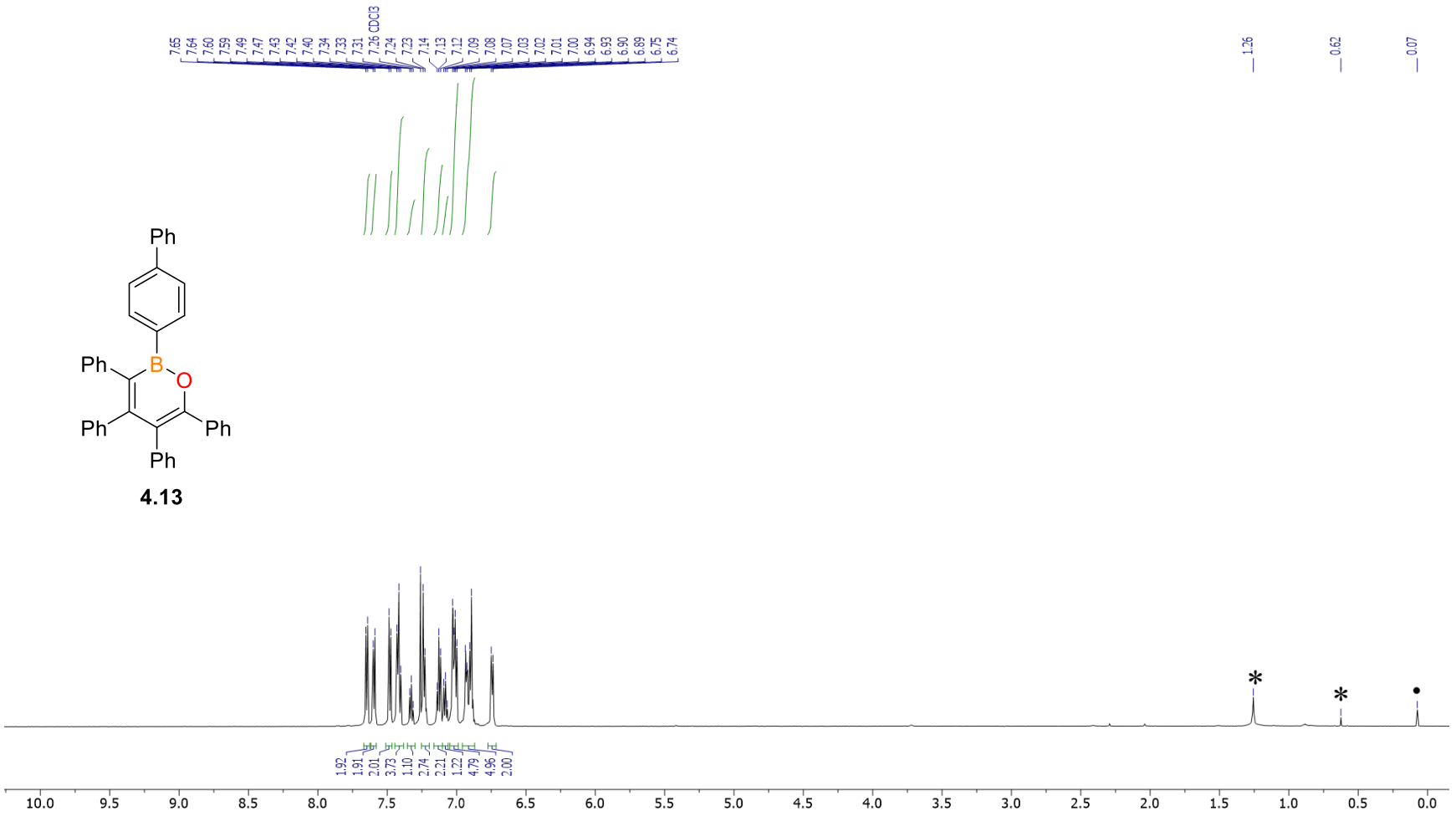

Figure C-11: ^{1}H NMR spectrum of **4.13** in $CDCl_3$ (* *n*-pentane, • grease).

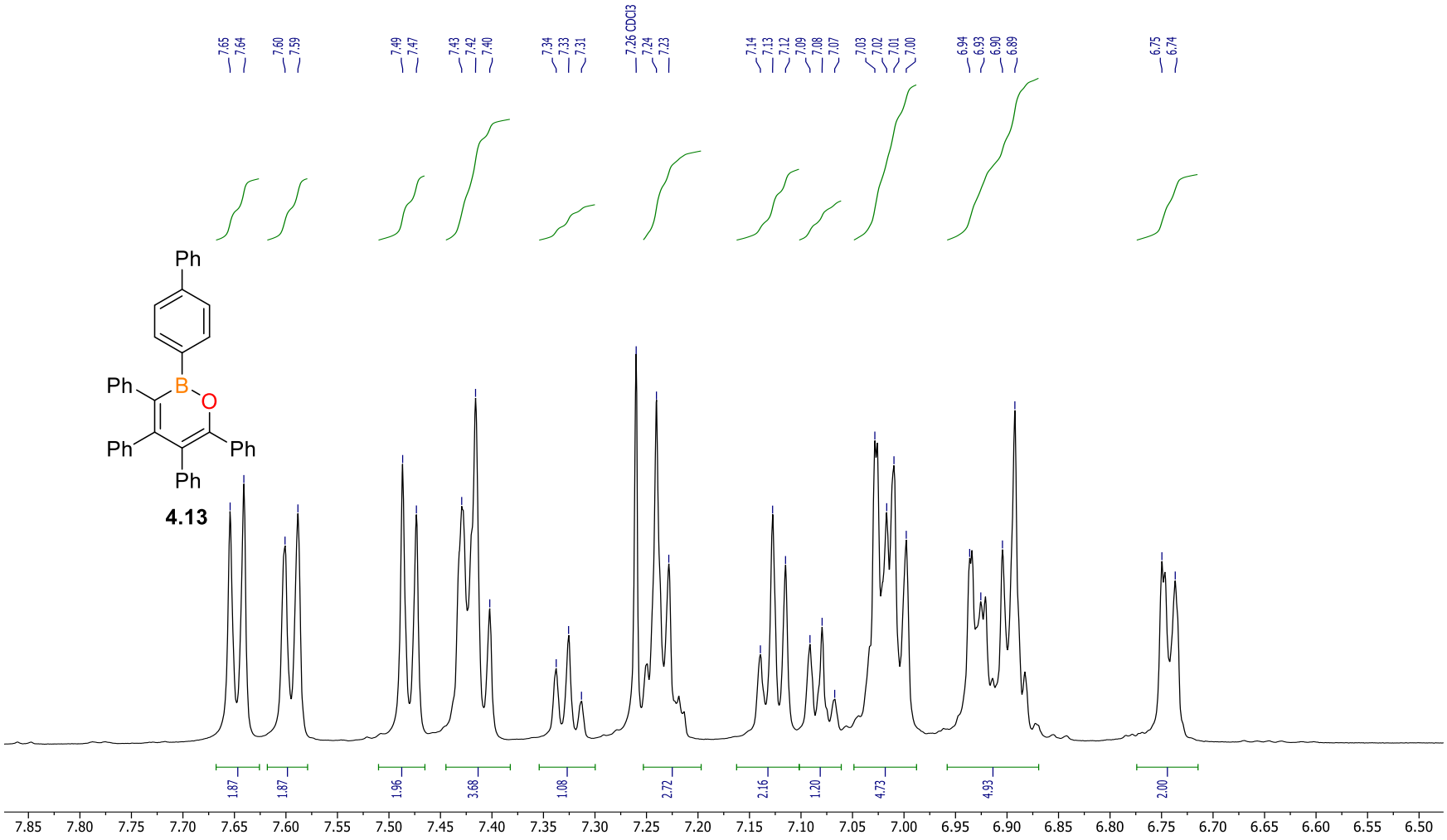

Figure C-12: Expansion of ^{1}H NMR spectrum of **4.13** in $CDCl_3$.

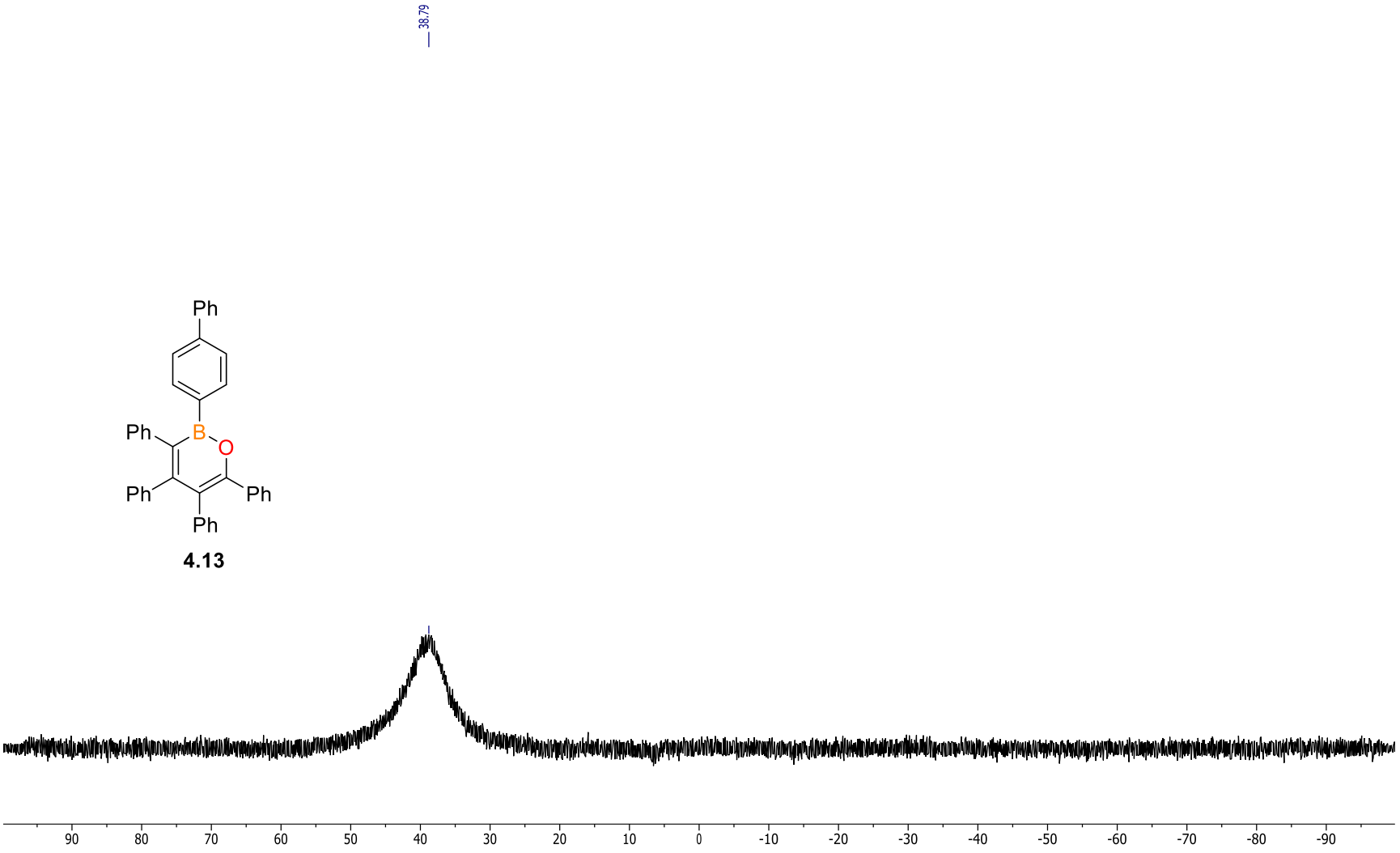

Figure C-13: $^{11}B\{^{1}H\}$ NMR spectrum of **4.13** in $CDCl_3$.

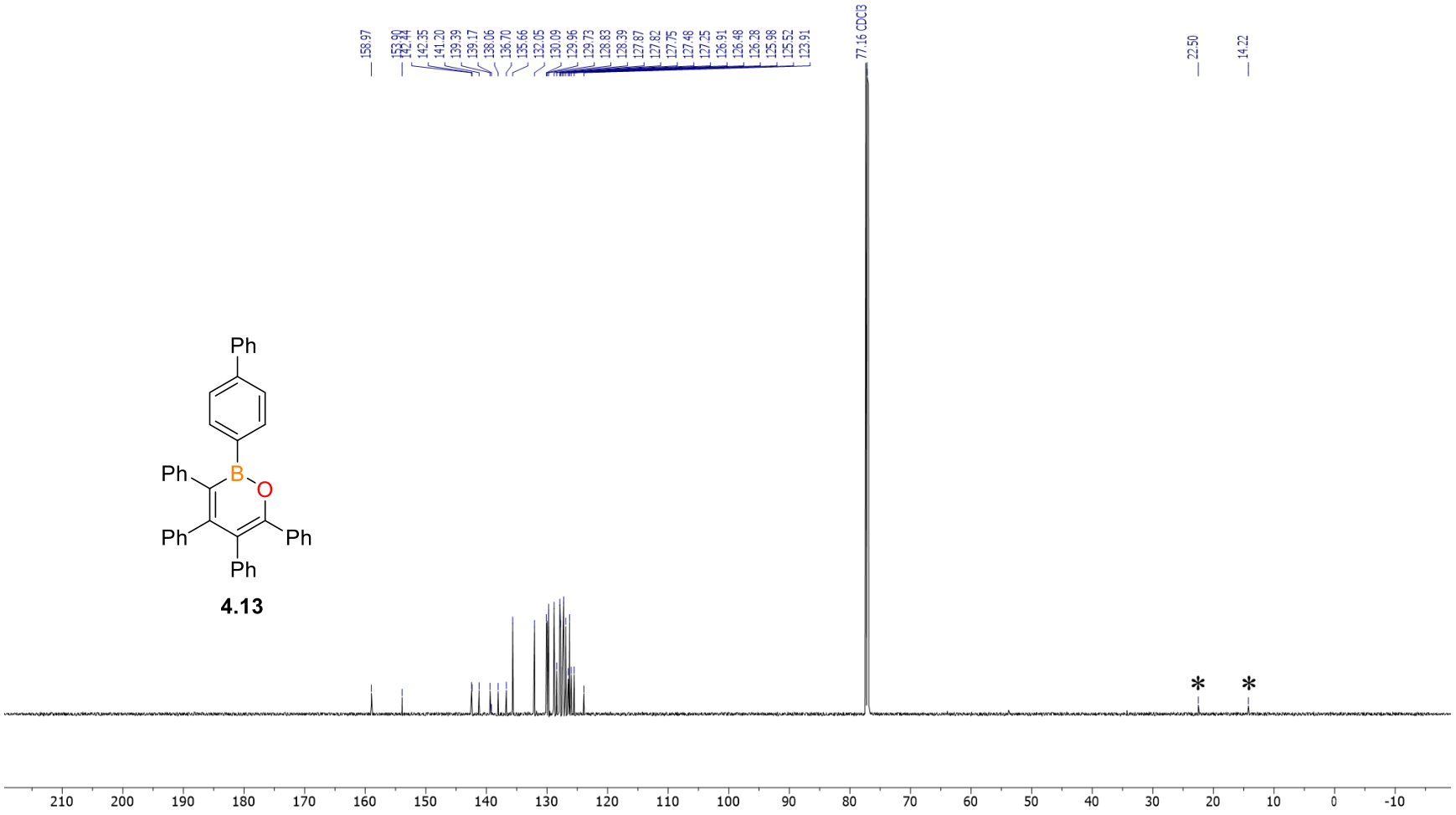

Figure C-14: $^{13}C\{^{1}H\}$ NMR spectrum of **4.13** in $CDCl_3$ (**n*-pentane).

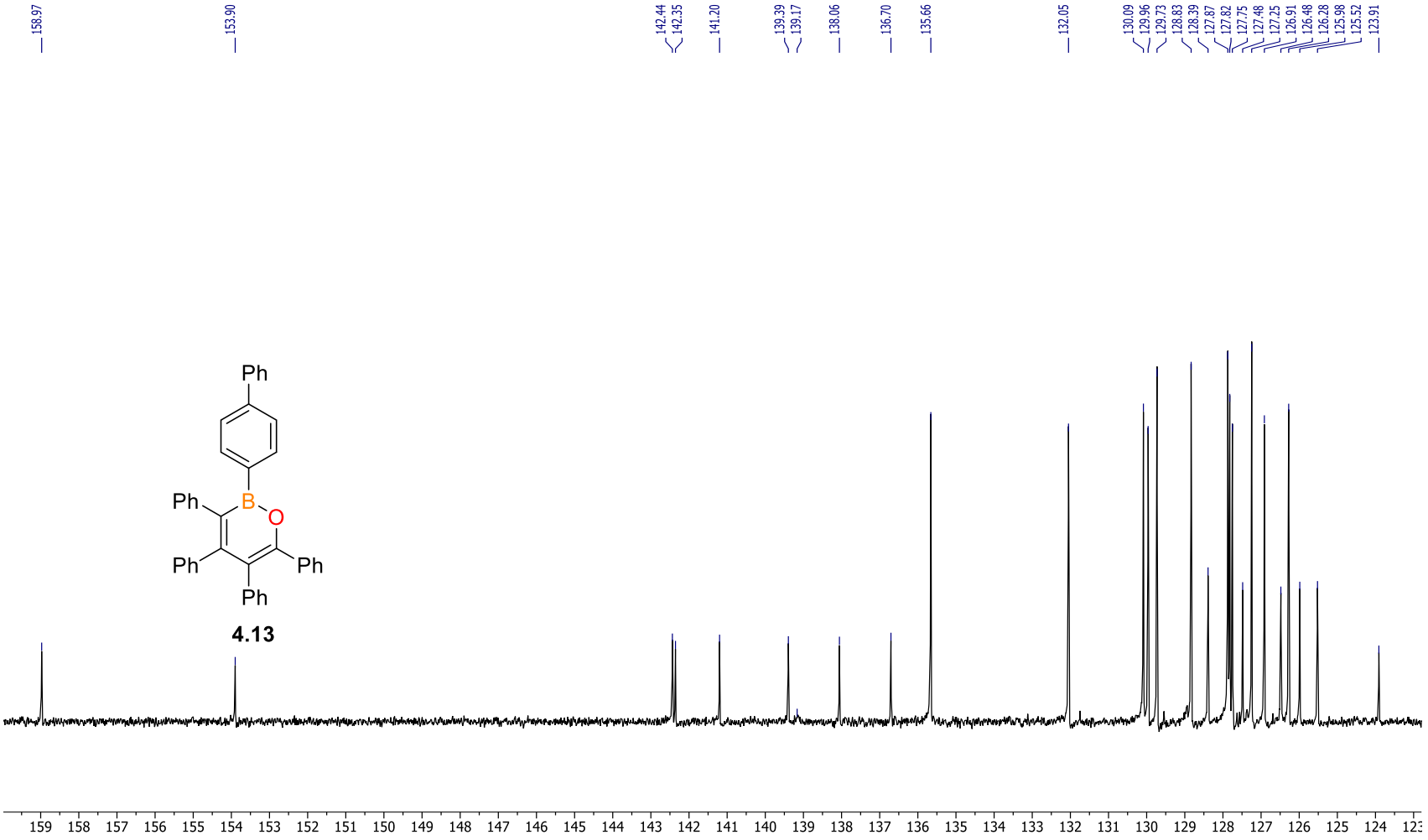

Figure C-15: Expansion of $^{13}C\{^{1}H\}$ NMR spectrum of **4.13** in $CDCl_3$.

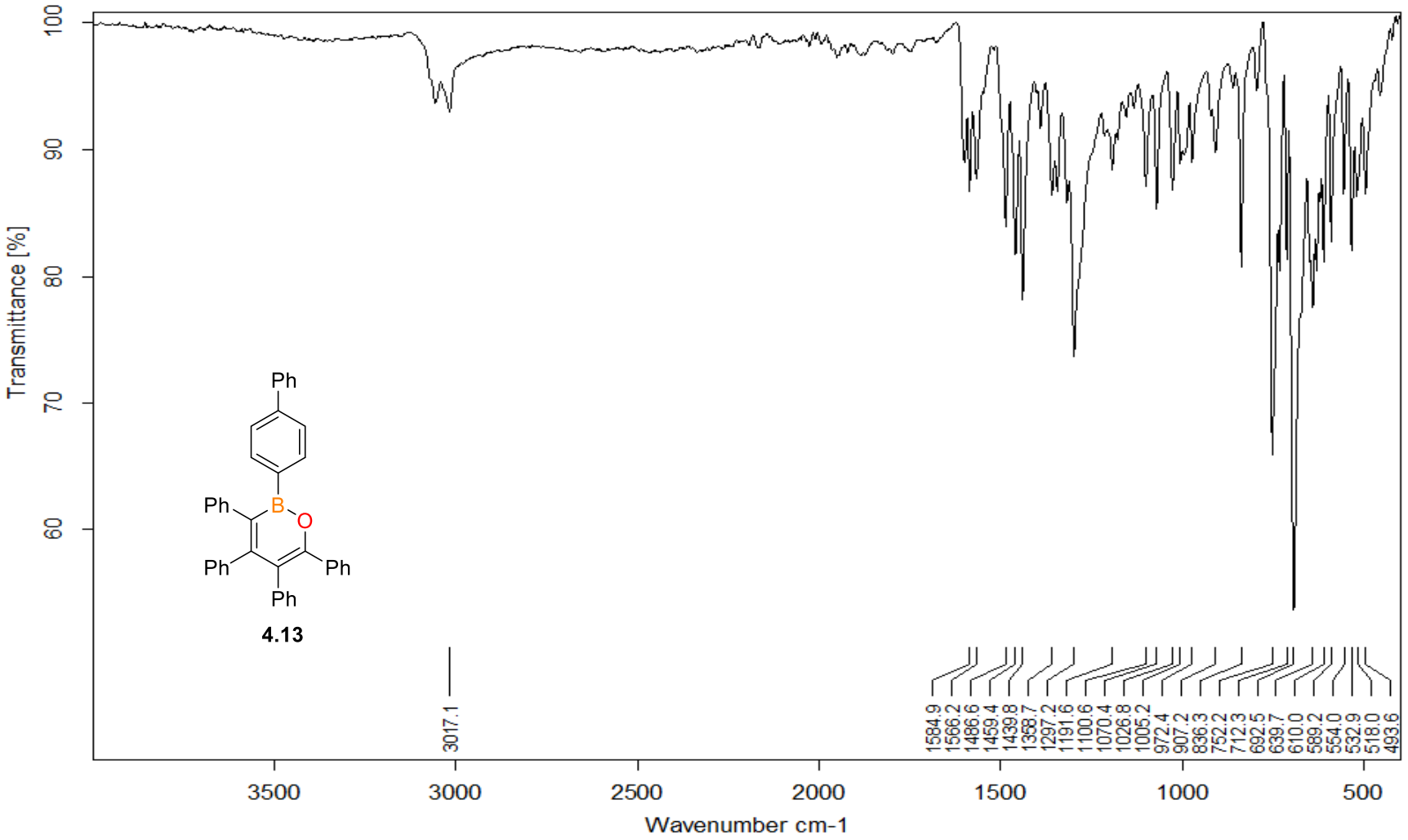

Figure C-16: FT-IR spectrum of **4.13**.

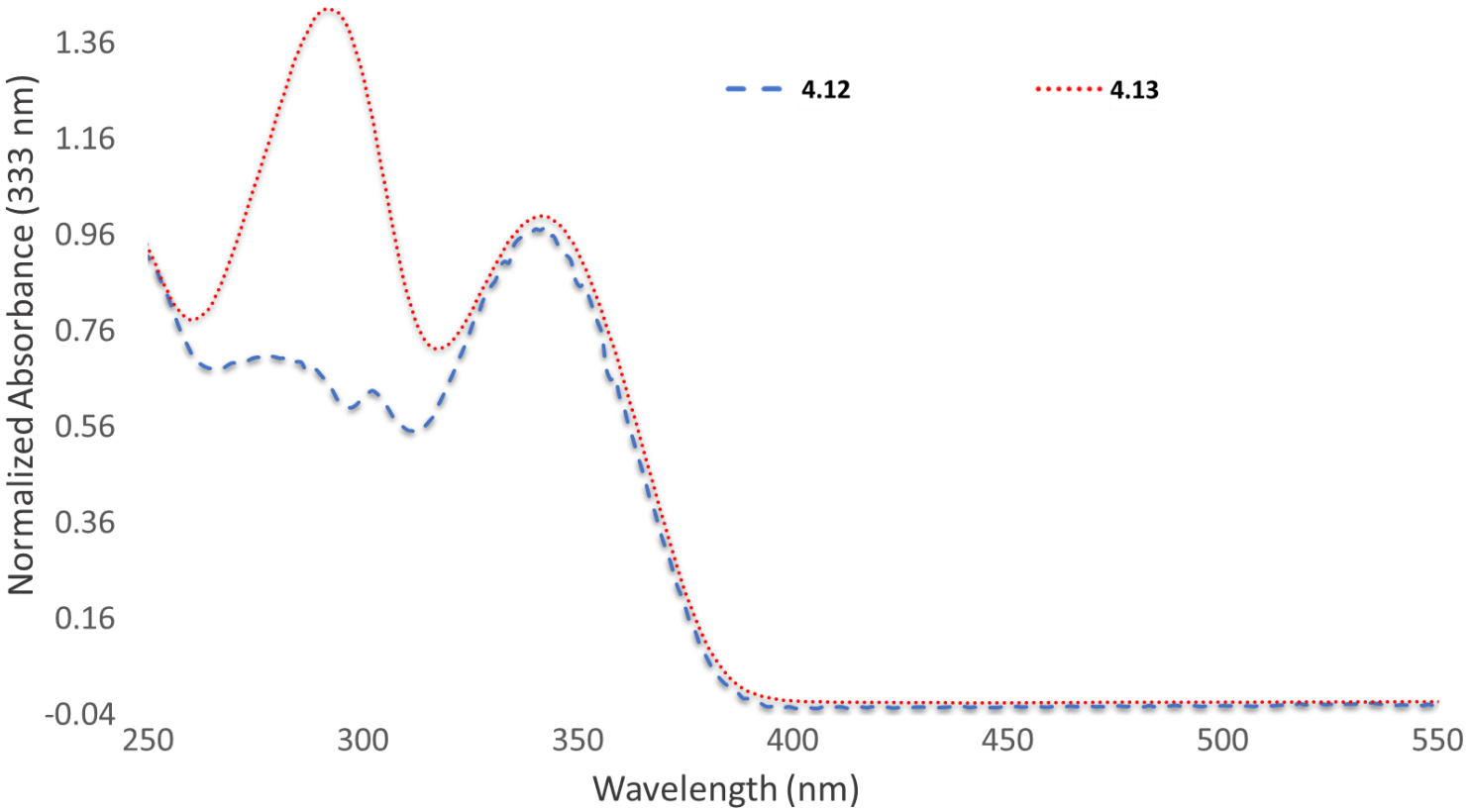

4.12 (333 nm): ε = 12,000 $Lmol^{-1}$ cm^{-1}; (305 nm): ε = 7500 $Lmol^{-1}$ cm^{-1}; (282 nm): ε = 5600 $Lmol^{-1}$ cm^{-1}

4.13 (333 nm): ε = 11,000 $Lmol^{-1}$ cm^{-1}; (295 nm): ε = 17,000 $Lmol^{-1}$ cm^{-1}

Figure C-17: Normalized absorption spectrum of **4.12** and **4.13** in CH_2Cl_2 (normalized at the 333 nm peak).

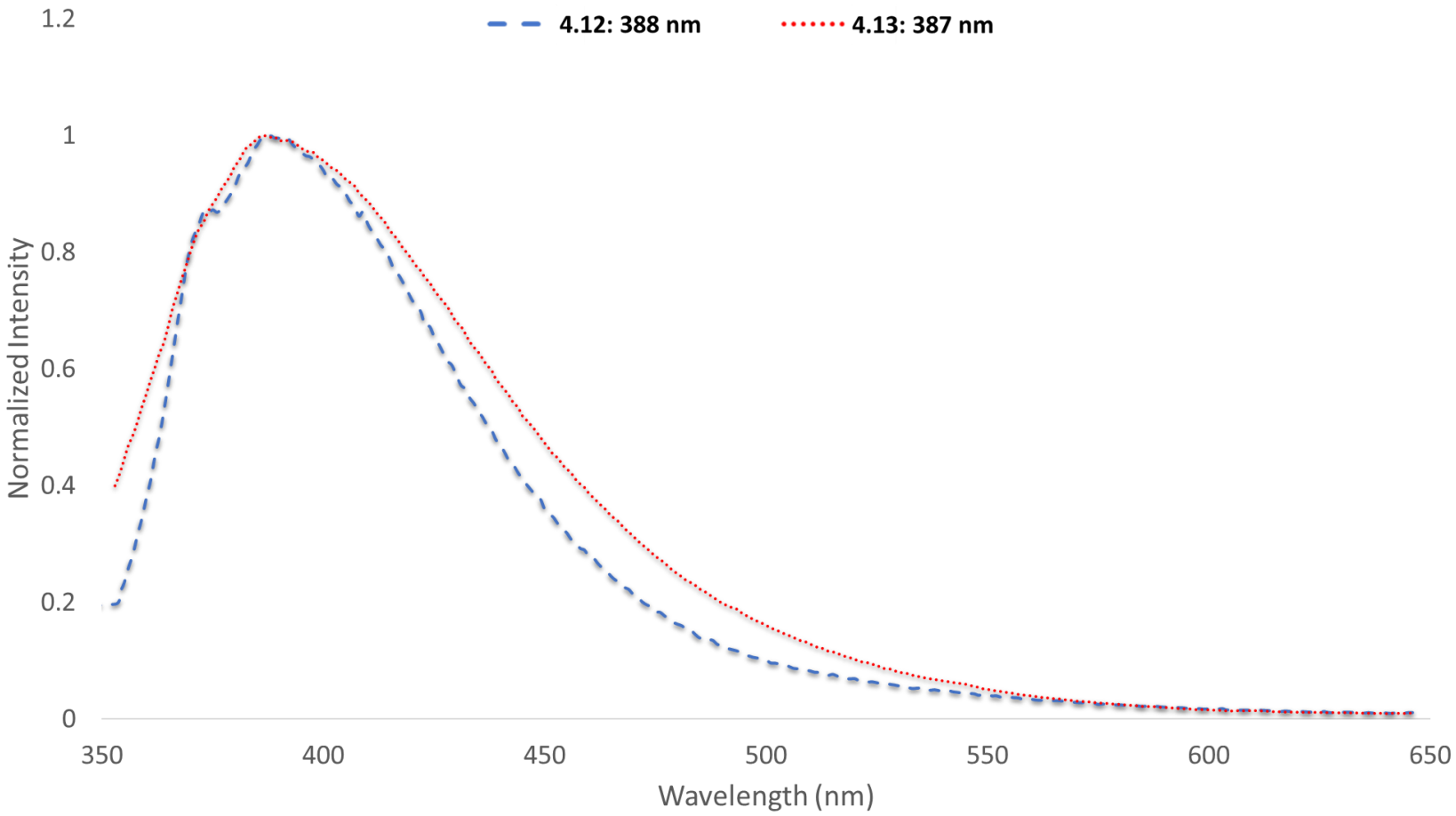

Figure C-18: Normalized emission spectra of **4.12** and **4.13** in CH_2Cl_2 (both compounds excited at 333 nm). Concentrations of samples **4.12**: 6.66×10^{-7} M; **4.13**: 6.58×10^{-7} M.

Table C-1: Coordinates of the HSE06/6-311+G(d,p) Geometry of **4.2** Simulated in C1 Symmetry.

Center Number	Atomic Number	Atomic Type	Coordinates (Angstroms) X	Y	Z
1	6	0	0.397343	-1.034286	0.006079
2	6	0	1.831846	1.366935	0.005033
3	6	0	0.478838	1.393573	0.004814
4	6	0	-0.250708	0.168294	0.005349
5	1	0	-0.187411	-1.948899	0.006505
6	1	0	2.453605	2.255443	0.004641
7	1	0	-0.028157	2.350431	0.004230
8	1	0	-1.337385	0.224128	0.005175
9	5	0	1.909040	-1.014922	0.006259
10	1	0	2.654896	-1.944609	0.006829
11	8	0	2.528709	0.233333	0.005703
12	0	0	1.117336	0.150963	0.005841
13	0	0	1.117336	0.150963	1.005841
14	0	0	1.117336	0.150963	-0.994159

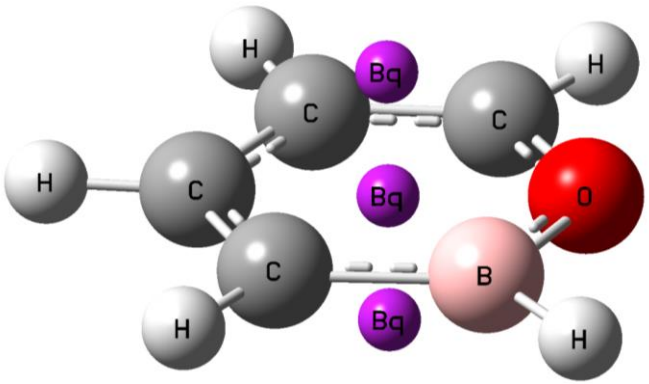

Figure C-19: Computed optimized structure of **4.2** displaying ghost atom positioning within the central ring.

Table C-2: Coordinates of the HSE06/6-311+G(d,p) Geometry of **4.6** Simulated in C1 Symmetry.

Center Number	Atomic Number	Atomic Type	Coordinates (Angstroms) X	Y	Z
1	6	0	2.313696	-0.847202	-0.000463
2	6	0	1.773142	0.392019	-0.001105
3	6	0	0.352766	0.539059	-0.001205
4	6	0	-0.467297	-0.550492	-0.000671
5	1	0	3.380991	-1.040332	-0.000355
6	1	0	2.428808	1.253684	-0.001530
7	1	0	-0.053200	1.548485	-0.001728
8	1	0	-1.540973	-0.387702	-0.000774
9	5	0	0.174720	-1.927553	0.000021
10	8	0	1.575983	-1.953950	0.000063
11	6	0	-0.529866	-3.315570	0.000705
12	6	0	0.210024	-4.507233	0.001273
13	6	0	-1.927638	-3.418374	0.000767
14	6	0	-0.416966	-5.745876	0.001873
15	1	0	1.294184	-4.453776	0.001239
16	6	0	-2.562650	-4.654051	0.001364
17	1	0	-2.532006	-2.516012	0.000338
18	6	0	-1.806697	-5.821572	0.001918
19	1	0	0.175413	-6.655351	0.002306
20	1	0	-3.646535	-4.708725	0.001398
21	1	0	-2.299313	-6.788681	0.002386
22	0	0	0.917534	-0.713656	-0.031292
23	0	0	0.917534	-0.713656	-1.031292
24	0	0	0.917534	-0.713656	0.968708

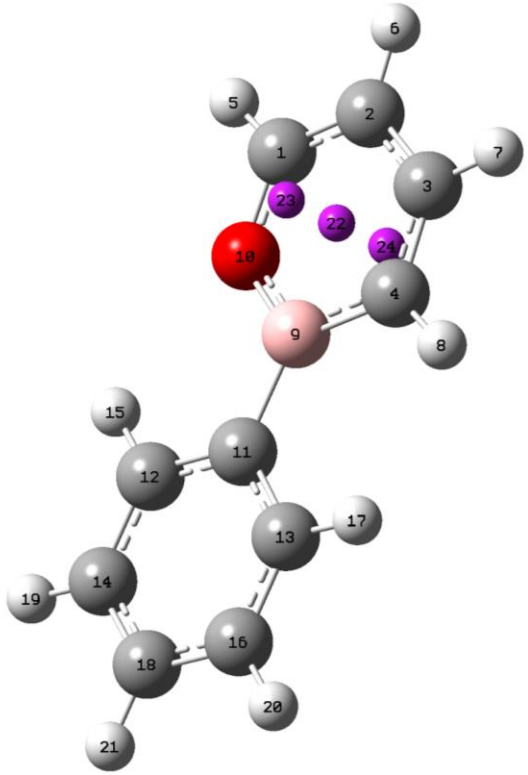

Figure C-20: Computed optimized structure of **4.6** displaying ghost atom positioning within the central ring.

Table C-3: Coordinates of the HSE06/6-311+G(d,p) Geometry of Hexaphenylbenzene Simulated in C1 Symmetry.

Center Number	Atomic Number	Atomic Type	Coordinates (Angstroms) X	Y	Z
1	6	0	0.698849	-0.795613	0.001780
2	6	0	2.104734	-0.795723	-0.000351
3	6	0	2.807484	0.421975	0.000629
4	6	0	2.104920	1.639783	0.000926
5	6	0	0.699038	1.639888	-0.002570
6	6	0	-0.003713	0.422190	-0.000737
7	6	0	-0.047814	-2.086315	0.009502
8	6	0	0.041650	-2.970957	-1.066810
9	6	0	-0.851754	-2.435899	1.096095
10	6	0	-0.657810	-4.171108	-1.059506
11	1	0	0.667879	-2.715922	-1.915489
12	6	0	-1.545592	-3.639160	1.108859
13	1	0	-0.934432	-1.756280	1.937909
14	6	0	-1.452662	-4.510679	0.029534
15	1	0	-0.578355	-4.844742	-1.906515
16	1	0	-2.163567	-3.894607	1.963483
17	1	0	-1.996924	-5.449238	0.036838
18	6	0	2.851560	2.930505	0.007753
19	6	0	3.654474	3.281440	1.094673
20	6	0	2.763047	3.813846	-1.069705
21	6	0	4.348271	4.484730	1.106610
22	1	0	3.736391	2.602849	1.937389
23	6	0	3.462475	5.014021	-1.063222
24	1	0	2.137600	3.557761	-1.918645
25	6	0	4.256324	5.354927	0.026132
26	1	0	4.965447	4.741242	1.961492
27	1	0	3.383781	5.686623	-1.911122
28	1	0	4.800564	6.293504	0.032793
29	6	0	-1.495015	0.422301	-0.001466
30	6	0	-2.207304	-0.093633	-1.085596
31	6	0	-2.208292	0.938334	1.081964
32	6	0	-3.596430	-0.090555	-1.088863
33	1	0	-1.665934	-0.502598	-1.932413
34	6	0	-3.597422	0.935442	1.083874
35	1	0	-1.667695	1.347236	1.929303
36	6	0	-4.296752	0.422490	-0.002836
37	1	0	-4.133075	-0.493562	-1.941559

38	1	0	-4.134844	1.338525	1.936044
39	1	0	-5.381722	0.422561	-0.003365
40	6	0	2.851194	-2.086552	-0.006502
41	6	0	3.655091	-2.437537	-1.092678
42	6	0	2.761573	-2.969919	1.070842
43	6	0	4.348750	-3.640910	-1.104014
44	1	0	3.737884	-1.758919	-1.935287
45	6	0	3.460861	-4.170179	1.064967
46	1	0	2.135361	-2.713789	1.919204
47	6	0	4.255685	-4.511142	-0.023659
48	1	0	4.966700	-3.897461	-1.958326
49	1	0	3.381291	-4.842802	1.912768
50	1	0	4.799818	-5.449784	-0.029847
51	6	0	-0.047408	2.930712	-0.010983
52	6	0	0.041172	3.815289	1.065457
53	6	0	-0.850215	3.280503	-1.098348
54	6	0	-0.658059	5.015568	1.057531
55	1	0	0.666525	3.560097	1.914736
56	6	0	-1.543823	4.483890	-1.111727
57	1	0	-0.932194	2.600944	-1.940279
58	6	0	-1.451790	5.355336	-0.032265
59	1	0	-0.579309	5.689148	1.904649
60	1	0	-2.160914	4.739496	-1.966943
61	1	0	-1.995874	6.293994	-0.040053
62	6	0	4.298785	0.421856	0.001348
63	6	0	5.011007	-0.092939	1.086065
64	6	0	5.012135	0.936523	-1.082685
65	6	0	6.400133	-0.090071	1.089317
66	1	0	4.469583	-0.500856	1.933351
67	6	0	6.401263	0.933403	-1.084610
68	1	0	4.471594	1.344548	-1.930483
69	6	0	7.100526	0.421602	0.002687
70	1	0	6.936722	-0.492174	1.942474
71	1	0	6.938739	1.335413	-1.937253
72	1	0	8.185496	0.421502	0.003204
73	0	0	1.354410	0.443517	0.011111
74	0	0	1.354410	0.443517	1.000000
75	0	0	1.354410	0.443517	-1.000000

.

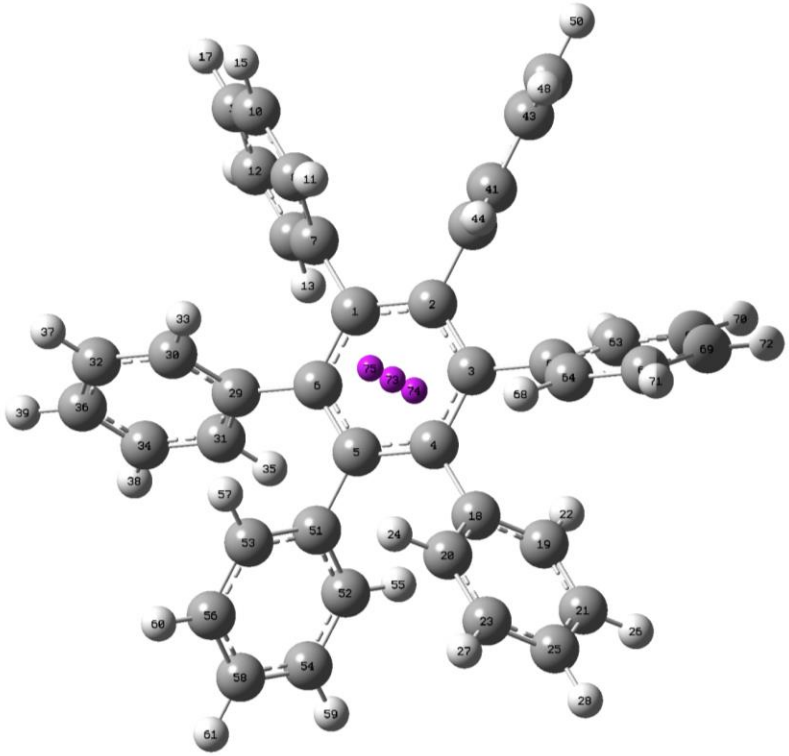

Figure C-21: Computed optimized structure of hexaphenylbenzene displaying ghost atom positioning within the central ring.

Table C-4: Coordinates of the HSE06/6-311+G(d,p) Geometry of Hexaphenyl-1,2-azaborine (**5.1**) Simulated in C1 Symmetry.

Center Number	Atomic Number	Atomic Type	Coordinates (Angstroms) X	Y	Z
1	6	0	2.193775	0.298714	0.006791
2	6	0	1.503179	1.492731	0.009507
3	6	0	0.066211	1.515976	-0.002862
4	6	0	-0.665744	0.341593	-0.009056
5	6	0	-0.649893	-2.385902	-0.021382
6	6	0	-0.455982	-3.347615	-1.021488
7	6	0	-1.562645	-2.692781	0.997097
8	6	0	-1.138786	-4.558329	-1.007038
9	1	0	0.243346	-3.151263	-1.829174
10	6	0	-2.231706	-3.910581	1.031740
11	1	0	-1.760790	-1.960967	1.775182
12	6	0	-2.024515	-4.847276	0.025402
13	1	0	-0.974375	-5.280948	-1.800295
14	1	0	-2.925873	-4.123344	1.838668
15	1	0	-2.552985	-5.795096	0.042936
16	6	0	3.683782	0.278488	0.028168
17	6	0	4.409392	0.768141	-1.058234
18	6	0	4.377405	-0.208748	1.137458
19	6	0	5.798162	0.765327	-1.039887
20	1	0	3.878735	1.160463	-1.919204
21	6	0	5.765815	-0.206485	1.158680
22	1	0	3.825773	-0.588835	1.990752
23	6	0	6.480660	0.278026	0.068768
24	1	0	6.347961	1.149379	-1.892701
25	1	0	6.290761	-0.584465	2.029705
26	1	0	7.565428	0.278178	0.084996
27	6	0	-0.621092	2.840780	-0.019603
28	6	0	-1.416294	3.202707	-1.108298
29	6	0	-0.496742	3.734731	1.045302
30	6	0	-2.064733	4.430764	-1.136261
31	1	0	-1.529722	2.511220	-1.936730
32	6	0	-1.155546	4.957323	1.024816
33	1	0	0.121160	3.469506	1.896854
34	6	0	-1.938827	5.311702	-0.068112
35	1	0	-2.676043	4.696657	-1.992473
36	1	0	-1.052567	5.637426	1.864088
37	1	0	-2.449313	6.268916	-0.086372
38	6	0	2.294806	-2.121439	-0.050548

39	6	0	3.013641	-2.459273	-1.192150
40	6	0	2.288835	-2.976455	1.045198
41	6	0	3.736079	-3.645155	-1.230062
42	1	0	3.006716	-1.791236	-2.046289
43	6	0	3.008705	-4.163602	1.002262
44	1	0	1.709319	-2.711494	1.922647
45	6	0	3.736348	-4.499930	-0.133527
46	1	0	4.297404	-3.902369	-2.122007
47	1	0	2.996897	-4.828807	1.858998
48	1	0	4.298881	-5.426781	-0.165666
49	6	0	-2.151743	0.366500	0.017429
50	6	0	-2.851909	0.957589	1.074014
51	6	0	-2.889319	-0.239671	-1.003886
52	6	0	-4.240738	0.951474	1.103707
53	1	0	-2.298576	1.426539	1.881073
54	6	0	-4.278314	-0.236812	-0.982569
55	1	0	-2.363706	-0.719689	-1.823148
56	6	0	-4.960883	0.358306	0.072542
57	1	0	-4.762286	1.414183	1.935532
58	1	0	-4.829079	-0.707934	-1.790413
59	1	0	-6.045715	0.356256	0.093276
60	6	0	2.266697	2.774946	0.024603
61	6	0	3.039635	3.137574	1.129145
62	6	0	2.214327	3.647275	-1.064910
63	6	0	3.747134	4.333349	1.143413
64	1	0	3.087402	2.472373	1.985255
65	6	0	2.921810	4.842480	-1.054546
66	1	0	1.608934	3.386209	-1.926951
67	6	0	3.691610	5.190188	0.050200
68	1	0	4.342898	4.596023	2.011605
69	1	0	2.869444	5.505871	-1.911728
70	1	0	4.243376	6.124357	0.059304
71	5	0	0.075945	-0.987420	-0.020360
72	7	0	1.521867	-0.907318	-0.009053
73	0	0	0.699907	0.271937	-0.000661
74	0	0	0.699907	0.271937	-0.995809
75	0	0	0.699907	0.271937	0.991061

.

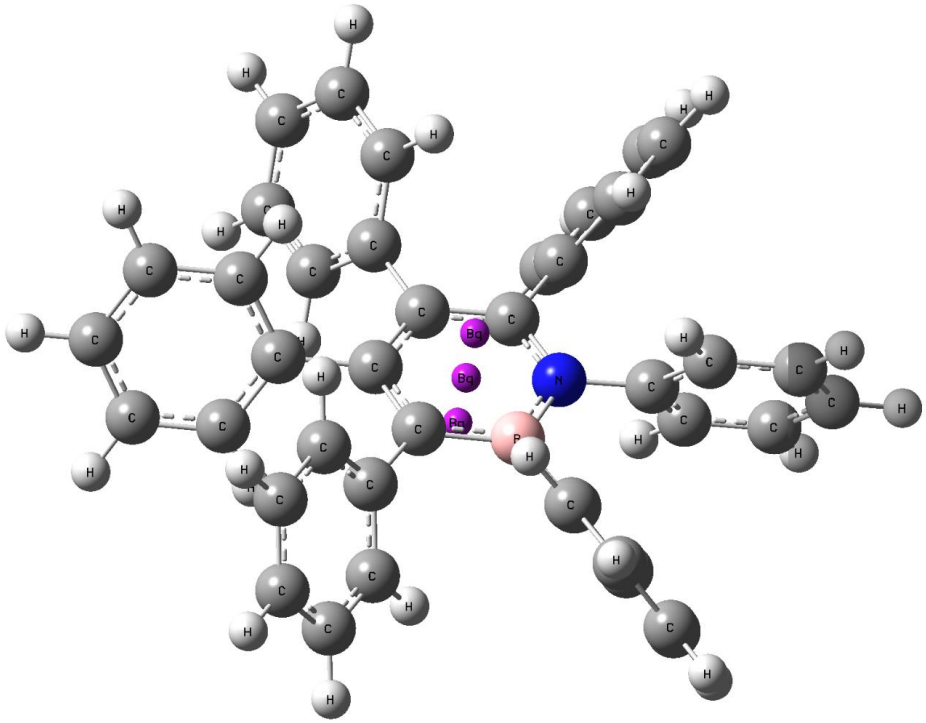

Figure C-22: Computed optimized structure of hexaphenyl-1.2-azaborine (**5.1**) displaying ghost atom positioning within the central ring.

Table C-5: Coordinates of the HSE06/6-311+G(d,p) Geometry of **4.12** Simulated in C1 Symmetry.

Center Number	Atomic Number	Atomic Type	Coordinates (Angstroms) X	Y	Z
1	6	0	1.408961	1.107799	-0.088849
2	6	0	0.748718	2.308586	-0.037103
3	6	0	-0.699999	2.321911	-0.012457
4	6	0	-1.433889	1.151674	-0.010585
5	5	0	-0.652785	-0.157407	0.025852
6	8	0	0.732174	-0.042656	-0.033386
7	6	0	-1.158090	-1.632271	0.134779
8	6	0	-0.335556	-2.678585	-0.312965
9	6	0	-2.392886	-1.977970	0.703242
10	6	0	-0.731197	-4.005804	-0.213990
11	1	0	0.630296	-2.440908	-0.748109
12	6	0	-2.786674	-3.305737	0.820308
13	1	0	-3.055521	-1.200183	1.067198
14	6	0	-1.960074	-4.322988	0.356270
15	1	0	-0.080748	-4.795070	-0.577573
16	1	0	-3.743277	-3.547043	1.272628
17	1	0	-2.271394	-5.359457	0.439784
18	6	0	-2.918348	1.169369	-0.010603
19	6	0	-3.646720	1.711121	1.052690
20	6	0	-3.623657	0.599822	-1.075170
21	6	0	-5.035928	1.688248	1.049116
22	1	0	-3.116343	2.150603	1.890931
23	6	0	-5.012859	0.586265	-1.085375
24	1	0	-3.072527	0.161126	-1.901314
25	6	0	-5.725234	1.129318	-0.021643
26	1	0	-5.582015	2.110910	1.886301
27	1	0	-5.540137	0.144346	-1.924660

28	1	0	-6.810056	1.114631	-0.025634
29	6	0	2.864303	0.881341	-0.191375
30	6	0	3.701273	1.688298	-0.968543
31	6	0	3.418479	-0.219316	0.473370
32	6	0	5.057891	1.410224	-1.061365
33	1	0	3.289224	2.530030	-1.511364
34	6	0	4.777541	-0.486068	0.388876
35	1	0	2.772448	-0.862587	1.059794
36	6	0	5.603298	0.328829	-0.377800
37	1	0	5.691353	2.041099	-1.675843
38	1	0	5.192284	-1.335614	0.921163
39	1	0	6.665250	0.118294	-0.448205
40	6	0	1.514127	3.584175	0.004012
41	6	0	2.348502	3.868209	1.086951
42	6	0	1.416284	4.520544	-1.028375
43	6	0	3.073634	5.052513	1.134700
44	1	0	2.431750	3.147959	1.894714
45	6	0	2.142632	5.703427	-0.983490
46	1	0	0.766673	4.318082	-1.873472
47	6	0	2.974226	5.973768	0.098306
48	1	0	3.717867	5.255210	1.983977
49	1	0	2.057264	6.417605	-1.795903
50	1	0	3.539843	6.898907	0.133829
51	6	0	-1.387271	3.645724	-0.002029
52	6	0	-2.193549	4.026792	-1.075656
53	6	0	-1.249134	4.518229	1.078724
54	6	0	-2.841337	5.255607	-1.072654
55	1	0	-2.314553	3.352373	-1.916841
56	6	0	-1.908585	5.740565	1.088849
57	1	0	-0.620805	4.236702	1.917376
58	6	0	-2.703456	6.115328	0.011147
59	1	0	-3.461132	5.538572	-1.917102
60	1	0	-1.796409	6.404533	1.939634
61	1	0	-3.213849	7.072686	0.016709
62	0	0	-0.028822	1.049494	0.008684
63	0	0	-0.028822	1.049494	-0.991316
64	0	0	-0.028822	1.049494	1.008684

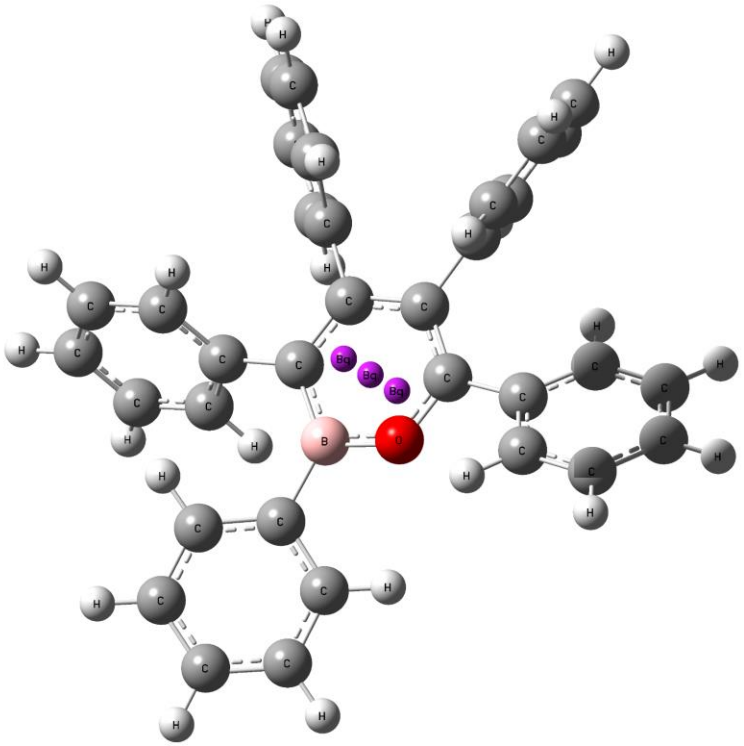

Figure C-23: Computed optimized structure of **4.12** displaying ghost atom positioning within the central ring.

Table C-6: Coordinates of the HSE06/6-311+G(d,p) Geometry of **4.13** Simulated in C1 Symmetry.

Center Number	Atomic Number	Atomic Type	Coordinates (Angstroms) X	Y	Z
1	6	0	-0.318282	-0.630638	-0.051679
2	6	0	1.296533	1.705251	-0.202112
3	6	0	-0.062846	1.826124	-0.069537
4	6	0	-0.879913	0.630928	-0.009529
5	5	0	1.203775	-0.711534	-0.099836
6	8	0	1.877575	0.502416	-0.189614
7	6	0	2.149685	-1.952631	-0.046274
8	6	0	1.786965	-3.172102	0.543539
9	6	0	3.450864	-1.858518	-0.564721
10	6	0	2.674494	-4.235870	0.613663
11	1	0	0.791555	-3.296784	0.955901
12	6	0	4.335090	-2.924464	-0.513380
13	1	0	3.774760	-0.923510	-1.011523
14	6	0	3.963828	-4.135641	0.081282
15	1	0	2.353716	-5.170464	1.062939
16	1	0	5.339183	-2.810268	-0.910091
17	6	0	4.905728	-5.271257	0.148221
18	6	0	4.959959	-6.092533	1.279736
19	6	0	5.768075	-5.554371	-0.916597
20	6	0	5.846039	-7.159601	1.344787
21	1	0	4.317121	-5.875129	2.126578
22	6	0	6.653984	-6.621826	-0.852562
23	1	0	5.724200	-4.945136	-1.813607
24	6	0	6.697173	-7.429383	0.278654
25	1	0	5.878257	-7.778117	2.235828
26	1	0	7.307360	-6.829350	-1.693729
27	1	0	7.389264	-8.263226	0.329046
28	6	0	-1.157956	-1.854318	-0.017899
29	6	0	-1.973869	-2.158040	1.076177
30	6	0	-1.114510	-2.759026	-1.083377
31	6	0	-2.724663	-3.326852	1.102305
32	1	0	-2.015430	-1.471581	1.915261
33	6	0	-1.872862	-3.922863	-1.063328
34	1	0	-0.474802	-2.545203	-1.934057
35	6	0	-2.680013	-4.212904	0.031288
36	1	0	-3.348439	-3.545122	1.963132
37	1	0	-1.827865	-4.608508	-1.903306
38	1	0	-3.268432	-5.124201	0.050676

39	6	0	-2.358847	0.798940	0.085413
40	6	0	-3.183642	0.351507	-0.947731
41	6	0	-2.944125	1.392180	1.205270
42	6	0	-4.562449	0.500828	-0.866967
43	1	0	-2.739035	-0.119972	-1.817888
44	6	0	-4.323638	1.527749	1.293108
45	1	0	-2.313976	1.749431	2.013149
46	6	0	-5.137153	1.086739	0.255123
47	1	0	-5.189467	0.151596	-1.680701
48	1	0	-4.763713	1.984505	2.173432
49	1	0	-6.214326	1.198099	0.321303
50	6	0	2.286041	2.789936	-0.356424
51	6	0	3.540547	2.645864	0.247933
52	6	0	2.038157	3.928879	-1.128737
53	6	0	4.508875	3.630275	0.109908
54	1	0	3.748040	1.754800	0.829464
55	6	0	3.013990	4.904683	-1.275876
56	1	0	1.082988	4.047283	-1.625233
57	6	0	4.248780	4.764482	-0.651537
58	1	0	5.471378	3.509002	0.595647
59	1	0	2.808861	5.777632	-1.886379
60	1	0	5.007221	5.532031	-0.764157
61	6	0	-0.688060	3.173370	0.027290
62	6	0	-0.393204	4.004379	1.110163
63	6	0	-1.576889	3.634729	-0.946910
64	6	0	-0.964534	5.266544	1.214653
65	1	0	0.295664	3.655809	1.873107
66	6	0	-2.146360	4.897535	-0.845505
67	1	0	-1.821265	2.998501	-1.791126
68	6	0	-1.842157	5.718163	0.235774
69	1	0	-0.722794	5.898371	2.063041
70	1	0	-2.831880	5.240931	-1.613275
71	1	0	-2.289079	6.703548	0.315412
72	0	0	0.489289	0.509824	-0.073490
73	0	0	0.489289	0.509824	-1.073490
74	0	0	0.489289	0.509824	0.926510

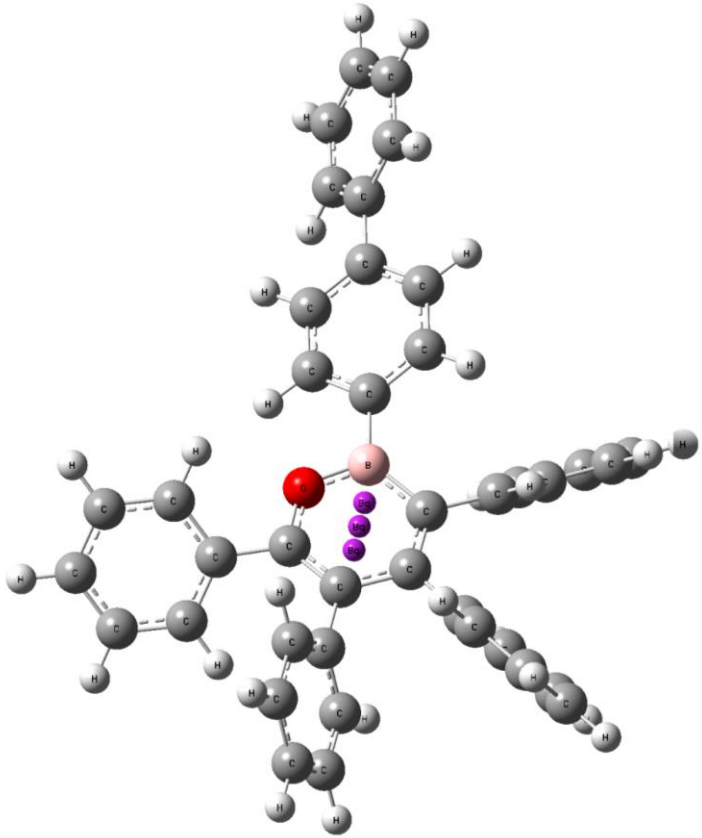

Figure C-24: Computed optimized structure of **4.13** displaying ghost atom positioning within the central ring.

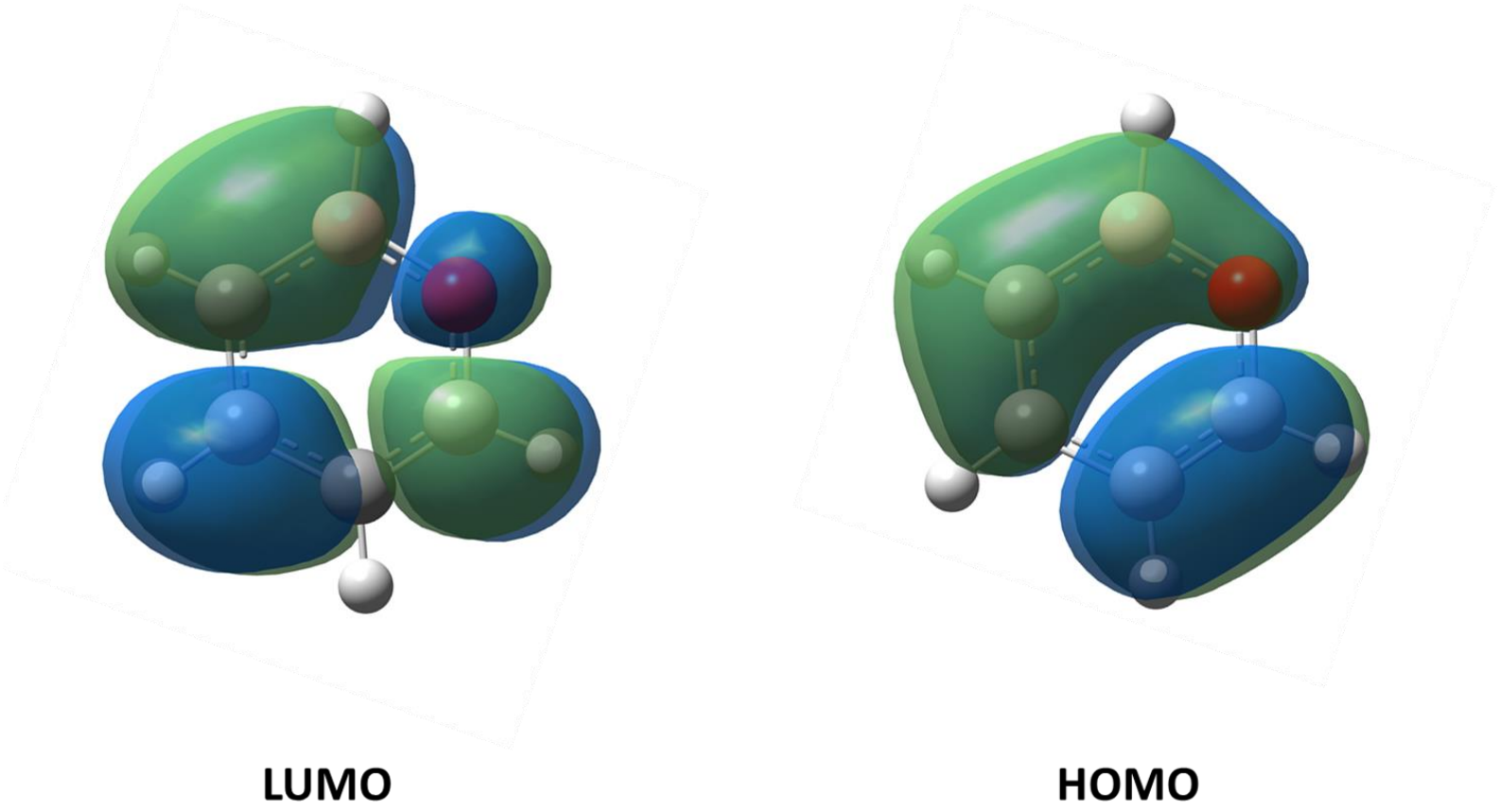

Figure C-25: Frontier orbitals of **4.2** depicting contributions to the aromaticity at an isovalue of 0.02 a.u.

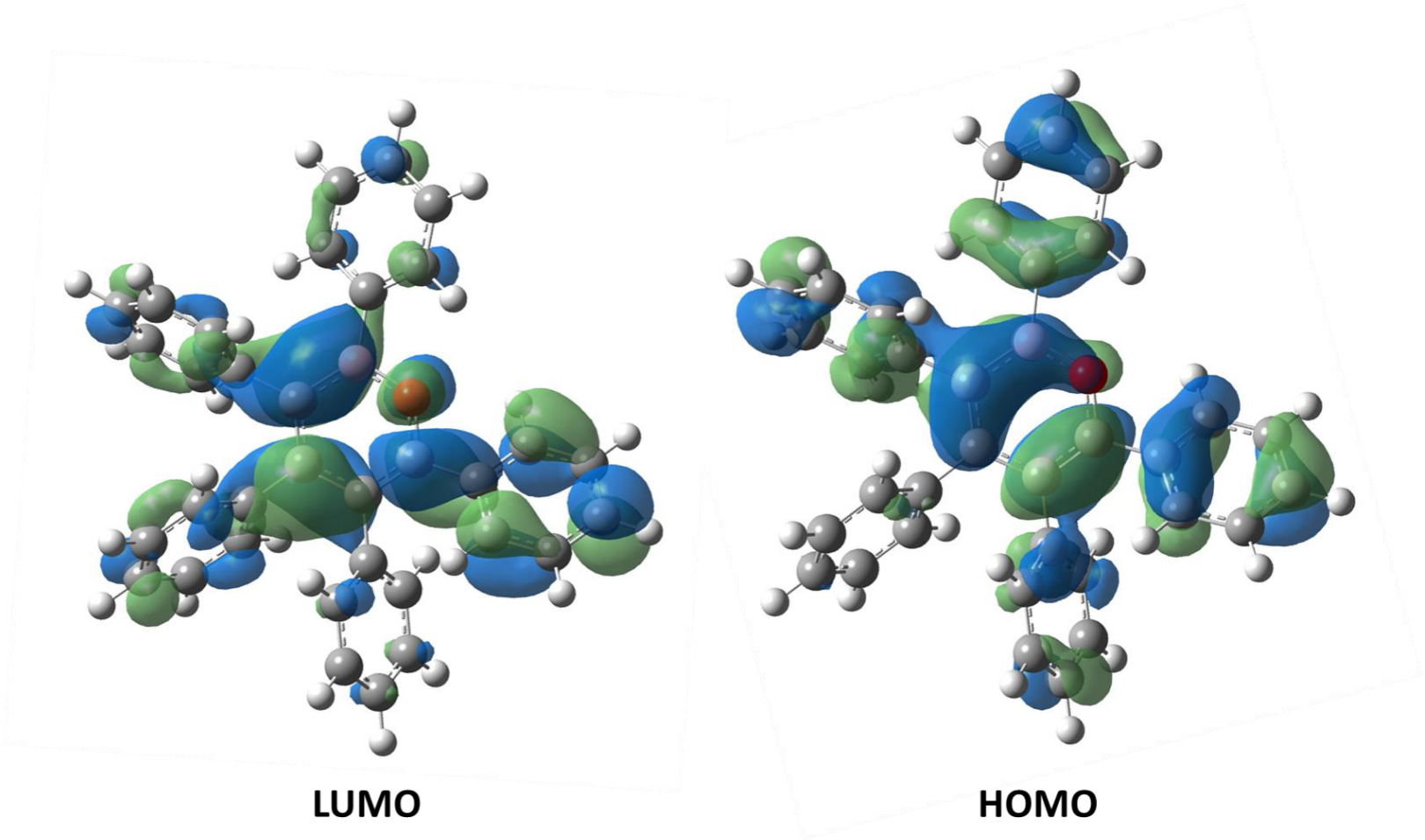

Figure C-26: Frontier orbitals of **4.12** depicting contributions to the aromaticity at an isovalue of 0.02 a.u.

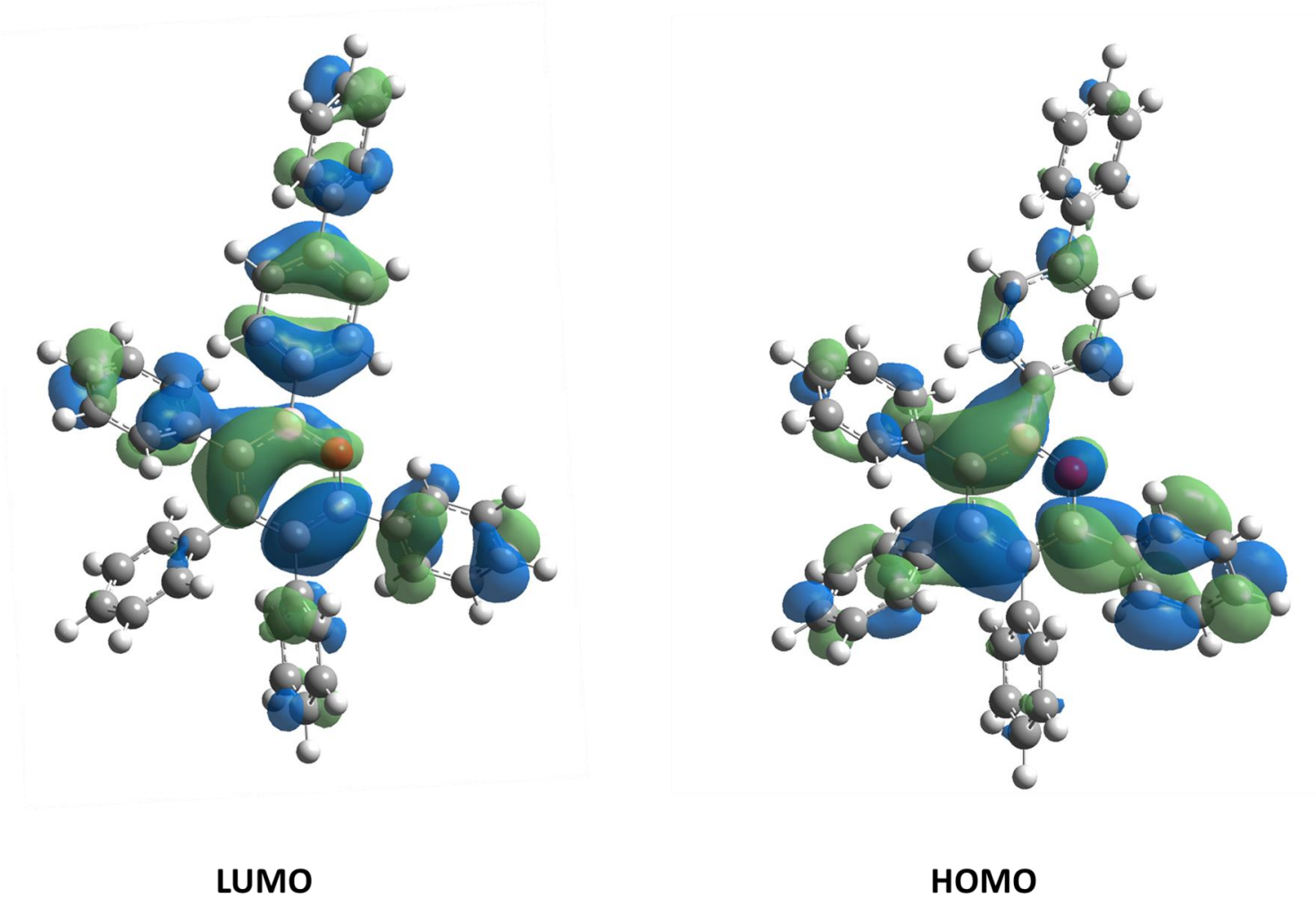

Figure C-27: Frontier orbitals of **4.13** depicting contributions to the aromaticity at an isovalue of 0.02 a.u.

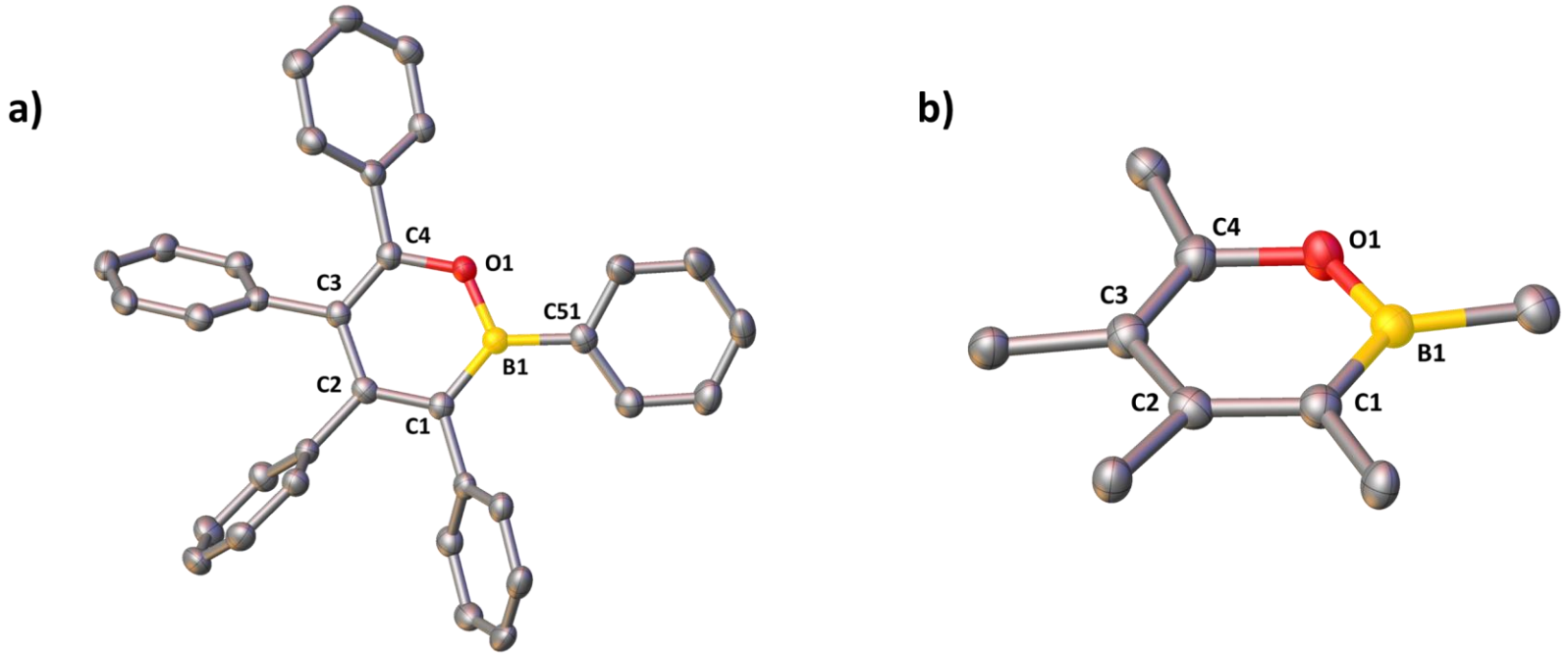

Figure C-28: a) Solid-state structure of **4.12**. Thermal ellipsoids are drawn at the 50% probability level and hydrogen atoms have been omitted for clarity. Selected bond lengths (Å) and angles (˚): B(1)-O(1) 1.388(17), B(1)-C(1) 1.510(19), C(1)-C(2) 1.388(18), C(2)-C(3) 1.449(17), C(3)-C(4) 1.379(18), C(4)-O(1) 1.360(15), B(1)-C(51) 1.567(2), O(1)-B(1)-C(51) 112.40(11), O(1)-B(1)-C(1) 116.70(12), C(51)-B(1)-C(1) 130.88(12), C(4)-C(3)-C(2) 118.93(12), C(3)-C(2)-C(1) 121.56(11), C(2)-C(1)-B(1) 117.58(11); b) Simplified view along the BOC_4 plane of **4.12** (carbon atoms from aryl groups except *ipso* carbons have been removed).

Note: Similar boron heterocycles bearing phenyl groups on boron and carbon atoms within the ring have shown disorder. Therefore, the bond distances and bond angles are not discussed in detail. However, the structure confirms the identity of **4.12**.

Table C-7: Crystallographic Data for **4.12** and **4.13**.

Entry	**4.12**	**4.13**
CCDC	1457937	1457938
Empirical formula	$C_{34}H_{25}BO$	$C_{40}H_{29}BO$
FW (g/mol)	460.35	536.44
Crystal system	Triclinic	Triclinic
Space group	*P-1*	*P-1*
a (Å)	9.7747(5)	10.5923(10)
b (Å)	11.2285(5)	11.7946(7)
c (Å)	12.0790(6)	12.5909(7)
α (deg)	86.439(2)	91.861(2)
β (deg)	70.815(1)	94.751(2)
γ (deg)	85.025(1)	113.478(2)
V (Å^3)	1246.59(11)	1434.13(14)
Z	2	2
D_c (mg m^{-3})	1.226	1.242
radiation, λ (Å)	0.71073	0.71073
temp (K)	150(2)	150(2)
$R1[I>2\sigma I]^a$	0.0470	0.0434
$wR2(F^2)^a$	0.1190	0.1281
GOF $(S)^a$	1.014	1.064

[a] $R1(F[\mathrm{I} > 2(\mathrm{I})]) = \sum\|\|F_o| - |F_c\|\|/ \sum |F_o|$; $wR2(F^2\ [\text{all data}]) = [w(F_o^2 - F_c^2)^2]^{1/2}$; $S(\text{all data}) = [w(F_o^2 - F_c^2)^2/(n - p)]^{1/2}$ (n = no. of data; p = no. of parameters varied; $w = 1/[^2(F_o^2) + (aP)^2 + bP]$ where $P = (F_o^2 + 2F_c^2)/3$ and a and b are constants suggested by the refinement program.

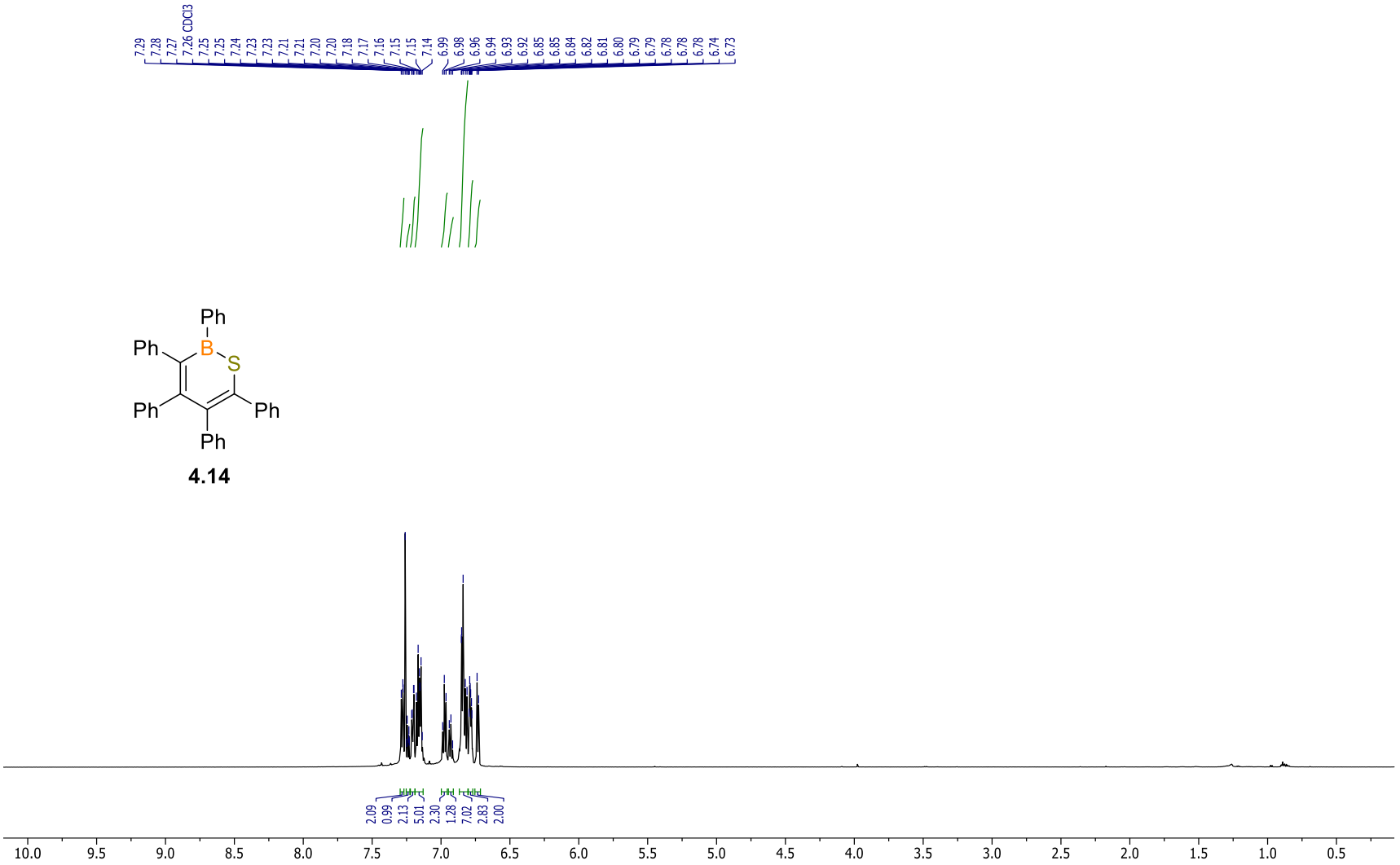

Figure C-29: ^{1}H NMR spectrum of the reaction of **4.14** in $CDCl_3$.

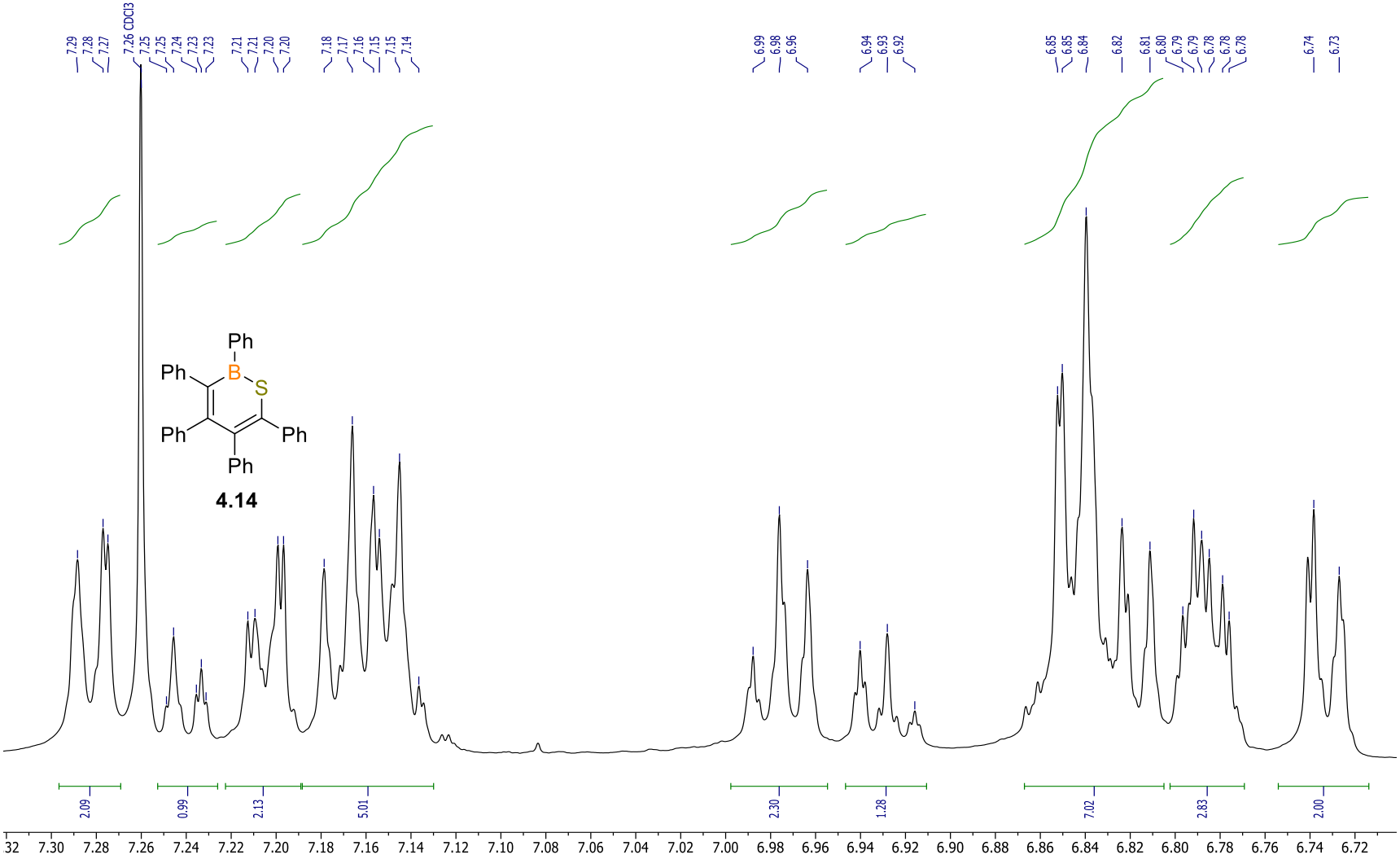

Figure C-30: Expansion of aryl region of ^{1}H NMR spectrum of **4.14** in $CDCl_3$.

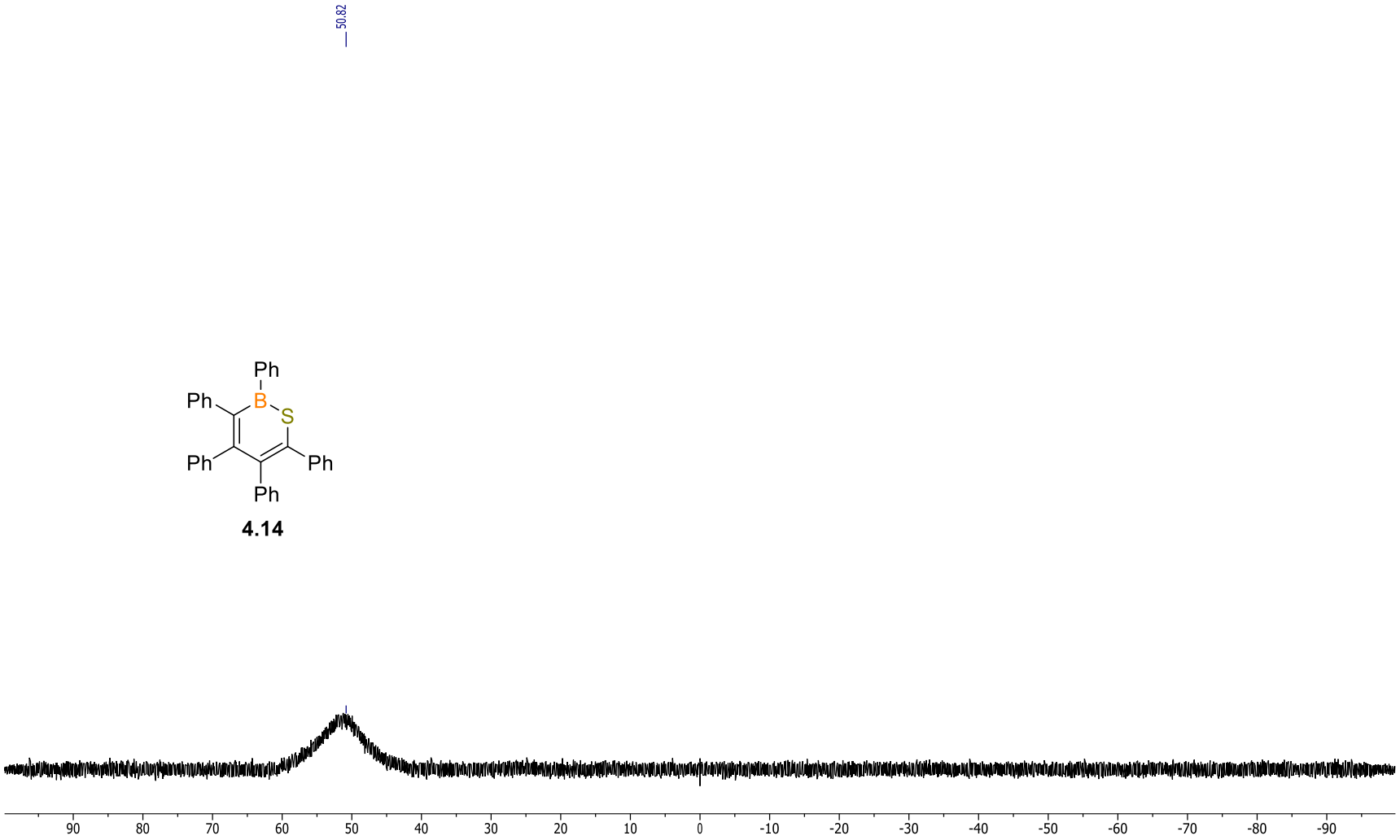

Figure C-31: $^{11}B\{^{1}H\}$ NMR spectrum of **4.14** in $CDCl_3$.

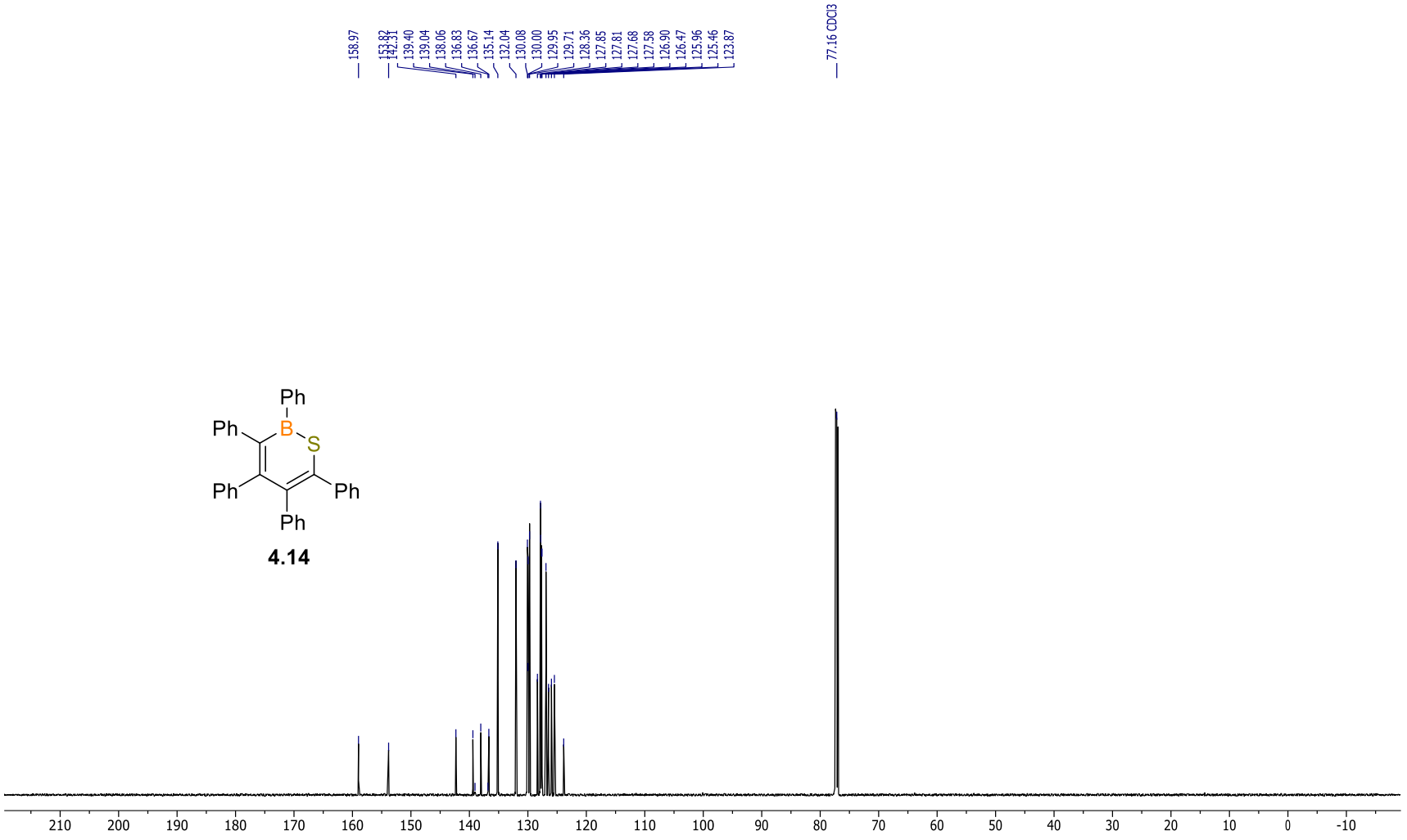

Figure C-32: $^{13}C\{^{1}H\}$ NMR spectrum of **4.14** in $CDCl_3$.

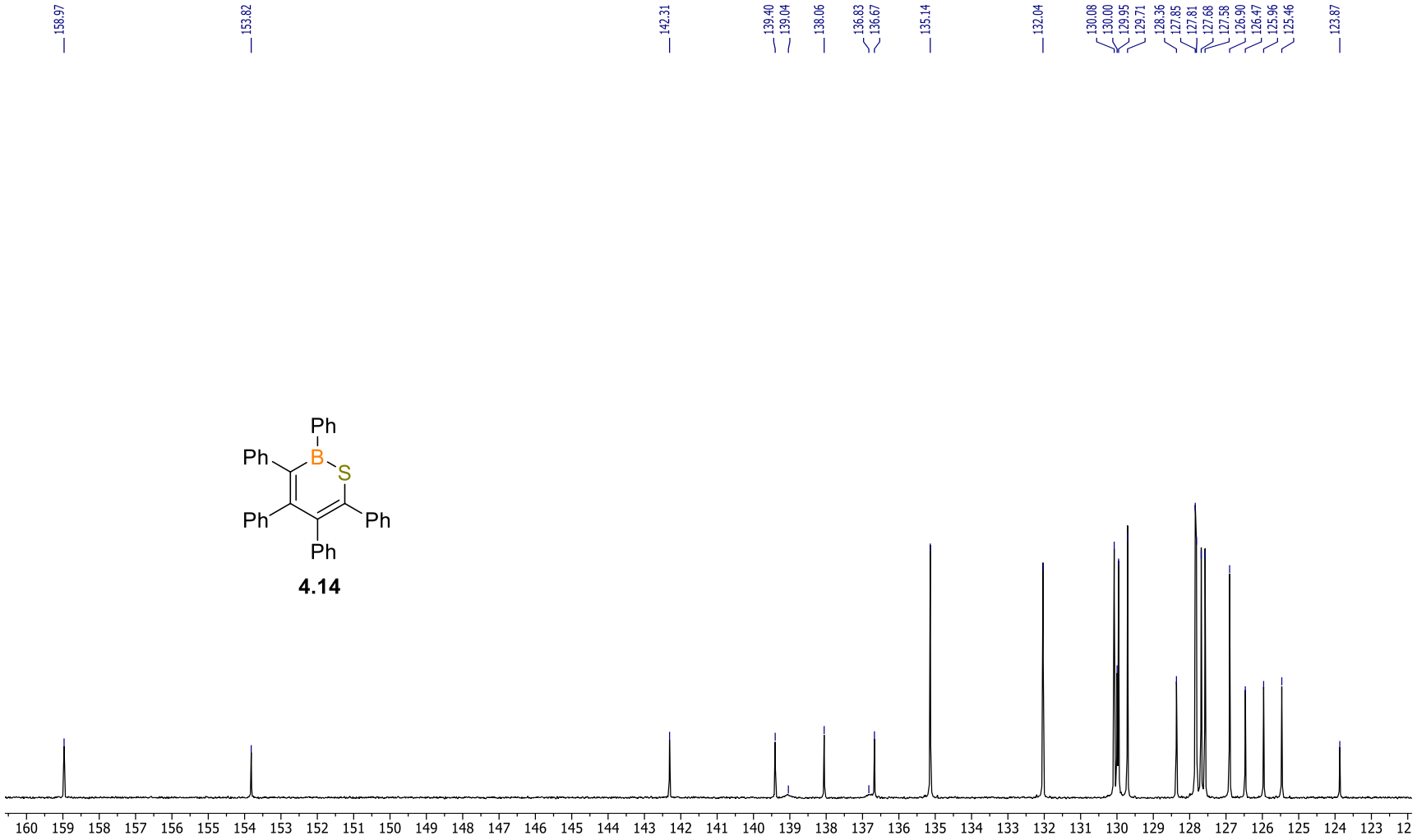

Figure C-33: Expansion of $^{13}C\{^{1}H\}$ NMR spectrum of **4.14** in $CDCl_3$.

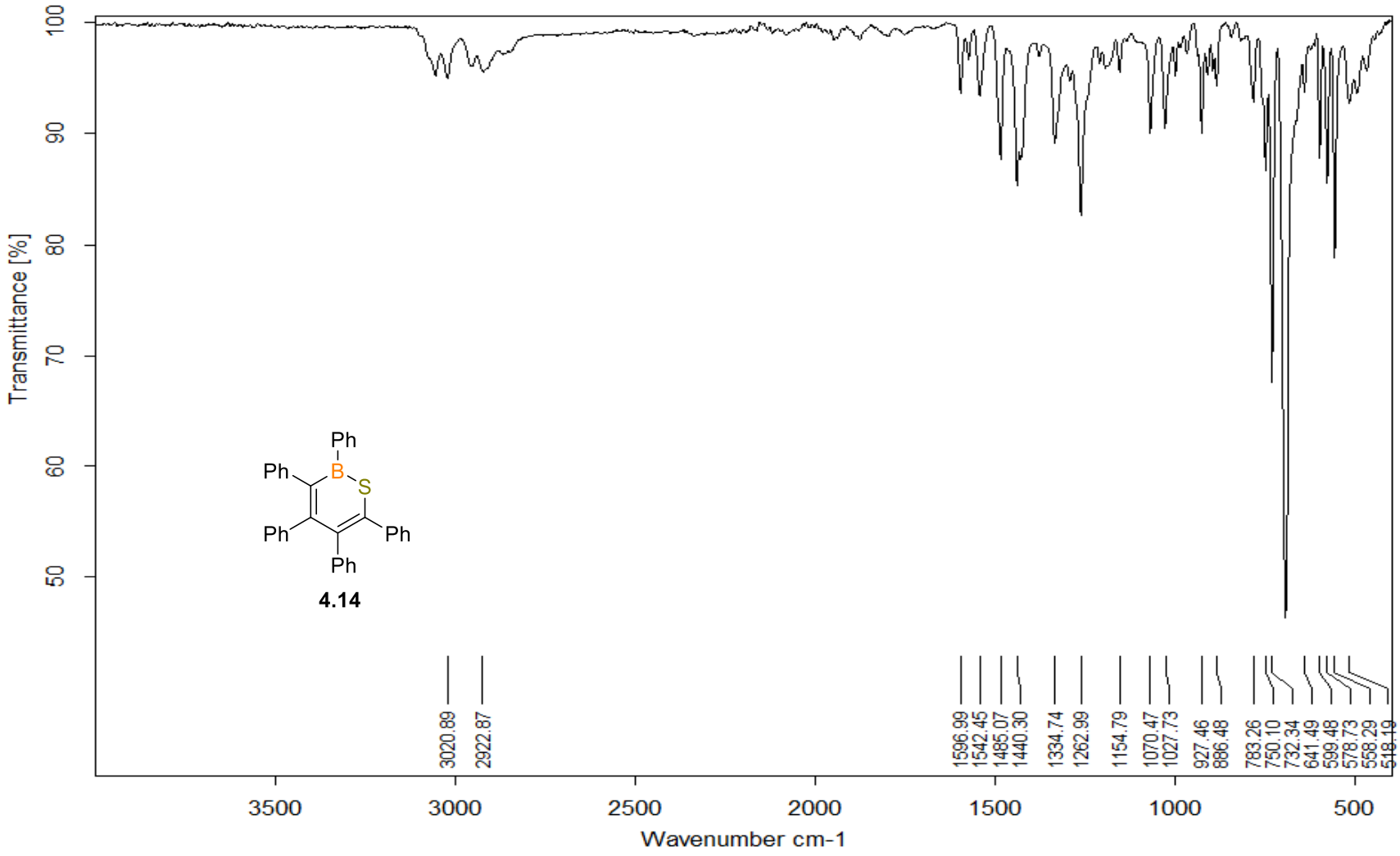

Figure C-34: FT-IR spectrum of **4.14**.

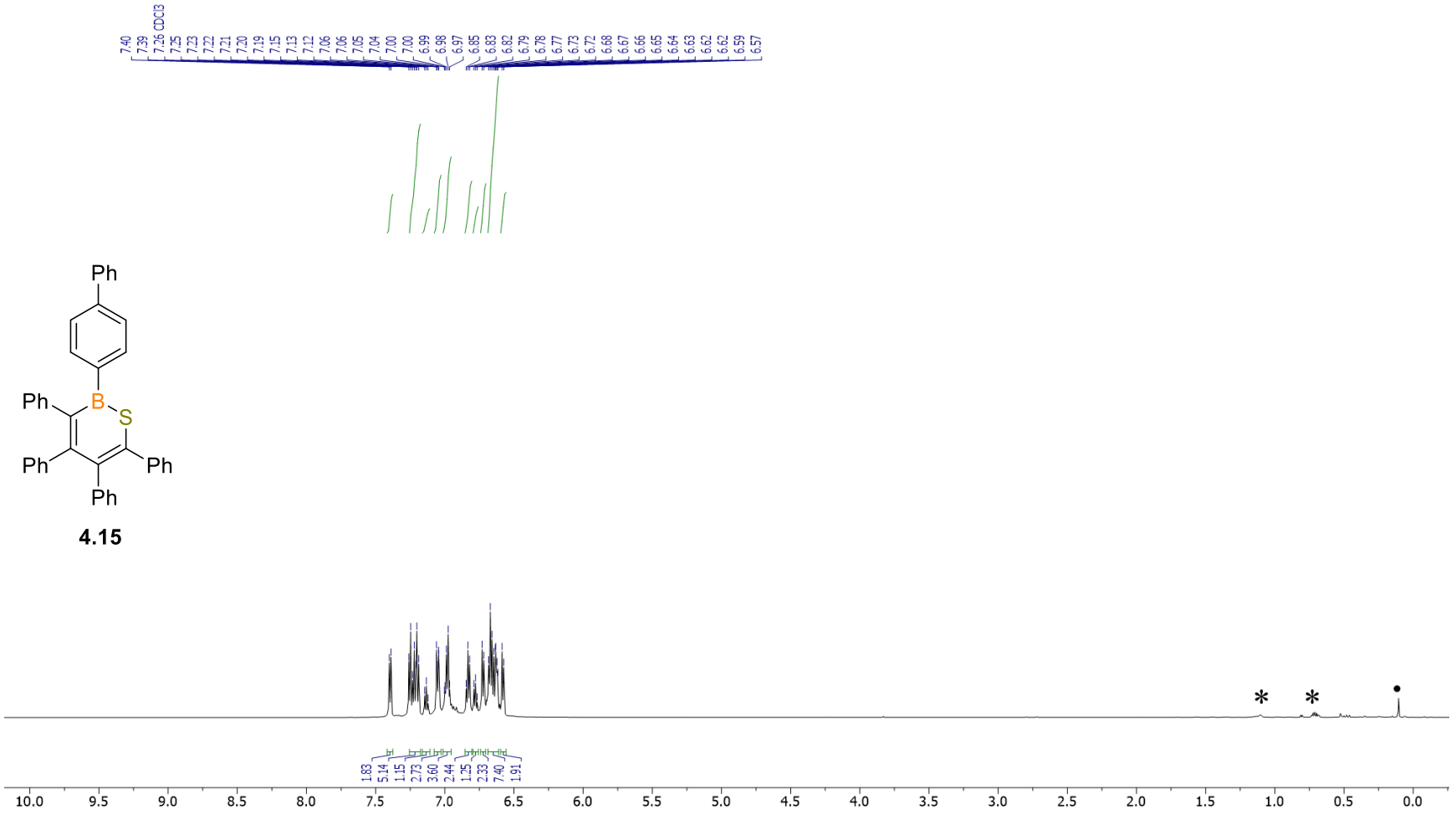

Figure C-35: ^{1}H NMR spectrum of **4.15** in $CDCl_3$ (* *n*-pentane, • grease).

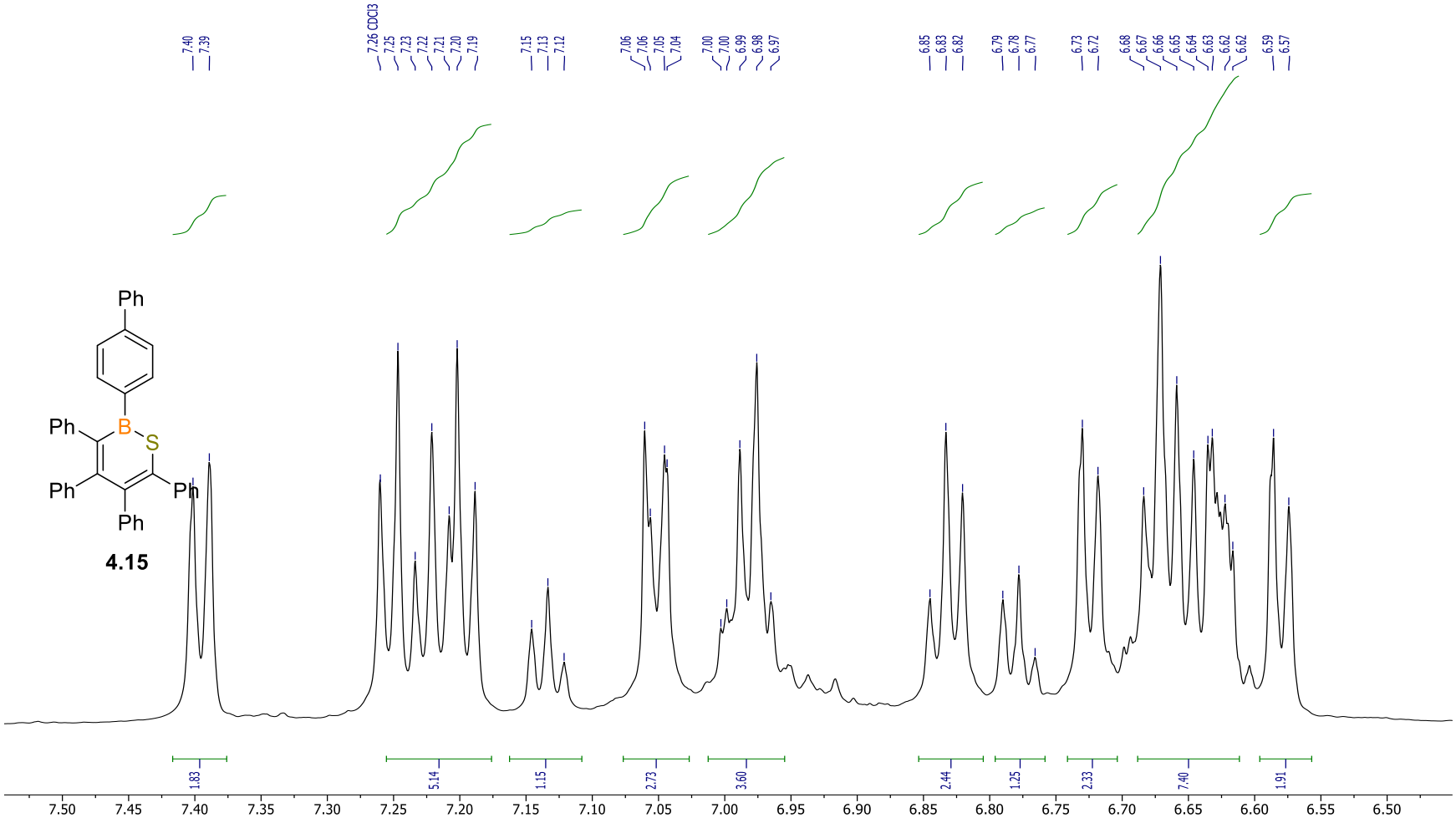

Figure C-36: Expansion of ^{1}H NMR spectrum of **4.15** in $CDCl_3$.

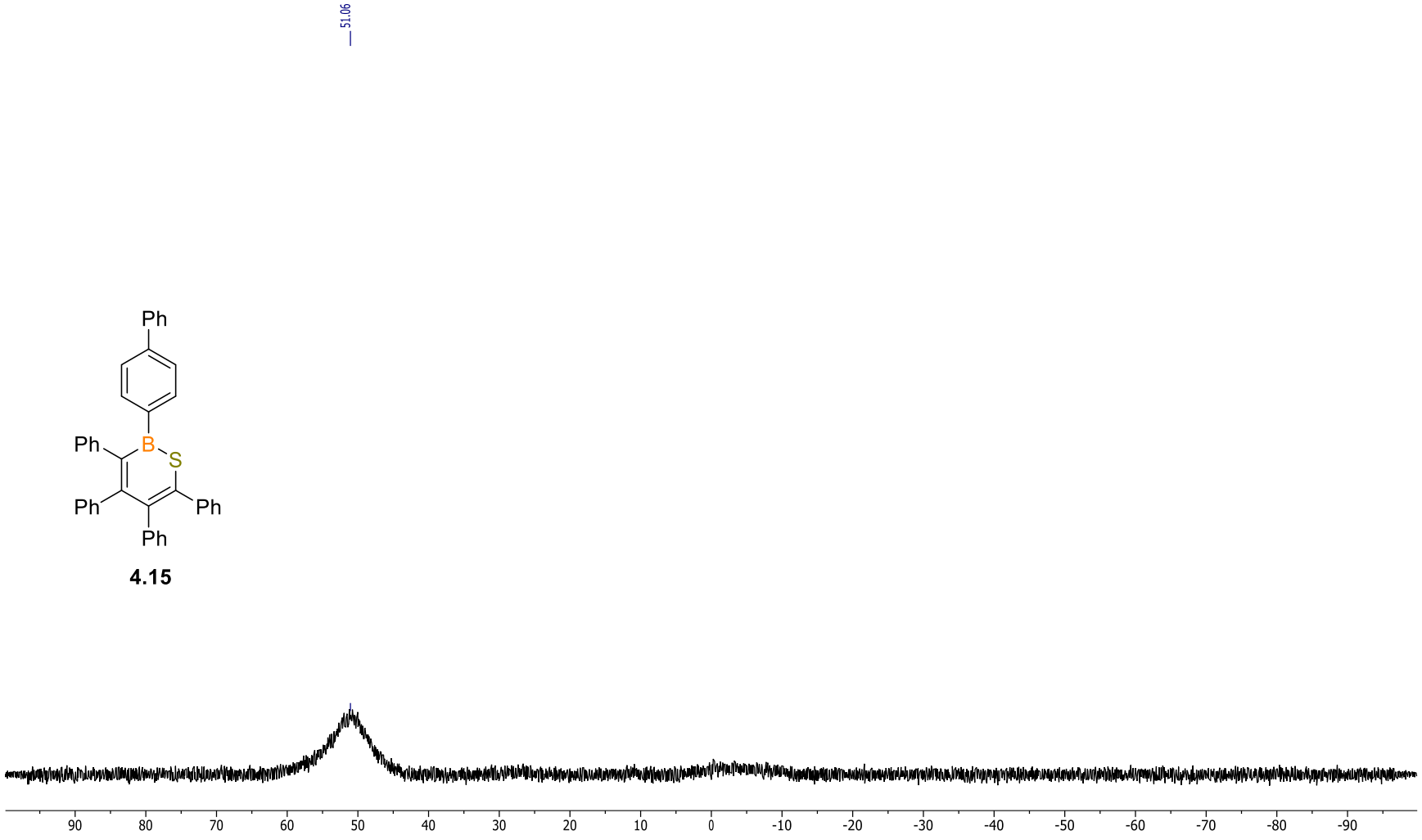

Figure C-37: $^{11}B\{^{1}H\}$ NMR spectrum of **4.15** in $CDCl_3$.

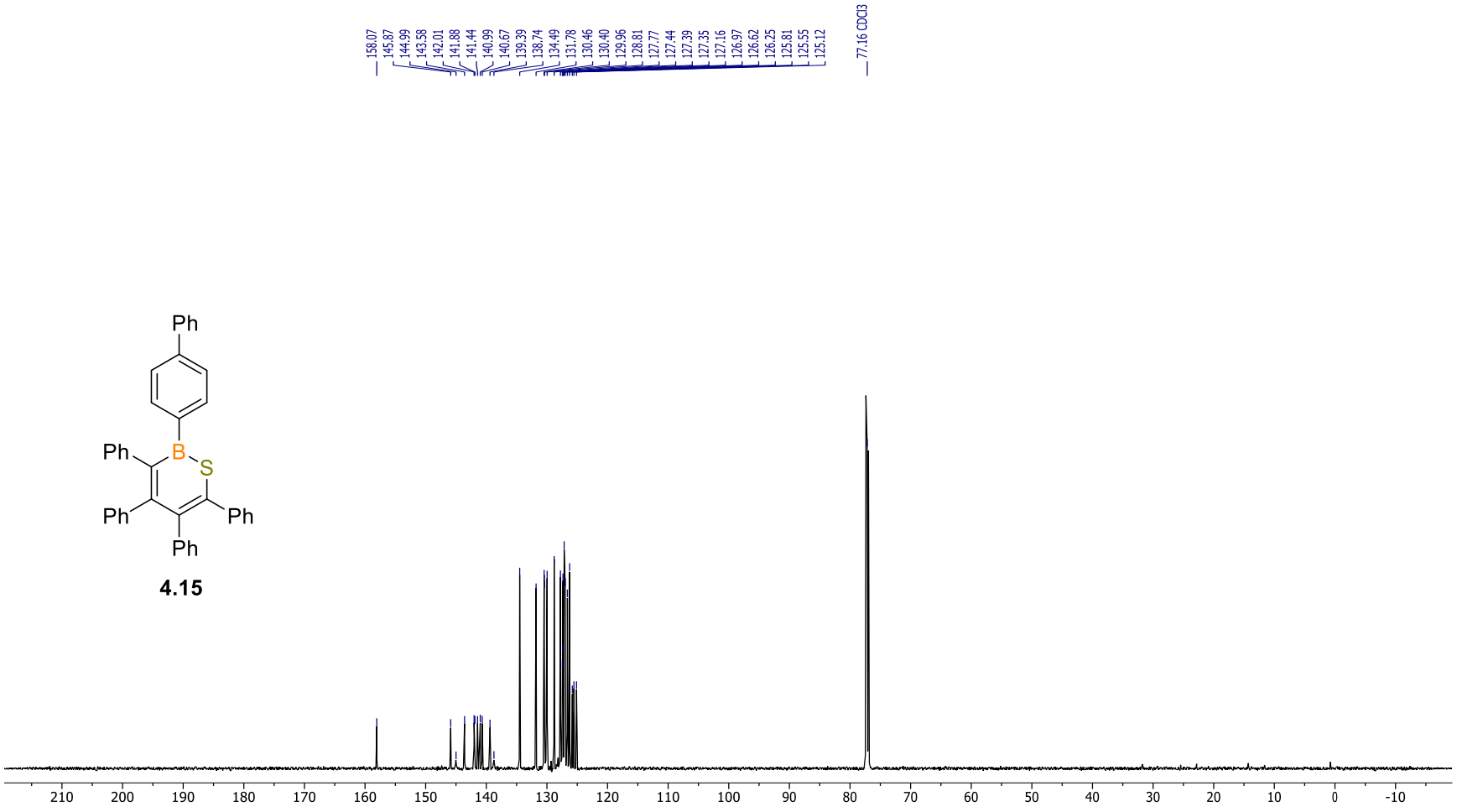

Figure C-38: $^{13}C\{^{1}H\}$ NMR spectrum of **4.15** in $CDCl_3$.

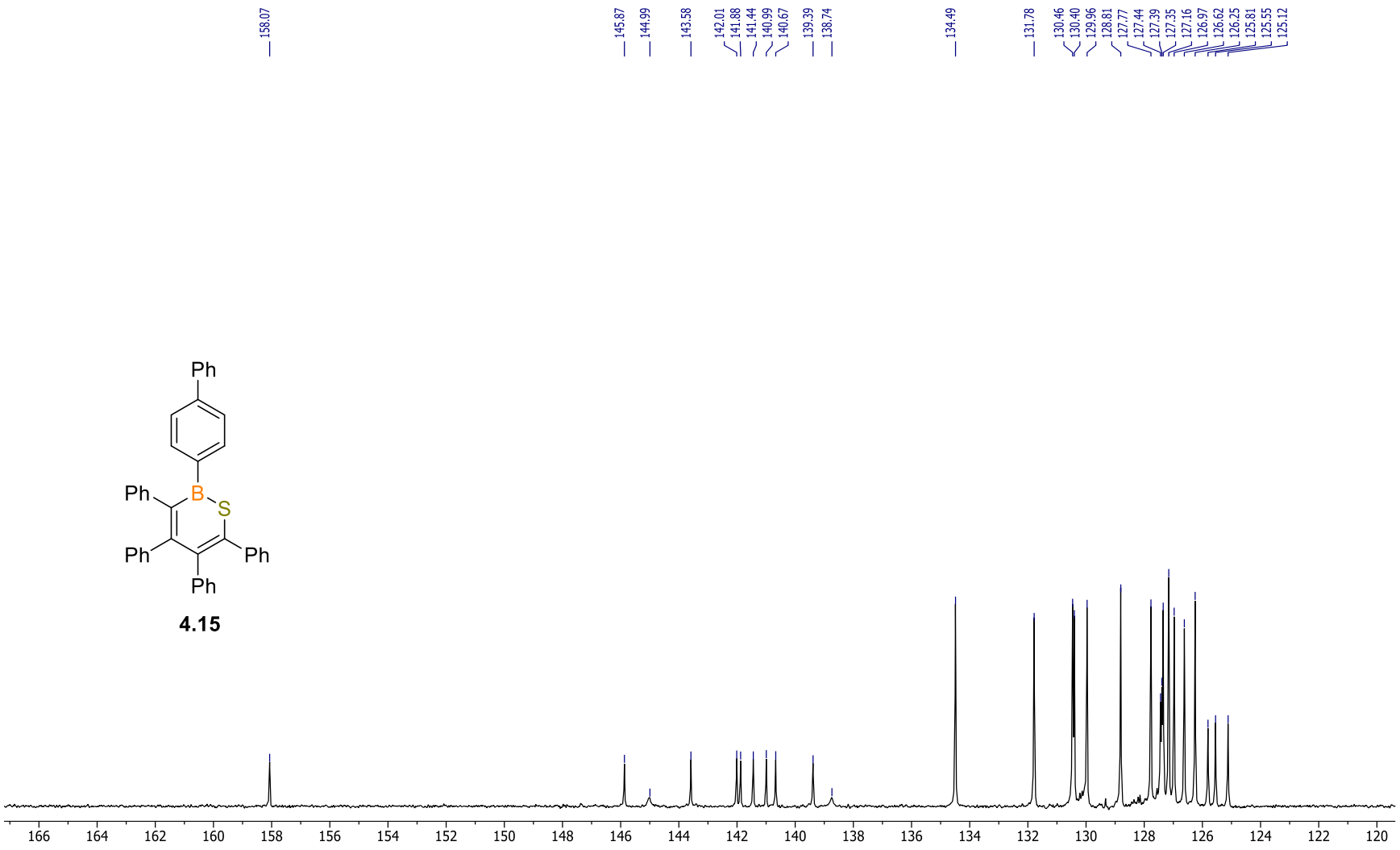

Figure C-39: Expansion of $^{13}C\{^{1}H\}$ NMR spectrum of **4.15** in $CDCl_3$.

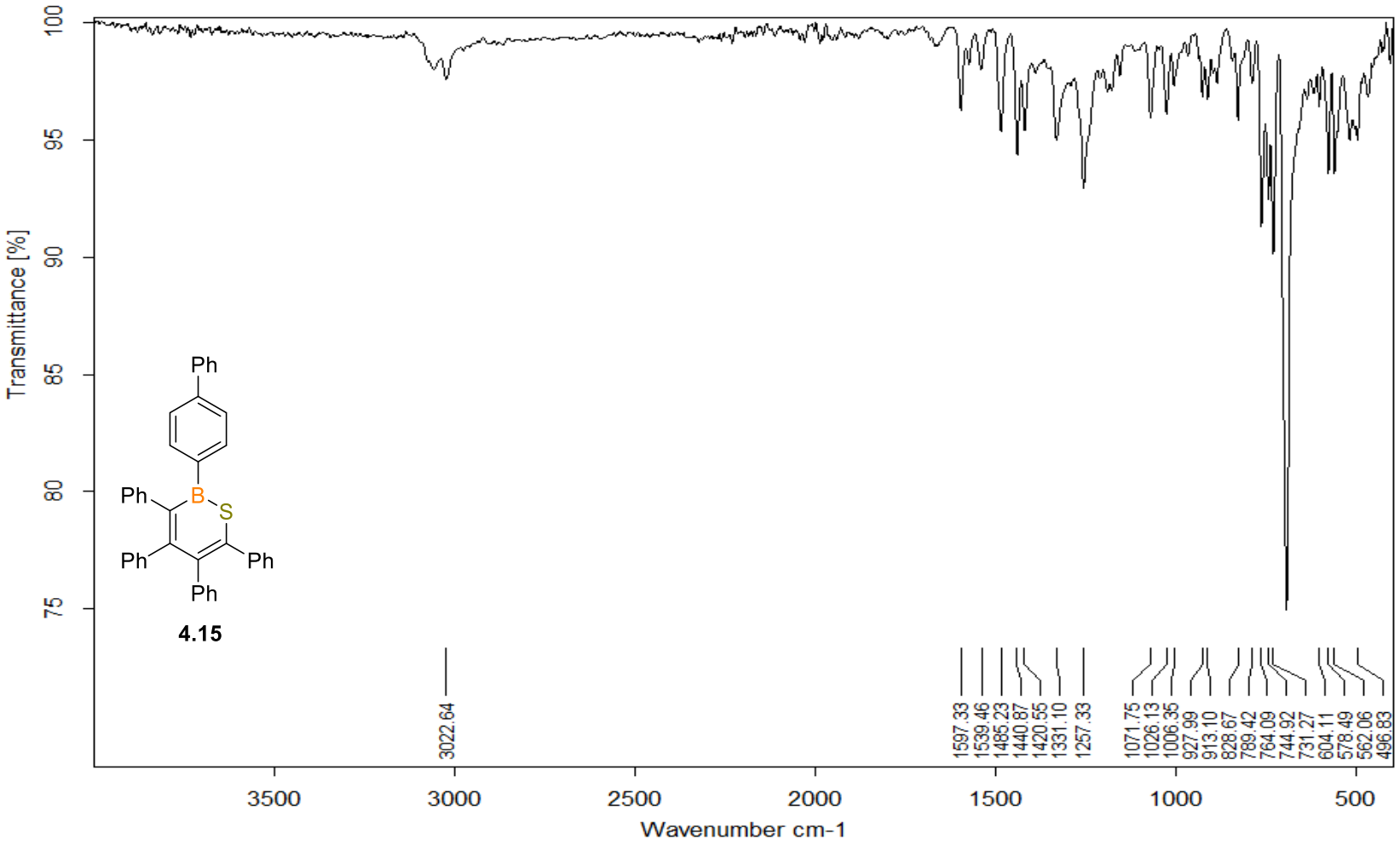

Figure C-40: FT-IR spectrum of **4.15**.

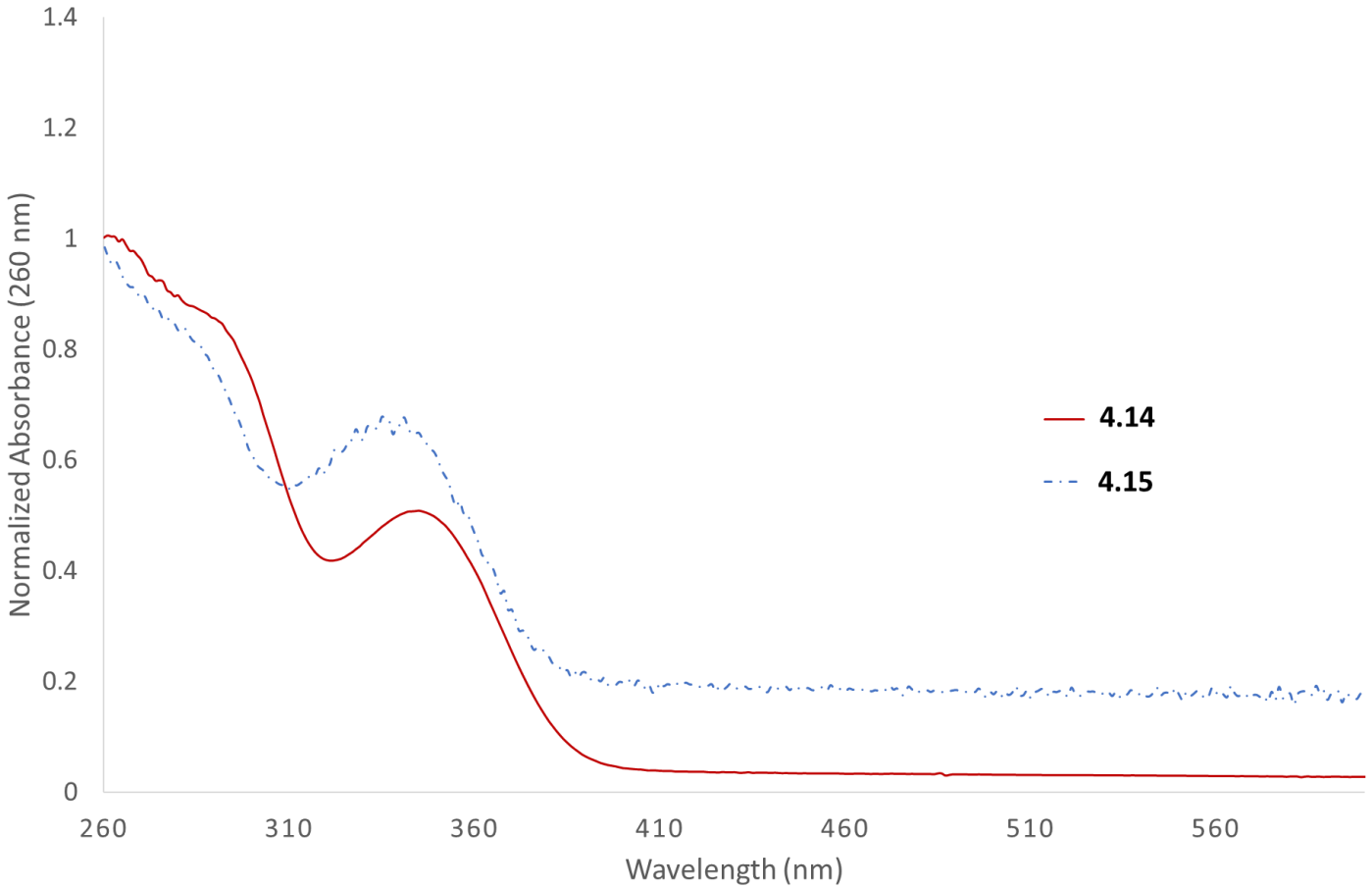

4.14 (340 nm): ε = 11,000 $Lmol^{-1}$ cm^{-1}; (260 nm): ε = 4,200 $Lmol^{-1}$ cm^{-1}

4.15 (345 nm): ε = 10,000 $Lmol^{-1}$ cm^{-1}; (260 nm): ε = 17,000 $Lmol^{-1}$ cm^{-1}

Figure C-41: Normalized absorption spectrum of **4.14** and **4.15** in CH_2Cl_2 (normalized at the 260 nm shoulder).

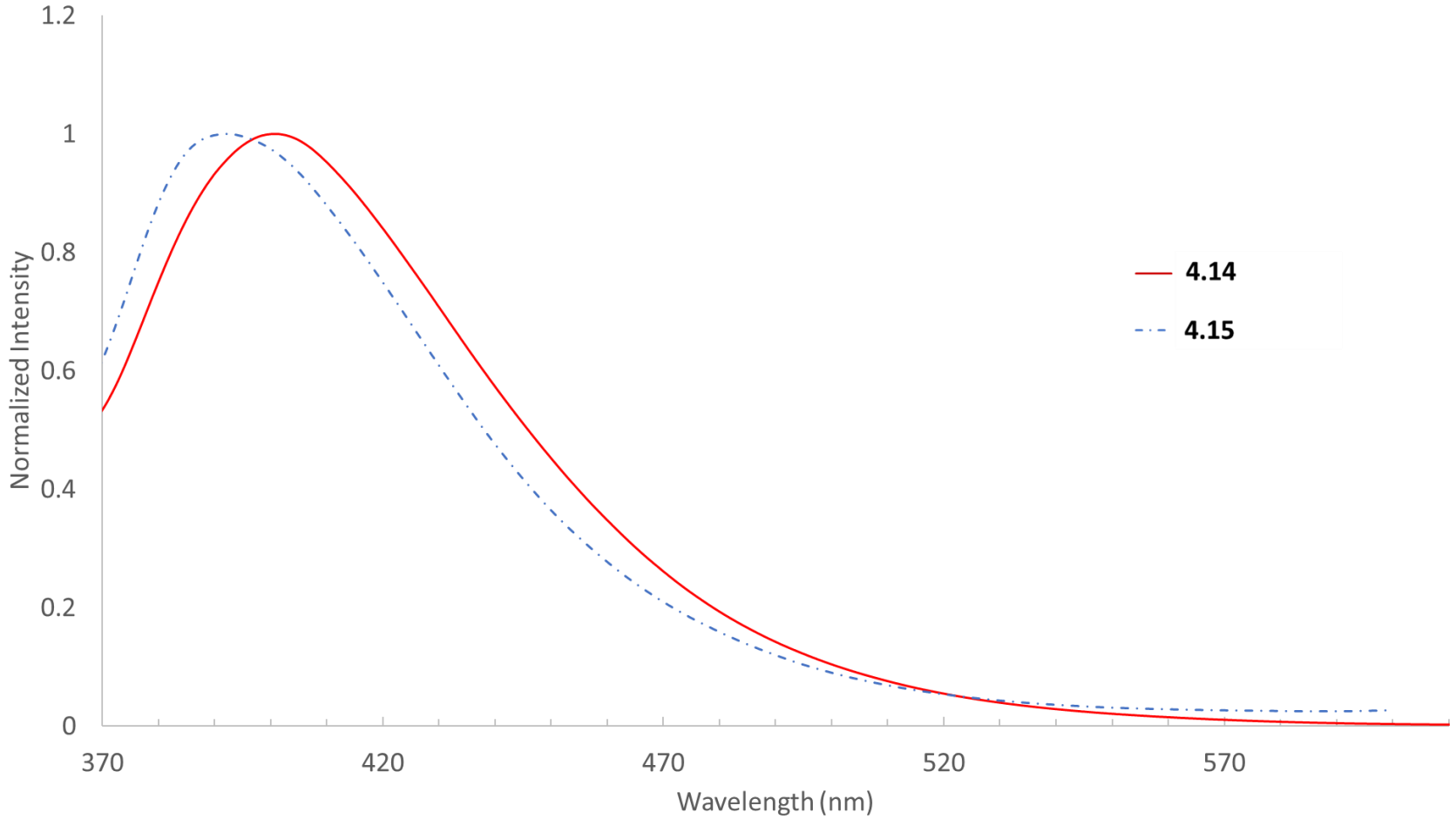

Figure C-42: Normalized emission spectra of **4.14** and **4.15** in CH_2Cl_2 (compounds excited at 340 and 345 nm respectively). Concentrations of samples **4.14**: 1.55×10^{-7} M; **4.15**: 9.33×10^{-7} M.

Table C-8: Coordinates of the HSE06/6-311+G(d,p) Geometry of **4.11** Simulated in C1 Symmetry.

Center Number	Atomic Number	Atomic Type	Coordinates (Angstroms) X	Y	Z
1	6	0	1.562864	2.368292	-1.275456
2	6	0	1.622986	2.969046	-0.069571
3	6	0	1.094967	2.390279	1.128769
4	6	0	0.475196	1.184064	1.212476
5	1	0	1.976205	2.841426	-2.159653
6	1	0	2.098616	3.942914	-0.007715
7	1	0	1.211552	2.981883	2.034683
8	1	0	0.144267	0.915967	2.213595
9	5	0	0.233401	0.22825	0.030876
10	16	0	0.857504	0.827018	-1.610396
11	7	0	-0.411768	-1.033088	0.112707
12	6	0	-0.930324	-1.519265	1.400961
13	1	0	-0.715316	-0.742247	2.133462
14	6	0	-0.63017	-1.963742	-1.010688
15	1	0	-1.13867	-2.831252	-0.580219
16	6	0	-0.212392	-2.780918	1.878689
17	1	0	-0.394789	-3.636543	1.221026
18	1	0	0.866579	-2.613936	1.929388
19	1	0	-0.563353	-3.058453	2.877187
20	6	0	-2.448454	-1.695722	1.389768
21	1	0	-2.801329	-1.96927	2.388602
22	1	0	-2.942152	-0.765971	1.09591
23	1	0	-2.770819	-2.485305	0.704047
24	6	0	0.671304	-2.498395	-1.606638
25	1	0	1.249925	-1.720473	-2.108831
26	1	0	1.299204	-2.936001	-0.826584
27	1	0	0.448867	-3.275627	-2.344349
28	6	0	-1.576126	-1.40709	-2.073581
29	1	0	-1.148079	-0.554374	-2.604378
30	1	0	-1.799341	-2.181543	-2.81409
31	1	0	-2.516929	-1.085082	-1.62047
32	0	0	0.836324	1.537531	-0.208005
33	0	0	1.738119	1.105367	-0.208005
34	0	0	-0.027439	2.041429	-0.208005

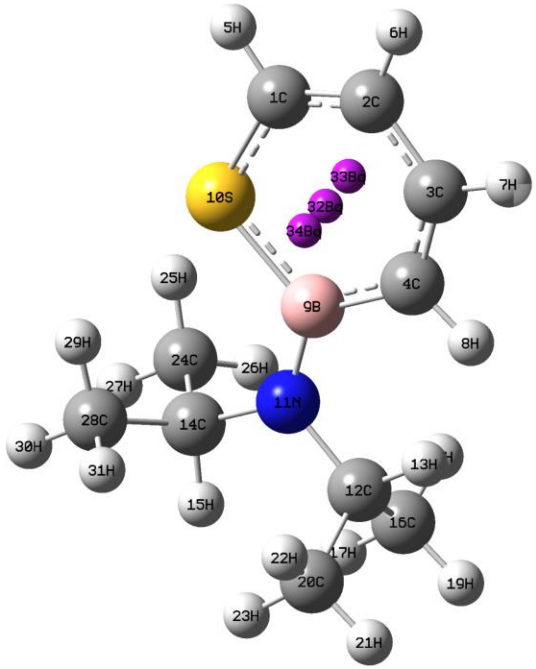

Figure C-43: Computed optimized structure of **4.11** displaying ghost atom positioning within the central ring.

Table C-9: Coordinates of the HSE06/6-311+G(d,p) Geometry of **4.14** Simulated in C1 Symmetry.

Center Number	Atomic Number	Atomic Type	Coordinates (Angstroms) X	Y	Z
1	6	0	2.47066	0.921773	-0.010996
2	6	0	1.676818	2.041651	0.002293
3	6	0	0.226361	2.010864	0.008779
4	6	0	-0.541819	0.858491	0.005561
5	5	0	0.062109	-0.541778	0.004643
6	16	0	1.855916	-0.69797	0.013102
7	6	0	-0.691634	-1.914994	0.01464
8	6	0	-1.805084	-2.135521	0.840403
9	6	0	-0.250206	-2.988852	-0.774176
10	6	0	-2.438107	-3.370818	0.88422
11	1	0	-2.181875	-1.328212	1.459827
12	6	0	-0.893107	-4.220667	-0.749623
13	1	0	0.606373	-2.854838	-1.429073
14	6	0	-1.987862	-4.416241	0.084475
15	1	0	-3.291306	-3.516391	1.538998
16	1	0	-0.53728	-5.029399	-1.379914
17	1	0	-2.489476	-5.378298	0.110161
18	6	0	3.955009	0.952919	-0.06275
19	6	0	4.624729	1.594203	-1.108242
20	6	0	4.706174	0.290918	0.912239
21	6	0	6.011337	1.585457	-1.166956
22	1	0	4.053048	2.098881	-1.878549
23	6	0	6.09419	0.292872	0.857878
24	1	0	4.19641	-0.219274	1.723159
25	6	0	6.751366	0.940215	-0.181794
26	1	0	6.515916	2.084189	-1.987757
27	1	0	6.662669	-0.215246	1.629712
28	1	0	7.835251	0.938464	-0.227074
29	6	0	2.363461	3.370912	0.02607
30	6	0	3.12594	3.74551	1.133253
31	6	0	2.269134	4.254108	-1.051055
32	6	0	3.776148	4.972885	1.166483
33	1	0	3.211217	3.064687	1.97425
34	6	0	2.922923	5.478894	-1.022348
35	1	0	1.676266	3.979674	-1.917392
36	6	0	3.67735	5.843782	0.08777
37	1	0	4.363186	5.247612	2.036729
38	1	0	2.84051	6.152052	-1.86936
39	1	0	4.185307	6.802151	0.11118
40	6	0	-2.030019	0.959533	0.01894
41	6	0	-2.776093	0.450572	-1.047303

42	6	0	-2.716302	1.507509	1.106413
43	6	0	-4.164	0.509364	-1.039706
44	1	0	-2.259029	0.001608	-1.889614
45	6	0	-4.104671	1.554648	1.121924
46	1	0	-2.154619	1.898941	1.948081
47	6	0	-4.83468	1.060453	0.046367
48	1	0	-4.723208	0.114946	-1.88194
49	1	0	-4.617806	1.981943	1.977418
50	1	0	-5.918809	1.100832	0.056607
51	6	0	-0.468596	3.33591	0.007959
52	6	0	-1.223522	3.731053	-1.09711
53	6	0	-0.389071	4.191753	1.107349
54	6	0	-1.878105	4.956075	-1.106634
55	1	0	-1.30095	3.069313	-1.953496
56	6	0	-1.054091	5.410986	1.104469
57	1	0	0.197592	3.899428	1.972079
58	6	0	-1.797768	5.799413	-0.004424
59	1	0	-2.45811	5.248983	-1.975632
60	1	0	-0.98713	6.061632	1.970221
61	1	0	-2.313199	6.75406	-0.008568
62	0	0	1.032008	0.646188	0.004849
63	0	0	1.032008	0.646188	1.004849
64	0	0	1.032008	0.646188	-0.995151

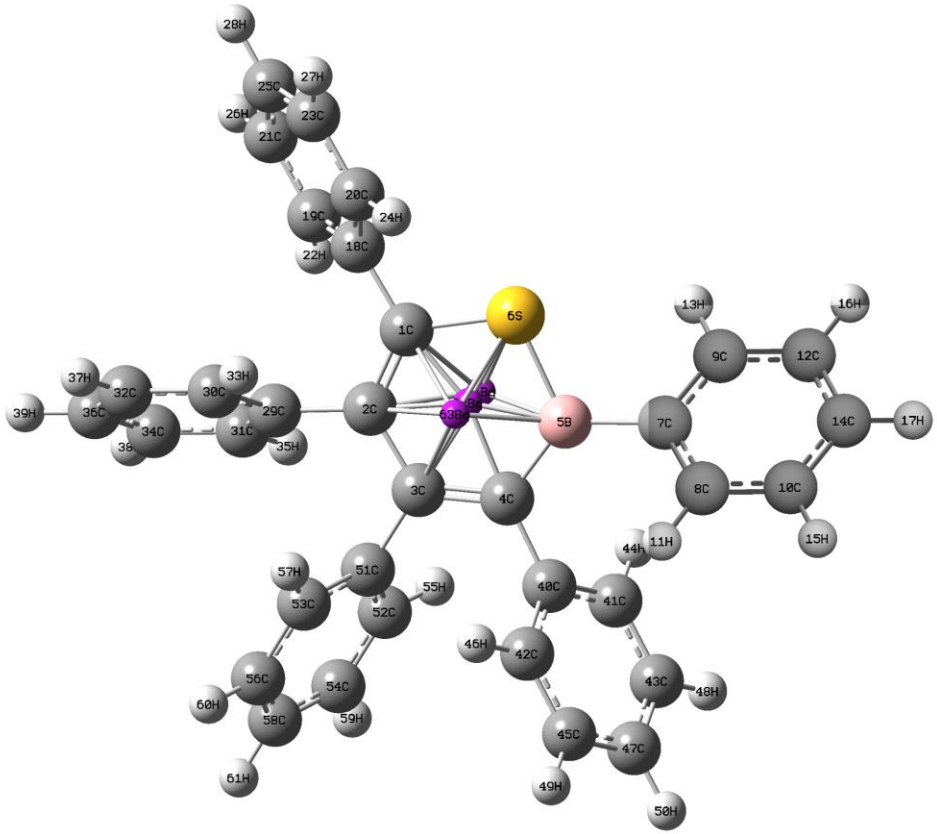

Figure C-44: Computed optimized structure of **4.14** displaying ghost atom positioning within the central ring.

Table C-10: Coordinates of the HSE06/6-311+G(d,p) Geometry of **4.15** Simulated in C1 Symmetry.

Center Number	Atomic Number	Atomic Type	Coordinates (Angstroms) X	Y	Z
1	6	0	2.073677	1.543772	-0.066151
2	6	0	1.29148	2.6706	-0.016156
3	6	0	-0.158944	2.65361	0.020362
4	6	0	-0.93866	1.509219	0.007059
5	5	0	-0.349154	0.10289	-0.033429
6	16	0	1.443634	-0.070133	-0.059188
7	6	0	-1.115126	-1.262091	-0.039742
8	6	0	-2.232795	-1.489986	0.778148
9	6	0	-0.686059	-2.333575	-0.838308
10	6	0	-2.874954	-2.718175	0.80449
11	1	0	-2.61364	-0.688693	1.402751
12	6	0	-1.33877	-3.557388	-0.831205
13	1	0	0.177935	-2.207266	-1.484953
14	6	0	-2.445162	-3.775454	-0.004738
15	1	0	-3.74666	-2.850735	1.437518
16	1	0	-0.968532	-4.366023	-1.453494
17	6	0	3.55691	1.561171	-0.149084
18	6	0	4.210344	2.212095	-1.198855
19	6	0	4.322078	0.875932	0.798523
20	6	0	5.595142	2.189719	-1.288531
21	1	0	3.62733	2.734849	-1.948306
22	6	0	5.708518	0.864075	0.713304
23	1	0	3.824826	0.358028	1.612322
24	6	0	6.349647	1.521102	-0.330323
25	1	0	6.086878	2.69625	-2.112345
26	1	0	6.288314	0.337638	1.464146
27	1	0	7.432187	1.508623	-0.399685
28	6	0	-0.839245	3.985394	0.066761
29	6	0	-0.723123	4.812393	1.184805
30	6	0	-1.615998	4.41658	-1.009261
31	6	0	-1.37301	6.038978	1.22877
32	1	0	-0.11921	4.491492	2.027234
33	6	0	-2.255455	5.649091	-0.97212
34	1	0	-1.722355	3.777567	-1.879653
35	6	0	-2.138346	6.463669	0.148307
36	1	0	-1.277094	6.666718	2.108574
37	1	0	-2.852725	5.970476	-1.819081
38	1	0	-2.642047	7.424032	0.180159
39	6	0	-2.425291	1.62426	0.048523
40	6	0	-3.193516	1.14598	-1.01623
41	6	0	-3.088356	2.152444	1.15994

42	6	0	-4.580598	1.214208	-0.982971
43	1	0	-2.694273	0.713052	-1.877475
44	6	0	-4.475935	2.209381	1.200528
45	1	0	-2.509227	2.520321	2.000402
46	6	0	-5.228163	1.744816	0.127071
47	1	0	-5.157388	0.842927	-1.823845
48	1	0	-4.970999	2.620776	2.074265
49	1	0	-6.31162	1.792114	0.157386
50	6	0	1.99143	3.992727	0.013934
51	6	0	2.783009	4.342817	1.108594
52	6	0	1.881055	4.89338	-1.047113
53	6	0	3.445681	5.563437	1.145488
54	1	0	2.881059	3.648419	1.937014
55	6	0	2.547361	6.111296	-1.014968
56	1	0	1.265661	4.638137	-1.903582
57	6	0	3.330595	6.451893	0.082839
58	1	0	4.055366	5.819003	2.005945
59	1	0	2.452125	6.79817	-1.849534
60	1	0	3.848315	7.404945	0.109128
61	6	0	-3.139024	-5.079057	0.011136
62	6	0	-3.320641	-5.81084	-1.167573
63	6	0	-3.630919	-5.616131	1.20579
64	6	0	-3.97121	-7.037538	-1.152257
65	1	0	-2.969407	-5.400199	-2.108731
66	6	0	-4.281224	-6.842916	1.221888
67	1	0	-3.478462	-5.076208	2.13472
68	6	0	-4.454488	-7.559366	0.042681
69	1	0	-4.109428	-7.584362	-2.079302
70	1	0	-4.646417	-7.245497	2.161069
71	1	0	-4.962645	-8.517704	0.054746
72	0	0	0.605558	1.437619	-0.00354
73	0	0	0.605558	1.437619	0.99646
74	0	0	0.605558	1.437619	-1.00354

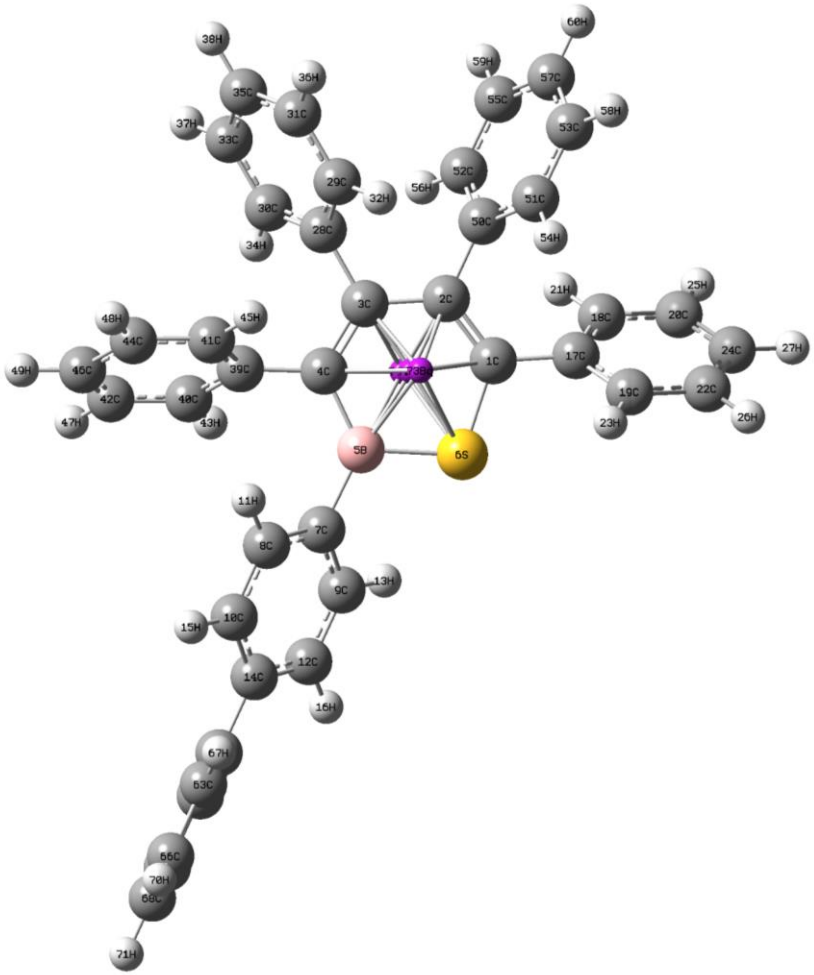

Figure C-45: Computed optimized structure of **4.15** displaying ghost atom positioning within the central ring.

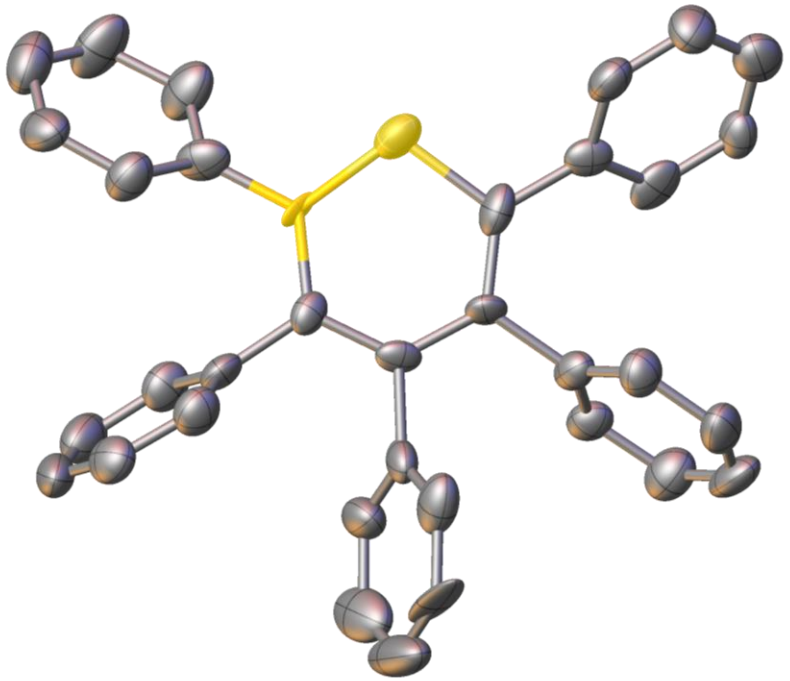

Figure C-46: Solid-state structure of **4.14**. Thermal ellipsoids are drawn at the 50% probability level and hydrogen atoms have been omitted for clarity.

Note: Similar boron heterocycles bearing phenyl groups on boron and carbon atoms within the ring have shown disorder. Therefore, the bond distances and bond angles are not discussed in detail. However, the structure confirms the identity of **4.14**.

Table C-11: Crystallographic Data for **4.14** and **4.15**.

Entry	**3.16**	**3.17**
CCDC	1507212	1507213
Empirical formula	$C_{34}H_{25}BS$	$C_{40}H_{29}BS$
FW (g/mol)	476.41	552.50
Crystal system	Triclinic	Triclinic
Space group	*P-1*	$P2_1/n$
a (Å)	10.572(8)	9.4650(7)
b (Å)	11.407(8)	20.4026(13)
c (Å)	12.957(10)	15.6377(6)
α (deg)	63.900(16)	90
β (deg)	73.750(18)	102.068(2)
γ (deg)	70.575(16)	90
V (Å^3)	1306.8(17)	2953.1(3)
Z	2	4
D_c (mg m^{-3})	1.211	1.243
radiation, λ (Å)	0.71073	0.71073
temp (K)	150(2)	150(2)
$R1[I>2\sigma I]^a$	0.0921	0.0482
$wR2(F^2)^a$	0.3193	0.1232
GOF $(S)^a$	1.122	1.057

[a] $R1(F[\mathrm{I} > 2(\mathrm{I})]) = \sum\|\|F_o| - |F_c\|\|/ \sum |F_o|$; $wR2(F^2$ [all data]$) = [w(F_o^2 - F_c^2)^2]^{1/2}$; S(all data$) = [w(F_o^2 - F_c^2)^2/(n - p)]^{1/2}$ (n = no. of data; p = no. of parameters varied; $w = 1/[^2(F_o^2) + (aP)^2 + bP]$ where $P = (F_o^2 + 2F_c^2)/3$ and a and b are constants suggested by the refinement program.

APPENDIX D

Supplementary Information for Chapter Five

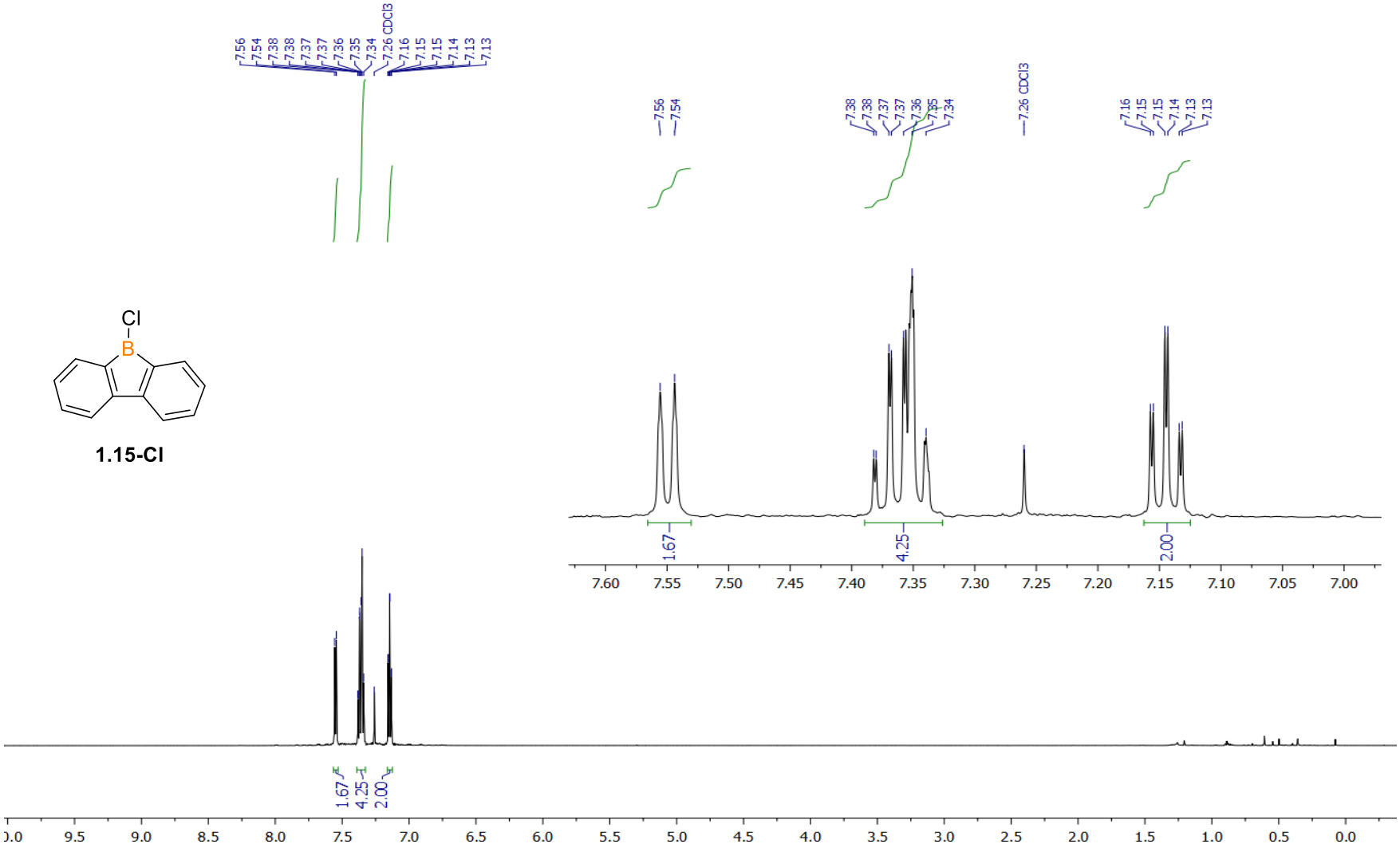

Figure D-1: ^{1}H NMR spectrum of **1.15-Cl** in $CDCl_3$.

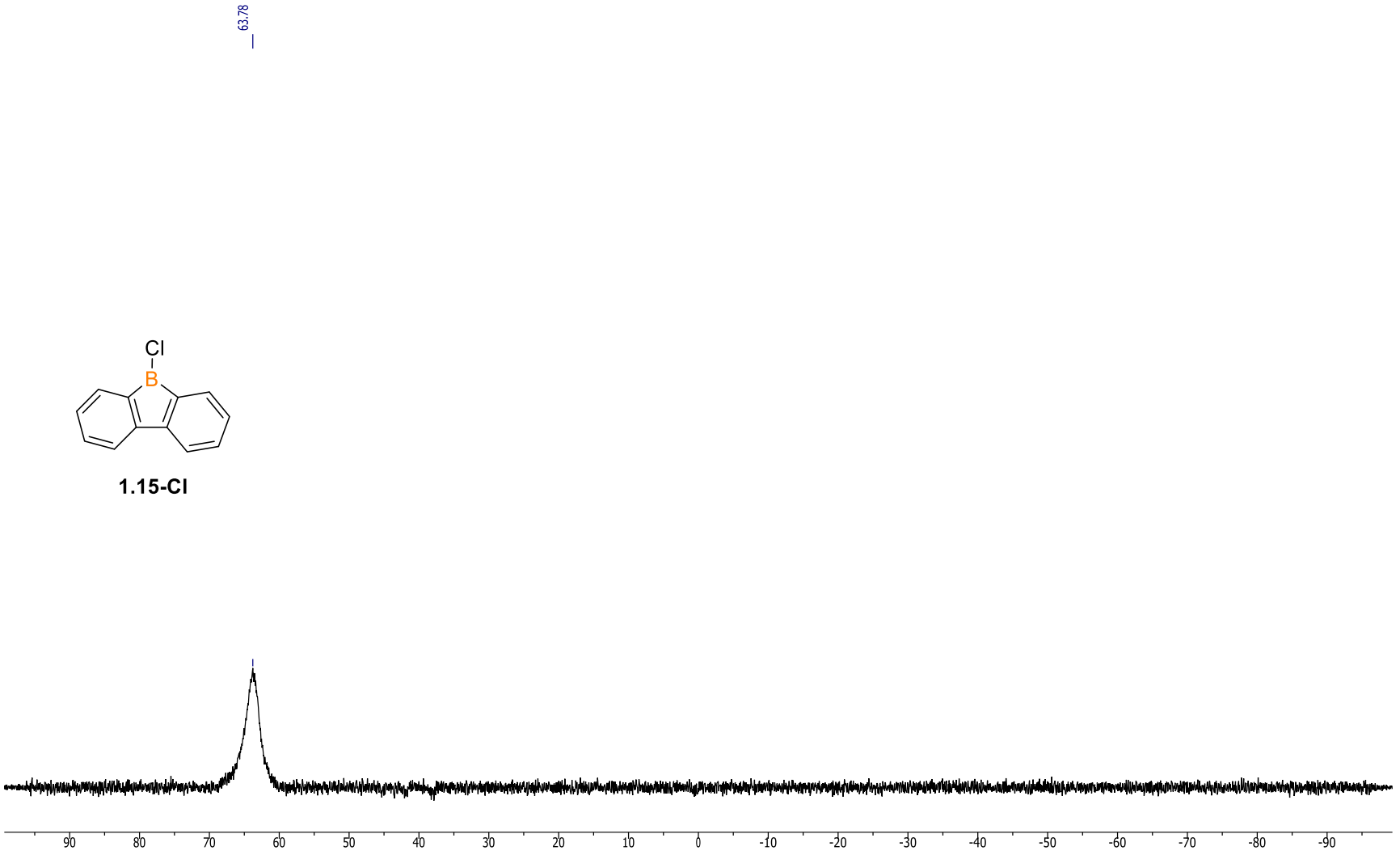

Figure D-2: $^{11}B\{^{1}H\}$ NMR spectrum of **1.15-Cl** in $CDCl_3$.

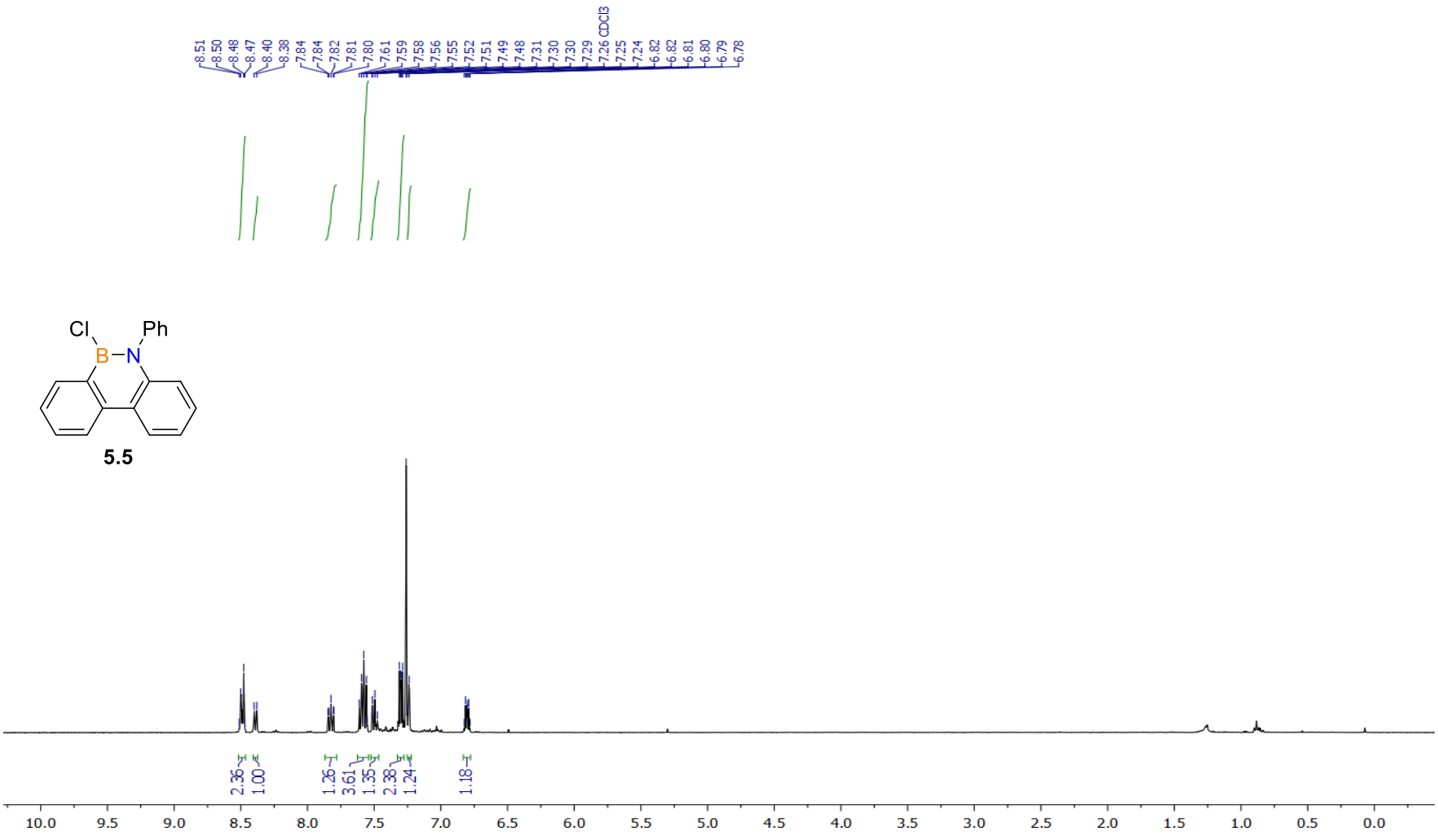

Figure D-3: ^{1}H NMR spectrum of **5.5** in $CDCl_3$.

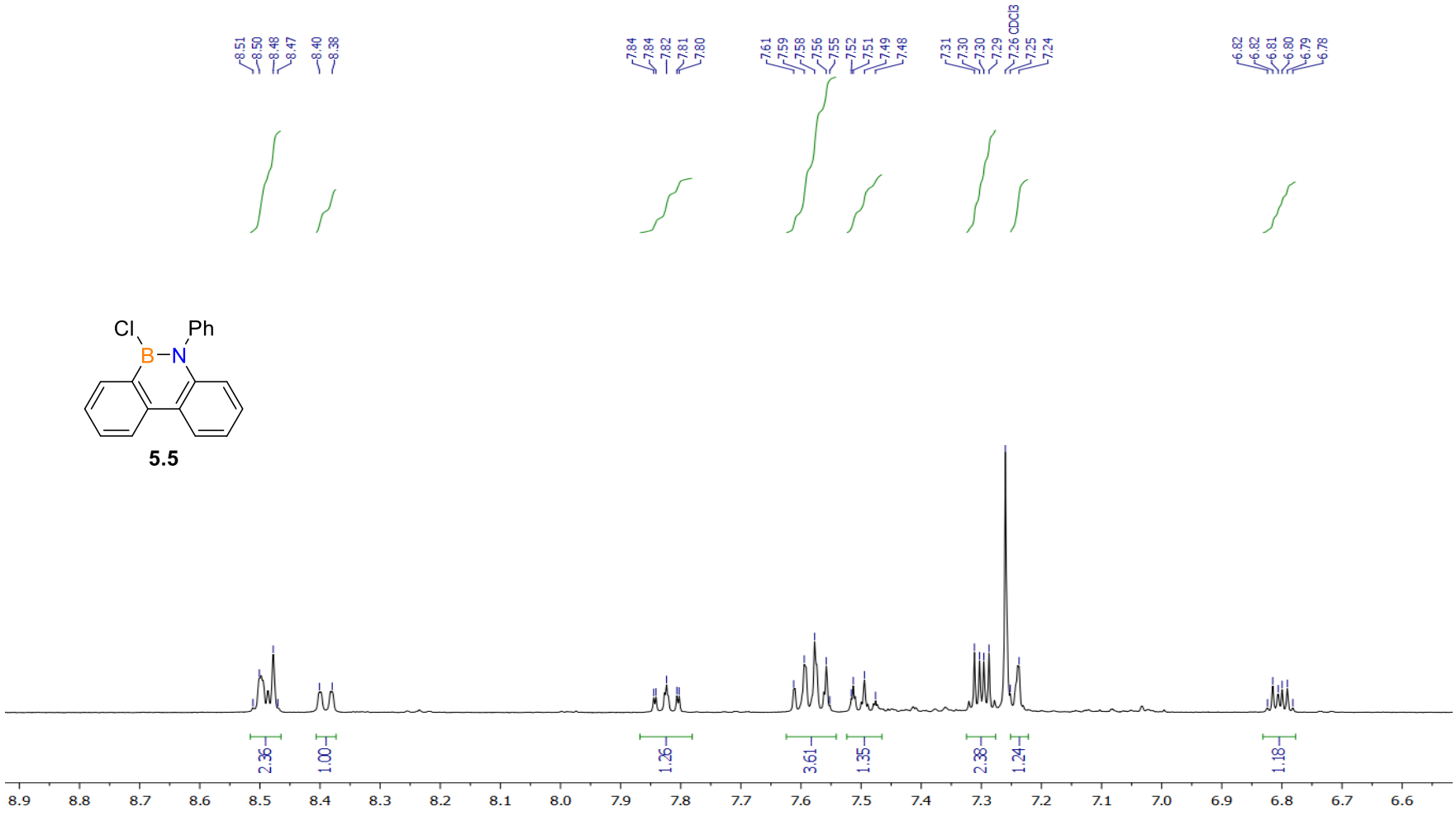

Figure D-4: Expansion of ^{1}H NMR spectrum of **5.5** in $CDCl_3$ (aryl region) .

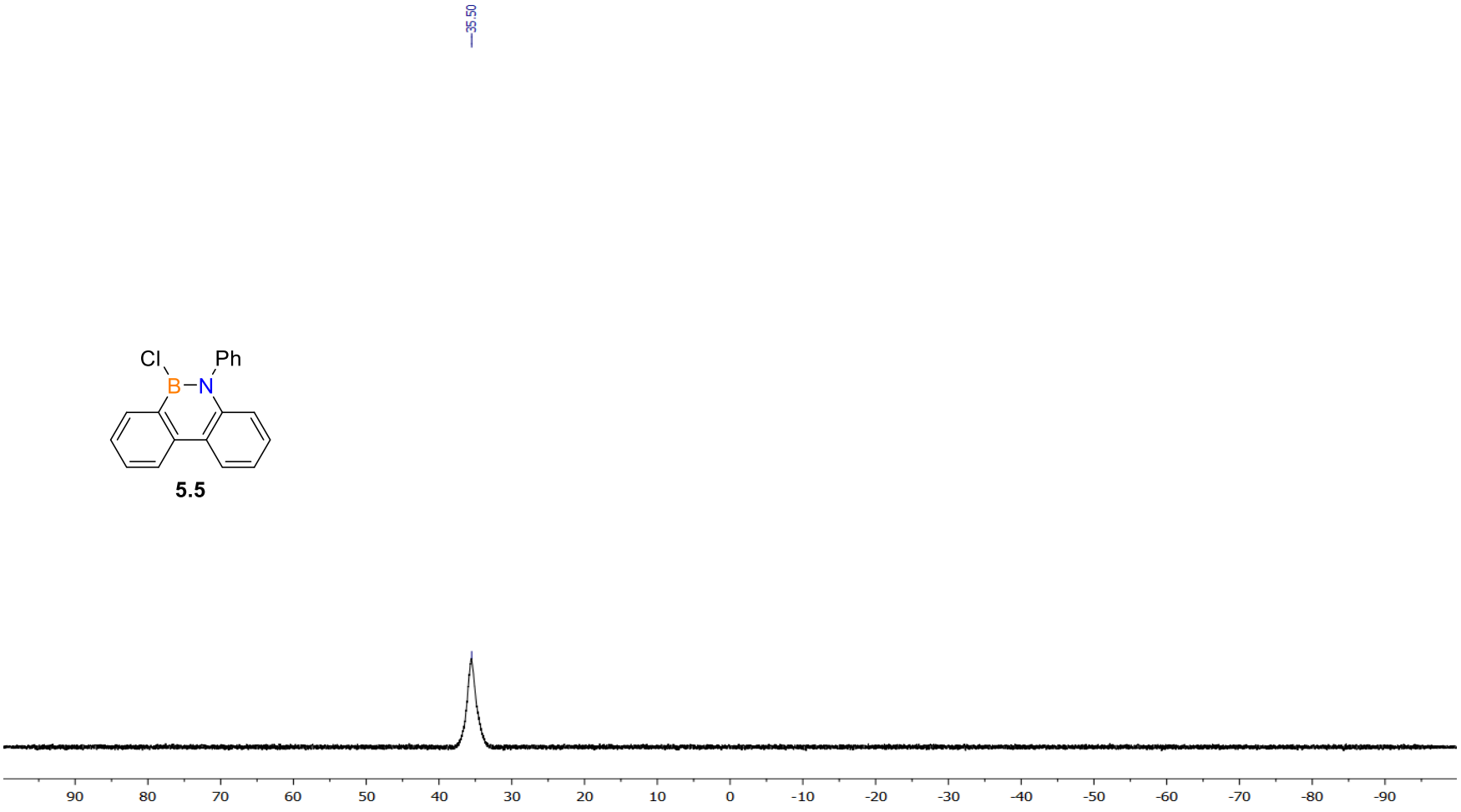

Figure D-5: $^{11}B\{^{1}H\}$ NMR spectrum of **5.5** in $CDCl_3$.

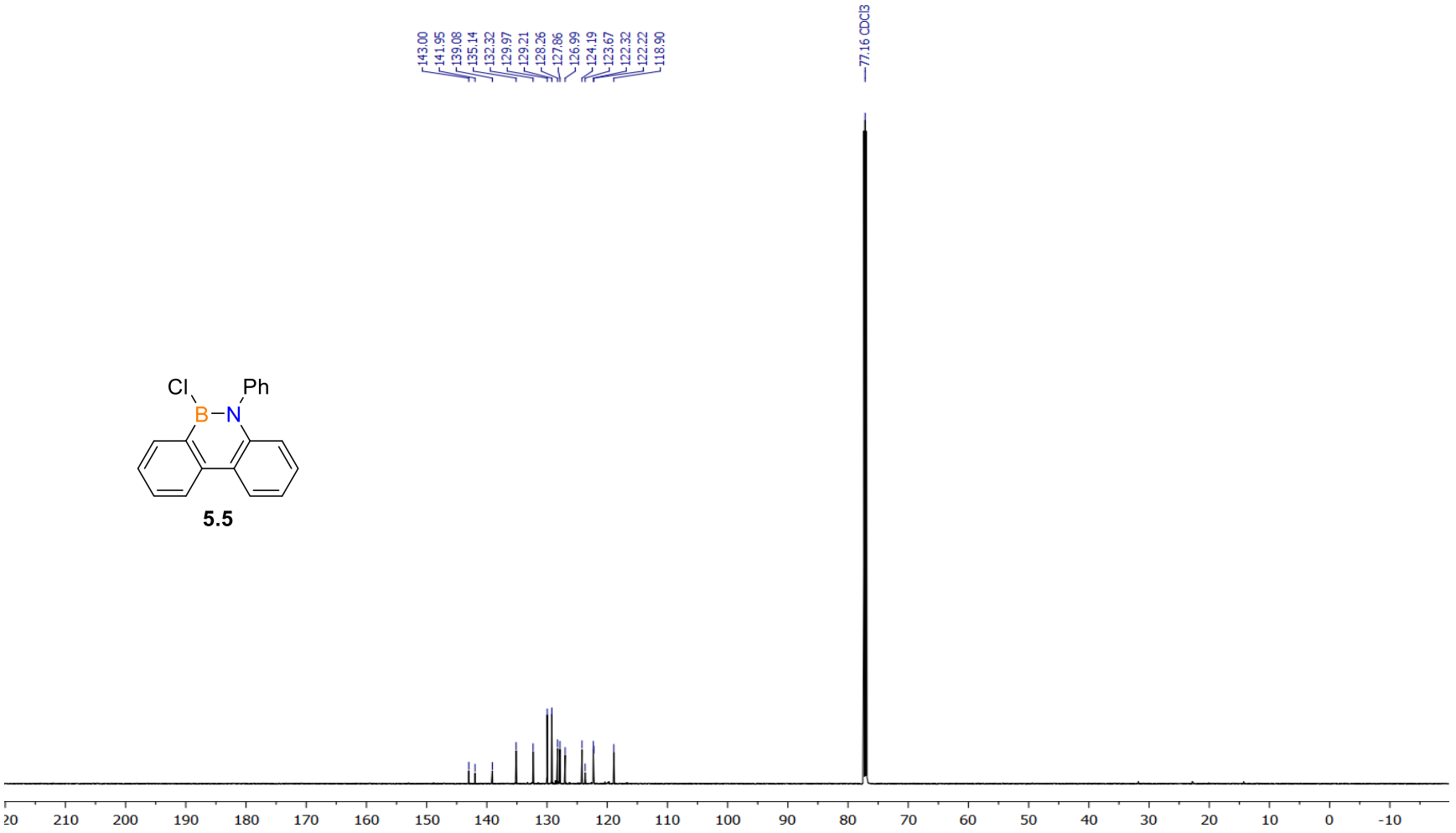

Figure D-6: $^{13}C\{^{1}H\}$ NMR spectrum of **5.5** in $CDCl_3$.

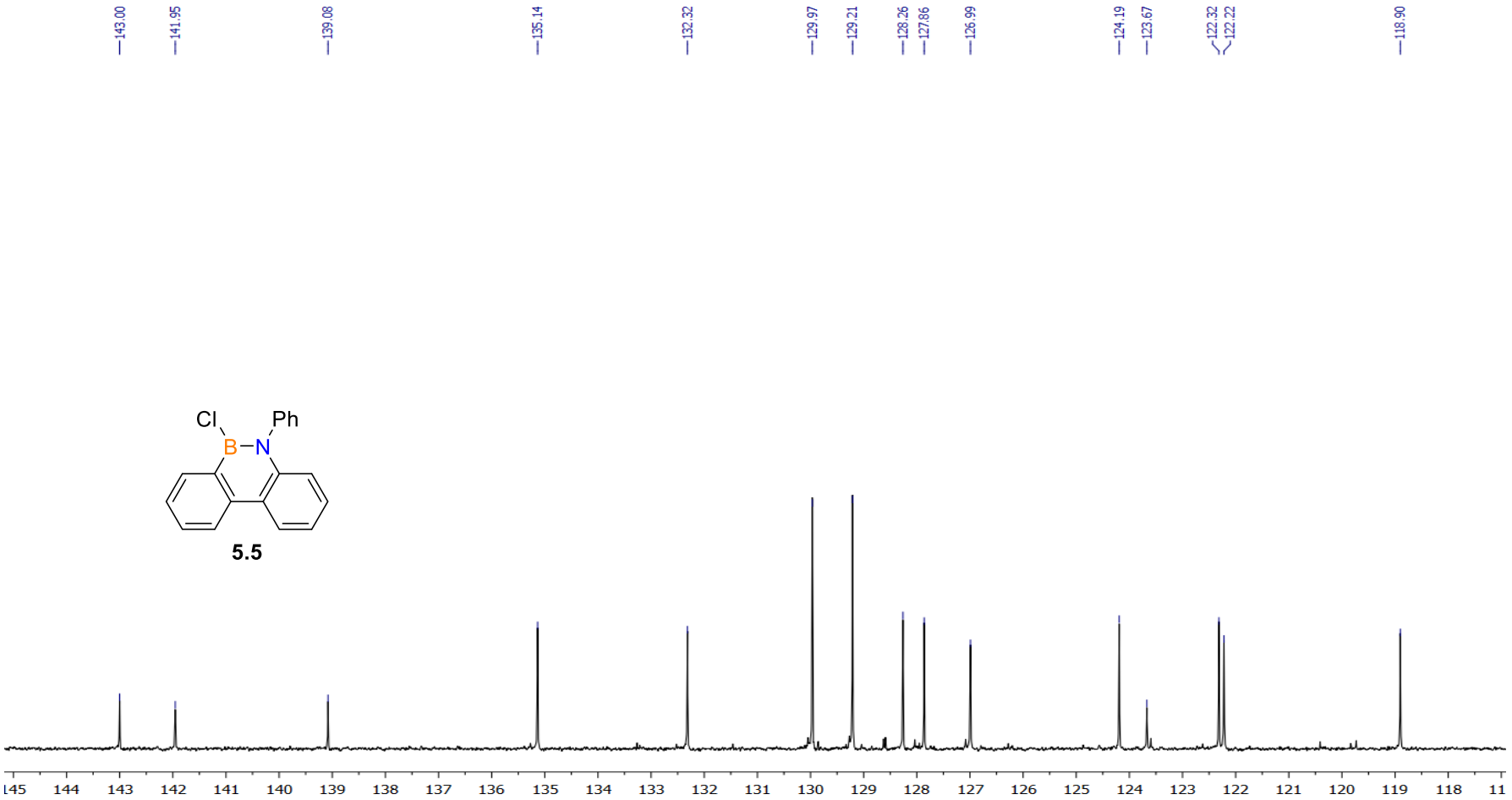

Figure D-7: Expansion of $^{13}C\{^{1}H\}$ NMR spectrum of **5.5** in $CDCl_3$ (aryl region).

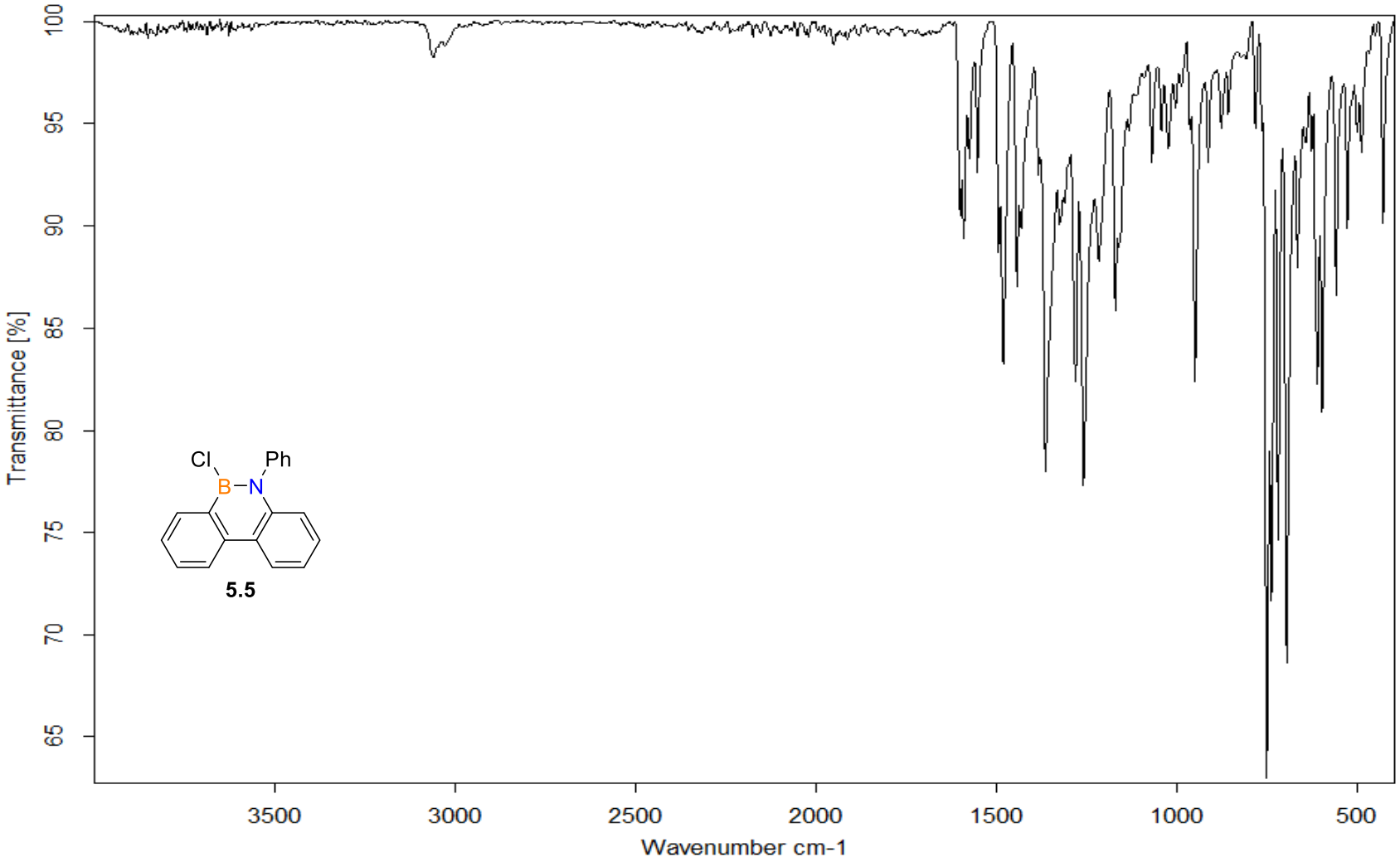

Figure D-8: FT-IR spectrum of **5.5**.

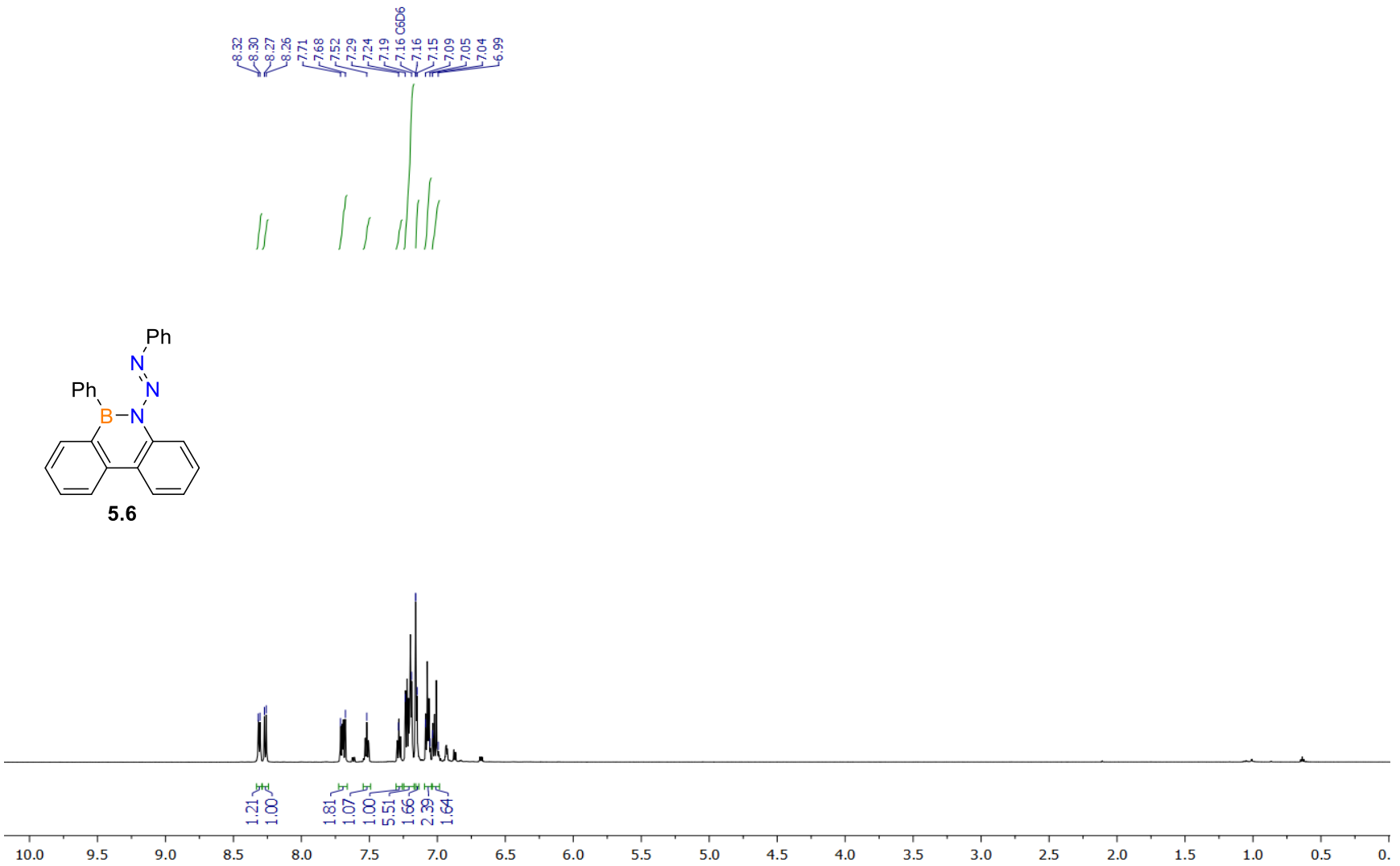

Figure D-9: ^{1}H NMR spectrum of **5.6** in C_6D_6.

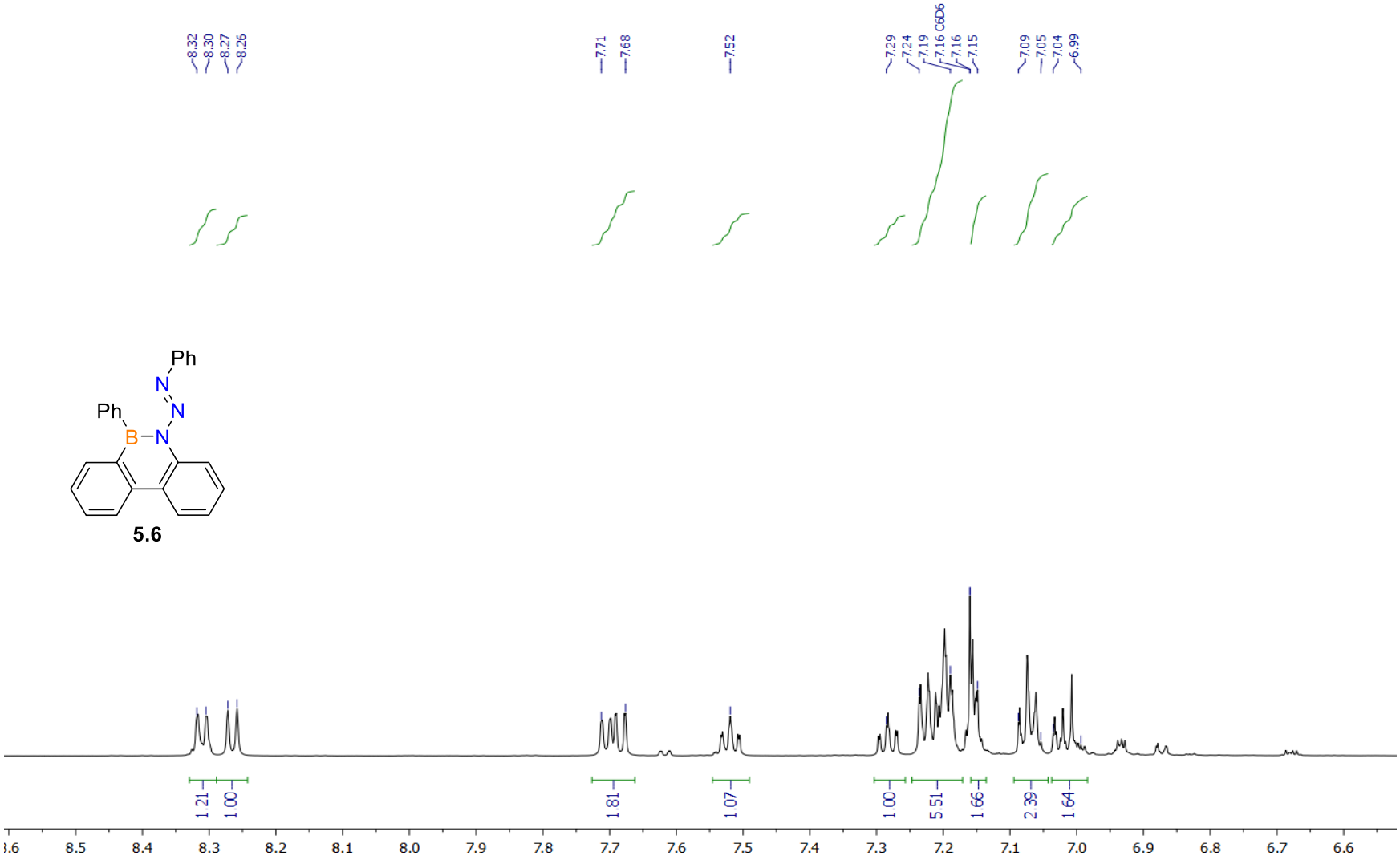

Figure D-10: Expansion of ^{1}H NMR spectrum of **5.6** in C_6D_6 (aryl region).

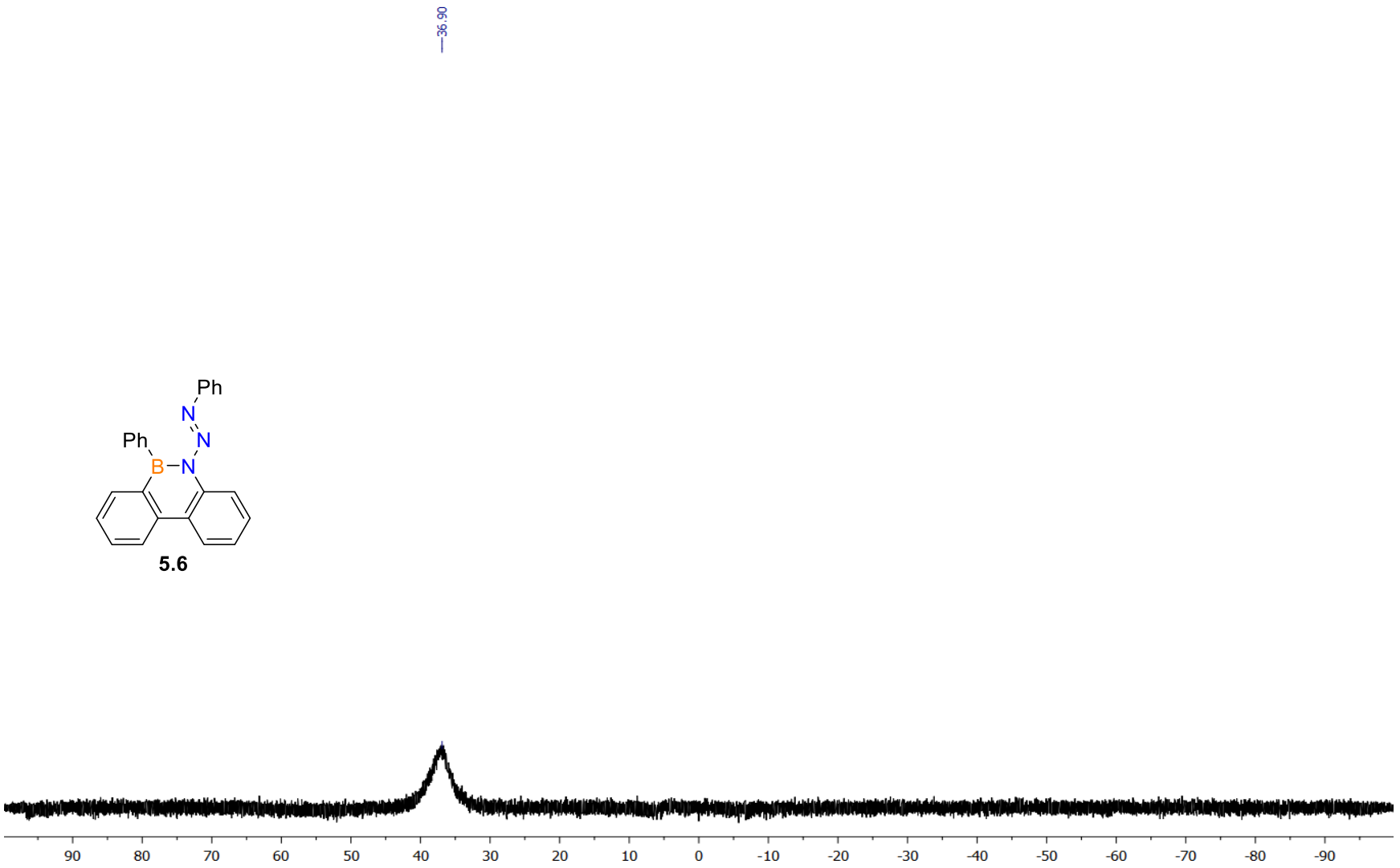

Figure D-11: $^{11}B\{^{1}H\}$ NMR spectrum of **5.6** in $CDCl_3$.

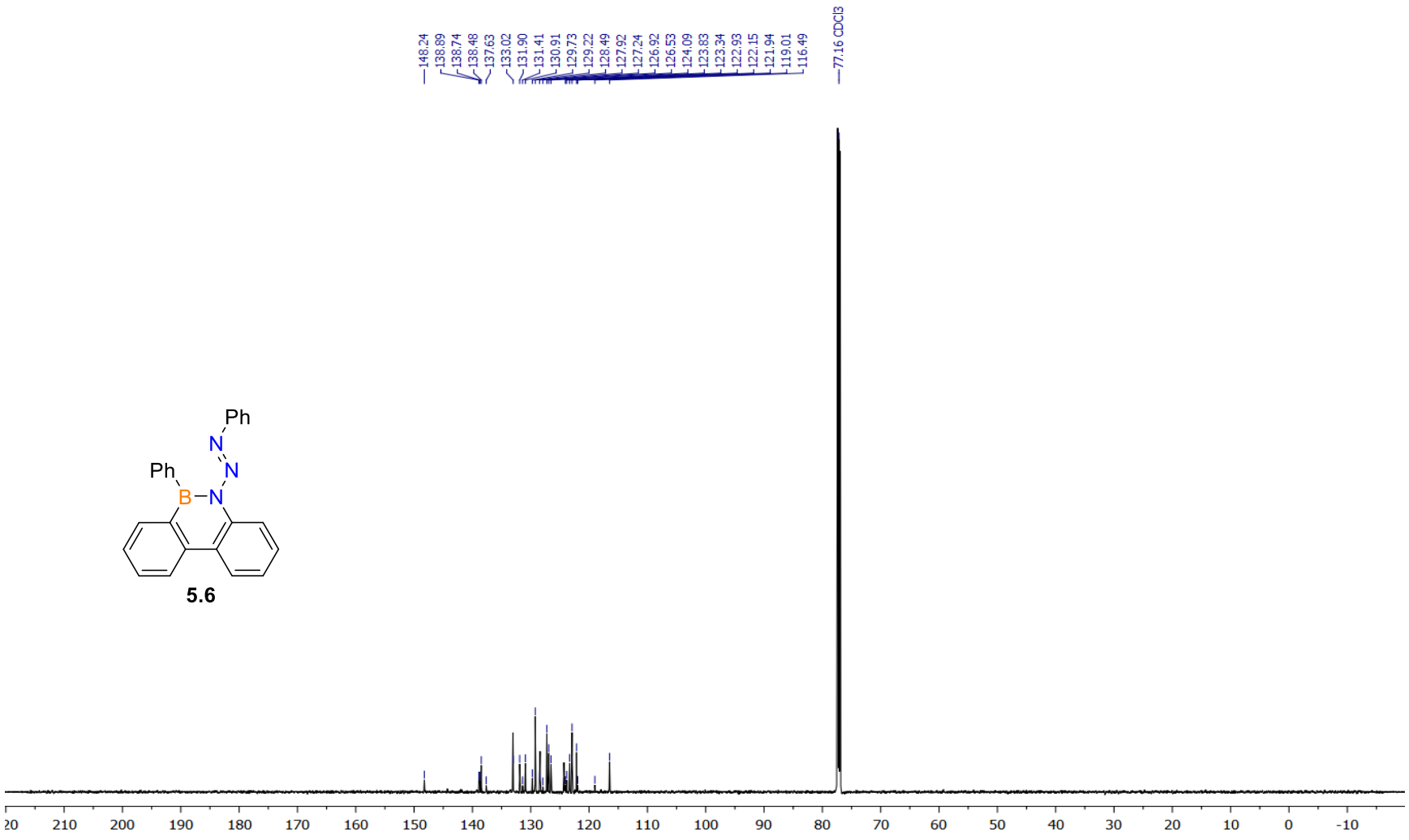

Figure D-12: $^{13}C\{^{1}H\}$ NMR spectrum of **5.6** in $CDCl_3$.

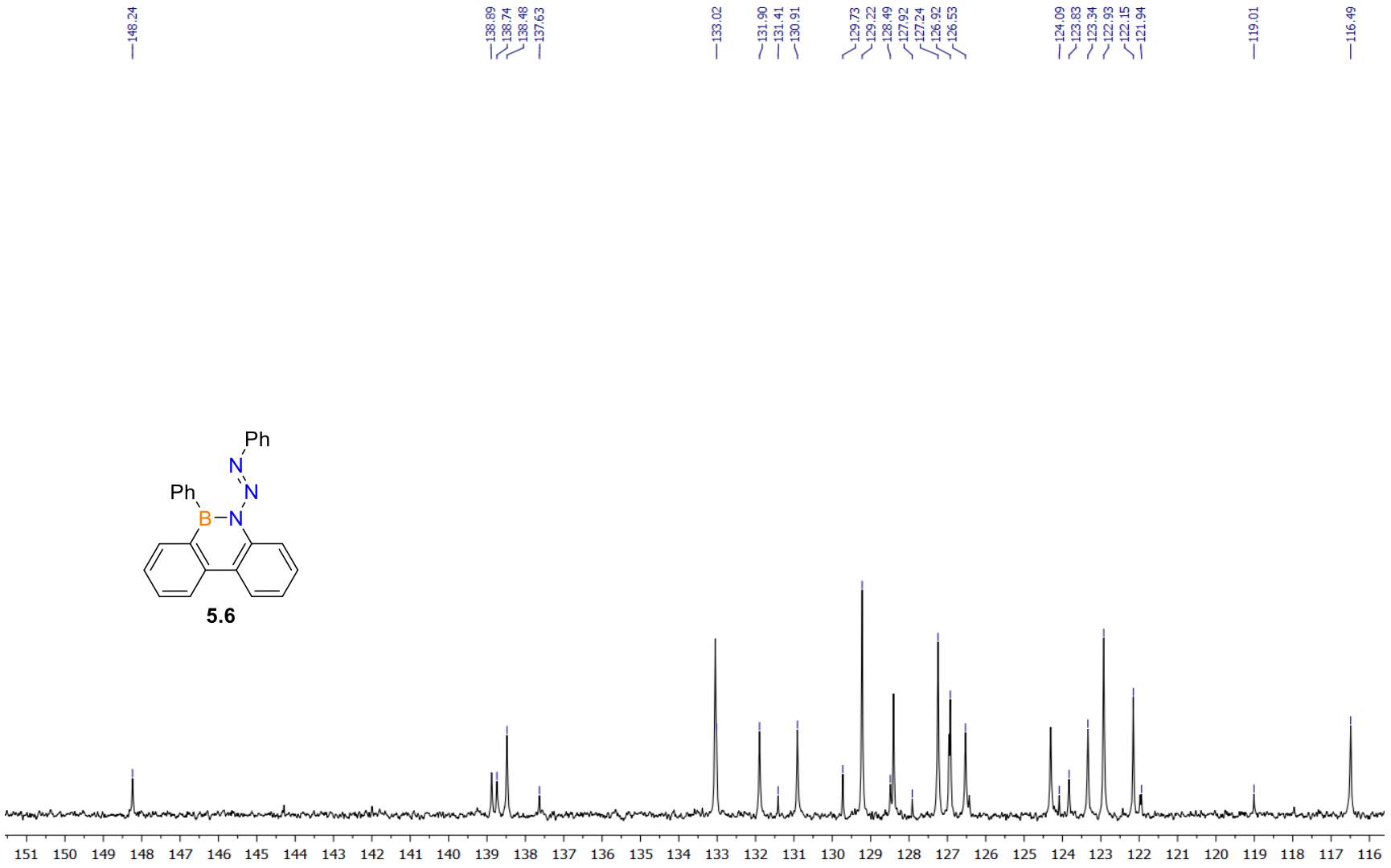

Figure D-13: Expansion of $^{13}C\{^{1}H\}$ NMR spectrum of **5.6** in $CDCl_3$ (aryl region).

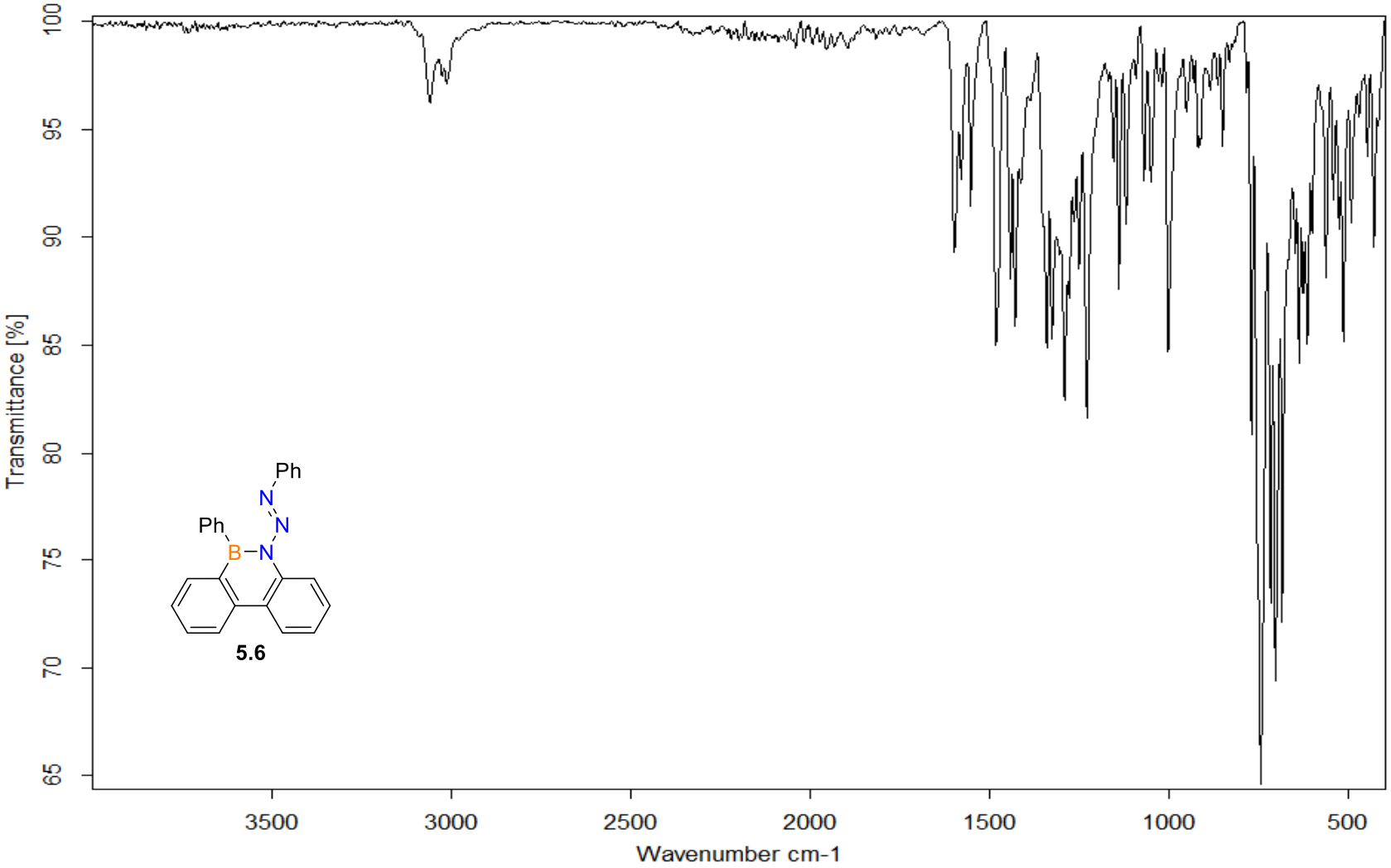

Figure D-14: FT-IR spectrum of **5.6**.

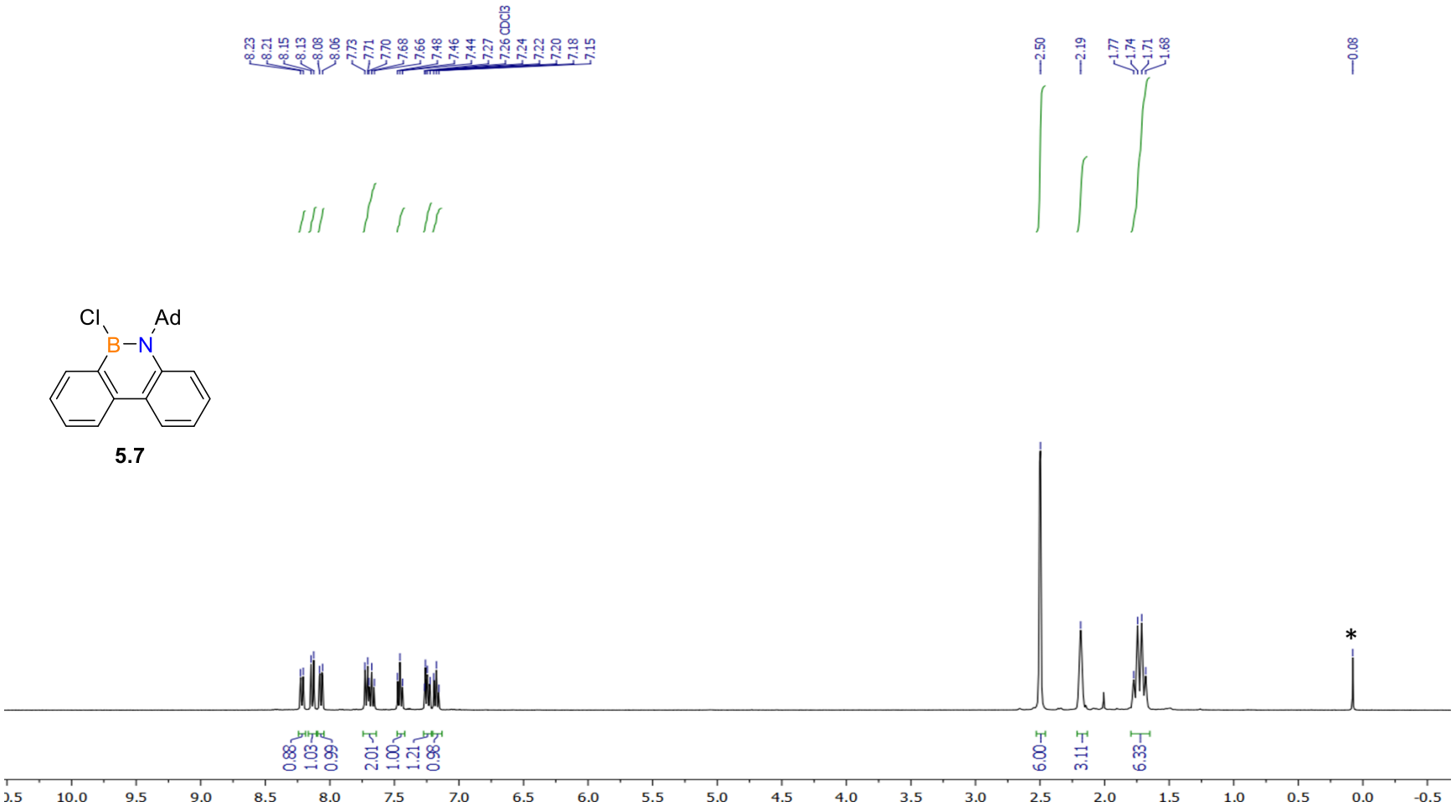

Figure D-15: ^{1}H NMR spectrum of **5.7** in $CDCl_3$ (*grease).

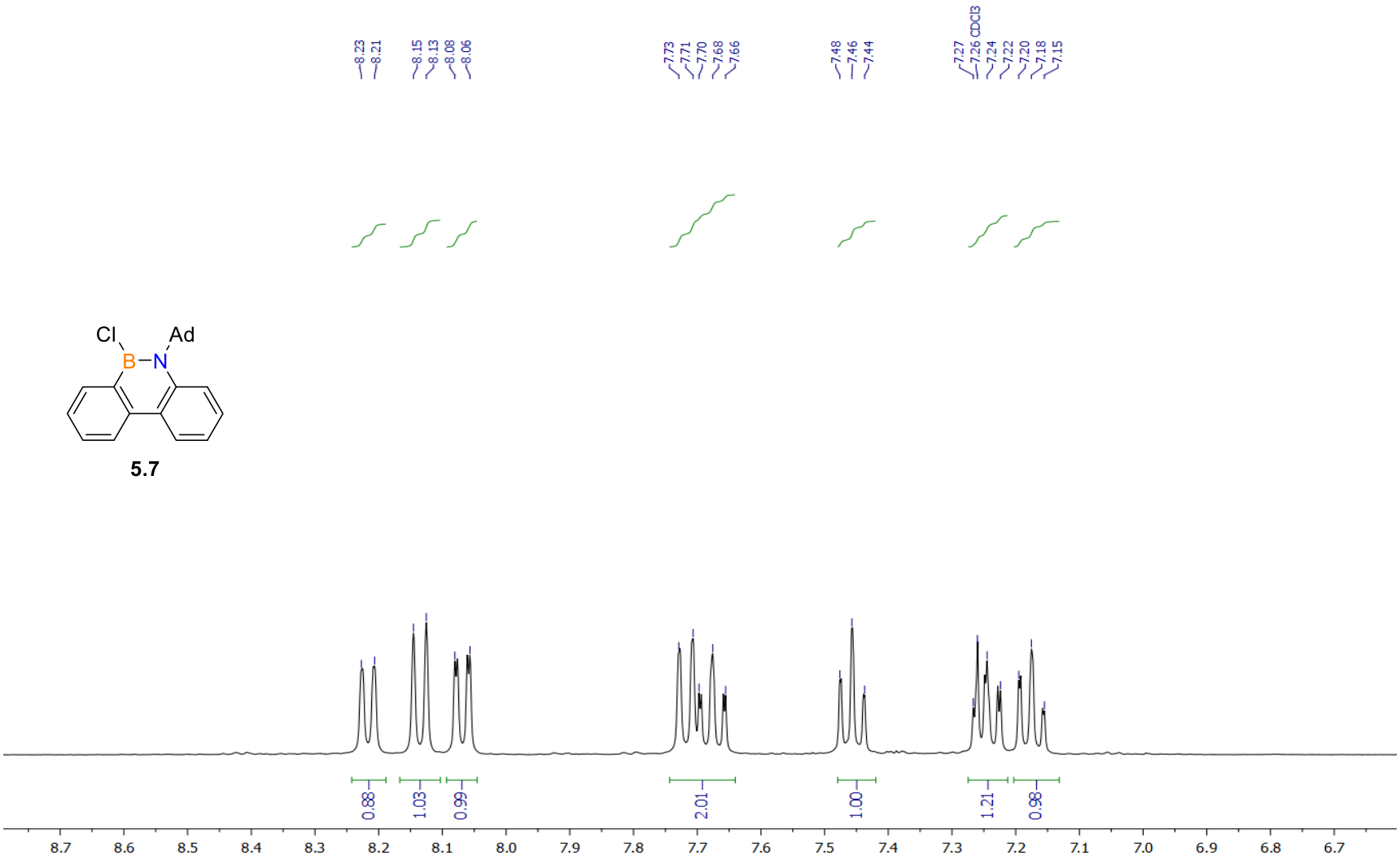

Figure D-16: Expansion of ^{1}H NMR spectrum of **5.7** in $CDCl_3$ (aryl region).

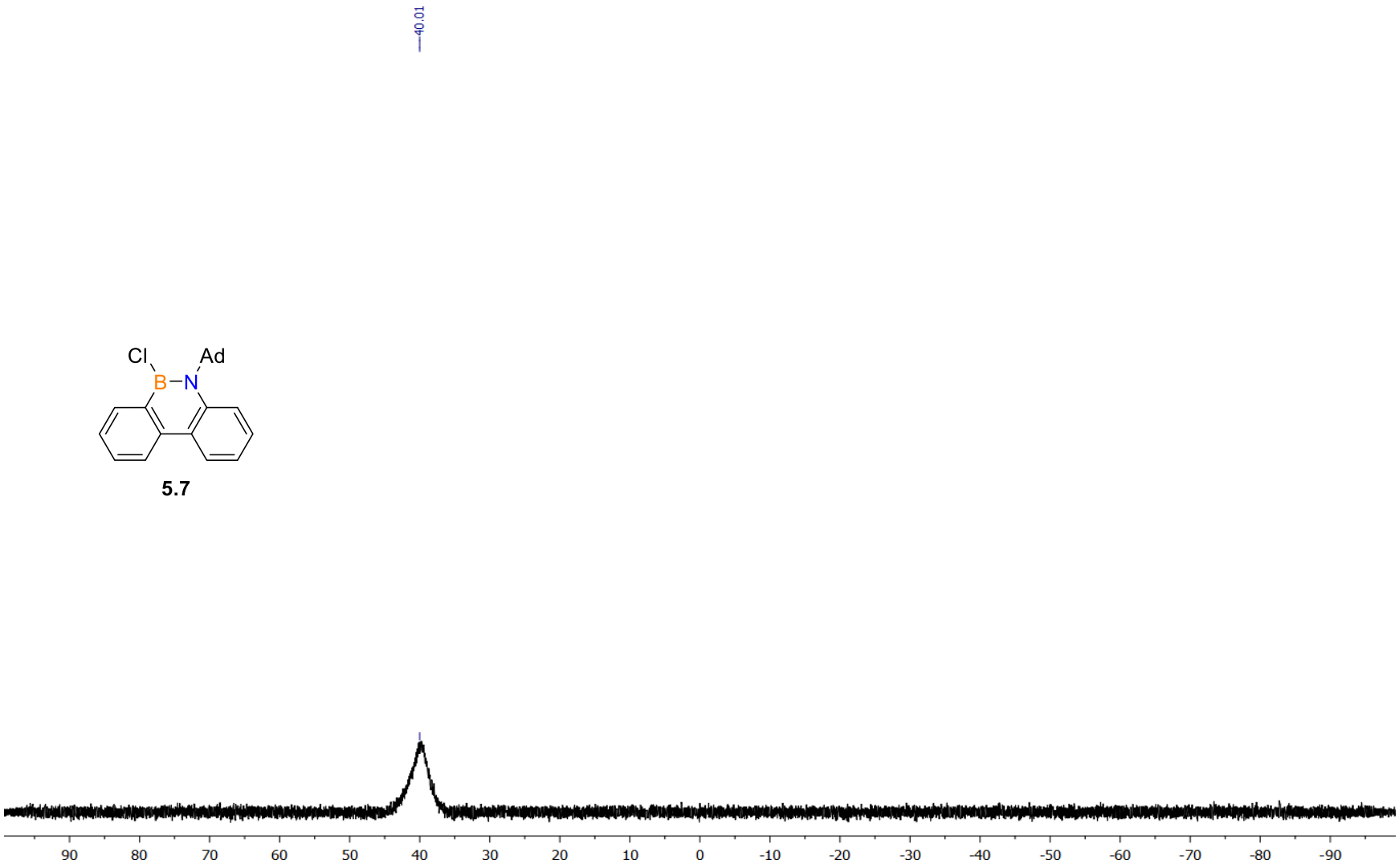

Figure D-17: $^{11}B\{^{1}H\}$ NMR spectrum of **5.7** in $CDCl_3$.

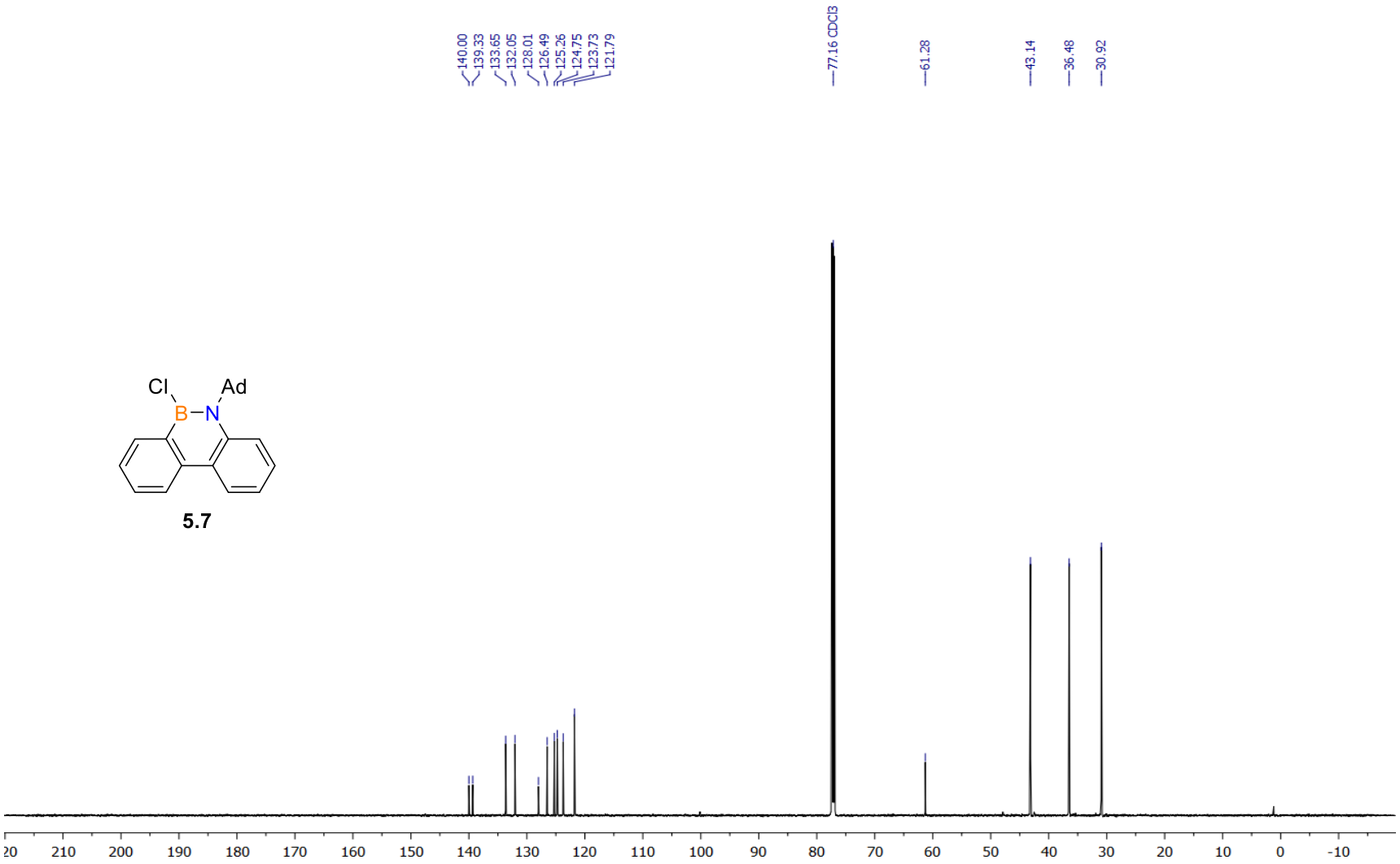

Figure D-18: $^{13}C\{^{1}H\}$ NMR spectrum of **5.7** in $CDCl_3$ (*grease).

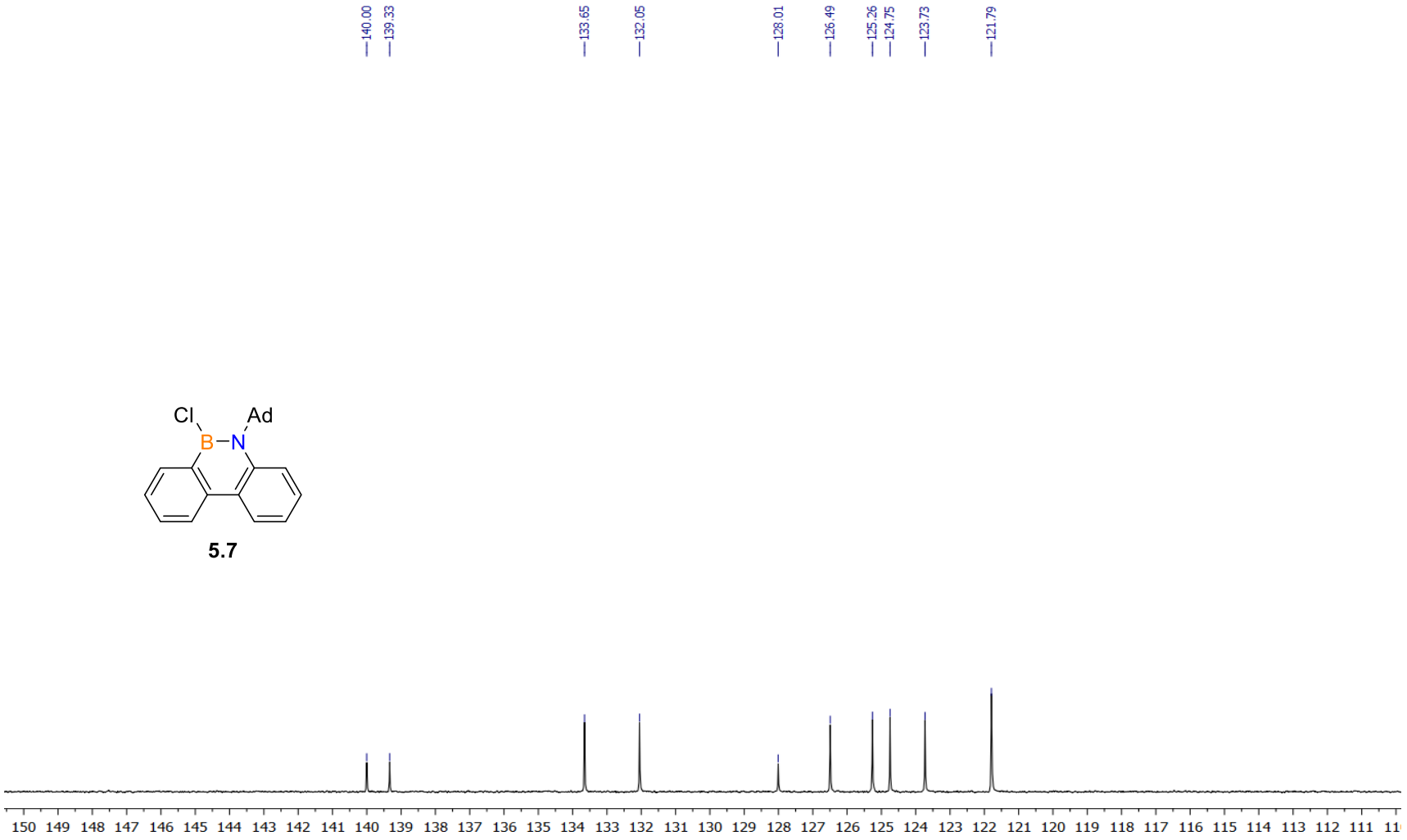

Figure D-19: Expansion of $^{13}C\{^{1}H\}$ NMR spectrum of **5.7** in $CDCl_3$ (aryl region).

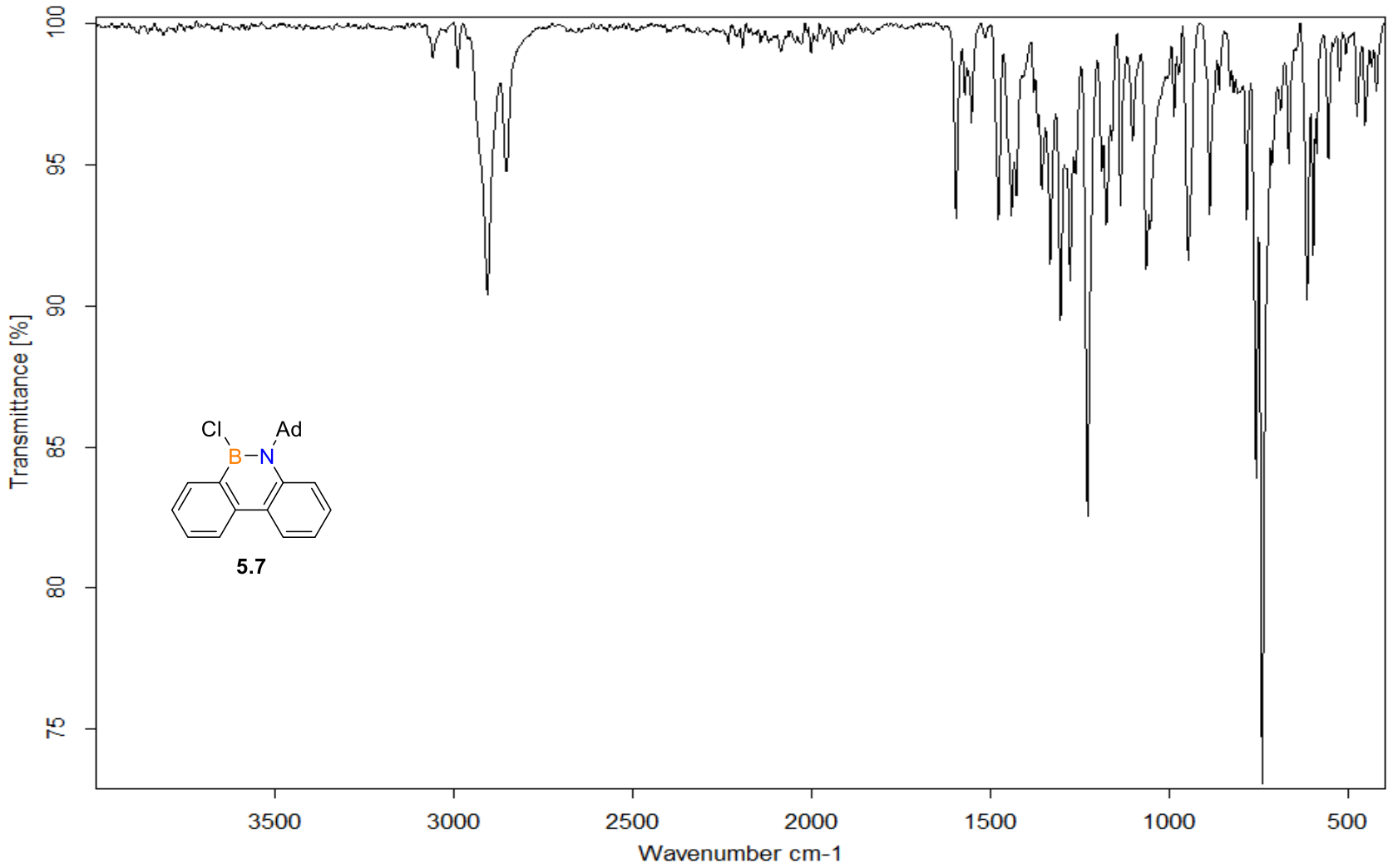

Figure D-20: FT-IR spectrum of **5.7**.

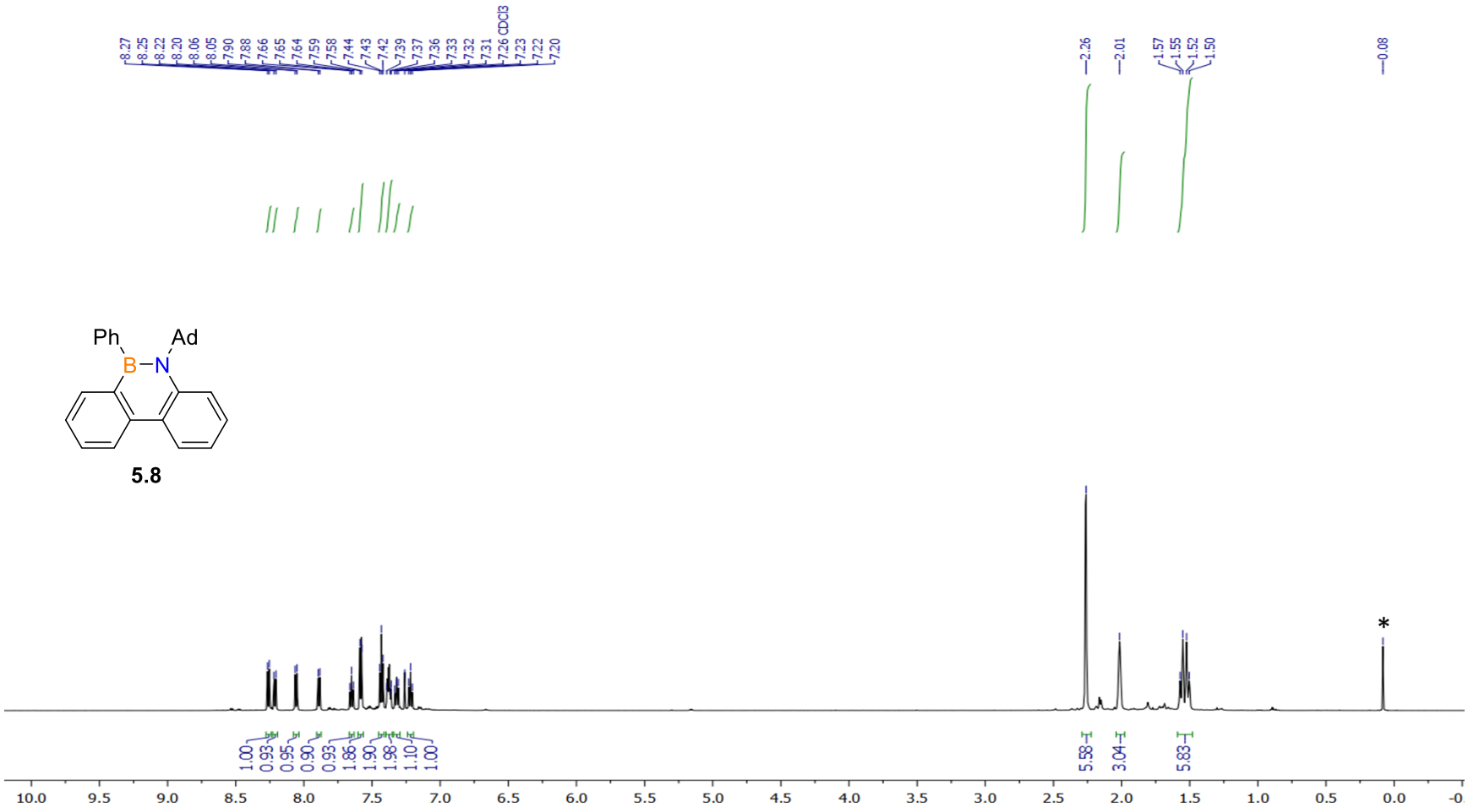

Figure D-21: ^{1}H NMR spectrum of **5.8** in $CDCl_3$ (*grease).

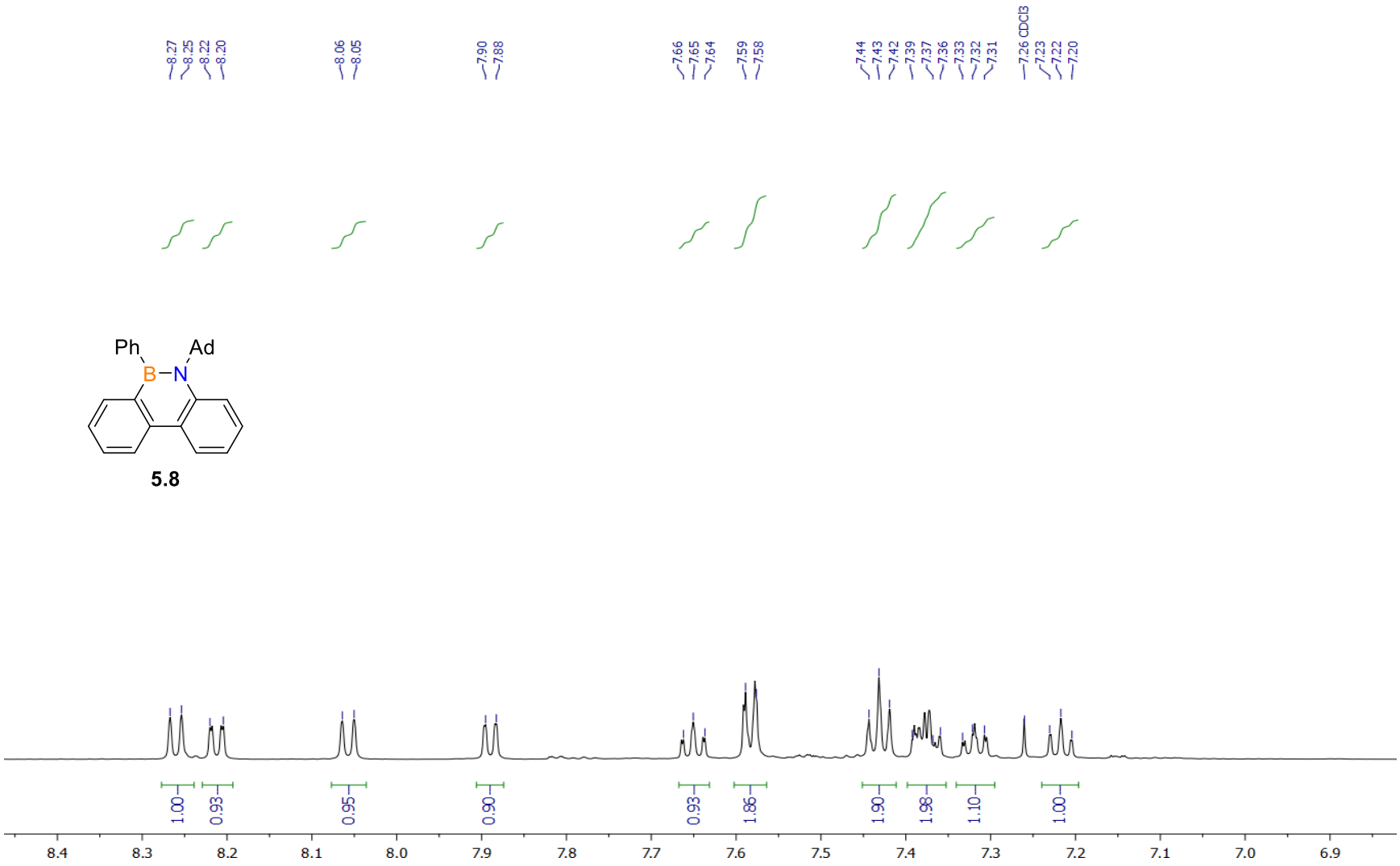

Figure D-22: Expansion of ^{1}H NMR spectrum of **5.8** in $CDCl_3$ (aryl region).

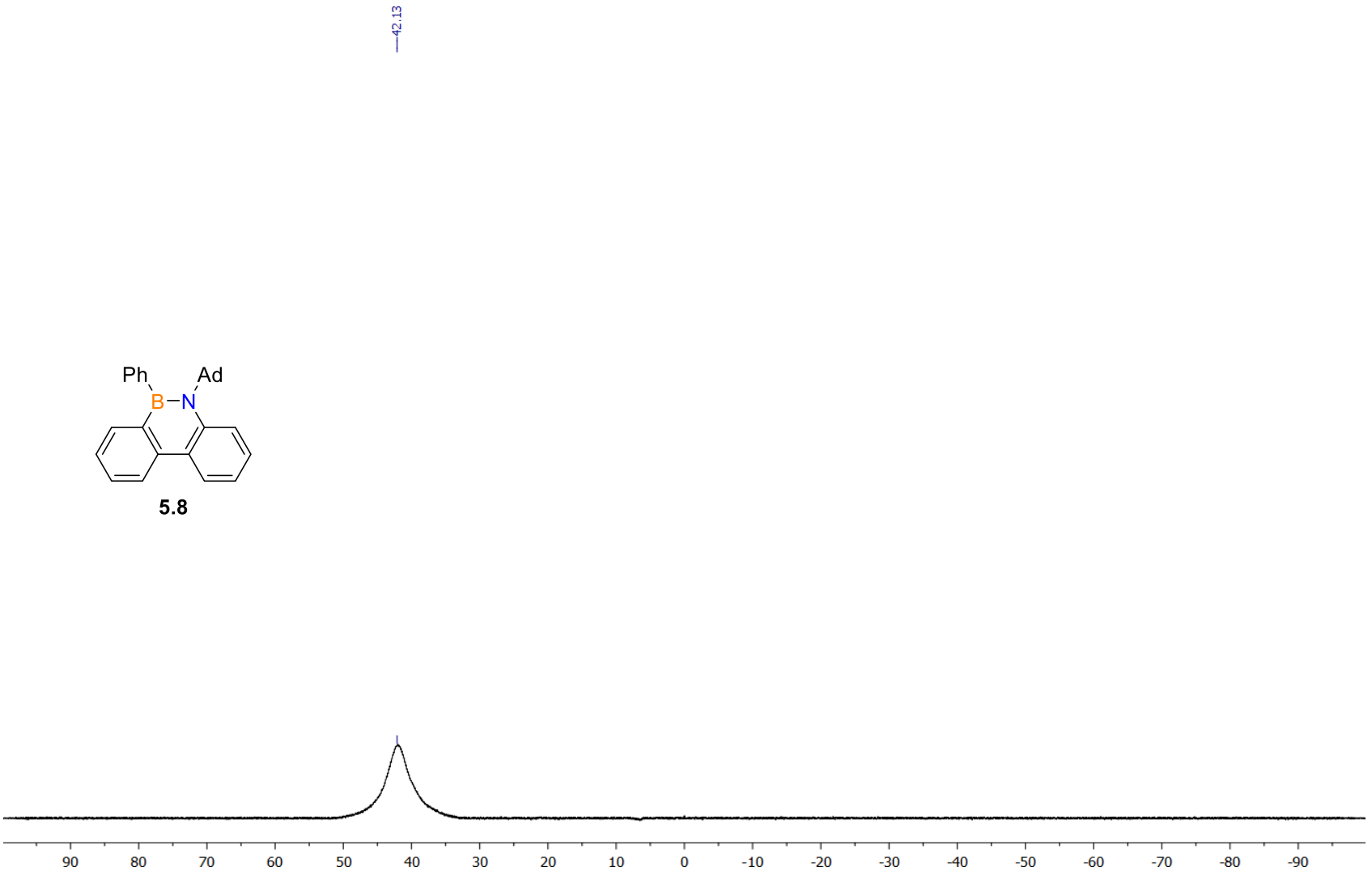

Figure D-23: $^{11}B\{^{1}H\}$ NMR spectrum of **5.8** in $CDCl_3$.

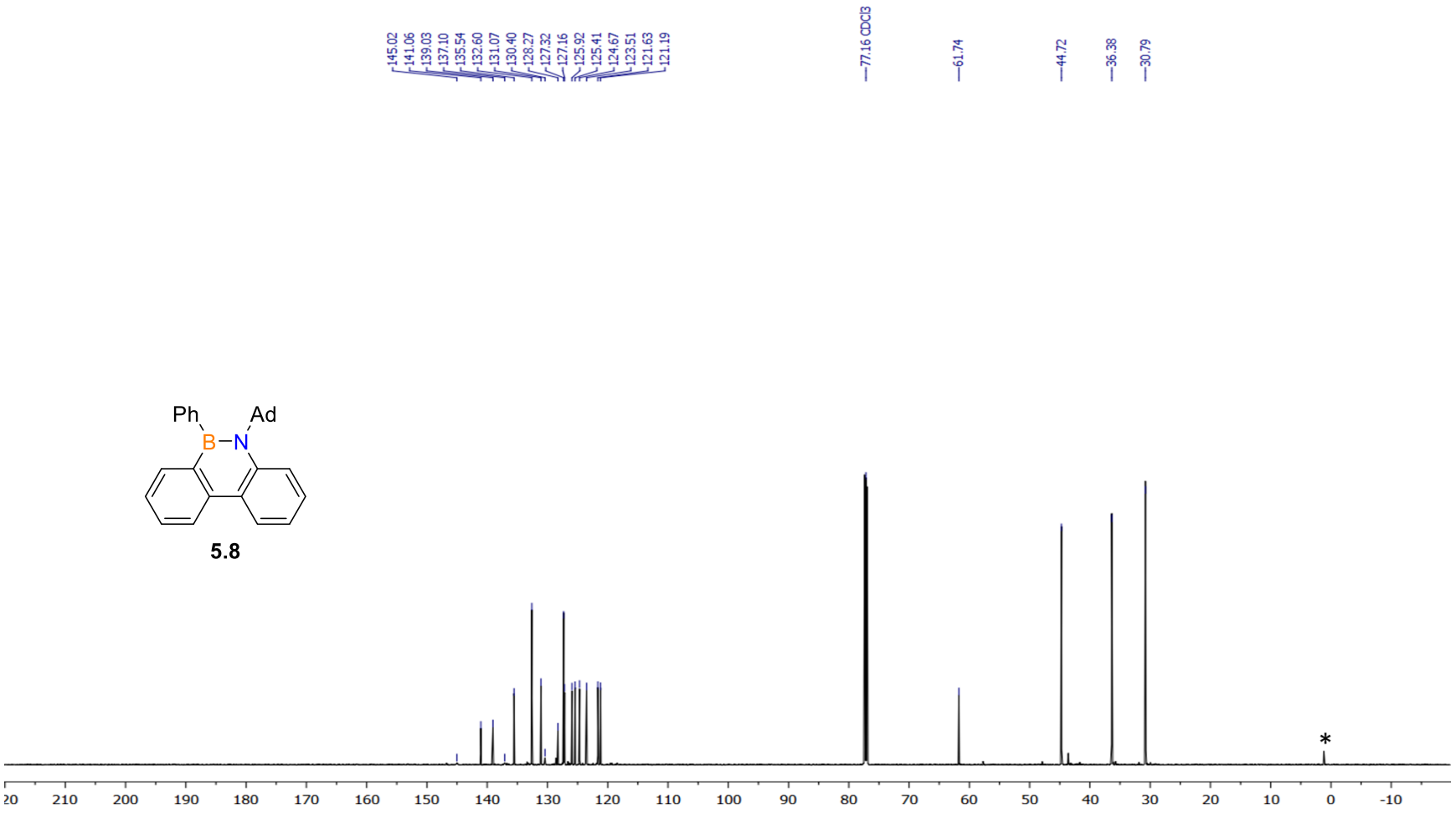

Figure D-24: $^{13}C\{^{1}H\}$ NMR spectrum of **5.8** in $CDCl_3$ (*grease).

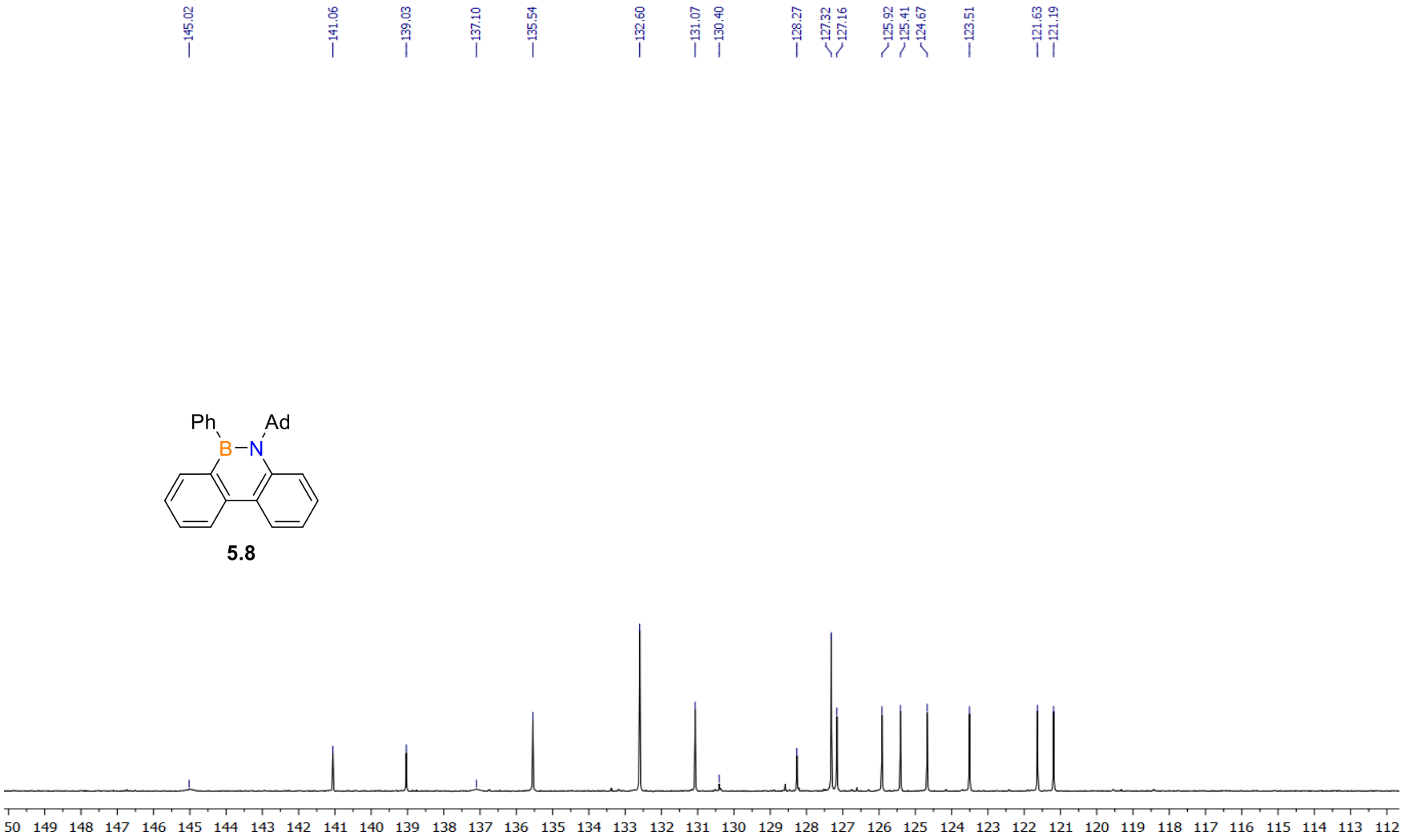

Figure D-25: Expansion of $^{13}C\{^{1}H\}$ NMR spectrum of **5.8** in $CDCl_3$ (aryl region).

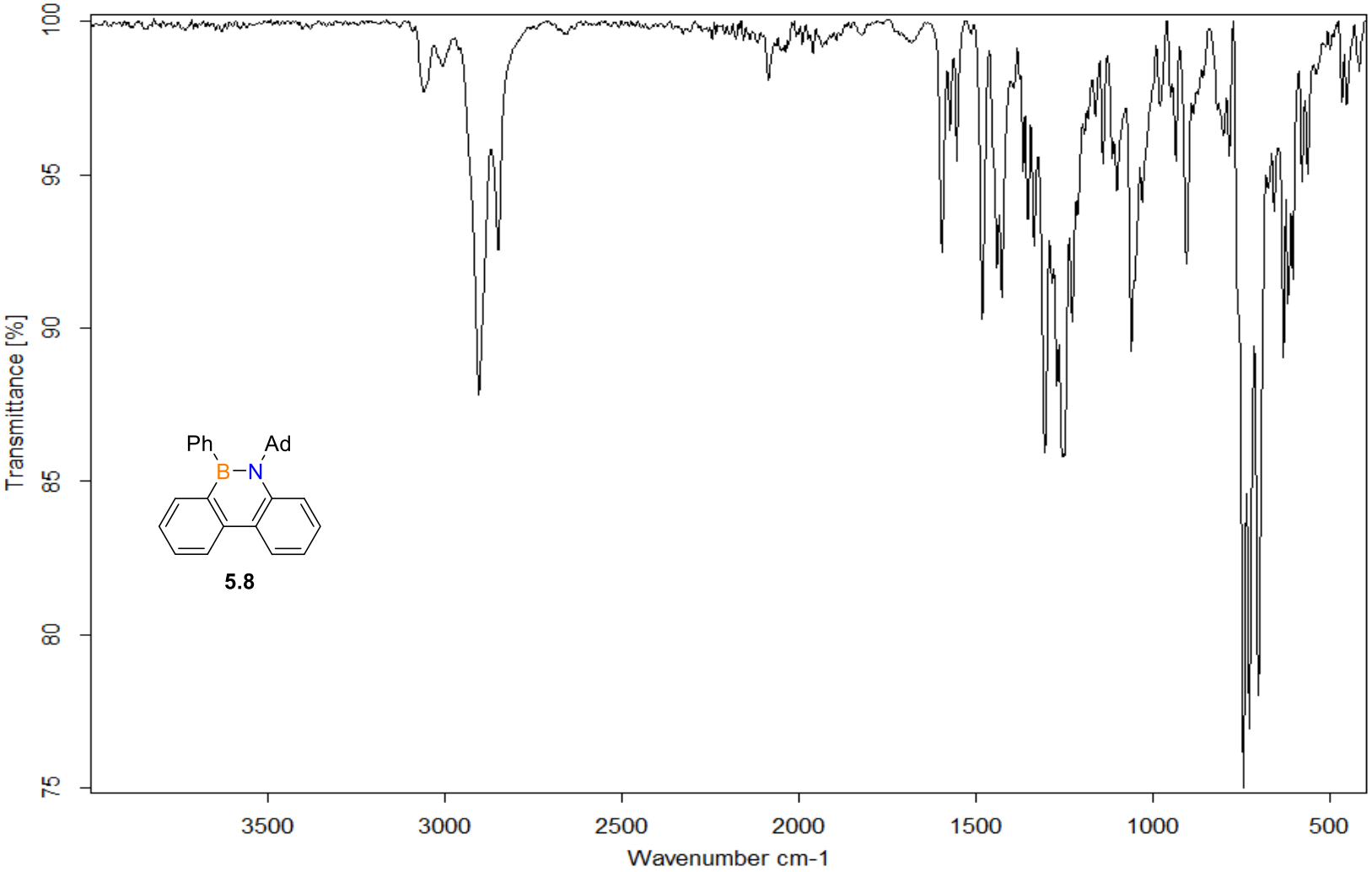

Figure D-26: FT-IR spectrum of **5.8**.

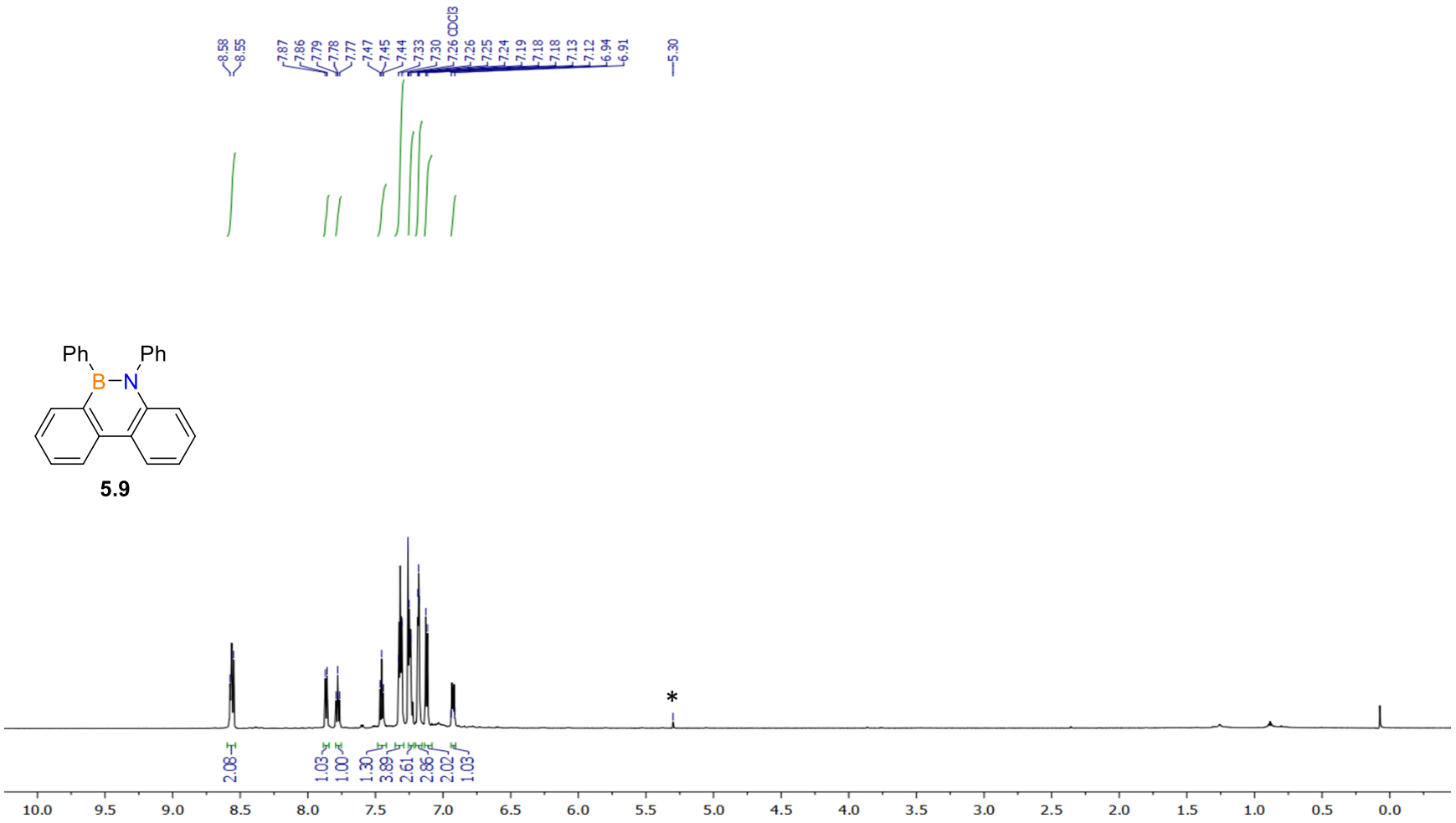

Figure D-27: ^{1}H NMR spectrum of **5.9** in $CDCl_3$ (*CH_2Cl_2)..

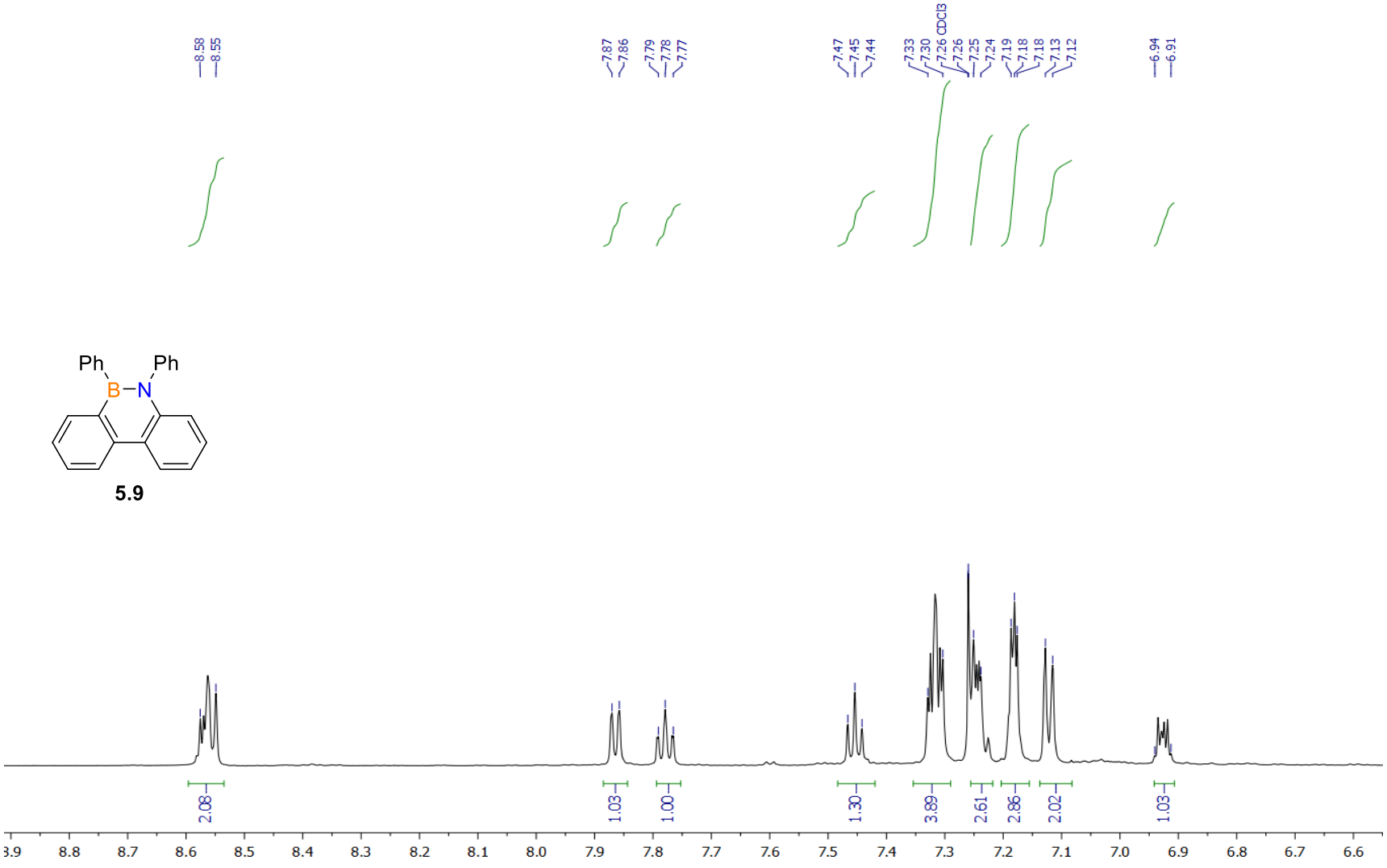

Figure D-28: Expansion of ^{1}H NMR spectrum of **5.9** in $CDCl_3$ (aryl region).

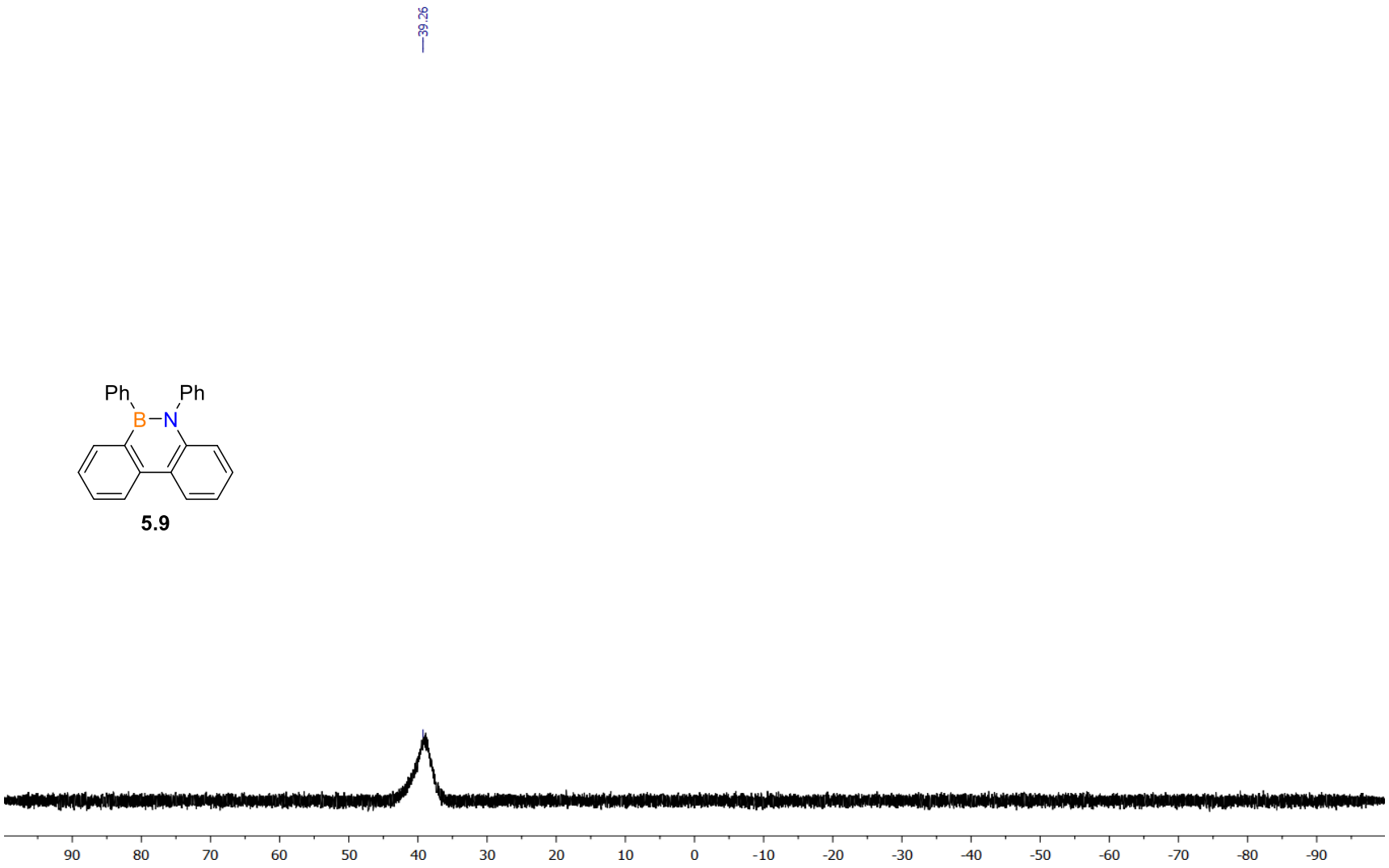

Figure D-29: $^{11}B\{^{1}H\}$ NMR spectrum of **5.9** in $CDCl_3$.

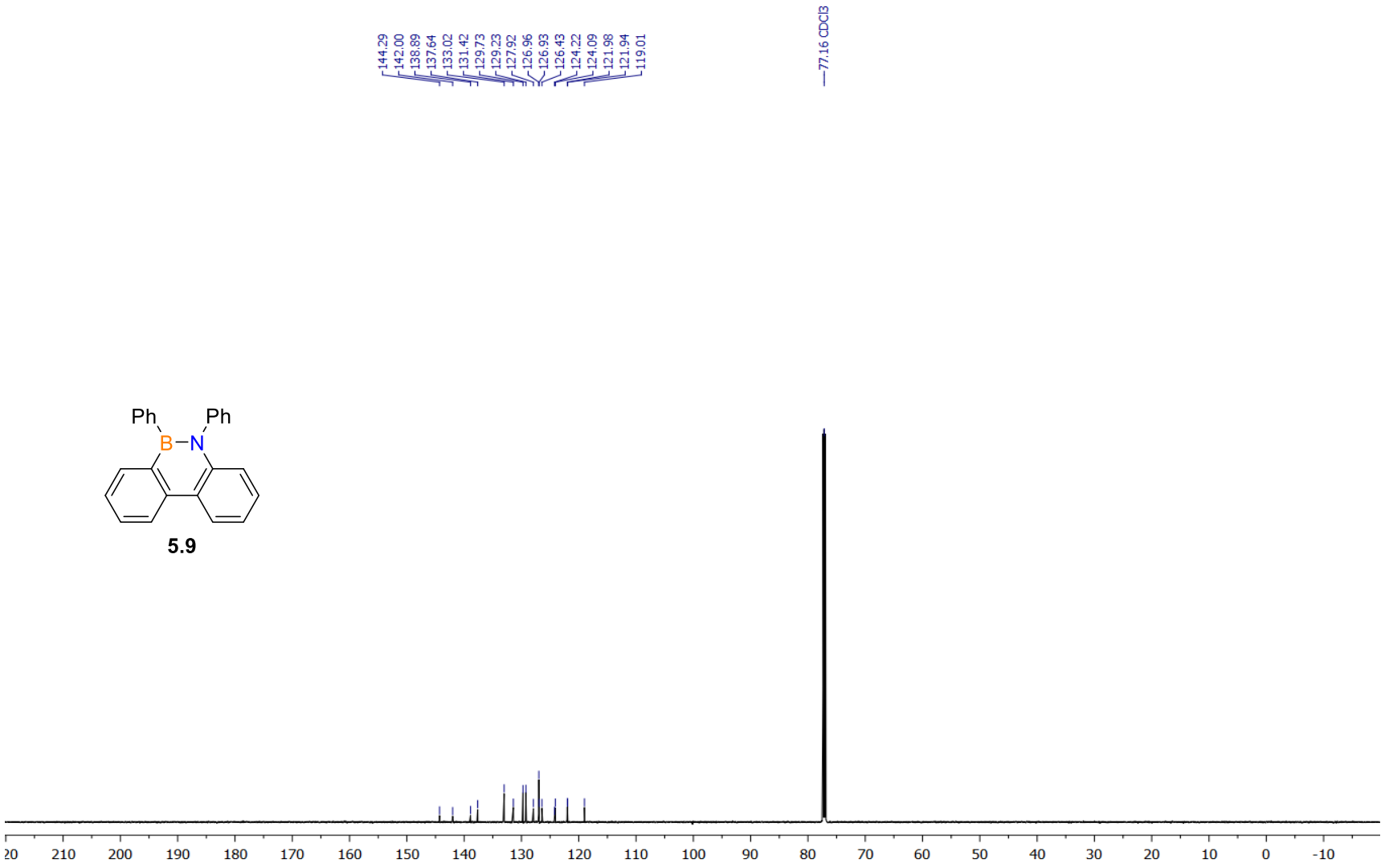

Figure D-30: $^{13}C\{^{1}H\}$ NMR spectrum of **5.9** in $CDCl_3$.

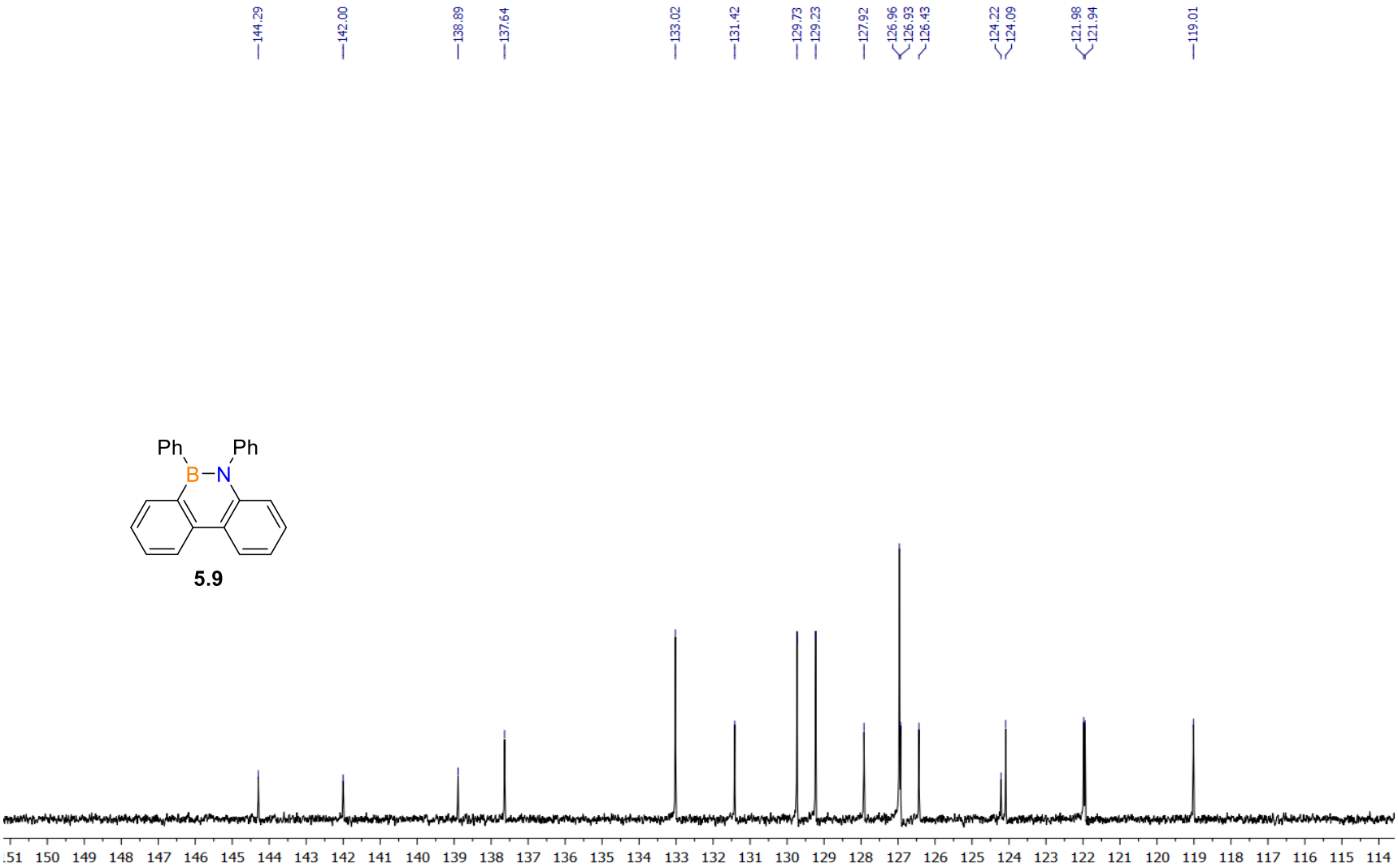

Figure D-31: Expansion of $^{13}C\{^{1}H\}$ NMR spectrum of **5.9** in $CDCl_3$ (aryl region).

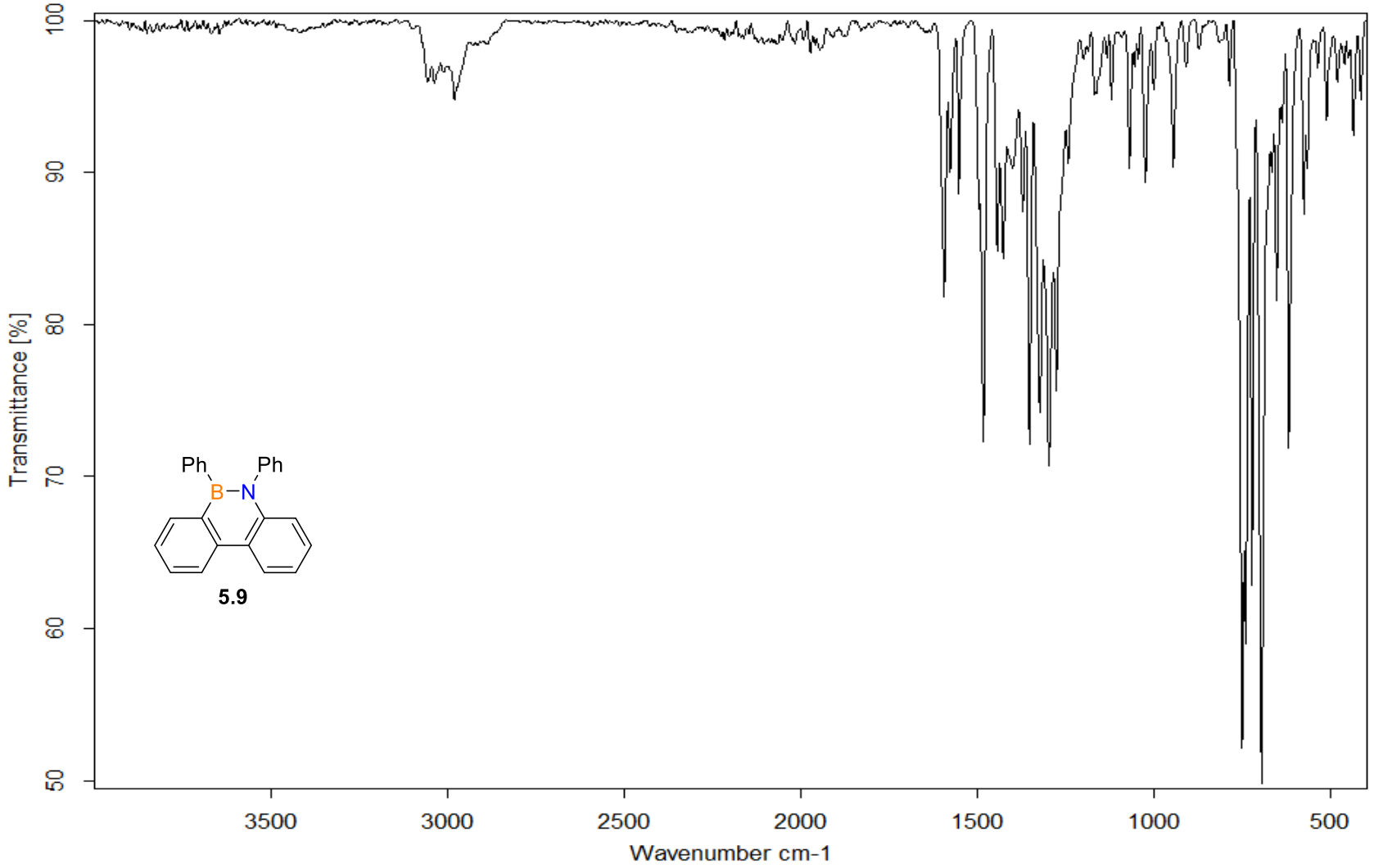

Figure D-32: FT-IR spectrum of **5.9**.

Gutmann-Beckett Studies

For the Gutmann−Beckett studies, samples were prepared in a 1:1 stoichiometric ratio of Lewis acid/Et_3PO. Subsequent $^{31}P\{^1H\}$ NMR spectroscopy was done in C_6D_6. Samples were prepared in a glovebox under a nitrogen atmosphere. Single crystals for X-ray diffraction studies were grown from a dichloromethane solution of the adduct by vapor diffusion into hexanes.

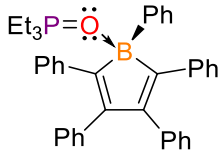

1.7-Ph·OPEt$_3$

^{1}H NMR (600 MHz, $CDCl_3$): δ 7.68 (d, *J* = 6.0 Hz, 2H), δ 7.25 (d, *J* = 6.0 Hz, 1H), 7.11-7.00 (m, 12H), 6.91-6.86 (m, 8H), 6.79 (t, *J* = 6.0 Hz, 2H, 1.72 (dq, *J* = 18.0, 6.0 Hz, 6H), 1.04 (dt, *J* = 18.0, 6.0 Hz, 9H)

$^{31}P\{^1H\}$ NMR (243 MHz, C_6D_6): δ 76.6 (br)

$^{11}B\{^1H\}$ NMR (193 MHz, C_6D_6): δ 7.4 (br)

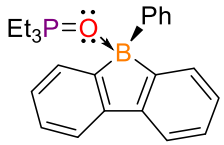

1.15-Ph·OPEt$_3$

^{1}H NMR (600 MHz, C_6D_6): δ 7.84 (d, *J* = 6.0 Hz, 2H), 7.81 (d, *J* = 6.0 Hz, 2H), 7.67 (d, *J* = 6.0 Hz, 2H), 7.42-7.39 (m, 2H), 7.35-7.32 (m, 2H), 7.27-7.23 (m, 3H), 0.85-0.82 (m, 6H), 0.40-0.28 (m, 9H)

$^{31}P\{^1H\}$ NMR (243 MHz, C_6D_6): δ 74.1 (br)

$^{11}B\{^1H\}$ NMR (193 MHz, C_6D_6): δ 6.0 (br)

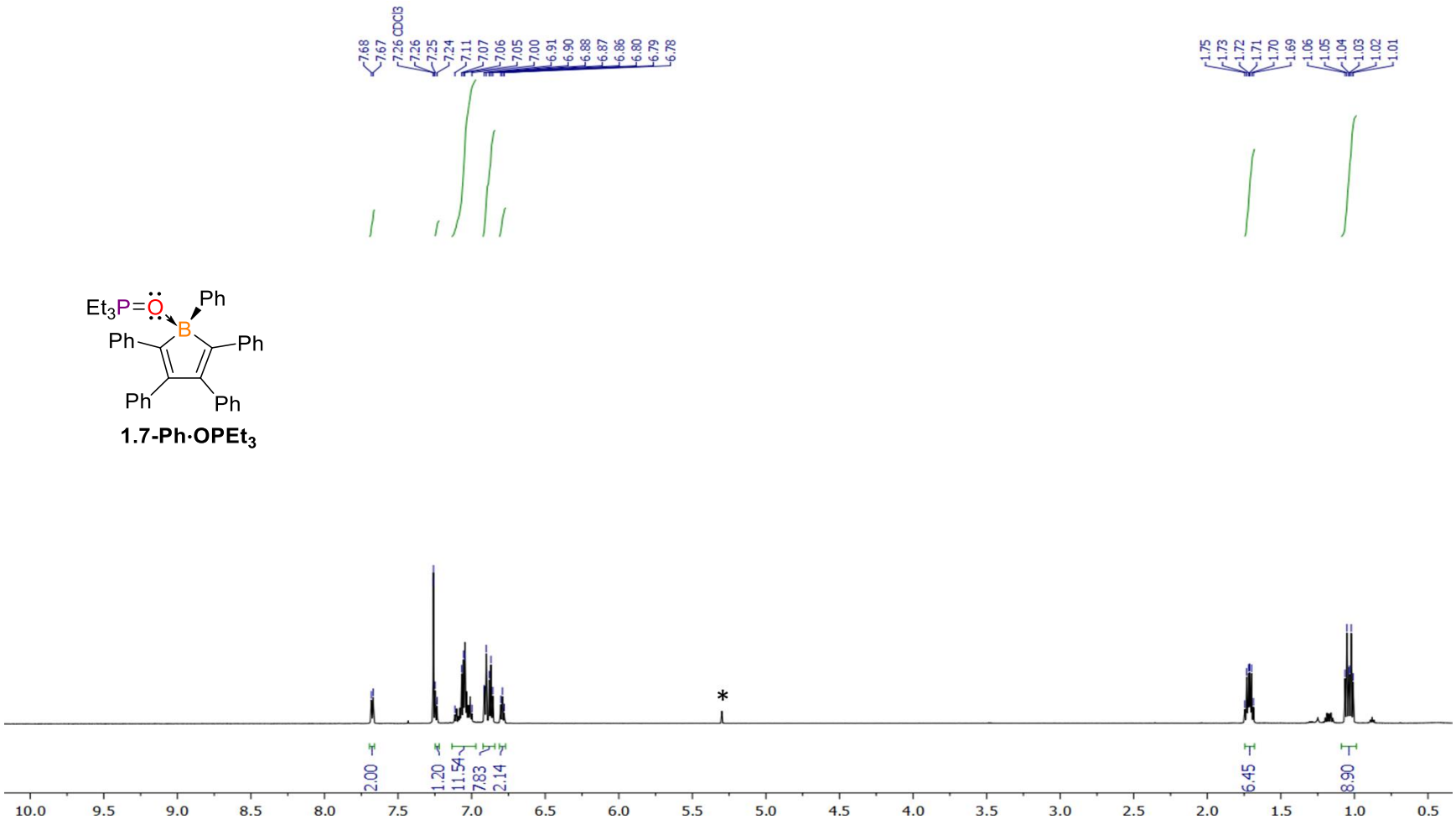

Figure D-33: ^{1}H NMR spectrum of **1.7-Ph·OPEt$_3$** in $CDCl_3$ (*CH_2Cl_2).

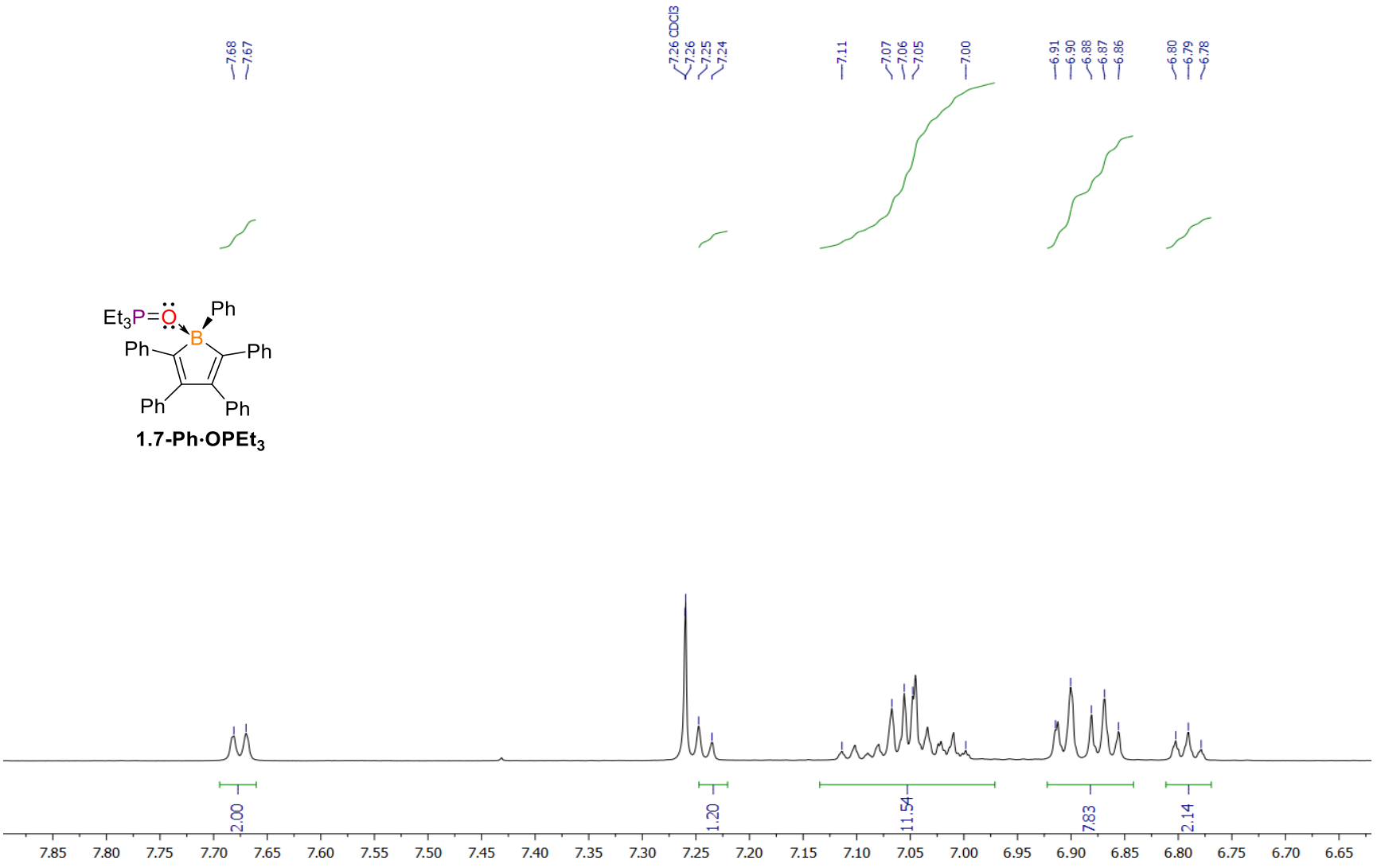

Figure D-34: Expansion of ^{1}H NMR spectrum of **1.7-Ph·OPEt$_3$** in $CDCl_3$.

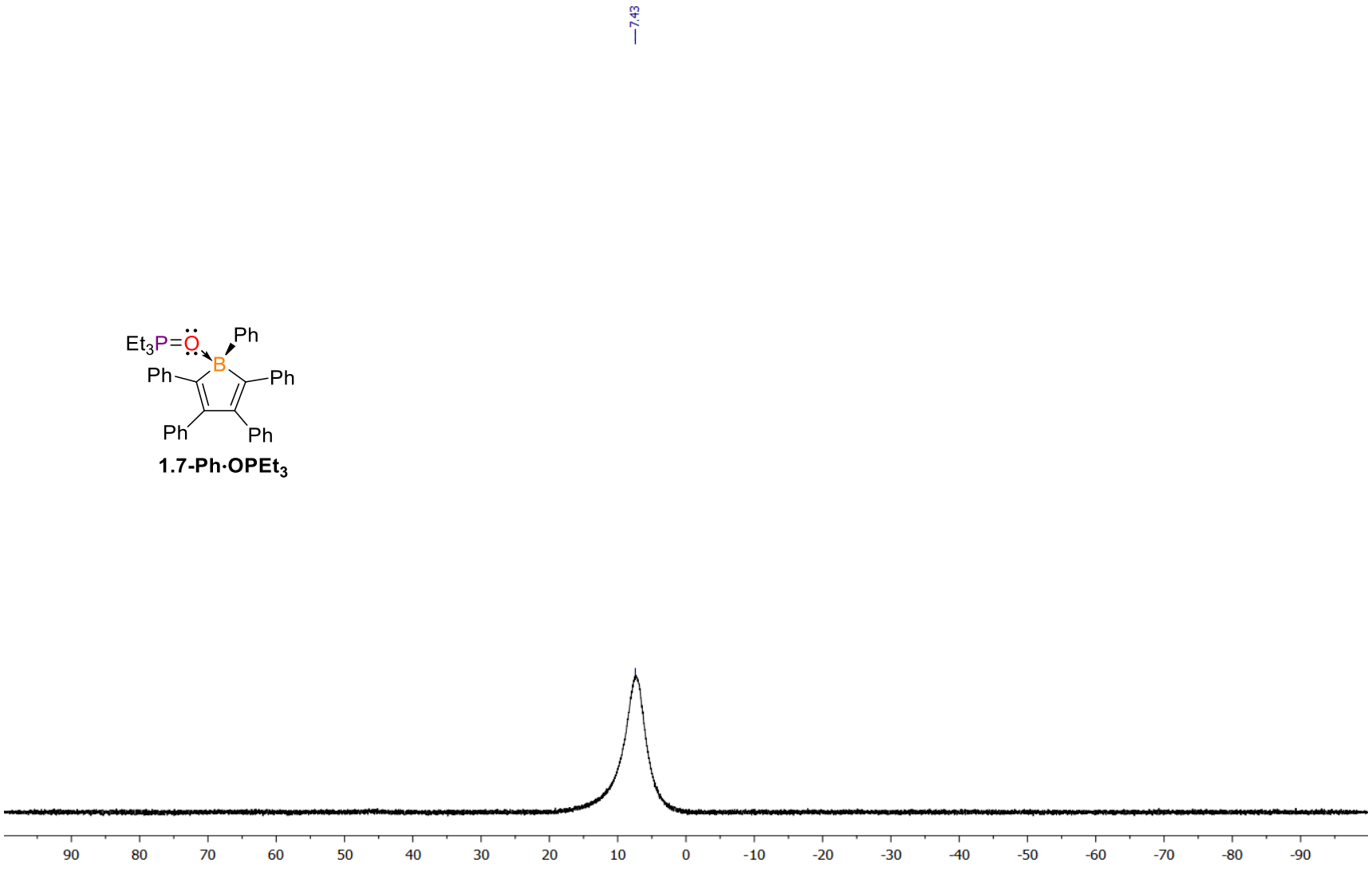

Figure D-35: $^{11}B\{^{1}H\}$ NMR spectrum of **1.7-Ph·OPEt3** in C_6D_6.

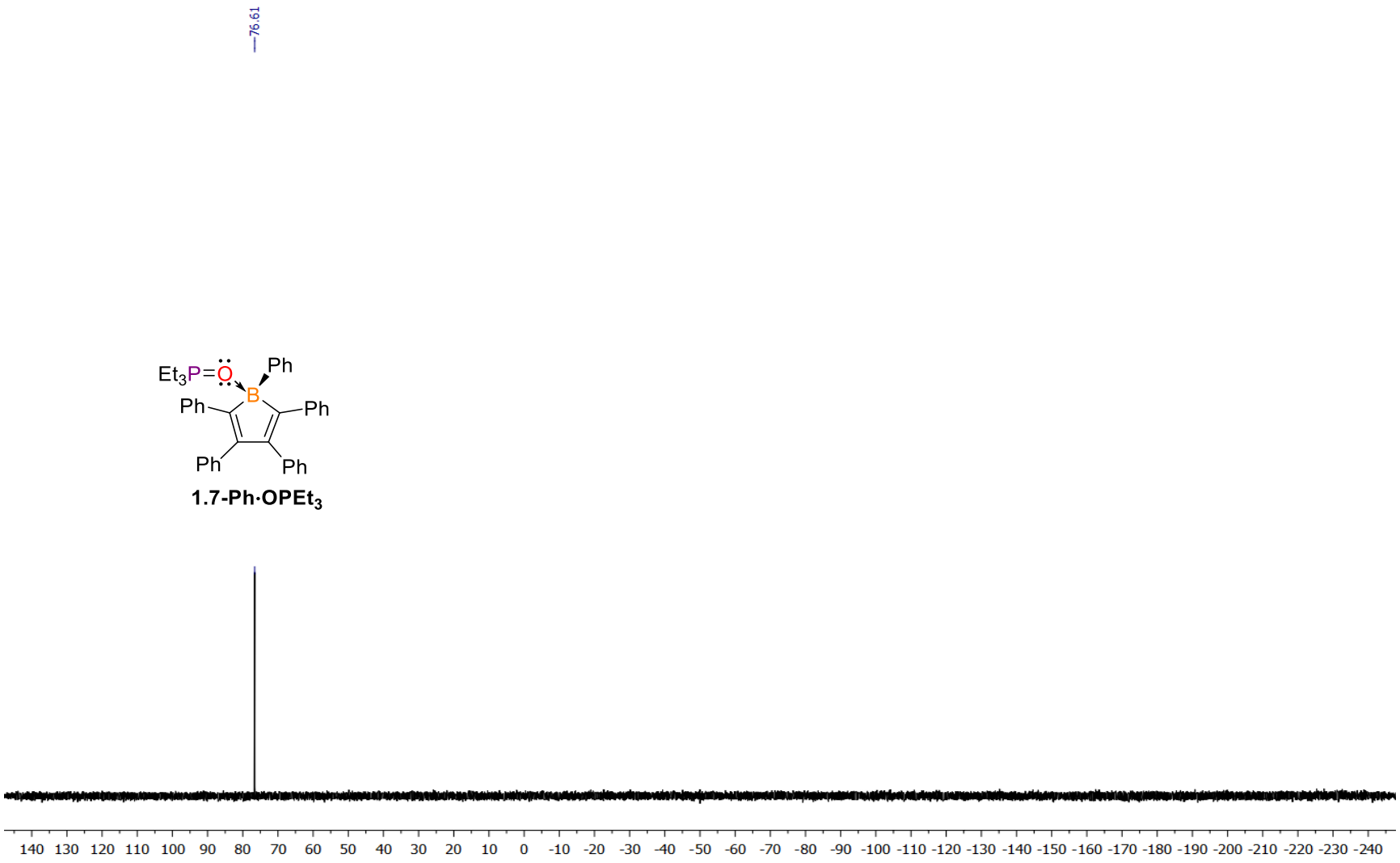

Figure D-36: ^{31}P NMR spectrum of **1.7-Ph·OPEt3** in C_6D_6.

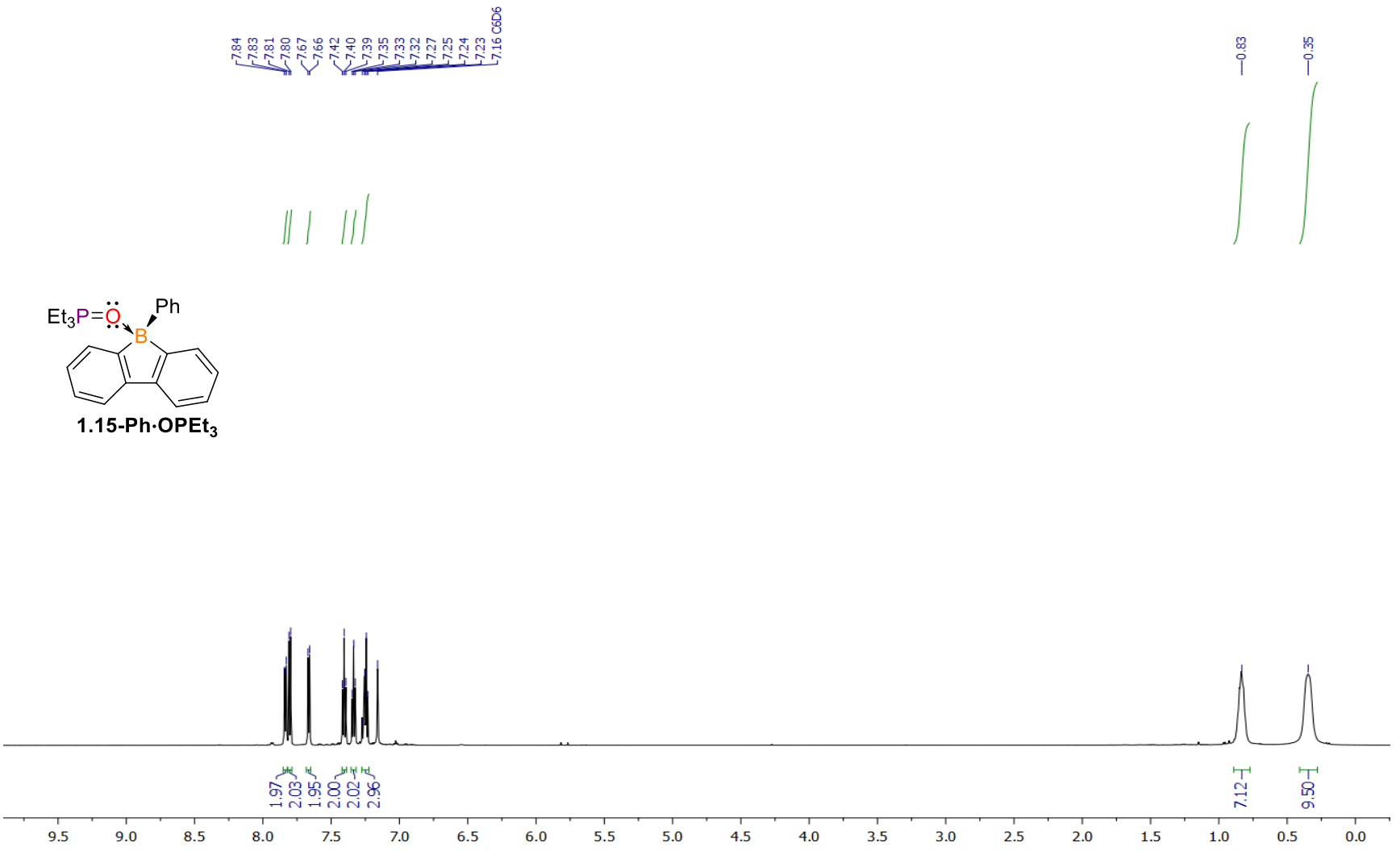

Figure D-37: ^{1}H NMR spectrum of **1.15-Ph·OPEt$_3$** in C_6D_6.

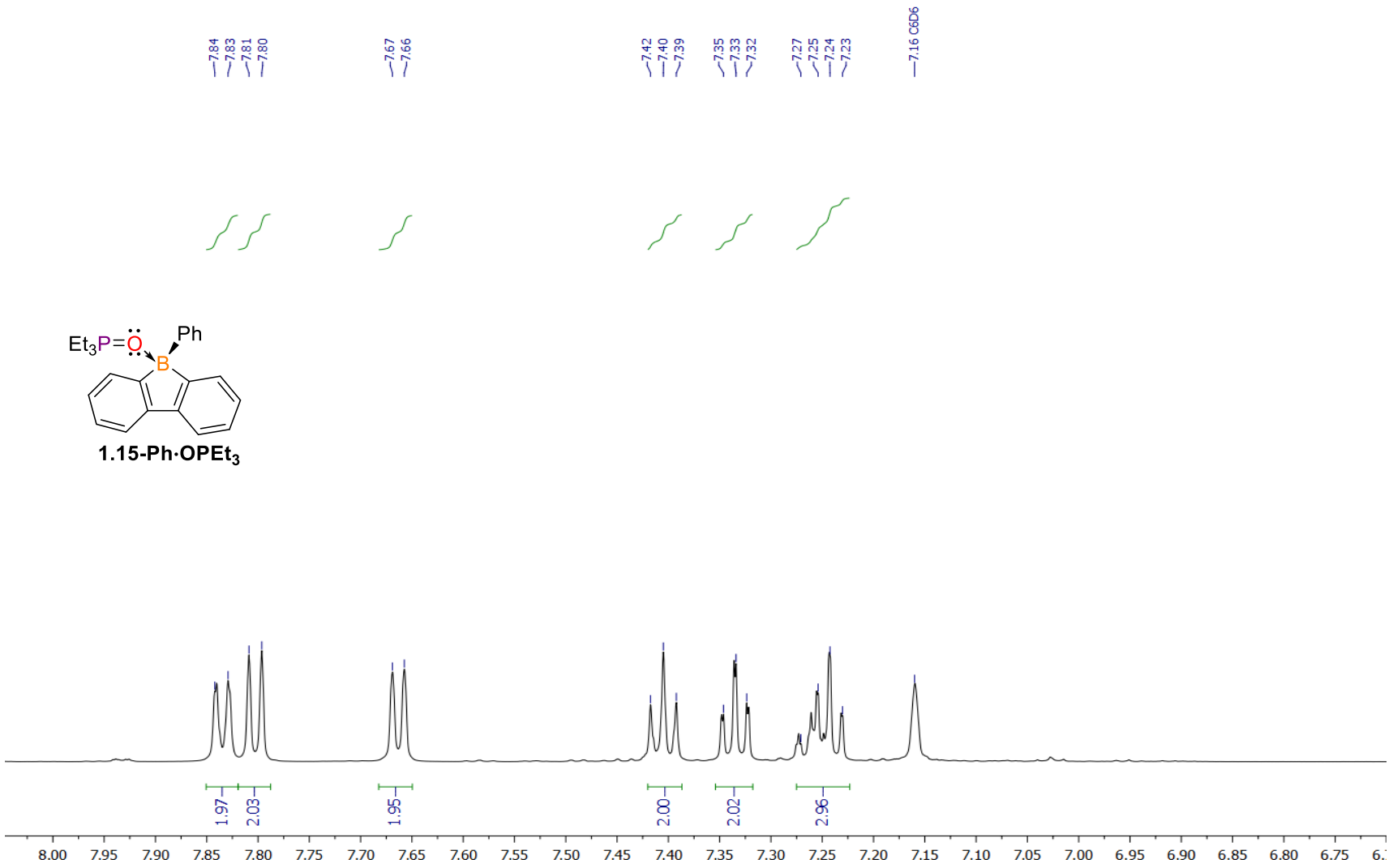

Figure D-38: Expansion of ^{1}H NMR spectrum of **1.15-Ph·OPEt$_3$** in C_6D_6 (aryl region).

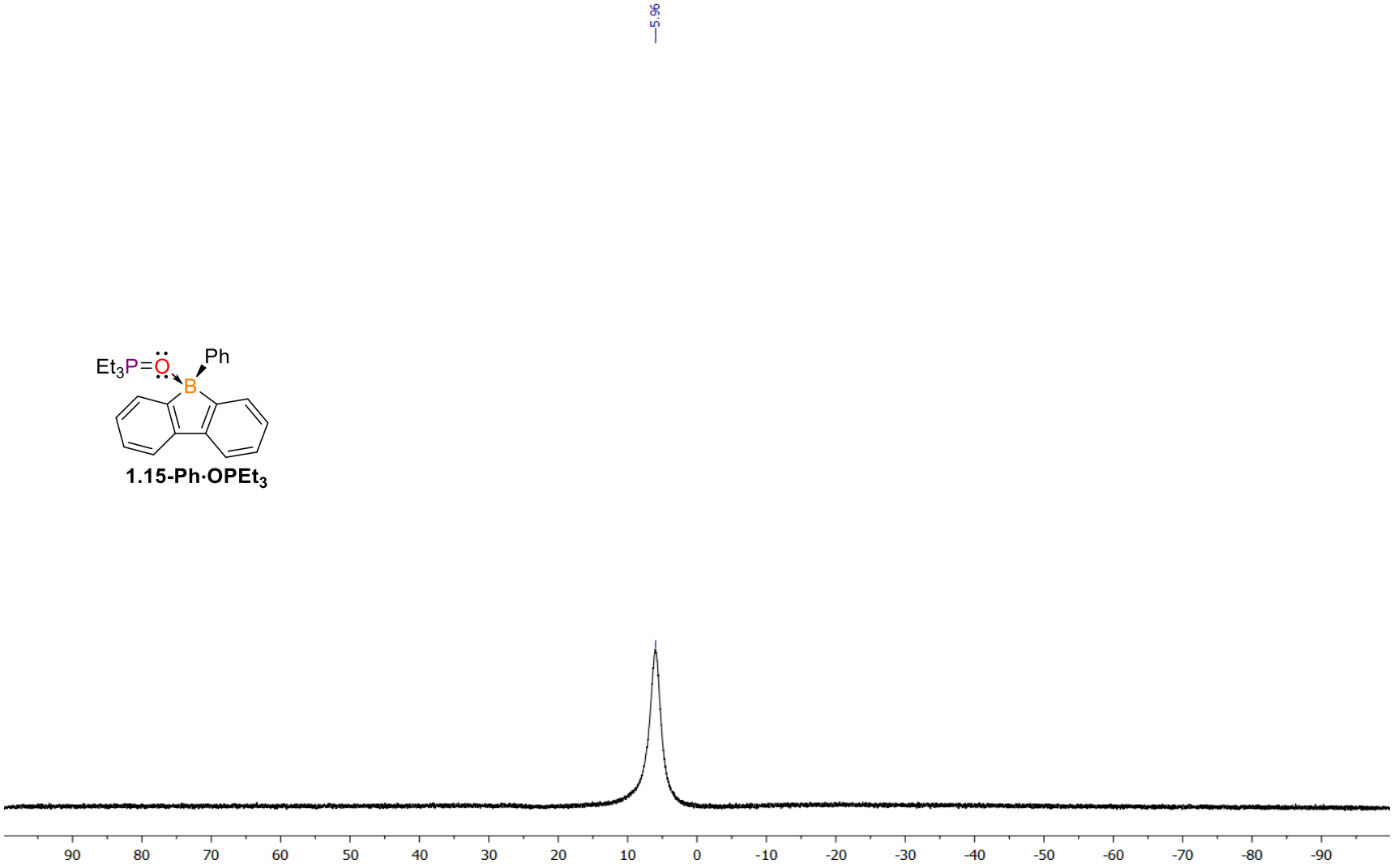

Figure D-39: $^{11}B\{^{1}H\}$ NMR spectrum of **1.15-Ph·OPEt3** in C_6D_6.

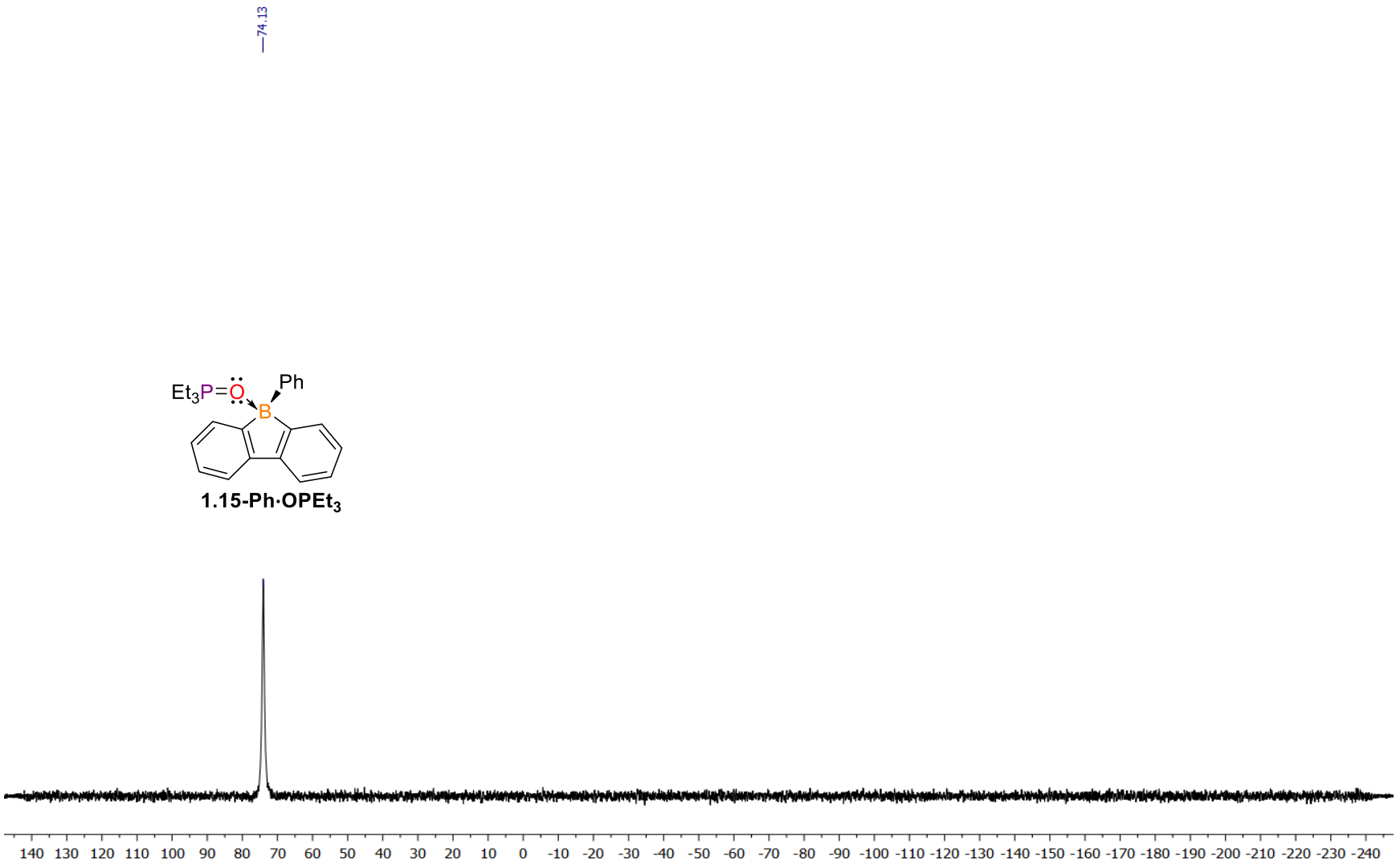

Figure D-40: ^{31}P NMR spectrum of **1.15-Ph·OPEt$_3$** in C_6D_6.

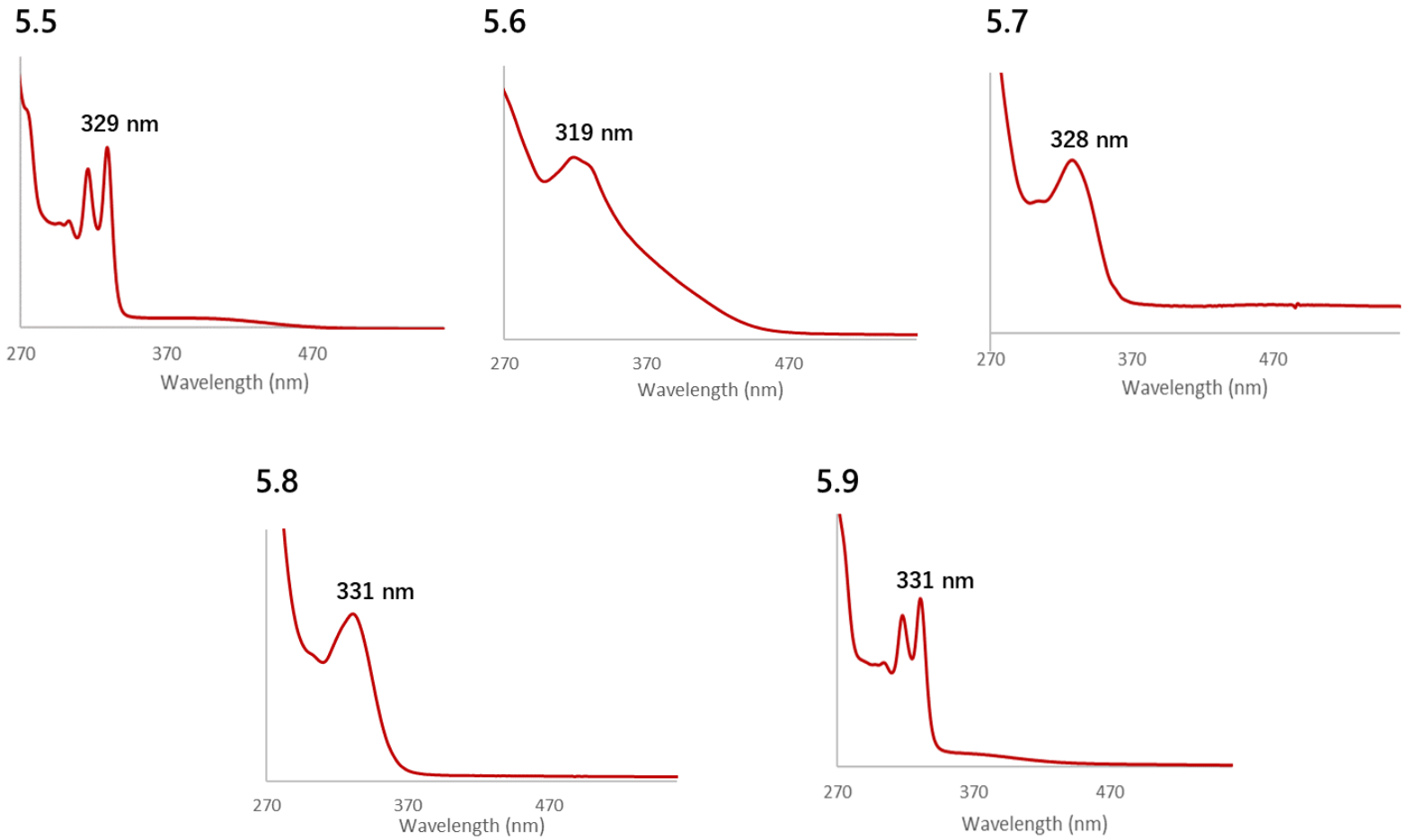

Figure D-41: Normalized absorption spectra of **5.5-5.9** in CH_2Cl_2 under an N_2 atmosphere (spectra have their respective λ_{max} listed above their respective peaks).

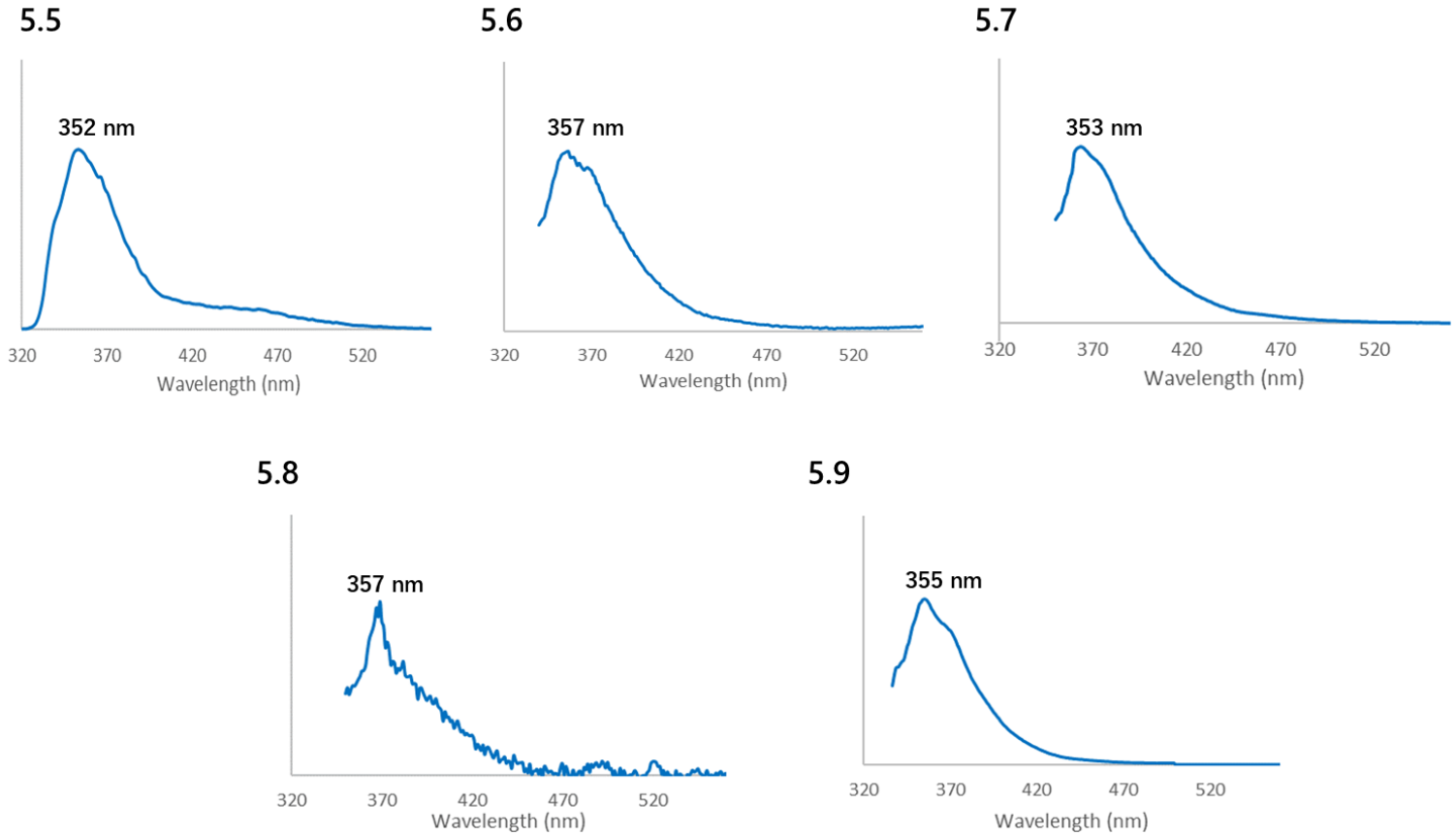

Figure D-42: Normalized emission spectra of **5.5-5.9** in CH_2Cl_2 under an N_2 atmosphere (all emission spectra excited at their respective λ_{max} and correspondingly labeled).

Table D-1: Crystallographic Data for **5.5-5.9**, **1.7-Ph·OPEt$_3$**, and **1.15-Ph·OPEt$_3$**.

Entry	**5.5**	**5.6**	**5.7**	**5.8**	**5.9**	**1.7-Ph·OPEt$_3$**	**1.15-·OPEt$_3$**
CCDC	1819488	1819489	1819490	1819491	1819492	1819493	1819494
Empirical formula	$C_{18}H_{13}BClN$	$C_{24}H_{18}BN_3$	$C_{22}H_{23}BClN$	$C_{28}H_{28}BN$	$C_{24}H_{18}BN$	$C_{40}H_{40}BOP$	$C_{24}H_{28}BOP$
FW (g/mol)	289.55	359.22	347.67	389.32	331.20	578.50	374.24
Crystal system	Monoclinic	Triclinic	Monoclinic	Monoclinic	Tetragonal	Monoclinic	Monoclinic
Space group	*P2$_1$/n*	*P-1*	*P2$_1$/c*	*P2$_1$/c*	*I4$_1$/a*	*P2$_1$/n*	*Pn*
a (Å)	11.4311(11)	8.3238(12)	13.679(15)	15.8892(14)	26.7935(17)	9.0948(3)	9.8145(9)
b (Å)	7.5161(6)	9.5871(14)	12.5898(13)	12.4193(10)	26.7935(17)	36.1717(13)	15.5763(15)
c (Å)	17.3831(16)	11.8893(15)	10.2613(10)	11.0719(9)	9.9207(13)	10.2433(4)	13.7943(13)
α (deg)	90	83.315(4)	90	90	90	90	90
β (deg)	101.691(3)	81.252(4)	97.732(3)	104.771(3)	90	110.991(2)	90.023(3)
γ (deg)	90	76.743(5)	90	90	90	90	90
V (Å^3)	1462.5(2)	909.5(2)	1751.1(3)	2112.6(3)	7122.0(13)	3146.2(2)	2108.8(3)
Z	4	2	4	4	16	4	4
D_c (mg m^{-3})	1.315	1.312	1.319	1.224	1.236	1.221	1.179
radiation, λ (Å)	0.71073	0.71073	0.71073	0.71073	0.71073	0.71073	0.71073
temp (K)	150(2)	150(2)	150(2)	150(2)	150(2)	150(2)	150(2)
$R1[I>2\sigma I]^a$	0.0481	0.0640	0.0433	0.0499	0.0928	0.0445	0.0492
$wR2(F^2)^a$	0.1053	0.1861	0.1221	0.1109	0.2264	0.1197	0.1104
GOF (S)^a	1.046	1.153	1.147	1.042	1.221	1.110	1.025

[a] $R1(F[\mathrm{I} > 2(\mathrm{I})]) = \sum\|\|F_o| - |F_c\|\|/ \sum |F_o|$; $wR2(F^2$ [all data]$) = [w(F_o^2 - F_c^2)^2]^{1/2}$; S(all data$) = [w(F_o^2 - F_c^2)^2/(n - p)]^{1/2}$ (n = no. of data; p = no. of parameters varied; $w = 1/[^2(F_o^2) + (aP)^2 + bP]$ where $P = (F_o^2 + 2F_c^2)/3$ and a and b are constants suggested by the refinement program.

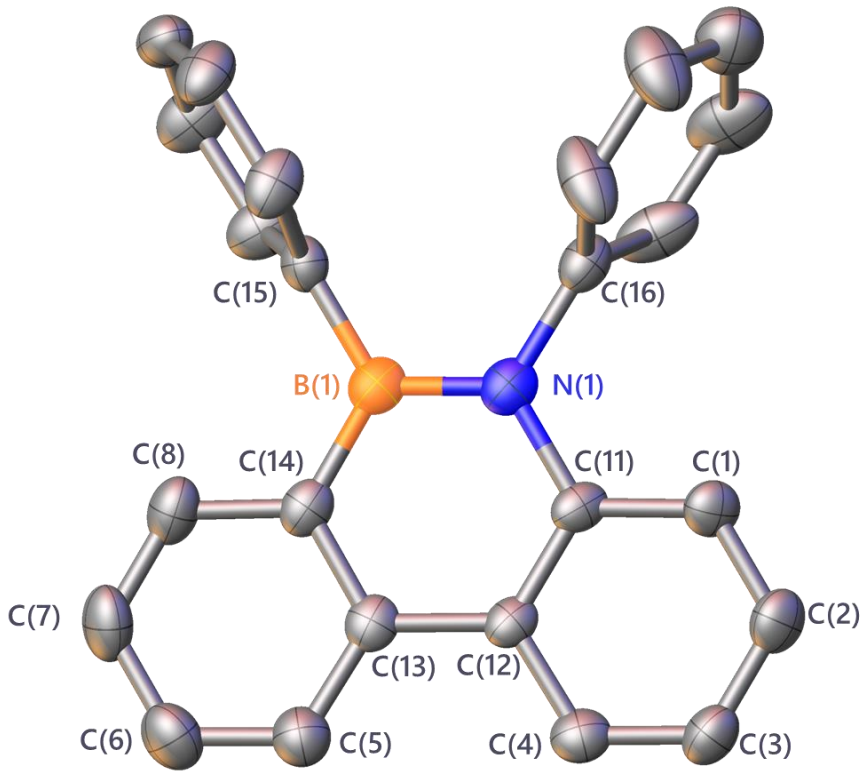

Figure D-43: Solid-state structure of **5.9**. Thermal ellipsoids are drawn at the 50% probability level and hydrogen atoms have been omitted for clarity.

Note: Similar boron heterocycles bearing phenyl groups on boron and nitrogen atoms within the ring have shown disorder. Therefore, the bond distances and bond angles are not discussed in detail. However, the structure confirms the identity of **5.9**. The disorder was modeled using EADP on both boron and nitrogen atoms.

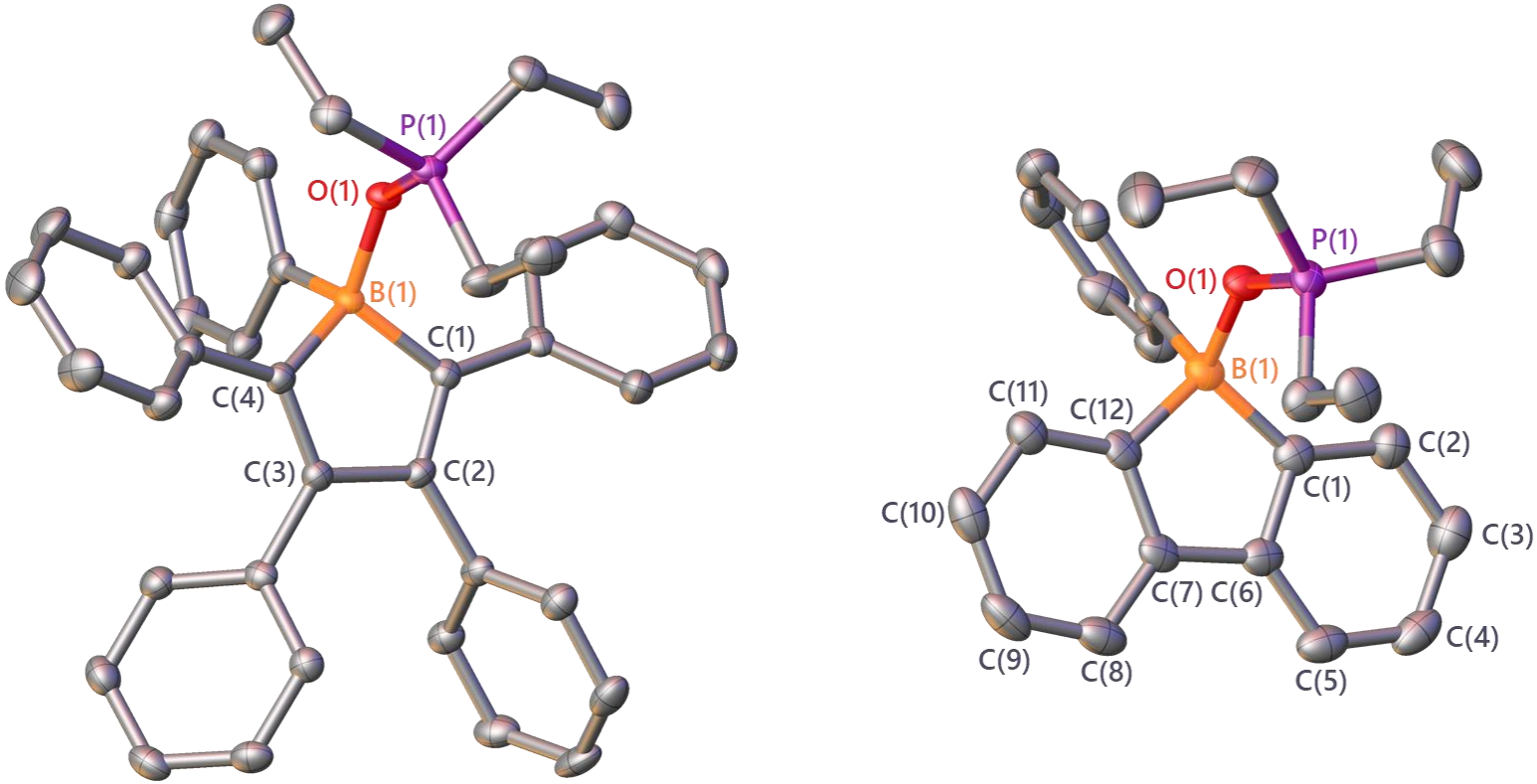

Figure D-44: Solid-state structures of **1.7-Ph·OPEt$_3$** and **1.15-Ph·OPEt$_3$**. Thermal ellipsoids are drawn at the 50% probability level and hydrogen atoms have been omitted for clarity.

APPENDIX E

Supplementary Information for Chapter Six

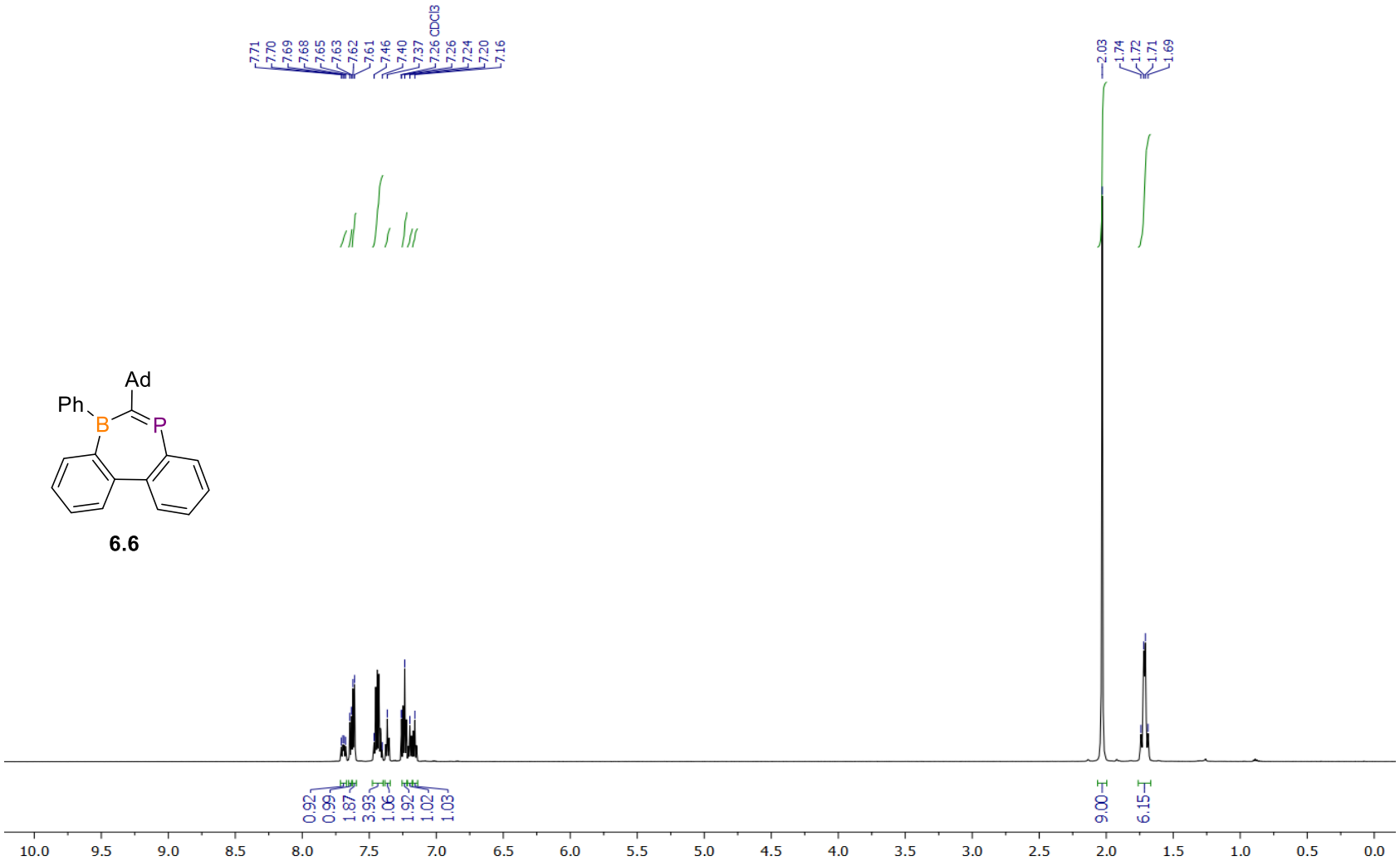

Figure E-1: ^{1}H NMR spectrum of **6.6** in $CDCl_3$.

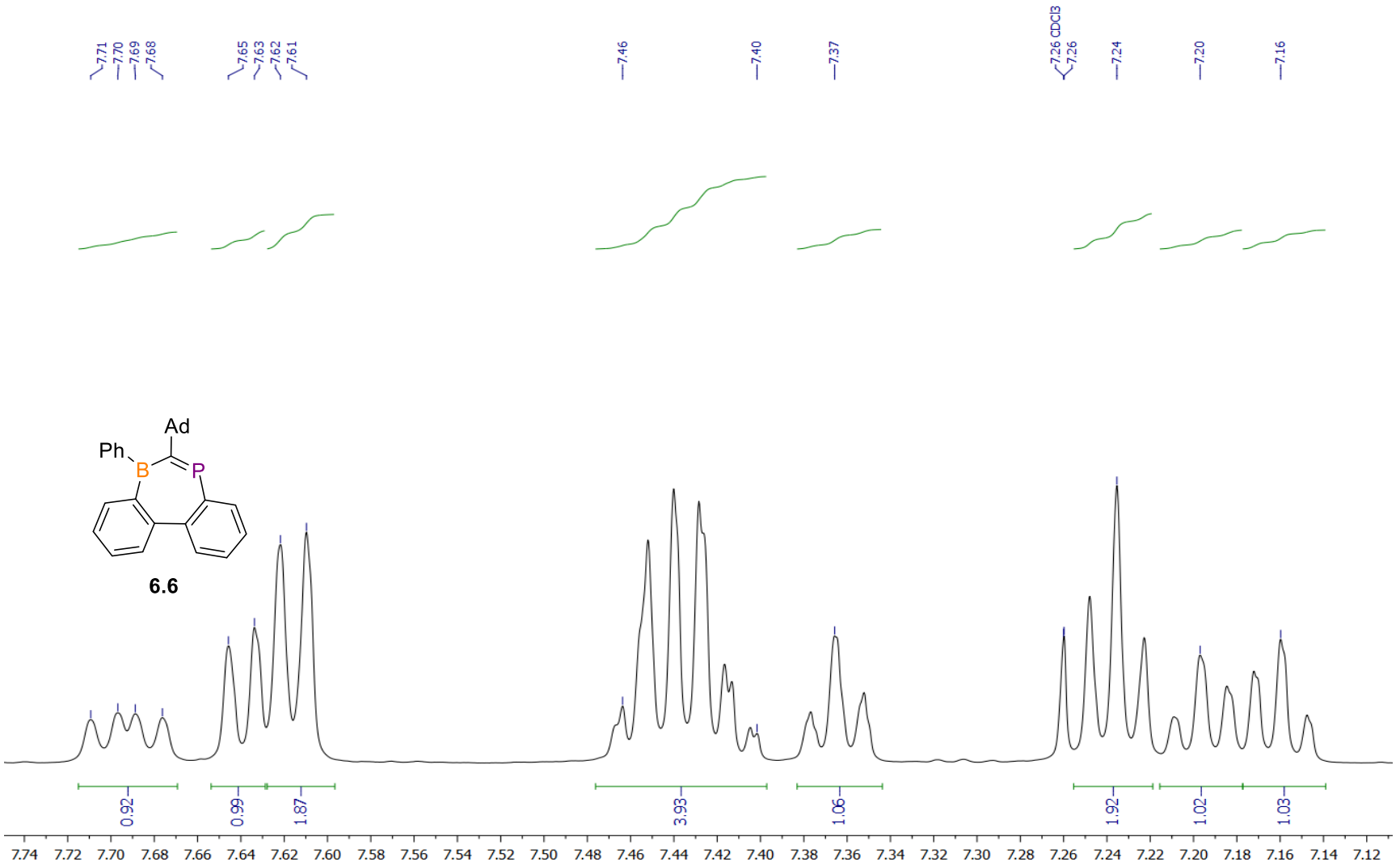

Figure E-2: Expansion of ^{1}H NMR spectrum of **6.6** in $CDCl_3$.

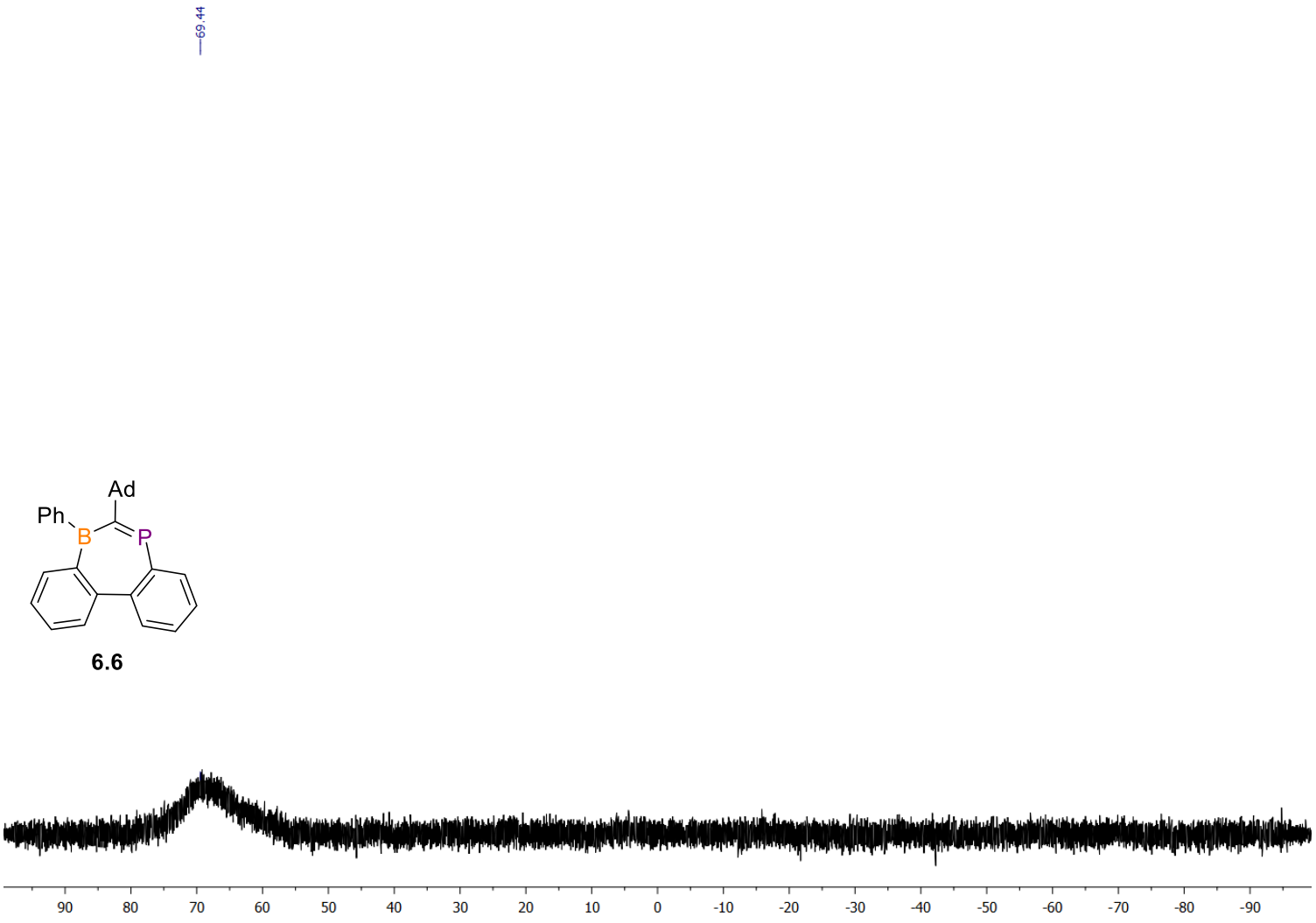

Figure E-3: $^{11}B\{^{1}H\}$ NMR spectrum of **6.6** in $CDCl_3$.

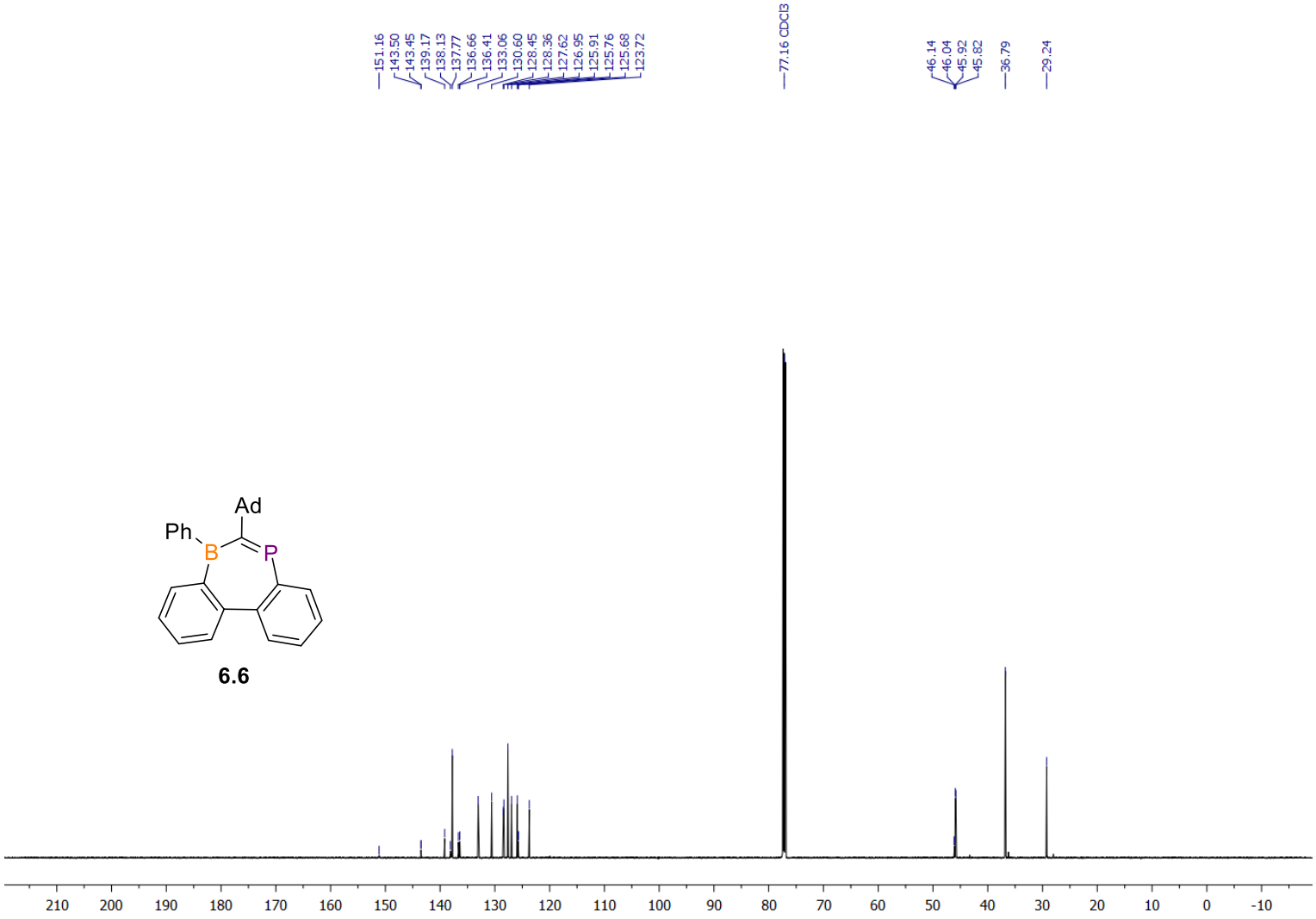

Figure E-4: $^{13}C\{^{1}H\}$ NMR spectrum of **6.6** in $CDCl_3$.

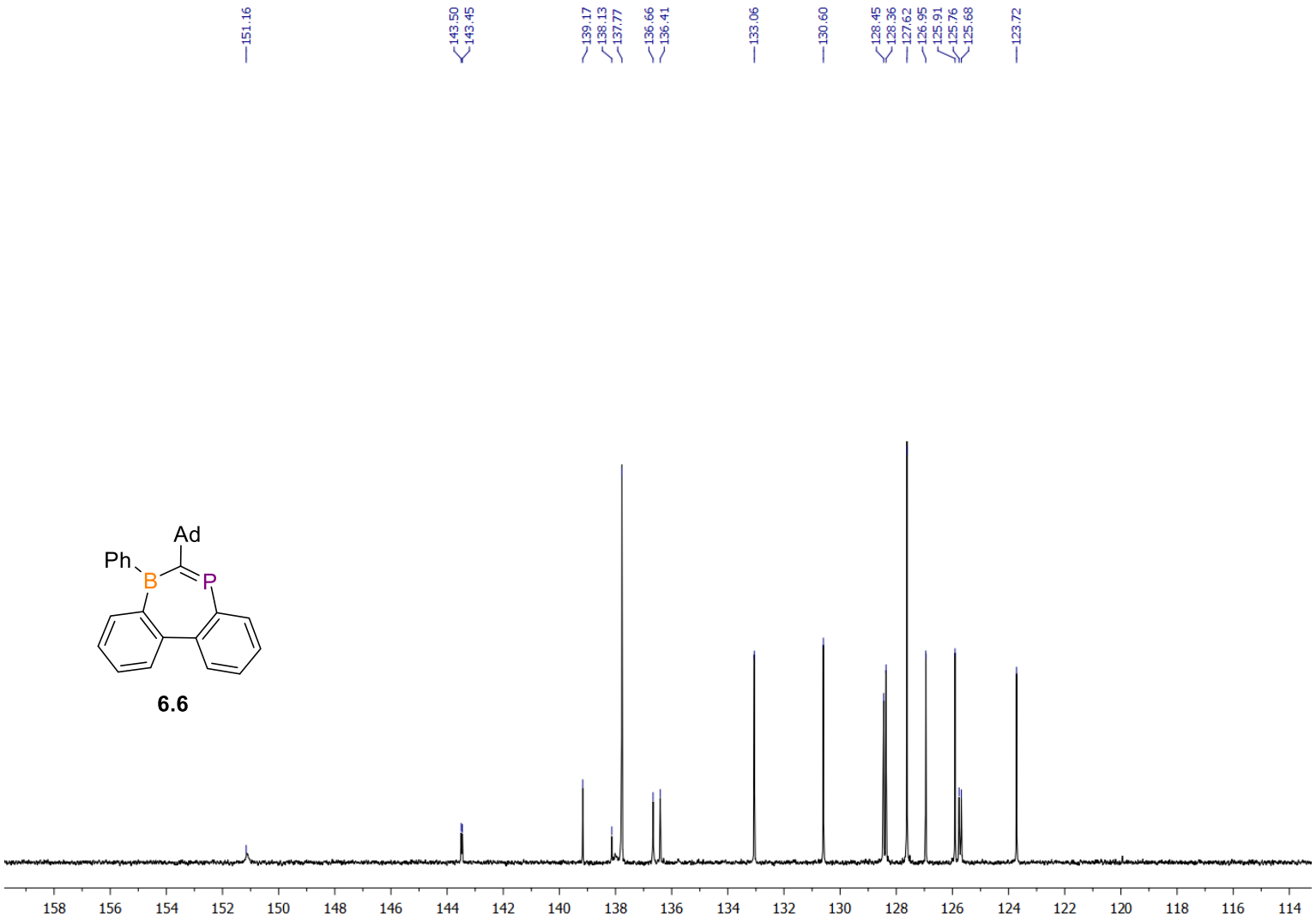

Figure E-5: Expansion of $^{13}C\{^{1}H\}$ NMR spectrum of **6.6** in $CDCl_3$ (aryl region).

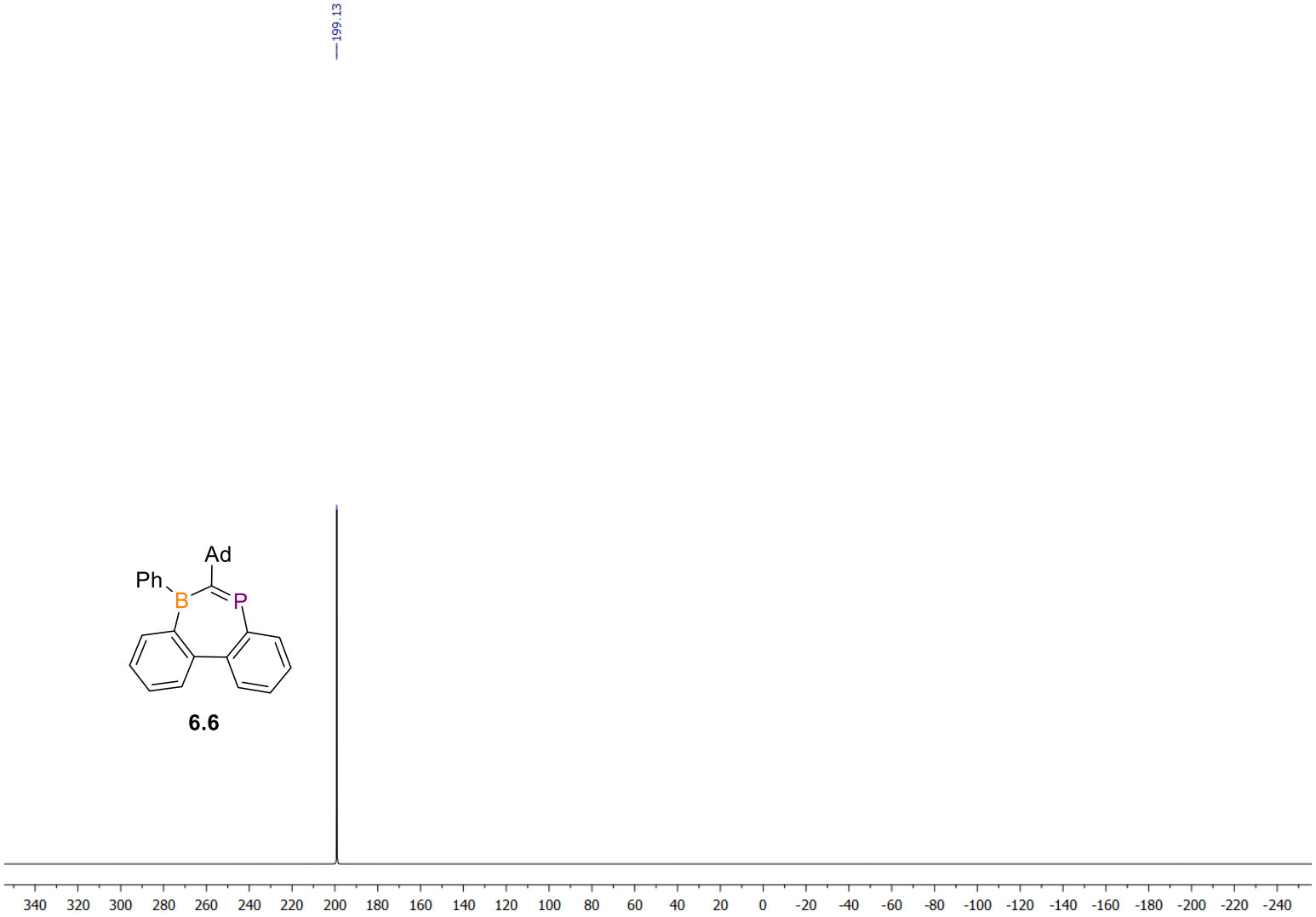

Figure E-6: ^{31}P NMR spectrum of **6.6** in $CDCl_3$.

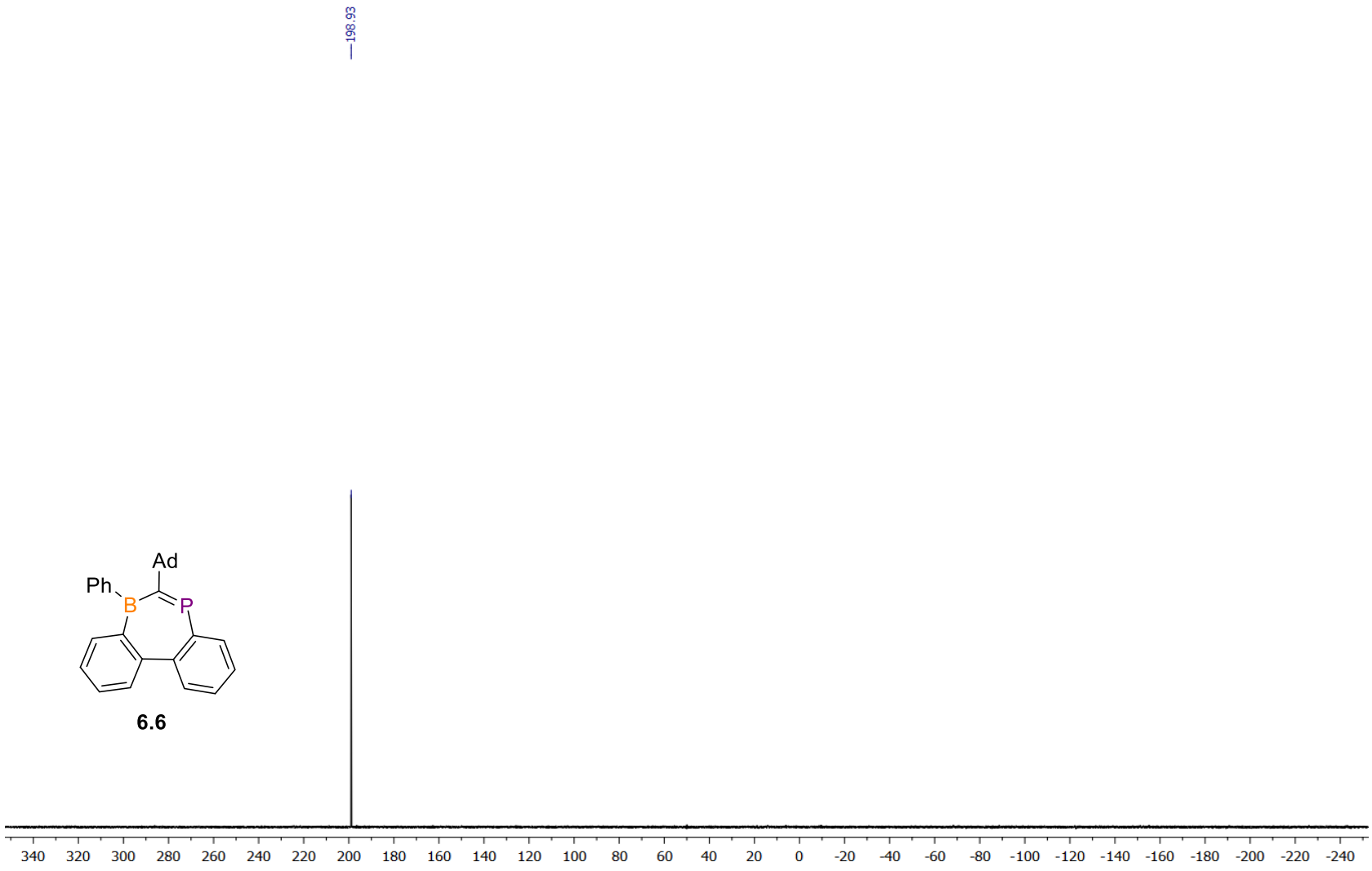

Figure E-7: $^{31}P\{^{1}H\}$ NMR spectrum of **6.6** in $CDCl_3$.

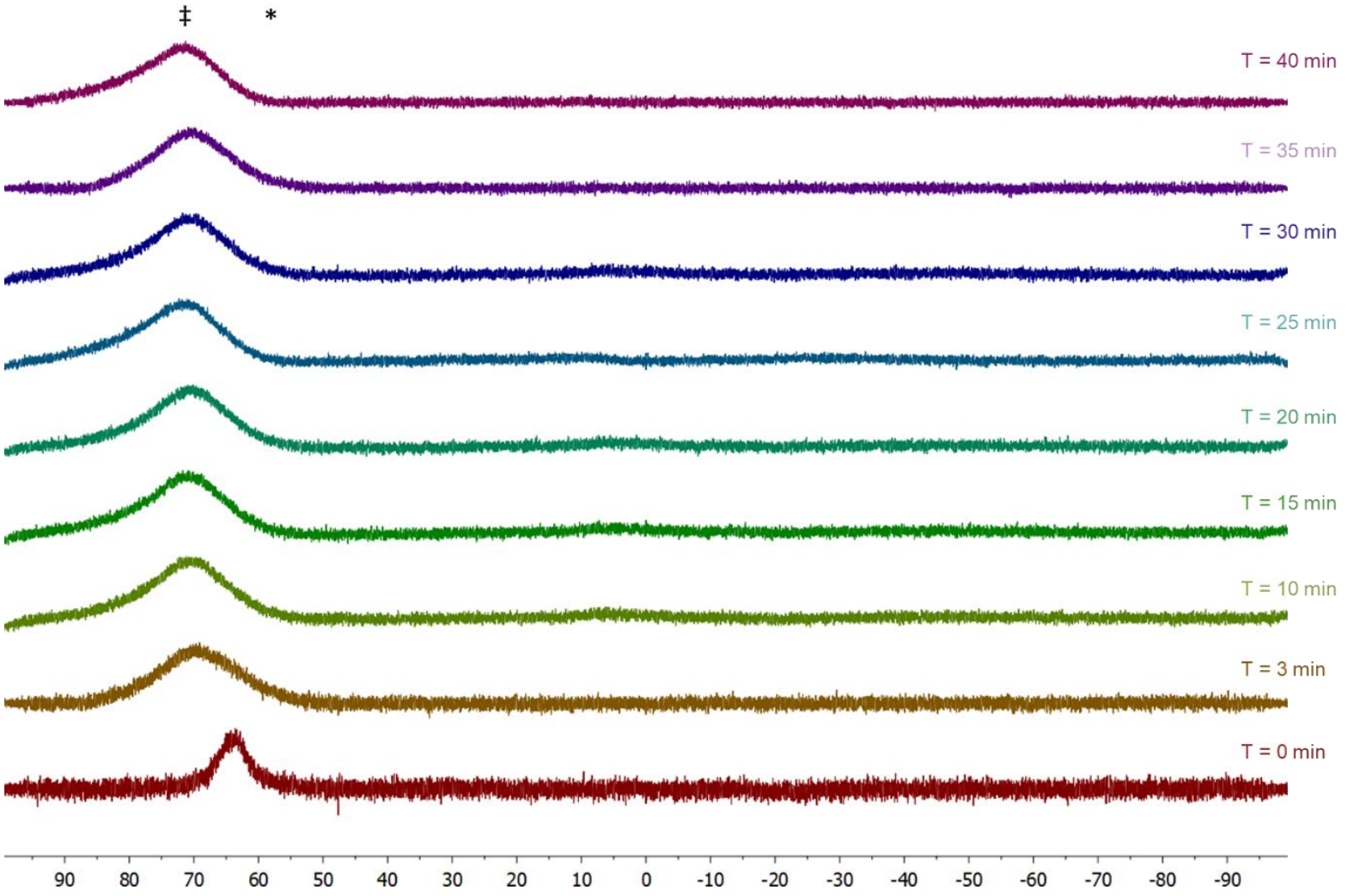

Figure E-8: $^{11}B\{^{1}H\}$ NMR stacked plot of in situ reaction of **6.6** with 1-adamantylphoshaalkyne (‡ = **6.6**, * = **1.15-Ph**).

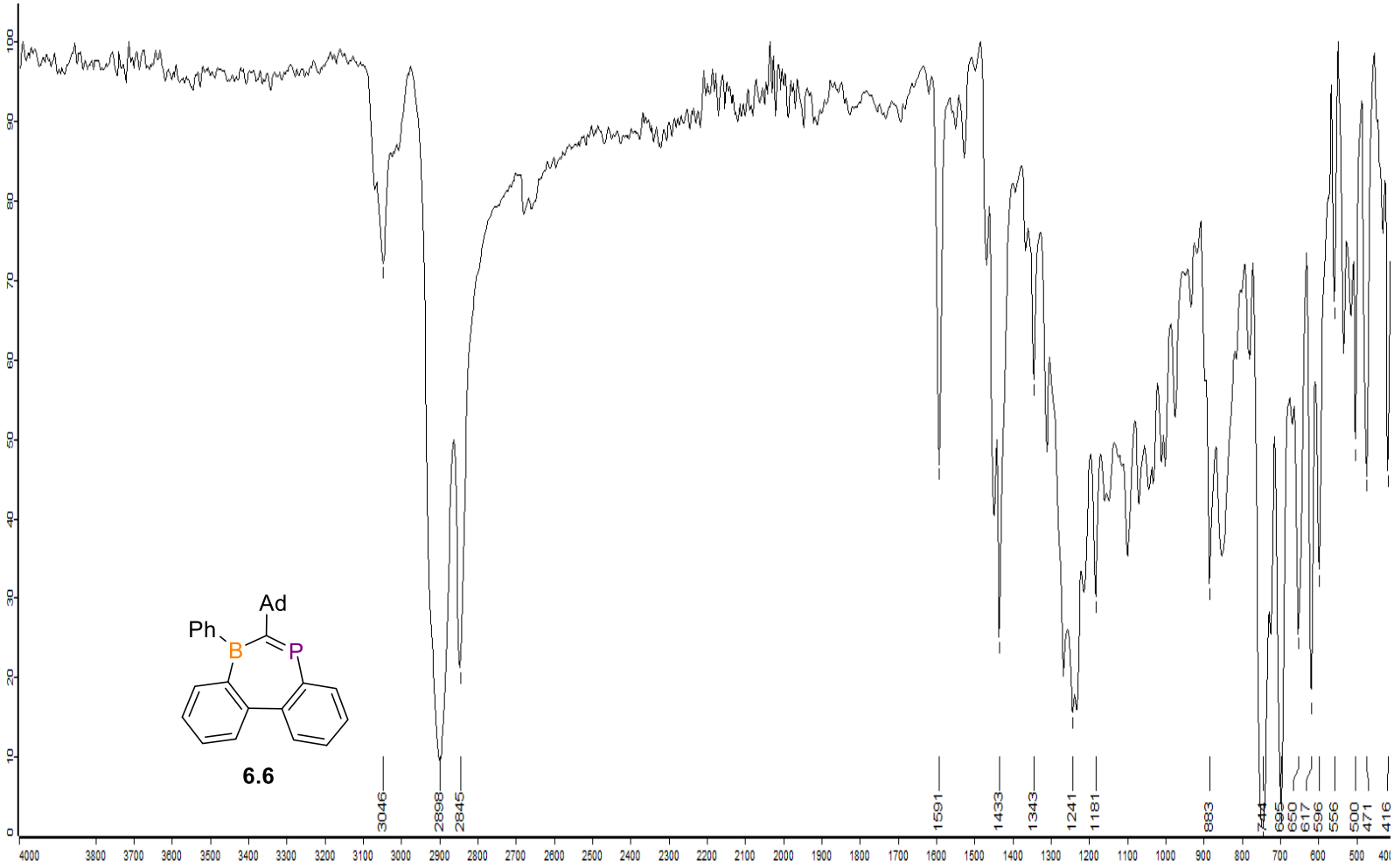

Figure E-9: FT-IR spectrum of **6.6**.

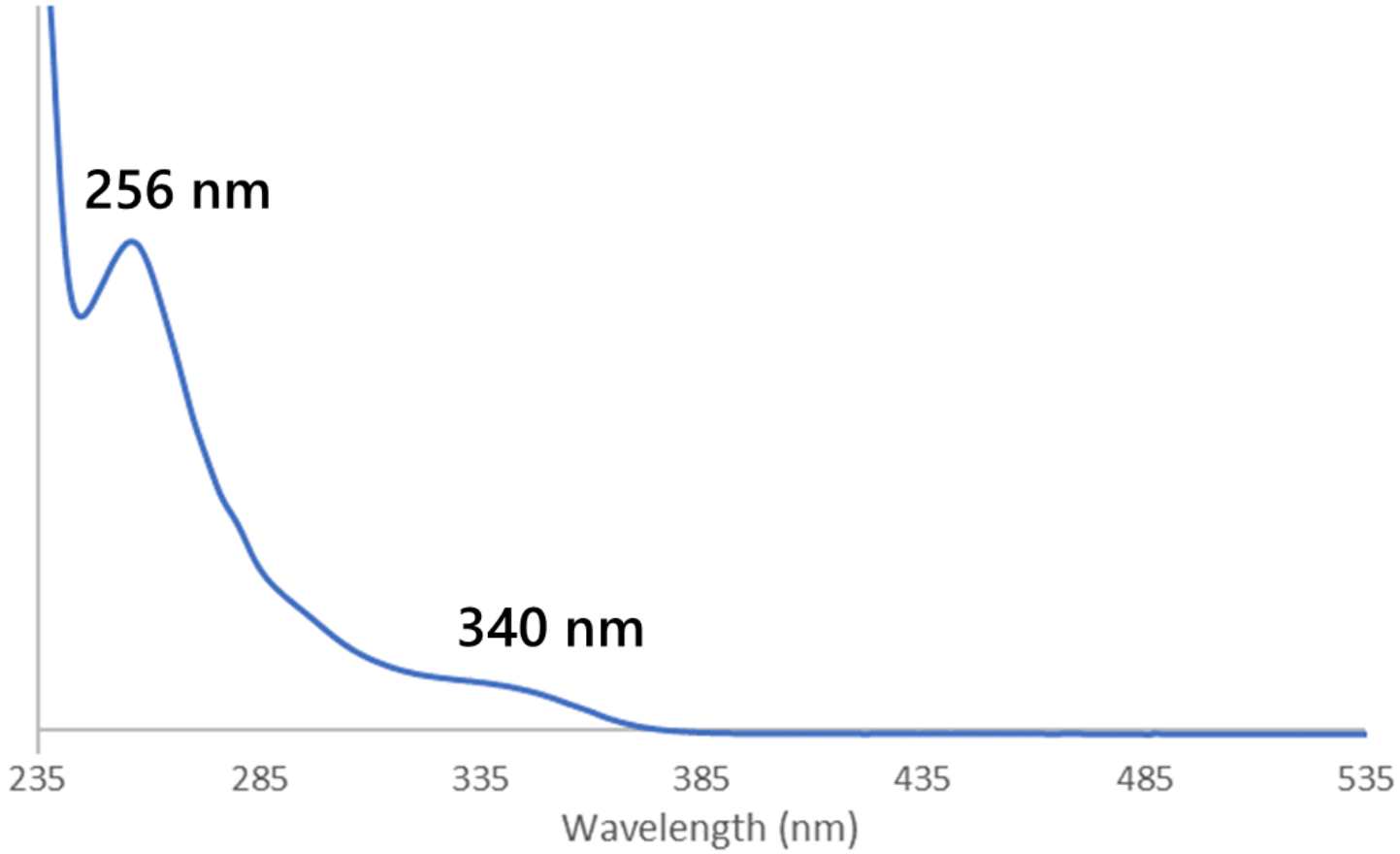

Figure E-10: Normalized absorption spectrum of **6.6** in CH_2Cl_2 under an N_2 atmosphere (spectrum has the respective λ_{max} listed above the respective peaks).

Table E-1: Crystallographic Data for **6.6**.

Entry	**6.6**
CCDC	1837570
Empirical formula	$C_{29}H_{28}BP$
FW (g/mol)	418.29
Crystal system	Triclinic
Space group	*P-1*
a (Å)	8.8815(7)
b (Å)	11.795(1)
c (Å)	12.1256(10)
α (deg)	113.894(2)
β (deg)	98.665(2)
γ (deg)	93.102(2)
V (Å^3)	1138.77(16)
Z	2
D_c (Mg m^{-3})	1.220
$2\theta_{max}$	27.916
μ	0.135
No. reflections	33232
No. independent reflections	5456
radiation, λ (Å)	0.71073
temp (K)	150(2)
$R1[I>2\sigma I]^a$	0.0373
$wR2(F^2)^a$	0.0995
GOF (S)^a	1.034

^{a} $R1(F[\mathrm{I} > 2(\mathrm{I})]) = \sum\|\|F_o| - |F_c\|\|/ \sum |F_o|$; $wR2(F^2$ [all data]$) = [w(F_o^2 - F_c^2)^2]^{1/2}$; S(all data) $= [w(F_o^2 - F_c^2)^2/(n - p)]^{1/2}$ (n = no. of data; p = no. of parameters varied; $w = 1/[^2(F_o^2) + (aP)^2 + bP]$ where $P = (F_o^2 + 2F_c^2)/3$ and a and b are constants suggested by the refinement program.

Table E-2: Calculated Frontier Molecular Orbitals for Reactants, Intermediates and Products (B3LYP/def2-TZVP).

Frontier Molecular Orbitals	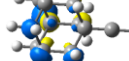	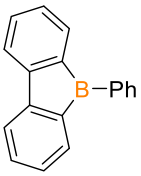	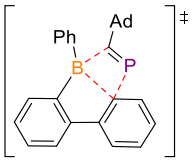 $TS_{4.1}$	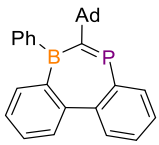 **6.6**
LUMO+3		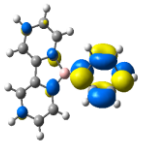	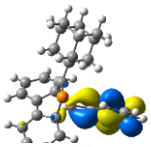	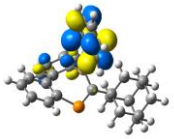
LUMO+2		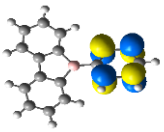		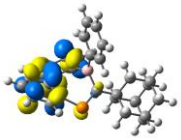
LUMO+1	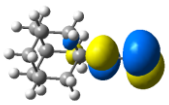	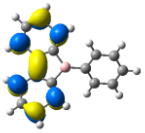	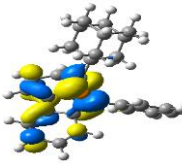	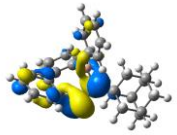
LUMO	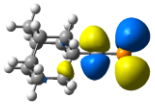	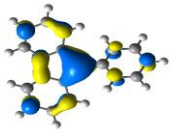	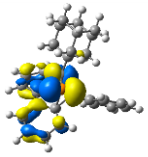	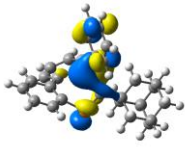
HOMO	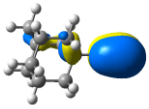	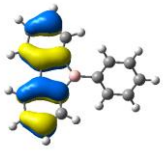	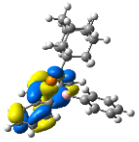	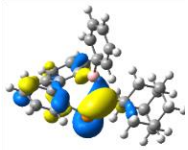
HOMO-1	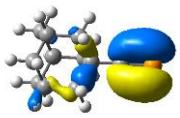	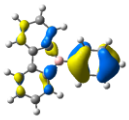	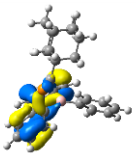	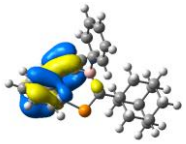
HOMO-2	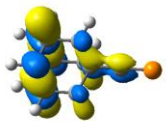	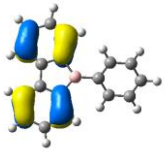	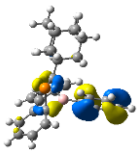	
HOMO-3	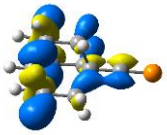	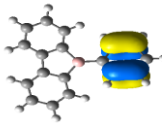	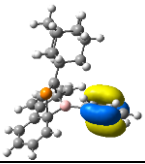	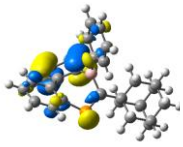

Table E-3: HOMO and LUMO Energies Gaps for Reactants and Products (B3LYP/def2-TZVP (dichloromethane solvent, SMD, units of eV).

Molecules	HOMO	LUMO	HOMO/LUMO gap
1-adamantylphosphaalkyne	-7.05	-1.09	5.96
9-phenyl-9-borafluorene (**1**)	-6.09	-2.46	3.63
TS1	-5.92	-1.71	4.21
Product (**2**)	-6.07	-1.82	4.25

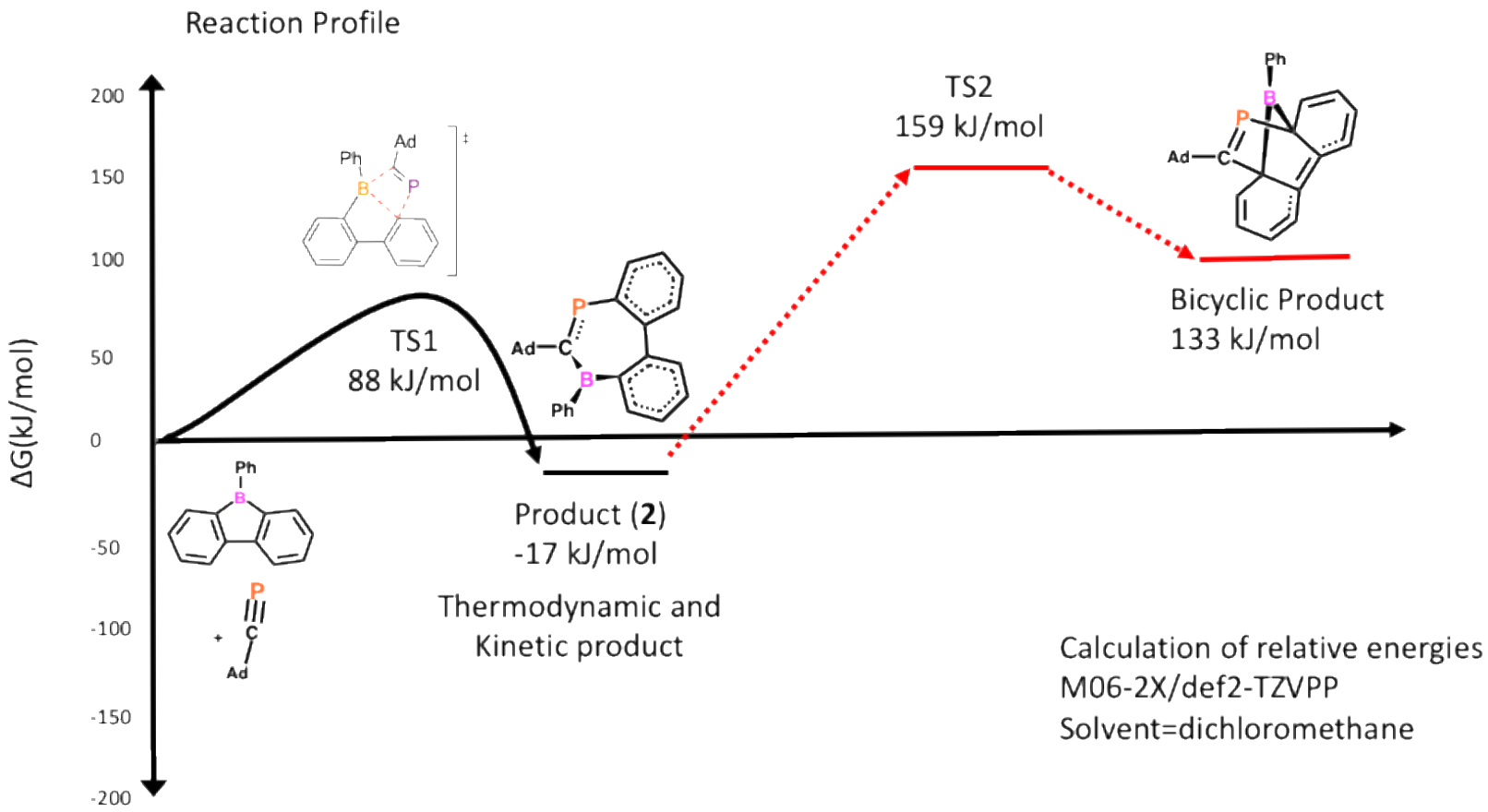

Scheme E-1: Mechanism of reaction of **1.15-Ph** with 1-adamantylphosphaalkyne.

Note: We attempted to model a significant number of configurations, however no adduct (phosphorus of the phosphaalkyne bound directly to the boron center of **1.15-Ph**) was able to be located. The pathway through TS1 is the most feasible computed pathway.

APPENDIX F

Supplementary Information for Chapter Seven

Table F-1: Attempted transmetallation reaction of **Me_2Sn(7.2)** with boranes.

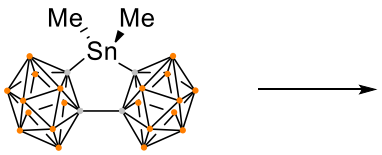

Me_2Sn[7.2]

● = BH ● = C

$RBCl_2$	Solvent	Temp	Time	Result
Ph	CH_2Cl_2, PhMe	23 °C	72 h	NR
Ph	PhMe	100 °C	72 h	NR
p-Tolyl	CH_2Cl_2, PhMe	23 °C	72 h	NR
p-Tolyl	PhMe	100 °C	72 h	NR
Mes	CH_2Cl_2, PhMe	23 °C	72 h	NR
Mes	PhMe	100 °C	72 h	NR
$^{i}Pr_2N$	CH_2Cl_2, PhMe	23 °C	72 h	NR
$^{i}Pr_2N$	PhMe	100 °C	72 h	NR
NPh_3	CH_2Cl_2, PhMe	23 °C	72 h	NR
NPh_3	PhMe	100 °C	72 h	NR
Trip	CH_2Cl_2, PhMe	23 °C	72 h	NR
Trip	PhMe	100 °C	72 h	NR

BR_3	Solvent	Temp	Time	Result
Cl	CH_2Cl_2, PhMe	23 °C	72 h	NR
Cl	PhMe	100 °C	72 h	NR
Br	CH_2Cl_2, PhMe	23 °C	72 h	NR
Br	PhMe	100 °C	72 h	NR
I	CH_2Cl_2, PhMe	23 °C	72 h	NR
I	PhMe	100 °C	72 h	NR

Table F-2: Attempted transmetallation reaction of **Li_2(7.2)** with boranes.

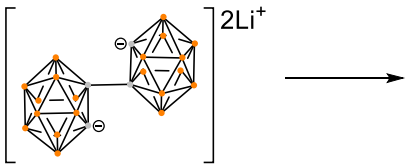

Li_2[7.2]

● = BH ● = C

$RBCl_2$	Solvent	Temp	Time	Result
Ph	THF, PhMe	23 °C	48 h	Decomp
Ph	PhMe	100 °C	72 h	NR
Ph	THF	-78 °C	72 h	Decomp
p-Tolyl	THF, PhMe	23 °C	48 h	NR
p-Tolyl	PhMe	100 °C	72 h	NR
p-Tolyl	THF	-78 °C	72 h	Decomp
Mes	THF, PhMe	23 °C	48 h	NR
Mes	PhMe	100 °C	72 h	Decomp
Mes	THF	-78 °C	72 h	Decomp
$^{i}Pr_2N$	THF, PhMe	23 °C	48 h	NR
$^{i}Pr_2N$	PhMe	100 °C	72 h	Decomp
$^{i}Pr_2N$	THF	-78 °C	72 h	NR
NPh_3	THF, PhMe	23 °C	48 h	NR
NPh_3	PhMe	100 °C	72 h	Decomp
NPh_3	THF	-78 °C	72 h	NR
Trip	THF, PhMe	23 °C	48 h	NR
Trip	PhMe	100 °C	72 h	Decomp
Trip	THF	-78 °C	72 h	NR

BR_3	Solvent	Temp	Time	Result
Cl	THF, PhMe	23 °C	48 h	NR
Cl	PhMe	100 °C	72 h	Decomp
Cl	THF	-78 °C	72 h	NR
Br	THF, PhMe	23 °C	48 h	NR
Br	PhMe	100 °C	72 h	Decomp
Br	THF	-78 °C	72 h	NR
I	THF, PhMe	23 °C	48 h	NR
I	PhMe	100 °C	72 h	Decomp
I	THF	-78 °C	72 h	NR
F	THF, PhMe	23 °C	48 h	NR
F	PhMe	100 °C	72 h	Multiple products
F	THF	-78 °C	72 h	NR

Decomposition was identified as the **nido-B compound.*

Table F-3: Attempted transmetallation reaction of **DME_2Mg(7.2)** with boranes.

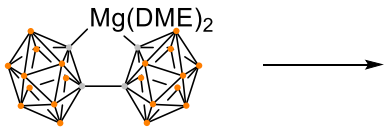

$(DME)_2Mg$[7.2]

● = BH ● = C

$RBCl_2$	Solvent	Temp	Time	Result
Ph	CH_2Cl_2, PhMe	23 °C	72 h	NR
Ph	PhMe	100 °C	72 h	NR
p-Tolyl	CH_2Cl_2, PhMe	23 °C	72 h	NR
p-Tolyl	PhMe	100 °C	72 h	NR
Mes	CH_2Cl_2, PhMe	23 °C	72 h	NR
Mes	PhMe	100 °C	72 h	NR
$^{i}Pr_2N$	CH_2Cl_2, PhMe	23 °C	72 h	NR
$^{i}Pr_2N$	PhMe	100 °C	72 h	NR
NPh_3	CH_2Cl_2, PhMe	23 °C	72 h	NR
NPh_3	PhMe	100 °C	72 h	NR
Trip	CH_2Cl_2, PhMe	23 °C	72 h	NR
Trip	PhMe	100 °C	72 h	NR

BR_3	Solvent	Temp	Time	Result
Cl	CH_2Cl_2, PhMe	23 °C	72 h	NR
Cl	PhMe	100 °C	72 h	NR
Br	CH_2Cl_2, PhMe	23 °C	72 h	NR
Br	PhMe	100 °C	72 h	NR
I	CH_2Cl_2, PhMe	23 °C	72 h	NR
I	PhMe	100 °C	72 h	NR

Table F-4: Attempted transmetallation reaction of **K_2(7.2)** with boranes.

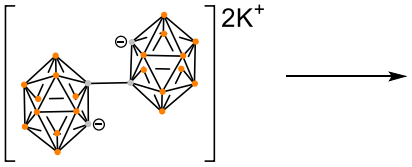

$RBCl_2$	Solvent	Temp	Time	Result
Ph	THF, PhMe	23 °C	48 h	Decomp
Ph	PhMe	100 °C	72 h	NR
Ph	THF	-78 °C	72 h	Decomp
p-Tolyl	THF, PhMe	23 °C	48 h	NR
p-Tolyl	PhMe	100 °C	72 h	NR
p-Tolyl	THF	-78 °C	72 h	Decomp
Mes	THF, PhMe	23 °C	48 h	NR
Mes	PhMe	100 °C	72 h	Decomp
Mes	THF	-78 °C	72 h	Decomp
$^{i}Pr_2N$	THF, PhMe	23 °C	48 h	**$^{11}B\{^{1}H\}$ 32.9 ppm**
$^{i}Pr_2N$	PhMe	100 °C	72 h	NR
$^{i}Pr_2N$	THF	-78 °C	72 h	**$^{11}B\{^{1}H\}$ 32.9 ppm**
NPh_3	THF, PhMe	23 °C	48 h	NR
NPh_3	PhMe	100 °C	72 h	Decomp
NPh_3	THF	-78 °C	72 h	NR
Trip	THF, PhMe	23 °C	48 h	NR
Trip	PhMe	100 °C	72 h	Decomp
Trip	THF	-78 °C	72 h	NR

BR_3	Solvent	Temp	Time	Result
Cl	THF, PhMe	23 °C	48 h	NR
Cl	PhMe	100 °C	72 h	Decomp
Cl	THF	-78 °C	72 h	NR
Br	THF, PhMe	23 °C	48 h	NR
Br	PhMe	100 °C	72 h	Decomp
Br	THF	-78 °C	72 h	NR
I	THF, PhMe	23 °C	48 h	NR
I	PhMe	100 °C	72 h	Decomp
I	THF	-78 °C	72 h	NR
F	THF, PhMe	23 °C	48 h	NR
F	PhMe	100 °C	72 h	Multiple products
F	THF	-78 °C	72 h	NR

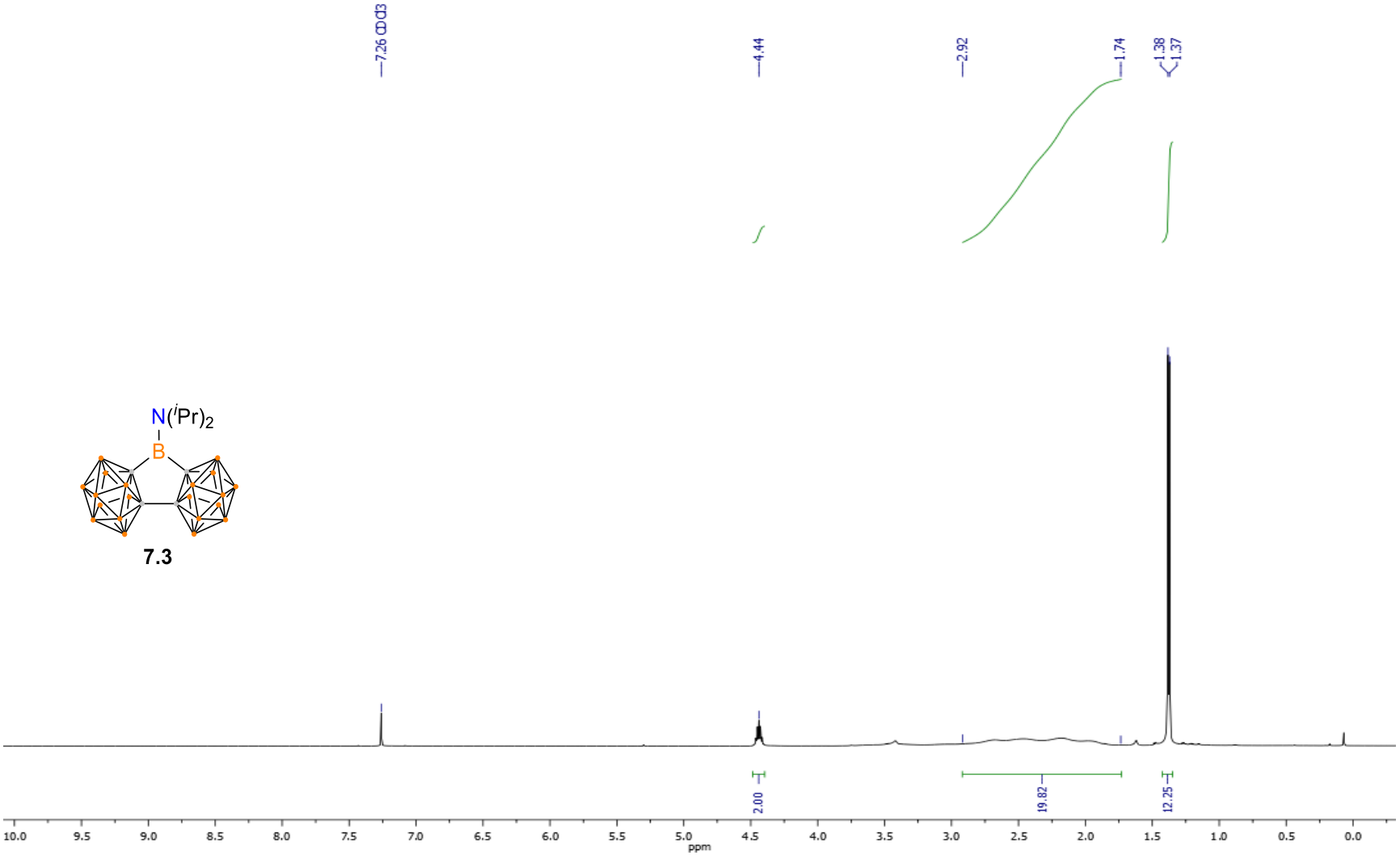

Figure F-1: ^{1}H NMR spectrum of **7.3** in $CDCl_3$.

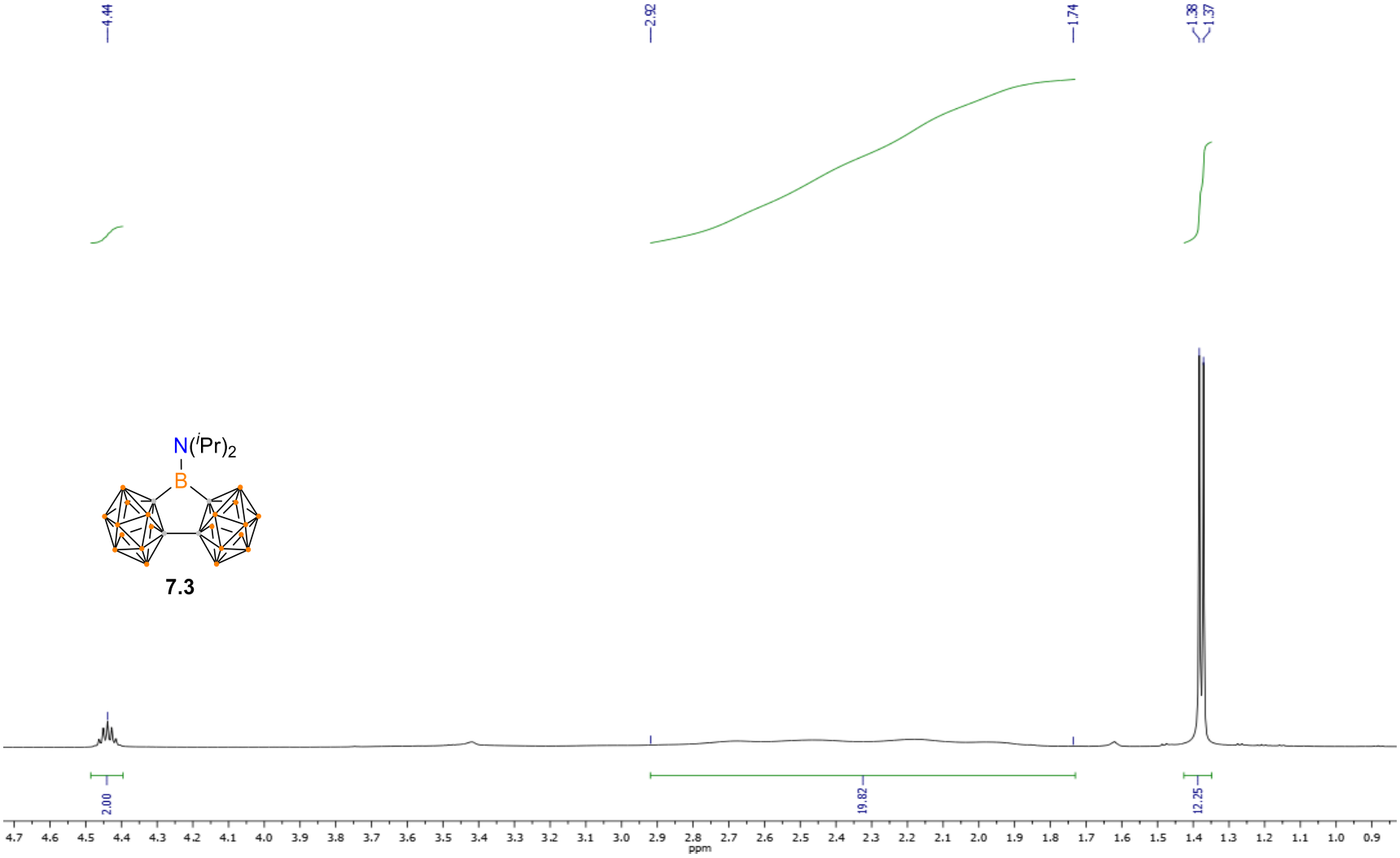

Figure F-2: Expansion of the ^{1}H NMR spectrum of **7.3** in $CDCl_3$.

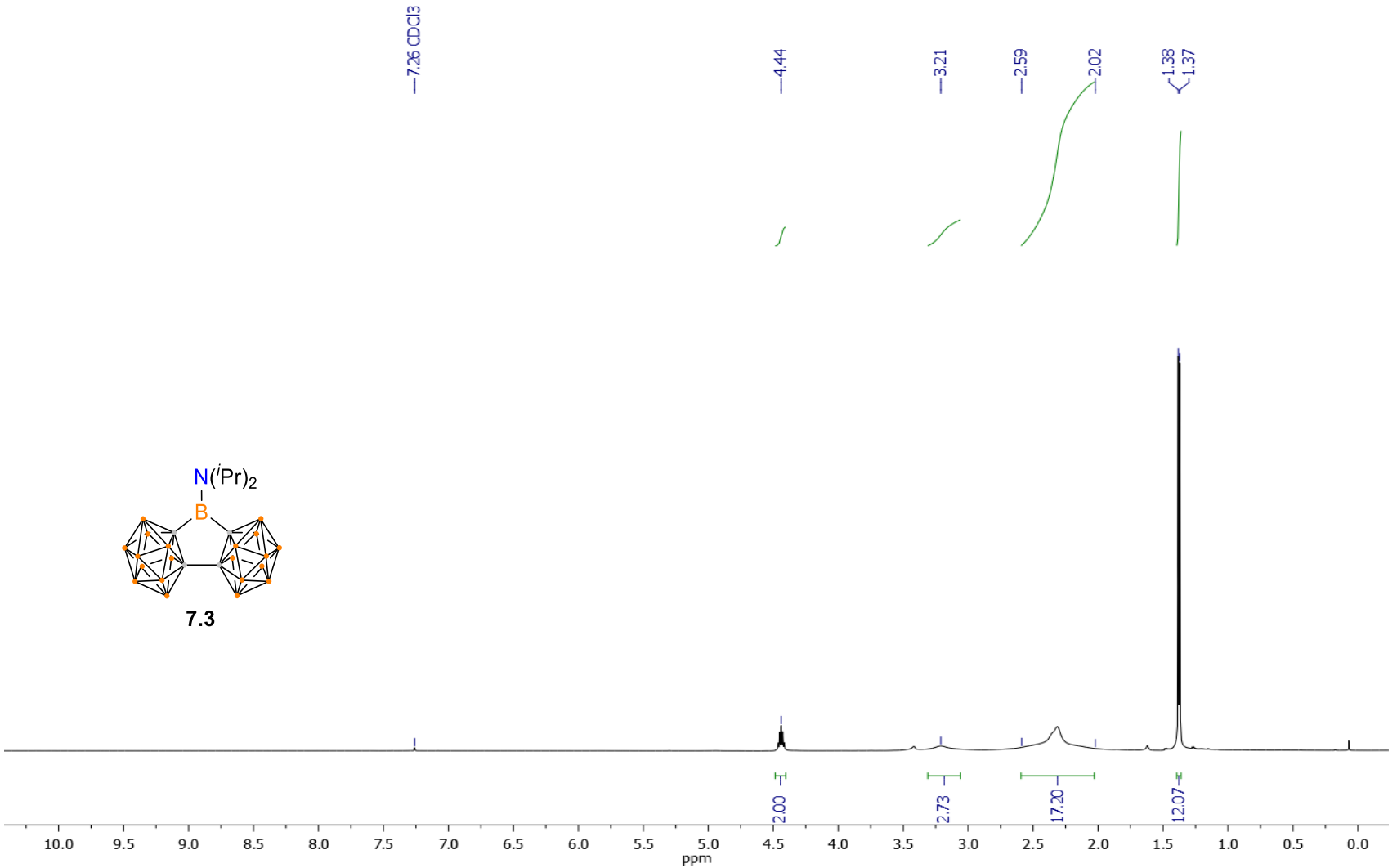

Figure F-3: $^{1}H\{^{11}B\}$ NMR spectrum of **7.3** in $CDCl_3$.

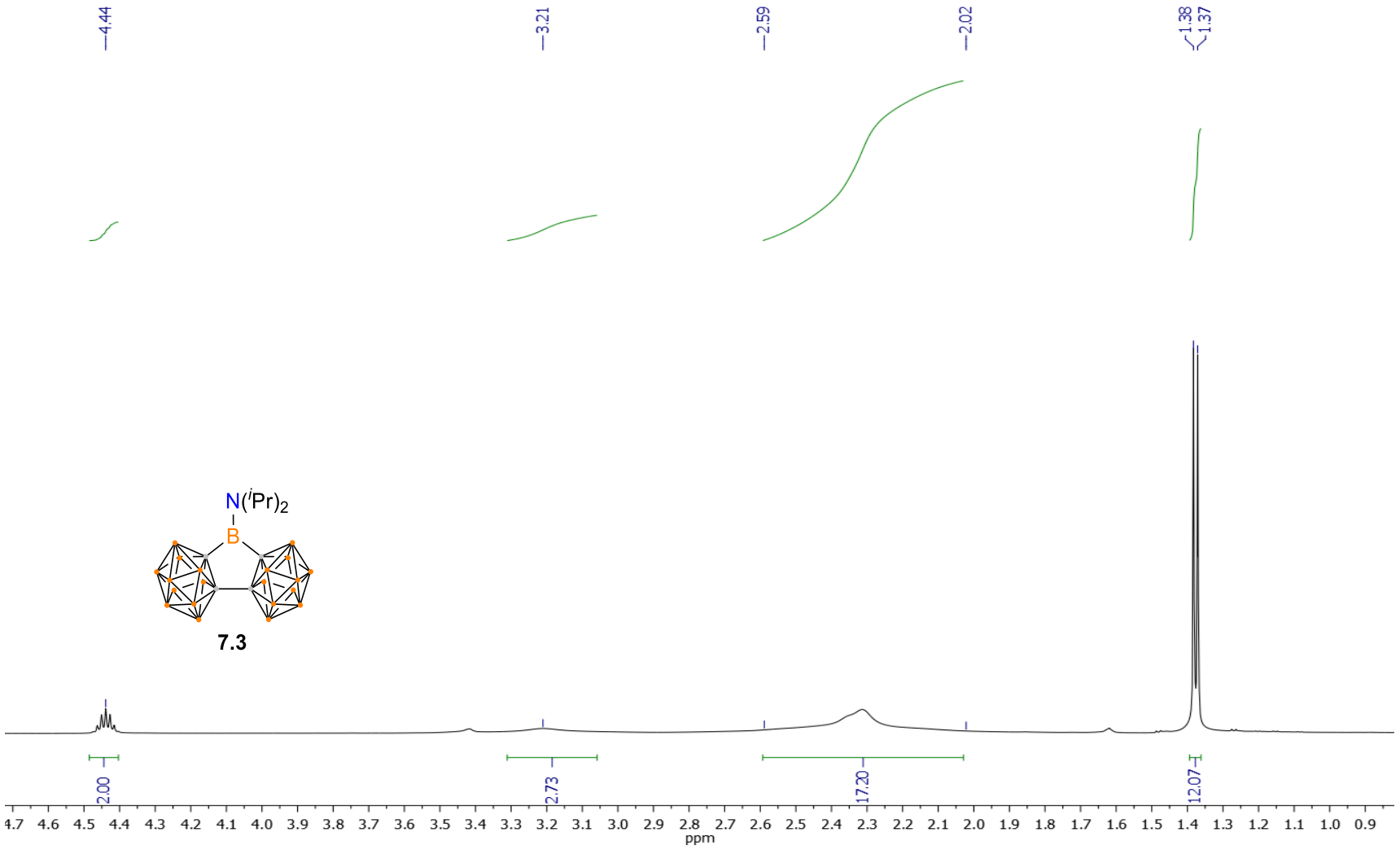

Figure F-4: Expansion of the $^{1}H\{^{11}B\}$ NMR spectrum of **7.3** in $CDCl_3$.

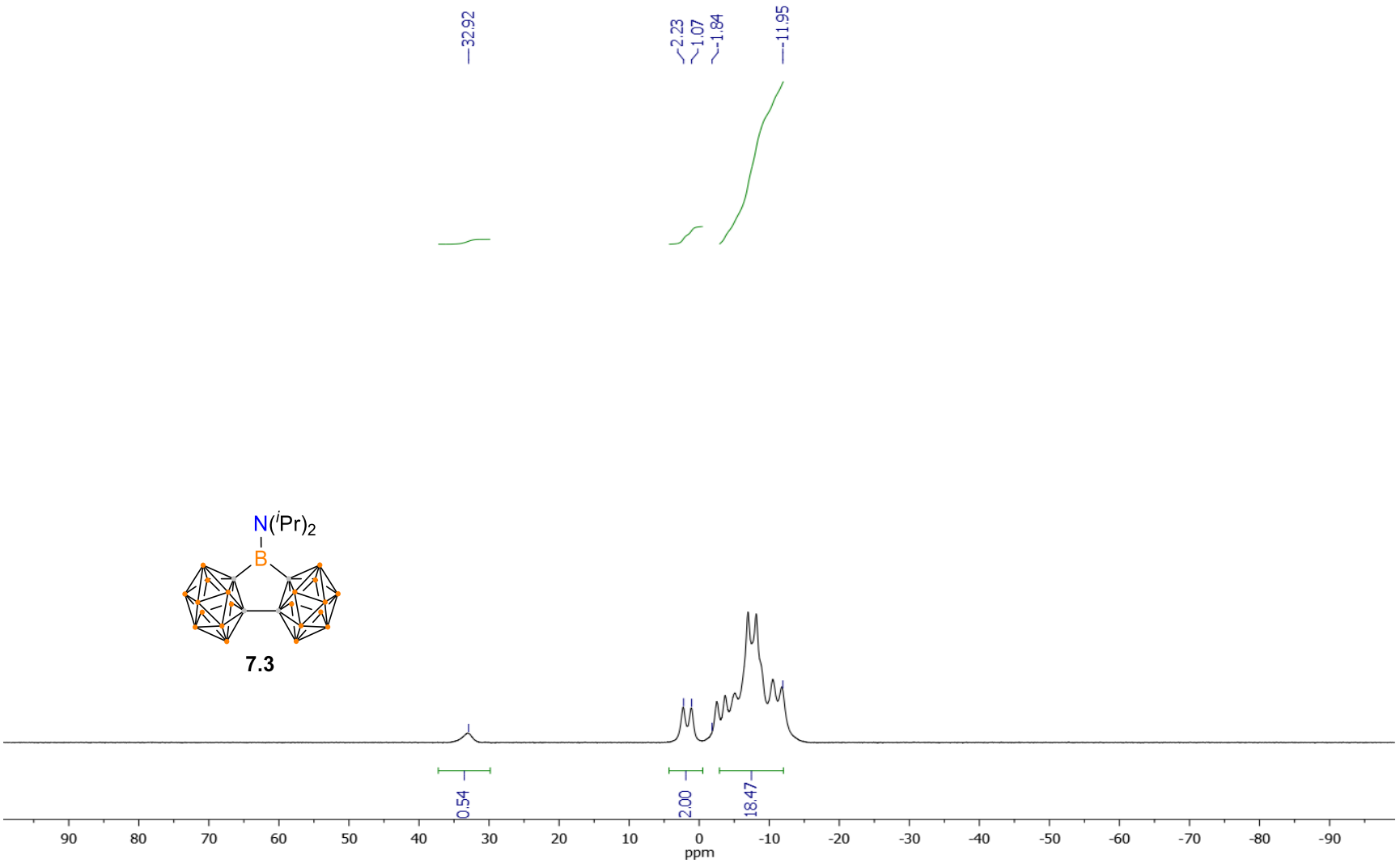

Figure F-5: ^{11}B NMR spectrum of **7.3** in $CDCl_3$.

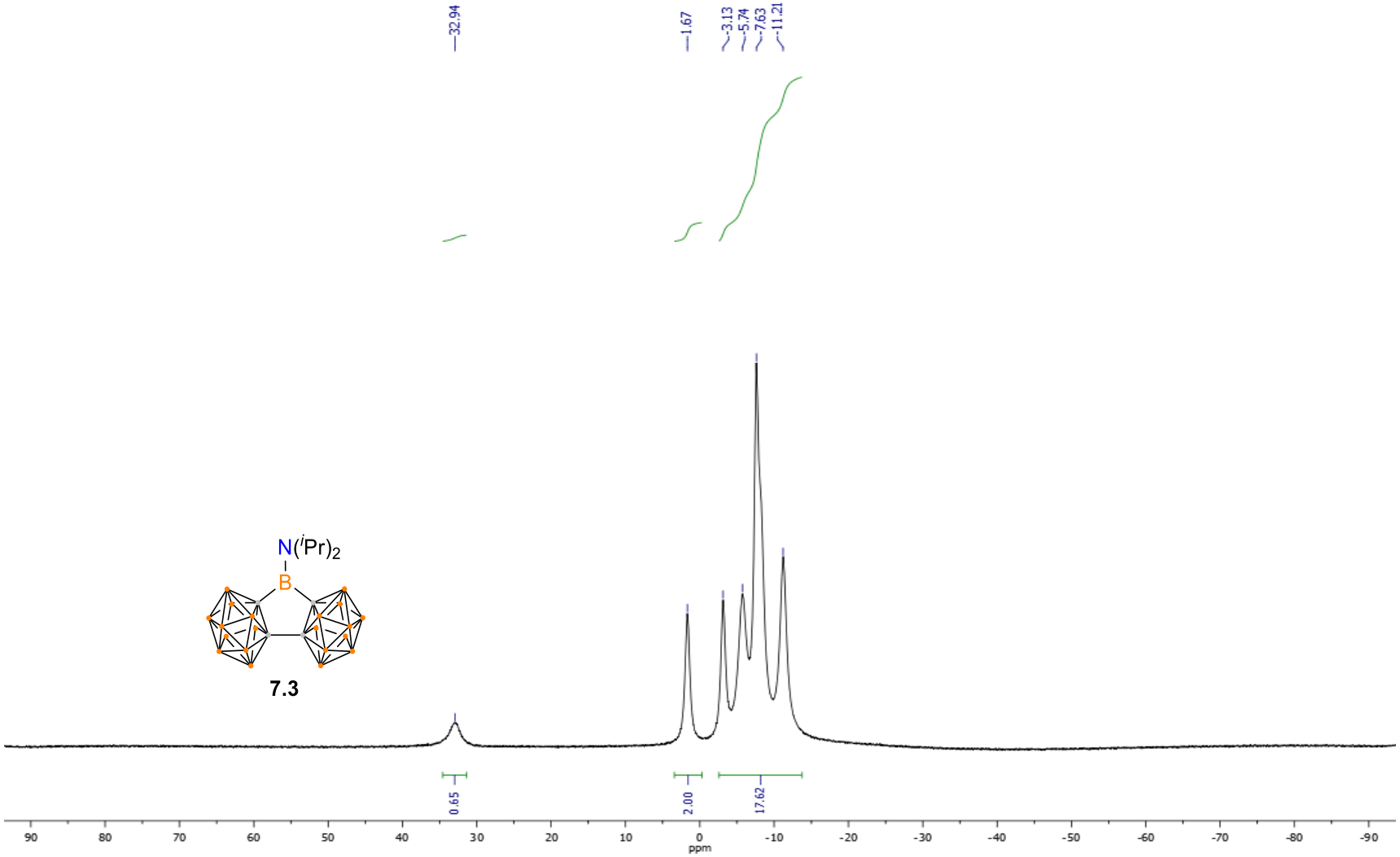

Figure F-6: $^{11}B\{^{1}H\}$ NMR spectrum of **7.3** in $CDCl_3$.

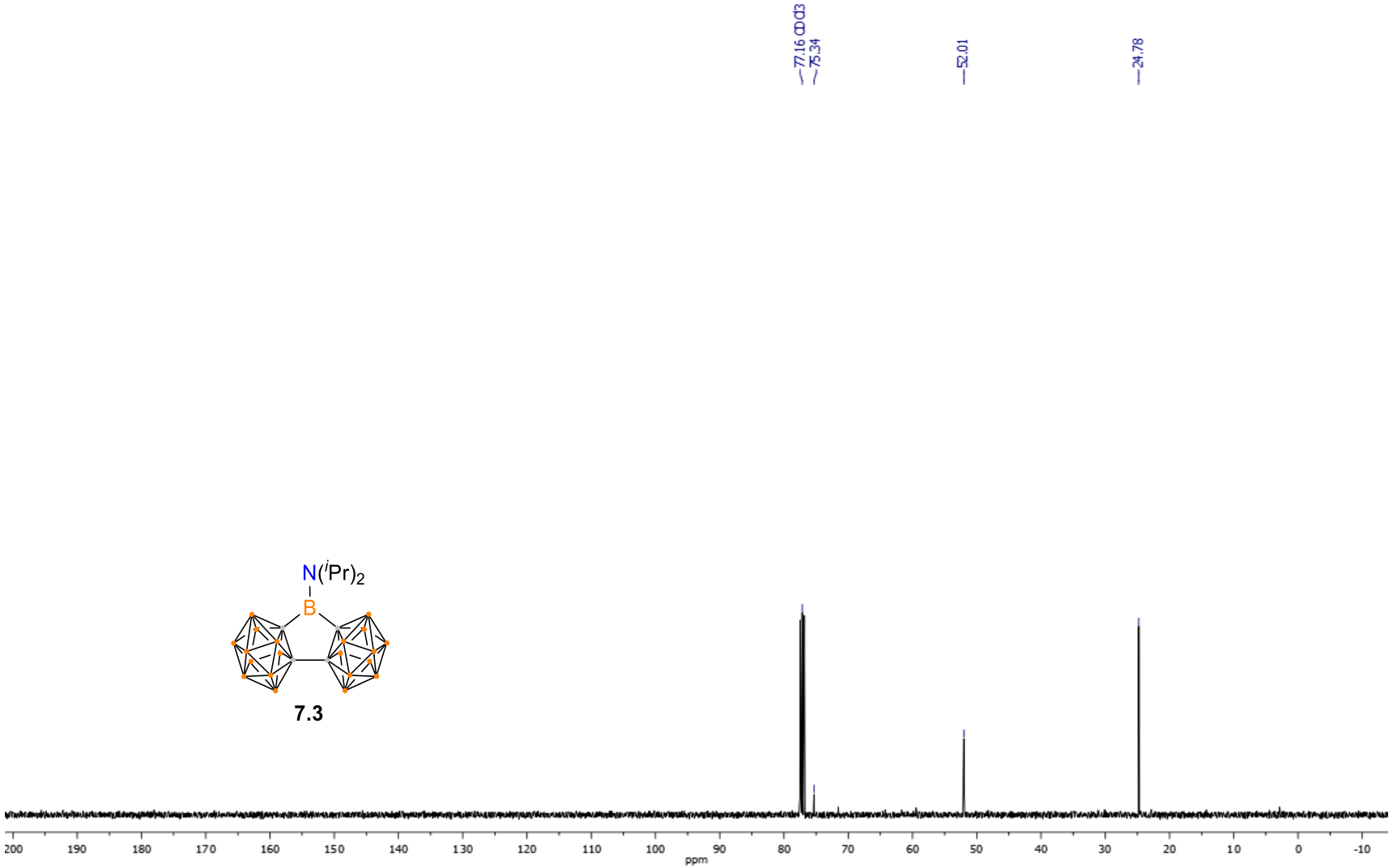

Figure F-7: $^{13}C\{^{1}H\}$ NMR spectrum of **7.3** in $CDCl_3$.

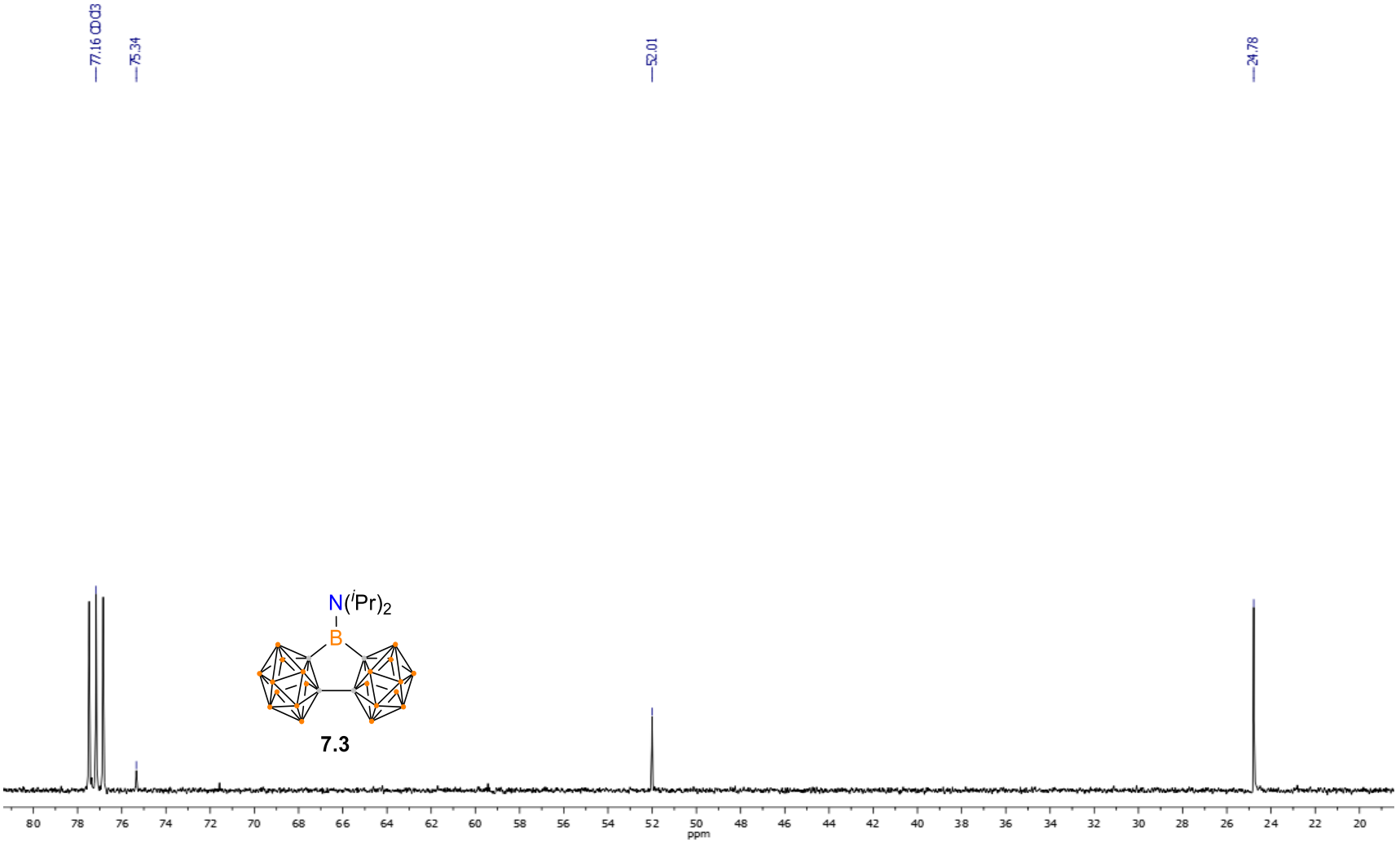

Figure F-8: Expansion of $^{13}C\{^{1}H\}$ NMR spectrum of **7.3** in $CDCl_3$ (aryl region).

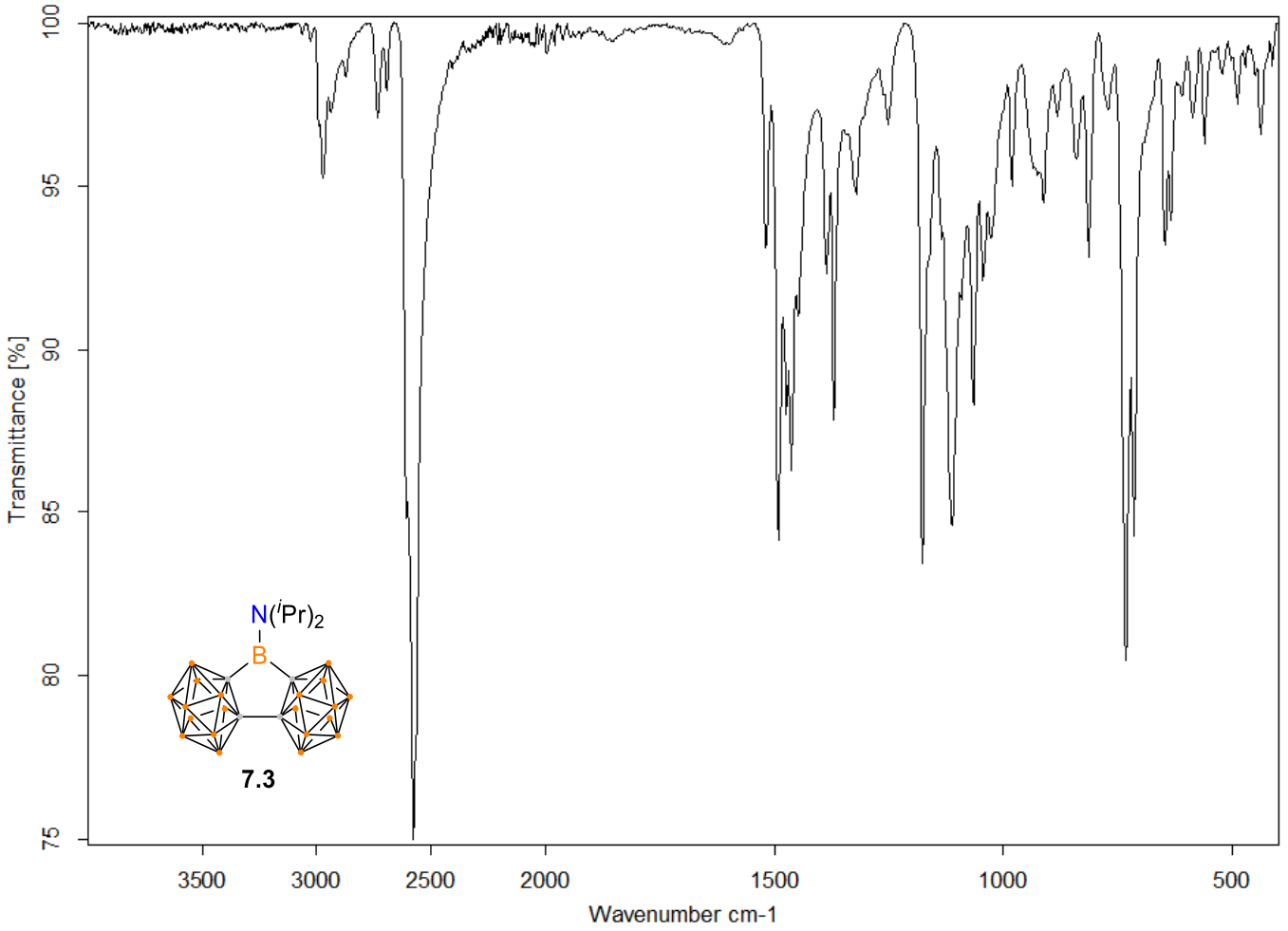

Figure F-9: FT-IR spectrum of **7.3**.

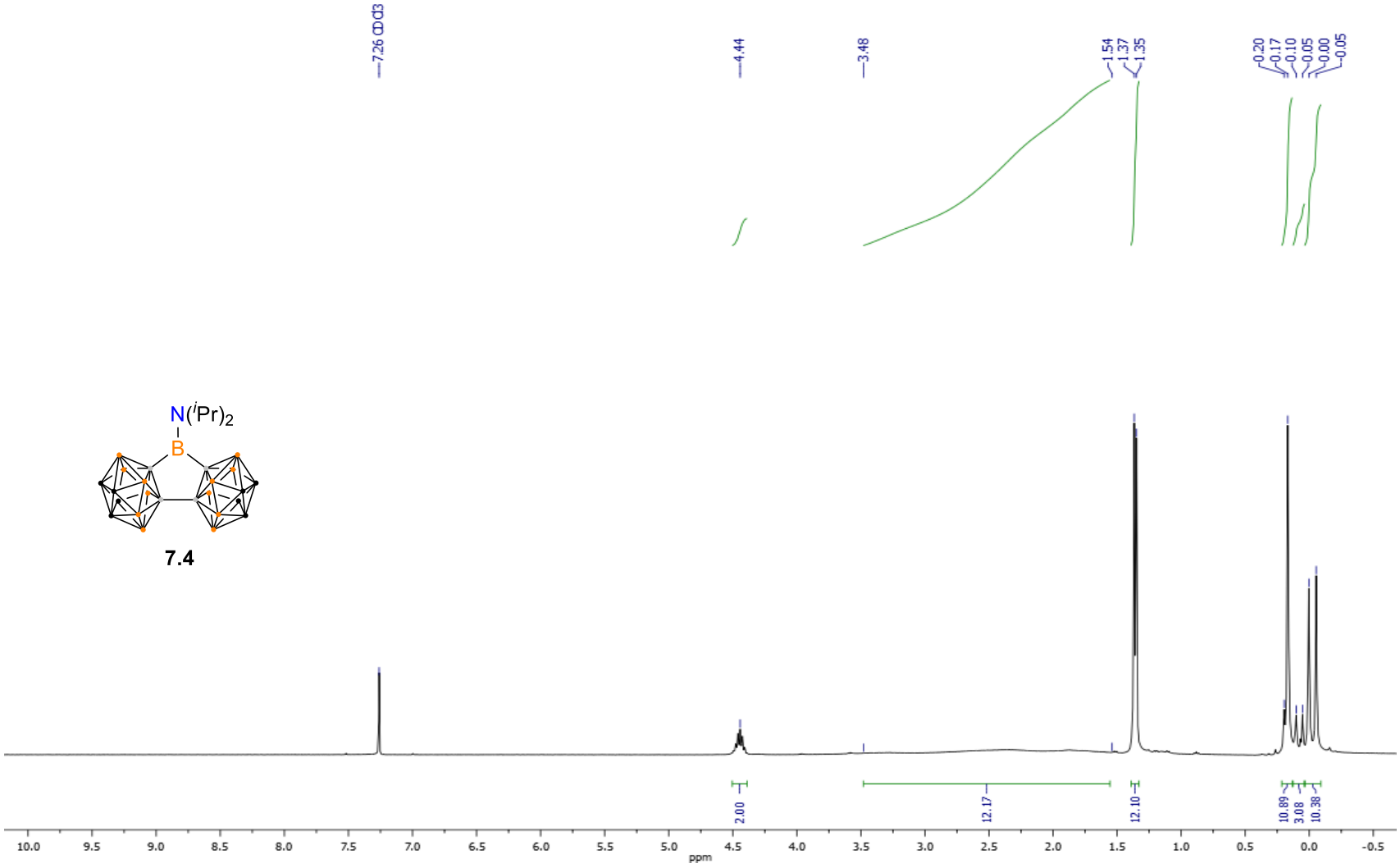

Figure F-10: ^{1}H NMR spectrum of **7.4** in $CDCl_3$.

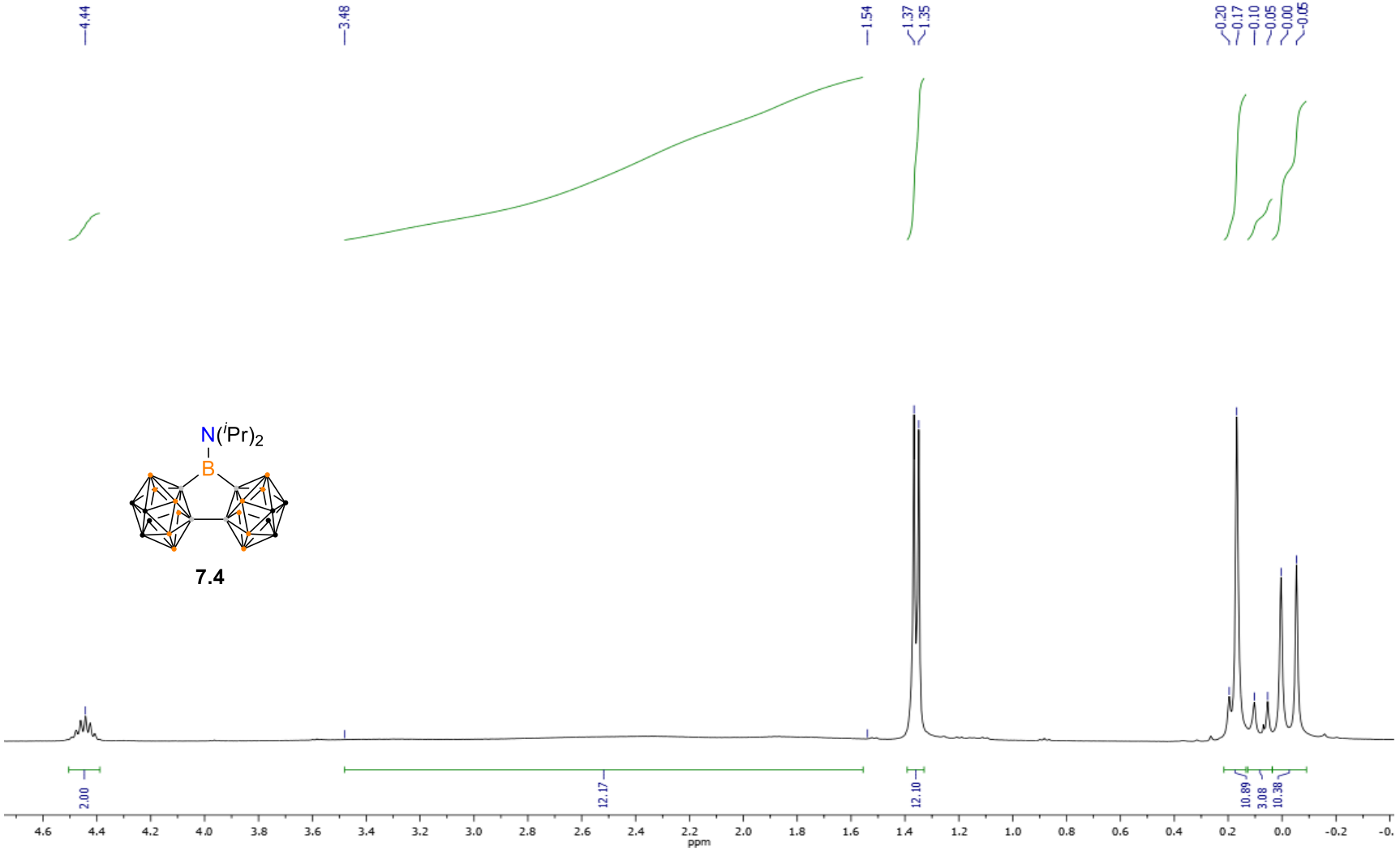

Figure F-11: Expansion of the ^{1}H NMR spectrum of **7.4** in $CDCl_3$.

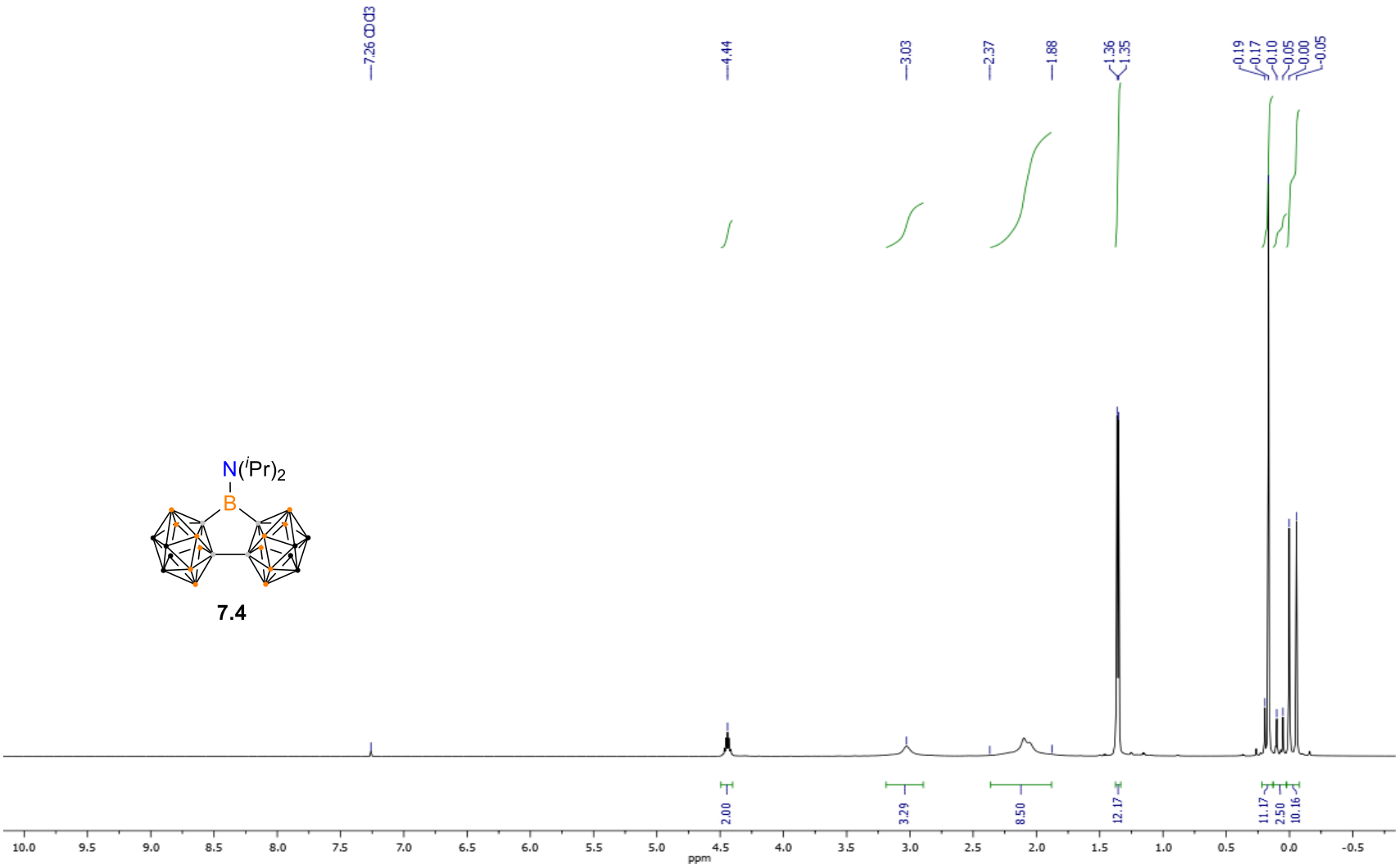

Figure F-12: $^{1}H\{^{11}B\}$ NMR spectrum of **7.4** in $CDCl_3$.

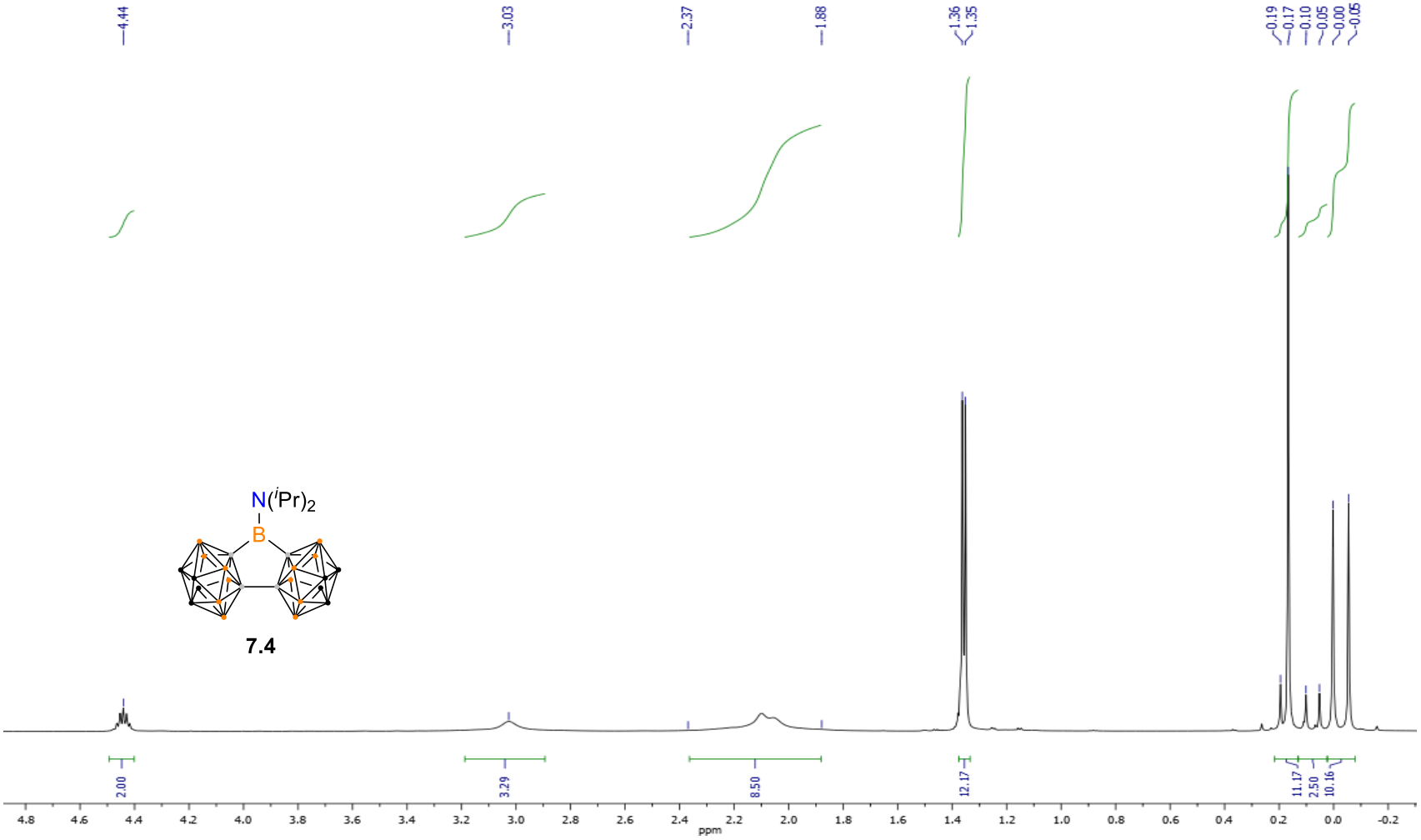

Figure F-13: Expansion of the ^{1}H NMR spectrum of **7.4** in $CDCl_3$.

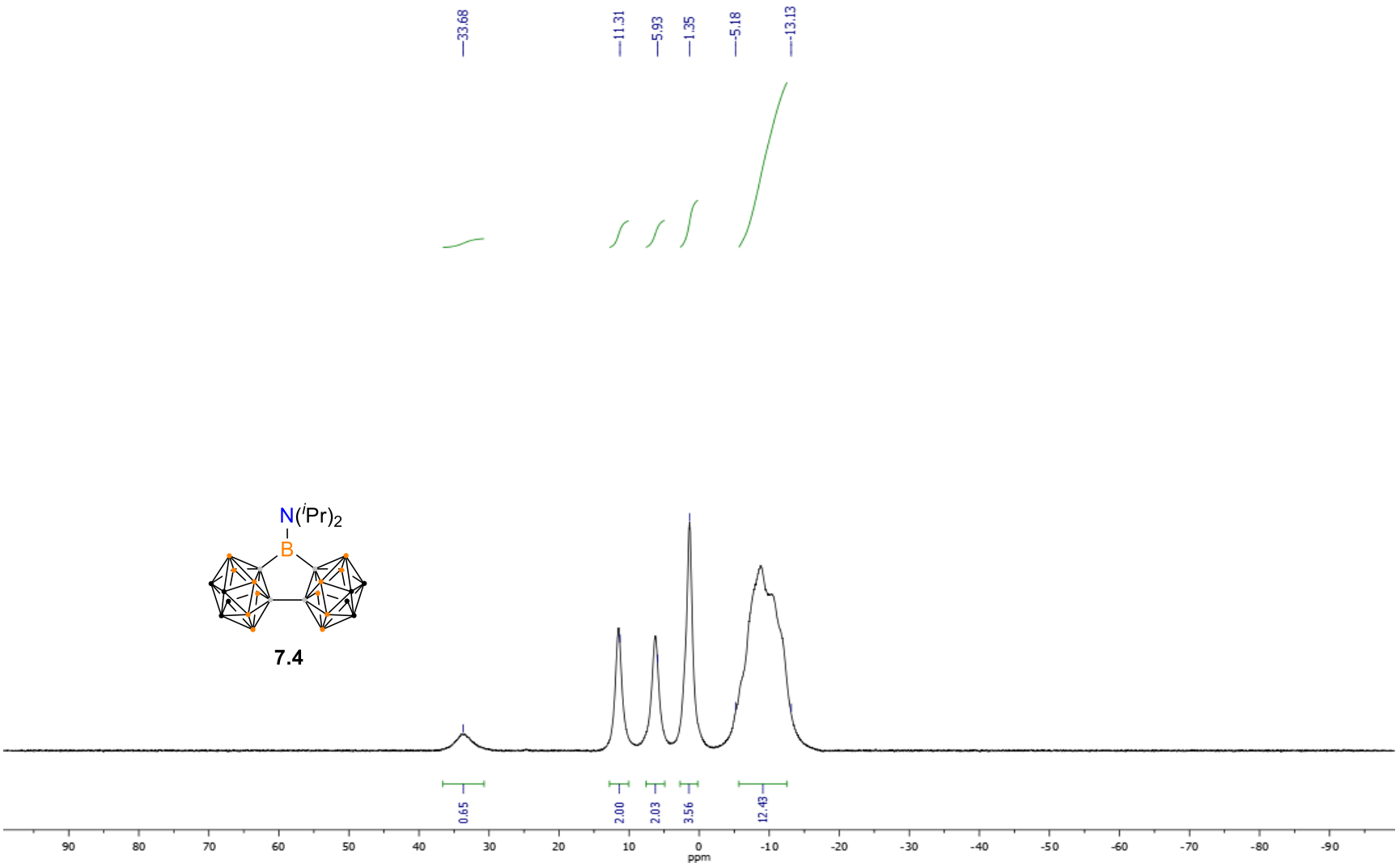

Figure F-14: ^{11}B NMR spectrum of **7.4** in $CDCl_3$.

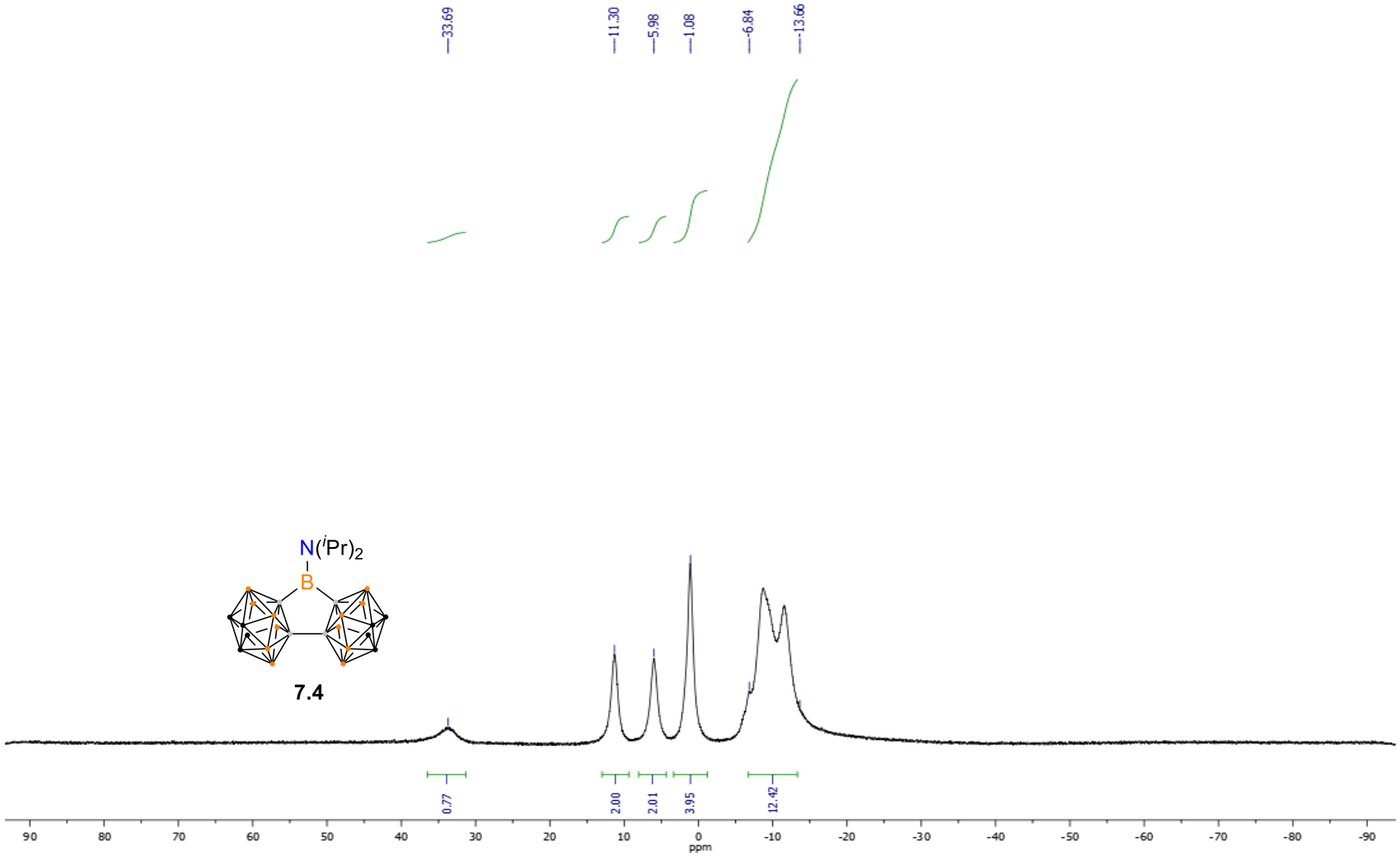

Figure F-15: $^{11}B\{^{1}H\}$ NMR spectrum of **7.4** in $CDCl_3$.

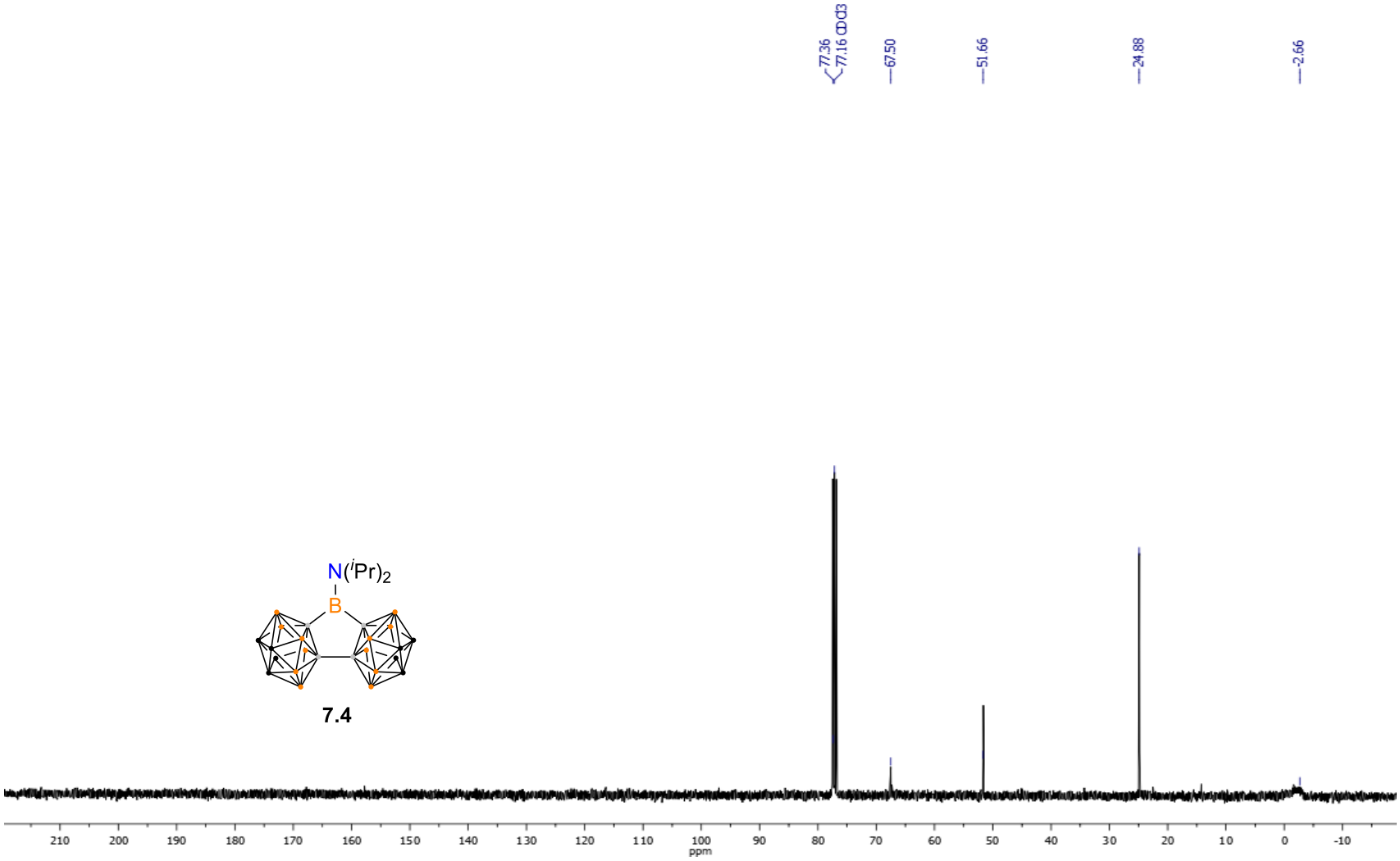

Figure F-16: $^{13}C\{^{1}H\}$ NMR spectrum of **7.4** in $CDCl_3$.

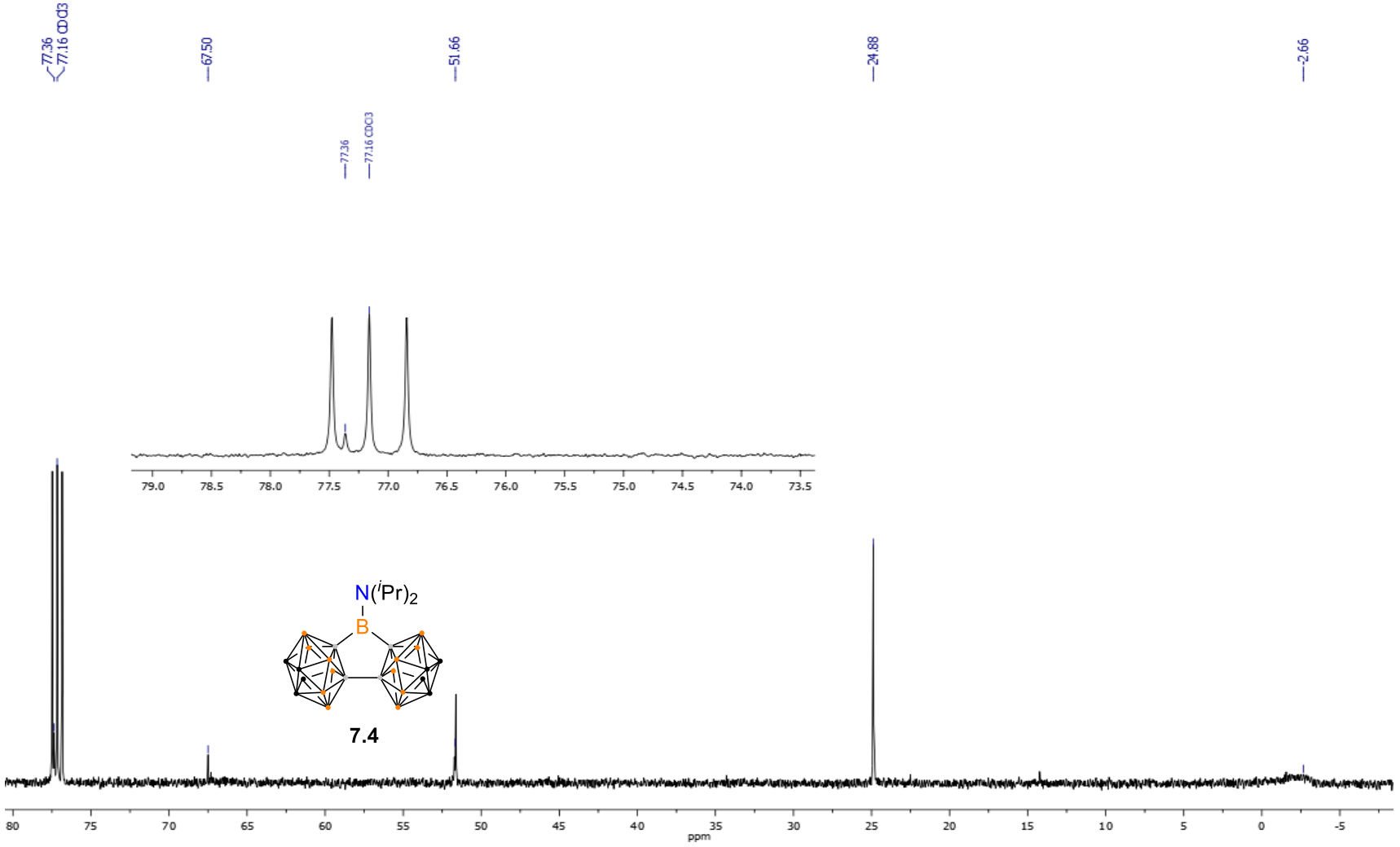

Figure F-17: Expansion of $^{13}C\{^{1}H\}$ NMR spectrum of **7.4** in $CDCl_3$ (aryl region).

Table F-5: Crystallographic Data for **7.3** and **7.4**.

Entry	**7.3**	**7.4**
CCDC	1884761	1884762
Empirical formula	$C_{10}H_{34}B_{21}N$	$C_{18}H_{36}B_{21}N$
FW (g/mol)	395.39	493.49
Crystal system	Triclinic	Monoclinic
Space group	*P-1*	$P2_1/n$
a (Å)	10.5847(11)	11.7390(7)
b (Å)	10.7181(11)	16.5577(11)
c (Å)	12.7511(13)	19.2181(13)
α (deg)	93.570(6)	90
β (deg)	109.312(5)	96.680(2)
γ (deg)	116.930(6)	90
V (Å^3)	1177.9(2)	3710.1(4)
Z	2	4
D_c (mg m^{-3})	1.115	0.883
radiation, λ (Å)	0.71073	0.71073
temp (K)	150(2)	150(2)
$R1[I>2\sigma I]^a$	0.0546	0.0988
$wR2(F^2)^a$	0.1399	0.2898
GOF $(S)^a$	1.055	1.048

[a] $R1(F[\mathrm{I} > 2(\mathrm{I})]) = \sum\|\|F_o| - |F_c\|\|/ \sum |F_o|$; $wR2(F^2\ [\text{all data}]) = [w(F_o^2 - F_c^2)^2]^{1/2}$; $S(\text{all data}) = [w(F_o^2 - F_c^2)^2/(n - p)]^{1/2}$ (n = no. of data; p = no. of parameters varied; $w = 1/[^2(F_o^2) + (aP)^2 + bP]$ where $P = (F_o^2 + 2F_c^2)/3$ and a and b are constants suggested by the refinement program.

Coordinates for geometry optimized structures of **1.15-N(^{i}Pr)$_2$**, **7.3**, and **7.4**.

1.15-N(^{i}Pr)$_2$

N	-3.15442387	9.96704909	3.51892173
C	-4.66959764	11.49289484	2.20047046
H	-4.05728387	12.40166500	2.16391970
H	-5.72402248	11.79735301	2.12541361
H	-4.42709274	10.87580411	1.32575656
C	-4.45130418	10.69376783	3.49500131
H	-5.19903505	9.89283350	3.51062950
H	-0.28285940	8.50749397	4.40053722
C	-1.70343919	10.66055216	5.46245407
H	-2.36477922	11.37952211	5.96038679
H	-0.66640406	10.94106178	5.69996069
H	-1.89503190	9.66483075	5.88279547
C	-1.89970213	10.64523864	3.93825661
H	-1.10871781	10.01499179	3.51656644
C	-1.68358763	12.03084312	3.31718306
H	-1.76825976	11.99202667	2.22396841
H	-0.66904668	12.37240121	3.56626518
H	-2.38419766	12.78483337	3.69730239
C	-4.24564551	7.76634151	2.39727186
H	-3.99565604	4.49614567	1.31594564
C	-2.33916157	6.35237326	2.71610788
C	-4.73702629	11.53425415	4.74578463
H	-4.64171652	10.93152680	5.65763616
H	-5.77043694	11.90427210	4.69047495
H	-4.08118014	12.40937914	4.83328068
B	-3.11219846	8.61280649	3.12740904
C	-1.90974755	7.58287793	3.28965339
H	1.14322008	6.50974744	4.40864525
C	-1.53047539	5.21563193	2.72971871
C	-0.26840266	5.27951327	3.33277827
C	0.16555294	6.46797661	3.92511610
C	-0.65230045	7.60775466	3.90717322
H	0.37232744	4.39604815	3.34922981
H	-1.87459760	4.27979171	2.28469703
C	-3.70621868	6.46850351	2.16662363
H	-7.25320043	7.27822861	0.83299220
C	-5.52496736	8.03525336	1.89243278
C	-6.25611712	7.04920628	1.21291845
C	-5.71058864	5.77849416	1.01432804
C	-4.42574995	5.48499719	1.48693636
H	-6.28309881	5.01652713	0.48215902
H	-5.98174128	9.01895941	2.00583399

7.3

N	-3.09410817	9.87831787	3.52897163
C	-3.96573152	11.60024356	1.91469165
H	-3.25782676	12.41988166	2.08546121
H	-4.91137537	12.03936405	1.56488383
H	-3.57341013	10.96111115	1.11185173
C	-4.23975472	10.77376897	3.17853963
H	-5.05239586	10.08863605	2.92074446
C	-1.85838527	7.52130179	3.18373204
C	-2.18256904	10.42304743	5.81170124
H	-2.85179991	11.23637798	6.11646680
H	-1.22516762	10.56184170	6.33469397
H	-2.61478888	9.46999108	6.14624616

C	-1.92191337	10.39660222	4.29963195
H	-1.14022161	9.64798157	4.14236127
C	-1.34685370	11.71524006	3.78124685
H	-1.11394140	11.65550752	2.71001685
H	-0.40974802	11.91812035	4.31912013
H	-2.01373321	12.57042404	3.95145969
C	-4.40418471	7.76947071	2.51294378
C	-3.91111904	6.21323127	2.27054557
C	-2.40375563	6.11243450	2.51643022
C	-4.76702994	11.62750501	4.33220983
H	-5.01208002	11.01140981	5.20712079
H	-5.69102598	12.12143109	3.99954496
H	-4.06725789	12.41598399	4.63810993
B	-3.11632236	8.54841725	3.12515463
B	-1.40214875	7.17582377	1.55448123
H	-1.86225194	7.85617459	0.71183452
B	-1.24161592	5.41480358	1.46928513
H	-1.63538767	4.85428385	0.49843056
B	0.11413482	4.97576239	2.53571366
H	0.80092076	4.03413829	2.28876912
B	-5.70945629	8.13948754	1.42803014
H	-5.78477559	9.24438389	0.99282938
B	-4.37031579	7.14641420	0.88159980
H	-3.56534177	7.53052337	0.11615316
B	-5.10328403	5.08409876	2.75616646
H	-4.73690888	4.06262083	3.23965301
B	-4.79163158	5.43294238	1.03996737
H	-4.21363807	4.64757593	0.36141332
B	-5.99246125	6.64208957	0.49838301
H	-6.33813403	6.68616102	-0.64104299
B	-7.03550446	7.03975138	1.87266116
H	-8.17129767	7.37163950	1.73087408
B	-6.03037860	7.78801569	3.12250360
H	-6.31927279	8.64634771	3.89519162
B	-4.88782272	6.58187428	3.67405759
H	-4.41371725	6.65669358	4.74840377
B	-6.50163839	6.07632634	3.26697193
H	-7.21697633	5.71153172	4.14710972
B	-6.46322007	5.36219415	1.64161251
H	-7.18203728	4.46653106	1.32412901
B	-0.22687057	7.82719247	2.67367950
H	0.09546307	8.96152158	2.51135917
B	0.19176238	6.47548322	1.59022631
H	0.90406203	6.64286975	0.65000451
B	0.74306190	6.47373367	3.27781008
H	1.88728817	6.63329988	3.57006745
B	-1.55986222	4.74866356	3.08905090
H	-2.16882039	3.73675501	3.21689112
B	-1.92843084	6.09332877	4.18310100
H	-2.72700318	6.00821962	5.04098291
B	-0.55190947	7.17639727	4.27676970
H	-0.44708903	7.84313407	5.25704110
B	-0.32720558	5.40782072	4.20299034
H	0.00817974	4.79474662	5.16802831

7.4

C	6.09095469	11.53162286	6.08272552
H	5.98560440	10.71504617	6.81280457
H	5.53554744	11.22968664	5.18226660
H	5.57981736	12.41030273	6.50354531
C	9.55272085	12.74482404	3.92748528
B	10.32197462	13.09624643	2.54466266

C	11.91932554	13.12135162	2.81675292
C	15.88988002	14.11278773	1.67284181
H	15.92481090	13.49744698	0.76131789
H	16.85268141	13.97677311	2.18787036
H	15.83763324	15.16456315	1.35386409
C	15.54142478	10.89932746	2.99805188
H	15.22395227	9.93943153	3.43089082
H	16.52259911	11.14467737	3.43144077
H	15.69607534	10.73977321	1.92074225
C	12.09414801	12.85657342	4.43891106
C	10.74526781	12.46503623	5.03646309
C	8.70752649	10.92889381	8.38566397
H	9.00536457	11.64116976	9.16963393
H	9.27799903	10.00343970	8.55422148
H	7.64556846	10.69213467	8.55136201
C	8.39926618	8.96750641	5.48790848
H	7.72672238	8.70098950	4.65918606
H	7.87805644	8.71293755	6.42292284
H	9.28111509	8.31371909	5.41944953
C	7.82569527	14.21555833	7.52326889
H	7.33368324	13.67643816	8.34657082
H	7.05752462	14.83402692	7.03545617
H	8.55973386	14.89976381	7.97347730
N	9.71035578	13.32993777	1.31719788
C	14.41324791	16.36560372	3.95357059
H	14.52177573	16.61838556	5.01863838
H	13.72014454	17.09684161	3.51216019
H	15.39579431	16.52122359	3.48356592
C	16.17183024	13.59076585	5.17970473
H	16.08681494	14.32478849	5.99485502
H	16.99106790	13.92801558	4.52703815
H	16.48670576	12.63884110	5.63255864
B	7.61915939	11.83059768	5.75957310
B	8.28072166	11.59146033	4.13088606
H	7.69823886	11.22549604	3.15716260
B	13.36673514	12.64233047	2.00201391
H	13.28358033	12.16289836	0.91395896
B	14.66420358	13.71176358	2.60330076
B	14.49076562	12.06172856	3.27181544
B	14.80496298	13.44301983	4.38198800
B	13.24872801	13.90697480	5.12333057
H	13.06306823	14.30695641	6.22850554
B	13.91482687	14.86832165	3.75719599
B	13.03166623	14.33770919	2.29562039
H	12.68360536	15.07143030	1.42270878
B	12.78012476	11.69830038	3.35218874
H	12.30632462	10.62805517	3.23196091
B	13.60944284	12.19999011	4.82779241
H	13.66751215	11.42796386	5.73109634
B	12.20910421	14.49076441	3.82443472
H	11.32249535	15.25672565	3.95070055
B	9.66051003	13.78223868	5.32713314
H	10.02146984	14.89707162	5.22165606
B	8.49950973	13.20187973	6.49983101
B	10.22627883	12.72972998	6.62740825
H	11.01189919	13.16959403	7.40512865
B	8.95531541	11.51744067	6.93076672
B	10.40758434	11.08814129	5.98657876
H	11.31764333	10.39962600	6.32370584
B	9.94602354	11.10465877	4.28435608
H	10.46924739	10.48311423	3.43107585
B	8.79203094	10.50784975	5.45572686

B	8.10784132	13.22204124	4.75256303
H	7.39221374	14.02288381	4.23511894
C	10.54275904	13.35118706	0.07585189
C	10.25890149	14.51578732	-0.87354280
C	10.54256138	11.99574226	-0.64426849
C	7.50517910	12.69832858	0.21138749
C	7.85628964	15.02707842	1.18373320
C	8.23268377	13.54090260	1.25970747
H	11.56477257	13.50288150	0.43523999
H	9.28255514	14.43718847	-1.36936444
H	11.02719689	14.51318671	-1.66003393
H	10.31533720	15.47969890	-0.35137269
H	10.74242519	11.18218336	0.06659331
H	11.34384606	11.99077779	-1.39770468
H	9.59626143	11.78593400	-1.15745679
H	6.42279248	12.81597476	0.36279734
H	7.74702290	11.63291918	0.31986900
H	7.72774684	13.00890176	-0.81785875
H	6.78520421	15.13525918	1.40888930
H	8.03694273	15.46422400	0.19460007
H	8.41823854	15.60512770	1.93011656
H	7.87030805	13.18989069	2.23040274

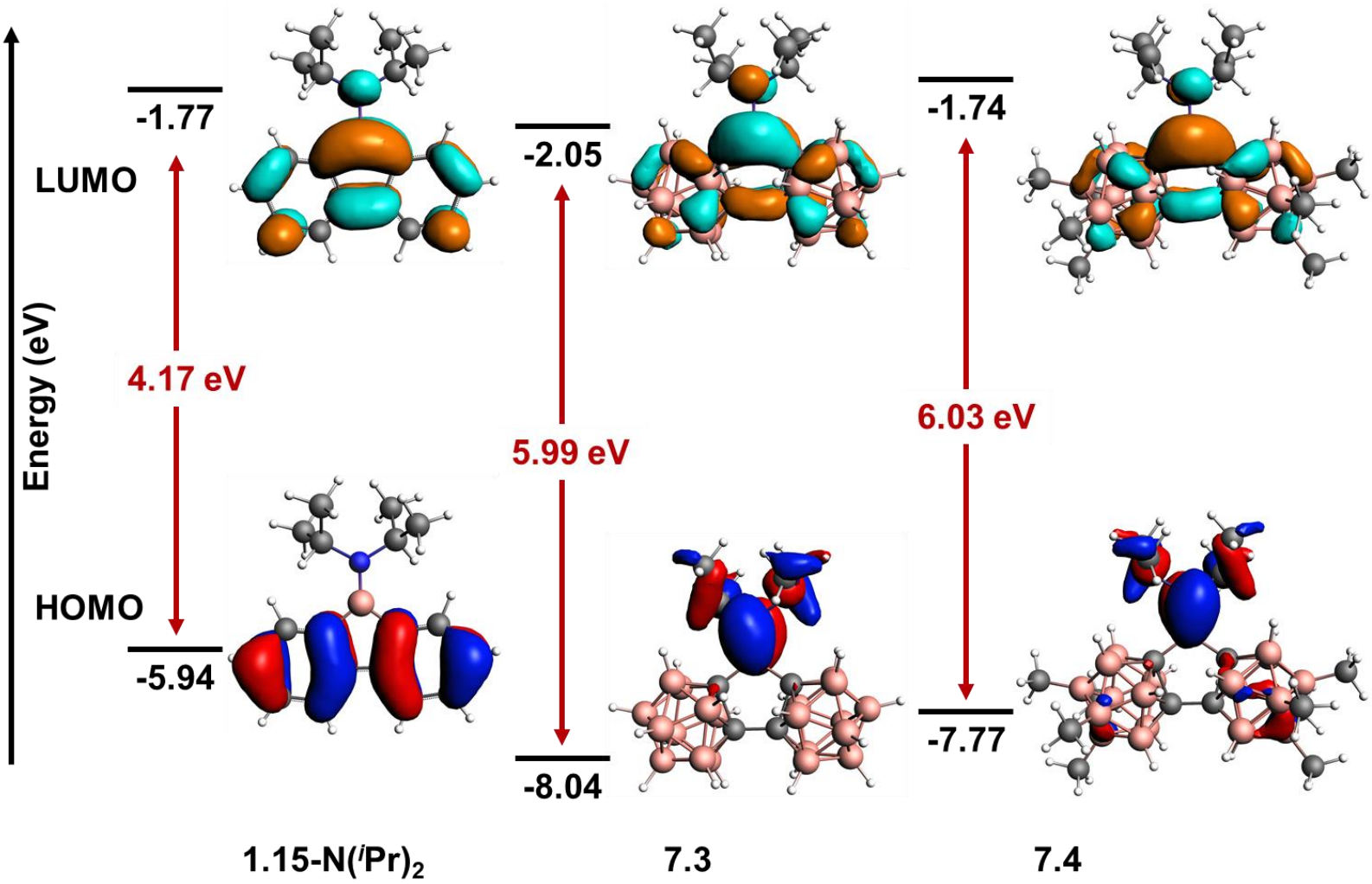

Figure F-18: HOMO and LUMO diagrams for **1.15-N(^{i}Pr)$_2$**,**7.3**, and **7.4**.

APPENDIX G

Synthesis of **1.10** and **1.7-Ph**

General Considerations. All manipulations were performed using Schlenk techniques under a dry argon atmosphere, under an inert atmosphere in an argon-filled MBraun LABstar Pro glovebox, in a nitrogen-filled MBraun Unilab glovebox. Solvents were purchased from commercial sources as anhydrous grade, and dried further using a JC Meyer Solvent System with dual columns packed with solvent-appropriate drying agents. Diphenylacetylene was purchased from Alfa Aesar, dimethyltin dichloride from TCI, lithium pellets from Acros, and dichlorophenylborane from Beantown Chemicals. All reagents were used as received and stored in an argon-filled glovebox. $CDCl_3$ for NMR spectroscopy was purchased from Cambridge Isotope Laboratories and dried by stirring for 3 days over CaH_2, distilled, and stored over 4 Å molecular sieves. Multinuclear NMR spectra were recorded on a Bruker 400 MHz spectrometer.

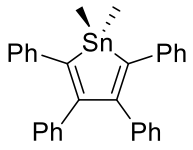

1.10

Synthesis of **1.10** (Video Experimental): In an argon-filled glovebox, diphenylacetylene (10.0 g, 56.1 mmol), lithium pellets (0.390 g, 56.1 mmol), and a medium-sized stir bar were added to a 200-mL Schlenk flask. Diethyl ether (80 mL) was added to the flask *via* cannula transfer (under positive pressure) on an argon Schlenk line. The reaction mixture was stirred vigorously (700 rpm) at room temperature (22 – 27 ˚C) for 16 h to give a yellowish-brown suspension. The yellowish-brown suspension was added to a 500 mL Schlenk flask containing dimethyltin dichloride (6.16 g, 28.0 mmol) in THF (100 mL) *via* cannula transfer (under positive pressure) on the Schlenk line. The combination of both mixtures resulted in a bright yellow solution that was immediately dried *in vacuo*. Ethanol

(100 mL) was added to the flask and the yellow solid was collected on a glass frit. The solid was washed with ethanol (2 × 100 mL) and dried *in vacuo* to give the desired 1,1-dimethyl-2,3,4,5-tetraphenylstannole. Yield: 10.3 g, 73%.

^{1}H NMR (400 MHz, $CDCl_3$): δ 7.09-7.06 (m, 4H), 7.01-6.93 (m, 8H), 6.87-6.85 (m, 4H), 6.81-6.76 (m, 4H), 0.63 (s, $J_{Sn\text{-}C\text{-}H}$ = 28.0 Hz);

^{119}Sn{^{1}H} NMR (149 MHz, $CDCl_3$): δ 3.7; The spectroscopic data matches the literature values.

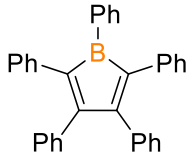

1.7-Ph

Synthesis of **1.7-Ph** (Video Experimental): In a nitrogen-filled glovebox, dichlorophenylborane (30.0 μL, 2.31 mmol) was added dropwise to a toluene solution of **1.10** (1.07 g, 2.11 mmol; 3 mL) at room temperature (20 – 25 ˚C) and stirred for 3 h. The resulting blue solution was centrifuged, a dark blue residue was isolated and washed with toluene (3 × 20 mL) and subsequently *n*-pentane (1 × 20 mL). Drying the solid *in vacuo* gave the desired pentaphenylborole. Yield: 0.78 g, 84%.

^{1}H NMR (400 MHz, $CDCl_3$): δ 7.43 (t, J = 4.0 Hz, 1H), 7.24-7.17 (m, 4H), 7.15-7.08 (m, 8H), 7.03 (t, J = 8.0 Hz, 4H), 6.90-6.88 (m, 4H), 6.76 (d, J = 4.0 Hz, 4H);

^{11}B NMR (128 MHz, $CDCl_3$): δ 66.7 (br); The spectroscopic data matches the literature values.

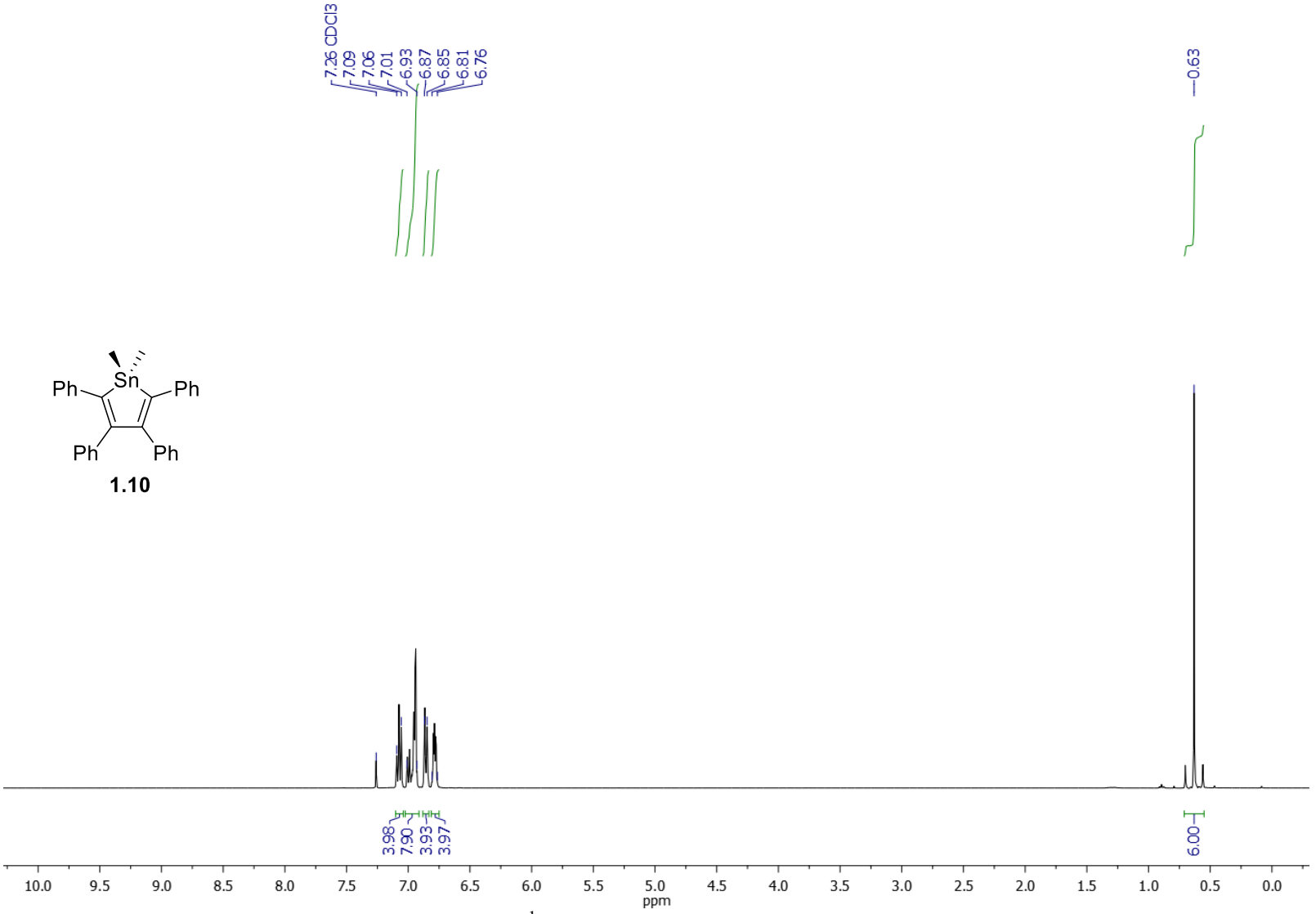

Figure G-1: ^{1}H NMR spectrum of **1.10** in $CDCl_3$.

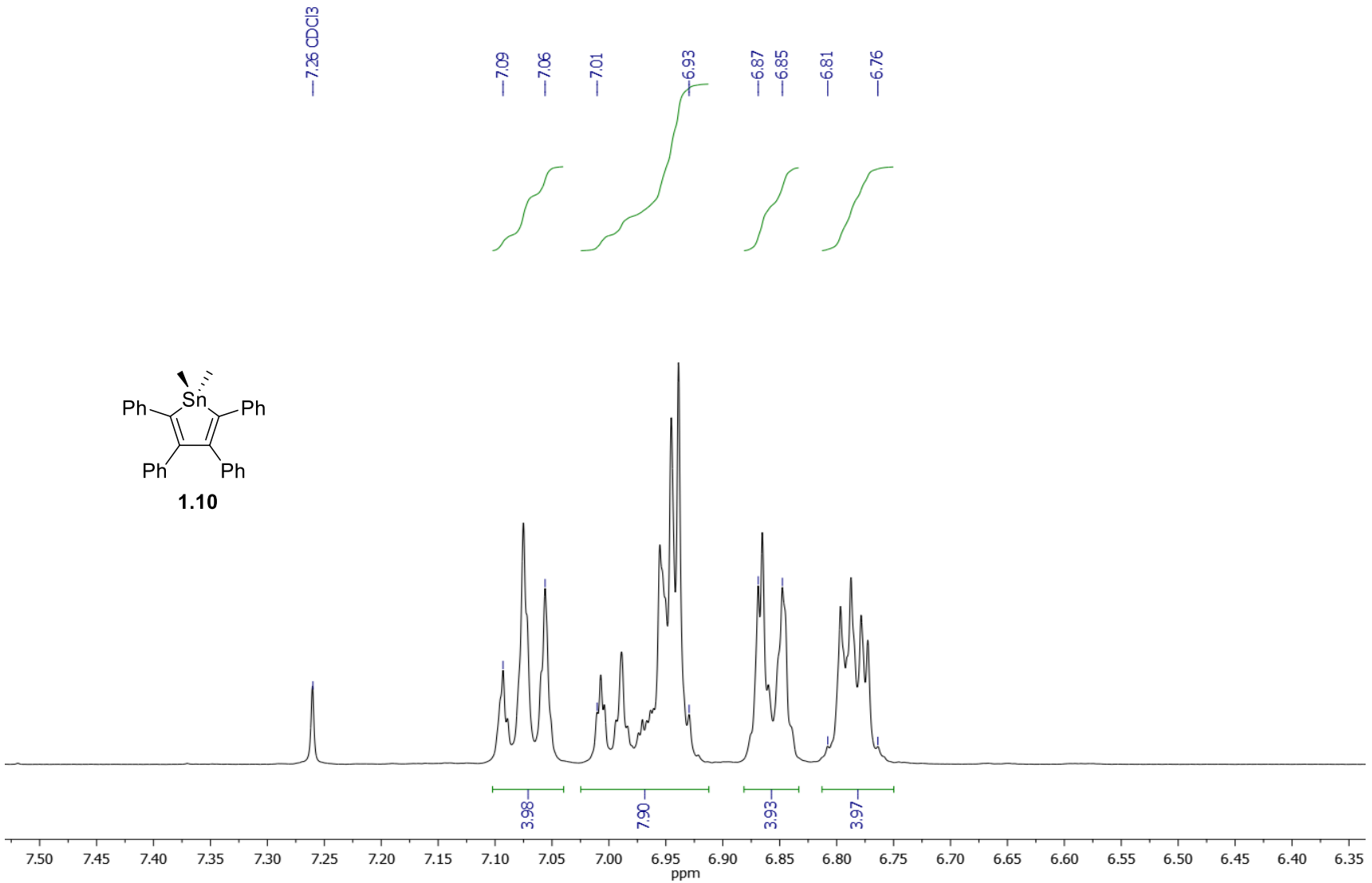

Figure G-2: Expansion of ^{1}H NMR spectrum of **1.10** in $CDCl_3$.

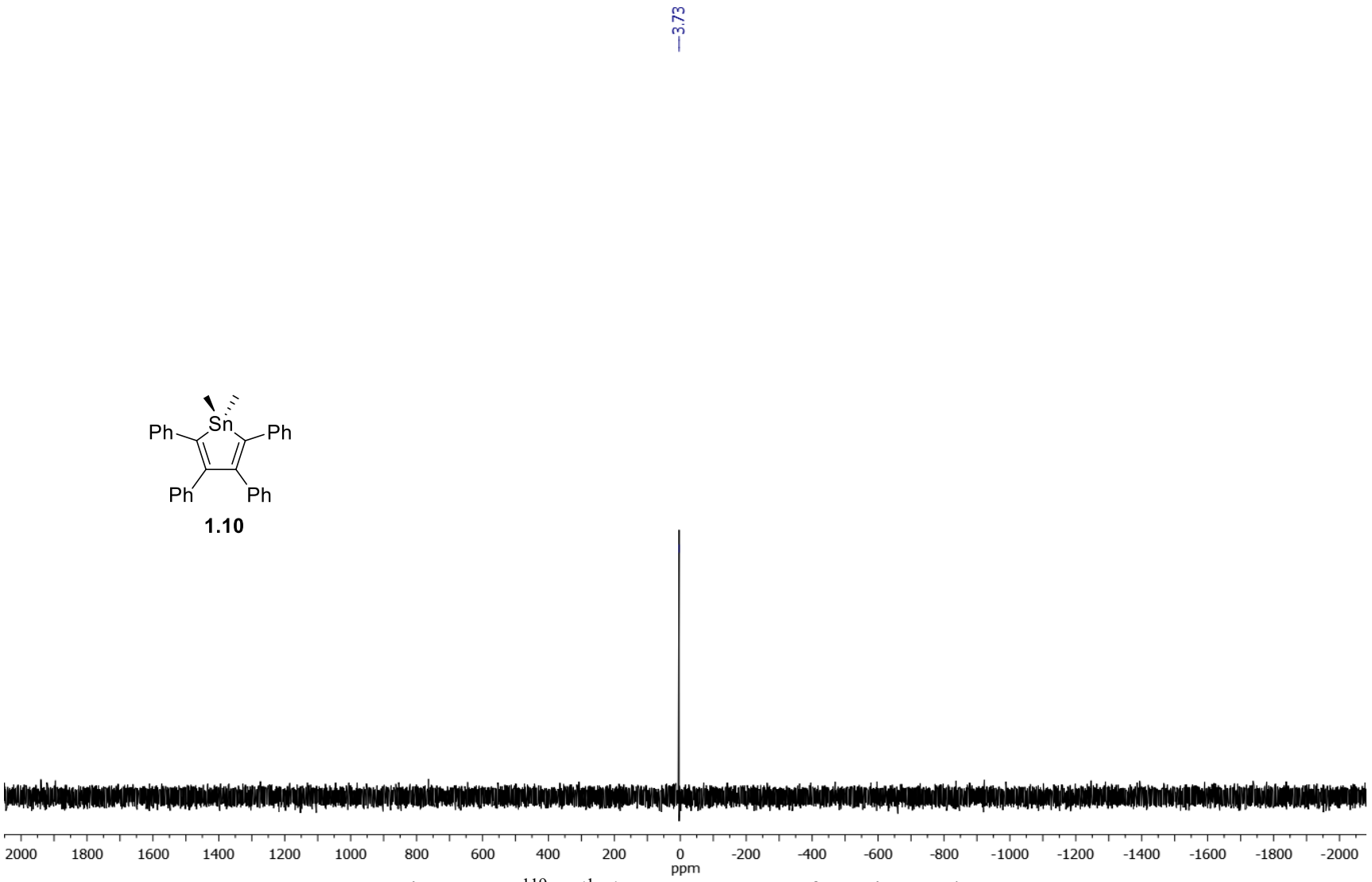

Figure G-3: $^{119}Sn\{^{1}H\}$ NMR spectrum of **1.10** in $CDCl_3$.

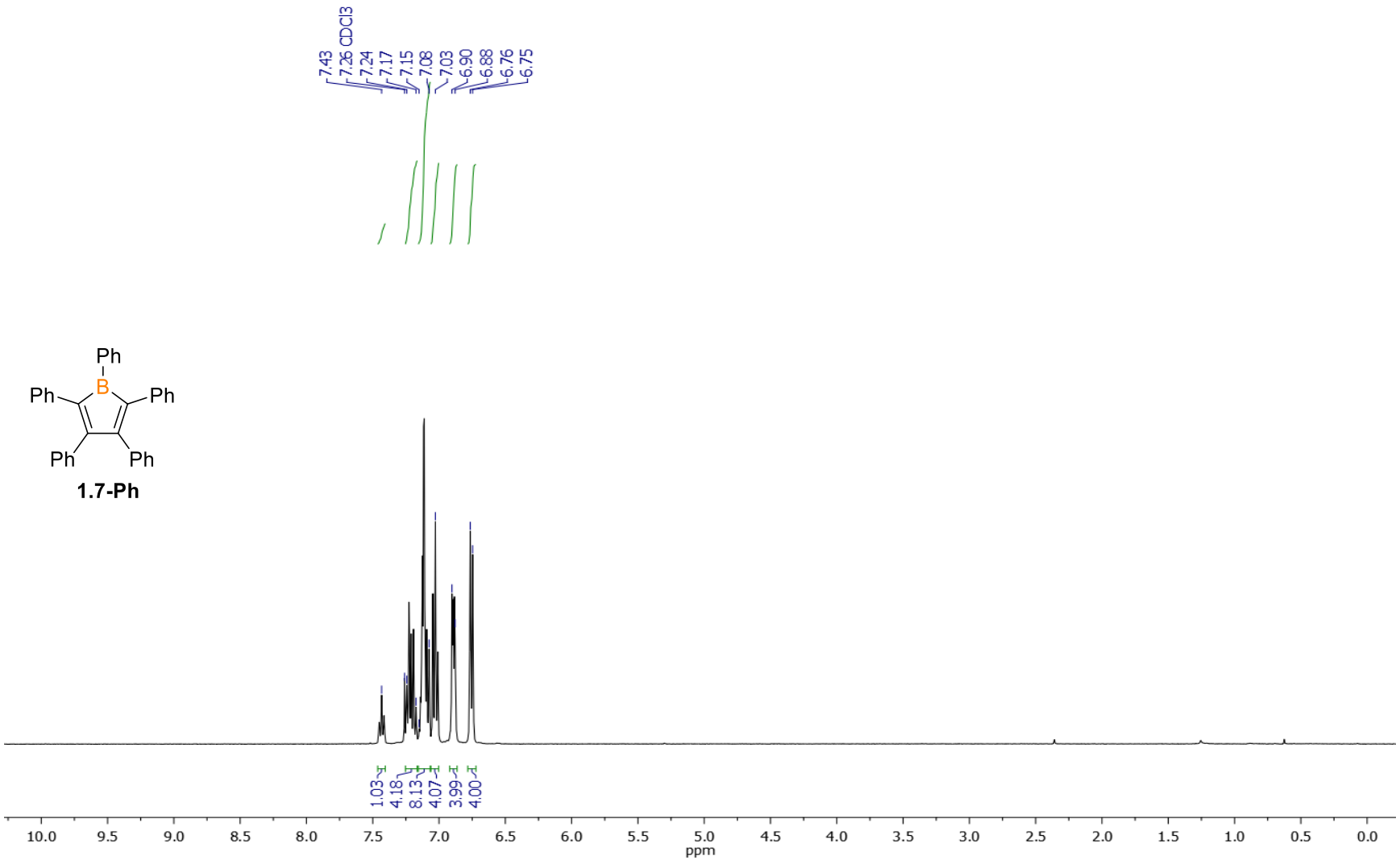

Figure G-4: ^{1}H NMR spectrum of **1.7-Ph** in $CDCl_3$.

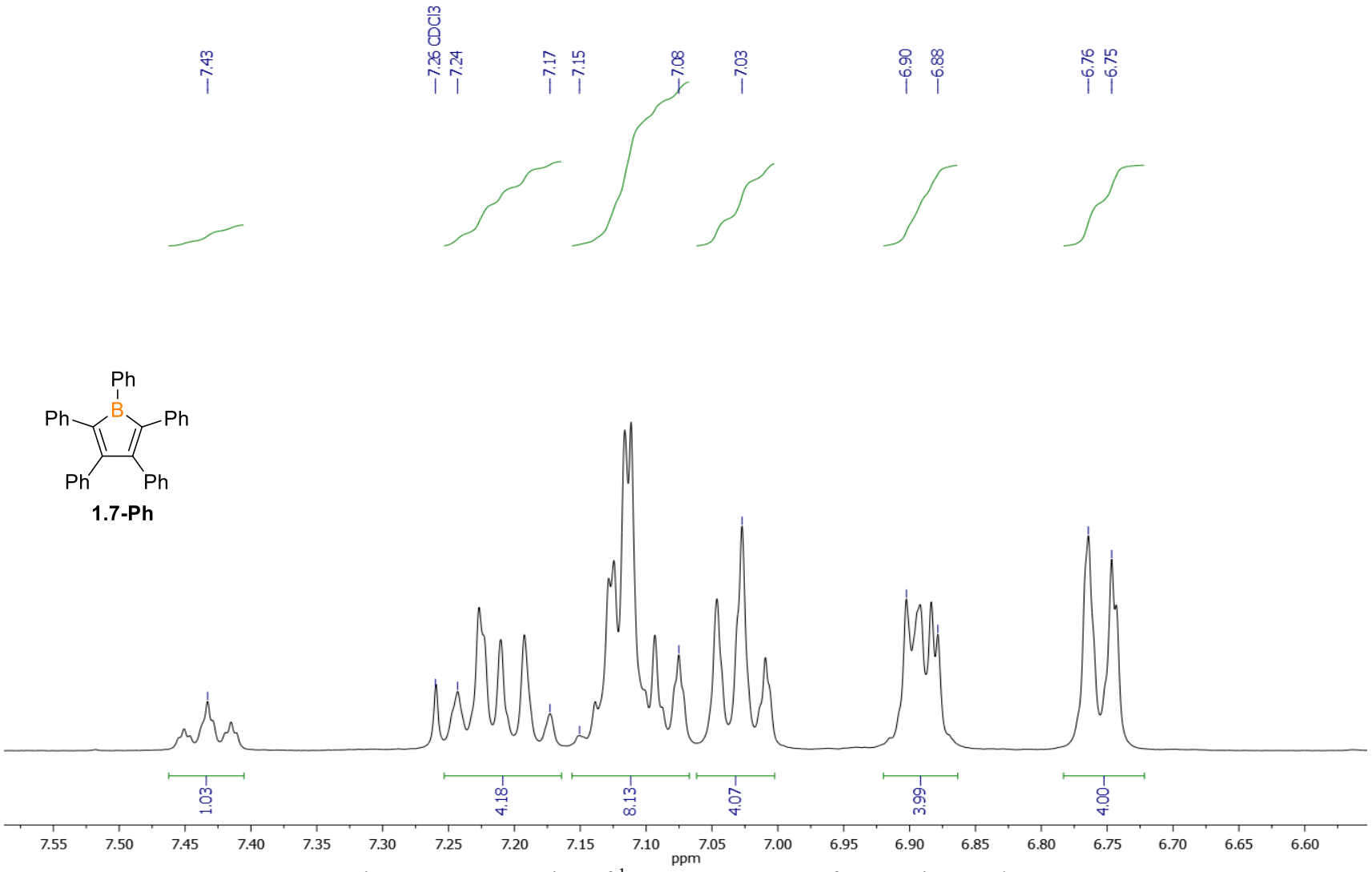

Figure G-5: Expansion of ^{1}H NMR spectrum of **1.7-Ph** in $CDCl_3$.

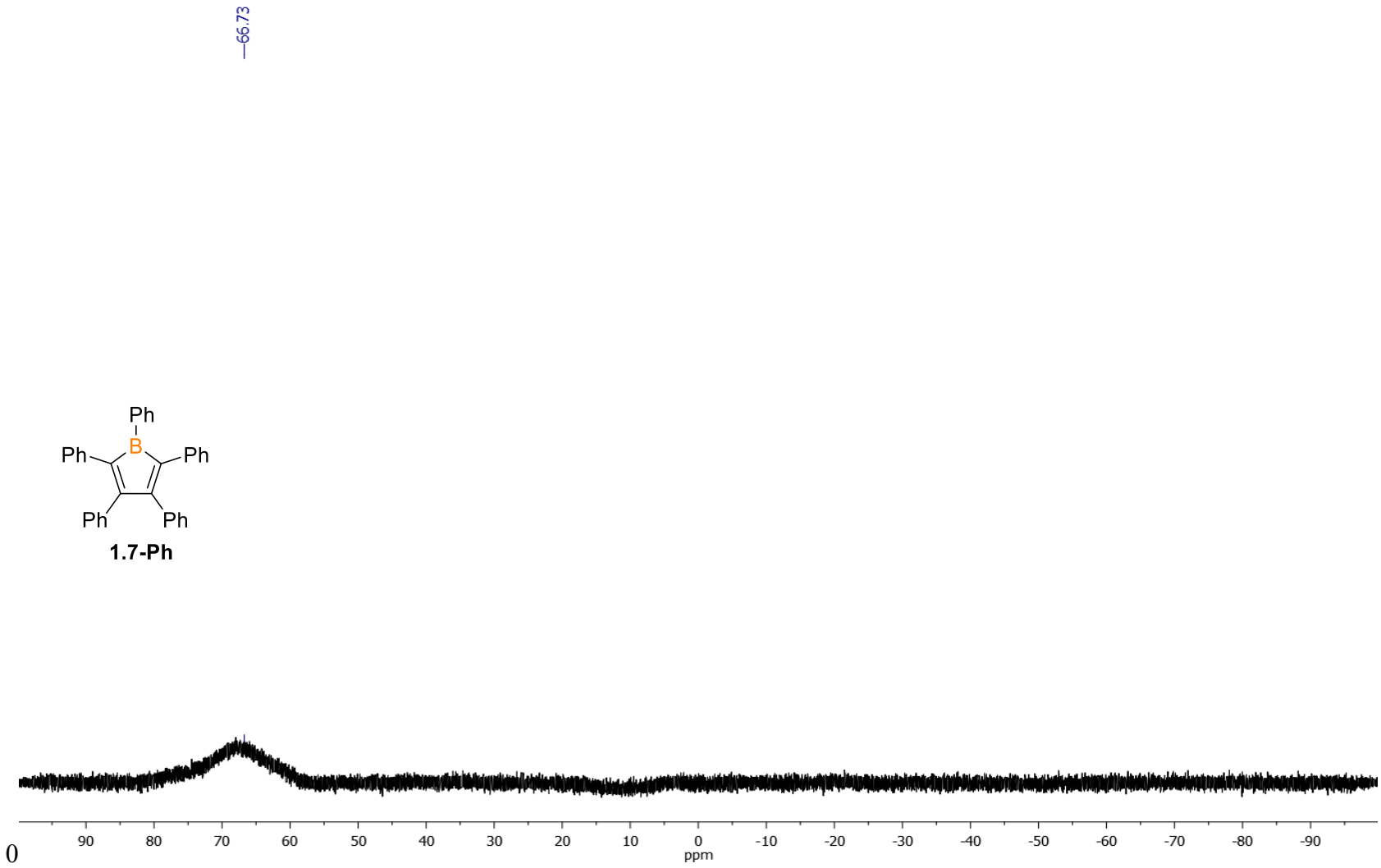

Figure G-6: ^{11}B NMR spectrum of **1.7-Ph** in $CDCl_3$.

BIBLIOGRAPHY

1. Wang, B. J.; Groziak, M. P., Chapter Two - Recent Developments in the Chemistry of Boron Heterocycles. In *Advances in Heterocyclic Chemistry*, Eric, F. V. S.; Christopher, A. R., Eds. Academic Press: 2016; Vol. Volume 118, pp 47-90.

2. Su, Y.; Kinjo, R., Small molecule activation by boron-containing heterocycles. *Chem. Soc. Rev.* **2019**.

3. Su, B.; Kinjo, R., Construction of Boron-Containing Aromatic Heterocycles. *Synthesis* **2017**, *49*, 2985-3034.

4. Yamaguchi, S.; Wakamiya, A., Boron as a key component for new π-electron materials. *Pure Appl. Chem.* **2006**, *78*, 1413.

5. Guo, X.; Baumgarten, M.; Müllen, K., Designing π-conjugated polymers for organic electronics. *Progress in Polymer Science* **2013**, *38*, 1832-1908.

6. Li, G.; Zhao, Y.; Li, J.; Cao, J.; Zhu, J.; Sun, X. W.; Zhang, Q., Synthesis, Characterization, Physical Properties, and OLED Application of Single BN-Fused Perylene Diimide. *J. Org. Chem.* **2015**, *80*, 196-203.

7. Entwistle, C. D.; Marder, T. B., Boron Chemistry Lights the Way: Optical Properties of Molecular and Polymeric Systems. *Angew. Chem. Int. Ed.* **2002**, *41*, 2927-2931.

8. Entwistle, C. D.; Marder, T. B., Applications of Three-Coordinate Organoboron Compounds and Polymers in Optoelectronics. *Chem. Mater.* **2004**, *16*, 4574-4585.

9. Ji, L.; Griesbeck, S.; Marder, T. B., Recent developments in and perspectives on three-coordinate boron materials: a bright future. *Chem. Sci.* **2017**, *8*, 846-863.

10. Giustra, Z. X.; Liu, S.-Y., The State of the Art in Azaborine Chemistry: New Synthetic Methods and Applications. *J. Am. Chem. Soc.* **2018**, *140*, 1184-1194.

11. Baldock, C.; Rafferty, J. B.; Sedelnikova, S. E.; Baker, P. J.; Stuitje, A. R.; Slabas, A. R.; Hawkes, T. R.; Rice, D. W., A mechanism of drug action revealed by structural studies of enoyl reductase. *Science* **1996**, *274*, 2107-2110.

12. Jinna, S.; Finch, J., Spotlight on tavaborole for the treatment of onychomycosis. *Drug Des Devel Ther* **2015**, *9*, 6185-6190.

13. Bodset, M. J. D.; Piers, W. E., B-N as a C-C substitute in aromatic systems. *Can. J. Chem.* **2009**, *87*, 8-29.

14. Morgan, M. M.; Piers, W. E., Efficient synthetic methods for the installation of boron-nitrogen bonds in conjugated organic molecules. *Dalton Trans.* **2016**, *45*, 5920-5924.

15. Campbell, P. G.; Marwitz, A. J. V.; Liu, S.-Y., Recent Advances in Azaborine Chemistry. *Angew. Chem. Int. Ed.* **2012**, *51*, 6074-6092.

16. Steffen, A.; Ward, R. M.; Jones, W. D.; Marder, T. B., Dibenzometallacyclopentadienes, boroles and selected transition metal and main group heterocyclopentadienes: Synthesis, catalytic and optical properties. *Coord. Chem. Rev.* **2010**, *254*, 1950-1976.

17. Braunschweig, H.; Kupfer, T., Recent developments in the chemistry of antiaromatic boroles. *Chem. Commun.* **2011**, *47*, 10903-10914.

18. Braunschweig, H.; Krummenacher, I.; Wahler, J., Chapter One - Free Boroles: The Effect of Antiaromaticity on Their Physical Properties and Chemical Reactivity. In *Adv. Organomet. Chem.*, Hill, A. F.; Fink, M. J., Eds. Academic Press: San Diego, CA, 2013; Vol. 61, pp 1-53.

19. Eisch, J. J.; Hota, N. H.; Kozima, S., Synthesis of pentaphenylborole, a potentially antiaromatic system. *J. Am. Chem. Soc.* **1969**, *91*, 4575-4577.

20. Braunschweig, H.; Fernández, I.; Frenking, G.; Kupfer, T., Structural Evidence for Antiaromaticity in Free Boroles. *Angew. Chem. Int. Ed.* **2008**, *47*, 1951-1954.

21. Barnard, J. H.; Yruegas, S.; Huang, K.; Martin, C. D., Ring expansion reactions of anti-aromatic boroles: a promising synthetic avenue to unsaturated boracycles. *Chem. Commun.* **2016**, *52*, 9985-9991.

22. Xi, Z., 1,4-Dilithio-1,3-dienes: Reaction and Synthetic Applications. *Acc. Chem. Res.* **2010**, *43*, 1342-1351.

23. Yan, X.; Xi, C., Conversion of Zirconacyclopentadienes into Metalloles: Fagan–Nugent Reaction and Beyond. *Acc. Chem. Res.* **2015**, *48*, 935-946.

24. Fagan, P. J.; Burns, E. G.; Calabrese, J. C., Synthesis of boroles and their use in low-temperature Diels-Alder reactions with unactivated alkenes. *J. Am. Chem. Soc.* **1988**, *110*, 2979-2981.

25. Braye, E. H.; Hübel, W.; Caplier, I., New Unsaturated Heterocyclic Systems. I. *J. Am. Chem. Soc.* **1961**, *83*, 4406-4413.

26. Brown, S. G.; Wei, P.; Beck, B. C.; Vohs, J. K.; Robinson, G. H., Synthesis and molecular structure of a novel ring-fused borane derivative $[(PhC)_8C_2H_5]B$. *J. Chem. Crystallogr.* **2001**, *31*, 467-470.

27. Eisch, J. J.; Galle, J. E.; Kozima, S., The physical and chemical consequences of cyclic conjugation in boracyclopolyenes. The antiaromatic character of pentaarylboroles. *J. Am. Chem. Soc.* **1986**, *108*, 379-385.

28. Braunschweig, H.; Chiu, C. W.; Wahler, J.; Radacki, K.; Kupfer, T., Chemical Reduction and Dimerization of 1-Chloro-2,3,4,5-tetraphenylborole. *Chem. Eur. J.* **2010**, *16*, 12229-12233.

29. Ansorg, K.; Braunschweig, H.; Chiu, C. W.; Engels, B.; Gamon, D.; Hügel, M.; Kupfer, T.; Radacki, K., The Pentaphenylborole–2,6-Lutidine Adduct: A System with Unusual Thermochromic and Photochromic Properties. *Angewandte Chemie* **2011**, *50*, 2833-2836.

30. Braunschweig, H.; Chiu, C. W.; Damme, A.; Ferkinghoff, K.; K. Kraft; Radacki, K.; Wahler, J., Unwinding Antiaromaticity in 1-Bromo-2,3,4,5-tetraphenylborole. *Organometallics* **2011**, *30*, 3210-3216.

31. Braunschweig, H.; Damme, A.; Gamon, D.; Kupfer, T.; Radacki, K., Synthesis and Coordination Chemistry of 1-Cymantrenyl-2,3,4,5-tetraphenylborole. *Inorg. Chem.* **2011**, *50*, 4250-4252.

32. Braunschweig, H.; Dyakonov, V.; Jimenez-Halla, J. O. C.; K. Kraft; Krummenacher, I.; Radacki, K.; Sperlich, A.; Wahler, J., An Isolable Radical Anion Based on the Borole Framework. *Angew. Chem. Int. Ed.* **2012**, *51*, 2977-2980.

33. Braunschweig, H.; Chiu, C. W.; Gamon, D.; Gruß, K.; Hörl, C.; Kupfer, T.; Radacki, K.; Wahler, J., Lewis Acid–Base Adducts of 1-Mesityl- and 1-Chloro-2,3,4,5-tetraphenylborole. *Eur. J. Inorg. Chem.* **2013**, 1525-1530.

34. Braunschweig, H.; Hörl, C.; Mailänder, L.; Radacki, K.; Wahler, J., Antiaromaticity to Aromaticity: From Boroles to 1,2-Azaborinines by Ring Expansion with Azides. *Chem. - Eur. J.* **2014**, *20*, 9858-9861.

35. Couchman, S. A.; Thompson, T. K.; Wilson, D. J. D.; Dutton, J. L.; Martin, C. D., Investigating the ring expansion reaction of pentaphenylborole and an azide. *Chem. Commun.* **2014**, *50*, 11724-11726.

36. Braunschweig, H.; Celik, M. A.; Hupp, F.; Krummenacher, I.; Mailänder, L., Formation of BN Isosteres of Azo Dyes by Ring Expansion of Boroles with Azides. *Angew. Chem. Int. Ed.* **2015**, *54*, 6347-6351.

37. Braunschweig, H.; Celik, M.; Dellermann, T.; Frenking, G.; Hammond, K.; Hupp, F.; Kelch, H.; Krummenacher, I.; Lindl, F.; Mailänder, L.; Müssig, J.; Ruppert, A., Scope of the Thermal Ring Expansion Reaction of Boroles with Organoazides. *Chem. - Eur. J.* **2017**, 8006-8013.

38. Barnard, J. H.; Brown, P. A.; Shuford, K. L.; Martin, C. D., 1,2-Phosphaborines: Hybrid Inorganic/Organic P–B Analogues of Benzene. *Angew. Chem. Int. Ed.* **2015**, *54*, 12083-12086.

39. Eisch, J. J.; Galle, J. E., Rearrangements of organometallic compounds. XIII. Boraaromatic systems. IV. Synthesis of heptaphenylborepin via the thermal rearrangement of heptaphenyl-7-borabicyclo[2.2.1]heptadiene. *J. Am. Chem. Soc.* **1975**, *97*, 4436-4437.

40. Baker, J. J.; Al Furaiji, K. H. M.; Liyanage, O. T.; Wilson, D. J. D.; Dutton, J. L.; Martin, C. D., Diverse Reactivity of Dienes with Pentaphenylborole and 1-Phenyl-2,3,4,5-Tetramethylborole Dimer. *Chem. - Eur. J.* **2019**, *25*, 1581-1587.

41. Wang, Z.; Zhou, Y.; Zhang, J.-X.; Krummenacher, I.; Braunschweig, H.; Lin, Z., DFT Studies on the Reactions of Boroles with Alkynes. *Chem. - Eur. J.* **2018**, *24*, 9612-9621.

42. Fukazawa, A.; Dutton, J. L.; Fan, C.; Mercier, L. G.; Houghton, A. Y.; Wu, Q.; Piers, W. E.; Parvez, M., Reaction of pentaarylboroles with carbon monoxide: an isolable organoboron carbonyl complex. *Chem. Sci.* **2012**, *3*, 1814-1818.

43. Wang, Z.; Zhou, Y.; Marder, T. B.; Lin, Z., DFT studies on reactions of boroles with carbon monoxide. *Org. Biomol. Chem.* **2017**, *15*, 7019-7027.

44. Araneda, J. F.; Piers, W. E.; Sgro, M. J.; Parvez, M., Ring Expansion Reactions of Electron-Rich Boron-Containing Heterocycles. *Organometallics* **2015**, *34*, 3408-3413.

45. Houghton, A. Y.; Karttunen, V. A.; Fan, C.; Piers, W. E.; Tuononen, H. M., Mechanistic Studies on the Metal-Free Activation of Dihydrogen by Antiaromatic Pentarylboroles. *J. Am. Chem. Soc.* **2013**, *135*, 941-947.

46. Houghton, A. Y. On the Syntheses and Reactions of Boroles and Boraindenes. Ph.D. Dissertation, University of Calgary, Calgary, AB, CA, 2014.

47. Houghton, A. Y.; Karttunen, V. A.; Piers, W. E.; Tuononen, H. M., Hydrogen activation with perfluorinated organoboranes: 1,2,3-tris(pentafluorophenyl)-4,5,6,7-tetrafluoro-1-boraindene. *Chem. Commun.* **2014**, *50*, 1295-1298.

48. Houghton, A. Y.; Hurmalainen, J.; Mansikkamäki, A.; Piers, W. E.; Tuononen, H. M., Direct observation of a borane–silane complex involved in frustrated Lewis-pair-mediated hydrosilylations. *Nat. Chem.* **2014**, *6*, 983-988.

49. Braunschweig, H.; Damme, A.; Hörl, C.; Kupfer, T.; Wahler, J., Si–H Bond Activation at the Boron Center of Pentaphenylborole. *Organometallics* **2013**, *32*, 6800-6803.

50. Caputo, B. C.; Manning, Z. J.; Barnard, J. H.; Martin, C. D., Reactions of Pentaphenylborole with Main Group Hydrides. *Polyhedron* **2016**, *114*, 273-277.

51. So, C. W.; Watanabe, D.; Wakamiya, A.; Yamaguchi, S., Synthesis and Structural Characterization of Pentaarylboroles and Their Dianions. *Organometallics* **2008**, *27*, 3496-3501.

52. Herberich, G. E.; Buller, B.; Hessner, B.; Oschmann, W., Derivative des borols: II. Pentaphenylborol: Synthese, reduktion zum dianion und komplexe von kobalt und platin. *J. Organomet. Chem.* **1980**, *195*, 253-259.

53. Braunschweig, H.; Chiu, C. W.; Wahler, J.; Radacki, K.; Kupfer, T., Chemical Reduction and Dimerization of 1-Chloro-2,3,4,5-tetraphenylborole. *Chem. - Eur. J.* **2010**, *16*, 12229-12233.

54. Braunschweig, H.; Chiu, C. W.; Gamon, D.; Kaupp, M.; Krummenacher, I.; Kupfer, T.; Müller, R.; Radacki, K., Synthesis, Structure, and Reactivity of Borole-Functionalized Ferrocenes. *Chem. - Eur. J.* **2012**, *18*, 11732-11746.

55. Braunschweig, H.; Damme, A.; Gamon, D.; Kelch, H.; Krummenacher, I.; Kupfer, T.; Radacki, K., Synthesis, Coordination Behavior, and Reduction Chemistry of Cymantrenyl-1,3-bis(2,3,4,5-tetraphenyl)borole. *Chem. - Eur. J.* **2012**, *18*, 8430-8436.

56. Huang, K.; Martin, C. D., Ring Expansion Reactions of Pentaphenylborole with Dipolar Molecules as a Route to Seven-Membered Boron Heterocycles. *Inorg. Chem.* **2015**, *54*, 1869-1875.

57. Huang, K.; Couchman, S. A.; Wilson, D. J. D.; Dutton, J. L.; Martin, C. D., Reactions of Imines, Nitriles, and Isocyanides with Pentaphenylborole: Coordination, Ring Expansion, C–H Bond Activation, and Hydrogen Migration Reactions. *Inorg. Chem.* **2015**, *54*, 8957-8968.

58. Huang, K.; Martin, C. D., Peculiar Reactivity of Isothiocyanates with Pentaphenylborole. *Inorg. Chem.* **2016**, *55*, 330-337.

59. Barnard, J. H.; Yruegas, S.; Couchman, S. A.; Wilson, D. J. D.; Dutton, J. L.; Martin, C. D., Reactivity of a Phosphaalkyne with Pentaarylboroles. *Organometallics* **2016**, *35*, 929–931.

60. Adiraju, V. A. K.; Martin, C. D., Isomer Dependence on the Reactivity of Diazenes with Pentaphenylborole. *Chem. -Eur. J* **2017**, *23*, 11437-11444.

61. Adiraju, V. A. K.; Martin, C. D., C-H addition reactivity of 2-phenylpyridine and 2,2-bipyridine with pentaphenylborole. *Dalton Trans.* **2017**, *46*, 10324-10331.

62. Bluer, K. R.; Laperriere, L. E.; Pujol, A.; Yruegas, S.; Adiraju, V. A. K.; Martin, C. D., Coordination and Ring Expansion of 1,2-Dipolar Molecules with 9-Phenyl-9-borafluorene. *Organometallics* **2018**, *37*, 2917-2927.

63. Köster, R.; Benedikt, G., 9-Borafluorenes. *Angew. Chem. Int. Ed.* **1963**, *2*, 323-324.

64. Iida, A.; Sokioka, A.; Yamaguchi, S., Heteroarene-fused boroles: what governs the antiaromaticity and Lewis acidity of the borole skeleton? *Chem. Sci.* **2012**, *3*, 1461-1466.

65. Yamaguchi, S.; Shirasaka, T.; Akiyama, S.; Tamao, K., Dibenzoborole-Containing π-Electron Systems: Remarkable Fluorescence Change Based on the "On/Off" Control of the pπ−π* Conjugation. *J. Am. Chem. Soc.* **2002**, *124*, 8816-8817.

66. Shoji, Y.; Shigeno, N.; Takenouchi, K.; Sugimoto, M.; Fukushima, T., Mechanistic Study of Highly Efficient Direct 1,2-Carboboration of Alkynes with 9-Borafluorenes. *Chem. - Eur. J.* **2018**, *24*, 13223-13230.

67. Smith, M. F.; Cassidy, S. J.; Adams, I. A.; Vasiliu, M.; Gerlach, D. L.; Dixon, D. A.; Rupar, P. A., Substituent Effects on the Properties of Borafluorenes. *Organometallics* **2016**, *35*, 3182-3191.

68. Biswas, S.; Oppel, I. M.; Bettinger, H. F., Synthesis and Structural Characterization of 9-Azido-9-Borafluorene, Monomer and Cyclotrimer of a Borole Azide. *Inorg. Chem.* **2010**, *49*, 4499-4506.

69. Romero, P. E.; Piers, W. E.; Decker, S. A.; Chau, D.; Woo, T. K.; Parvez, M., η^1 versus η^5 Bonding Modes in Cp*Al(I) Adducts of 9-Borafluorenes. *Organometallics* **2003**, *22*, 1266-1274.

70. Müller, M.; Maichle-Mössmer, C.; Bettinger, H. F., BN-Phenanthryne: Cyclotetramerization of an 1,2-Azaborine Derivative. *Angew. Chem. Int. Ed.* **2014**, *53*, 9380-9383.

71. Urban, M.; Durka, K.; Górka, P.; Wiosna-Sałyga, G.; Nawara, K.; Jankowski, P.; Lulinski, S., The effect of locking π-conjugation in organoboron moieties in the structures of luminescent tetracoordinate boron complexes. *Dalton Trans.* **2019**.

72. Yruegas, S.; Martinez, J. J.; Martin, C. D., Intermolecular insertion reactions of azides into 9-borafluorenes to generate 9,10-B,N-phenanthrenes. *Chem. Commun.* **2018**, *54*, 6808-6811.

73. Berger, C. J.; He, G.; Merten, C.; McDonald, R.; Ferguson, M. J.; Rivard, E., Synthesis and Luminescent Properties of Lewis Base-Appended Borafluorenes. *Inorg. Chem.* **2014**, *53*, 1475-1486.

74. Das, A.; Hübner, A.; Weber, M.; Bolte, M.; Lerner, H.-W.; Wagner, M., 9-H-9-Borafluorene dimethyl sulfide adduct: a product of a unique ring-contraction reaction and a useful hydroboration reagent. *Chem. Commun.* **2011**, *47*, 11339-11341.

75. Laperriere, L. E.; Yruegas, S.; Martin, C. D., Investigating the reactivity of 9-phenyl-9-borafluorene with N-H, O-H, P-H, and S-H bonds. *Tetrahedron* **2019**, *75*, 937-943.

76. Essex, L. A.; Taylor, J. W.; Harman, W. H., Nickel complexes of phosphine-appended benzannulated boron heterocycles. *Tetrahedron* **2019**, *75*, 2255-2260.

77. Cassidy, S. J.; Brettell-Adams, I.; McNamara, L. E.; Smith, M. F.; Bautista, M.; Cao, H.; Vasiliu, M.; Gerlach, D. L.; Qu, F.; Hammer, N. I.; Dixon, D. A.; Rupar, P. A., Boranes with Ultra-High Stokes Shift Fluorescence. *Organometallics* **2018**, *37*, 3732-3741.

78. Biswas, S.; Maichle-Mössmer, C.; Bettinger, H. F., Rearrangement from the heteroantiaromatic borole to the heteroaromatic azaborine motif. *Chem. Commun.* **2012**, *48*, 4564-4566.

79. Kashida, J.; Shoji, Y.; Fukushima, T., Synthesis and Reactivity of Cyclic Borane-Amidine Conjugated Molecules Formed by Direct 1,2-Carboboration of Carbodiimides with 9-Borafluorenes. *Chem. - Asian J.* **2019**, *14*, 1879-1885.

80. Bartholome, T. A.; Bluer, K. R.; Martin, C. D., Successive carbene insertion into 9-phenyl-9-borafluorene. *Dalton Trans.* **2019**, *48*, 6319-6322.

81. Beckett, M. A.; Strickland, G. C.; Holland, J. R.; Sukumar Varma, K., A convenient n.m.r. method for the measurement of Lewis acidity at boron centres: correlation of reaction rates of Lewis acid initiated epoxide polymerizations with Lewis acidity. *Polymer* **1996**, *37*, 4629-4631.

82. Childs, R. F.; Mulholland, D. L.; Nixon, A., The Lewis acid complexes of α,β-unsaturated carbonyl and nitrile compounds. A nuclear magnetic resonance study. *Can. J. Chem.* **1982**, *60*, 801-808.

83. Sivaev, I. B.; Bregadze, V. I., Lewis acidity of boron compounds. *Coord. Chem. Rev.* **2014**, *270-271*, 75-88.

84. Hückel, E., Quantentheoretische Beiträge zum Benzolproblem. *Zeitschrift für Physik* **1931**, *70*, 204-286.

85. Chen, Z.; Wannere, C. S.; Corminboeuf, C.; Puchta, R.; Schleyer, P. v. R., Nucleus-Independent Chemical Shifts (NICS) as an Aromaticity Criterion. *Chem. Rev.* **2005**, *105*, 3842-3888.

86. Stanger, A., Nucleus-Independent Chemical Shifts (NICS): Distance Dependence and Revised Criteria for Aromaticity and Antiaromaticity. *J. Org. Chem.* **2006**, *71*, 883-893.

87. Gershoni-Poranne, R.; Stanger, A., Magnetic criteria of aromaticity. *Chem. Soc. Rev.* **2015**, *44*, 6597-6615.

88. Schleyer, P. v. R.; Maerker, C.; Dransfeld, A.; Jiao, H.; van Eikema Hommes, N. J. R., Nucleus-Independent Chemical Shifts: A Simple and Efficient Aromaticity Probe. *J. Am. Chem. Soc.* **1996**, *118*, 6317-6318.

89. Zhang, W.; Yu, D.; Wang, Z.; Zhang, B.; Xu, L.; Li, G.; Yan, N.; Rivard, E.; He, G., Dibora[10]annulenes: Construction, Properties, and Their Ring-Opening Reactions. *Org. Lett.* **2019**, *21*, 109-113.

90. Jimenez-Halla, J. O. C.; Matito, E.; Sola, M.; Braunschweig, H.; Horl, C.; Krummenacher, I.; Wahler, J., A theoretical study of the aromaticity in neutral and anionic borole compounds. *Dalton Trans.* **2015**, *44*, 6740-6747.

91. Fallah-Bagher-Shaidaei, H.; Wannere, C. S.; Corminboeuf, C.; Puchta, R.; Schleyer, P. v. R., Which NICS Aromaticity Index for Planar π Rings Is Best? *Org. Lett.* **2006**, *8*, 863-866.

92. Herberich, G. E.; Hessner, B.; Ohst, H.; Raap, I. A., Borole derivatives: XI. 1-(Diisopropylamino)borole as ligand in transition metal complexes. Crystal and molecular structures of cis-$Cr(CO)_2(C_4H_4BN^iPr_2)_2$ and $Mn(CO)(C_4H_4BN^iPr_2)_2$. *J. Organomet. Chem.* **1988**, *348*, 305-316.

93. Braunschweig, H.; Kupfer, T., Direct functionalization at the boron center of antiaromatic chloroborole. *Chem. Commun.* **2008**, 4487-4489.

94. Braunschweig, H.; Chiu, C. W.; Radacki, K.; Brenner, P., Platinum Substituted Boroles. *Chem. Commun.* **2010**, *46*, 916-918.

95. Braunschweig, H.; Breher, F.; Chiu, C. W.; Gamon, D.; Nied, D.; Radacki, K., The reduction chemistry of ferrocenylborole. *Angew. Chem. Int. Ed.* **2010**, *49*, 8975-8978.

96. Iida, A.; Yamaguchi, S., Thiophene-Fused Ladder Boroles with High Antiaromaticity. *J. Am. Chem. Soc.* **2011**, *133*, 6952-6955.

97. Lo, P. K.; Lau, K. C., High-Level ab Initio Predictions for the Ionization Energies and Heats of Formation of Five-Membered-Ring Molecules: Thiophene, Furan, Pyrrole, 1,3-Cyclopentadiene, and Borole, $C_4H_4X/C_4H_4X^+$ (X = S, O, NH, CH_2, and BH). *J. Phys. Chem.* **2011**, *115*, 932-939.

98. Braunschweig, H.; Chiu, C. W.; Kupfer, T.; Radacki, K., NHC-Stabilized 1-Hydro-1H-borole and Its Nondegenerate Sigmatropic Isomers. *Inorg. Chem.* **2011**, *50*, 4247-4249.

99. Ansorg, K.; Braunschweig, H.; Chiu, C. W.; Engels, B.; Gamon, D.; Hugel, M.; Kupfer, T.; Radacki, K., The Pentaphenylborole–2,6-Lutidine Adduct: A System with Unusual Thermochromic and Photochromic Properties. *Angew. Chem. Int. Ed.* **2011**, *50*, 2833-2836.

100. Loginov, D. A.; Pronin, A. A.; Starikova, Z. A.; Vologzhanina, A. V.; Petrovskii, P. V.; Kudinov, A. R., (Methoxyborole)cobalt Complexes – Synthesis, Structures and Bonding. *Eur. J. Inorg. Chem.* **2011**, 5422-5429.

101. Araki, T.; Fukazawa, A.; Yamaguchi, S., Electron-Donating Tetrathienyl-Substituted Borole. *Angew. Chem. Int. Ed.* **2012**, *51*, 5484-5487.

102. Braunschweig, H.; Hörl, C.; Hupp, F.; Radacki, K.; Wahler, J., Borole-Derived Spirocyclic Tetraorganoborate. *Organometallics* **2012**, *31*, 8463-8466.

103. Araneda, J. F.; Neue, B.; Piers, W. E.; Parvez, M., Photochemical synthesis of a ladder diborole: a new boron-containing conjugate material. *Angew. Chem. Int. Ed.* **2012**, *51*, 8546-8550.

104. Chen, J.; Chen, S.; Liu, Z.; Feng, H.; Xie, Y.; King, R. B., Terminal versus bridging methylborole ligands and agostic hydrogen atoms in binuclear cobalt carbonyl derivatives. *J. Organomet. Chem.* **2012**, *721*, 104-112.

105. Chen, S.; Chen, J.; Liu, Z.; Feng, H.; Xie, Y.; King, R. B., Binuclear methylborole nickel carbonyls. *Inorg. Chim. Acta* **2012**, *387*, 195-203.

106. Feldmann, A.; Iida, A.; Fröhlich, R.; Yamaguchi, S.; Kehr, G.; Erker, G., Preparation of Dihydroborole Derivatives by a Simple 1,1-Carboboration Route. *Organometallics* **2012**, *31*, 2445-2451.

107. Braunschweig, H.; Damme, A.; Jimenez-Halla, J. O. C.; Hörl, C.; Krummenacher, I.; Kupfer, T.; Mailänder, L.; Radacki, K., 1-Heteroaromatic-Substituted Tetraphenylboroles; π–π Interactions Between Aromatic and Antiaromatic Rings Through a B–C Bond. *J. Am. Chem. Soc.* **2012**, *134*, 20169-20177.

108. Tai, T. B.; Huong, V. T. T.; Nguyen, M. T., Design of aromatic heteropolycyclics containing borole frameworks. *Chem. Commun.* **2013**, *49*, 11548-11550.

109. Bauer, J.; Braunschweig, H.; Hörl, C.; Radacki, K.; Wahler, J., Synthesis of Zwitterionic Cobaltocenium Borate and Borata-alkene Derivatives from a Borole-Radical Anion. *Chem. - Eur. J.* **2013**, *19*, 13396-13401.

110. Qu, Z. W.; Zhu, H., Toward Reversible Dihydrogen Activation by Borole Compounds. *J. Phys. Chem.* **2013**, *117*, 11989-11993.

111. Bertermann, R.; Braunschweig, H.; Dewhurst, R. D.; Hörl, C.; Kramer, T.; Krummenacher, I., Evidence for Extensive Single-Electron-Transfer Chemistry in Boryl Anions: Isolation and Reactivity of a Neutral Borole Radical. *Angew. Chem. Int. Ed.* **2014**, *53*, 5453-5457.

112. Araneda, J. F.; Piers, W. E.; Sgro, M. J.; Parvez, M., Bronsted acid-catalyzed skeletal rearrangements in polycyclic conjugated boracycles: a thermal route to a ladder diborole. *Chem. Sci.* **2014**, *5*, 3189-3196.

113. Ge, F.; Kehr, G.; Daniliuc, C. G.; Erker, G., Borole formation by 1,1-carboboration. *J. Am. Chem. Soc.* **2014**, *136*, 68-71.

114. Weber, L.; Halama, J.; Hanke, K.; Bohling, L.; Brockhinke, A.; Stammler, H.-G.; Neumann, B.; Fox, M. A., On the ambiguity of 1,3,2-benzodiazaboroles as donor/acceptor functionalities in luminescent molecules. *Dalton Trans.* **2014**, *43*, 3347-3363.

115. Ge, F.; Kehr, G.; Daniliuc, C. G.; Erker, G., Reactions of Boroles Formed by 1,1-Carboboration. *Organometallics* **2015**, *34*, 229-235.

116. Zhang, Z.; Edkins, R. M.; Haehnel, M.; Wehner, M.; Eichhorn, A.; Mailänder, L.; Meier, M.; Brand, J.; Brede, F.; Muller-Buschbaum, K.; Braunschweig, H.; Marder, T. B., Taming the beast: fluoromesityl groups induce a dramatic stability enhancement in boroles. *Chem. Sci.* **2015**, *6*, 5922-5927.

117. Braunschweig, H.; Krummenacher, I.; Mailänder, L.; Rauch, F., O,N,B-Containing eight-membered heterocycles by ring expansion of boroles with nitrones. *Chem. Commun.* **2015**, *51*, 14513-14515.

118. Braunschweig, H.; Hupp, F.; Krummenacher, I.; Mailänder, L.; Rauch, F., Ring Expansions of Boroles with Diazo Compounds: Steric Control of C or N Insertion and Aromatic/Nonaromatic Products. *Chem. - Eur. J.* **2015**, *21*, 17844-17849.

119. Fan, C.; Piers, W. E.; Parvez, M., Perfluoropentaphenylborole. *Angew. Chem. Int. Ed.* **2009**, *48*, 2955-2958.

120. Fan, C.; Mercier, L. G.; Piers, W. E.; Tuononen, H. M.; Parvez, M., Dihydrogen Activation by Antiaromatic Pentaarylboroles. *J. Am. Chem. Soc.* **2010**, *132*, 9604-9606.

121. Fan, C.; Piers, W. E.; Parvez, M.; McDonald, R., Divergent Reactivity of Perfluoropentaphenylborole with Alkynes. *Organometallics* **2010**, *29*, 5132-5139.

122. Welch, G. C.; Juan, R. R. S.; Masuda, J. D.; Stephan, D. W., Reversible, Metal-Free Hydrogen Activation. *Science* **2006**, *314*, 1124-1126.

123. Stephan, D. W.; Erker, G., Frustrated Lewis Pairs: Metal-free Hydrogen Activation and More. *Angew. Chem. Int. Ed.* **2010**, *49*, 46-76.

124. Stephan, D. W., "Frustrated Lewis Pair" hydrogenations. *Org. Biomol. Chem.* **2012**, *10*, 5740-5746.

125. Stephan, D. W., Frustrated Lewis pairs: A metal-free landmark. *Nat Chem* **2014**, *6*, 952-953.

126. Stephan, D. W., Frustrated Lewis Pairs: From Concept to Catalysis. *Acc. Chem. Res.* **2015**, *48*, 306-316.

127. Wilkins, L. C.; Wieneke, P.; Newman, P. D.; Kariuki, B. M.; Rominger, F.; Hashmi, A. S. K.; Hansmann, M. M.; Melen, R. L., Pathways to Functionalized Heterocycles: Propargyl Rearrangement using $B(C_6F_5)_3$. *Organometallics* **2015**, *34*, 5298-5309.

128. Bielawski, J.; Niedenzu, K., Boron-nitrogen compounds. 110. Reactions of boroxins and diboroxanes with pyrazole. *Inorg. Chem.* **1986**, *25*, 1771-1774.

129. Lange, T.; Böhme, U.; Roewer, G., Crystal structure of tetraphenyldiboroxane a monomer diboroxane. *Inorg. Chem. Commun.* **2002**, *5*, 377-379.

130. Kaufmann, L.; Lerner, H.-W.; Bolte, M., A new polymorph of tetraphenyldiboroxane. *Acta Crystallogr.* **2007**, *63*, 588-590.

131. Walkowiak, J.; Marciniec, B., A new catalytic method for the synthesis of boroxanes. *Tetrahedron Lett.* **2010**, *51*, 6177-6180.

132. Aldridge, S., Group III- B, Al, Ga, In, Tl. In *Organomet. Chem.*, Green, M., Ed. 2007; Vol. 33, pp 102-155.

133. Ashby, M. T.; Sheshtawy, N. A., Barriers to rotation about the B-X bonds of coordinatively unsaturated borates and thioborates R_2BXR' (X = O, S) are not measures of the relative strengths of their B:O and B:S π bonds. *Organometallics* **1994**, *13*, 236-243.

134. Franz, D.; Irran, E.; Inoue, S., Isolation of a Three-Coordinate Boron Cation with a Boron–Sulfur Double Bond. *Angew. Chem. Int. Ed.* **2014**, *53*, 14264-14268.

135. Rohr, A. D.; Banaszak Holl, M. M.; Kampf, J. W.; Ashe III, A. J., 2H-1,2-Thiaborin: A New Boron–Sulfur Heterocycle. *Organometallics* **2011**, *30*, 3698-3700.

136. The same low temperature $^{11}B\{^1H\}$ NMR spectroscopy experiments were performed for the reactions forming **2.13** and **2.14**, but intermediates were not observed.

137. Harshbarger, W.; Lee, G. H.; Porter, R. F.; Bauer, S. H., Structure of borazine. *Inorg. Chem.* **1969**, *8*, 1683-1689.

138. Jäschke, T.; Jansen, M., Synthesis, Crystal Structure, and Spectroscopic Characterization of the Borazine Derivatives $[B\{CH_2(SiCl_3)\}NH]_3$ and $[B\{CH_2(SiCl_2CH_3)\}NH]_3$. *Z. Anorg. Allg. Chem.* **2004**, *630*, 239-243.

139. Bourumeau, K.; Gaumont, A.-C.; Denis, J.-M., Hydrophosphination of α,β-unsaturated esters by primary phosphine-boranes; a useful entry to symmetrical and unsymmetrical phosphine-boranes. *Tetrahedron Lett.* **1997**, *38*, 1923-1926.

140. Dias, H. V. R.; Pestana, D. C.; Petrie, M.; Power, P. P., Synthesis and Reactions of Novel Boron-Phosphorus Compounds. *Phosphorus, Sulfur Silicon Relat. Elem.* **1990**, *51*, 87-91.

141. Geier, S. J.; Gilbert, T. M.; Stephan, D. W., Synthesis and Reactivity of the Phosphinoboranes $R_2PB(C_6F_5)_2$. *Inorg. Chem.* **2011**, *50*, 336-344.

142. Geier, S. J.; Gilbert, T. M.; Stephan, D. W., Activation of H_2 by Phosphinoboranes $R_2PB(C_6F_5)_2$. *J. Am. Chem. Soc.* **2008**, *130*, 12632-12633.

143. Power, W. P., Phosphorus-31 Solid-State NMR of a Phosphine-Borane Adduct: Phosphorus Chemical Shielding Trends in the Isoelectronic Series R_3PX, where X = BH_3, CH_2, NH, O. *J. Am. Chem. Soc.* **1995**, *117*, 1800-1806.

144. Pyykkö, P.; Atsumi, M., Molecular Single-Bond Covalent Radii for Elements 1–118. *Chem. - Eur. J.* **2009**, *15*, 186-197.

145. Frisch, M. J.; Trucks, G. W.; Schlegel, H. B.; Scuseria, G. E.; Robb, M. A.; Cheeseman, J. R.; Scalmani, G.; Barone, V.; Mennucci, B.; Petersson, G. A.; Nakatsuji, H.; Caricato, M.; Li, X.; Hratchian, H. P.; Izmaylov, A. F.; Bloino, J.; Zheng, G.; Sonnenberg, J. L.; Hada, M.; Ehara, M.; Toyota, K.; Fukuda, R.; Hasegawa, J.; Ishida, M.; Nakajima, T.; Honda, Y.; Kitao, O.; Nakai, H.; Vreven, T.; Montgomery Jr., J. A.; Peralta, J. E.; Ogliaro, F.; Bearpark, M.; Heyd, J. J.; Brothers, E.; Kudin, K. N.; Staroverov, V. N.; Kobayashi, R.; Normand, J.; Raghavachari, K.; Rendell, A.; Burant, J. C.; Iyengar, S. S.; Tomasi, J.; Cossi, M.; Rega, N.; Millam, J. M.; Klene, M.; Knox, J. E.; Cross, J. B.; Bakken, V.; Adamo, C.; Jaramillo, J.; Gomperts, R.; Stratmann, R. E.; Yazyev, O.; Austin, A. J.; Cammi, R.; Pomelli, C.; Ochterski, J. W.; Martin, R. L.; Morokuma, K.; Zakrzewski, V. G.; Voth, G. A.; Salvador, P.; Dannenberg, J. J.; Dapprich, S.; Daniels, A. D.; Farkas, Ö.; Foresman, J. B.; Ortiz, J. V.; Cioslowski, J.; Fox, D. J. Gaussian 09, Revision D.01 Gaussian, Inc.: Wallingford CT, 2009.

146. Zhao, Y.; Truhlar, D. G., The M06 suite of density functionals for main group thermochemistry, thermochemical kinetics, noncovalent interactions, excited states, and transition elements: two new functionals and systematic testing of four M06-class functionals and 12 other. *Theor. Chem. Acc.* **2008**, *120*, 215-241.

147. Hariharan, P. C.; Pople, J. A., The influence of polarization functions on molecular orbital hydrogenation energies. *Theoret. Chim. Acta* **1973**, *28*, 213-222.

148. Hehre, W. J.; Ditchfield, R.; Pople, J. A., Self—Consistent Molecular Orbital Methods. XII. Further Extensions of Gaussian—Type Basis Sets for Use in Molecular Orbital Studies of Organic Molecules. *J. Chem. Phys.* **1972**, *56*, 2257-2261.

149. Peng, C.; Ayala, P. Y.; Schlegel, H. B.; Frisch, M. J., Using redundant internal coordinates to optimize equilibrium geometries and transition states. *J. Comp. Chem.* **1996**, *17*, 49-56.

150. Eisch, J. J.; Galle, J. E.; Shafii, B.; Rheingold, A. L., Thermal generation and transformation of the borepin ring system; a paradigm of pericyclic processes. *Organometallics* **1990**, *9*, 2342-2349.

151. Braunschweig, H.; Maier, J.; Radacki, K.; Wahler, J., Ring Expansion of 7-Boranorbornadienes by Coordination with an N-Heterocyclic Carbene. *Organometallics* **2013**, *32*, 6353-6359.

152. Yruegas, S.; Patterson, D. C.; Martin, C. D., Oxygen insertion into boroles as a route to 1,2-oxaborines. *Chem. Commun.* **2016**, *52*, 6658-6661.

153. Zhang, Z.; Wang, Z.; Haehnel, M.; Eichhorn, A.; Edkins, R. M.; Steffen, A.; Krueger, A.; Lin, Z.; Marder, T. B., Synthesis and fluxional behaviour of novel chloroborole dimers. *Chem. Commun.* **2016**, *52*, 9707-9710.

154. Yruegas, S.; Martin, C. D., Expedient Synthesis of 1,2-Thiaborines via Sulfur Insertion into Boroles. *Chem. - Eur. J.* **2016**, *22*, 18358-18361.

155. Braunschweig, H.; Geethrani, K.; Jimenez-Halla, J. O. C.; Schäfer, M., Direct Synthetic Route to Functionalized 1,2-Azaborinines. *Angew. Chem. Int. Ed.* **2014**, *53*, 3500-3504.

156. Childers, M. I.; Longo, J. M.; Van Zee, N. J.; LaPointe, A. M.; Coates, G. W., Stereoselective Epoxide Polymerization and Copolymerization. *Chem. Rev.* **2014**, *114*, 8129-8152.

157. Herzberger, J.; Niederer, K.; Pohlit, H.; Seiwert, J.; Worm, M.; Wurm, F. R.; Frey, H., Polymerization of Ethylene Oxide, Propylene Oxide, and Other Alkylene Oxides: Synthesis, Novel Polymer Architectures, and Bioconjugation. *Chem. Rev.* **2016**, *116*, 2170-2243.

158. Faiz, S.; Zahoor, A. F., Ring opening of epoxides with C-nucleophiles. *Molec. Divers.* **2016**, *20*, 969-987.

159. Moloy, K. G., A Simple, Effective Boron-Halide Ethoxylation Catalyst. *Adv. Synth. Catal.* **2010**, *352*, 821-826.

160. Yruegas, S.; Huang, K.; Wilson, D. J. D.; Dutton, J. L.; Martin, C. D., Probing the reactivity of pentaphenylborole with N-H, O-H, P-H, and S-H bonds. *Dalton Trans.* **2016**, *45*, 9902-9911.

161. Brown, H. C.; Phadke, A. S.; Rangaishenvi, M. V., Ring enlargement of boracyclanes via sequential one carbon homologation. The first synthesis of boracyclanes in the strained medium ring range. *J. Am. Chem. Soc.* **1988**, *110*, 6263-6264.

162. On the basis of previous reactivity, the zwitterionic mechanism seems most likely, as only *cis* substituents are observed in the rapid reaction. We believe a radical process would result in a mixture of isomers, which is not observed experimentally by X-ray crystallography, ^{1}H NMR, or $^{13}C\{^{1}H\}$ NMR spectroscopy.

163. The reaction of **3.7** with 1 equiv of cyclohexene oxide, under the same reaction conditions as for the formation of **3.8**, did not lead to a ring expansion product similar to **3.8**. No reaction occurred even upon stirring for 24 h.

164. We have not, however, been able to optimize the geometry of this intermediate, and it may not be a distinct minimum on the potential energy surface of the reaction.

165. Becke, A. D., Density-functional exchange-energy approximation with correct asymptotic behavior. *Phys. Rev. A* **1988**, *38*, 3098-3100.

166. Marwitz, A. J. V.; Matus, M. H.; Zakharov, L. N.; Dixon, D. A.; Liu, S.-Y., A Hybrid Organic/Inorganic Benzene. *Angew. Chem. Int. Ed.* **2009**, *48*, 972-977.

167. Morgan, M. M.; Piers, W. E., Efficient synthetic methods for the installation of boron-nitrogen bonds in conjugated organic molecules. *Dalton Trans.* **2016**.

168. Escande, A.; Ingleson, M. J., Fused polycyclic aromatics incorporating boron in the core: fundamentals and applications. *Chem. Commun.* **2015**, *51*, 6257-6274.

169. III, A. J. A.; Fang, X.; Fang, X.; Kampf, J. W., Synthesis of 1,2-Dihydro-1,2-azaborines and Their Conversion to Tricarbonyl Chromium and Molybdenum Complexes. *Organometallics* **2001**, *20*, 5413-5418.

170. Abbey, E. R.; Zakharov, L. N.; Liu, S.-Y., Crystal Clear Structural Evidence for Electron Delocalization in 1,2-Dihydro-1,2-azaborines. *J. Am. Chem. Soc.* **2008**, *130*, 7250-7252.

171. Xu, S.; Zakharov, L. N.; Liu, S.-Y., A 1,3-Dihydro-1,3-azaborine Debuts. *J. Am. Chem. Soc.* **2011**, *133*, 20152-20155.

172. Braunschweig, H.; Damme, A.; Jimenez-Halla, J. O. C.; Pfaffinger, B.; Radacki, K.; Wolf, J., Metal-Mediated Synthesis of 1,4-Di-tert-butyl-1,4-azaborine. *Angew. Chem. Int. Ed.* **2012**, *51*, 10034-10037.

173. Chrostowska, A.; Xu, S.; Lamm, A. N.; Mazière, A.; Weber, C. D.; Dargelos, A.; Baylère, P.; Graciaa, A.; Liu, S.-Y., UV-Photoelectron Spectroscopy of 1,2- and 1,3-Azaborines: A Combined Experimental and Computational Electronic Structure Analysis. *J. Am. Chem. Soc.* **2012**, *134*, 10279-10285.

174. Xu, S.; Mikulas, T. C.; Zakharov, L. N.; Dixon, D. A.; Liu, S.-Y., Boron-Substituted 1,3-Dihydro-1,3-azaborines: Synthesis, Structure, and Evaluation of Aromaticity. *Angew. Chem. Int. Ed.* **2013**, *52*, 7527-7531.

175. Abbey, E. R.; Lamm, A. N.; Baggett, A. W.; Zakharov, L. N.; Liu, S.-Y., Protecting Group-Free Synthesis of 1,2-Azaborines: A Simple Approach to the Construction of BN-Benzenoids. *J. Am. Chem. Soc.* **2013**, *135*, 12908-12913.

176. Marwitz, A. J. V.; Jenkins, J. T.; Zakharov, L. N.; Liu, S.-Y., 1,2-Azaborine Cations. *Angew. Chem. Int. Ed.* **2010**, *49*, 7444-7447.

177. Wang, X. Y.; Lin, H. R.; Lei, T.; Yang, D. C.; Zhuang, F. D.; Wang, J. Y.; Yuan, S. C.; Pei, J., Azaborine Compounds for Organic Field-Effect Transistors: Efficient Synthesis, Remarkable Stability, and BN Dipole Interactions. *Angew. Chem. Int. Ed.* **2013**, *52*, 3117-3120.

178. Baggett, A. W.; Guo, F.; Li, B.; Liu, S.-Y.; Jäkle, F., Regioregular Synthesis of Azaborine Oligomers and a Polymer with a syn Conformation Stabilized by N-H···π Interactions. *Angew. Chem. Int. Ed.* **2015**, *54*, 11191-11195.

179. Liu, L.; Marwitz, A. J. V.; Matthews, B. W.; Liu, S.-Y., Boron Mimetics: 1,2-Dihydro-1,2-azaborines Bind inside a Nonpolar Cavity of T4 Lysozyme. *Angew. Chem. Int. Ed.* **2009**, *121*, 6949-6951.

180. Kahlert, J.; Austin, C. J. D.; Kassiou, M.; Rendina, L. M., The Fifth Element in Drug Design: Boron in Medicinal Chemistry. *Aust. J. Chem.* **2013**, *66*, 1118-1123.

181. Ingleson, M. J., Boron, aluminium, gallium, indium and thallium. *Annu. Rep., Sect A : Inorg. Chem.* **2013**, *109*, 28-52.

182. Baranac-Stojanović, M., Aromaticity and Stability of Azaborines. *Chem.-Eur. J.* **2014**, *20*, 16558-16565.

183. Braunschweig, H.; Hörl, C.; Mailänder, L.; Radacki, K.; Wahler, J., Antiaromaticity to Aromaticity: From Boroles to 1,2-Azaborinines by Ring Expansion with Azides. *Chem.-Eur. J.* **2014**, *20*, 9858-9861.

184. Burford, R. J.; Li, B.; Vasiliu, M.; Dixon, D. A.; Liu, S.-Y., Diels–Alder Reactions of 1,2-Azaborines. *Angew. Chem. Int. Ed.* **2015**, *54*, 7823-7827.

185. Molander, G. A.; Wisniewski, S. R.; Amani, J., Accessing an Azaborine Building Block: Synthesis and Substitution Reactions of 2-Chloromethyl-2,1-borazaronaphthalene. *Org. Lett.* **2014**, *16*, 5636-5639.

186. Amani, J.; Molander, G. A., Toward Efficient Nucleophilic Azaborine Building Blocks for the Synthesis of B–N Naphthyl (Hetero)arylmethane Isosteres. *Org. Lett.* **2015**, *17*, 3624-3627.

187. Letsinger, R. L.; Nazy, J. R., Organoboron Compounds. XI. Isomerization of 2,2'-Tolandiboronic Acid. *J. Am. Chem. Soc.* **1959**, *81*, 3013-3017.

188. Dewar, M. J. S.; Dietz, R., Aromatic boron-oxygen heterocycles. *Tetrahedron Lett.* **1959**, *1*, 21-23.

189. Dewar, M. J. S.; Dietz, R., 269. New heteroaromatic compounds. Part V. Some 9,10-boroxarophenanthrenes. *J. Chem. Soc.* **1960**, 1344-1347.

190. Davis, F. A.; Dewar, M. J. S., 10-Hydroxy-10,9-boroxarophenanthrene. A Lewis acid. *J. Org. Chem.* **1968**, *33*, 3324-3326.

191. Grisdale, P. J.; Williams, J. L. R., Boron photochemistry. V. Photochemical syntheses of the borazarophenanthrene, boroxarophenanthrene and the borathiarophenanthrene ring systems. *J. Org. Chem.* **1969**, *34*, 1675-1677.

192. Arcus, V. L.; Main, L.; Nicholson, B. K., ortho-Directed electrophilic boronation of a benzyl ketone: the preparation, X-ray crystal structure, and some reactions of 4-ethyl-1-hydroxy-3-(4-hydroxyphenyl)-2-oxa-1-boranaphthalene. *J. Organomet. Chem.* **1993**, *460*, 139-147.

193. Minyaev, R. M.; Minkin, V. I.; Gribanova, T. N.; Starikov, A. G., Novel aromatic oxaborabenzene and 9-oxa-1,8-diboranaphthalene systems: an ab initio study. *Mendeleev Commun.* **2001**, *11*, 43-44.

194. Zhou, Q. J.; Worm, K.; Dolle, R. E., 10-Hydroxy-10,9-boroxarophenanthrenes: Versatile Synthetic Intermediates to 3,4-Benzocoumarins and Triaryls. *J. Org. Chem.* **2004**, *69*, 5147-5149.

195. Paetzold, P.; Stanescu, C.; Stubenrauch, J. R.; Bienmüller, M.; Englert, U., 1-Azonia-2-boratanaphthalenes. *Z. Anorg. Allg. Chem.* **2004**, *630*, 2632-2640.

196. Sumida, Y.; Harada, R.; Kato-Sumida, T.; Johmoto, K.; Uekusa, H.; Hosoya, T., Boron-Selective Biaryl Coupling Approach to Versatile Dibenzoxaborins and Application to Concise Synthesis of Defucogilvocarcin M. *Org. Lett.* **2014**, *16*, 6240-6243.

197. Guo, R.; Li, K.-N.; Liu, B.; Zhu, H.-J.; Fan, Y.-M.; Gong, L.-Z., Asymmetric synthesis of heteroaryl atropisomers via a gold-catalyzed cycloisomerization-amination cascade reaction. *Chem. Commun.* **2014**, *50*, 5451-5454.

198. Budanow, A.; Sinke, T.; Lerner, H.-W., Packing considerations of 10-oxa-9-boraphenanthrene derivatives. *Acta. Cryst. C.* **2014**, *70*, 662-667.

199. Koster, R.; Pourzal, A.-A., Kondensationprodukte von Alkyl-phenylketonen. *Synthesis* **1973**, *11*, 674-676.

200. Chen, J.; Bajko, Z.; Kampf, J. W.; Ashe, A. J., 1,2-Dihydro-1,2-oxaborine: A Boron−Oxygen Heterocycle Isoelectronic with Benzene. *Organometallics* **2007**, *26*, 1563-1564.

201. Davis, F. A.; Dewar, M. J. S., New heteroaromatic compounds. XXX. A derivative of 10,9-borathiarophenanthrene. *J. Am. Chem. Soc.* **1968**, *90*, 3511-3515.

202. Barnes, S. S.; Vogels, C. M.; Decken, A.; Westcott, S. A., Addition of boranes to N-aryl-salicylaldimines: Intramolecular hydrogenation of imines. *Dalton Trans.* **2011**, *40*, 4707-4714.

203. Loh, Y. K.; Chong, C. C.; Ganguly, R.; Li, Y.; Vidovic, D.; Kinjo, R., 1,2,4,3-Triazaborole-based neutral oxoborane stabilized by a Lewis acid. *Chem. Commun.* **2014**, *50*, 8561-8564.

204. Han, R.; Hillhouse, G. L., Sulfur-Atom Transfer from Elemental Sulfur to Nickel−Carbon Bonds as a New Route to Reactive Nickel(II) Thiolates. *J. Am. Chem. Soc.* **1998**, *120*, 7657-7658.

205. Sahoo, S.; Mobin, S. M.; Ghosh, S., Direct insertion of sulfur, selenium and tellurium atoms into metallaborane cages using chalcogen powders. *J. Organomet. Chem.* **2010**, *695*, 945-949.

206. Wang, H.; Zhang, J.; Hu, H.; Cui, C., Access to BdS and BdSe Double Bonds via Sulfur and Selenium Insertion into a B-H Bond and Hydrogen Migration. *J. Am. Chem. Soc.* **2010**, *132*, 10998–10999.

207. Meng, L.; Fujikawa, T.; Kuwayama, M.; Segawa, Y.; Itami, K., Thiophene-Fused π-Systems from Diarylacetylenes and Elemental Sulfur. *J. Am. Chem. Soc.* **2016**, *138*, 10351-10355.

208. Nguyen, T. B., Recent Advances in Organic Reactions Involving Elemental Sulfur. *Adv. Synth. Catal.* **2017**, *359*, 1066-1130.

209. Mitzel, N. W.; Losehand, U., Dimethyl-, Disilyl- and Digermylsulfide: Different Intermolecular Contacts in the Solid State *Z. Naturforsch. B Chem. Sci* **2004**, 635.

210. Watson, M. D.; Fechtenkötter, A.; Müllen, K., Big Is Beautiful−"Aromaticity" Revisited from the Viewpoint of Macromolecular and Supramolecular Benzene Chemistry. *Chem. Rev.* **2001**, *101*, 1267-1300.

211. Anthony, J. E., Functionalized Acenes and Heteroacenes for Organic Electronics. *Chem. Rev.* **2006**, *106*, 5028-5048.

212. Liu, Z.; Marder, T. B., B□N versus C□C: How Similar Are They? *Angew. Chem. Int. Ed.* **2008**, *47*, 242-244.

213. Velinova, M.; Georgiev, V.; Todorova, T.; Madjarova, G.; Ivanova, A.; Tadjer, A., Boron–nitrogen- and boron-substituted anthracenes and -phenanthrenes as models for doped carbon-based materials. *J. Mol. Struct. (Theochem)* **2010**, *955*, 97-108.

214. Helten, H., B=N Units as Part of Extended π-Conjugated Oligomers and Polymers. *Chem. - Eur. J.* **2016**, *22*, 12972-12982.

215. von Grotthuss, E.; John, A.; Kaese, T.; Wagner, M., Doping Polycyclic Aromatics with Boron for Superior Performance in Materials Science and Catalysis. *Asian J. Org. Chem.* **2018**, *7*, 37-53.

216. Hashimoto, S.; Ikuta, T.; Shiren, K.; Nakatsuka, S.; Ni, J.; Nakamura, M.; Hatakeyama, T., Triplet-Energy Control of Polycyclic Aromatic Hydrocarbons by BN Replacement: Development of Ambipolar Host Materials for Phosphorescent Organic Light-Emitting Diodes. *Chem. Mater.* **2014**, *26*, 6265-6271.

217. Wang, B. J.; Groziak, M. P., Chapter Two - Recent Developments in the Chemistry of Boron Heterocycles. In *Advances in Heterocyclic Chemistry*, Eric, F. V. S.; Christopher, A. R., Eds. Academic Press: 2016; Vol. 118, pp 47-90.

218. Baumgartner, T.; Jaekle, F., *Main Group Strategies Towards Functional Hybrid Materials*. Wiley: 2018.

219. Braunschweig, H.; Hupp, F.; Krummenacher, I.; Mailänder, L.; Rauch, F., Ring Expansions of Boroles with Diazo Compounds: Steric Control of C or N Insertion and Aromatic/Nonaromatic Products. *Chem.-Eur. J.* **2015**, *21*, 17844-17849.

220. Yruegas, S.; Martin, C. D., Expedient Synthesis of 1,2-Thiaborines via Sulfur Insertion into Boroles. *Chem. -Eur. J.* **2016**, *22*, 18358-18361.

221. Braunschweig, H.; Celik, M.; Dellermann, T.; Frenking, G.; Hammond, K.; Hupp, F.; Kelch, H.; Krummenacher, I.; Lindl, F.; Mailänder, L.; Müssig, J.; Ruppert, A., Scope of the Thermal Ring Expansion Reaction of Boroles with Organoazides. *Chem. -Eur. J.* **2017**, 8006-8013.

222. Yruegas, S.; Wilson, C.; Dutton, J. L.; Martin, C. D., Ring Opening of Epoxides Induced by Pentaphenylborole. *Organometallics* **2017**, *36*, 2581-2587.

223. Adiraju, V. A. K.; Martin, C. D., Isomer Dependence on the Reactivity of Diazenes with Pentaphenylborole. *Chem.-Eur. J* **2017**, *23*, 11437-11444.

224. Giustra, Z. X.; Liu, S.-Y., The State of the Art in Azaborine Chemistry: New Synthetic Methods and Applications. *J. Am. Chem. Soc.* **2018**, *140*, 1184-1194.

225. Chase, P. A.; Piers, W. E.; Patrick, B. O., New Fluorinated 9-borafluorene lewis acids. *J. Am. Chem. Soc.* **2000**, *122*, 12911-12912.

226. Wakamiya, A.; Mishima, K.; Ekawa, K.; Yamaguchi, S., Kinetically stabilized dibenzoborole as an electron-accepting building unit. *Chem. Commun.* **2008**, 579-581.

227. Muhammad, S.; Janjua, M. R.; Su, Z., Investigation of Dibenzoboroles Having π-Electrons: Toward a New Type of Two-Dimensional NLO Molecular Switch? *J. Phys. Chem. C* **2009**, *113*, 12551–12557.

228. Adams, I. A.; Rupar, P. A., A Poly(9-Borafluorene) Homopolymer: An Electron-Deficient Polyfluorene with "Turn-On" Fluorescence Sensing of NH3 Vapor. *Macromol. Rapid Commun.* **2015**, *36*, 1336-1340.

229. Köster, R.; Willemsen, H.-G., Borverbindungen XXVIII1) 1,2-(2,2′-Biphenylylen)diborane(6). *Justus Liebigs Ann. Chem* **1974**, *1974*, 1843-1850.

230. Hübner, A.; Qu, Z. W.; Englert, U.; Bolte, M.; Lerner, H. W.; Holthausen, M. C.; Wagner, M., Main-chain boron-containing oligophenylenes via ring-opening polymerization of 9-H-9-borafluorene. *J. Am. Chem. Soc.* **2011**, *133*, 4596-609.

231. Hübner, A.; Diehl, A. M.; Lerner, H.-W.; Wagner, M., High-Temperature Reactivity of the Strongly Electrophilic Pristine 9H-9-Borafluorene. *Organometallics* **2013**, *32*, 6827-6833.

232. Hübner, A.; Bolte, M.; Lerner, H.-W.; Wagner, M., Extensive Structural Rearrangements upon Reduction of 9H-9-Borafluorene. *Angew. Chem. Int. Ed.* **2014**, *53*, 10408-10411.

233. Bettinger, H. F.; Müller, M., Pathways for the cyclotetramerization of dibenz[c,e][1,2]azaborine, a BN-phenanthryne. *J. Phys. Org. Chem.* **2015**, *28*, 97-103.

234. Shoji, Y.; Tanaka, N.; Muranaka, S.; Shigeno, N.; Sugiyama, H.; Takenouchi, K.; Hajjaj, F.; Fukushima, T., Boron-mediated sequential alkyne insertion and C–C coupling reactions affording extended π-conjugated molecules. *Nature Comm.* **2016**, *7*, 12704-12711.

235. Beckett, M. A.; Strickland, G. C.; Holland, J. R.; Varma, K. S., A convenient n.m.r method for the measurement of Lewis acidity at boron centres: correlation of reaction rates of Lewis acid initiated epoxide polymerizations with Lewis acidity. *Polymer* **1996**, *37*, 4629-4631.

236. It is unclear why incorporation of the γ-nitrogen of PhN_3 is observed in the reaction with **5.6** rather than α-nitrogen. Computational mechanistic studies are the subject of follow up work to provide insight into the kinetics and thermodynamics of these reactions."

237. Budanow, A.; von Grotthuss, E.; Bolte, M.; Wagner, M.; Lerner, H.-W., 10,9-Oxaboraphenanthrenes as luminescent fluorophores. *Tetrahedron* **2016**, *72*, 1477-1484.

238. Similar boron heterocycles bearing phenyl groups on adjacent boron and nitrogen atoms within the ring have shown disorder. Therefore, the bond distances and bond angles are not discussed in detail.

239. Zhou, W.-Q.; Peng, H.-P.; Xu, J.-K.; Xia, H.-Y.; Pu, S.-Z., Electrochemical polymerization of phenanthrene in mixed electrolytes of boron trifluoride diethyl etherate and concentrated sulfuric acid. *Polym. Int.* **2008**, *57*, 92-98.

240. Aldred, M. P.; Li, C.; Zhu, M.-Q., Optical Properties and Photo-Oxidation of Tetraphenylethene-Based Fluorophores. *Chem. - Eur. J.* **2012**, *18*, 16037-16045.

241. Dillon, K. B.; Mathey, F.; Nixon, J. F., *Phosphorus: The Carbon Copy: From Organophosphorus to Phospha-organic Chemistry*. Chichester: Wiley: 2001.

242. Simpson, M. C.; Protasiewicz, J. D., Phosphorus as a carbon copy and as a photocopy: New conjugated materials featuring multiply bonded phosphorus. *Pure Appl. Chem.* **2013**, *85*, 801-815.

243. Mädl, E.; Butovskii, M. V.; Balázs, G.; Peresypkina, E. V.; Virovets, A. V.; Seidl, M.; Scheer, M., Functionalization of a cyclo-P_5 Ligand by Main-Group Element Nucleophiles. *Angew. Chem. Int. Ed.* **2014**, *53*, 7643-7646.

244. Baudler, M., Chain and Ring Phosphorus Compounds—Analogies between Phosphorus and Carbon Chemistry. *Angew. Chem. Int. Ed.* **1982**, *21*, 492-512.

245. Gómez-Ruiz, S.; Hey-Hawkins, E., The unusual coordination chemistry of phosphorus-rich linear and cyclic oligophosphanide anions. *Coord. Chem. Rev.* **2011**, *255*, 1360-1386.

246. Donath, M.; Hennersdorf, F.; Weigand, J. J., Recent highlights in mixed-coordinate oligophosphorus chemistry. *Chem. Soc. Rev.* **2016**, *45*, 1145-1172.

247. Regitz, M.; Binger, P., Phosphaalkynes—Syntheses, Reactions, Coordination Behavior. *Angew. Chem. Int. Ed.* **1988**, *27*, 1484-1508.

248. Quin, L. D., *A Guide to Organophosphorus Chemistry*. New York: VCH, John Wiley & Sons: 2000.

249. Falconer, R. L.; Russell, C. A., 1,3,5-Triphosphabenzenes: Synthesis, reactivity and theory. *Coord. Chem. Rev.* **2015**, *297-298*, 146-167.

250. Gates, D. P., Expanding the Analogy Between P=C and C=C Bonds to Polymer Science. In *New Aspects in Phosphorus Chemistry V*, Majoral, J.-P., Ed. Springer Berlin Heidelberg: Berlin, Heidelberg, 2005; Vol. Chapter 4, pp 107-126.

251. Bates, J. I.; Dugal-Tessier, J.; Gates, D. P., Phospha-organic chemistry: from molecules to polymers. *Dalton Trans.* **2010**, *39*, 3151-3159.

252. Regitz, M., Phosphaalkynes: new building blocks in synthetic chemistry. *Chem. Rev.* **1990**, *90*, 191-213.

253. Nixon, J. F., Recent developments in the organometallic chemistry of phospha-alkynes, RC≡P. *Coord. Chem. Rev.* **1995**, *145*, 201-258.

254. Kamer, P. C. J.; van Leeuwen, P. W. N. M., *Phosphorus(III)Ligands in Homogeneous Catalysis: Design and Synthesis*. Oxford: Wiley-Blackwell: 2012.

255. Appel, R.; Knoll, F.; Ruppert, I., Phospha-alkenes and Phospha-alkynes, Genesis and Properties of the (p-p)π-Multiple Bond. *Angew. Chem. Int. Ed.* **1981**, *20*, 731-744.

256. Russell, C. A.; Townsend, N. S., Phosphaalkynes. In *Phosphorus(III) Ligands in Homogeneous Catalysis: Design and Synthesis*, Oxford: Wiley-Blackwell: 2012; Vol. Chapter 11, pp 343-354.

257. Balueva, A. S.; Nikonov, G. N.; Vul'fson, S. G.; Sarvarova, N. N.; Arbuzov, B. A., Reaction of 1-boryl-2-phosphinoethenes with carbon disulfide. *Russ. Chem. Bull.* **1990**, *39*, 2367-2370.

258. Longobardi, L. E.; Johnstone, T. C.; Falconer, R. L.; Russell, C. A.; Stephan, D. W., Hydroboration of Phosphaalkynes by $HB(C_6F_5)_2$. *Chem – Eur. J.* **2016**, *22*, 12665-12669.

259. Becker, G.; Becker, W.; Knebl, R.; Schmidt, H.; Hildenbrand, U.; Westerhausen, M., Alkylidynephosphines - Syntheses and Reactivity. *Phosphorus Sulfur Silicon Relat Elem.* **1987**, *30*, 349-352.

260. Yruegas, S.; Martinez, J. J.; Martin, C. D., Intermolecular insertion reactions of azides into 9-borafluorenes to generate 9,10-B,N-phenanthrenes. *Chem. Commun.* **2018**.

261. Chase, P. A.; Romero, P. E.; Piers, W. E.; Parvez, M.; Patrick, B. O., Fluorinated 9-borafluorenes vs. conventional perfluoroaryl boranes - Comparative Lewis acidity. *Can. J. Chem.* **2005**, *83*, 2098-2105.

262. Quin, L. D.; Verkade, J. G., *Phosphorus-31 NMR Spectral Properties in Compound Characterization and Structural Analysis*. New York: VCH, John Wiley & Sons: 1994.

263. Longobardi, L. E.; Russell, C. A.; Green, M.; Townsend, N. S.; Wang, K.; Holmes, A. J.; Duckett, S. B.; McGrady, J. E.; Stephan, D. W., Hydrogen Activation by an Aromatic Triphosphabenzene. *Journal of the American Chemical Society* **2014**, *136*, 13453-13457.

264. Miura-Akagi, P. M.; Nakashige, M. L.; Maile, C. K.; Oshiro, S. M.; Gurr, J. R.; Yoshida, W. Y.; Royappa, A. T.; Krause, C. E.; Rheingold, A. L.; Hughes, R. P.; Cain, M. F., Synthesis of a Tris(phosphaalkene)phosphine Ligand and Fundamental Organometallic Reactions on Its Sterically Shielded Metal Complexes. *Organometallics* **2016**, *35*, 2224-2231.

265. Magnuson, K. W.; Oshiro, S. M.; Gurr, J. R.; Yoshida, W. Y.; Gembicky, M.; Rheingold, A. L.; Hughes, R. P.; Cain, M. F., Streamlined Preparation and Coordination Chemistry of Hybrid Phosphine–Phosphaalkene Ligands. *Organometallics* **2016**, *35*, 855-859.

266. Wilson, D. W. N.; Hinz, A.; Goicoechea, J. M., An Isolable Phosphaethynolatoborane and Its Reactivity. *Angew. Chem. Int. Ed.* **2018**, *57*, 2188-2193.

267. Floch, P. L., Phosphaalkene, phospholyl and phosphinine ligands: New tools in coordination chemistry and catalysis. *Coord. Chem. Rev.* **2006**, *250*, 627-681.

268. Wang, Z.; Zhou, Y.; Zhang, J.-X.; Krummenacher, I.; Braunschweig, H.; Lin, Z., DFT Studies on the reactions of boroles with alkynes. *Chem – Eur. J.* **2018**.

269. Frisch, M. J.; Trucks, G. W.; Schlegel, H. B.; Scuseria, G. E.; Robb, M. A.; Cheeseman, J. R.; Scalmani, G.; Barone, V.; Petersson, G. A.; Nakatsuji, H.; Li, X.; Caricato, M.; Marenich, A. V.; Bloino, J.; Janesko, B. G.; Gomperts, R.; Mennucci, B.; Hratchian, H. P.; Ortiz, J. V.; Izmaylov, A. F.; Sonnenberg, J. L.; Williams; Ding, F.; Lipparini, F.; Egidi, F.; Goings, J.; Peng, B.; Petrone, A.; Henderson, T.; Ranasinghe, D.; Zakrzewski, V. G.; Gao, J.; Rega, N.; Zheng, G.; Liang, W.; Hada, M.; Ehara, M.; Toyota, K.; Fukuda, R.; Hasegawa, J.; Ishida, M.; Nakajima, T.; Honda, Y.; Kitao, O.; Nakai, H.; Vreven, T.; Throssell, K.; Montgomery Jr., J. A.; Peralta, J. E.; Ogliaro, F.; Bearpark, M. J.; Heyd, J. J.; Brothers, E. N.; Kudin, K. N.; Staroverov, V. N.; Keith, T. A.; Kobayashi, R.; Normand, J.; Raghavachari, K.; Rendell, A. P.; Burant, J. C.; Iyengar, S. S.; Tomasi, J.; Cossi, M.; Millam, J. M.; Klene, M.; Adamo, C.; Cammi, R.; Ochterski, J. W.; Martin, R. L.; Morokuma, K.; Farkas, O.; Foresman, J. B.; Fox, D. J. Gaussian 16 Rev. B.01, Wallingford, CT, 2016.

270. Fukui, K., The path of chemical reactions - the IRC approach. *Acc. Chem. Res.* **1981**, *14*, 363-368.

271. Schäfer, A.; Huber, C.; Ahlrichs, R., Fully optimized contracted Gaussian basis sets of triple zeta valence quality for atoms Li to Kr. *J. Phys. Chem.* **1994**, *100*, 5829-5835.

272. Marenich, A. V.; Cramer, C. J.; Truhlar, D. G., Universal Solvation Model Based on Solute Electron Density and on a Continuum Model of the Solvent Defined by the Bulk Dielectric Constant and Atomic Surface Tensions. *J. Phys. Chem. B* **2009**, *113*, 6378-6396.

273. Glendening, E. D., Reed, A. E., Carpenter, J. E., Weinhold, F., NBO Version 3.1.

274. Schleyer, P. v. R.; Najafian, K., Stability and Three-Dimensional Aromaticity of closo-Monocarbaborane Anions, $CB_{n-1}H_{n-}$, and closo-Dicarboranes, $C_2B_{n-2}H_n$. *Inorg. Chem.* **1998**, *37*, 3454-3470.

275. King, R. B., Three-Dimensional Aromaticity in Polyhedral Boranes and Related Molecules. *Chem. Rev.* **2001**, *101*, 1119-1152.

276. Chen, Z.; King, R. B., Spherical Aromaticity: Recent Work on Fullerenes, Polyhedral Boranes, and Related Structures. *Chem. Rev.* **2005**, *105*, 3613-3642.

277. Plesek, J., Potential applications of the boron cluster compounds. *Chem. Rev.* **1992**, *92*, 269-278.

278. Fox, M. A.; Hughes, A. K., Cage C・H···X interactions in solid-state structures of icosahedral carboranes. *Coord. Chem. Rev.* **2004**, *248*, 457-476.

279. Grimes, R. N., Carboranes in the chemist's toolbox. *Dalton Trans.* **2015**, *44*, 5939-5956.

280. Grimes, R. N., *Carboranes*. Academic Press: New York, 2016.

281. Estrada, J.; Lugo, C. A.; McArthur, S. G.; Lavallo, V., Inductive effects of 10 and 12-vertex closo-carborane anions: cluster size and charge make a difference. *Chem. Commun.* **2016**, *52*, 1824-1826.

282. Zakharkin, L. I.; Kovredov, A. I., Formation of biscarboranes during reaction of lithium carboranes with copper salts. *Bull. Acad. Sci. USSR, Div. Chem. Sci.* **1973**, *22*, 1396-1396.

283. Zakharkin, L. I.; Shemyakin, N. F., Synthesis of cyclic compounds that contain the carbon atoms of two o-carborane nuclei, a CH_2 group, and a heteroatom in the ring. *Bull. Acad. Sci. USSR, Div. Chem. Sci.* **1977**, *26*, 2184-2186.

284. Zakharkin, L. I.; Shemyakin, N. F., Synthesis of five- and seven-membered rings that contain the carbon atoms of two *o*-carborane nuclei and a heteroatom. *Bull. Acad. Sci. USSR, Div. Chem. Sci.* **1978**, *27*, 1267-1268.

285. Bokii, N. G.; Yanovskii, A. I.; Struchkov, Y. T.; Shemyakin, N. F.; Zakharkin, L. I., Crystal structures of $(CH_3)_2Ge(C_2B_{10}H_{10})_2PC_6H_5$ and $(CH_3)_2Sn(C_2B_{10}H_{10})_2CHOCH_3$, heterocyclic compounds with *o*-carborane ring carbon atoms in the heterocycle. *Bull. Acad. Sci. USSR, Div. Chem. Sci.* **1978**, *27*, 328-334.

286. Antipin, M. Y.; Furmanova, N. G.; Yanovskii, A. I.; Struchkov, Y. T., Crystal and molecular structure of bis(o-carboranyl)dimethylgermane. *Bull. Acad. Sci. USSR, Div. Chem. Sci.* **1978**, *27*, 1264-1267.

287. Zakharkin, L. I.; Shemyakin, N. F., Synthesis of five-membered heterocycles containing in the ring two carbon atoms of an *o*-carborane ring, two methylene groups, and atoms of Ni, Pd, Pt, Ti, Zr, Si, Ge, OR Sn. *Bull. Acad. Sci. USSR, Div. Chem. Sci.* **1981**, *30*, 1525-1527.

288. Zakharkin, L. I.; Shemyakin, N. F., Synthesis of heterocyclic compounds containing four carbon atoms of two *o*-carborane systems, a silicon atom, and a Ni, Co, Pd, or Cu atom in the ring. *Bull. Acad. Sci. USSR, Div. Chem. Sci.* **1984**, *33*, 2572-2573.

289. Love, R. A.; Bau, R., Crystal structure of the biscarborane complex $Co[B_{10}C_2H_{10}]_2)_2$. *J. Am. Chem. Soc.* **1972**, *94*, 8274-8276.

290. Harwell, D. E.; McMillan, J.; Knobler, C. B.; Hawthorne, M. F., Structural Characterization of Representative d7, d8, and d9 Transition Metal Complexes of Bis(*o*-carborane). *Inorg. Chem.* **1997**, *36*, 5951-5955.

291. Ren, S.; Xie, Z., A Facile and Practical Synthetic Route to 1,1′-Bis(*o*-carborane). *Organometallics* **2008**, *27*, 5167-5168.

292. Puga, A. V.; Teixidor, F.; Sillanpää, R.; Kivekäs, R.; Arca, M.; Barberà, G.; Viñas, C., From Mono- to Poly-Substituted Frameworks: A Way of Tuning the Acidic Character of C-H in o-Carborane Derivatives. *Chem. - Eur. J.* **2009**, *15*, 9755-9763.

293. Qiu, Z.; Ren, S.; Xie, Z., Transition Metal-Carboryne Complexes: Synthesis, Bonding, and Reactivity. *Acc. Chem. Res.* **2011**, *44*, 299-309.

294. Spokoyny, A. M.; Machan, C. W.; Clingerman, D. J.; Rosen, M. S.; Wiester, M. J.; Kennedy, R. D.; Stern, C. L.; Sarjeant, A. A.; Mirkin, C. A., A coordination chemistry dichotomy foricosahedral carborane-based ligands. *Nat. Chem.* **2011**, *3*, 590-596.

295. Ren, S.; Qiu, Z.; Xie, Z., Transition-Metal-Promoted or -Catalyzed Exocyclic Alkyne Insertion *via* Zirconacyclopentene with Carborane Auxiliary: Formation of Symmetric or Unsymmetric Benzocarboranes. *J. Am. Chem. Soc.* **2012**, *134*, 3242-3254.

296. Asay, M.; Kefalidis, C. E.; Estrada, J.; Weinberger, D. S.; Wright, J.; Moore, C. E.; Rheingold, A. L.; Maron, L.; Lavallo, V., Isolation of a Carborane-Fused Triazole Radical Anion. *Angew. Chem. Int. Ed.* **2013**, *125*, 11774-11777.

297. Chan, A. L.; Fajardo, J.; Wright, J. H.; Asay, M.; Lavallo, V., Observation of Room Temperature B–Cl Activation of the $HCB_{11}Cl_{11}^-$ Anion and Isolation of a Stable Anionic Carboranyl Phosphazide. *Inorg. Chem.* **2013**, *52*, 12308-12310.

298. Wright, J. H.; Kefalidis, C. E.; Tham, F. S.; Maron, L.; Lavallo, V., Click-Like Reactions with the Inert $HCB_{11}Cl_{11}^-$ Anion Lead to Carborane-Fused Heterocycles with Unusual Aromatic Character. *Inorg. Chem.* **2013**, *52*, 6223-6229.

299. Yao, Z.-J.; Zhang, Y.-Y.; Jin, G.-X., Pseudo-aromatic bis-*o*-carborane iridium and rhodium complexes. *J. Organomet. Chem.* **2015**, *798*, 274-277.

300. Lugo, C. A.; Moore, C. E.; Rheingold, A. L.; Lavallo, V., Synthesis of a Hybrid *m*-Terphenyl/*o*-Carborane Building Block: Applications in Phosphine Ligand Design. *Inorg. Chem.* **2015**, *54*, 2094-2096.

301. Wong, Y. O.; Smith, M. D.; Peryshkov, D. V., Synthesis of the First Example of the 12-Vertex-closo/12-Vertex-nido Biscarborane Cluster by a Metal-Free B−H Activation at a Phosphorus(III) Center. *Chem. - Eur. J.* **2016**, *22*, 6764-6767.

302. Zhao, D.; Zhang, J.; Lin, Z.; Xie, Z., Unique properties of C,C′-linked nido-biscarborane tetraanions. Synthesis, structure and bonding of ruthenium monocarbollide via unprecedented cage carbon extrusion. *Chem. Commun.* **2016**, *52*, 9992-9995.

303. Wong, Y. O.; Smith, M. D.; Peryshkov, D. V., Reversible water activation driven by contraction and expansion of a 12-vertex-closo-12-vertex-nido biscarborane cluster. *Chem. Commun.* **2016**, *52*, 12710-12713.

304. Axtell, J. C.; Kirlikovali, K. O.; Djurovich, P. I.; Jung, D.; Nguyen, V. T.; Munekiyo, B.; Royappa, A. T.; Rheingold, A. L.; Spokoyny, A. M., Blue Phosphorescent Zwitterionic Iridium(III) Complexes Featuring Weakly Coordinating nido-Carborane-Based Ligands. *J. Am. Chem. Soc.* **2016**, *138*, 15758-15765.

305. Dziedzic, R. M.; Martin, J. L.; Axtell, J. C.; Saleh, L. M. A.; Ong, T.-C.; Yang, Y.-F.; Messina, M. S.; Rheingold, A. L.; Houk, K. N.; Spokoyny, A. M., Cage-Walking: Vertex Differentiation by Palladium-Catalyzed Isomerization of B(9)-Bromo-meta-Carborane. *J. Am. Chem. Soc.* **2017**, *139*, 7729-7732.

306. Chan, T. L.; Xie, Z., Synthesis, structure and aromaticity of carborane-fused carbo- and heterocycles. *Chem. Sci.* **2018**, *9*, 2284-2289.

307. Cheng, R.; Li, B.; Wu, J.; Zhang, J.; Qiu, Z.; Tang, W.; You, S.-L.; Tang, Y.; Xie, Z., Enantioselective Synthesis of Chiral-at-Cage *o*-Carboranes *via* Pd-Catalyzed Asymmetric B–H Substitution. *J. Am. Chem. Soc.* **2018**, *140*, 4508-4511.

308. Quan, Y.; Qiu, Z.; Xie, Z., Transition-Metal-Catalyzed Selective Cage B−H Functionalization of *o*-Carboranes. *Chem. - Eur. J.* **2018**, *24*, 2795-2805.

309. Duttwyler, S., Recent advances in B–H functionalization of icosahedral carboranes and boranes by transition metal catalysis. *Pure Appl. Chem.* **2018**, *90*, 733.

310. Wiesboeck, R. A.; Hawthorne, M. F., Dicarbaundecaborane(13) and Derivatives. *J. Am. Chem. Soc.* **1964**, *86*, 1642-1643.

311. Spokoyny, A. M., New ligand platforms featuring boron-rich clusters as organomimetic substituents. *Pure Appl. Chem.* **2013**, *85*, 903-919.

312. Thiripuranathar, G.; Man, W. Y.; Palmero, C.; Chan, A. P. Y.; Leube, B. T.; Ellis, D.; McKay, D.; Macgregor, S. A.; Jourdan, L.; Rosair, G. M.; Welch, A. J., Icosahedral metallacarborane/carborane species derived from 1,1′-bis(*o*-carborane). *Dalton Trans.* **2015**, *44*, 5628-5637.

313. Martin, M. J.; Man, W. Y.; Rosair, G. M.; Welch, A. J., 1,1′-Bis(ortho-carborane) as a κ2 co-ligand. *J. Organomet. Chem.* **2015**, *798*, 36-40.

314. Riley, L. E.; Chan, A. P. Y.; Taylor, J.; Man, W. Y.; Ellis, D.; Rosair, G. M.; Welch, A. J.; Sivaev, I. B., Unprecedented flexibility of the 1,1′-bis(*o*-carborane) ligand: catalytically-active species stabilised by B-agostic B–H⇀Ru interactions. *Dalton Trans.* **2016**, *45*, 1127-1137.

315. Kirlikovali, K. O.; Axtell, J. C.; Gonzalez, A.; Phung, A. C.; Khan, S. I.; Spokoyny, A. M., Luminescent metal complexes featuring photophysically innocent boron cluster ligands. *Chem. Sci.* **2016**, *7*, 5132-5138.

316. Sivaev, I., Recent advances in the chemistry of 1,1'-bis(ortho-carborane). *Commun. Inorg. Synth.* **2016**, 21-28.

317. Riley, L. E.; Krämer, T.; McMullin, C. L.; Ellis, D.; Rosair, G. M.; Sivaev, I. B.; Welch, A. J., Large, weakly basic bis(carboranyl)phosphines: an experimental and computational study. *Dalton Trans.* **2017**, *46*, 5218-5228.

318. Thiripuranathar, G.; Chan, A. P. Y.; Mandal, D.; Man, W. Y.; Argentari, M.; Rosair, G. M.; Welch, A. J., Double deboronation and homometalation of 1,1′-bis(ortho-carborane). *Dalton Trans.* **2017**, *46*, 1811-1821.

319. Axtell, J. C.; Kirlikovali, K. O.; Dziedzic, R. M.; Gembicky, M.; Rheingold, A. L.; Spokoyny, A. M., Magnesium Reagents Featuring a 1,1′-Bis(*o*-carborane) Ligand Platform. *Eur. J. Inorg. Chem.* **2017**, 4411-4416.

320. Kirlikovali, K. O.; Axtell, J. C.; Anderson, K.; Djurovich, P. I.; Rheingold, A. L.; Spokoyny, A. M., Fine-Tuning Electronic Properties of Luminescent Pt(II) Complexes via Vertex-Differentiated Coordination of Sterically Invariant Carborane-Based Ligands. *Organometallics* **2018**, *37*, 3122-3131.

321. Chan, A. P. Y.; Rosair, G. M.; Welch, A. J., Heterometalation of 1,1′-Bis(ortho-carborane). *Inorg. Chem.* **2018**, *57*, 8002-8011.

322. Scholz, M.; Hey-Hawkins, E., Carbaboranes as Pharmacophores: Properties, Synthesis, and Application Strategies. *Chem. Rev.* **2011**, *111*, 7035-7062.

323. Issa, F.; Kassiou, M.; Rendina, L. M., Boron in Drug Discovery: Carboranes as Unique Pharmacophores in Biologically Active Compounds. *Chem. Rev.* **2011**, *111*, 5701-5722.

324. Zhu, L.; Lv, W.; Liu, S.; Yan, H.; Zhao, Q.; Huang, W., Carborane enhanced two-photon absorption of tribranched fluorophores for fluorescence microscopy imaging. *Chem. Commun.* **2013**, *49*, 10638-10640.

325. Leśnikowski, Z. J., Challenges and Opportunities for the Application of Boron Clusters in Drug Design. *J. Med. Chem.* **2016**, *59*, 7738-7758.

326. Dash, B. P.; Satapathy, R.; Gaillard, E. R.; Norton, K. M.; Maguire, J. A.; Chug, N.; Hosmane, N. S., Enhanced π-Conjugation and Emission via Icosahedral Carboranes:Synthetic and Spectroscopic Investigation. *Inorg. Chem.* **2011**, *50*, 5485-5493.

327. McArthur, S. G.; Geng, L.; Guo, J.; Lavallo, V., Cation reduction and comproportionation as novel strategies to produce high voltage, halide free, carborane based electrolytes for rechargeable Mg batteries. *Inorg. Chem. Front.* **2015**, *2*, 1101-1104.

328. Mukherjee, S.; Thilagar, P., Boron clusters in luminescent materials. *Chem. Commun.* **2016**, *52*, 1070-1093.

329. Núñez, R.; Tarrés, M.; Ferrer-Ugalde, A.; de Biani, F. F.; Teixidor, F., Electrochemistry and Photoluminescence of Icosahedral Carboranes, Boranes, Metallacarboranes, and Their Derivatives. *Chem. Rev.* **2016**, *116*, 14307-14378.

330. Li, X.; Yan, H.; Zhao, Q., Carboranes as a Tool to Tune Phosphorescence. *Chem. - Eur. J.* **2016**, *22*, 1888-1898.

331. Tu, D.; Shao, D.; Yan, H.; Lu, C., A carborane-incorporated mononuclear Co(II) complex showing zero-field slow magnetic relaxation. *Chem. Commun.* **2016**, *52*, 14326-14329.

332. Matsumoto, T.; Takamine, H.; Tanaka, K.; Chujo, Y., Design of bond-cleavage-induced intramolecular charge transfer emission with dibenzoboroles and their application to ratiometric sensors for discriminating chain lengths of alkanes. *Mater. Chem. Front.* **2017**, *1*, 2368-2375.

333. Yruegas, S.; Barnard, J. H.; Al-Furaiji, K.; Dutton, J. L.; Wilson, D. J. D.; Martin, C. D., Boraphosphaalkene Synthesis via Phosphaalkyne Insertion into 9-Borafluorene. *Organometallics* **2018**, *37*, 1515-1518.

334. Zhang, W.; Li, G.; Xu, L.; Zhuo, Y.; Wan, W.; Yan, N.; He, G., 9,10-Azaboraphenanthrene-containing small molecules and conjugated polymers: synthesis and their application in chemodosimeters for the ratiometric detection of fluoride ions. *Chem. Sci.* **2018**, *9*, 4444-4450.

335. Radtke, J.; Mellerup, S. K.; Bolte, M.; Lerner, H.-W.; Wang, S.; Wagner, M., Aryl Insertion vs Aryl–Aryl Coupling in C,C-Chelated Organoborates: The "Missing Link" of Tetraarylborate Photochemistry. *Org. Lett.* **2018**, *20*, 3966-3970.

336. Thanthiriwatte, K. S.; Gwaltney, S. R., Excitation Spectra of Dibenzoborole Containing π-Electron Systems: Controlling the Electronic Spectra by Changing the pπ−π* Conjugation. *J. Phys. Chem. A.* **2006**, *110*, 2434-2439.

337. Lorenz-Rothe, M.; Schellhammer, K. S.; Jägeler-Hoheisel, T.; Meerheim, R.; Kraner, S.; Hein, M. P.; Schünemann, C.; Tietze, M. L.; Hummert, M.; Ortmann, F.; Cuniberti, G.; Körner, C.; Leo, K., From Fluorine to Fluorene—A Route to Thermally Stable aza-BODIPYs for Organic Solar Cell Application. *Adv. Electron. Mater.* **2016**, *2*, 1600152-1600163.

338. Zhang, W.; Yu, D.; Wang, Z.; Zhang, B.; Xu, L.; Li, G.; Yan, N.; Rivard, E.; He, G., Dibora[10]annulenes: Construction, Properties, and Their Ring-Opening Reactions. *Org. Lett.* **2018**.

339. Reiner, J. R.; Alexander, R. P.; Schroeder, H., A New Series of Organoboranes. VIII. The Reaction of Phosgene with the Dilithium Salts of *o*- and *m*-Carborane. *Inorg. Chem.* **1966**, *5*, 1460-1462.

340. Popescu, A.-R.; Musteti, A. D.; Ferrer-Ugalde, A.; Viñas, C.; Núñez, R.; Teixidor, F., Influential Role of Ethereal Solvent on Organolithium Compounds: The Case of Carboranyllithium. *Chem. - Eur. J.* **2012**, *18*, 3174-3184.

341. Teixidor, F.; Vinas, C.; Rudolph, R. W., Rules for predicting the boron-11 NMR spectra of closo-boranes and closo-heteroboranes. *Inorg. Chem.* **1986**, *25*, 3339-3345.

342. Herzog, A.; Maderna, A.; Harakas, G. N.; Knobler, C. B.; Hawthorne, M. F., A Camouflaged nido-Carborane Anion: Facile Synthesis of Octa-B-methyl-1,2-dicarba-closo-dodecaborane(12) and Its Deboration Reaction. *Chem. - Eur. J.* **1999**, *5*, 1212-1217.

343. Araki, T.; Wakamiya, A.; Mori, K.; Yamaguchi, S., Elucidation of π-Conjugation Modes in Diarene-Fused 1,2-Dihydro-1,2-diborin Dianions. *Chem. - Asian J.* **2012**, *7*, 1594-1603.

344. Ge, F.; Kehr, G.; Daniliuc, C. G.; Mück-Lichtenfeld, C.; Erker, G., Trisubstituted Boroles by 1,1-Carboboration. *Organometallics* **2015**, *34*, 4205-4208.

345. Paetzold, P., New perspectives in boron-nitrogen chemistry - I. *Pure Appl. Chem.* **1991**, *63*, 345-350.

346. Hermanek, S., Boron-11 NMR spectra of boranes, main-group heteroboranes, and substituted derivatives. Factors influencing chemical shifts of skeletal atoms. *Chem. Rev.* **1992**, *92*, 325-362.

347. Heřmánek, S., NMR as a tool for elucidation of structures and estimation of electron distribution in boranes and their derivatives. *Inorganica Chim. Acta* **1999**, *289*, 20-44.

348. Teixidor, F.; Barberà, G.; Vaca, A.; Kivekäs, R.; Sillanpää, R.; Oliva, J.; Viñas, C., Are Methyl Groups Electron-Donating or Electron-Withdrawing in Boron Clusters? Permethylation of *o*-Carborane. *J. Am. Chem. Soc.* **2005**, *127*, 10158-10159.

349. te Velde, G.; Bickelhaupt, F. M.; Baerends, E. J.; Fonseca Guerra, C.; van Gisbergen, S. J. A.; Snijders, J. G.; Ziegler, T., Chemistry with ADF. *J. Comput. Chem.* **2001**, *22*, 931-967.

350. Fonseca Guerra, C.; Snijders, J. G.; te Velde, G.; Baerends, E. J., Towards an order-N DFT method. *Theor. Chem. Acc.* **1998**, *99*, 391-403.

351. ADF2014, SCM, Theoretical Chemistry, Vrije Universiteit, Amsterdam, The Netherlands, http://www.scm.com.

352. Grimme, S.; Huenerbein, R.; Ehrlich, S., On the Importance of the Dispersion Energy for the Thermodynamic Stability of Molecules. *ChemPhysChem* **2011**, *12*, 1258-1261.

353. Perdew, J. P.; Burke, K.; Ernzerhof, M., Generalized Gradient Approximation Made Simple. *Phys. Rev. Lett.* **1996**, *77*, 3865-3868.

354. Lee, C.; Sosa, C., Local density component of the Lee–Yang–Parr correlation energy functional. *J. Chem. Phys.* **1994**, *100*, 9018-9024.

355. Becke, A. D., Density-functional thermochemistry. III. The role of exact exchange. *J. Chem. Phys.* **1993**, *98*, 5648-5652.

356. Stephens, P. J.; Devlin, F. J.; Chabalowski, C. F.; Frisch, M. J., Ab Initio Calculation of Vibrational Absorption and Circular Dichroism Spectra Using Density Functional Force Fields. *J. Phys. Chem.* **1994**, *98*, 11623-11627.

357. Yruegas, S.; Axtell, J. C.; Kirlikovali, K. O.; Spokoyny, A. M.; Martin, C. D., Synthesis of 9-borafluorene analogues featuring a three-dimensional 1,1′-bis(*o*-carborane) backbone. *Chem. Commun.* **2019**, *55*, 2892-2895.

358. Sheldrick, G. M., A short history of SHELX. *Acta Cryst.* **2008**, *A64*, 112-122.

359. Dolomanov, O. V.; Bourhis, L. J.; Gildea, R. J.; Howard, J. A. K.; Puschmann, H., OLEX2: a complete structure solution, refinement and analysis program. *J. Appl. Crystallogr.* **2009**, *42*, 339-341.

360. Spek, A., Structure validation in chemical crystallography. *Acta Cryst.* **2009**, *65*, 148-155.

ABOUT THE AUTHOR

Samantha (Sam) was born in Laredo, TX, a small border town in Southwest Texas, on April 15th, 1992. Sam attended John B. Alexander High School where she graduated as part of the Mighty Bulldog Class of 2010 while also enrolled in the Magnet for Health Science program.

Sam began her undergraduate career as a Regents' Scholar at Texas A&M University as part of the Fightin' Texas Aggie Class of 2014 where she received her Bachelor of Arts in Chemistry and minored in English and Psychology. Fascinated by chemical reactions, she became interested in undergraduate research and matriculated into Professor Oleg V. Ozerov's group in 2011 where she studied the solubility of carborane salts of electrophilic transition metal pincer complexes. Sam's experience doing undergraduate research encouraged her to apply to graduate school to obtain a Ph.D. in chemistry.

In the fall of 2014, Sam joined the lab of Professor Caleb D. Martin in the Department of Chemistry and Biochemistry at Baylor University in Waco, Texas. Upon completion of her PhD, she will begin a post-doctoral research position in the laboratory of Professor Paul J. Chirik, The Edwards S. Sanford Professor of Chemistry, at Princeton University in September 2019. After living in Texas for so long, she is excited to move to New Jersey and experience winter for the first time with her significant other Josh Cox and two dogs Sherlock and Hercule.